UNIVERSITY OF SOUTHAMPTON

# Adaptive IIR Filtering for Acoustic Echo Cancellation on a Mobile Handset

by

Edward Peter Craney

A Thesis submitted for the degree of

**Doctor of Philosophy**

Faculty of Engineering and Applied Science
Institute of Sound and Vibration Research

October 2003

UNIVERSITY OF SOUTHAMPTON

ABSTRACT

FACULTY OF ENGINEERING AND APPLIED SCIENCE
INSTITUTE OF SOUND AND VIBRATION RESEARCH

Doctor of Philosophy

**ADAPTIVE IIR FILTERING FOR ACOUSTIC ECHO CANCELLATION ON A MOBILE HANDSET**

by Edward Peter Craney

This thesis is concerned with the problem of acoustic echo cancellation in mobile handsets. The acoustic echo path in a mobile handset is due to the acoustic coupling between the loudspeaker and microphone, which changes depending on the particular handset design and on the handset orientation. To cancel this echo effectively, the nature of this acoustic echo path in normal use must be fully understood. This thesis identifies the possible echo sources on a mobile handset and reports on echo path measurements taken from a typical handset design in various handset orientations. It has been found that resonant acoustic echo path responses are obtained in normal handset use.

The resonant nature of the echo path response motivates an investigation of IIR filter models, as well as more traditional FIR models of the echo path. From the reported results of offline modelling experiments it is clear that, not only do IIR filter models give benefits in terms of complexity and performance over FIR models, but that the IIR filter model also needs to be adaptive.

The modelling performances of adaptive FIR and both Equation Error and Output Error adaptive IIR algorithms have been investigated in this thesis. The steady state performance of certain Output Error adaptive IIR algorithms has been shown to be superior to equivalent adaptive FIR algorithms, both in the presence and the absence of microphone disturbance noise. The tracking performance of these Output Error adaptive IIR algorithms for different time variations in the echo path response, also show that these algorithms can also have better tracking performance than equivalent adaptive FIR algorithms.

In the handset acoustic echo cancellation application robust operation for input speech signals is necessary at low echo to microphone noise levels. A modified form of the NLMS Newton Simplified Gradient Output Error adaptive IIR algorithm is developed in this thesis to satisfy these requirements.

# Acknowledgements

This thesis would not exist without the support and help of my family, the university staff and my friends.

Joanne, my wife, has been extremely supportive in many ways and deserves a special mention, if not a medal. Her patience and encouragement has been there for me when it counted.

My supervisor, Professor Steve Elliott, also deserves being singled out as a person who has provided professional support and encouragement over the 7 long years of my part-time PhD.

Thank you all.

# Chapter 1

## 1. An Introduction to Echo Cancellation

An echo of a transmitted signal can be a disturbing phenomenon for virtually all types of communication. The greater the amplitude of the echo signal and time delay between a signal being transmitted and the echo component being received the greater the disturbing effect will be on the quality and reliability of communication. Echo cancellation simply mimics the echo path function in a communication system to cancel any echo components [1.1]. The principle of echo cancellation is illustrated below in Figure 1.1,

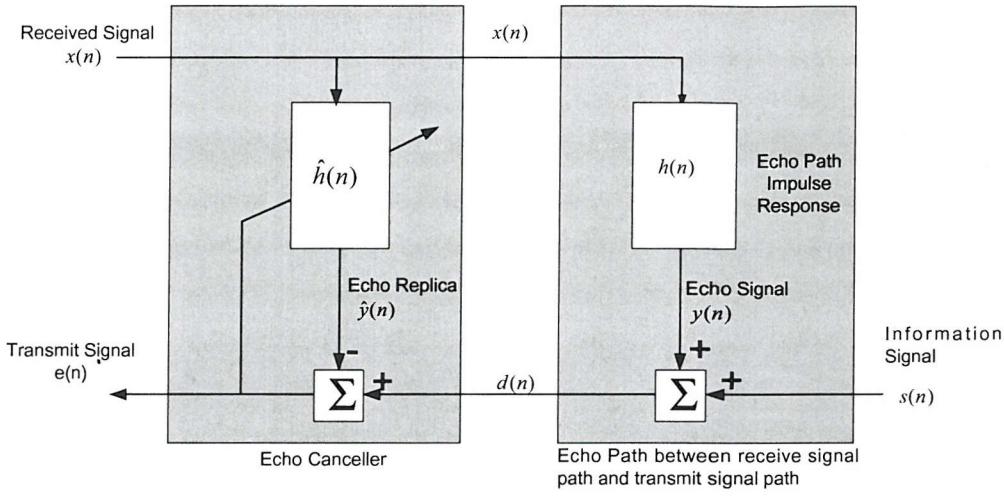


**Figure 1.1 : General configuration of an Echo Canceller**

In Figure 1.1 an echo path, $h(n)$, exists between the received signal path and the transmit signal path of a particular communications system. As a result the signal information $s(n)$ to be transmitted is corrupted by an echo signal $y(n)$. In order to cancel the echo signal $y(n)$, an adaptive filter model is normally used to model the echo path $h(n)$, as the echo path normally varies with time. The output of the adaptive filter $\hat{y}(n)$ is a replica of the echo signal $y(n)$ and can then be subtracted form corrupted signal $d(n)$ to ideally leave no echo signal and only the signal information $s(n)$ to be transmitted [1.1].

The type of echo cancellation used depends on the echo generating mechanism that creates the echo path $h(n)$. In general there are 3 different types of echo cancellation - Acoustic Echo Cancellation, Line Echo Cancellation and Digital Echo Cancellation.

The echo path generating mechanism that must be modelled in the case of Line Echo Cancellation is the result of impedance mismatches in 2 to 4 wire hybrids on the PSTN. During telephone calls on the PSTN electrical echo signals are generated on the receiver of the caller due to these impedance mismatches, which if not attenuated can be disruptive for long echo delays [1.1],[1.2].

In 4 wire subscriber loops which are used for digital data transmission over the PSTN via modems, the echo generating mechanism is the result of impedance mismatches in the local hybrid of the modem set on access to the 2 wire loop, and from impedance mismatches in the modem hybrid at the group

switching centre. Digital Echo Cancellation is required to increase the signal to echo ratio for reliable modem data transmission [1.3].

The echo path generating mechanism for the Acoustic Echo Cancellation (AEC) application is a result of the acoustic coupling path between the loudspeaker and microphone arrangement as part of the communications system [1.4],[1.5] .For hands free applications the acoustic echo path may be the result of acoustic coupling between a loudspeaker and microphone enclosure in a room, office or car [1.5],[1.6],[1.7]. For Acoustic Echo Cancellation (AEC) on a mobile handset the echo path generating mechanism to be modelled is the acoustic path between handset loudspeaker and microphone within the operating environment of the user.

This thesis is concerned with the cancellation of acoustic echo signals on mobile handsets using adaptive IIR filtering techniques. To the authors knowledge no results currently exist for acoustic echo cancellation on mobile handsets, which makes this area exciting and attractive to research.

## 1.1. Acoustic Echo Cancellation on Mobile Handsets

Consider the problem of acoustic echo on a mobile handset as illustrated in Figure 1.2.

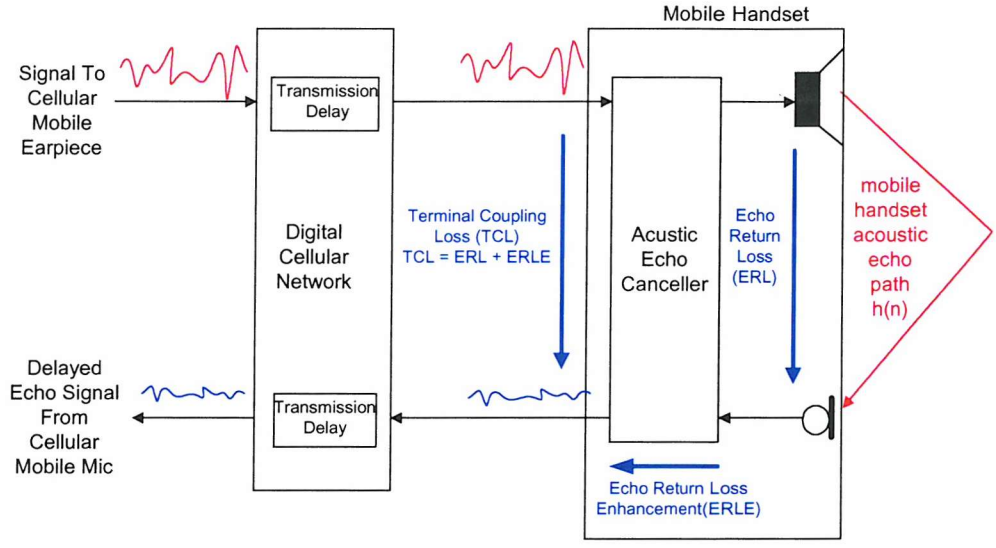


**Figure 1.2: Acoustic Echo Cancellation on a mobile handset**

The acoustic echo path of the mobile handset is a result of acoustic coupling between the loudspeaker and microphone on the handset. When a call is made with the mobile handset, speech signals sent by a user at the other end of the call to the mobile handset loudspeaker will result in an acoustic echo signal being returned to the handset microphone. This echo signal is due to the presence of an acoustic echo path, which produces this acoustic coupling between the loudspeaker and microphone on the handset.

This acoustic echo signal will then be returned to the user at the other end of the call, delayed by the round trip network delay (which for GSM can be up to 200ms [1.6]). Depending on the level of these echo signals returned, significant degradation of the speech call can occur. The effects of time delay and echo for PSTN telephone connections has been studied in [1.8],[1.9]. In order to prevent any degradation in speech quality during a call, the terminal coupling loss of the handset must remain below a certain level.

For GSM and third generation mobile handsets, to deal with calls that may have delays up to 300ms, this terminal coupling loss level is specified as 46dB [1.10],[1.11].

The terminal coupling loss (TCL) of a mobile handset is defined as the overall attenuation of echo signals on the handset picked up by the handset microphone, and transmitted over the network. The echo return loss (ERL) of the mobile handset is the physical echo loss of the handset design due to the casing, etc. This echo return loss is due to the acoustic echo path of the mobile handset. Where the echo return loss of the mobile handset is insufficient to give the required terminal coupling loss level of -46dB, additional echo return loss enhancement (ERLE) in form of an acoustic echo canceller is required.

To effectively cancel the acoustic echo signals on a mobile handset the acoustic echo cancellation device within a mobile handset must model the acoustic echo path of the mobile handset. As the acoustic echo path of a mobile handset may vary quickly depending on the handset position in normal use, the echo cancellation device must be capable of track these changes in order to provide sufficient terminal coupling loss at all times [1.11]. Adaptive filtering techniques would normally be applied within the acoustic echo cancellation device in order to track any echo path changes in normal handset use. This thesis is concerned with the application of adaptive IIR filtering techniques to this problem.

## 1.2. Overview of Thesis

The work described in this thesis was carried out between October 1996 and October 2002 on a part time basis. The aims of this work can be summarised as follows: -

- **To develop adaptive IIR filtering techniques suitable for acoustic echo cancellation on mobile handsets and to investigate their benefits in terms of performance over more traditional adaptive FIR filtering techniques.**

From the work carried out in this thesis the main contributions are: -

- The nature of the acoustic echo path of a typical mobile handset design in normal handset use has been recorded and analysed (chapter2). The variations of both echo path response and resulting terminal coupling loss that an echo canceller must deal with in normal handset use have been identified. A proposal is made for a more robust set of standard test conditions than are used in [1.10] and [1.11], to ensure the handset terminal coupling loss remains below 46dB during normal handset use.
- Modelling experiments have been carried out (chapter 4) showing the benefit of fixed IIR filter models over more traditional FIR filter models for the cancellation of acoustic echoes on mobile handsets under stationary conditions. It is shown that an adaptive model is needed to ensure the terminal coupling loss of a mobile handset remains below 46dB during normal handset use.
- Adaptive Filtering simulations have been used (chapter 5) to show that adaptive IIR filtering techniques can give the performance advantages predicted for fixed IIR filter models under stationary conditions. The effects of adaptive algorithm parameters on the steady state modelling performance of adaptive IIR algorithms have been analysed. The modelling performance of

adaptive IIR algorithms in the presence of echo path output noise for this application has been established. It is clear from the results presented an output error adaptive IIR algorithm is required for the handset acoustic echo application, and that LMS Newton based adaption schemes are required. A proposal is made on the most suitable adaptive IIR algorithm for modelling the acoustic echo path of a mobile handset under stationary conditions.

- The effects of time variations in the echo path response and non-stationary speech input signals on the tracking performance of output error adaptive IIR algorithms suitable for this application area are investigated (chapter 6). The effect of input SNR and output ENR on modelling performance when using speech signals is also investigated. It is shown that an output error adaptive IIR algorithm has benefits in tracking performance over more traditional FIR adaptive filtering algorithms. A robust output error adaptive IIR algorithm is proposed suitable for the handset acoustic echo cancellation application.

Chapter 2, which follows this introductory chapter, deals with measuring and analysing the acoustic echo path response of a mobile handset for different handset positions and configurations. The handset configurations used represent the extreme positions possible in normal handset use and as such should also contain the likely possible variation in handset response in normal handset use The main purpose of this chapter is to determine the echo path response and terminal coupling loss behaviour of a mobile handset in normal use. The possible echo path sources of a typical mobile handset design are firstly identified based on the typical construction of a modern mobile handset design. Next the measurement process is outlined.

From the measurements recorded in chapter 2 the echo path sources (or echo path generating mechanisms) responsible for the variation of terminal coupling loss and echo path response of a handset in normal use are identified. The echo path response of a mobile handset is identified to be linear in nature. It is clear that echo cancellation is required in normal handset use for the mobile handset designs tested, and that a linear echo canceller should be used for this application. It can also be observed that resonant echo path responses can be produced for the handset designs and configurations tested, indicating that an IIR filter structure may be beneficial for use in an echo canceller for this application.

Finally in chapter 2 the effects of echo reflections from the user, and the external environment on the acoustic echo path response of a mobile handset are considered. Non-anechoic environments are used with different user handset positions. From the echo path measurements recorded throughout chapter 2 it is clear the single test condition of [1.10] used to establish the handset terminal coupling loss does not deal with the possible echo path variations in normal handset use observed from the measurements in this chapter. Using the non-anechoic echo path measures presented in the final sections of chapter 2 as a reference of how the mobile handset echo response can actually vary in normal use, a more robust set of fixed handset orientations are proposed for use in [1.10] and [1.11] to ensure a handset design will have sufficient terminal coupling loss in normal handset use. Adaptive algorithms developed in later chapters must remain stable and provide sufficient ERLE performance for the echo path responses of these fixed handset orientations, thus ensuring they will remain stable and provide sufficient terminal coupling loss in actual normal handset use.

Chapter 3 deals with adaptive filter theory for FIR and IIR filter models. The theory presented will be applied later the thesis to the handset acoustic echo cancellation problem when the performance of FIR and IIR filter models and adaptive filtering algorithms will be studied. Chapter 3 is split into three main parts. The first part begins with introducing FIR least squares optimal filtering concepts, which leads to the well-known normal equations [1.12]. Steepest descent and Newton iterative solutions to the normal equations are then presented from which the most commonly used gradient-based adaptive FIR filtering algorithms are derived. The second part is an extension of FIR least squares optimal filtering concepts to cover Output Error IIR least squares optimal filtering and the most commonly used gradient based adaptive Output Error IIR filtering algorithms. The final part of the chapter is used to cover Equation Error IIR least squares optimal filtering and the most commonly used gradient based adaptive Equation Error IIR filtering algorithms. At the end of this chapter a useful summary is given of all adaptive algorithms presented in this chapter in tabulated form.

The choice of whether an FIR or IIR filter model should be used for acoustic echo cancellation is commonly based on modelling experiments carried out for the acoustic echo path responses from hands-free telephony and teleconferencing applications [1.13], [1.14]. This basis is incorrect as the suitability of IIR filter models depends largely on the nature of the acoustic echo path of the particular application area. chapter 4 presents the results of offline modelling experiments using FIR and IIR filter models to model the echo path responses measured in chapter 2. From the results presented it can be seen there is a clear benefit in the use of IIR filter models for acoustic echo cancellation on a mobile handset, particularly for those handsets which employ wideband speech codecs for higher speech quality. Further, an analysis of the zero and pole vectors of the IIR filter models, and the ERLE gain achievable from fixed IIR filter models and fixed pole models, illustrates clearly the need of a fully adaptive IIR filter model for this application.

Chapter 5 follows on from the work carried out in chapter 4 by examining the steady state modelling performance of the adaptive FIR and IIR filtering algorithms when modelling the echo path response of a mobile handset. To the author's knowledge no literature exists on the modelling performance of adaptive algorithms for the handset acoustic echo cancellation application. The first part of chapter 5 examines the achievable steady state ensemble averaged echo return loss enhancement and convergence performance of adaptive FIR and IIR algorithms under stationary conditions, over a range of model orders. A system identification configuration is used with no output noise, stationary input signals and a non-time varying echo path response. The handset echo path responses used in the offline modelling experiments of chapter 4 are re-used here. The adaptive FIR and IIR algorithms employed are a subset of those presented in chapter 3.

From the results presented in the first part of chapter 5 it is clear the same gains in steady state modelling performance as presented in chapter 4 can be achieved for adaptive IIR algorithms. However from the results presented it is clear that faster LMS Newton based adaption schemes of chapter 3 are necessary for adaptive IIR algorithms in order to achieve these gains, and to get closer to the convergence performance achieved by adaptive FIR algorithms. The most suitable model order for adaptive FIR algorithms, Equation Error adaptive IIR algorithms and Output Error adaptive IIR algorithms can be

identified from the results presented to meet the required echo return loss enhancement of each echo path modelled.

As the handset acoustic echo cancellation may have to operate in noisy environments it is necessary that any adaptive IIR algorithms used in the echo canceller must be robust to echo path output noise. The second part of chapter 5 thus looks at the modelling performance of equation and output error adaptive IIR filtering algorithms when modelling the echo paths presented in chapter 4 in the presence of echo path output noise. Using the model orders identified in the first part of chapter 5 the modelling performance of the LMS Newton adaptive algorithms presented in chapter 3 is established. At low echo to noise ratios it is clear an output error adaptive IIR algorithm is required to maintain modelling performance gains over equivalent adaptive FIR algorithms in the presence of echo path output noise. From the LMS Newton based adaptive IIR algorithms presented in chapter 3, only the Output Error Simplified Gradient LMS and NLMS Newton adaptive IIR algorithms provides sufficient modelling performance in the presence of echo path output noise.

So far in the thesis only stationary input signals and non-time varying acoustic echo path responses have been modelled. In the real handset acoustic echo cancellation application time variations will exist both in the handset acoustic echo path to be modelled and the input signals present. Chapter 6 addresses some of the more real world issues for acoustic echo cancellation on a mobile handset using adaptive IIR algorithms. The adaptive IIR algorithms used are Output Error Simplified Gradient LMS and NLMS Newton adaptive IIR algorithms of chapter 5. Chapter 6 is split into 3 parts. The first part of chapter 6 deals with the tracking performance of adaptive IIR algorithms for a time varying acoustic echo path response. As the handset will not have a fixed orientation during a call, time variations in the acoustic path to be modelled will arise. The effect of both linear and non-linear time variations on the tracking performance of adaptive IIR algorithms is analysed. From the results presented it is clear that adaptive IIR algorithms have similar tracking performance to adaptive FIR algorithms with the same number of coefficients.

In the final part of chapter 6 the effect of time varying inputs signals on the modelling performance of adaptive IIR algorithms is addressed. As non-stationary speech signals will be present in the actual handset echo cancellation application, it is important to establish the performance of adaptive IIR algorithms with real speech signals. Additionally the effects of low input SNR and output ENR on the performance of adaptive IIR algorithms is studied. A modified Simplified Gradient NLMS Newton adaptive IIR algorithm is proposed for robust acoustic echo cancellation on a mobile handset.

Finally, chapter 7 summarises the main results presented in this thesis, and draws overall conclusions. Some directions for future research into acoustic echo cancellation on mobile handsets are also suggested.

# Chapter 2

## 2. The Acoustic Echo Path of a Mobile Handset

### 2.1. Introduction

The main objective of this thesis is to develop adaptive IIR filtering techniques for acoustic echo cancellation on mobile handsets. In order to accomplish this it is necessary to understand the behaviour of the echo path response of a typical mobile handset design in normal use. In addition it is necessary to determine the level of Echo Return Loss Enhancement (ERLE) typically needed by an acoustic echo canceller for this application to ensure the terminal coupling loss requirements of can be satisfied at all times. To do this the echo path response of a typical mobile handset design must be measured and analysed. The main focus of this Chapter is to measure and characterise the echo path response, and terminal coupling loss of a typical mobile handset design. To the authors knowledge no results to date have been published on the nature of the acoustic echo path of a mobile handset in normal use.

Chapter 2 is divided into 5 main sections. Section 2.2 begins by firstly discussing the possible sources of echo on a mobile handset. A discussion is presented on how these sources may influence the overall echo path response and terminal coupling loss of a mobile handset, depending on the handset orientation. It is thus important to identify which of these echo path sources will dominate in normal handset use as this will greatly influence the design of the most suitable echo canceller. Section 2.3 then outlines the measurement process and equipment configuration used to record acoustic echo path impulse response data from a typical mobile handset design. The calculation of echo path impulse and frequency response information from this recorded data is explained. Finally definitions for the Terminal Coupling Loss (TCL) of a mobile handset and the Echo Return Loss Enhancement (ERLE) are presented. The calculation of the Terminal Coupling Loss (TCL) level from echo path frequency response information is explained.

In normal handset use the handset position with respect to the user's head will not remain fixed. Different handset orientations are also possible for future mobile applications other than speech, such as video telephony. A large number of handset orientations are hence possible and complete measurement of the echo path response of a handset in normal use is a difficult one. As a solution to this problem a set of fixed handset configurations are proposed. This novel set of test configurations not only represent extreme handset orientations in normal use, but also allows the dominating echo sources of a mobile handset to be clearly identified. Later in the chapter it will be shown that when actual echo path responses from reverberant environments are considered these fixed handset orientations do represent the likely variation possible in normal handset use.

The results of anechoic echo path measurements from these fixed handset positions are presented in Section 2.5. From the results the dominant echo path sources are identified. It is clear that acoustic echo cancellation is needed in normal handset use, despite providing sufficient echo loss during the single fixed handset orientation described in the relevant standard [2.1]. It is also clear that the acoustic echo path of a mobile handset is largely linear in nature. From the results presented it can be observed that resonant echo path responses are possible from a mobile handset depending on the handset orientation and whether any

obstructions or seals exist on the handset transducers. This motivates the study of IIR filter structures and adaptive IIR algorithms for this application in later chapters. At the end of this section a characterisation of the acoustic echo path response of a mobile handset response is made. The results presented in this section of course only directly apply to handsets of similar construction to the handset design measured for this thesis. It is, however, expected the conclusions drawn from these echo path results will apply to most mobile handset designs.

Finally Section 2.6 addresses the impact of echo reflections from the user and the external environment on the acoustic echo path response required to be modelled by an echo canceller. Here the issue of the single test position of [2.1] to represent the handset terminal coupling loss in normal handset use is raised. It is clear from the results presented that a ***set*** of handset test positions is needed to capture the likely variation of handset echo response during normal use. The handset test positions discussed earlier in the chapter are proposed as a ***more robust set of test configurations*** for [2.1] and [2.2] to test whether the terminal coupling loss of a mobile handset remains below 46dB.

## 2.2. Echo Path Sources on a Mobile Handset

Before considering actual echo path measurements let us look at the design of a typical mobile handset. The normal construction of a mobile handset consists of a removable front plastic casing, which is secured to a base unit housing all handset electronics as illustrated in Figure 2.1.

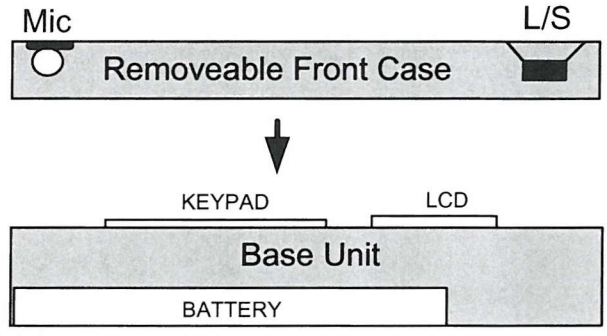


**Figure 2.1: Mobile handset constuction**

The handset loudspeaker is normally permanently attached to the front casing. The handset microphone can either be permanently attached to the front casing as illustrated in Figure 2.1, or permanently attached to the base unit, where a sealing contact with the front unit is made only when the front case is firmly attached to the base unit. The trend for modern mobile handsets is for the overall mobile size/volume to reduce, which normally reduces the relative distance between microphone and loudspeaker in the front case. As new multimedia applications arise such as mobile internet and video telephony the increased functionality of the mobile and increased LCD area needed will fundamentally restrict the size of a typical mobile handset in the future.

In addition to mobile handsets, cordless telephony in the home is also becoming popular, where newer cordless handset designs are designed to look more like the size of older mobile handset designs. It is expected this trend will continue in the future, and these cordless handset designs will face similar echo problems to modern GSM handsets.

The mobile handset design used for the measurement and analysis of handset acoustic impulse responses in this document is the NEC G9 mobile handset. The NEC G9 has approximate dimensions 13cm x 5 cm x 2.5cm (length x breadth x height/width). At the time that the echo path measurements were taken this handset design was considered typical of the handset designs available in the market place. At the time of writing this Ph.D. thesis, however, this handset may be considered to be an older handset design. Indeed by current GSM handset designs this handset may be considered large by comparison, however it is still typical of the size of DECT cordless handsets currently available for the use in the home or office. This size is also comparable to newer third generation designs beginning to emerge in the marketplace.

From a consideration of the construction of a mobile handset design the most probable echo path sources on a mobile handset are defined in Figure 2.2.

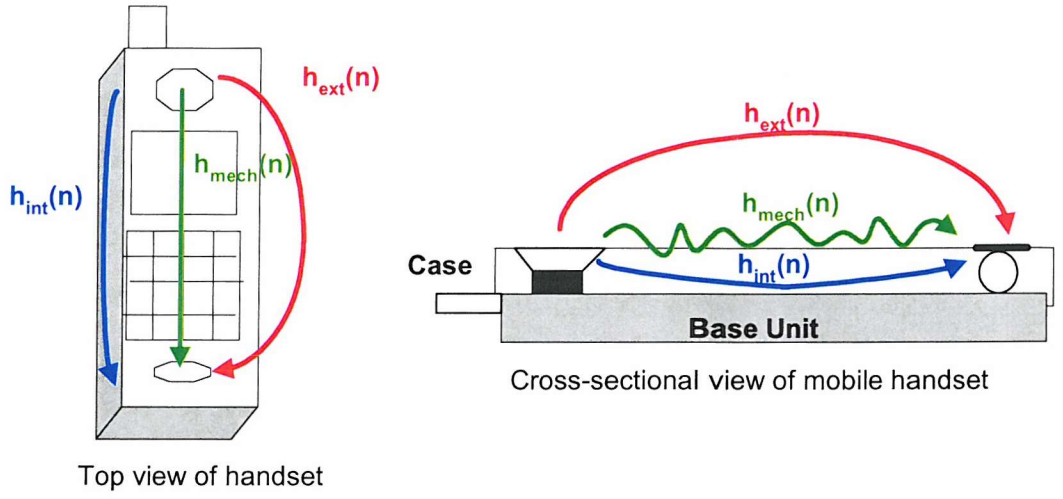


**Figure 2.2: Echo path sources on a mobile handset**

These three possible echo sources are defined as the external acoustic echo path $h_{ext}(n)$, the internal acoustic echo path $h_{\text{int}}(n)$, and the casing and structural mechanical echo path $h_{mech}(n)$.

The external acoustic echo path, $h_{ext}(n)$, is due to acoustic coupling from the loudspeaker in the handset earpiece to the microphone in the handset mouthpiece through the external environment. An external echo path is inevitable when a direct air gap exists between handset loudspeaker and microphone for sound to propagate. No external echo path components would be expected to arrive at the handset microphone until sound propagates across the distance from the loudspeaker to microphone in the air gap in this condition. For a distance of 10cm this would be approximately 0.34ms. An alternative source of external echo may also be due to propagation of sound in other transmission mediums. For example, if the handset is placed face down on a rigid surface while the handset loudspeaker is in operation, no direct air gap may exist, but sound may still propagate from the loudspeaker to the microphone through the rigid surface, creating an external echo path.

It is assumed at this stage that the impact of echo reflections from the external environment may be neglected. The impact of echo reflections from the external environment will be considered later, when the echo path impulse responses in non-anechoic environments are analyzed. The external acoustic echo path

on a mobile handset will be the main echo source for mobile applications such as hands free video telephony.

The internal acoustic path, $h_{\text{int}}(n)$, is due to the internal air cavity, which may exist in a handset design between the removable front casing and the base unit. Pressure fluctuations from the handset loudspeaker into the internal air cavity, may be picked up by the handset microphone, resulting in an internal echo path being created. Depending on the size and construction of the air cavity, and propagation characteristics within the cavity, resonant modes may appear in the echo path response due to the existence of sealed enclosure. This may only occur when a loudspeaker or microphone obstruction or seal is in place on the handset to form a sealed enclosure. For example, for an internal echo path enclosure that has a dominant length dimension of 10cm, the dominant fundamental frequency would approximately 1.7kHz.

The mechanical echo path, $h_{mech}(n)$, is a result of the propagation of vibrations from the handset loudspeaker when in operation to the handset microphone through the handset front casing or base unit. This mechanical coupling may be non-linear in nature [2.3]. It is expected both the internal and external echo path sources would be linear in nature.

The combination of echo path sources $h_{ext}(n), h_{\text{int}}(n)$ and $h_{mech}(n)$ for a particular mobile handset will determine the overall acoustic impulse response $h(n)$ as illustrated in Figure 2.3.

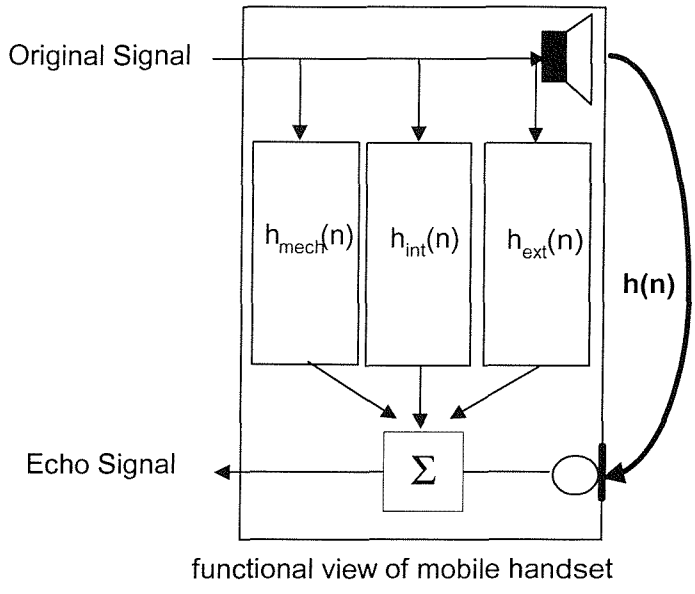


**Figure 2.3: Functional view of the acoustic echo path on a mobile handset**

The overall acoustic echo path response may be written as,

$$h(n) = h_{ext}(n) + h_{\text{int}}(n) + h_{mech}(n), \tag{2.1}$$

To illustrate how these echo path sources described above may influence the overall Terminal Coupling Loss (TCL) level of the mobile handset in normal use, let us consider some examples.

Consider a handset placed firmly to the user's head and ear as shown in Figure 2.4a. This situation is typical during a normal speech call if perhaps the user's environment is noisy. Due the handset earpiece being effectively sealed or obstructed by the user's ear, external echo path contributions would be expected to be low. The overall Terminal Coupling Loss (TCL) level for the handset in this position would as a result be mainly a function of the internal echo path and mechanical echo path components. If mechanical echo path contributions can be neglected, internal echo path contributions would dominate the echo path response and hence overall Terminal Coupling Loss (TCL) level for the handset. If a strong internal echo path exists in the handset design, linear acoustic echo cancellation may be required.

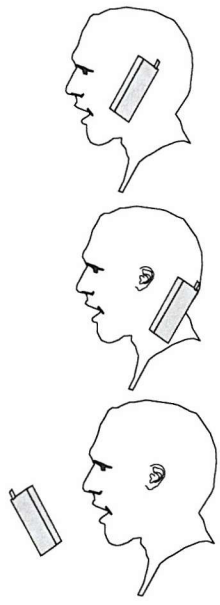

**(a) Handset placed firmly to user's ear and head**

$h_{ext}(n)$ small as external path attenuated
$h_{\text{int}}(n)$ unattenuated perhaps augmented
$h_{mech}(n)$ attenuated



**(b) Handset placed away from user's ear and head**

$h_{ext}(n)$ larger as external path unattenuated
$h_{\text{int}}(n)$ unattenuated
$h_{mech}(n)$ unattenuated



**(c) Handset placed in front of user's head , far away from user's ear.**

$h_{ext}(n)$ large as clear external path present
$h_{\text{int}}(n)$ unattenuated
$h_{mech}(n)$ unattenuated

**Figure 2.4: Illustration of how echo path sources may influence Terminal Coupling Loss of a handset in normal use**

Now consider the placement of the handset away from the user's head and ear as shown in Figure 2.4b. This situation may occur depending on the preference of the user not to place the handset firmly to their head and ear. A direct air gap may exist in this handset configuration resulting in a larger contribution from the external echo path components to the overall Terminal Coupling Loss (TCL) level for the handset in this position. Echo path contributions from the internal and mechanical echo path sources would remain unchanged. Assuming a weak internal echo path in this handset configuration, and that mechanical echo path contributions can be neglected in the handset design, external echo path contributions would dominate the echo path response and hence overall Terminal Coupling Loss (TCL) level for the handset. The presence of external echo path contributions in this handset configuration may require the use of linear acoustic echo cancellation to increase the overall echo loss of the handset.

Finally consider the placement of the handset away from the user's head and ear as shown in Figure 2.4c. This situation may exist for mobile PDA's or future mobile handsets where video telephony is used. A direct air gap will exist in this handset configuration resulting in a large contribution from the external echo path components to the overall Terminal Coupling Loss (TCL) level for the handset in this position. Echo path contributions from the internal and mechanical echo path sources would remain unchanged. Again assuming a weak internal echo path in this handset configuration, and that non-linear mechanical

echo path contributions can be neglected in the handset design, external echo path contributions would dominate the echo path response and hence overall Terminal Coupling Loss (TCL) level for the handset. The presence of strong external echo path contributions in this handset configuration will require the use of linear acoustic echo cancellation to increase the overall echo loss of the handset.

In the next sections of this Chapter we will look at how the acoustic echo path response of a typical mobile handset design is measured. We will also look at how the resulting Terminal Coupling Terminal Loss is calculated.

## 2.3. Echo Path Impulse Response Measurement Process

Many different methods exist for the measurement of the frequency response in a loudspeaker microphone arrangement [2.4]. One of the most common methods that is widely available in most commercial FFT based analysers, is based on random signal excitation input signal to a linear system and the calculation of auto and cross spectral densities[2.5][2.6]. This technique forms the basis of echo path Many different methods exist for the measurement of the frequency response in a loudspeaker microphone arrangement [2.4]. One of the most common methods that is widely available in most commercial FFT based analysers, is based on random signal excitation input signal to a linear system and the calculation of auto and cross spectral densities[2.5][2.6]. This technique forms the basis of echo path response measurements in this Chapter.

### 2.3.1. Estimation of system response using random signal excitation

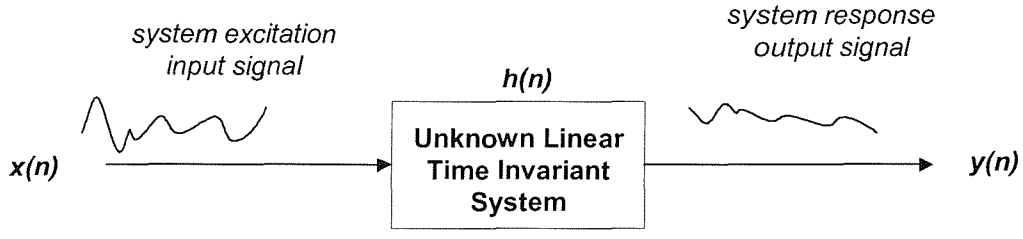


**Figure 2.5: Estimation of impulse response *h(n)* using a random signal excitation**

Consider the basic input-output relationship of Figure 2.5, described in terms of a convolution sum in the time domain as,

$$y(n) = \sum_{m=0}^{\infty} h(m)x(n-m), \tag{2.2}$$

Where the input signal $x(n)$ is a random stationary process, the measurement of the system response $h(n)$ requires use of statistical parameters such as the auto-correlation of the input $x(n)$ and the auto-correlation of the system output $y(n)$ defined as[2.5],

$$r_{xx}(k) = E[x(n)x(n+k)] = \sum_{k=0}^{\infty} x(n)x(n+k), \tag{2.3}$$

$$r_{yy}(k) = E[y(n)y(n+k)] = \sum_{k=0}^{\infty} y(n)y(n+k), \tag{2.4}$$

Using equation (2.1) the cross-correlation may be defined as[2.5],

$$r_{xy}(k) = \sum_{m=0}^{\infty} h(m) r_{xx}(k-m), \tag{2.5}$$

Taking the Fast Fourier Transform (FFT) of both sides of (2.5) gives the Cross Spectral Density,

$$S_{xy}(\omega) = H(\omega) S_{xx}(\omega), \tag{2.6}$$

where $S_{xx}(\omega)$ is the Auto Spectral Density. Re-arranging (2.6) gives the complex frequency response $H(\omega)$ of the unknown system as,

$$H(\omega) = \frac{S_{xy}(\omega)}{S_{xx}(\omega)}, \tag{2.7}$$

Equation (2.7) defines the unknown complex frequency response $H(\omega)$ of the system in terms of the complex cross-power spectrum $S_{xy}(\omega)$ and the auto spectrum of the input excitation signal $S_{xx}(\omega)$. The unknown impulse response of the system $h(n)$ may then be computed using the Inverse Fast Fourier Transform (IFFT) of (2.7) as,

$$h(n) = IFFT[H(\omega)], \tag{2.8}$$

In practice estimates of the auto and cross spectrums are computed from finite sampled data records $x(n)$ and $y(n)$ [2.6]. Denoting the estimates of auto and cross spectrums as $\hat{S}_{xy}(\omega)$ and $\hat{S}_{xx}(\omega)$ we get the transfer function estimate,

$$H_1(\omega) = \frac{\hat{S}_{xy}(\omega)}{\hat{S}_{xx}(\omega)}, \tag{2.9}$$

where $H_1(e^{j\omega})$ is an estimate of the complex frequency response $H(e^{j\omega})$. A common technique used to estimate $\hat{S}_{xy}(\omega)$ and $\hat{S}_{xx}(\omega)$ is the Welch method of spectrum estimation[2.7]. The unknown impulse response estimate of the system may then be computed using an Inverse Fast Fourier Transform (IFFT) from(2.9) as follows,

$$\hat{h}(n) = IFFT[H_1(\omega)], \tag{2.10}$$

Equations (2.9) and (2.10) provide an unbiased estimate of the complex frequency response and impulse response of an unknown system.

Consider now the problem of estimating the unknown acoustic echo path impulse response *h(n)* from the data signals $x(n)$ and $d(n)$ of Figure 2.6. Due to measurement noise and ambient noise picked up by the microphone in the handset, the output of the echo path $d(n)$ can be regarded as the true output of the echo path $y(n)$, superimposed on which would be some uncorrelated output noise $v(n)$ as shown in Figure 2.6.

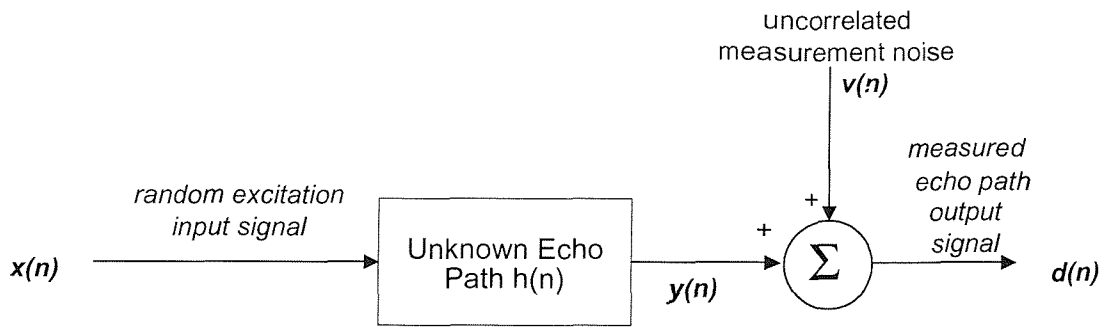


**Figure 2.6: Echo path impulse estimation in presence of output noise**

The measured echo path output $d(n)$ of Figure 2.6 recorded may be expressed as,

$$d(n) = y(n) + v(n), \tag{2.11}$$

Assuming the measurement noise $v(n)$ is uncorrelated with the input signal $x(n)$,

$$E[v(n)x(n+m)] = 0, \tag{2.12}$$

$$E[V^*(\omega)X(\omega)] = 0, \tag{2.13}$$

The cross spectral density between input signal input *x(n)* and measured output *d(n)* becomes [2.5],

$$S_{xd}(\omega) = E[X^*(\omega)(Y(\omega)+V(\omega))] = E[X^*(\omega)Y(\omega)] = S_{xy}(\omega) = H(e^{j\omega})S_{xx}(\omega), \tag{2.14}$$

From (2.14) the same relationship exists between the cross spectrum of input $x(n)$ and measured output $d(n)$ as exists in equation (2.6). Equation (2.9) and (2.10) thus provide an unbiased estimate of the complex frequency response and impulse response of an unknown system with respect to any output noise in the system. As the amount of averaging used in the computation of cross and auto power spectrum estimates $\hat{S}_{xd}(\omega)$ and $\hat{S}_{xx}(\omega)$ in (2.9) is increased [2.7] the impulse response estimate $\hat{h}(n)$ of (2.10) should converge to the actual impulse response of the unknown system $h(n)$ [2.5].

### 2.3.2. Estimation of the coherence function

When the output of a linear system is corrupted with un-corrected measurement noise as shown in Figure 2.6 the power spectrum of the output signal becomes,

$$S_{dd}(\omega) = S_{yy}(\omega) + S_{nn}(\omega), \tag{2.15}$$

From the FFT of both sides of equation (2.3) the auto spectrum of the actual output $y(n)$ can be shown to be,

$$S_{yy}(\omega) = |H(\omega)|^2 S_{xx}(\omega), \tag{2.16}$$

Using equation (2.9), relation (2.14) and equation (2.15) the auto-spectrum of the output $y(n)$ becomes,

$$S_{yy}(\omega) = |H(\omega)|^2 S_{xx}(\omega) = \frac{|S_{xd}(\omega)|^2}{S_{xx}(\omega)}, \tag{2.17}$$

The ratio of power output of the system relating to the input, to the total output power at frequency ω is defined as,

$$\gamma^2_{xd}(\omega) = \frac{S_{yy}(\omega)}{S_{dd}(\omega)} = \frac{|S_{xd}(\omega)|^2}{S_{xx}(\omega)S_{dd}(\omega)}, \tag{2.18}$$

Equation (2.18) is termed the ***coherence function*** relating actual system output $y(n)$ linearly derived from input $x(n)$ and the measured system output $d(n)$. The coherence function is often used as a quality indicator when performing transfer function estimates, and has a range of 0 to 1. A level of 1 indicates all of the output power at frequency $\omega$ is due to the input excitation signal only, with negligible measurement noise present.

The noise process $v(n)$ thus far has been interpreted as the system output measurement noise, but can be more widely interpreted as any ***non-coherent*** contributions to the output of the system such as non-linearities in the system response. The coherence in equation (2.18) may hence be defined as the ratio of output power linearly derived from the excitation signal $x(n)$, to the total output power measured. A high level of coherence across all frequencies is a good indication of system linearity.

### 2.3.3. Echo Path Response Measurements using MATLAB and SIGLAB

#### 2.3.3.1. Equipment Set-up

To record the acoustic impulse response of a mobile handset the measurement set-up Figure 2.7 was used. All handset impulse response measurements recorded in this document were recorded in the University of Southampton anechoic chamber (which has a cut-off frequency of about 100Hz).

#### 2.3.3.2. Audio Bandwidth and Sample Rate

At the time of writing this thesis most mobile handsets incorporate narrowband (telephone bandwidth) codecs, which employ an audio sample rate of 8000Hz, and a bandwidth around 300-3400Hz. This is still true for most GSM handsets in the marketplace today and for fixed telephone lines. To see clearly the characteristics of the acoustic echo path response a sample rate of 12.8kHz is used. The echo path responses presented in this chapter are converted to the 8000Hz sample rate later in the thesis in chapter 4 for FIR and IIR modeling experiments, since the main focus during this thesis is acoustic echo cancellation on mobile handsets with narrowband.

Due to the increasing market penetration of ISDN, Broadband Internet, audio and video conferencing, and newly emerging third generation mobile applications, wideband speech codecs have been developed to provide higher fidelity speech [2.12]. These wideband codecs operate at a 16kHz sample rate with a bandwidth of 50-7000Hz. The higher sample rate of 12.8kHz used for echo path measurements presented in this chapter will be close to the actual responses required to be modelled by an echo canceller in future mobile handset designs (of similar construction) which use these wideband codec

devices. To show the application of results presented in thesis also apply to wideband codec systems the echo path responses presented in this chapter are converted to a 16000Hz sample rate in chapter 4 for FIR and IIR modeling experiments.

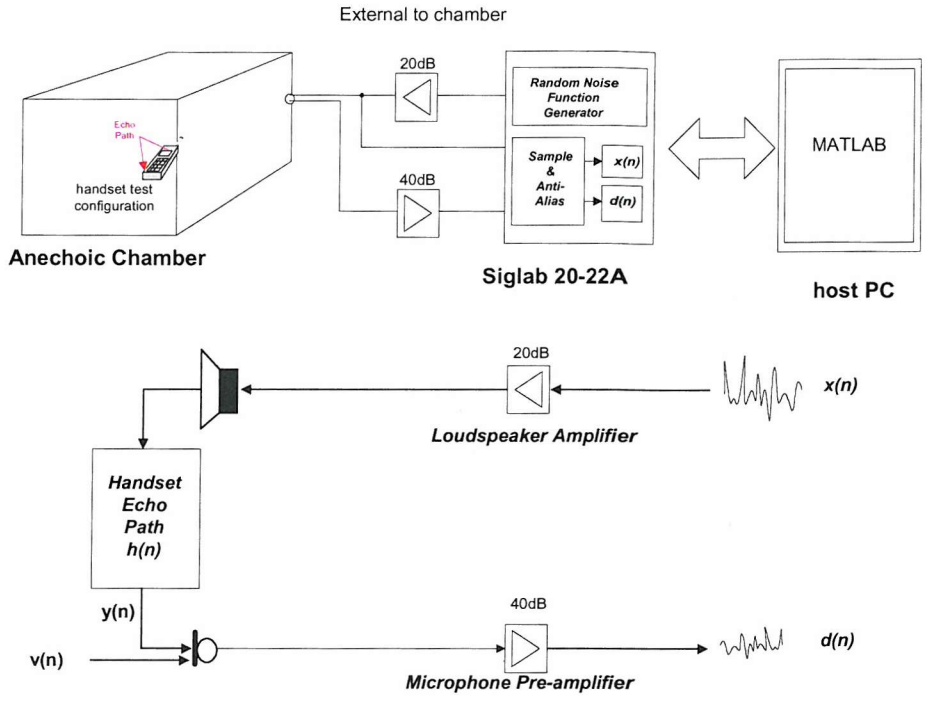


**Figure 2.7: Handset echo path measurement layout**

#### 2.3.3.3. Measurement Procedure

The first step in generating echo path impulse responses was to inject a band limited Gaussian white noise signal into the handset loudspeaker, and record simultaneously both this original noise signal $x(n)$ (before loudspeaker) , and the signal $d(n)$ returning through the handset microphone after amplification. Both signals $x(n)$ and $d(n)$ are recorded at a sampling frequency of 12.8kHz, for a duration of 25secs (320,000 samples at 12.8kHz sample rate) using the Siglab 20-22A unit [2.8],[2.9]. The Siglab unit uses a fixed sampling rate of 51.2kHz and a $4^{th}$ order analogue anti-aliasing filter to band limit recorded data to 12.8kHz. The AD 2105 is then used to perform multi-stage digital decimation filtering to get the relevant sample rate. In our case this is a 12.8kHz sample rate for echo loss measurements.

Using the MATLAB signal processing toolbox functions[2.10], the echo path impulse response estimate $\hat{h}(n)$, of equation (2.10) is computed as shown below in Figure 2.8. The auto and cross power spectrum estimates $\hat{S}_{xx}(\omega)$ and $\hat{S}_{xd}(\omega)$ were computed from the input and output data sets $x(n)$ and $d(n)$ using the Welch's method with a Hanning window type used. A Hanning window size of 1024 samples and overlap of 512 samples were used in the calculation of the complex frequency response estimator $H_1(e^{j\omega})$ using equation (2.9). Approximately 600 averages were used in the computation of

auto- and cross-spectrum estimates for $H_1(e^{j\omega})$ to get accurate results for the echo path frequency response.

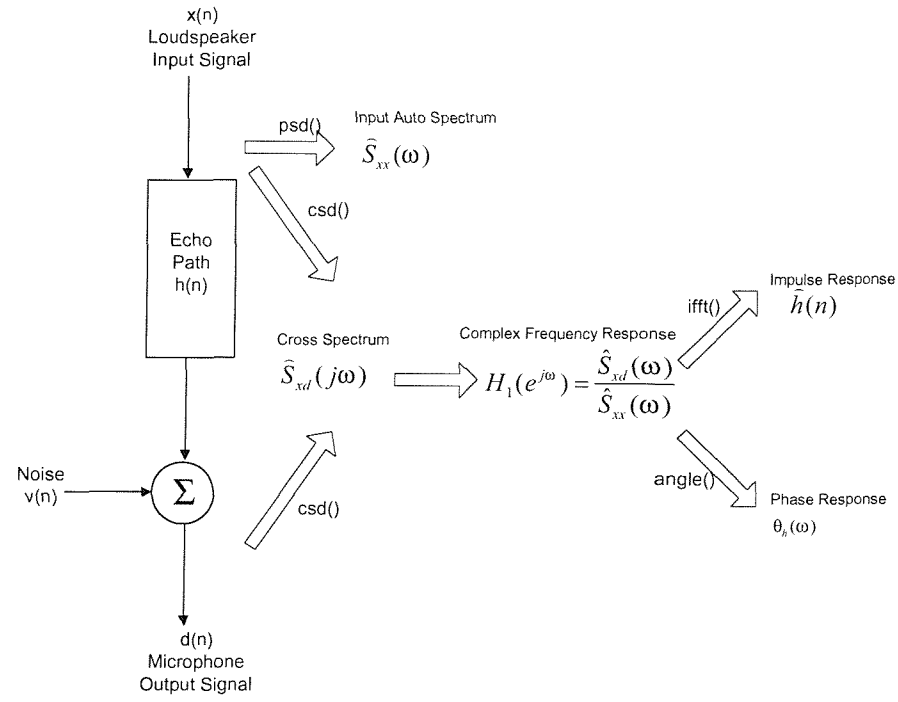


**Figure 2.8: Estimation of unknown echo impulse response using MATLAB and the SIGAB 20-22A unit**

The echo path phase response is calculated from the complex frequency response estimate $H_1(e^{j\omega})$ and the acoustic echo path impulse response estimate $\hat{h}(n)$ is calculated from (2.10).

The coherence function $\gamma^2_{xd}(\omega)$ of (2.18) for an echo path impulse response measurement is computed from input and output data sets *x(n)* and *d(n)*, using estimates for the auto and cross power spectrums $S_{xx}(\omega)$, $S_{yy}(\omega)$ and $S_{xd}(\omega)$. The estimates $\hat{S}_{xx}(\omega)$, $\hat{S}_{yy}(\omega)$ and $\hat{S}_{xd}(\omega)$ are calculated from *x(n)* and *d(n)* using the Welch's method as discussed earlier using a Hanning window size of 1024 and overlap of 512 samples [2.5],[2.7]. Approximately 600 averages were used in the computation of auto and cross spectrums for an accurate coherence function measurement. The coherence function is a particularly useful indication as to whether any non-linear components exist in the echo path response measured.

### 2.3.4. Calculation of the Terminal Coupling Loss (TCL) and Echo Return Loss Enhancement (ERLE)

The Terminal Coupling Loss (TCL) level of a mobile handset is currently defined as the integral of the power transfer characteristic *A(f)* weighted by a –3dB/octave slope starting at 300Hz and extending to 3400Hz [2.1],[2.11] - where a –3dB/octave slope corresponds to a $1/f$ dependence of the input power

spectral density, i.e. the input is assumed to be band limited pink noise. This definition is based on narrowband codec systems with an audio bandwidth of 300-3400Hz.

For the measured handset acoustic echo path responses, the function *A(f)* becomes the echo path frequency response $|H_1(e^{j2\pi f})|^2$ giving the Terminal Coupling Loss (TCL) equation,

$$TCL_{dB} = 3.85 - 10\log_{10}\left[\int_{300}^{3400} \frac{|H(e^{j2\pi f})|^2}{f} df\right], \tag{2.19}$$

Equation (2.19) is simply the ratio of input and output powers of the echo path for a band limited pink noise input signal in the range 300 to 3400Hz [2.11] .The input signal characteristics are defined as,

$$X(f) = \begin{cases} \frac{\sigma_x^2}{f}, & 300 \le f \le 3400 \\ 0, & f < 300, f > 3400 \end{cases}, \tag{2.20}$$

The signal characteristics of (2.20) approximate the long-term average spectrum characteristics of a speech signal. The actual test signal of [2.1] used in TCL measurements is an artificial speech signal, whose long-term spectrum approximates the characteristics of (2.20). For the purposes of echo loss measurement and preliminary modelling results contained in this thesis, an implementation of the band limited pink noise signal of (2.20) in MATLAB is used.

To compute the Terminal Coupling Loss (TCL) level of (2.19) in practice using N+1 discrete samples of $|H_1(e^{j2\pi f})|^2$ uniformly spaced in the range 300 to 3400Hz, the following approximation is used [2.11],

$$TCL_W(dB) = 3.24 - 10\log_{10}\left[\sum_{i=1}^{N}\left(|H(i)|^2 + |H(i-1)|^2\right)\left(\log_{10} f(i) - \log_{10} f(i-1)\right)\right] \tag{2.21}$$

where $|H_1(0)|^2$ is the echo path power response at frequency 300 Hz, and $|H_1(N)|^2$ is the echo path power response at frequency 3400 Hz.

In the same way the Terminal Coupling Loss (TCL) level can be defined as a ratio of ratio of input and output powers, the Echo Return Loss Enhancement (ERLE) may also defined as ratio of powers. It is common practice to calculate this Echo Return Loss Enhancement (ERLE) using time averages across the data records as follows,

$$ERLE_{dB} = 10\log_{10}\left[\frac{E[d^2(n)]}{E[e^2(n)]}\right] \approx 10\log_{10}\left[\frac{\sum_{m=0}^{M-1} d^2(m)}{\sum_{m=0}^{M-1} e^2(m)}\right], \tag{2.22}$$

where M represents the length of input and output recorded sequences *x(n)* and *d(n)*.

For wideband codec systems the Terminal Coupling Loss definition in [2.1] may be modified to account for the higher audio bandwidth of 50- 7000Hz.

### 2.3.5. Calculation of the Effective Impulse Response Duration

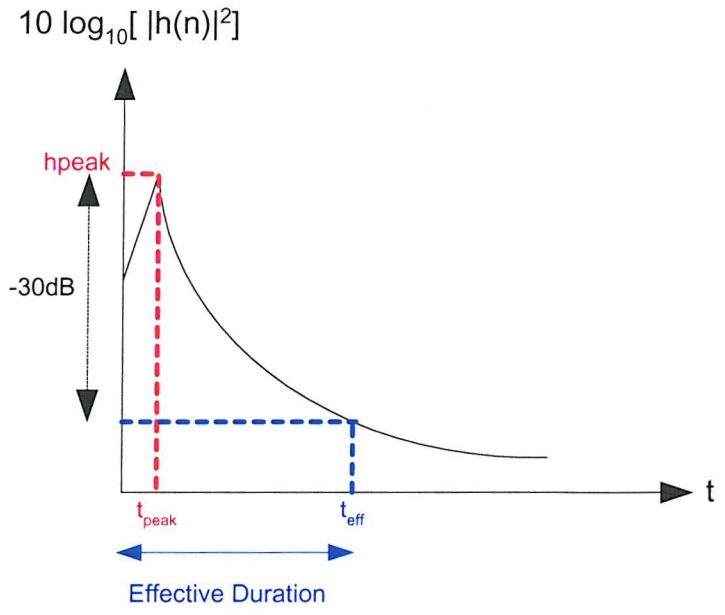


**Figure 2.9 : Effective Duration of an echo path impulse response**

From Figure 2.9 it can be clearly seen the effective duration $t_{eff}$ of an echo path response is defined is the time taken for the echo path impulse response to decay to 30dB below the main peak energy of the response.

The effective duration $t_{eff}$ determines the effective impulse duration required to be modelled by an echo canceller. This of course can be related to the number of feedforward filter model coefficients required to model the echo path response effectively.

## 2.4. Handset Test Configurations

The actual echo path impulse response of a mobile handset will depend on the handset orientation. In normal handset use, the handset orientation is dependent on the user and the mobile application being used. For example in normal speech conversation the user may place the handset in a $45^{o}$ position close to the user's head and ear, whereas in new multimedia applications such as mobile video telephony the handset will most likely be placed vertically (or horizontally) in front of the user's head. A large number of possible handset orientations are hence possible. The task of determining the echo loss performance of a mobile handset in normal use is a difficult one.

The main aim of this section is to define fixed test handset orientations that are repeatable, and representative of the possible handset variations in normal handset use, to allow the dominating echo path sources on a mobile handset to be identified. With this aim in mind the following set of handset orientations are defined. These handset orientations are designed to take into account all possible handset transducer sealing or obstruction possibilities, for all mobile applications (not just speech services) so that the full variation of the handset echo path response in normal use will be observed.

1. The artificial ear sealed test configuration of [2.1]and [2.2].
2. The face up handset configuration, with no transducer seals.
3. The face up handset configuration, with adhesive tape sealing the loudspeaker port
4. The face up handset configuration, with adhesive tape sealing both the loudspeaker and microphone ports
5. The face up handset configuration, with adhesive tape sealing the microphone port
6. The face down handset configuration as defined in stability tests of [2.1]and [2.2] to give worst-case acoustic conditions.

We shall see later in the Chapter that this set of handset orientations allows the handset echo path loss in normal handset use to be more robustly estimated in normal handset use. Currently only the single test condition specified in [2.1]and [2.2] is used.

### 2.4.1. The Artificial Ear Sealed Handset Configuration.

Currently the echo loss performance for GSM mobile handsets is determined by using the test configuration specified in [2.1]. This test configuration is used to represent the typical handset placement for a speech only service, where the handset is placed firmly against the user's ear during a call, normally in a slanted $45^{o}$ position. The test configuration used is shown in Figure 2.10. The mobile handset loudspeaker is sealed to an artificial ear, which approximates the acoustic impedance of the inner ear.

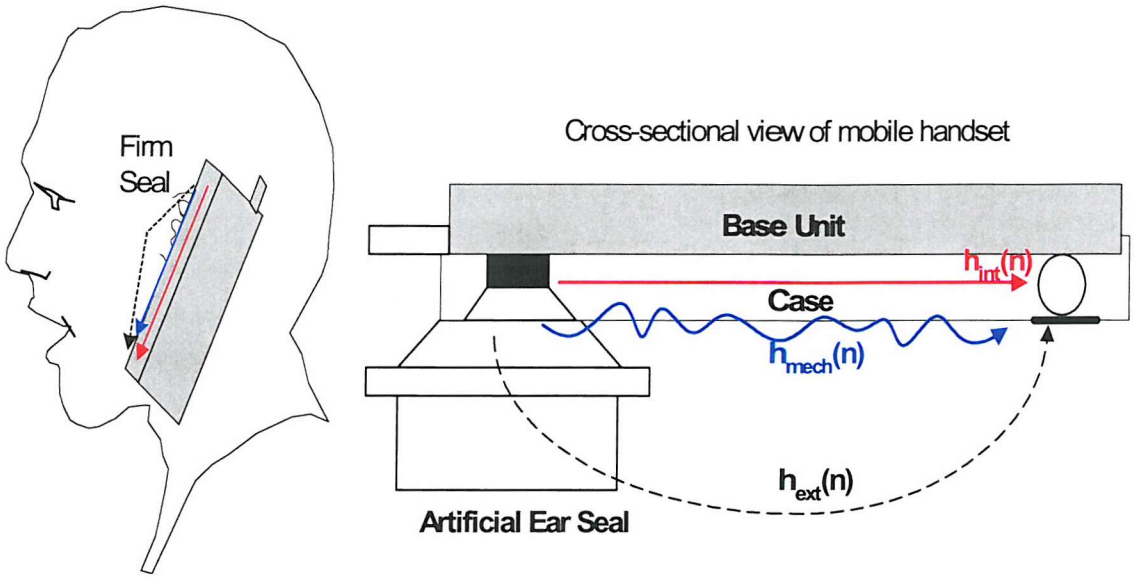


**Figure 2.10: The artificial ear sealed echo loss test configuration of [2.1].**

This handset configuration is used to represent the firm placement of a mobile handset to a user's ear. The internal and mechanical echo path echo path sources are likely to be the main sources of echo in this handset configuration due to heavy attenuation of external path components.

During a speech call or different mobile application the actual handset orientation may not remain firmly against the user's head and ear. No account of this can be made during the echo loss test of [2.1], thus the single test condition is not a very robust method to ensure the echo loss performance for the handset remains below the required levels in normal handset use.

In this handset configuration the external echo path will be heavily attenuated and the internal echo path or mechanical echo path sources may dominate the echo response of the handset.

### 2.4.2. Face Up No Seals Handset Configuration

In this handset configuration all echo path sources will be present. This configuration covers the condition where a partial or full direct path exists between the handset loudspeaker and microphone ports. This may occur during a speech call due to a loose placement of handset to the user's head and ear. In different mobile applications such as a mobile video telephony, this condition is very likely since the handset is likely to be placed in directly front of the user as illustrated in Figure 2.11.

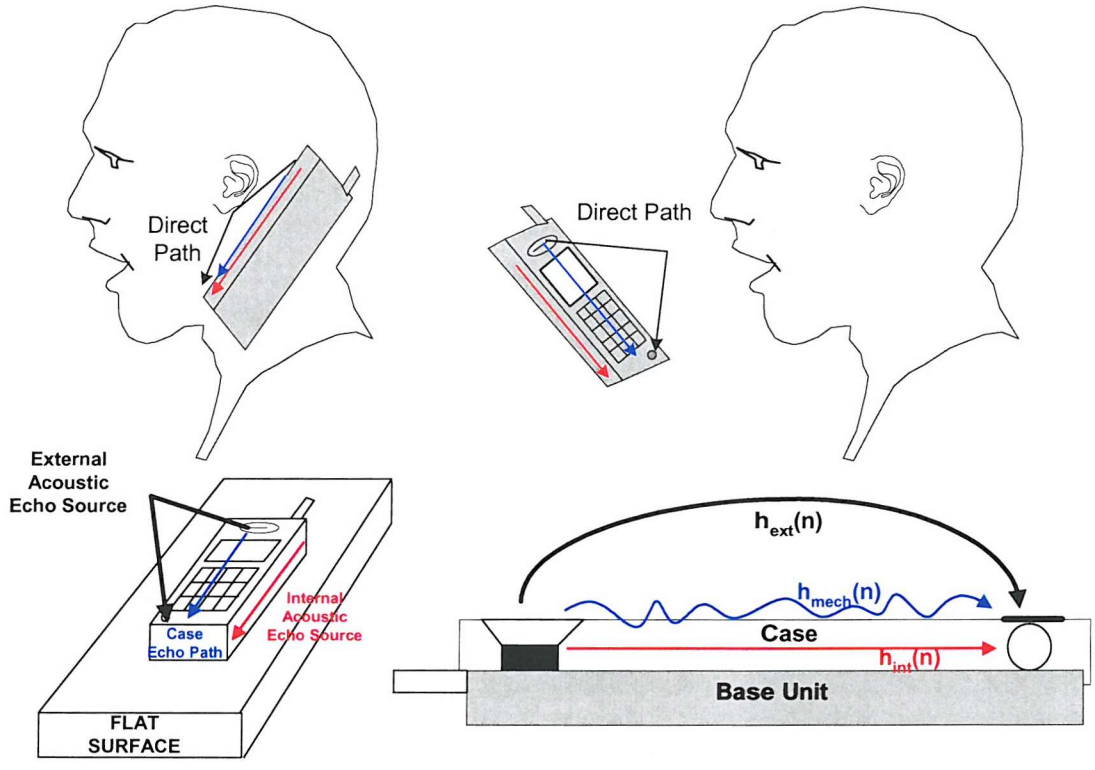


**Figure 2.11: No obstruction or sealed handset configuration.**

This handset configuration represents the condition where a direct air gap exists between the handset loudspeaker and microphone for sound to travel. The external echo path contributions will be a significant contribution to the overall echo path response in this handset configuration.

Identification of the external echo path contributions will be possible in this handset configuration by comparing the echo path response with the artificial ear sealed handset configuration response of 2.4.1 where the external echo path contributions are expected to be low. The presence of case echo path components can be also established by analysing the coherence of the measurement and the absence of any components during the time taken for sound to propagate from handset loudspeaker to microphone.

### 2.4.3. Face Up Handset Configuration with the Handset Loudspeaker Sealed with Tape

This configuration covers the condition where an imperfect seal or obstruction exists on the handset loudspeaker, which can occur in normal use, in assembly, or as a result misalignment of front casing with base unit during front casing replacement by user. To represent this condition of an imperfect seal or obstruction adhesive tape is placed over the handset loudspeaker as illustrated in Figure 2.12.

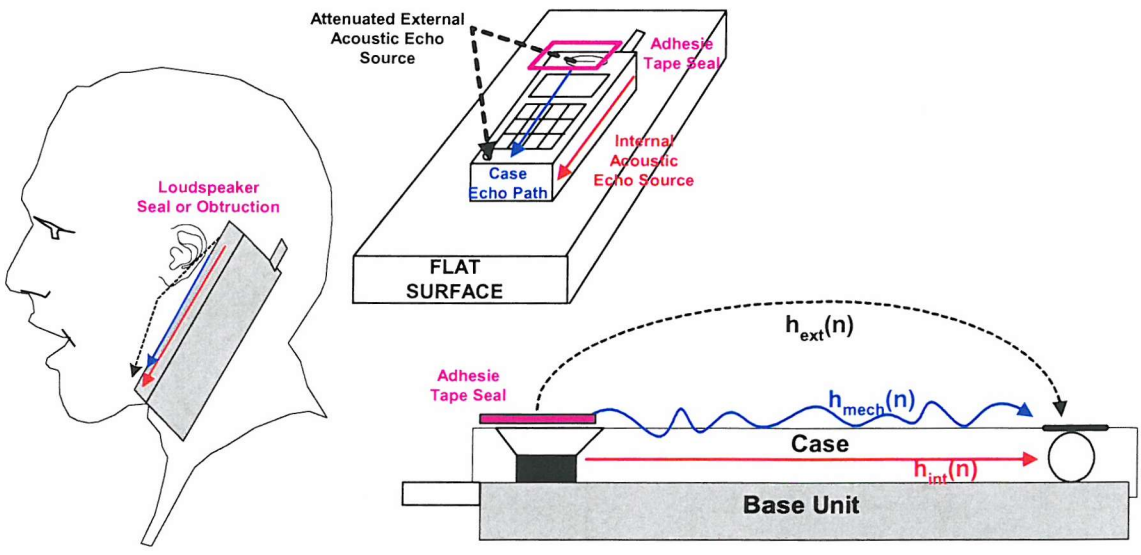


**Figure 2.12: Loudspeaker sealed handset configuration.**

This handset configuration represents the condition where an imperfect seal exists on the handset loudspeaker. The case and external echo path contributions will be significantly reduced due to the presence of the tape seal. However the internal echo path may become augmented due to pressure fluctuations from loudspeaker propagating in air cavity of handset.

Identification of the external and internal echo path contributions will be possible in this handset configuration by comparing the echo path response with the artificial ear sealed handset and face up no sealed configuration responses of 2.4.1 and 2.4.2.

The presence of a loudspeaker seal or obstruction will result in the external (and case) echo path source being attenuated. It is possible that the internal echo path may become augmented if the presence of a loudspeaker seal creates an enclosure where pressure fluctuations from loudspeaker propagate in air cavity of handset resulting in resonant modes in the echo path response. Comparison with handset configuration of 2.4.1 and 2.4.2 should show augmentation of internal echo path components.

### 2.4.4. Face Up Handset Configuration with the Handset Microphone Sealed with Tape

This configuration covers the condition where a seal or obstruction exists on the handset microphone, which can occur in normal use, in assembly, or as a result misalignment of front casing with base unit during front casing replacement by user. To represent this condition adhesive tape is placed over the handset microphone as illustrated in Figure 2.13.

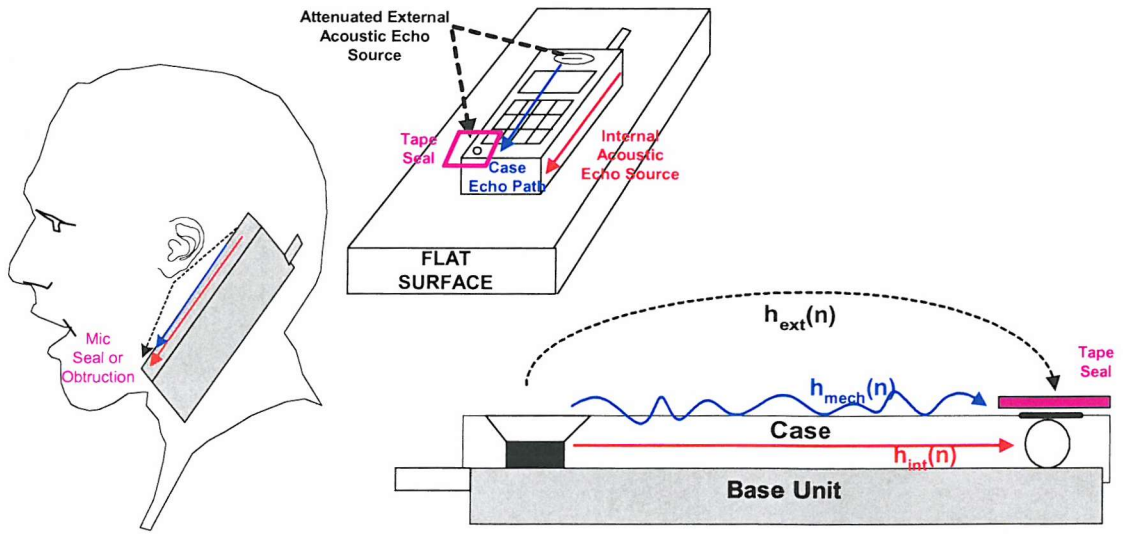


**Figure 2.13: Microphone obstruction or sealed handset configuration.**

This handset configuration represents the condition in which a microphone obstruction or seal exists on the handset during a call. Adhesive tape seals on the handset microphone shall be used to represent this condition. The internal echo path is expected to form a large part of the echo path response in this handset configuration, assuming negligible case echo path components.

This handset configuration represents the condition where only a microphone obstruction or seal exists on the handset during a call. An adhesive tape seal on the handset microphone is used to represent this condition.

The presence of a microphone seal or obstruction will result in the external echo path source being attenuated. It is possible that the internal echo path may become augmented if the presence of a microphone seal creates an enclosure resulting in resonant modes in the echo path response. Comparison with handset configurations of 2.4.1 to 2.4.3 should show augmentation of internal echo path components.

### 2.4.5. Face Up Handset Configuration with the Handset Microphone and Loudspeaker Sealed with Tape

This configuration covers the condition where a seal or obstruction exists on both the handset loudspeaker and microphone, which can occur in normal use, in assembly, or as a result misalignment of front casing with base unit during front casing replacement by user. To represent this condition adhesive tape is placed over both the handset microphone and loudspeaker as illustrated in Figure 2.14.

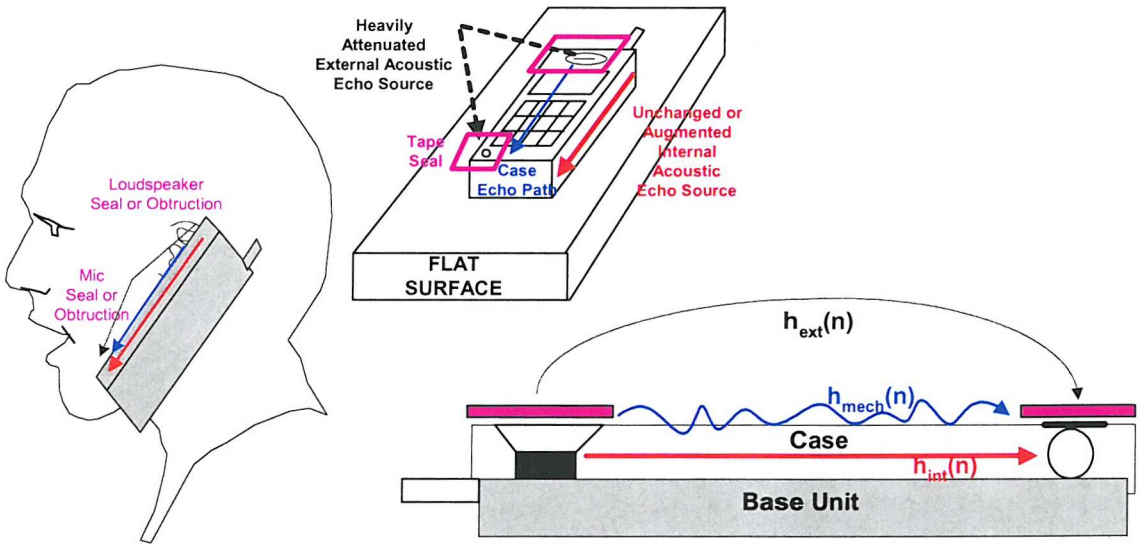


**Figure 2.14: Microphone and loudspeaker obstruction or sealed handset configuration.**

This handset configuration represents the condition in which both a microphone and loudspeaker obstruction or seal exists on the handset during a call. Adhesive tape seals on the handset microphone and loudspeaker shall be used to represent this condition. The internal echo path is expected to form a large part of the echo path response in this handset configuration, assuming negligible case echo path components.

The presence of a both a microphone and loudspeaker seal or obstruction will result in the external echo path source being heavily attenuated. This allows the internal echo path components to be identified. It is possible the presence of both a microphone and loudspeaker seal will create an internal enclosure within the handset, resulting in resonant modes being set-up as sound re-radiated from the loudspeaker propagates in the internal air cavity. The handset echo path response may become resonant in nature when placed in this handset configuration.

### 2.4.6. Face Down Handset Configuration

In this handset configuration the handset is placed face down on a rigid surface as illustrated in Figure 2.15. This configuration represents the condition where the user may place the handset face down during a normal conversation. This handset configuration also represents the stability tests of [2.1] and [2.2]. It is expected that this handset condition will be representative of the worst-case acoustic condition during a call [2.2].

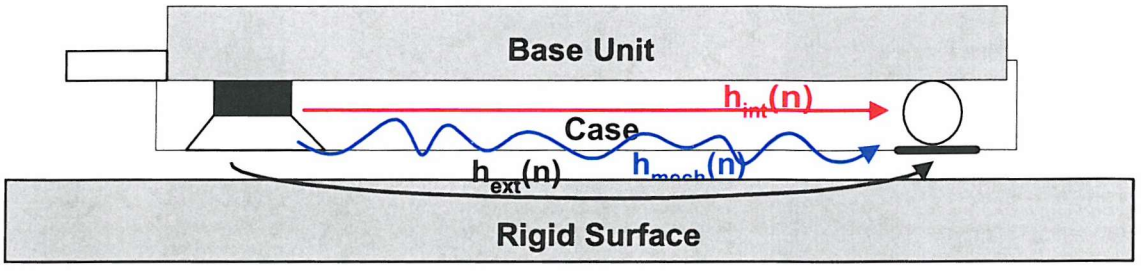


**Figure 2.15: Face Down handset configuration.**

This handset configuration represents the condition a partial or no air gap may exist between handset loudspeaker and microphone. The external echo path may be augmented due to existence of a propagation path through the rigid surface from loudspeaker to microphone.

The echo path response of this handset configuration will depend both on the handset shape or design, and the properties of the rigid surface on which the handset is placed. For handset designs like the one tested in this thesis a number of possibilities could exist for which echo path source dominates the overall echo path response for this handset configuration.

One likely possibility is that the external echo path source will dominate, which consist mainly of the propagation through the rigid surface used, and/or across any direct air gap that may exist depending on the shape of the handset. Another possibility depending on the handset design and the rigid surface used is that a microphone and loudspeaker seal or obstruction may result when placed on the rigid surface. This could result in the external echo path source being heavily attenuated, allowing the internal echo path components to be identified.

The presence of any non-linear contributions from propagation through the rigid surface or across the handset casing in this handset configuration can be established by analyzing the coherence of the measurement.

## 2.5. Results of Anechoic Acoustic Echo Path Impulse Response Measurements

This section of the report presents the echo path responses of the NEC G9 mobile handset in the test configurations described in the last section. Five mobile handsets of the same type were used. No significant differences in responses were noticed from these handsets. It is expected the results presented in this section will be the same for other handset designs of similar construction.

The Terminal Coupling Loss (TCL) levels calculated for each echo path response measured in this chapter are displayed in Table 1 below. The required Echo Return Loss enhancement levels for each echo path response, to ensure that the requirements of [2.1] and [2.2] are satisfied, are also shown in Table 1.

| Handset Configuration | TCL(dB) | Required ERLE (dB) |
|---|---|---|
| G9 artificial ear loudspeaker sealed test configuration | 46.18 | 0 |
| G9 face up configuration with no transducer seals | 32.95 | 13.05 (13) |
| G9 face up configuration with a loudspeaker seal | 41.73 | 4.27 (4) |
| G9 face up configuration with a microphone seal | 40.2 | 5.8 (6) |
| G9 face up configuration with a microphone and loudspeaker seal | 37.38 | 8.62 (9) |
| G9 face down on a flat rigid surface | 30.31 | 15.69 (16) |

**Table 1: Terminal Coupling Loss(TCL) and required Echo Return Loss Enhancement(ERLE) levels calculated for NEC G9 echo path responses.**

To simplify the ERLE requirements for future Chapters the required ERLE levels from Table 1 are rounded up to the nearest integer level (shown in brackets). From Table 1 it can be clearly see that additional Echo Return Loss Enhancement (ERLE) up to 16dB will be required for normal handset use to ensure that the 46dB Terminal Coupling loss requirement of [2.1] for the handset design tested.

The echo loss results in Table 1 for the mobile handset tested show that no additional ERLE is needed for the artificial ear sealed test configuration of [2.1] and [2.2]. However for the other echo paths tested additional ERLE is needed. Only when we consider the full range of echo path responses possible in normal handset use for this handset, do we see the full range of ERLE levels needed for this application. An echo canceller must be designed to meet the ERLE requirements of all echo paths tested in Table 1, not just the artificial ear sealed test configuration of [2.1].

The results of Table 1 demonstrate that using the set of handset configurations described in the last section to establish the echo loss performance of a mobile handset is a more robust method than the single

test configuration of [2.1]. Indeed we can say that, when only the artificial ear sealed test configuration of [2.1] is used to establish the echo loss performance of a mobile handset, in normal handset use the levels of echo loss for the handset cannot be guaranteed to remain below the required levels of [2.1].

Let us now look at the actual echo path response results. Let us first look at the artificial ear sealed response of [2.1] discussed in Section 2.4.1. Figure 2.16 shows the coherence function, frequency response, and echo path impulse response measured for this handset test configuration. A high level of coherence across all frequencies can be observed. Areas of low coherence can be attributed to the echo path response being low, where the resulting output SNR for the measurement may be low. The frequency response in Figure 2.16(a) shows the echo path loss across the frequency range of 0 to 6400Hz and as a result shows negative y-axis values, unlike the Terminal Coupling Loss value which is defined to be positive in [2.1]. This is the same form used for all results presented in this chapter. For narrowband codecs the main region of concern is the audio range of 0 to 4kHz. Above 3.6kHz, the frequency response will be heavily filtered by the narrowband codec ADC filter response. As most of the energy of the frequency response resides above 3 kHz, the resulting Terminal Coupling Loss measured in the region 300 to 3400Hz for this echo path response is large (indicating high echo path loss). Looking more closely at the frequency response in Figure 2.16, low level peaks can be observed around 400, 1400 and 1900Hz in this handset configuration.

From the echo path impulse response in Figure 2.16(c) there exists a delay period with little impulse response activity of approximately 0.4ms, which corresponds to the time taken for sound to travel the loudspeaker to microphone distance in air. A high level of coherence can also be observed across most frequencies in Figure 2.16(a) (except those due to low signal to noise levels due to the lower level echo path response). Since any mechanical vibrations travelling along the handset case would most likely arrive during this observed delay period, and would be non-linear in nature, it can be concluded that no case ( $h_{mech}(n)$ ) echo path source terms exist in this handset configuration. This is also the case for the other handset orientations tested in this chapter. Only the internal and external acoustic path sources are significant for the handset design tested.

At this point an important conclusion can be drawn, given that no non-linear mechanical component $h_{mech}(n)$ exists in the handset responses measured, and that the coherence measures are close to unity for all measurements. Based on the handset design tested it can be concluded that the handset echo path impulse response to be modelled by an echo canceller is linear in nature. A linear acoustic echo canceller is required for the mobile handset acoustic echo cancellation application.

Consider next the face up no seals handset response of Section 2.4.2. Figure 2.17 shows the echo path measurements for this handset test configuration. A high level of coherence across all frequencies can be observed in Figure 2.17(a). The echo path frequency response of Figure 2.17(b) has a general high pass characteristic with most energy in the response above 2200Hz, with a low-level peak can be observed around 1600Hz.

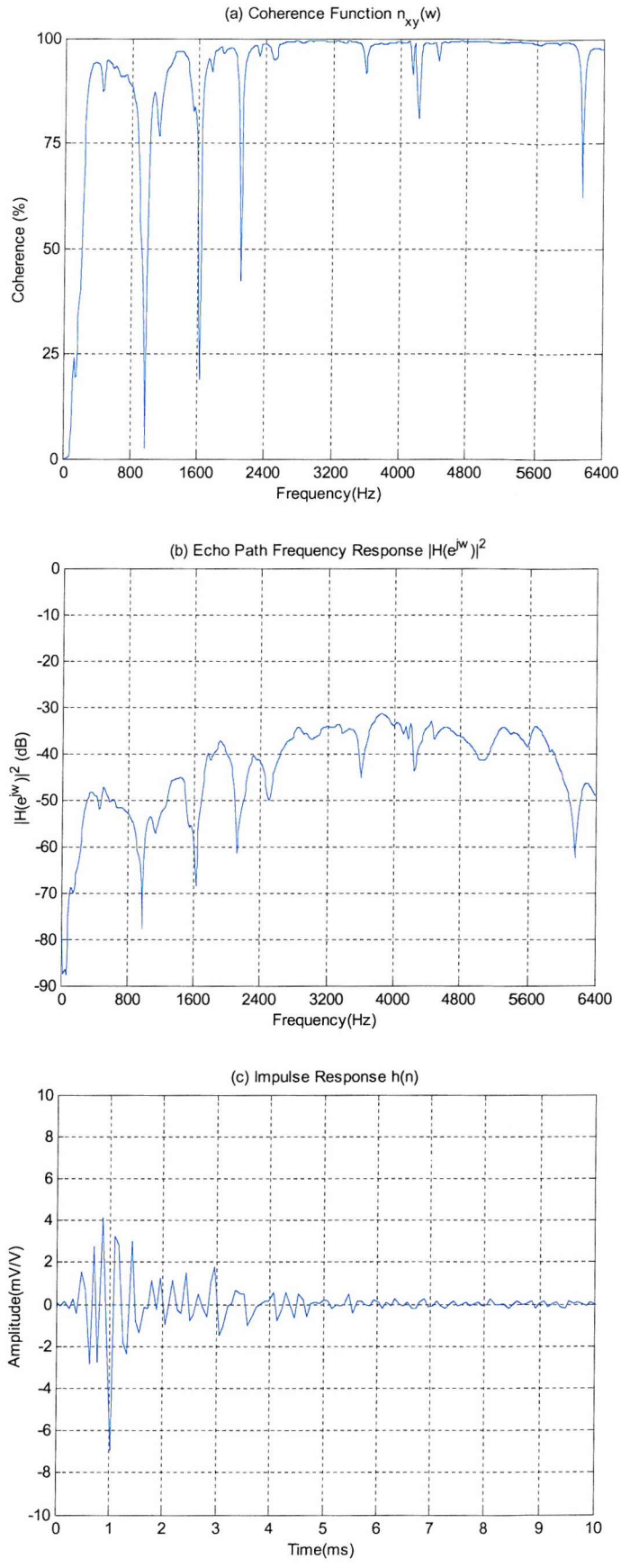


**Figure 2.16: Echo path results for the artificial ear sealed handset configuration,** showing a) the coherence function, (b) frequency response characteristic, and (c) the echo path impulse response.

The impulse response of Figure 2.17(c) contains significant energy from 0 to 0.8ms (responsible for the general high pass characteristic) and decays relatively quickly after this. A delay period of around 0.4ms exists before any response activity as in the artificial ear sealed response.

In Figure 2.18 the echo path frequency responses, phase responses, and impulse responses of the artificial ear sealed and face up no seals handset configurations are superimposed on the same axes for comparison purposes. Both phase responses in Figure 2.18(b) are clearly not linear, and the artificial ear sealed handset configuration introduces more phase delay. The largest phase transition is around the frequency response peak at 1900Hz. From the frequency responses of both handset configurations in Figure 2.18(a) it is clear to see the higher acoustic coupling and lower terminal coupling loss level of the face up no seals handset configuration.

The impulse responses of the artificial ear sealed and face up handset echo path responses are superimposed in Figure 2.18(c). The main contribution of external echo path source component ( $h_{ext}(n)$ ) to the calculated terminal coupling loss level can be easily identified. This is the region of significant impulse response activity in the face up no seals echo path response up to 0.8ms in duration and is responsible for the general high pass nature of the frequency response. As expected this component is heavily attenuated when the handset is placed in the artificial ear sealed handset configuration resulting in a much lower terminal coupling loss level. Without the main external echo path source contribution (and with case and structural components neglected) the low terminal coupling loss of the artificial ear sealed configuration can be attributed to the internal echo path component ( $h_{\text{int}}(n)$ ). At this point it is unclear as to nature of the internal echo path $h_{\text{int}}(n)$ depending on the type of transducer seal or obstruction. The total effective duration of these echo path responses are approximately 3ms for the face up no seals handset response and 5.4ms for the artificial ear sealed handset configuration. As we will see in the next Chapter the effective impulse response duration required to be modelled for satisfactory ERLE, will depend on both the effective impulse response duration and the terminal coupling loss level calculated.

Consider next the measurement results for the loudspeaker adhesive tape sealed handset configuration of Section 2.4.3. These results are presented in Figure 2.19. It is clear from these results when an adhesive seal is placed on the handset loudspeaker a resonant echo path response is produced. From Figure 2.19(b) several distinct resonant peaks exist in the terminal coupling loss measurement band, at around 1900 and 4100Hz in this handset configuration. For the terminal coupling loss level calculated for this echo path response the higher energy peak around 4100Hz will not be taken into account resulting in a lower level. In practice, as we shall see in later Chapters, when handset ADC codec filters are applied all frequency response information above 3.6kHz will be heavily filtered out.

The resulting echo path response in Figure 2.19(c) consists of a small delay period of approximately 0.4ms followed by exponentially decaying resonant response. This response directly reflects the two main resonant peaks in the echo path frequency response in Figure 2.19(b). In particular the 4100Hz peak, which is 10dB stronger, would have major impact on the echo path to be modelled if

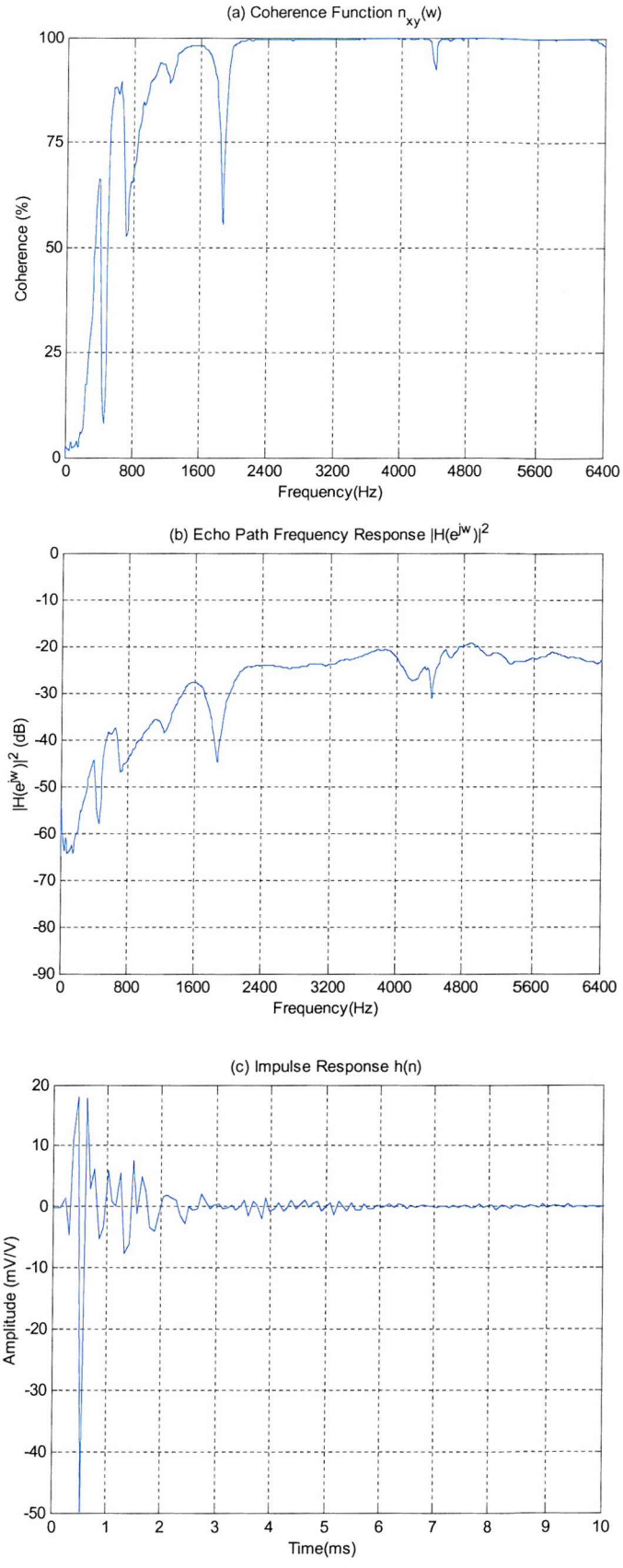


**Figure 2.17: Echo path results for the face up no seals handset configuration,** showing a) the coherence function, (b) frequency response characteristic, and (c) the echo path impulse response.

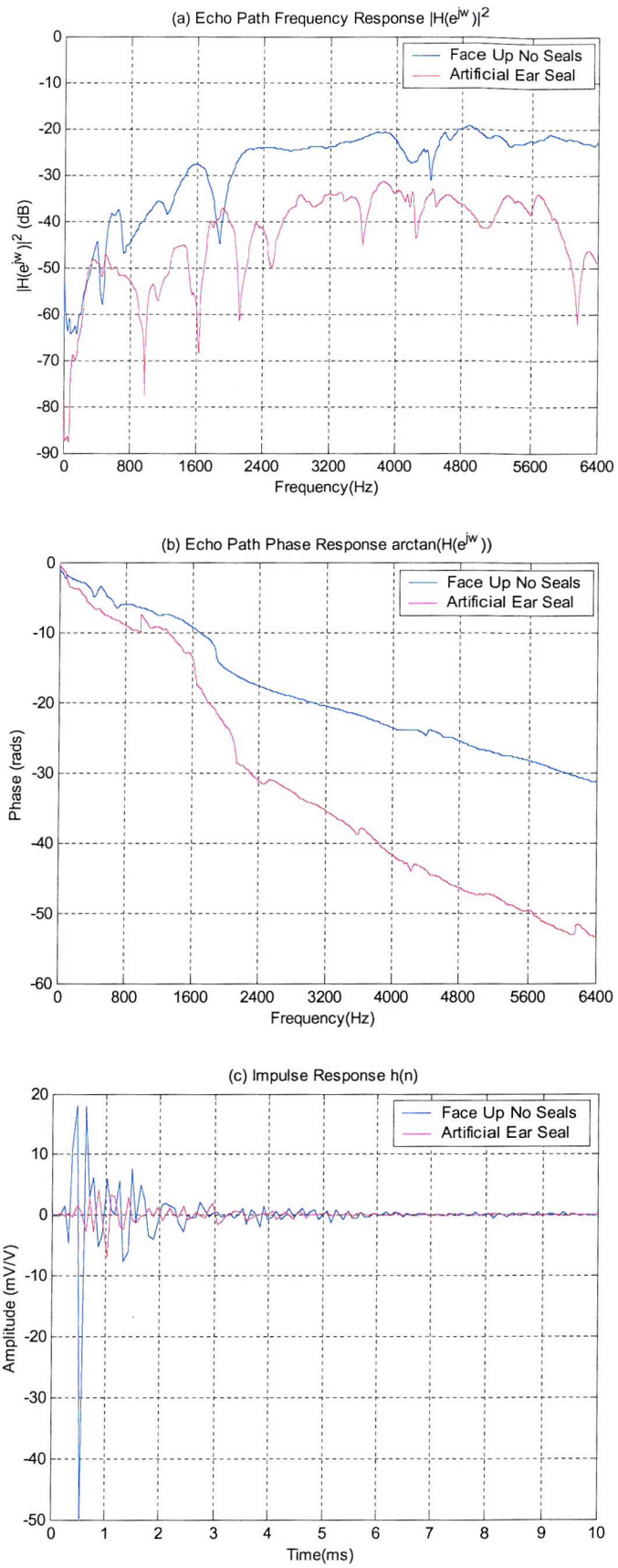


**Figure 2.18: Echo path results for the artificial ear sealed and face up no seals handset configurations superimposed,** showing (a) the frequency response characteristics, (b) the phase responses, and (c) the echo path impulse responses.

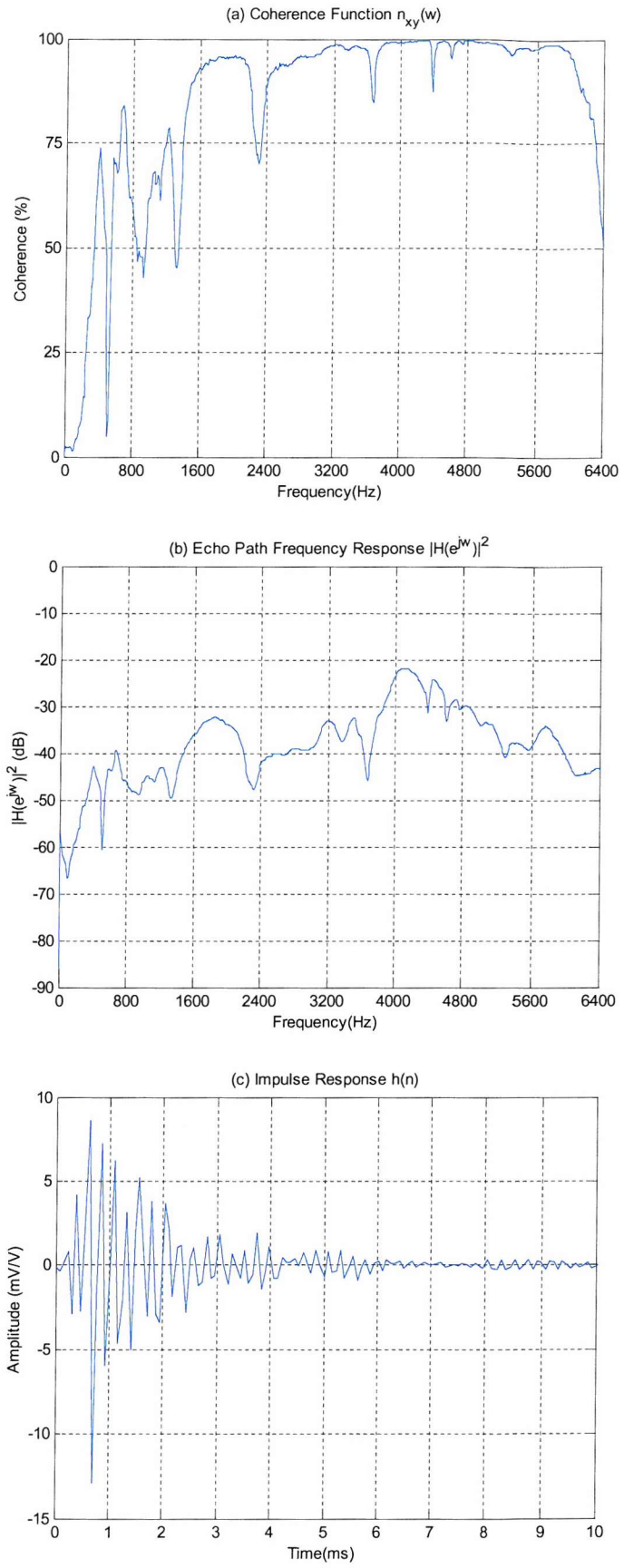


**Figure 2.19: Echo path results for the loudspeaker adhesive tape sealed handset configuration,** showing a) the coherence function, (b) frequency response characteristic, and (c) the echo path impulse response.

the echo path was sampled above 8.2 kHz as in wideband codec systems. As can be observed in Figure 2.19(c), the decaying oscillations have a strong 4100Hz component. The total effective duration of this echo path response is as a result slightly longer, at approximately 6.3ms.

In order to explain which echo sources are most active in this handset configuration, the echo path results for the loudspeaker adhesive tape sealed handset configuration in Figure 2.20, along with the artificial ear sealed and face up no seals handset responses for comparison purposes. From Figure 2.20(a) it can be seen that when a loudspeaker adhesive tape seal is applied as opposed to an artificial ear seal on the handset loudspeaker, the resonant peak around 1900Hz becomes augmented. To a lesser extent the peak around 400Hz also becomes augmented. This results in a lower terminal coupling loss for the loudspeaker adhesive tape sealed handset configuration of approximately 42dB. Apart from the main resonant peaks in the loudspeaker adhesive tape sealed echo path frequency response, the frequency response of the face up no seals handset response can be clearly observed to be much higher overall across the measurement band 300 to 3400Hz. This results in a higher terminal coupling loss for the face up no seals handset configuration of approximately 33dB. From Figure 2.20(b) a similar phase response for both the loudspeaker adhesive tape sealed response and the face up no seal response is obtained.

When an adhesive tape seal (or artificial ear seal) is applied to a handset, from Figure 2.20(b) it can be seen the main external echo path component ( $h_{ext}(n)$ ) identified earlier is heavily attenuated. With the absence of case and structural echo path components, the main resonant peaks at around 1900Hz and 4100Hz in the frequency response, when adhesive tape seal is applied, can be concluded to be due to the internal echo path component ( $h_{\text{int}}(n)$ ). When the seal is applied pressure fluctuations in the internal air cavity of the handset increase give rise these dominate resonant peaks in the frequency response discussed earlier. An internal echo path component term giving rise to peaks around 400Hz and 1900Hz is clearly visible in both the loudspeaker artificial ear seal and adhesive tape sealed responses. The strength of these peaks and the impact on the overall echo path response and terminal coupling loss clearly depends on the type of seal applied. The impact of the internal echo path component ( $h_{\text{int}}(n)$ ) clearly depends on the type of loudspeaker seal used.

When both a loudspeaker and microphone adhesive tape seal are applied to the handset, resonant peaks in the frequency response at 500, 2000, 3500 and 4200 Hz are produced as shown in Figure 2.21(a). Like the loudspeaker sealed handset configuration, the terminal coupling loss level of approximately 40dB calculated using (2.21) does not take into account the higher energy peak around 4200Hz (which will be filtered out by the narrowband ADC codec). In the resulting echo path impulse response of Figure 2.21(c), the 4200Hz peak, which is 15dB above the other peaks, has a strong effect on the form of the impulse response. For wideband codec mobiles this would have a strong impact on the echo path to be modelled. The total effective duration of this echo path response is as a result slightly longer, at approximately 5ms. Due to the absence of external echo path components, and similar resonant peaks in the frequency response as in the artificial ear sealed and loudspeaker tape sealed responses, the internal echo path component term can be concluded to dominate this echo path response.

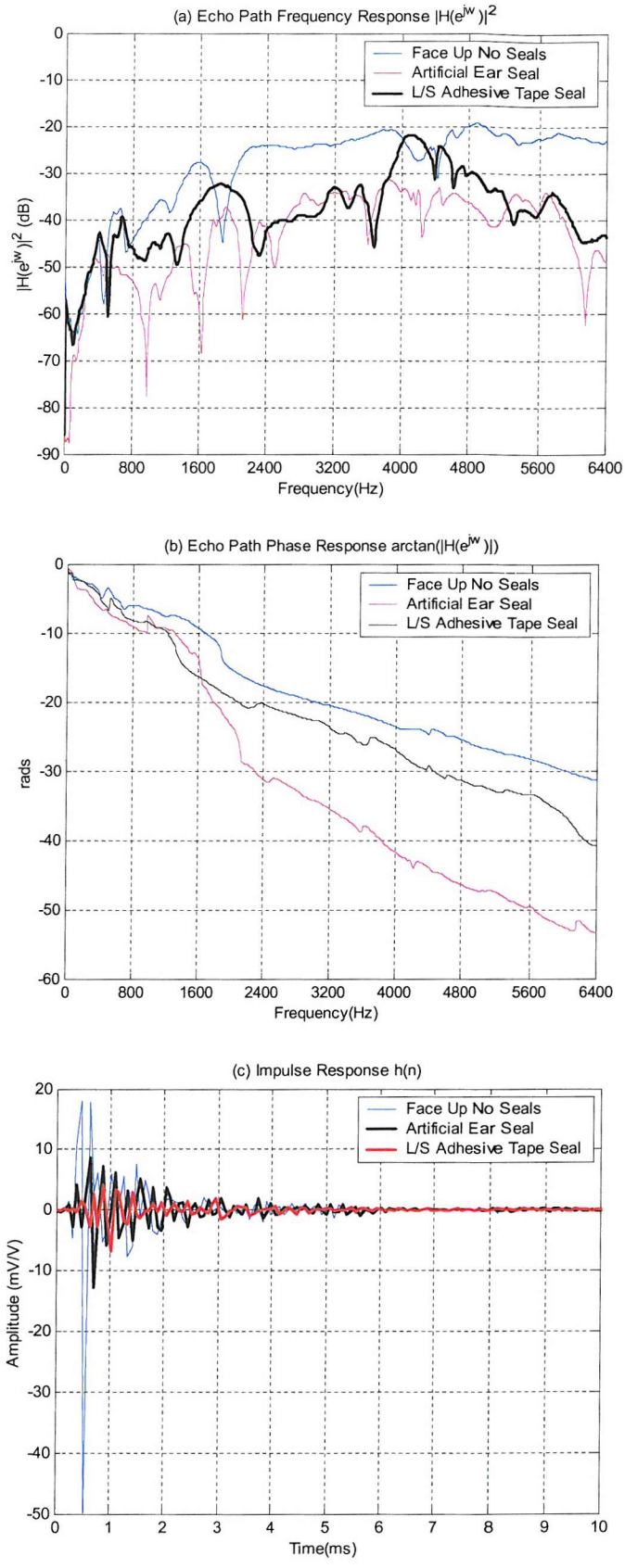


**Figure 2.20: Echo path results for the artificial ear sealed, face up no seals and loudspeaker adhesive tape sealed handset configurations superimposed,** showing (a) the frequency response characteristics, (b) the phase responses, and (c) the echo path impulse responses.

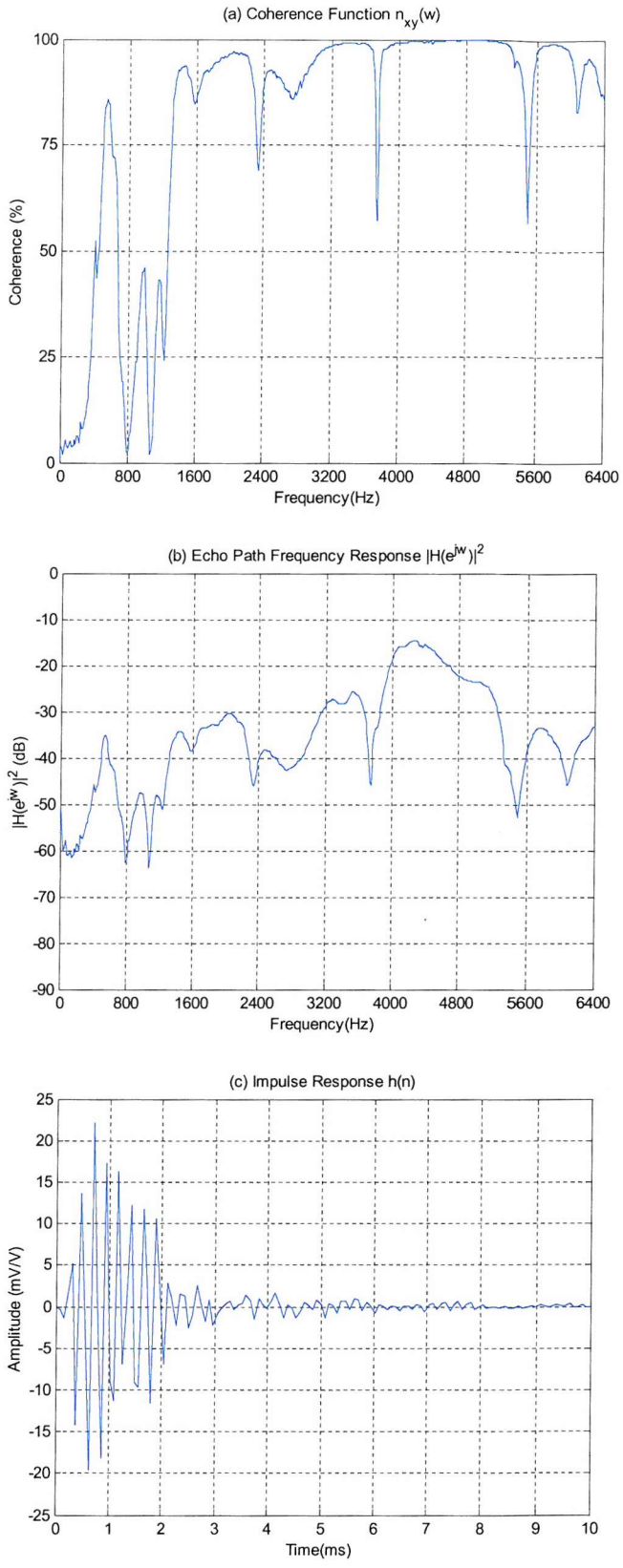


**Figure 2.21 : Echo path results for the loudspeaker and microphone adhesive tape sealed handset configuration,** showing a) the coherence function, (b) frequency response characteristic, and (c) the echo path impulse response.

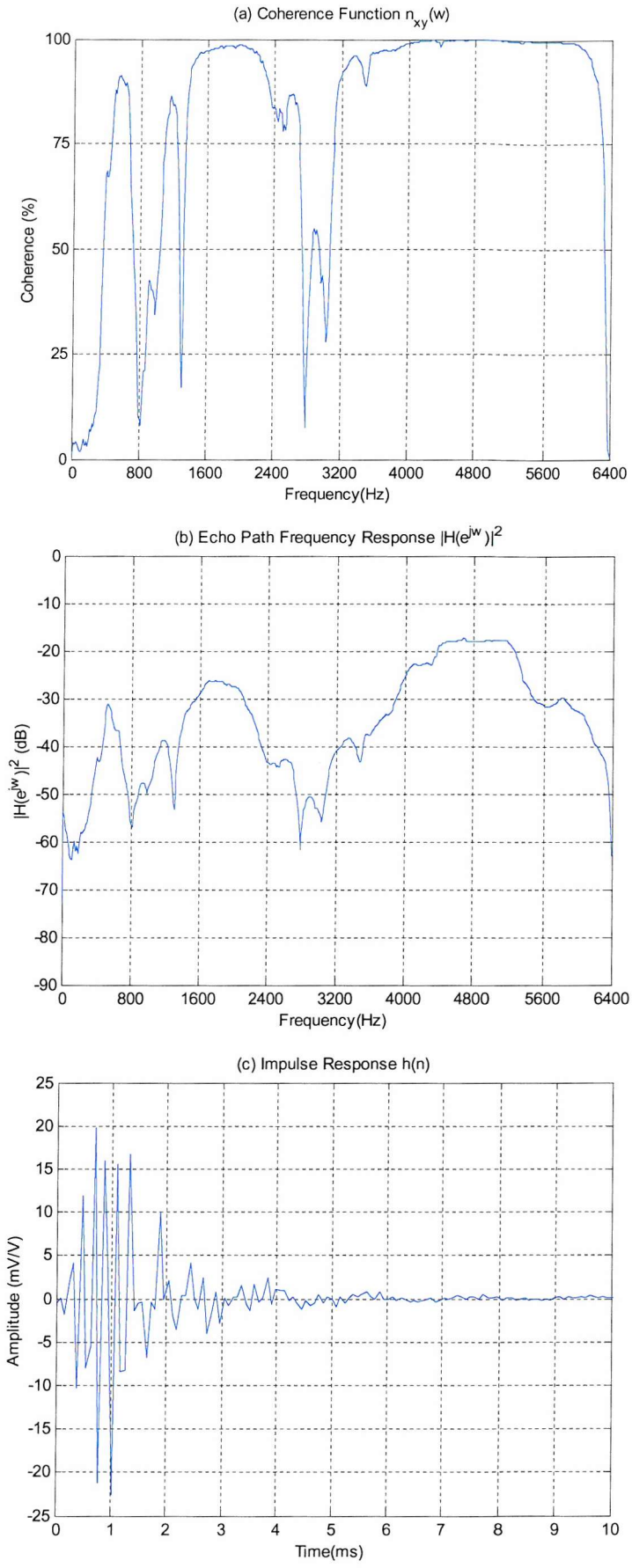


**Figure 2.22: Echo path results for the microphone adhesive tape sealed handset configuration,** showing a) the coherence function, (b) frequency response characteristic, and (c) the echo path impulse response.

When a microphone adhesive tape seal is applied to the handset, similar resonant peaks in the frequency response at 500, 1800, and between 4400 to 5200 Hz are produced as shown in Figure 2.22(a). The higher frequency response peaks have a large impact on the echo path response to be modelled as shown in Figure 2.22(c). The total effective duration of this echo path response is as a result slightly longer, at approximately 6.3ms. Again the internal echo path component term can be concluded to dominate this echo path response, resulting in a lower Terminal Coupling Loss of approximately 37dB.

In Figure 2.23 the frequency, phase and impulse responses of all the handset responses that have either a microphone or loudspeaker seal, or both, are superimposed on the same axes. From the frequency responses of Figure 2.23(a) the similar trend in the echo path response behaviour discussed earlier can be seen more clearly. The peaks around the frequencies of 500, 1800 and 4200Hz become augmented when either the handset loudspeaker or microphone (or both) contain an adhesive tape seal. With no casing or structural echo path components, and negligible external echo path components, this echo path behaviour can be concluded to be due to the internal echo path component ( $h_{\text{int}}(n)$ ). Depending on which seal is used, pressure fluctuations in the internal air cavity of the handset increase give rise these dominate resonant peaks in the frequency response. The adhesive tape sealed handset configurations of Section 2.4.3 to 2.4.5 are used to represent obstructions or imperfect seals that may occur in normal handset use. From the measurements in Figure 2.23 it can be seen that the internal echo path component is very significant when modelling the echo path of a mobile handset in normal use. The resonant impulse responses and low terminal coupling loss that arise from these handset configurations motivate the study of adaptive IIR algorithms for this application.

Finally consider the face down handset echo path response of Section 2.4.6. Figure 2.24 shows the coherence function, frequency response and echo path impulse responses measured for this handset configuration. It can be clearly seen the echo path response when placed down on a flat rigid surface is resonant in nature. The total effective duration of this echo path response is the longest, at approximately 7.3ms. From the frequency response of Figure 2.24(b) peaks around the frequencies of 700, 1200, 2000, 2600, 3000, 3900 and 4500Hz can be observed. As a result a lower Terminal Coupling Loss of 30dB was calculated for this handset configuration. Like other handset responses this value only takes account of the narrowband codec ADC bandwidth range, and does not account for the strong high frequency information above 3400HZ in this echo path response. For wideband codec mobiles the echo path frequency information above 3400Hz would also have to be modelled. Due to the high effective impulse response duration and lowest Terminal Coupling loss, this is clearly the worst case acoustic condition required to be modelled in normal handset use. The strong frequency response peaks around 500Hz, 2000Hz and 4000Hz like the adhesive tape sealed responses indicates a strong internal echo path component. The absence of any strong external echo path components as in the face up no seals responses suggests no direct air gap exists for sound to propagate in this handset configuration. High coherence levels across all frequencies also suggest that no strong non-linear terms have been introduced in this handset configuration. Additional resonances at 1200, 2600 and 3000Hz, and echo delay terms after 7.5ms in the impulse response may be attributed to additional external echo path components.

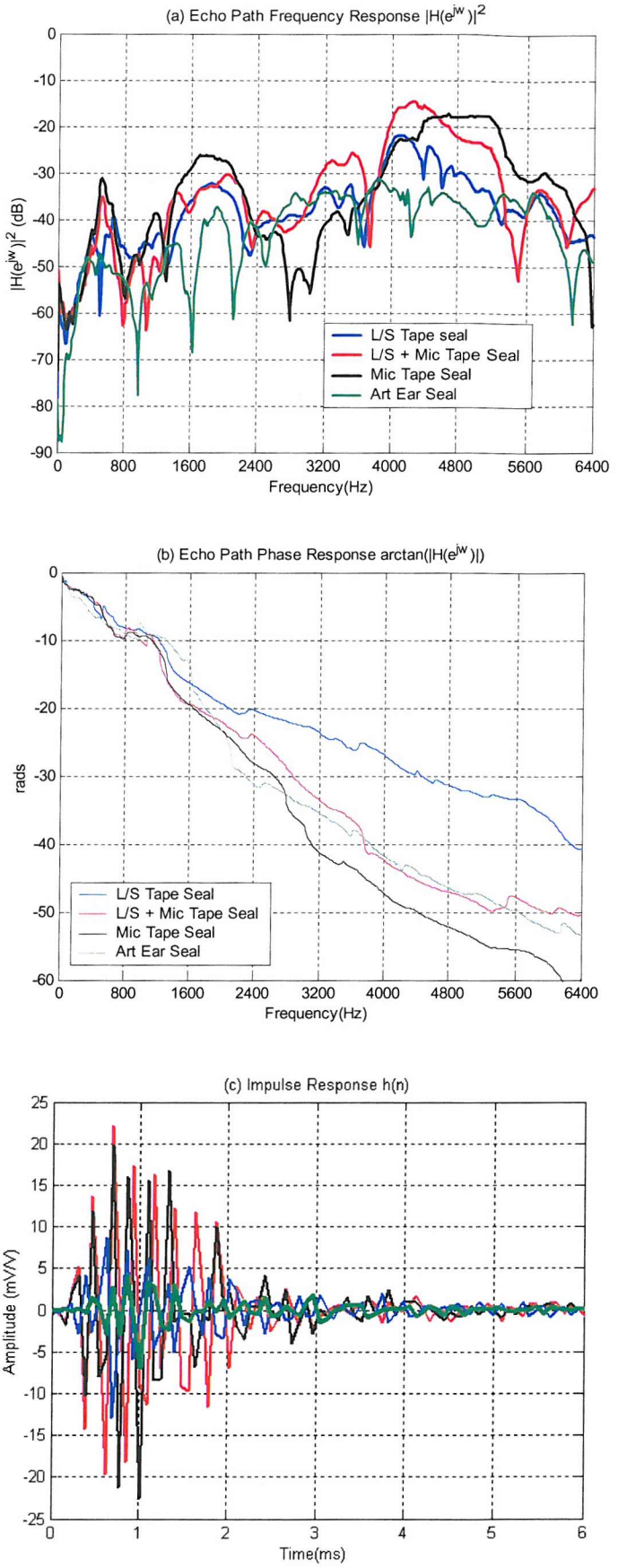


**Figure 2.23: Echo path results for the artificial ear sealed, loudspeaker tape sealed, loudspeaker and microphone tape sealed microphone tape sealed handset configurations superimposed,** showing (a) the frequency response characteristics, (b) the phase responses, and (c) the echo path impulse responses.

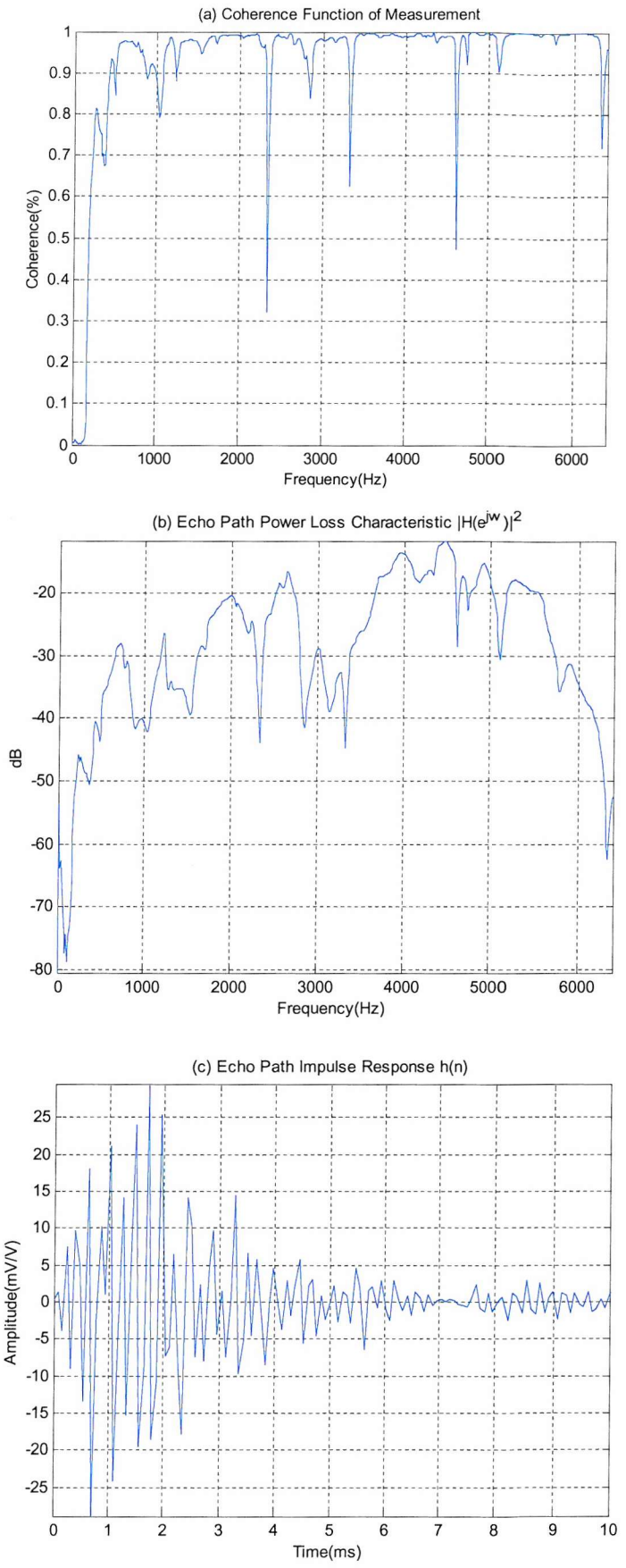


**Figure 2.24: Echo path results for the face down on a rigid surface handset configuration [2.1],** showing a) the coherence function, (b) frequency response characteristic, and (c) the echo path impulse response.

These additional components are likely to be due to the propagation of sound through the rigid surface used, and across any indirect air gap between the handset and rigid surface (echo reflections).

### 2.5.1. Summary of Anechoic Acoustic Echo Path Impulse Response Measurements

In summary the acoustic echo path response of a mobile handset in normal handset use may be characterised as shown in Table 2 below.

| Handset Orientation in Normal Use | Dominant Echo Path Sources | Echo Path Impulse Response Characteristics | Effective Echo Path Duration | ERLE needed |
|---|---|---|---|---|
| No loudspeaker or microphone seals or obstructions. | External echo path $h_{ext}(n)$ | Large period of impulse response activity after initial delay period, followed by exponentially decaying tail | Up to 3ms | Up to 16dB |
| Direct air gap between handset loudspeaker and microphone. | | | | |
| Loose placement of handset to user's ear | | | | |
| Firm placement of handset to user's ear | Internal echo path $h_{int}(n)$ | Small amplitude decaying oscillatory impulse response after initial delay period | Up to 5.2ms | Up to 6dB |
| Loudspeaker seal or obstruction | | | | |
| **Microphone obstruction and/or Loudspeaker seal or obstruction** | **Internal echo path $h_{int}(n)$** | **Decaying oscillatory impulse response after initial delay period** | **Up to 6.3ms** | **Up to 12dB** |
| **Handset placed face down** | **Internal echo path $h_{int}(n)$ and External echo path $h_{ext}(n)$** | **Decaying oscillatory impulse response after initial delay period** | **Up to 7.3ms** | **Up to 16dB** |

Table 2: General characteristics of the acoustic echo path of a mobile handset

It is expected the handset echo path behaviour summarised in Table 2 below may be applicable to all mobile handsets of similar construction. In the next section it will be shown that the fixed set of handset orientations discussed in this section are needed to represent the full echo path variation in normal handset use.

## 2.6. Results of Actual Acoustic Echo Path Impulse Response Measurements in a Reverberant Environment

So far we have looked at the nature of how the acoustic echo path response of a mobile handset changes in normal use depending on the handset orientation. To do this we have used a fixed set of handset configurations to represent the full variation in handset echo path response possible in normal handset use. What has not yet been established is that the fixed handset configurations used in this section are actually representative of the maximum variation in echo path possible in actual normal use. In a simple attempt to establish this, the anechoic echo path responses from the fixed sets of handset configurations (discussed in the last section) will be compared with actual handset echo path responses as follows.

Actual echo path responses were recorded in an office against the head and ear of 3 different user's with the same type of mobile handset in an attempt to capture the actual variation in the echo path response between different users in normal use during a call. To reduce the number of measurements to be performed only the handset orientations against each user's ear are used. Each handset position represents the typical comfortable position used/preferred by each user during a call at different locations in a quiet office environment. The echo path response results for each user are shown in Figure 2.25 for one location. From the acoustic echo path impulse results presented, the Terminal Coupling Loss levels calculated are shown in Table 3 below.

| Handset Configuration | TCL(dB) | $\frac{\sum\lvert h_{10-50}\rvert^2}{\sum\lvert h_{0-10}\rvert^2}$ | Required ERLE (dB) |
|---|---|---|---|
| Echo Path Response Measurements User 1 | 32.83 | -22.2dB | 13.17 (13) |
| Echo Path Response Measurements User 2 | 37.28 | -19.8dB | 8.72 (9) |
| Echo Path Response Measurements User 3 | 37.76 | -18.8dB | 8.24 (8) |

**Table 3: Terminal Coupling Loss(TCL) and required Echo Return Loss Enhancement(ERLE) levels calculated for NEC G9 echo path responses in an office environment.**

From Table 3 it can be seen the echo path response varies between different users in normal use when placed in a typical handset position for a regular speech call. For all users additional ERLE is required to maintain the 46dB requirement of [2.1]. These results also neglect the possible variation in a handset echo path response from specific applications such as hands free video telephony. As for the adhesive tape sealed anechoic handset echo path responses of the last section a notable resonant peak around 1800Hz exists in all measurements. For these measurements the internal echo path component appears to dominate the overall echo path response and terminal coupling loss. The impulse responses obtained all show similar trends, a small delay period of 0.4ms, following by exponentially decaying oscillatory impulse response.

The impact of the head and body of the mobile handset user, and the non-anechoic environment in which a mobile handset is used can be seen in the echo path impulse responses of Figure 2.26. Here the time scale has been extended from those results of Figure 2.25. The main source of echo reflections occurs in the echo path responses after a time of 10ms. This would correspond to reflections due to the environment in which the handset is used such as walls, ceilings and furniture greater than 3-4m away. These reflections are very small in comparison to the anechoic region of the responses up to 10ms. In Table 3 the ratio of echo path impulse response energy from 10 to 50ms (echo reflections) to anechoic echo path impulse response energy from 0 to 10 ms ($\frac{\sum |h_{10-50}|^2}{\sum |h_{0-10}|^2}$) is computed in decibels. It is clear that the level of echo reflections after 10ms is small in comparison to the anechoic region up to 10ms. The acoustic echo cancellation device employed within the handset device is normally designed to cancel out only the anechoic echo path response of the handset, which is only the period up to approximately 7ms in duration due to the handset itself. The echo reflections after 10ms due to the environment can hence effectively be ignored, as they will have no impact on the design of the acoustic echo canceller.

Echo reflections due to the head and body of the mobile handset user would occur before a period of 7ms as the user's body would normally be within 1m of the mobile even for hands free applications. However, from Figure 2.26 it can be seen for the speech application that the echo reflections within the anechoic response region up to 7ms are small or negligible, and will have little impact on the design of an acoustic echo canceller. Even for hands free video telephony applications echo reflections will be also be small within the anechoic response region due to the relatively low power handset loudspeaker output and the higher attenuation of echo paths due to the larger potential travelling distance of the echo reflections. Echo reflections can hence also be ignored for this application.

The set of anechoic handset responses discussed in the last section and the non-anechoic echo path responses of this section are plotted on the same axes in. From Figure 2.27 it can be clearly seen how the fixed set of handset configurations proposed in section 2.4 can more adequately deal with the variation in echo path response in normal use during a speech call for the three user positions measured. This is in sharp contrast to the incapability of the single test configuration of [2.1] to accurately reflect the actual variation of a handset response in normal use.

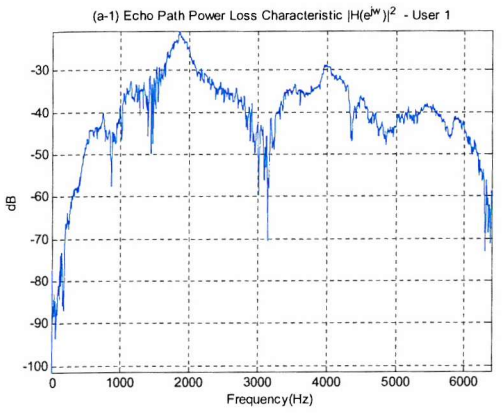


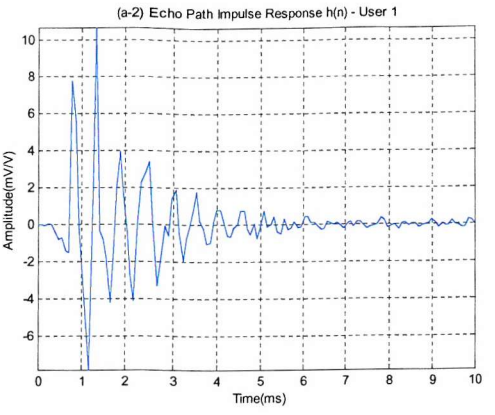


(a) Echo Path Response Measurements User 1

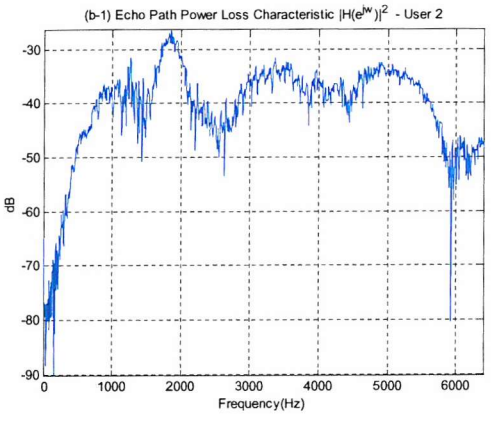


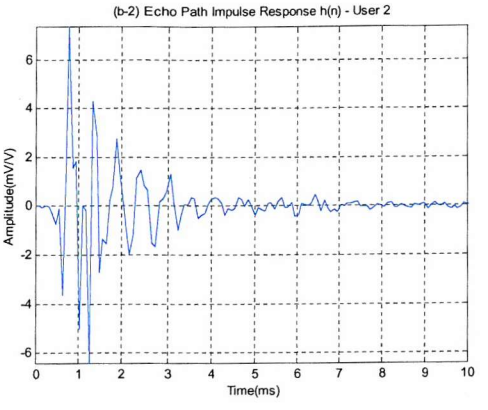


(b) Echo Path Response Measurements User 2

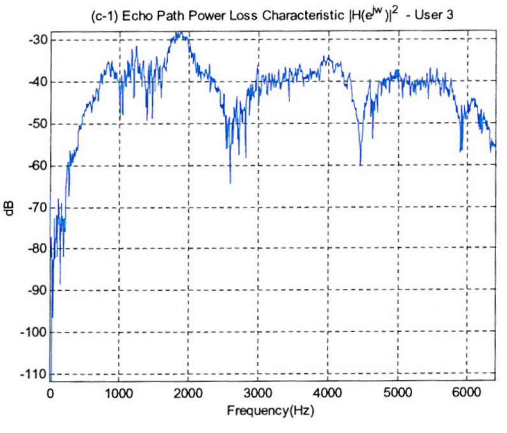


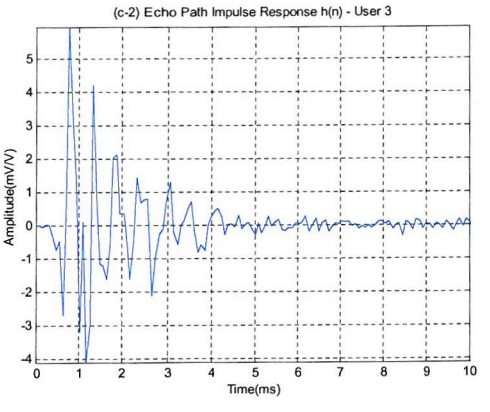


(c ) Echo Path Response Measurements User 3

**Figure 2.25: Echo path loss characteristics and impulse responses in a reverberant environment**

In (a) to (c) above show the echo path response measurements of 3 different users in a reverberant environment. Each handset is placed against the head and ear of the user. A non-anechoic environment is used to record these responses.

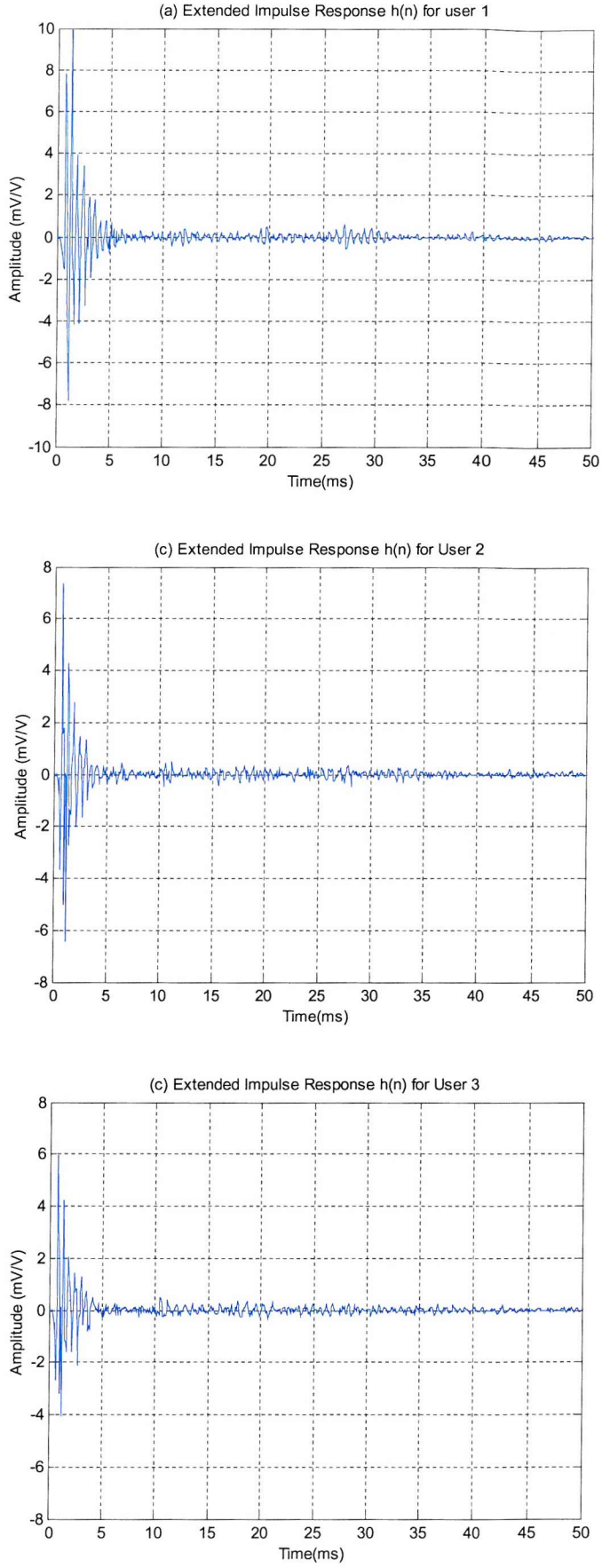


**Figure 2.26: Echo path impulse responses in a reverberant environment for different users.**

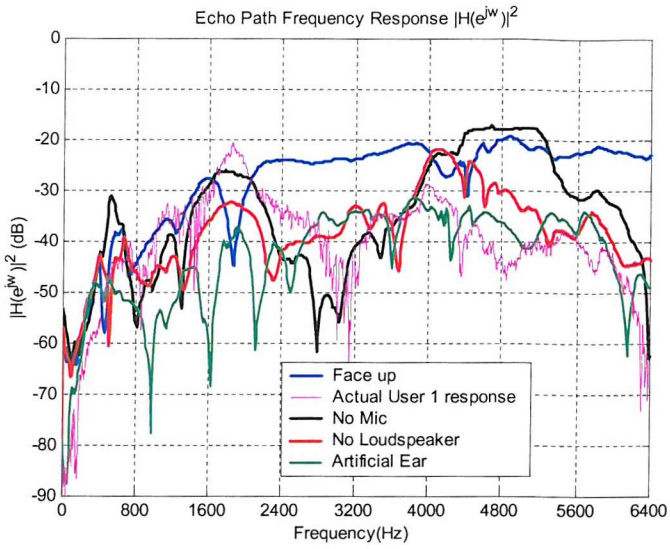


(a) Comparison of Anechoic and Actual (user1) echo path frequency response measurements

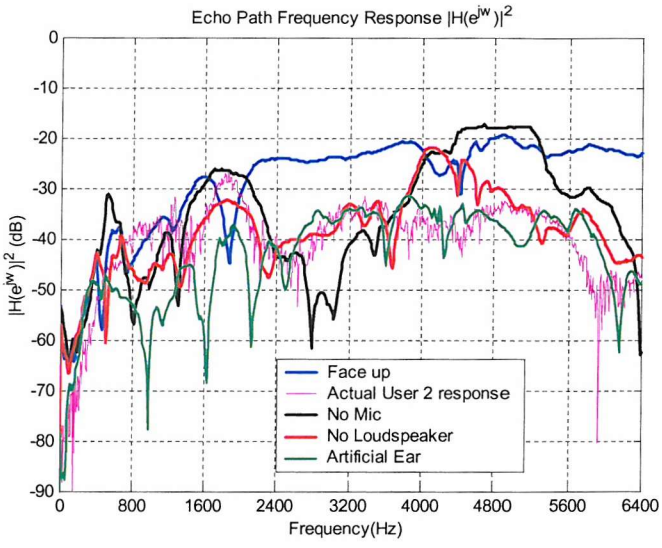


(b) Comparison of Anechoic and Actual (user2) echo path frequency response measurements

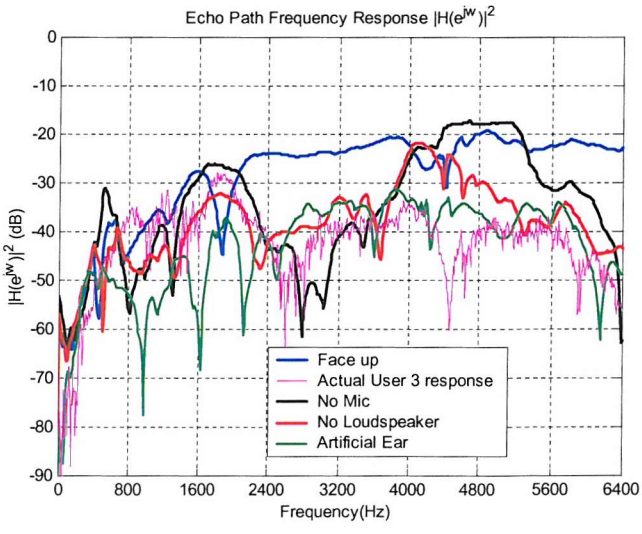


(c) Comparison of Anechoic and Actual (user3) echo path frequency response measurements

**Figure 2.27: Comparison of anechoic echo path results and actual echo path measurements.**

## 2.7. Overall Summary of Handset Acoustic Echo Path Results

The following points can be summarised from the results presented in this Chapter,

1. It has been clearly demonstrated that acoustic echo cancellation is needed for both handset designs tested to ensure the 46dB requirement of [2.1] is satisfied in normal handset use. It is expected this important result would also be true for other handset designs of similar construction.
2. It is clear that in normal handset use the single test condition of [2.1] is not sufficient to ensure the echo loss requirements of [2.1] are satisfied in normal handset use. The fixed set of anechoic handset configurations proposed in the section 2.4 to establish the echo loss performance of a mobile handset in normal use have been demonstrated to be a more robust method than the single test configuration of [2.1]. This is especially true for future mobile applications as the role of the mobile moves away from the more traditional speech services to offer new data services such as hands free video telephony [2.2]
3. The echo path response of the mobile handset design tested has been shown to be linear in nature and the echo path sources responsible for the acoustic echo path have been identified. It is expected this important result would also be true for other handset designs of similar construction.
4. The effect of echo reflections from the environment, and the user's head and body, has been analysed using echo path measurements in a reverberant environment. Echo reflections have been concluded to have negligible impact on the echo path modelled by an acoustic echo canceller.

In Chapter 4 we follow on from the results of this Chapter and will look at how to effectively model the acoustic echo path of a mobile handset, using the echo path results of this Chapter. The effects of the mobile handset codec device filtering and sampling rate on the echo path response to be modelled will also be taken into consideration.

# Chapter 3

## 3. Adaptive Filter Theory

In this chapter we will review some of the theory and techniques commonly used for adaptive FIR and IIR filtering. We shall firstly look at adaptive FIR filtering theory. Extensions are then made to adaptive IIR filtering theory and algorithms. No attempt is made in this chapter to discuss the advantages and disadvantages of each, since there are a large number of algorithms. Also their performance will depend on the conditions under which they are used. The conditions of interest here are those described n chapter 5, where simulations of their performance can be found.

### 3.1. Adaptive FIR Filtering

Figure 3.1 shows a typical system identification configuration for a FIR adaptive filter modelling an echo path impulse response.

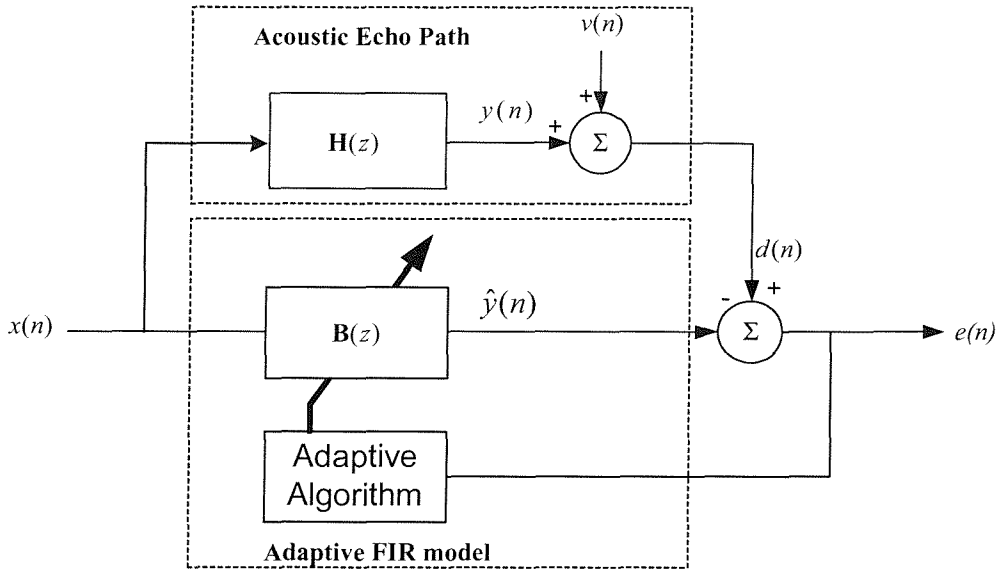


**Figure 3.1 : System Identification of echo path using an FIR adaptive filter.**

The FIR adaptive filter will attempt to adjust the FIR filter coefficient values to minimise the error signal $e(n)$. In system identification theory the criterion normally used to select the FIR model coefficient values would be minimisation of the mean square error.

In this section we will present the optimal FIR filter design that minimises the mean square error (MSE) for the system identification configuration of Figure 3.1. We will see how this optimal FIR filter design is specified in terms of the solution to the well-known normal equations in [3.1]and [3.2], often termed the "Wiener filter" solution. Iterative solutions to the normal equations are then presented which are used to adapt the coefficients of the FIR filter to track changes in the optimal solution as new data arrives. From these iterative solutions we will derive the most commonly used gradient based adaptive FIR filtering algorithms.

### 3.1.1. The Optimal FIR Filter

Consider the output of the echo path, $d(n)$, which contains both the echo signal to be cancelled $y(n)$ and a disturbance source $v(n)$ as follows,

$$d(n) = y(n) + v(n), \tag{3.1.1}$$

where the disturbance source $v(n)$ may be interpretated to include not only an additive disturbance source picked up by the handset microphone at the output of the echo path, but also undermodelling noise caused by the FIR filter model being of lower order than that of the echo path to be modelled [3.3]. Rewriting (3.1.2) we get

$$d(n) = y(n) + v(n) = \mathbf{h}^T \mathbf{x}_o(n) + v(n) = \sum_{i=0}^{L-1} h(i)x(n-i) + v(n), \tag{3.1.2}$$

where $\mathbf{h}$ is a vector of L echo path response samples given by,

$$\mathbf{h} = [h(0), h(1), ...., h(L-1)]^T, \tag{3.1.3}$$

and where $\mathbf{x}_o(n)$ is a vector of L past input samples given by,

$$\mathbf{x}_o(n) = [x(n), x(n-1), ....., x(n-L+1)]^T, \tag{3.1.4}$$

and T denotes matrix transposition.

To cancel this echo signal $d(n)$, a replica of the echo signal, $\hat{y}(n)$, must be created by the FIR filter which models the echo path transfer function, and subtracted from $d(n)$. For a fixed time invariant FIR filter of order M the output of the FIR model filter $\hat{y}(n)$ at time index $n$ becomes,

$$\hat{y}(n) = \mathbf{b}^T \mathbf{x}(n) = \sum_{i=0}^{M-1} b_i x(n-i), \tag{3.1.5}$$

where $\mathbf{x}(n)$ is a vector of M past input samples defined similarly to (3.1.4) and $\mathbf{b}$ is a vector of FIR filter model coefficients given by,

$$\mathbf{b}(n) = [b_0, b_1, ...., b_{M-1}]^T, \tag{3.1.6}$$

Consider the error signal $e(n)$,

$$e(n) = d(n) - \hat{y}(n) = d(n) - \sum_{i=0}^{M-1} b_i x(n-i), \tag{3.1.7}$$

Using (3.1.2), the error signal of (3.1.7) can be re-written as,

$$e(n) = \sum_{i=0}^{M-1} (h(i) - b_i)x(n-i) + \sum_{j=M}^{L-1} h(j)x(n-j) + v(n), \tag{3.1.8}$$

For appropriate selection of FIR model coefficient values, the greater the number of coefficients M in the FIR model to match the activity of the impulse response samples $h(n)$, the smaller the error or mismatch signal $e(n)$ would be. For a minimum error signal, the coefficients of the FIR model simply become the impulse response samples. In practise however the model order M will be smaller than L. In

system identification theory the cost function normally used to select the FIR model coefficient values would be **minimisation** of the mean square error [3.4].

Consider the design of a FIR model of order M to minimise the mean square error. The cost function $F$ to be minimised is denoted as,

$$F = E[e^2(n)], \tag{3.1.9}$$

where $E$ denotes an average over ensembles of the random error sequence $e(n)$ at time $n$. Rewriting (3.1.9) using (3.1.8) we get ,

$$F = E\left[\left(\sum_{i=0}^{M-1}(h(i)-b_i)x(n-i)+\sum_{j=M}^{L-1}h(j)x(n-j)+v(n)\right)^2\right], \tag{3.1.10}$$

Since the filter coefficients of $\mathbf{h}$ are assumed to be time invariant, and assuming the disturbance signal $v(n)$ is an additive white noise signal independent of the input process $x(n)$, we then may write,

$$F = E[y^2(n)] - 2E\left[y(n)\sum_{i=0}^{M-1}b_i x(n-i)\right] + E\left[\sum_{i=0}^{M-1}b_i x(n-i)\sum_{i=0}^{M-1}b_i(n)x(n-i)\right] + E[v^2(n)] \tag{3.1.11}$$

,

Equation (3.1.11) is termed the mean square error surface. Re-writing (3.1.11) in more compact form we get,

$$F = E[y^2(n)] - 2\mathbf{b}^T\mathbf{r}_{yx} + \mathbf{b}^T\mathbf{R}_{xx}\mathbf{b} + E[v^2(n)], \tag{3.1.12}$$

where $\mathbf{R}_{xx}$ is an M x M autocorrelation matrix of the input signal $x(n)$ defined as,

$$\mathbf{R}_{xx} = E[\mathbf{x}(n)\mathbf{x}^T(n)], \tag{3.1.13}$$

and where $\mathbf{r}_{\hat{y}x}$ is a cross correlation vector between input signal $x(n)$ and the output of the echo path model $y(n)$ as defined as,

$$\mathbf{r}_{yx} = E[y(n)\mathbf{x}(n)], \tag{3.1.14}$$

We can see from (3.1.12), the mean square error surface is a quadratic function of the FIR filter coefficients $b_i$. Since the cost function $F$ *is a quadratic* function of the coefficients there will exist a single global minimum solution with no local minima (provided $\mathbf{R}_{xx}$ is non-singular and $x(n)$ is persistently exciting) corresponding to the optimum weight vector $\mathbf{b}_{opt}$, at which the gradient of $F$ will be zero. Therefore to find $\mathbf{b}_{opt}$ which minimises this cost function $F$, the gradient $F$ can be calculated with respect to the filter coefficients, and equated to zero. The gradient is calculated by differentiating $F$ with respect to the filter coefficients $b_i$. Differentiating $F$ in (3.1.12) with respect to each coefficient $b_i$ of the FIR model, and equating to zero yields [3.1],

$$\frac{\partial F}{\partial b_i} = -\mathbf{r}_{yx} + \mathbf{R}_{xx}\mathbf{b} = 0, \tag{3.1.15}$$

giving,

$$\mathbf{R}_{xx}\mathbf{b} = \mathbf{r}_{yx}, \tag{3.1.16}$$

Equation (3.1.16) represents a set of equations known as the ***normal equations*** or discrete time ***Wiener-Hopf equations*** [3.1]. The term ***normal equations*** comes from the orthogonality of the input signal and the output error which results when the derivative of $F$ *in* (3.1.12) with respect to the filter coefficients is equated to zero as follows,

$$\frac{\partial F}{\partial b_i} = \frac{\partial E[e^2(n)]}{\partial b_i} = 2E[e(n)\frac{\partial e(n)}{\partial b_i}] = 0 \quad , i = 0...M , \tag{3.1.17}$$

Using (3.1.7) we get,

$$\frac{\partial F}{\partial b_i} = \frac{\partial E[e^2(n)]}{\partial b_i} = -2E[e(n)x(n-i)] = 0 \quad , i = 0...M , \tag{3.1.18}$$

Equation (3.1.18) is the *orthogonality principle* [3.2], and requires the input to the FIR filter and estimation error to be orthogonal over the length of the filter.

The solution to (3.1.16) represents the optimal least squares filter coefficients. The optimal least squares filter coefficients selected to minimise the mean square error (MSE are found by solving (3.1.18) for $\boldsymbol{b}$ as follows,

$$\mathbf{b}_{opt} = \mathbf{R}_{xx}^{-1}\mathbf{r}_{yx} , \tag{3.1.19}$$

Equation (3.1.19) is the solution to the problem of designing a linear time invariant FIR filter to minimise the mean square error (MSE) for wide-sense stationary input signals. From Equation (3.1.19) we can see the selection of FIR model coefficients $\mathbf{b}_{opt}$ to minimise the mean square error (MSE) involves a direct matrix inversion. From (3.1.12) and (3.1.19) we can see the disturbance signal $v(n)$ only adds a constant offset term to the mean square error surface, and will no effect the selection of optimum filter coefficients to minimise $F$.

At this point it is worth noting that a special case of (3.1.19) exists where $x(n)$ is unit variance white noise. This results in $\mathbf{R}_{xx} = \mathbf{I}$, and $\mathbf{b}_{opt}$ from (3.1.14) and (3.1.19) simply becomes the first M coefficients of the impulse response $\mathbf{h}$ to be modelled.

### 3.1.2. Adaptive FIR Filtering

We have seen so far how the optimal FIR filter coefficients may be designed to minimise the mean square error for stationary input signals using a direct solution of the normal equations in (3.1.17). However in most applications the input signals that arise will be statistically non-stationary. Although the normal equations of (3.1.16) can be formulated for non-stationary inputs, the calculation of non-stationary correlation coefficients presents difficulties when replacing ensemble averages with time averages [3.2]. For non-stationary input signals such as speech in many Acoustic Echo Cancellation applications a "local stationarity" may be assumed over which the speech signals properties change slowly with time. In this way the input signals may be segmented into smaller intervals or windows, where the optimum FIR coefficients are updated using the direct solution of (3.1.19) in each time interval segment or window. However since this involves calculation and construction of an autocorrelation matrix, and a matrix

inversion in each time window for the direct solution of (3.1.19), computational complexity would be very high, and hence would be unsuitable for real time Acoustic Echo Cancellation applications. A more complete solution to the problem of minimising the mean square error for time varying input signals would be to provide a continuously adaptive filter which tracks changes in the optimal solution, as each new data sample becomes available. This leads us to look at iterative solutions to the normal equations of (3.1.16).

#### 3.1.2.1. Iterative Solutions to the Normal Equations

To recap, our objective is to choose the filter coefficients $\mathbf{b}_n$ at each iteration n, to minimise the mean squared error cost function cost function of (3.1.9),

$$F = E[e^2(n)], \tag{3.1.9}$$

We have already seen that the cost function $F$ is a quadratic function of the coefficients $\mathbf{b}$, and can be thought of as an M dimensional parabolic surface. The purpose of an iterative solution is from an initial filter weight vector estimate $\mathbf{b}_0$ to search the function $F$ by successively updating this filter weight vector estimate to force the filter to the optimal solution at the minimum point $F_{\min}$ on the M dimensional parabolic surface.

A general iterative formula that can be used to find the solution to the normal equations of (3.1.16) to minimise the mean square error cost function of (3.1.9) is given by [3.2],[3.4],

$$\mathbf{b}_{n+1} = \mathbf{b}_n - \mu_n \mathbf{p}_n, \tag{3.1.20}$$

where $\mathbf{b}_n$ denotes the $n^{th}$ update of the FIR filter coefficient vector $\mathbf{b}$ at iteration n, $\mu_n$ is a step size parameter to control the size of change in $\mathbf{b}_{n+1}$ from $\mathbf{b}_n$, and $\mathbf{p}_n$ is a vector which controls the search direction on the mean squared error surface of (3.1.12).

Since the mean square error surface of (3.1.12) has a unique global minimum solution a widely used general class of algorithms are those that iterate on **the gradient of the mean squared error** [3.2]. Adaptive algorithms derived from gradient search methods have found widespread use in the area of Acoustic Echo Cancellation [3.5]. Throughout the thesis we will concentrate on adaptive algorithms derived from gradient search iterative solutions to the normal equations. These gradient search methods are characterised by search directions $\mathbf{p}_n$ of the form,

$$\mathbf{p}_n = \mathbf{D}_n \nabla F_n, \tag{3.1.21}$$

where $\mathbf{D}_n$ is an (M x M) weighting matrix, and $\nabla F_n$ is the gradient of the mean squared error cost function $F$ with respect to the filter coefficient vector $\mathbf{b}_n$ at each iteration(or time index) n. $\nabla F_n$ can be represented as,

$$\nabla F_n = \frac{\partial F_n}{\partial \mathbf{b}_n} = \left( \frac{\partial F_n}{\partial b(0)_n}, \frac{\partial F_n}{\partial b(1)_n} \ldots, \frac{\partial F_n}{\partial b(M-1)_n} \right), \tag{3.1.22}$$

A large number of adaptive algorithms can be derived from different choices of $\mathbf{D}_n$ and $\alpha_n$. Let us now consider the most common gradient search methods. The first gradient search method to be considered is the well-known method of Steepest Descent, from which we will derive the LMS (Least Mean Squares) adaptive filtering algorithm [3.1],[3.2]. The LMS adaptive FIR filter and its variants are most widely used adaptive FIR filtering algorithms in Acoustic Echo Cancellation due to their simplicity and low complexity[3.5],[3.6]. The second iterative method that we will consider is the Newton method from which we will derive LMS-Newton adaptive filtering algorithms [3.2],[3.7],[3.8],[3.9].

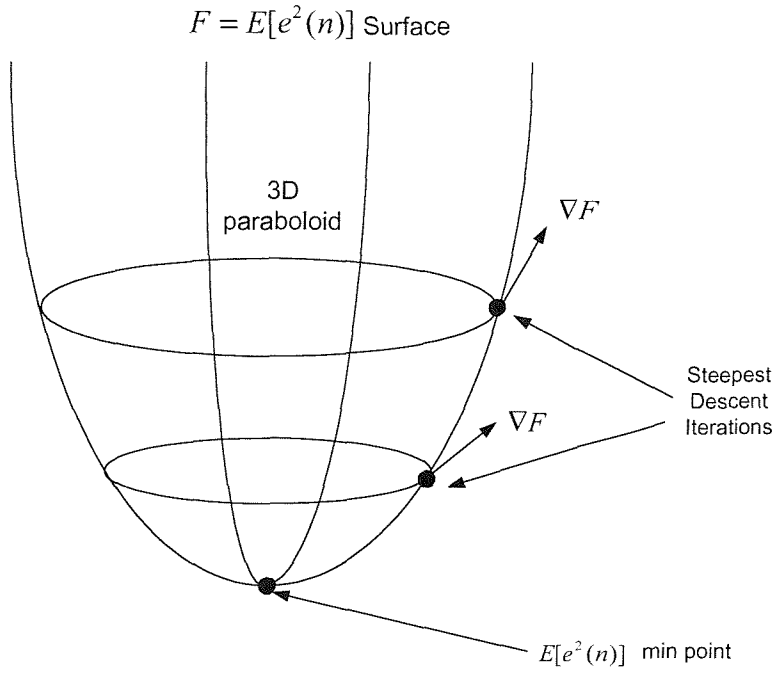


**Figure 3.2 : Illustration of Steepest Descent Method**

The mean squared error surface canbe viewed as (M+1) – dimensional paraboloid, where M is the number of FIR filter coefficients. The optimum set of coefficients corresponds to the bottom of the bowl. Note the gradient $\nabla F$ points in opposite direction to the bottom, thus the steepest descent method goes in a direction opposite to the gradient of the mean square error surface.

### 3.1.2.2. The method of Steepest Descent and the LMS adaptive algorithm

The steepest descent method produces an iterative estimate of optimal FIR coefficients, where every iteration n the filter coefficient vector $\mathbf{b}_n$ is changed by a small amount in a direction opposite to the gradient of the cost function $F$, and by a distance proportional to the magnitude of the gradient. This is illustrated in Figure 3.2. Mathematically the weight vector is altered as follows,

$$\mathbf{b}_{n+1} = \mathbf{b}_n - \frac{\mu}{2}\nabla F_n, \tag{3.1.23}$$

In comparison to the general equations of (3.1.20) and (3.1.21) for the steepest descent method of (3.1.23) we have $\mathbf{D}_n = \mathbf{I}$, $\mathbf{p}_n = \nabla F_n$ and $\mu_n = \frac{\mu}{2}$, where $\mathbf{I}$ is the identity matrix and $\mu$ is a constant

of proportion. The 2 is introduced into (3.1.23) for convenience. The term steepest descent arises from the fact that in the neighbourhood of $\mathbf{b}_n$ the gradient is normal to lines of equal cost, thus the gradient direction is the line of steepest ascent (in cost terms). The gradient of the mean square error surface $\nabla F_n$ using (3.1.17) and re-writing using vector notation we get,

$$\nabla F_n = 2E[e(n)\nabla e(n)] = -2E[e(n)\mathbf{x}(n)], \tag{3.1.24}$$

Using (3.1.24) and (3.1.12) in (3.1.23) we get [3.2],

$$\mathbf{b}_{n+1} = \mathbf{b}_n + \mu E[e(n)\mathbf{x}(n)] = \mathbf{b}_n + \mu(\mathbf{r}_{dx} - \mathbf{R}_{xx}\mathbf{b}_n), \tag{3.1.25}$$

Provided that the stepsize $\mu$ is not too large equation (3.1.25) will eventually converge to the optimal solution. However in the region of the local minimum where the gradient will be low the method may converge slowly. For zero-mean and jointly stationary input signals convergence will occur provided that,

$$0 < \mu < \frac{2}{\lambda_{\max}}, \tag{3.1.26}$$

where $\lambda_{\max}$ is the maximum eigenvalue of $\mathbf{R}_{xx}$ [3.2]. The issue of convergence rate will be studied in more detail later in the thesis for both adaptive FIR and IIR filters derived from this steepest descent method of (3.1.25).

Equation (3.1.25) gives an iterative solution for the stationary (fixed) normal equations. However to design an filter based on the steepest descent method which is responsive to changes on the input signal environment some dependence on the input data is needed in the iteration of (3.1.25). Re-writing (3.1.25) to replace the fixed auto and cross-correlation matrices by time estimates we get,

$$\mathbf{b}_{n+1} = \mathbf{b}_n + \mu(\hat{\mathbf{r}}_{dx}(n) - \hat{\mathbf{R}}_{xx}(n)\mathbf{b}_n), \tag{3.1.27}$$

where time estimates $\hat{\mathbf{R}}_{xx}(n)$ and $\hat{\mathbf{r}}_{dx}(n)$ are computed using a finite time window on sequences $x(n)$ and $d(n)$ [3.2]. Equation (3.1.27) despite having time dependency will still be very computationally expensive and unsatisfactory for real time implementation as estimates $\hat{\mathbf{R}}_{xx}(n)$ and $\hat{\mathbf{r}}_{dx}(n)$ must be calculated every data sample. To overcome this we can replace the gradient $\nabla F_n$ by an estimate. One such estimate of $\nabla F_n$ is to replace $E[e(n)\mathbf{x}(n)]$ in (3.1.24), which is generally unknown, with an estimate such as the sample mean as follows,

$$\hat{E}[e(n)\mathbf{x}(n)] = \frac{1}{L}\sum_{l=0}^{L-1} e(n-l)\mathbf{x}(n-l), \tag{3.1.28}$$

Incorporating this estimate into (3.1.25) gives,

$$\mathbf{b}_{n+1} = \mathbf{b}_n + \frac{\mu}{P}\sum_{p=0}^{P-1} e(n-p)\mathbf{x}(n-p), \tag{3.1.29}$$

A special case of (3.1.29) occurs if we consider the one-point sample mean (P=1), which involves replacing the gradient estimate $\nabla F_n$ in (3.1.24) by an instantaneous value,

$$\nabla \hat{F}_n = \frac{\partial e^2(n)}{\partial \mathbf{b}_n} = -2\mathbf{x}(n)e(n), \tag{3.1.30}$$

giving the filter update equation,

$$\mathbf{b}_{n+1} = \mathbf{b}_n + \mu \mathbf{x}(n)e(n), \tag{3.1.31}$$

Equation (3.1.31) is known as the LMS algorithm [3.1],[3.2],[3.3]. From (3.1.31) we can see that the LMS algorithm is very computationally simple requiring only M multiplications and M additions per time update. Intuitively the LMS algorithm updates the filter weight vector $\mathbf{b}_n$ at each time step n, to keep the filter as close as possible to the instantaneous solution of the normal equations. The weight vector is altered only by a small amount $\mu$ in order to ensure that the new weight vector is influenced by all previous error values and not just $e(n)$. This ensures the weight vector will converge to the optimal weight vector solution without excessive random wandering.

Consider the convergence of the LMS algorithm in the mean. Let us re-write the LMS solution of (3.1.31) using (3.1.5) and (3.1.7) giving,

$$\mathbf{b}_{n+1} = \mathbf{b}_n + \mu \mathbf{x}(n)\left[d(n) - \mathbf{b}_n^T \mathbf{x}(n)\right]. \tag{3.1.32}$$

Taking expectations of both sides this gives,

$$E[\mathbf{b}_{n+1}] = E\left[\mathbf{b}_n + \mu \mathbf{x}(n)\left[d(n) - \mathbf{b}_n^T \mathbf{x}(n)\right]\right]. \tag{3.1.33}$$

Using (3.1.13), (3.1.14) and (3.1.16) this becomes,

$$E[\mathbf{b}_{n+1}] = E[\mathbf{b}_n] - \mu \mathbf{R}_{xx}\left[\mathbf{b}_n - \mathbf{b}_{opt}\right]. \tag{3.1.34}$$

An error vector $\tilde{\boldsymbol{\varepsilon}}_n$ which represents the expectation of the difference between each element of the filter coefficient vector $\mathbf{b}_n$ and the optimal solution $\mathbf{b}_{opt}$ of (3.1.19), can now be defined as [3.1],

$$\tilde{\boldsymbol{\varepsilon}}_{n+1} = E\left[\mathbf{b}_{n+1} - \mathbf{b}_{opt}\right] = (\mathbf{I} - \mu \mathbf{R}_{xx})E\left[\mathbf{b}_n - \mathbf{b}_{opt}\right] = (\mathbf{I} - \mu \mathbf{R}_{xx})\tilde{\boldsymbol{\varepsilon}}_n. \tag{3.1.35}$$

A unitary similarity transform can be used to factorise the correlation matrix $\mathbf{R}_{xx}$ as follows [3.1],[3.2],

$$\mathbf{R}_{xx} = \mathbf{Q}.\boldsymbol{\Lambda}.\mathbf{Q}^T, \tag{3.1.36}$$

where $\mathbf{Q}$ is a matrix whose columns are the eigenvectors of $\mathbf{R}_{xx}$, and $\boldsymbol{\Lambda}$ is a diagonal matrix whose elements consist of the eigenvalues of $\mathbf{R}_{xx}$, corresponding to each eigenvector of $\mathbf{Q}$ [3.1],[3.2]. $\boldsymbol{\Lambda}$ is also referred to as the spectral matrix. Substituting (3.1.35) into (3.1.36) this gives

$$\tilde{\boldsymbol{\varepsilon}}_{n+1} = \left(\mathbf{I} - \mu \mathbf{Q}.\boldsymbol{\Lambda}.\mathbf{Q}^T\right)\tilde{\boldsymbol{\varepsilon}}_n. \tag{3.1.37}$$

If we now define a rotated error vector as,

$$\boldsymbol{\varepsilon}_n = \mathbf{Q}^T \tilde{\boldsymbol{\varepsilon}}_n, \tag{3.1.38}$$

we can compose a decoupled difference equation for each element $\varepsilon_n(j)$ of the rotated error vector $\boldsymbol{\varepsilon}_n$ as follows,

$$\varepsilon_n(j) = (1 - \mu\lambda_j)^n \varepsilon_0(j) \quad , j = 0,1...M, \tag{3.1.39}$$

where $\lambda_j$ is the $j^{th}$ eigenvalue of $\mathbf{R}_{xx}$. Consequently each coefficient $j$ of vector $\mathbf{b}_n$, denoted $b_n(j)$, will converge "in the mean", to the corresponding coefficient of optimal solution $b_{opt}(j)$ provided that,

$$\left|(1-\mu\lambda_j)\right|<1, \tag{3.1.40}$$

For a positive definite matrix $\mathbf{R}_{xx}$ the LMS algorithm will "converge in the mean" provided that [3.11],

$$0<\mu<\frac{2}{\lambda_{\max}}. \tag{3.1.41}$$

The result of (3.1.41)mirrors the result for the steepest descent algorithm in (3.1.26). However in most applications the knowledge of the maximum eigenvalue $\lambda_{\max}$ of $\mathbf{R}_{xx}$ is not known. One way to overcome this problem is to use the trace of positive definite matrix $\mathbf{R}_{xx}$ as a conservative estimate of $\lambda_{\max}$ giving [3.11],

$$0<\mu<\frac{2}{tr[\mathbf{R}_{xx}]}, \tag{3.1.42}$$

where

$$tr[\mathbf{R}_{xx}]=\sum_{i=1}^{M}\lambda_i. \tag{3.1.43}$$

From (3.1.43) we can see the trace of $\mathbf{R}_{xx}$ is greater than the maximum eigenvalue $\lambda_{\max}$ of $\mathbf{R}_{xx}$, since $\lambda_i>0$ for positive definite matrix $\mathbf{R}_{xx}$. Using the fact $\mathbf{R}_{xx}$ has a Toeplitz form all the elements on the main diagonal are equal to $\mathbf{r}_{xx}(0)$. Since $\mathbf{r}_{xx}(0)$ is itself equal to the mean square power of the input signal $x(n)$ at each of the M taps of the FIR filter then,

$$tr[\mathbf{R}_{xx}]=\sum_{i=1}^{M}\lambda_i=M\mathbf{r}_{xx}(0)=ME[x^2(n)]. \tag{3.1.44}$$

Equation (3.1.42) then becomes [3.11],

$$0<\mu<\frac{2}{M.E[x^2(n)]}. \tag{3.1.45}$$

We can see that from (3.1.45) the stability condition for convergence of the LMS algorithm "in the mean", has a dependence on the adaptive filter length M, and the input power of signal $x(n)$. If we consider the convergence time of the LMS algorithm we can see from (3.1.39) the rate of decay of each coefficient error term $\varepsilon_n(j)$ will depend on the magnitude of term $\left|(1-\mu\lambda_j)\right|$. The larger the stepsize $\mu$ within the limits of (3.1.45) the faster convergence will be. From (3.1.39) we can see the LMS algorithm generally converges in the mean to the optimum solution in a non-uniform manner, as some coefficients will converge quicker then others if the eigenvalues of $\mathbf{R}_{xx}$ are distinct. The overall convergence time is limited by the slowest mode of convergence, which is determined by the smallest eigenvalue. This non-uniform convergence is known as the ***eigenvalue disparity problem***. For signals with a large eigenvalue spread such as coloured noise signals or speech convergence time for the LMS

algorithm can be slow. This is one of the main problems with the application of LMS based algorithms for Acoustic Echo Cancellation. The eigenvalue spread of the correlation matrix $\mathbf{R}_{xx}$ is defined as [3.11].

$$\chi(\mathbf{R}_{xx}) = \frac{\lambda_{\max}}{\lambda_{\min}}, \tag{3.1.46}$$

where $\lambda_{\max}$ and $\lambda_{\max}$ are the maximum and minimum values of the correlation matrix $\mathbf{R}_{xx}$. Equation (3.1.46) is also termed the condition number of the correlation matrix $\mathbf{R}_{xx}$. If the condition number is large the correlation matrix is ***ill conditioned*** and solving equations in $\mathbf{R}^{-1}_{xx}$ may not be possible. For an ill conditioned correlation matrix in (3.1.19) it may not be possible to find the optimal filter weight solution or even to find an iterative estimate using an adaptive filter. For large condition numbers the LMS algorithm would be expected to converge slowly as the eigenvalue spread would be large. The eigenvalue spread would be greater than unity for correlated signals such as speech. For condition numbers close to unity the LMS algorithm would be expected to converge quickly as the error terms in (3.1.39) for each coefficient would converge with a similar time constant. The eigenvalue spread would be close to unity for uncorrelated signals such as white noise.

Another important point to consider is the misadjustment $\mathcal{M}$ of the LMS algorithm from the minimum mean squared error $F_{\min}$ obtained by the optimal solution of (3.1.19), which can be approximately written as [3.11],

$$\mathcal{M} = \frac{F_{\infty}}{F_{\min}} \cong \frac{1}{2}\mu.M.E[x^2(n)] \cong \frac{\mu}{\mu_{\max}}. \tag{3.1.47}$$

where $F_{\infty}$ is the steady state excess mean square error. We can see from (3.1.47) that the steady state mean squared error performance of the LMS adaptive filter is also dependent on the adaptive filter length M (and the input power of signal $x(n)$), in addition to the stepsize $\mu$. In general a trade off is necessary between filter length M and stepsize $\mu$ in the LMS adaptive algorithm to get the desired convergence time and steady state error.

### 3.1.2.3. The Normalised LMS (NLMS) adaptive algorithm

For Acoustic Echo Cancellation applications another limitation of the LMS algorithm is that the input signals of interest often are speech signals which can vary in power over a wide range. The update term in the LMS equation of (3.1.30) as a result will then vary with signal power of $x(n)$ and presents a problem for choosing a fixed step size $\tilde{\mu}$ (which from (3.1.45) is dependent on input signal power and adaptive filter length), generally resulting in poor convergence performance. By normalising the update of (3.1.31) to compensate for the dependency on the length of the adaptive filter and the input signal power of $x(n)$ we get,

$$\mathbf{b}_{n+1} = \mathbf{b}_n + \frac{\tilde{\mu}}{M.E[x^2(n)]}\mathbf{x}(n)e(n). \tag{3.1.48}$$

Equation (3.1.48) is termed the Normalised LMS (NLMS) algorithm and $\tilde{\mu}$ is now termed the normalised stepsize such that [3.2],[3.11],

$$\tilde{\mu} = \mu M.E[x^2(n)]. \tag{3.1.49}$$

The term $M.E[x^2(n)]$ is normally calculated by using an unbiased time average of the measured data. A convenient estimate is given by [3.2],

$$M.E[x^2(n)] = \sum_{j=0}^{M-1} x^2(n-j) = \mathbf{x}^T(n)\mathbf{x}(n). \tag{3.1.50}$$

Incorporating this in (3.1.48) we get the NLMS algorithm filter update,

$$\mathbf{b}_{n+1} = \mathbf{b}_n + \frac{\tilde{\mu}}{\delta + \mathbf{x}^T(n)\mathbf{x}(n)}\mathbf{x}(n)e(n), \tag{3.1.51}$$

where $\delta$ is a small positive constant to prevent division by zero when the input signal is zero or low in power. The convergence range of the NLMS algorithm in the mean square now becomes [3.2],

$$0 < \tilde{\mu} < 2. \tag{3.1.52}$$

Despite a small increase in complexity in the NLMS algorithm over the LMS algorithm, and the eigenvalue disparity problem, the NLMS algorithm is still computationally simple, as is often used in many Acoustic Echo Cancellation applications[3.6].

### 3.1.3. Newton's Method and the LMS-Newton (LMSN) algorithm

Consider Newton's method that provides an iterative technique for finding the solution to quadratic function $f(x) = 0$ as illustrated in Figure 3.3.

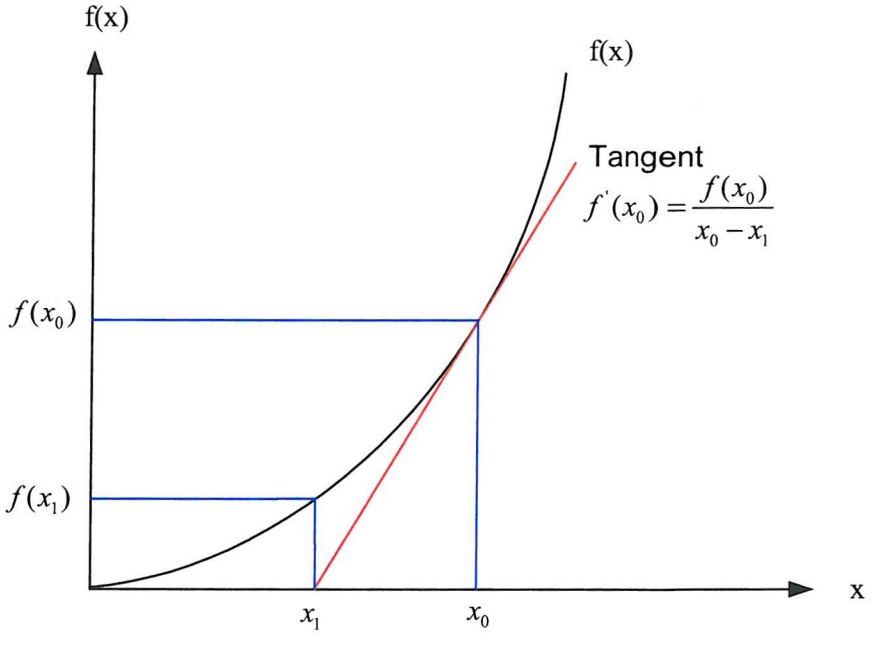


**Figure 3.3 : Newton's Gradient Search Method**

This method consists of starting with an initial guess $x_0$ and then using the first derivative $f'(x)$ to compute the new estimate $x_1$. The next point $x_2$ is then computed using $x_1$ as the initial guess and so on, giving the general formula [3.4],

$$x_{n+1} = x_n - \frac{f(x_n)}{f'(x_n)} = x_n - \frac{f(x_n)}{\partial f(x_n) / \partial x_n}. \tag{3.1.53}$$

Recall from (3.1.12) the mean square error surface $F$ can be written as a quadratic function of the filter coefficients as,

$$F = E[y^2(n)] - 2\mathbf{b}^T\mathbf{r}_{yx} + \mathbf{b}^T\mathbf{R}_{xx}\mathbf{b} + E[v^2(n)]. \tag{3.1.11}$$

In earlier sections the minimum of the mean square error surface $F$ with respect to the filter coefficients $\mathbf{b}$ can be written as $\nabla F_n = \frac{\partial F_n}{\partial \mathbf{b}_n} = 0$. To apply the Newton iteration to the problem of optimal filter design to find the solution to $\nabla F_n = \frac{\partial F_n}{\partial \mathbf{b}_n} = 0$, we can use $f(\mathbf{b}_n) = \nabla F_n = \frac{\partial F_n}{\partial \mathbf{b}_n}$ in (3.1.53) and iterate over $\mathbf{b}_n$ instead of $x_n$ giving the formula,

$$\mathbf{b}_{n+1} = \mathbf{b}_n - \frac{\frac{\partial F_n}{\partial \mathbf{b}_n}}{\frac{\partial^2 F_n}{\partial \mathbf{b}_n \partial \mathbf{b}_n^T}} = \mathbf{b}_n - \mathbf{H}^{-1}(\mathbf{b}_n)\nabla \mathbf{F}_n. \tag{3.1.54}$$

where $\mathbf{H}(b_n)$ is the Hessian matrix of the mean square error surface $F$, which is defined as the second derivative of $F$ with respect to the filter coefficients as follows,

$$H(\mathbf{b}_n) = \frac{\partial^2 F_n}{\partial \mathbf{b}_n \partial \mathbf{b}^T{}_n}. \tag{3.1.55}$$

From (3.1.12) the Hessian matrix $\mathbf{H}(\mathbf{b}_n)$ can be computed to be,

$$H(\mathbf{b}_n) = \frac{\partial}{\partial \mathbf{b}_n}[2\mathbf{R}_{xx}\mathbf{b}_n - 2\mathbf{r}_{xd}] = 2\mathbf{R}_{xx}. \tag{3.1.56}$$

Substituting (3.1.56) into (3.1.54) we get an iterative solution to the normal equations using Newton's method as follows,

$$\mathbf{b}_{n+1} = \mathbf{b}_n - \frac{1}{2}\mathbf{R}_{xx}^{-1}\nabla \mathbf{F}_n. \tag{3.1.57}$$

Comparing (3.1.57) to (3.1.20) and (3.1.21) we have $\mathbf{D}_n = \mathbf{R}_{xx}^{-1}$, $\mathbf{p}_n = \nabla \mathbf{F}_n$ and $\mu_n = 1$. By weighting the gradient search direction in Newton's method by the inverse of the estimated Hessian of the cost function $F$ in (3.1.55), the search direction always points to the minimum of the cost function $F$. This search direction is in sharp contrast to the steepest descent method of (3.1.23), which points to the maximum direction of change, and will result in an accelerated search. The search direction of Newton's method in (3.1.57), and the steepest descent method of (3.1.23) will only coincide when the eigenvalue spread of the correlation matrix is unity. Where the eigenvalue spread of the correlation matrix increases

above unity the search directions will differ. Newton's method of (3.1.57) can be expected to converge much quicker due to weighting by $\mathbf{R}_{xx}^{-1}$, which essentially not only modifies the search direction, but also equalises the eigenvalues of the correlation matrix in each direction.

Equation (3.1.57) despite having possibility of improved convergence is still idealised in that the update requires both the calculation of the correlation matrix $\mathbf{R}_{xx}$ and $\nabla\mathbf{F}_n$, and the inversion of $\mathbf{R}_{xx}$. As we have already discussed for the optimal solution in (3.1.19) and the steepest descent method in (3.1.27) earlier in the chapter this can be computationally very expensive and is unsuitable for real time implementation. In practice as seen already in the LMS algorithm in (3.1.31) it is necessary to use an instantaneous estimate for the gradient $\nabla F_n$ defined in (3.1.30) and introducing a time estimates as in (3.1.27) gives,

$$\mathbf{b}_{n+1} = \mathbf{b}_n + \mu\hat{\mathbf{R}}_{xx}^{-1}(n)\mathbf{x}(n)e(n), \tag{3.1.58}$$

where $\hat{\mathbf{R}}_{xx}^{-1}(n)$ is an estimate of the inverse of the correlation matrix $\mathbf{R}_{xx}^{-1}$. Equation (3.1.58) is termed the LMS-Newton (LMSN) algorithm[3.2],[3.4],[3.7],[3.8]. As the introduction of instantaneous estimate of $\nabla F_n$ defined in (3.1.30) will introduce noise into the coefficient vector update, so an update constant $\mu$ is introduced in (3.1.58) to allow a greater control of the algorithm update. Using the same procedure as in the LMS algorithm in it can be shown that the LMS-Newton (LMSN) method will converge in the mean provided that [3.2],

$$|1-\mu| < 1. \tag{3.1.59}$$

that is,

$$0 < \mu < 2. \tag{3.1.60}$$

Additionally the convergence rate in the mean of each coefficient is identical, and from (3.1.59) depends on $|1-\mu|$. As a result the convergence of the LMS-Newton (LMSN) algorithm is independent of the eigenvalue spread of the correlation matrix $\mathbf{R}_{xx}$. This is the key advantage of the LMS-Newton (LMSN) method and as we have already pointed contrasts sharply to the LMS algorithm, where the convergence of each coefficient in the mean from (3.1.40) is dependent on the eigenvalue spread of correlation matrix $\mathbf{R}_{xx}$. The Misadjustment $\mathcal{M}$ of the LMS-Newton (LMSN) algorithm, for a small $\mu$, can be approximately written as,

$$\mathcal{M} = \frac{F_\infty}{F_{\min}} \cong \frac{1}{2}\mu.M.E[x^2(n)] \cong \frac{\mu}{\mu_{\max}}. \tag{3.1.61}$$

From (3.1.61)we can see that the Misadjustment of the LMS-Newton (LMSN) algorithm is identical to the Misadjustment of the LMS algorithm. Thus for the same adaption rate $\mu$ the LMS-Newton (LMSN) algorithm will suffer no eigenvalue disparity, and at the same time achieve comparable steady state Misadjustment to the LMS algorithm.

Despite the advantages of the LMS-Newton (LMSN) algorithm from (3.1.58) we can see an estimate of the inverse of the correlation matrix $\hat{\mathbf{R}}_{xx}^{-1}(n)$ is required every update period. Using the

Robbins-Monro procedure an estimate of the correlation matrix every update period $\hat{\mathbf{R}}_{xx}(n)$ is given by [3.8],

$$\hat{\mathbf{R}}_{xx}(n) = \hat{\mathbf{R}}_{xx}(n-1) + \alpha(n)\left[\mathbf{x}(n)\mathbf{x}^T(n) - \hat{\mathbf{R}}_{xx}(n-1)\right], \tag{3.1.62}$$

where $\alpha(n)$ is a convergence factor. This will result in a good estimate for $\mathbf{R}_{xx}$, which is positive definite provided the input signal $x(n)$ is persistently exciting of order [3.8]. To obtain an estimate of the inverse of the correlation matrix $\hat{\mathbf{R}}_{xx}^{-1}(n)$ the matrix inversion lemma can be used yielding [3.2],[3.11],

$$\hat{\mathbf{R}}_{xx}^{-1}(n) = \frac{1}{1-\alpha(n)}\left( \hat{\mathbf{R}}_{xx}^{-1}(n-1) - \frac{\hat{\mathbf{R}}_{xx}^{-1}(n-1)\mathbf{x}(n)\mathbf{x}^T(n)\hat{\mathbf{R}}_{xx}^{-1}(n-1)}{\frac{1-\alpha(n)}{\alpha(n)} + \mathbf{x}^T(n)\hat{\mathbf{R}}_{xx}^{-1}(n-1)\mathbf{x}(n)} \right), \tag{3.1.63}$$

If $\alpha(n) = \alpha$ for all n, such that,

$$\alpha(n) = \alpha = 1 - \lambda = 2\mu, \tag{3.1.64}$$

equation (3.1.63) becomes,

$$\hat{\mathbf{R}}_{xx}^{-1}(n) = \frac{1}{\lambda}\left( \hat{\mathbf{R}}_{xx}^{-1}(n-1) - \frac{\hat{\mathbf{R}}_{xx}^{-1}(n-1)\mathbf{x}(n)\mathbf{x}^T(n)\hat{\mathbf{R}}_{xx}^{-1}(n-1)}{\frac{\lambda}{\alpha} + \mathbf{x}^T(n)\hat{\mathbf{R}}_{xx}^{-1}(n-1)\mathbf{x}(n)} \right), \tag{3.1.65}$$

It can be shown that with the settings of (3.1.64) the LMS-Newton (LMSN) algorithm minimises a weighted sum of posteriori errors $\xi(n)$, defined by,

$$\xi(n) = \sum_{i=1}^{n} \lambda^{n-i}\left[d(i) - \mathbf{w}^T(n)\mathbf{x}(i)\right]^2, \tag{3.1.66}$$

where $\lambda$ is termed the forgetting factor which weights the most recent errors. This is useful to exclude old data that is less appropriate in non-stationary environments. Equation (3.1.66) is the objective function of the well-known exponentially weighted Recursive Least Squares (RLS) algorithm, which can be obtained, after some manipulation, by substituting (3.1.66) into (3.1.58) [3.2]. The LMSN algorithm can hence be regarded as either a gradient descent method, which uses noisy estimates for the input correlation matrix $R_{xx}$ and the gradient vector $\nabla F_n$, or a deterministic least squares algorithm when (3.1.64) is satisfied.

Like the LMS algorithm however the use of a fixed stepsize control $\mu$ in the LMSN algorithm of (3.1.57) presents difficulties for using the algorithm in a non-stationary environment whose characteristics are unknown. The normalisation of $\hat{\mathbf{R}}_{xx}^{-1}(n)$ in (3.1.57) alone is ineffective for faster time variations in the input signal $x(n)$. Instead an additional variable stepsize control $\mu(n)$ can be used that is adjusted each iteration according to a certain optimality criterion. A variable stepsize $\mu(n)$ that can be chosen to yield zero a posteriori error regardless of how $\hat{\mathbf{R}}_{xx}^{-1}(n)$ is estimated is given by [3.9],

$$\mu(n) = \frac{1}{\mathbf{x}^T(n)\hat{\mathbf{R}}_{xx}^{-1}(n)\mathbf{x}(n)}, \tag{3.1.67}$$

Incorporating (3.1.67) into (3.1.57) and including an additional factor $\mu$ to control misadjustment at the expense of convergence speed gives [3.9],

$$\mathbf{b}_{n+1} = \mathbf{b}_n + \mu \frac{\hat{\mathbf{R}}_{xx}^{-1}(n)\mathbf{x}(n)e(n)}{\mathbf{x}^T(n)\hat{\mathbf{R}}_{xx}^{-1}(n)\mathbf{x}(n)}. \tag{3.1.68}$$

Equation (3.1.68) shall be termed the Normalised LMS-Newton method (NLMSN) and is almost identical in form and complexity to the exponentially weighted Recursive Least Squares (RLS) algorithm [3.2].

### 3.1.4. Adaptive FIR Algorithm Summary

A complete summary of the FIR adaptive algorithms detailed in the thesis can be formulated in general form as shown in the table below,

<table>
<tr><td colspan="3">Initialisation: $\mathbf{b}_n = \mathbf{0}, \ \forall n < 0$<br>$\hat{y}(n) = \mathbf{b}_n^T \mathbf{x}(n)$<br>$e(n) = d(n) - \hat{y}(n)$</td></tr>
<tr><td>Algorithm</td><td>$\mathbf{H}_n$</td><td>$\mu(n)$</td></tr>
<tr><td>FIR LMS</td><td>$\mathbf{I}$</td><td>$\mu$</td></tr>
<tr><td>FIR NLMS</td><td>$\mathbf{I}$</td><td>$\frac{\mu}{\mathbf{x}^T(n)\mathbf{x}(n)}$</td></tr>
<tr><td>FIR LMSN</td><td>$\mathbf{R}_{xx}^{-1}(n)$</td><td>$\mu$</td></tr>
<tr><td>FIR NLMSN</td><td>$\mathbf{R}_{xx}^{-1}(n)$</td><td>$\frac{\mu}{\mathbf{x}^T(n)\mathbf{R}_{xx}^{-1}(n)\mathbf{x}(n)}$</td></tr>
<tr><td colspan="3">$\mathbf{b}_{n+1} = \mathbf{b}_n + \mu(n)\mathbf{H}_n\mathbf{x}(n)e(n)$</td></tr>
</table>

**Table 3-1: FIR adaptive algorithm summary**

In addition to the algorithms detailed in this section many other variants may be derived form using different formulations and implementations of $\mu(n)$ and $\mathbf{H}_n$ [3.4],[3.9],[3.10],[3.11].

## 3.2. Output Error Adaptive IIR Filtering

There are two error signal formulations normally used for adaptive IIR filtering - Equation Error and Output Error. This section describes the most common adaptive IIR filtering algorithms based on the output error formulation [3.3],[3.12],[3.13],[3.15].

### 3.2.1. The Optimal Output Error IIR Filter

Consider an adaptive IIR filter model based on the output error formulation as shown below.

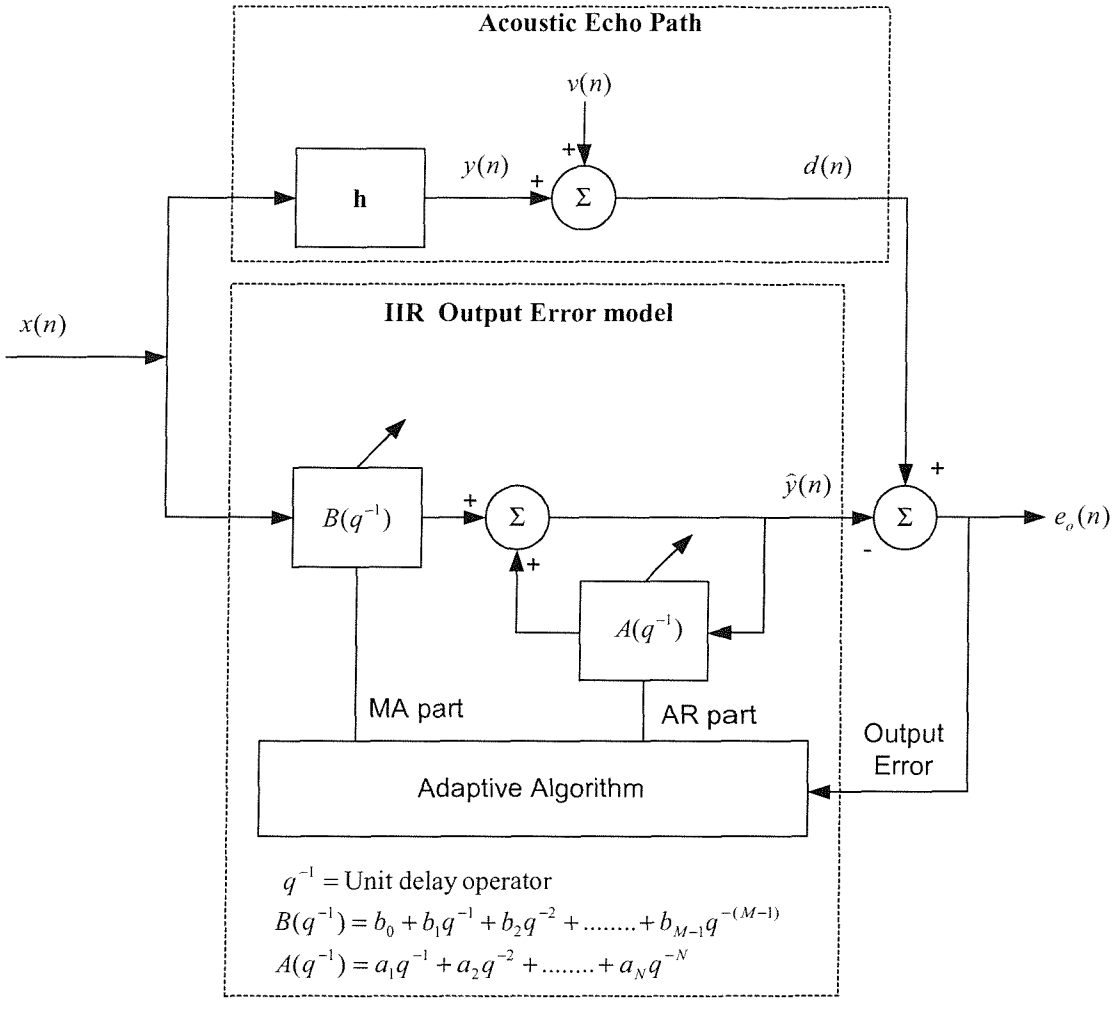


**Figure 3.4 : System Identification of echo path using output error adaptive IIR filter**

The same echo path model described by equation (3.1.1) and (3.1.2) is used for the unknown echo path to be modelled. Like the FIR filter to cancel the echo signal $d(n)$, a replica of the echo path output, $\hat{y}(n)$, must be created by the IIR output error filter which models the echo path transfer function and

subtracted from $d(n)$. For a fixed time invariant output error IIR filter model of order (M, N), the output $\hat{y}(n)$ becomes,

$$\hat{y}(n) = \mathbf{B}(q^{-1})x(n) + \mathbf{A}(q^{-1})y(n) = \sum_{i=0}^{M-1} b_i x(n-i) + \sum_{j=1}^{N} a_j \hat{y}(n-j). \tag{3.2.1}$$

Re-writing (3.2.1) more compactly using vector notation we get,

$$\hat{y}(n) = \boldsymbol{\theta}^T \boldsymbol{\varphi}_o. \tag{3.2.2}$$

where $\boldsymbol{\theta}$ is a (M+N) x 1 coefficient vector defined as:

$$\boldsymbol{\theta} = [b_0, b_1, ..., b_{M-1}, a_1, a_2, ..., a_N]^T, \tag{3.2.3}$$

with $\boldsymbol{\varphi}_o$ being a (M+N) x 1 information regression vector defined as:

$$\boldsymbol{\varphi}_o = [x(n), ..., x(n-M+1), \hat{y}(n-1), ..., \hat{y}(n-N)]^T = [\mathbf{x}(n)^T, \hat{\mathbf{y}}(n-1)^T]^T, \tag{3.2.4}$$

where $\mathbf{x}(n)$ is a Mx1 vector of echo path input samples defined as:

$$\mathbf{x}(n) = [x(n), x(n-1), ....., x(n-M+1)]^T, \tag{3.2.5}$$

and $\hat{\mathbf{y}}(n-1)$ is a Nx1 vector of IIR filter model output samples defined as:

$$\hat{\mathbf{y}}(n-1) = [\hat{y}(n-1), ....., \hat{y}(n-N)]^T, \tag{3.2.6}$$

Equation (3.2.2) has the form of linear regression. However since previous filter outputs in $\hat{\mathbf{y}}(n-1)$ of the regression vector $\boldsymbol{\varphi}_o$ depend on previous model coefficient values, equation (3.2.2) is not a linear regression. The filter output $\hat{y}(n)$ is a non-linear function of $\boldsymbol{\theta}$, and equation (3.2.2) is often termed a pseudo-linear regression [3.12]. Consider the output error signal $e_o(n)$,

$$e_o(n) = d(n) - \hat{y}(n) = d(n) - \boldsymbol{\theta}^T \boldsymbol{\varphi}_o, \tag{3.2.7}$$

For a minimum output error signal the fixed output error IIR filter coefficients must be chosen to minimise some cost function. Like we have already seen for the optimal FIR filter model the cost function normally used in system identification theory is the minimisation of the mean square error.

Consider now the design of an output error IIR filter model of order (M,N) to minimise the mean square error. The cost function $F$ to be minimised is denoted as,

$$F = E[e_o^2(n)], \tag{3.2.8}$$

Rewriting (3.2.8) using (3.2.2) and (3.2.7) we get an equation for the cost function $F$ in terms of the filter coefficient vector $\boldsymbol{\theta}$, which is termed the Mean Square Output Error (MSOE) Surface, as follows [3.2],[3.12],

$$F = E[e_o^{\,2}(n)] = E\left[\left(d(n) - \boldsymbol{\theta}^T \boldsymbol{\varphi}_o\right)^2\right], \tag{3.2.9}$$

Re-writing (3.2.9) and assuming that $v(n)$ is an additive white noise disturbance signal independent of input process $x(n)$ and hence information regression vector $\boldsymbol{\varphi}_o$ we get,

$$F = E[y^2(n)] - 2\boldsymbol{\theta}^T E[y(n)\boldsymbol{\varphi}_o] + \boldsymbol{\theta}^T E\left[\boldsymbol{\varphi}_o^{\,T} \boldsymbol{\varphi}_o\right]\boldsymbol{\theta} + E[v^2(n)], \tag{3.2.10}$$

Simplifying (3.2.10) we get,

$$F = E[y^2(n)] - 2\boldsymbol{\theta}^T \mathbf{r}_{y\boldsymbol{\varphi}_o} + \boldsymbol{\theta}^T \mathbf{R}_{\boldsymbol{\varphi}_o\boldsymbol{\varphi}_o} \boldsymbol{\theta} + E[v^2(n)], \tag{3.2.11}$$

where $\mathbf{R}_{\boldsymbol{\varphi}_o\boldsymbol{\varphi}_o}$ is a (M+N) x (M+N) covariance matrix defined as [3.13]:

$$\mathbf{R}_{\boldsymbol{\varphi}_o\boldsymbol{\varphi}_o} = E[\boldsymbol{\varphi}_o \boldsymbol{\varphi}_o^T] = \begin{bmatrix} \mathbf{R}_{xx} & \mathbf{R}_{x\hat{y}} \\ \mathbf{R}_{x\hat{y}}^T & \mathbf{R}_{\hat{y}\hat{y}} \end{bmatrix}, \tag{3.2.12}$$

and $\mathbf{r}_{y\boldsymbol{\varphi}_o}$ is a cross correlation vector defined as:

$$r_{y\boldsymbol{\varphi}_o} = E[y(n)\boldsymbol{\varphi}_o(n)], \tag{3.2.13}$$

with:

$$\mathbf{R}_{xx} = \text{M x M autocorrelation matrix } E[\mathbf{x}(n)\mathbf{x}^T(n)], \tag{3.2.14}$$

$$\mathbf{R}_{x\hat{y}} = \text{M x N cross correlation matrix } E[\mathbf{x}(n)\hat{\mathbf{y}}^T(n-1)], \tag{3.2.15}$$

$$\mathbf{R}_{\hat{y}\hat{y}} = \text{N x N autocorrelation matrix } E[\hat{\mathbf{y}}(n-1)\hat{\mathbf{y}}^T(n-1)], \tag{3.2.16}$$

From equation (3.2.11) to (3.2.16) we can clearly see that $\mathbf{r}_{y\boldsymbol{\varphi}_o}$, $\mathbf{R}_{x\hat{y}}$ and $\mathbf{R}_{\hat{y}\hat{y}}$ depend on $\hat{\mathbf{y}}(n-1)$, which in turn are functions of the filter coefficient vector $\boldsymbol{\theta}$. The Mean Square Output Error surface for the Output Error IIR filter model, unlike the FIR filter model, is hence a non-quadratic function of the filter coefficients $b_i$ and $a_j$. As a result a single unique solution "may not" exist in $F$ with respect to $\boldsymbol{\theta}$, and may correspond to local minima on the cost function rather than a global solution with respect to the filter coefficients. However to minimise this cost function $F$ with respect to the filter coefficient vector we can differentiate $F$ in (3.2.9) with respect to $\boldsymbol{\theta}$, and equate to zero. This yields,

$$\frac{\partial F}{\partial \boldsymbol{\theta}} = \frac{\partial E[e_o^2(n)]}{\partial \boldsymbol{\theta}} = 2E\left[ e_o(n) \frac{\partial e_o(n)}{\partial \boldsymbol{\theta}} \right], \tag{3.2.17}$$

But,

$$\frac{\partial e_o(n)}{\partial \boldsymbol{\theta}} = -\frac{\partial \hat{y}(n)}{\partial \boldsymbol{\theta}}, \tag{3.2.18}$$

Combining (3.2.9), (3.2.17) and (3.2.18), and equating to zero we get,

$$\frac{\partial F}{\partial \boldsymbol{\theta}} = \frac{\partial E[e_o^2(n)]}{\partial \boldsymbol{\theta}} = -2E\left[ e_o(n) \frac{\partial \hat{y}(n)}{\partial \boldsymbol{\theta}} \right] = \mathbf{0}. \tag{3.2.19}$$

Unlike the FIR model a direct derivative of $\hat{y}(n)$ from (3.2.2) with respect to the model coefficients $\boldsymbol{\theta}$ cannot be applied, as regression vector $\boldsymbol{\varphi}_o$ is also dependent on $\boldsymbol{\theta}$. Using (3.2.1) and separating derivatives of $\hat{y}(n)$ with respect to the coefficients $b_i$ and $a_j$ we get [3.14],

$$\frac{\partial \hat{y}(n)}{\partial b_i} = x(n-i) + \sum_{m=1}^{N} a_m \frac{\partial \hat{y}(n-m)}{\partial b_i} \qquad ;0 \le i \le M-1. \tag{3.2.20}$$

$$\frac{\partial \hat{y}(n)}{\partial a_j} = \hat{y}(n-j) + \sum_{m=1}^{N} a_m \frac{\partial \hat{y}(n-m)}{\partial a_j} \qquad ;1 \le j \le N. \tag{3.2.21}$$

Combining equation (3.2.19), (3.2.20) and (3.2.21) we get,

$$E\left\{e_o(n)\left[x(n-i)+\sum_{m=1}^{N}a_m\frac{\partial\hat{y}(n-m)}{\partial b_i}\right]\right\}=0 \quad ;0\le i\le M-1. \tag{3.2.22}$$

$$E\left\{e_o(n)\left[\hat{y}(n-j)+\sum_{m=1}^{N}a_m\frac{\partial\hat{y}(n-m)}{\partial a_j}\right]\right\}=0 \quad ;1\le j\le N. \tag{3.2.23}$$

Equation (3.2.22) and (3.2.23) are the recursive form of the normal equations of (3.1.15). Direct solution of (3.2.21) would yield the optimum output error IIR model filter coefficients. However as this equation is non-linear with respect to the filter coefficients $b_i$ and $a_j$ local minima may exist. A direct solution of (3.2.21) may be very difficult to solve directly in this fashion. The computation involved in such an attempt would also be extremely high. As a result the direct solution of (3.2.21) is generally not used. Instead the use of iterative solutions to the recursive normal equations of (3.2.21) is normally employed. In the next section adaptive IIR solutions are presented to the recursive normal equations.

Note that the disturbance term $E[v^2(n)]$ in (3.2.11) makes no contribution to these systems of equations in (3.2.22) and (3.2.23) that determine the optimal IIR filter coefficients. This can be seen more clearly by re-writing the cost function F using Parseval's theorem [3.13],

$$F=\frac{1}{2\pi}\int_{-2\pi}^{2\pi}S_{xx}(e^{j\omega})\left[\left|H(e^{j\omega})\right|^2-\frac{\left|B(e^{j\omega})\right|^2}{\left|1-A(e^{j\omega})\right|^2}\right]d\omega+\frac{1}{2\pi}\int_{-2\pi}^{2\pi}S_{vv}(e^{j\omega})d\omega. \tag{3.2.24}$$

This disturbance term $\frac{1}{2\pi}\int_{-2\pi}^{2\pi}S_{vv}(e^{j\omega})d\omega$ in (3.2.24) only adds a constant term to the mean square error surface and does not effect the locations of the minimum points. Minimisation of the mean square output error surface with respect to filter coefficients $b_i$ and $a_j$ shall not vary with the disturbance signal $v(n)$.

### 3.2.2. The method of Steepest Descent and the Simplified Gradient LMS Output Error adaptive IIR algorithm

Earlier in the Chapter we have seen the steepest descent update to the normal equations of (3.1.16) was given by (3.1.23) for a FIR adaptive filter. For an Output Error adaptive IIR filter the steepest descent update for the iterative solution to the recursive normal equations of (3.2.21) is similarly given by,

$$\boldsymbol{\theta}_{n+1}=\boldsymbol{\theta}_n-\frac{\mu}{2}\nabla F_n, \tag{3.2.25}$$

where $\mu$ is a step size parameter to control the size of change in $\boldsymbol{\theta}_{n+1}$ from $\boldsymbol{\theta}_n$. The gradient of the mean square output error surface $\nabla F_n$ using (3.2.16) and (3.2.17) can be written as,

$$\nabla F_n=-2E[e_o(n)\nabla\hat{y}(n)], \tag{3.2.26}$$

giving the iteration,

$$\boldsymbol{\theta}_{n+1} = \boldsymbol{\theta}_n + \mu E[e_o(n)\nabla\hat{y}(n)]. \tag{3.2.27}$$

Since $E[e(n)\nabla\hat{y}(n)]$ is generally unknown an estimate can be used. In line with the FIR LMS philosophy used earlier in the chapter the gradient $\nabla F_n$ is replaced by an instantaneous estimate,

$$\nabla F_n = -2e_o(n)\nabla\hat{y}(n), \tag{3.2.28}$$

where,

$$\nabla\hat{y}(n) = \frac{\partial\hat{y}(n)}{\partial\boldsymbol{\theta}_n}, \tag{3.2.29}$$

giving the coefficient update,

$$\boldsymbol{\theta}_{n+1} = \boldsymbol{\theta}_n + \mu e_o(n)\frac{\partial\hat{y}(n)}{\partial\boldsymbol{\theta}_n}, \tag{3.2.30}$$

Consider the gradient estimate of (3.2.28). As the output $\hat{y}(n)$ itself depends on previous outputs, which in turn depends on previous coefficient values, the derivative of the output, $\frac{\partial\hat{y}(n)}{\partial\boldsymbol{\theta}_n}$, in (3.2.30), is itself recursive. Expanding the derivative of the output using (3.2.20) and (3.2.21), and introducing time dependency we get,

$$\frac{\partial\hat{y}(n)}{\partial b_i(n)} = x(n-i) + \sum_{m=1}^{N} a_m(n)\frac{\partial\hat{y}(n-m)}{\partial b_i(n)} \quad ;0 \le i \le M-1, \tag{3.2.31}$$

$$\frac{\partial\hat{y}(n)}{\partial a_j(n)} = \hat{y}(n-j) + \sum_{m=1}^{N} a_m(n)\frac{\partial\hat{y}(n-m)}{\partial a_j(n)} \quad ;1 \le j \le N, \tag{3.2.32}$$

Equation (3.2.31), (3.2.32) and equation (3.2.30) represent the IIR LMS algorithm. This algorithm, as the name suggests, is the recursive output error form of the FIR LMS algorithm of (3.1.31) [3.2],[3.12],[3.14],[3.15]. From (3.2.31) and (3.2.32) we can see that the derivatives on the right hand side of these equations use current values, at time n, for coefficients $b_i$ and thus cannot be simplified to the form of a filter using delay operator notation. In to simplify the IIR LMS algorithm the stepsize $\alpha$ in (3.2.30) can be chosen to be sufficiently small to allow the following assumption can be made[3.12],

$$\boldsymbol{\theta}_n \cong \boldsymbol{\theta}_{n-1} \cong \ldots \cong \boldsymbol{\theta}_{n-N+1}. \tag{3.2.33}$$

This allows the derivatives in equation (3.2.31) and (3.2.32) to be reformulated to become recursive in form giving [3.2],[3.12],[3.14],

$$\frac{\partial\hat{y}(n)}{\partial b_i(n)} = x(n-i) + \sum_{m=1}^{N} a_m(n)\frac{\partial\hat{y}(n-m)}{\partial b_i(n-m)} \quad ;0 \le i \le M-1. \tag{3.2.34}$$

$$\frac{\partial\hat{y}(n)}{\partial a_j(n)} = \hat{y}(n-j) + \sum_{m=1}^{N} a_m(n)\frac{\partial\hat{y}(n-m)}{\partial a_j(n-m)} \quad ;1 \le j \le N. \tag{3.2.35}$$

.Rewriting (3.2.34) and (3.2.35) gives[3.12],

$$\frac{\partial\hat{y}(n)}{\partial b_i(n)} = x_f(i,n) = x(n-i) + \sum_{m=1}^{N} a_m(n)x_f(i,n-m) \quad ;0 \le i \le M-1. \tag{3.2.36}$$

$$\frac{\partial\hat{y}(n)}{\partial a_j(n)} = \hat{y}_f(j,n) = \hat{y}(n-j) + \sum_{m=1}^{N} a_m(n)\hat{y}_f(j,n-m) \quad ;1 \le j \le N. \tag{3.2.37}$$

Writing (3.2.36) and (3.2.37) in more compact form gives,

$$\frac{\partial \hat{y}(n)}{\partial b_i(n)} = \left( \frac{1}{1-\mathbf{A}(n,q^{-1})} \right) x(n-i) \quad ;0 \le i \le M-1. \tag{3.2.38}$$

$$\frac{\partial \hat{y}(n)}{\partial a_j(n)} = \left( \frac{1}{1-\mathbf{A}(n,q^{-1})} \right) \hat{y}(n-j) \quad ;1 \le j \le N. \tag{3.2.39}$$

Combining (3.2.38) and (3.2.39) and substituting into (3.2.30) gives the modified filter update,

$$\boldsymbol{\theta}_{n+1} = \boldsymbol{\theta}_n + \mu e_o(n) \boldsymbol{\varphi}_{FG}(n), \tag{3.2.40}$$

where $\boldsymbol{\varphi}_{FG}(n)$ is defined as,

$$\boldsymbol{\varphi}_{FG}(n) = \left( \frac{1}{1-\mathbf{A}(n,q^{-1})} \right) \boldsymbol{\varphi}_o(n). \tag{3.2.41}$$

Equation (3.2.40) represents the Full Gradient IIR LMS algorithm [3.12][3.14][3.15]. The structure of the Full Gradient IIR LMS algorithm is illustrated in Figure 3.5. From (3.2.40) and Figure 3.5 it can be seen the all pole filter operates on each element of information vector $\boldsymbol{\varphi}_o(n)$. The simplification of the gradient in (3.2.34) and (3.2.35) and the slowly varying filter weights assumption of (3.2.33) required for the devopment of the Full Gradient IIR LMS algorithm is reasonable in many applications. Where the assumption of (3.2.33) doesn't hold, only a small degradation in performance is observed in practice

Despite simplifications used in the Full Gradient IIR LMS algorithm, the gradient of (3.2.38) and (3.2.39) still requires a significant amount computation and storage, since N+M parallel shift variant AR filters are required of order N for each element in the adaptive filter information vector $\boldsymbol{\varphi}_o(n)$. If we again use the slowly varying filter weights assumption in (3.2.33) such that stepsize $\mu$ is sufficiently small so that coefficients $\mathbf{A}(n,q^{-1})$ in (3.2.38) and (3.2.39) do not vary significantly over intervals of N, each parallel AR filter in (3.2.34) and (3.2.35) can be assumed to be shift invariant. This results in

$$\frac{\partial \hat{y}(n)}{\partial b_i(n)} = \left( \frac{1}{1-\mathbf{A}(n-i,q^{-1})} \right) x(n-i) \quad ;0 \le i \le M-1, \tag{3.2.42}$$

$$\frac{\partial \hat{y}(n)}{\partial a_j(n)} = \left( \frac{1}{1-\mathbf{A}(n-j,q^{-1})} \right) \hat{y}(n-j) \quad ;1 \le j \le N, \tag{3.2.43}$$

The gradient of the output from (3.2.42) and (3.2.43)may then be estimated by filtering only the input $x(n)$ and output $\hat{y}(n-1)$ and using shifted versions of these signals. This gives,

$$\frac{\partial \hat{y}(n)}{\partial b_i(n)} = x_f(n-i) \quad ;0 \le i \le M-1. \tag{3.2.44}$$

and

$$\frac{\partial \hat{y}(n)}{\partial a_j(n)} = \hat{y}_f(n-j) \quad ;1 \le j \le N, \tag{3.2.45}$$

where

$$x_f(n) = x(n) + \sum_{m=1}^{N} a_m(n)\, x_f(n-m), \tag{3.2.46}$$

$$\hat{y}_f(n) = \hat{y}(n-1) + \sum_{m=1}^{N} a_m(n)\,\hat{y}_f(n-m)\,. \tag{3.2.47}$$

Re-writing the simplified gradient of (3.2.44)and (3.2.45) in more compact form gives,

$$\frac{\partial \hat{y}(n)}{\partial \boldsymbol{\theta}_n} = \boldsymbol{\varphi}_f(n)\,, \tag{3.2.48}$$

where,

$$\boldsymbol{\varphi}_f = [\mathbf{x}_f(n)^T, \hat{\mathbf{y}}_f(n)^T]^T\,, \tag{3.2.49}$$

and $\mathbf{x}_f(n)$ is a Mx1 vector of filtered echo path input samples defined as:

$$\mathbf{x}_f(n) = [x_f(n), ....., x_f(n-M+1)]^T\,, \tag{3.2.50}$$

and $\hat{\mathbf{y}}_f(n)$ is a Nx1 vector of filtered IIR filter model output samples defined as:

$$\hat{\mathbf{y}}_f(n) = [\hat{y}_f(n), ....., \hat{y}_f(n-N+1)]^T\,, \tag{3.2.51}$$

Substituting (3.2.48) into (3.2.30) gives the simplified filter update,

$$\boldsymbol{\theta}_{n+1} = \boldsymbol{\theta}_n + \mu e_o(n)\boldsymbol{\varphi}_f(n)\,, \tag{3.2.52}$$

Equation (3.2.52) represents the Simplified Gradient adaptive IIR LMS algorithm [3.12]. This simplification in (3.2.37) introduces essentially no degradation in performance over the Full Gradient IIR LMS filter update of (3.2.40), and is normally used in practice. The structure of the Simplified Gradient adaptive IIR LMS algorithm is illustrated in Figure 3.6.

In terms of the stability of the Simplified Gradient IIR LMS algorithm of (3.2.52) it can be shown that with a sufficiently small stepsize $\mu$ the adaption algorithm can be modelled using the Ordinary Differential Equation (ODE) method [3.12]. Using this method together with the direct or indirect method of Lyapunov it can be demonstrated the differential equation derived from the adaption algorithm of (3.2.41) will converge to a minimum (local or global) of the cost function $F$. However this method does not clearly reveal the range of stepsize $\mu$ for convergence. To obtain approximate bounds for the stepsize $\mu$ local linearisation assumptions can be made about a minimum point on the cost function $F$ as follows. In doing this we will also see that the Simplified Gradient IIR LMS algorithm, like the FIR LMS algorithm, has dependence on the eigenvalue spread of the correlation matrix of the information regression vector.

Suppose parameter vector $\boldsymbol{\theta}_*$ corresponds to a local minimum on the cost function to $F$. If parameter vector lies in the local neighbourhood of we may use a Taylor series expansion of the filter output about the minimum point $\boldsymbol{\theta} = \boldsymbol{\theta}_*$ as [3.13],

$$\hat{y}(n\,|\,\boldsymbol{\theta}) = \hat{y}(n\,|\,\boldsymbol{\theta}_* + \Delta\boldsymbol{\theta}) = \hat{y}(n\,|\,\boldsymbol{\theta}_*) + \Delta\boldsymbol{\theta}^T \left.\frac{d\hat{y}(n\,|\,\boldsymbol{\theta})}{d\boldsymbol{\theta}}\right|_{\boldsymbol{\theta}=\boldsymbol{\theta}_*} + \Delta\boldsymbol{\theta}^T O(\Delta\boldsymbol{\theta})\,, \tag{3.2.53}$$

Performing a first order linearisation on (3.2.53) we neglect higher order terms $\Delta\boldsymbol{\theta}^T O(\Delta\boldsymbol{\theta})$ giving,

$$\hat{y}(n\,|\,\boldsymbol{\theta}) = \hat{y}(n\,|\,\boldsymbol{\theta}_* + \Delta\boldsymbol{\theta}) = \hat{y}(n\,|\,\boldsymbol{\theta}_*) + \Delta\boldsymbol{\theta}^T \left.\frac{d\hat{y}(n\,|\,\boldsymbol{\theta})}{d\boldsymbol{\theta}}\right|_{\boldsymbol{\theta}=\boldsymbol{\theta}_*}\,, \tag{3.2.54}$$

Consider then the output error, which can be assumed to be quadratic locally,

$$e(n) = y(n) - \hat{y}(n \mid \boldsymbol{\theta}) = e_*(n) + (\boldsymbol{\theta}_n - \boldsymbol{\theta}_*)\boldsymbol{\varphi}_f, \tag{3.2.55}$$

where $e_*(n)$ denotes minimum output error obtained at minimum point on $F$ when $\boldsymbol{\theta}_*$ is used. Inserting (3.2.55) into (3.2.52) we get,

$$\boldsymbol{\theta}_{n+1} = \boldsymbol{\theta}_n + \mu\boldsymbol{\varphi}_f(n)\boldsymbol{\varphi}_f^T(n)(\boldsymbol{\theta}_n - \boldsymbol{\theta}_*) + e_*(n)\boldsymbol{\varphi}_f(n), \tag{3.2.56}$$

Offsetting both sides of (3.2.56) by $\boldsymbol{\theta}_*$ and taking expectations we get,

$$E[\boldsymbol{\theta}_* - \boldsymbol{\theta}_{n+1}] = \left(1 - \mu\mathbf{R}_{\varphi_f\varphi_f}(n)\right)E[\boldsymbol{\theta}_* - \boldsymbol{\theta}_n], \tag{3.2.57}$$

where the term $E[e_*(n)\boldsymbol{\varphi}_f(n)]$ vanishes near any local minimum and $\mathbf{R}_{\varphi_f\varphi_f}(n)$ is the correlation matrix of the filtered information regression vector defined as,

$$\mathbf{R}_{\varphi_f\varphi_f}(n) = E[\boldsymbol{\varphi}_f(n)\boldsymbol{\varphi}_f{}^T(n)] = \begin{bmatrix} \mathbf{R}_{x_f x_f}(n) & \mathbf{R}_{x_f \hat{y}_f}(n) \\ \mathbf{R}^T_{x_f \hat{y}_f}(n) & \mathbf{R}_{\hat{y}_f \hat{y}_f}(n) \end{bmatrix}, \tag{3.2.58}$$

with:

$$\mathbf{R}_{x_f x_f}(n) = \text{M x M autocorrelation matrix } E[\mathbf{x}_f(n)\mathbf{x}_f{}^T(n)], \tag{3.2.59}$$

$$\mathbf{R}_{x_f \hat{y}_f} = \text{M x N cross correlation matrix } E[\mathbf{x}_f(n)\hat{\mathbf{y}}_f{}^T(n)], \tag{3.2.60}$$

$$\mathbf{R}_{\hat{y}_f \hat{y}_f} = \text{N x N autocorrelation matrix } E[\hat{\mathbf{y}}_f(n)\hat{\mathbf{y}}_f{}^T(n)], \tag{3.2.61}$$

If we now define an error vector $\boldsymbol{\varepsilon}_n$ which represents the difference between the expected value of each element in filter coefficient vector $\boldsymbol{\theta}_n$ and the solution $\boldsymbol{\theta}_*$,

$$\boldsymbol{\varepsilon}_n = E[\boldsymbol{\theta}_* - \boldsymbol{\theta}_n]. \tag{3.2.62}$$

Equation (3.2.57) now becomes,

$$\boldsymbol{\varepsilon}_{n+1} = \left(1 - \mu\mathbf{R}_{\varphi_f\varphi_f}(n)\right)\boldsymbol{\varepsilon}_n. \tag{3.2.63}$$

Equation (3.2.63) takes the form of a discrete time homogenous system, which is stable, provided the eigenvalues of the correlation matrix $\mathbf{R}_{\varphi_f\varphi_f}(n)$ all have a magnitude, less than unity. For convergence the stepsize must $\mu$ then satisfy,

$$0 < \mu < \frac{2}{\lambda_{\max}}, \tag{3.2.64}$$

where $\lambda_{\max}$ is the maximum eigenvalue of the correlation matrix $\mathbf{R}_{\varphi_f\varphi_f}(n)$. For a positive definite matrix $\mathbf{R}_{\varphi_f\varphi_f}(n)$ the upper bound of (3.2.64) can be reduced to,

$$0 < \mu < \frac{2}{\left\|\boldsymbol{\varphi}_f(n)\right\|_2^2}, \tag{3.2.65}$$

where $\left\|\boldsymbol{\varphi}_f(n)\right\|_2$ is the $l_2$ norm of filtered information vector $\boldsymbol{\varphi}_f(n)$ defined in (3.2.49). This normalisation factor $\left\|\boldsymbol{\varphi}_f(n)\right\|_2$ is time varying and can alternatively be written as,

$$\left\|\varphi_f(n)\right\|_2^2 = \varphi^T{}_f(n)\varphi_f(n) = \sum_{i=0}^{M-1} x_f^2(n-i) + \sum_{j=0}^{N-1} y_f^2(n-j), \tag{3.2.66}$$

Note that the bounds for convergence in the mean in (3.2.65) are overly generous due to our linearisation assumption in (3.2.54). In practice decreasing the upper bound by a factor of 10 or so is advised. Often a stable bound for stepsize is chosen for the particular application area on a trial and error (instability) basis.

From (3.2.63) we can see the convergence in the mean for each coefficient error term for the Simplified Gradient adaptive IIR LMS algorithm will be dependent on the eigenvalue spread of the correlation matrix $\mathbf{R}_{\varphi_f\varphi_f}(n)$. The eigenvalue spread for a correlation matrix is defined earlier in (3.1.46). This coupled with the fact the stepsize must be sufficiently small to be very much less than the limits of (3.2.65) for stability in practice, is the main reason why adaptive IIR output error algorithms converge much slower than their FIR counterparts.

Equation (3.2.40) and equation (3.2.52) are specified in a group adaption form where the same stepsize $\mu$ is used to control the adaption of all coefficients in the IIR filter coefficient vector $\boldsymbol{\theta}_n$. We shall see later in the Chapter 5 that homogenous adaption forms will be used due to echo path attenuation [3.16]. A homogenous adaption form uses separate stepsize factors, $\mu_{MA}$ and $\mu_{AR}$, to control adaption of the feedforward and feedback parts of the coefficient vector.

### 3.2.3. The Simplified Gradient NLMS Output Error adaptive IIR algorithm

In the same way the LMS algorithm of (3.1.31) will vary with the power of the input signal $x(n)$ the simplified gradient adaptive IIR LMS algorithm will vary with the power of the information regression vector $\boldsymbol{\varphi}_f(n)$, which comprises both input and output samples. This, like the FIR LMS, presents a problem for choosing a fixed step size $\mu$. By incorporating normalisation into the filter update, proportional to the power of the information vector $\boldsymbol{\varphi}_f(n)$, the filter update can be made independent of input and output signal powers [3.17],[3.18]. For the IIR LMS algorithm of (3.2.52) normalisation by the $l_2$ norm of filtered information vector $\boldsymbol{\varphi}_f(n)$ gives the filter update,

$$\boldsymbol{\theta}_{n+1} = \boldsymbol{\theta}_n + \frac{\mu}{\delta + \varphi_f^T(n)\varphi_f(n)} e_o(n)\varphi_f(n), \tag{3.2.67}$$

where $\delta$ is a small positive constant to prevent division by zero when information vector power is zero. Equation (3.2.67) is called the simplified gradient adaptive IIR Normalised LMS (NLMS) algorithm.

As for the FIR NLMS algorithm, the stepsize normalisation in (3.2.67) effectively gives increased convergence rate performance over the LMS based algorithm of (3.2.52) for the same stepsize parameter $\mu$ without affecting the convergence properties [3.17]. However like the LMS counterpart of (3.2.52) the NLMS adaption form of (3.2.67) will still suffer from the same dependency on the eigenvalue spread of the correlation matrix $\mathbf{R}_{\varphi_f\varphi_f}$.

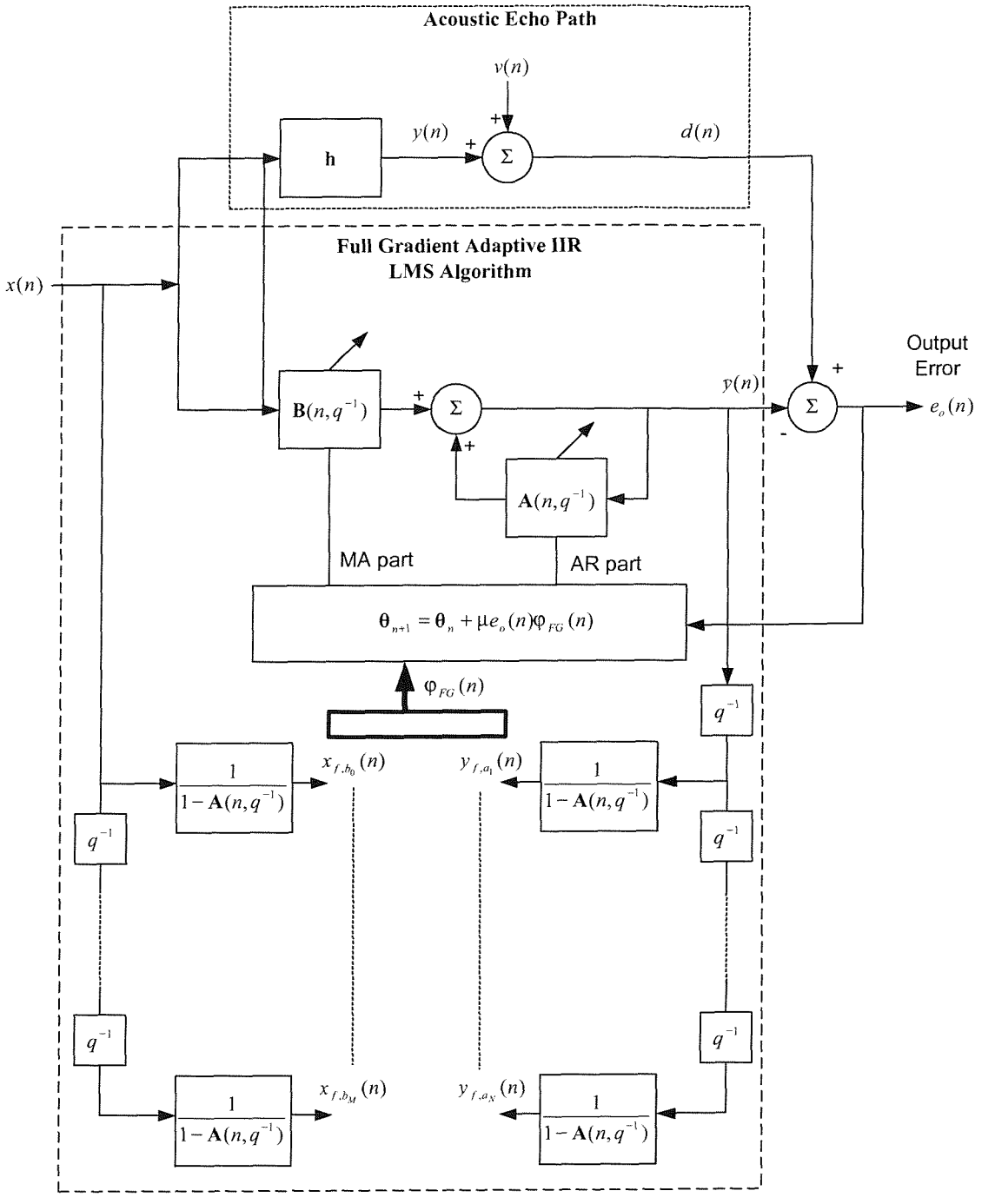


**Figure 3.5 : The Full Gradient Adaptive IIR LMS algorithm structure**

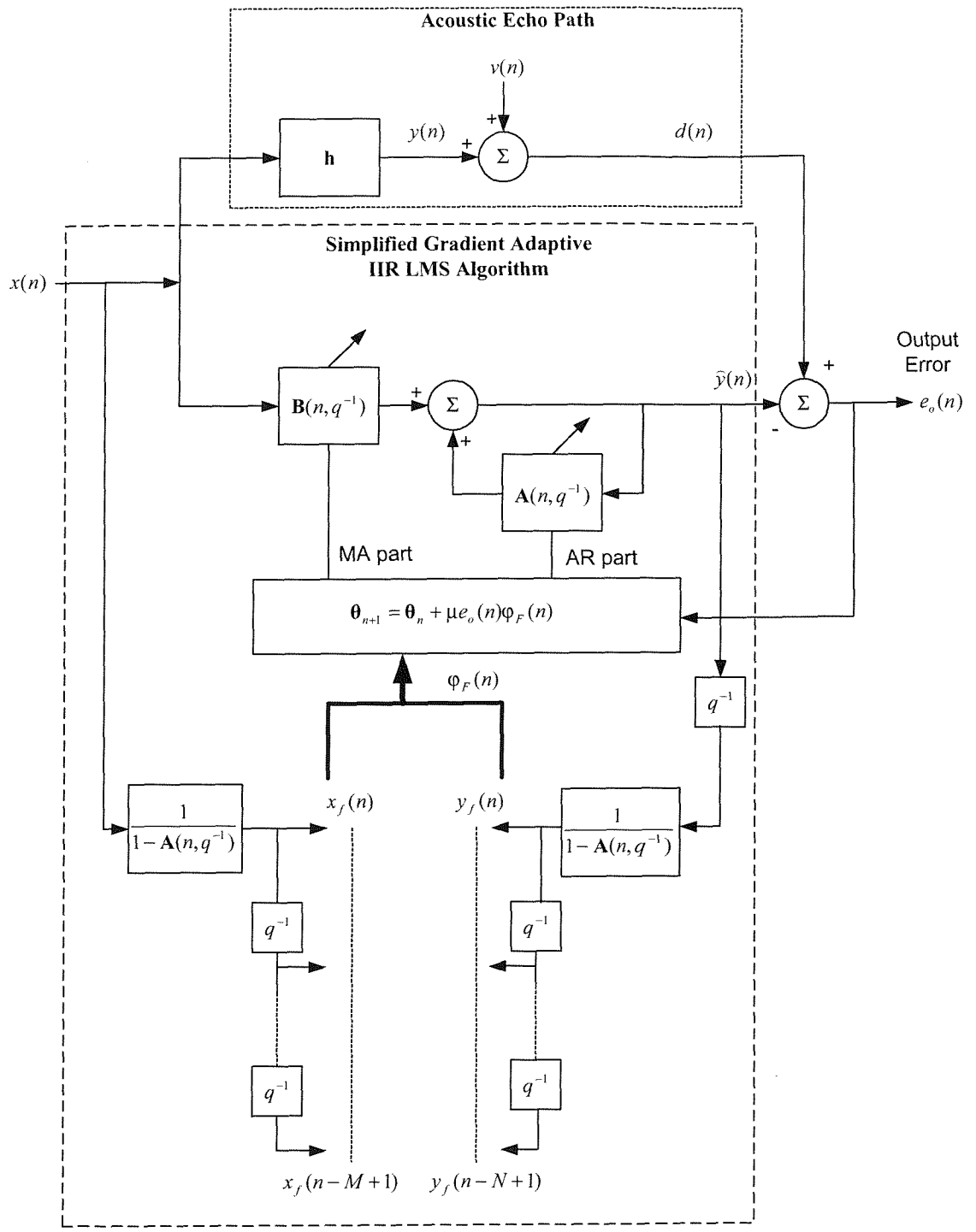


**Figure 3.6 : The Simplified Gradient Adaptive IIR LMS algorithm structure**

The same normalised stepsize $\mu$ is used to control the adaption of all coefficients in the IIR filter coefficient vector $\boldsymbol{\theta}_n$ in equation (3.2.67). In Chapter 5, because of differences in the magnitude of the input and output of the echo path, separate stepsizes will be used for feedforward and feedback coefficients.

### 3.2.4. Newton's method and the Simplified Gradient LMS Newton adaptive IIR algorithm

Mathematically the iterative solution to the recursive normal equations of (3.2.21) using Newton's Method is given by [3.12],

$$\boldsymbol{\theta}_{n+1} = \boldsymbol{\theta}_n - \mathbf{H}^{-1}(\boldsymbol{\theta}_n)\nabla F_n, \tag{3.2.68}$$

where $\mathbf{H}(\boldsymbol{\theta}_n)$ is the Hessian matrix of the mean squared error cost function $F$ of (3.2.11) and is $\mathbf{H}^{-1}(\boldsymbol{\theta}_n)$ its inverse. The Hessian matrix is defined in (3.1.55) as the second derivative of the cost function with respect to the filter coefficients. Using (3.2.26) and the simplification of (3.2.48) the Hessian matrix can be computed as follows,

$$\mathbf{H}(\boldsymbol{\theta}_n) = \frac{\partial^2 F}{\partial \boldsymbol{\theta}_n \partial \boldsymbol{\theta}_n} = \frac{\partial}{\partial \boldsymbol{\theta}_n}[-2E[e_o(n)\nabla \hat{y}(n)]] = \left[-2\frac{\partial \hat{y}(n)}{\partial \boldsymbol{\theta}_n}^T \boldsymbol{\varphi}_f(n)\right], \tag{3.2.69}$$

giving

$$\mathbf{H}(\boldsymbol{\theta}_n) = 2\mathbf{R}_{\varphi_f\varphi_f}, \tag{3.2.70}$$

Substituting (3.2.70) into (3.2.68) we get an equation for the solution to the recursive normal equations using Newton's method as ,

$$\boldsymbol{\theta}_{n+1} = \boldsymbol{\theta}_n - \frac{1}{2}\mathbf{R}^{-1}_{\varphi_f\varphi_f}\nabla F_n. \tag{3.2.71}$$

Comparing (3.2.71) to (3.2.25) we can see that Newton's method can be expected to converge quicker due to the weighting by $\mathbf{R}^{-1}_{\varphi_f\varphi_f}$ which essentially modifies the search direction to point to a minimum (local or global) point on the cost function $F$ [3.19]. In addition this weighting will equalise the eigenvalues of the correlation matrix each direction so each coefficient error term will converge uniformly. Incorporating time dependency into (3.2.71) and using an instantaneous estimate for $\nabla F$ as similarly done for the Simplified Gradient LMS algorithm in (3.2.28) gives,

$$\boldsymbol{\theta}_{n+1} = \boldsymbol{\theta}_n + \mu\hat{\mathbf{R}}^{-1}_{\varphi_f\varphi_f}(n)\boldsymbol{\varphi}_f(n)e(n). \tag{3.2.72}$$

where $\hat{\mathbf{R}}^{-1}_{\varphi_f\varphi_f}(n)$ is an estimate of the inverse of the correlation matrix $\mathbf{R}^{-1}_{\varphi_f\varphi_f}$. Equation (3.2.72) is named the Simplified Gradient LMS Newton adaptive IIR algorithm. It is also termed the Recursive Prediction Error algorithm [3.12]. Like the FIR LMS Newton algorithm of (3.1.58) an update constant $\mu$ has been introduced to allow a greater degree of control of the algorithm since a noisy instantaneous gradient estimate is used.

Using local stationarity assumptions, as done for the Simplified Gradient LMS algorithm earlier in the chapter, bounds on the stepsize can be derived for convergence in the mean of the Simplified Gradient LMS Newton algorithm of (3.2.72). Convergence in the mean about a local minimum point on the cost function $F$ will occur provided,

$$|1-\mu|<1. \tag{3.2.73}$$

or,

$$0<\mu<2. \tag{3.2.74}$$

Like the Simplified Gradient LMS algorithm the bounds of (3.2.74) will be optimistic due to the linearisation assumptions used and in practice the stepsize $\mu$ may have to be much less than the upper limit of (3.2.74) for convergence. We shall see in chapters 5 and 6 the stable range for stepsize $\mu$ for robust Acoustic Echo Cancellation on a mobile handset.

From (3.2.72) we can see the weighting by $\hat{\mathbf{R}}^{-1}_{\varphi_f\varphi_f}(n)$ essentially will ideally make the Simplified Gradient LMS Newton algorithm independent of the eigenvalue spread of the covariance matrix $\hat{\mathbf{R}}_{\varphi_f\varphi_f}(n)$. This is a major advantage of the Simplified Gradient LMS Newton algorithm over the Simplified Gradient LMS and Normalised LMS (NLMS) algorithms of (3.2.52) and (3.2.67) because of their dependence of convergence speed on the eigenvalue spread of the covariance matrix $\hat{\mathbf{R}}_{\varphi_f\varphi_f}(n)$. Since the stepsize $\mu$ has to be sufficiently small for stability, a slower convergence speed may result for the Simplified Gradient LMS and NLMS algorithms for coloured input signals when the eigenvalue spread is greater than unity. However due to the requirement of the computation of an estimate of the inverse covariance matrix $\hat{\mathbf{R}}^{-1}_{\varphi_f\varphi_f}(n)$ every iteration n, the Simplified Gradient LMS Newton algorithm of (3.2.72) has a far higher computational requirement. To reduce complexity of the inverse covariance matrix calculation the same techniques employed for the FIR LMS Newton algorithm can be used. Using the matrix inversion lemma, the inverse covariance estimate $\hat{\mathbf{R}}^{-1}_{\varphi_f\varphi_f}(n)$ may be computed as follows [3.19],

$$\hat{\mathbf{R}}^{-1}_{\varphi_f\varphi_f}(n)=\frac{1}{\lambda}\left(\hat{\mathbf{R}}^{-1}_{\varphi_f\varphi_f}(n-1)-\frac{\hat{\mathbf{R}}^{-1}_{\varphi_f\varphi_f}(n-1)\varphi_f(n)\varphi_f{}^{T}(n)\hat{\mathbf{R}}^{-1}_{\varphi_f\varphi_f}(n-1)}{\frac{\lambda}{\alpha}+\varphi_f{}^{T}(n)\hat{\mathbf{R}}^{-1}_{\varphi_f\varphi_f}(n-1)\varphi_f(n)}\right), \tag{3.2.75}$$

where $\lambda$ is termed the forgetting factor which weights the most recent output errors. This is useful to exclude old data that is less appropriate in non-stationary environments. $\alpha$ is a convergence factor.

Like the FIR LMS Newton algorithm the choice of fixed stepsize $\mu$ in (3.2.72) can be difficult for non-stationary environments and signals where fast time variations can be encountered. Normalisation by $\hat{\mathbf{R}}^{-1}_{\varphi_f\varphi_f}(n)$ in (3.2.72) is ineffective for faster time variations in the input signal. Instead a variable convergence factor $\mu(n)$ can be chosen to minimise a posteriori error as follows [3.8],

$$\mu(n) = \frac{1}{\varphi_f{}^T(n)\hat{\mathbf{R}}^{-1}_{\varphi_f\varphi_f}(n)\varphi_f(n)}. \tag{3.2.76}$$

Introducing (3.2.76)into (3.2.72) we get,

$$\boldsymbol{\theta}_{n+1} = \boldsymbol{\theta}_n + \mu \frac{\hat{\mathbf{R}}^{-1}_{\varphi_f\varphi_f}(n)\varphi_f(n)e(n)}{\varphi_f{}^T(n)\hat{\mathbf{R}}^{-1}_{\varphi_f\varphi_f}(n)\varphi_f(n)}. \tag{3.2.77}$$

Equation (3.2.77) is termed the Simplified Gradient Normalised IIR LMS Newton adaptive IIR algorithm and incorporates an additional reduction factor, $\mu$, like the FIR Normalised LMS Newton algorithm to control convergence speed at the expense of steady state error.

### 3.2.5. The method of Steepest Descent and the Pseudo Linear Regression (PLR) LMS Output Error adaptive IIR algorithm

Consider the equation of the cost function of (3.2.11),

$$F = E[y^2(n)] - 2\boldsymbol{\theta}^T\mathbf{r}_{y\varphi_o} + \boldsymbol{\theta}^T\mathbf{R}_{\varphi_o\varphi_o}\boldsymbol{\theta} + E[v^2(n)], \tag{3.2.11}$$

Feintuch proposed a further simplification of (3.2.52) by assuming the statistics $\mathbf{r}_{d\varphi_o}$, $\mathbf{R}_{xy}$ and $\mathbf{R}_{yy}$ in (3.2.11) are constants with respect to $\boldsymbol{\theta}$, and that previous output samples do not depend on $\boldsymbol{\theta}$. The resulting gradient of the cost function $F$ with respect to the coefficients $b_i$ and $a_j$ may then be written as,

$$\frac{\partial F}{\partial \boldsymbol{\theta}} = -2\mathbf{r}_{y\varphi_o} + 2\mathbf{R}_{\varphi_o\varphi_o}\boldsymbol{\theta} = 0, \tag{3.2.78}$$

This gives the modified optimal solution for a recursive output error filter,

$$\boldsymbol{\theta}_{opt} = \mathbf{R}^{-1}_{\varphi_o\varphi_o}\mathbf{r}_{y\varphi_o}, \tag{3.2.79}$$

Earlier assumptions and equation (3.2.54) implies that the following orthogonality principle holds [3.20],

$$\frac{\partial F}{\partial \boldsymbol{\theta}_n} = -2E[e_o(n)\varphi_o(n)] = 0. \tag{3.2.80}$$

In finding the steepest descent iterative solution to (3.2.79) we use the general iterative solution as follows [3.2],

$$\boldsymbol{\theta}_{n+1} = \boldsymbol{\theta}_n - \frac{\mu}{2}\nabla F_n, \tag{3.2.81}$$

where the gradient of the mean square output error surface $\nabla F_n$ from (3.2.80) can be written as,

$$\nabla F_n = -2E[e_o(n)\varphi_o(n)], \tag{3.2.82}$$

Since $E[e(n)\varphi_o(n)]$ is generally unknown an estimate can be used. In line with the FIR LMS philosophy the gradient $\nabla F_n$ is replaced by an instantaneous estimate,

$$\nabla F_n = -2e_o(n)\varphi_o, \tag{3.2.83}$$

giving the coefficient update,

$$\boldsymbol{\theta}_{n+1} = \boldsymbol{\theta}_n + \mu e_o(n)\varphi_o(n). \tag{3.2.84}$$

Equation (3.2.84) is known as Feintuch's Recursive LMS algorithm or more commonly in system identification and control literature as the Pseudo Linear Regression (PLR) LMS algorithm [3.12],[3.20]. The general structure of the Pseudo Linear Regression algorithm is shown in Figure 3.7.

Despite the mathematically invalidity of the assumptions made by Feintuch [3.21],[3.22], the above algorithm is the most computationally simple output error adaptive IIR algorithm, and does have the tendency to produce a stable IIR adaptive filter. In addition, by comparing (3.2.84) with (3.2.52) we can see the Pseudo Linear Regression algorithm has no AR filtering of the information vector $\varphi_o(n)$. For echo path models with low amounts of feedback, where $\sum_{m=1}^{N} a_m(n)$ is small, then Feintuch's approximation of (3.2.84) may be valid.

It has been shown that for equation (3.2.84) to convergence (to global or local minimum on error mean square surface) the following strict positive real condition should in general be satisfied [3.12], [3.23],[3.24],

$$\mathrm{Re}\left[\frac{1}{1-\mathbf{A}_*(z^{-1})}\right] > 0 \ , |z| = 1, \tag{3.2.85}$$

where Re(u) denotes the real part of u and $1-\mathbf{A}_*(z^{-1})$ denotes the poles of the system to be modelled.

Equation (3.2.85) is derived from Popov's hyperstability theorem [3.23], and implies the poles of the unknown echo path to be modelled must satisfy this hyperstability region to ensure convergence. This hyperstability region is always subset of the stability region within the unit circle of the complex Z domain. Equation (3.2.85) provides a guideline for ensuring convergence of (3.2.59) with a sufficiently small choice of step-size $\mu$. However the algorithm may converge in some cases despite violation of this condition if the adaptive model has sufficient degrees of freedom to approximate the echo path being modelled [3.20],[3.22]. For a stationary input sequence $x(n)$, convergence and stability will be achieved if the stepsize $\mu$ is chosen to be [3.25],

$$\mu \le \frac{1}{\|\varphi_o(n)\|_2^2} \ , \forall n, \tag{3.2.86}$$

where $\|\varphi_o(n)\|_2$ is the $l_2$ norm of information vector $\varphi_o(n)$, and the echo path to be modelled satisfies [3.25],

$$0 < \mathrm{Re}\left[\frac{1}{1-\mathbf{A}_*(z^{-1})}\right] < 2 \ , |z| = 1, \tag{3.2.87}$$

As the echo path to be modelled is generally unknown equation (3.2.87) represents the main drawback of the Pseudo Linear Regression LMS algorithm. Similar to the Simplified Gradient LMS algorithm of (3.2.52), the convergence speed of the Psudo Linear Regression LMS algorithm will be

dependent on eigenvalue spread of the information vector correlation matrix $\mathbf{R}_{\varphi_o\varphi_o}$. The stepsize $\mu$ of (3.2.87) is in practice is normally selected to be very much less than the upper bound of (3.2.86) for stability. Equation (3.2.84) is in a group adaption form, where the same stepsize $\mu$ is used to control the adaption of all coefficients in the IIR filter coefficient vector $\boldsymbol{\theta}_n$. A homogenous form will be used in later chapters to echo path attenuation [3.16].

### 3.2.6. The Pseudo Linear Regression (PLR) NLMS Output Error adaptive IIR algorithm

As already mentioned for the LMS adaptive FIR and Simplified Graident LMS adaptive IIR algorithms, choosing a fixed step size $\alpha$ is a problem when non-stationary signals are used, as the power of the input signal will vary. To overcome this power variation in the input signal $x(n)$ (and the output signal $y(n)$ in the case of output error adaptive IIR algorithms), a normalisation proportional to the power of the information vector $\boldsymbol{\varphi}_o(n)$, can be incorporated into the Pseudo Linear Regression LMS algorithm as follows,

$$\boldsymbol{\theta}_{n+1} = \boldsymbol{\theta}_n + \frac{\mu}{\delta + \boldsymbol{\varphi}_o^T(n)\boldsymbol{\varphi}_o(n)} e_o(n)\boldsymbol{\varphi}_o(n), \tag{3.2.88}$$

where $\delta$ is a small positive constant to prevent division by zero when information vector power is zero. Equation (3.2.88) is termed Pseudo Linear Regression Normalised LMS (NLMS) adaptive IIR algorithm.

From (3.2.88) it can be seen that the stepsize $\mu$ is normalised by the $l_2$ norm of the information vector $\boldsymbol{\varphi}_o(n)$. Despite becoming invariant to input signal power variations the same dependency on the eigenvalue spread of the correlation matrix $\mathbf{R}_{\varphi_o\varphi_o}$ will still exist as for the Pseudo Linear Regression LMS algorithm. As for the Simplified Gradient NLMS algorithm, equation (3.2.88) is in a group adaption form. We will see in later chapters that homogenous adaption forms need to be used for output error LMS based algorithms due to echo path attenatuation.

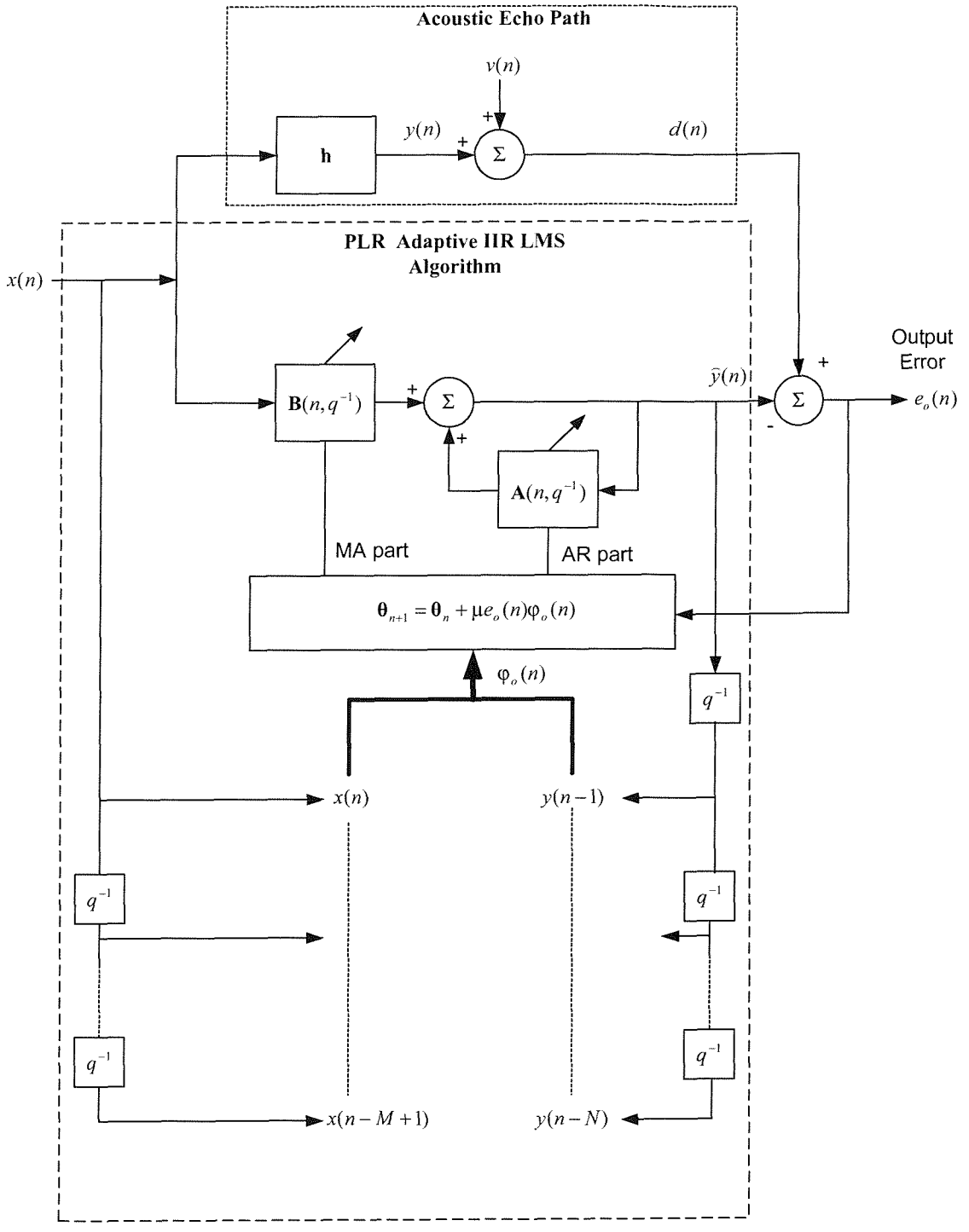


**Figure 3.7 : The Pseudo Linear Regression (PLR) Adaptive IIR LMS algorithm structure**

### 3.2.7. Newton's method and the Pseudo Linear Regression LMS Newton (PLR LMSN) Output Error adaptive IIR algorithm

Mathematically the iterative solution to the recursive normal equations of (3.2.21) using Newton's Method is given by [3.12],

$$\boldsymbol{\theta}_{n+1} = \boldsymbol{\theta}_n - \mathbf{H}^{-1}(\boldsymbol{\theta}_n)\nabla F_n, \tag{3.2.89}$$

where $\mathbf{H}(\boldsymbol{\theta}_n)$ is the Hessian matrix of the mean squared error cost function $F$ of (3.2.11) and is $\mathbf{H}^{-1}(\boldsymbol{\theta}_n)$ its inverse. The Hessian matrix is defined in (3.1.55) as the second derivative of the cost function with respect to the filter coefficients. Using Feintuch's simplifications of (3.2.78) the Hessian matrix can be computed as follows,

$$\mathbf{H}^{-1}(\boldsymbol{\theta}_n) = \frac{\partial^2 F}{\partial \boldsymbol{\theta}_n \partial \boldsymbol{\theta}_n} = \frac{\partial}{\partial \boldsymbol{\theta}_n}\left[-2\mathbf{r}_{d\boldsymbol{\varphi}_o} + 2\mathbf{R}_{\boldsymbol{\varphi}_o\boldsymbol{\varphi}_o}\boldsymbol{\theta}\right], \tag{3.2.90}$$

giving

$$\mathbf{H}(\boldsymbol{\theta}_n) = 2\mathbf{R}_{\boldsymbol{\varphi}_o\boldsymbol{\varphi}_o}, \tag{3.2.91}$$

Substituting (3.2.91) into (3.2.89) we get an equation for the solution to the recursive normal equations using Newton's method as ,

$$\boldsymbol{\theta}_{n+1} = \boldsymbol{\theta}_n - \frac{1}{2}\mathbf{R}^{-1}_{\boldsymbol{\varphi}_o\boldsymbol{\varphi}_o}\nabla F_n. \tag{3.2.92}$$

Comparing (3.2.92) to (3.2.84) we can see that Newton's method can be expected to converge quicker due to the weighting by $\mathbf{R}_{\boldsymbol{\varphi}_o\boldsymbol{\varphi}_o}$ which essentially modifies the search direction to point to a minimum (local or global) point on the cost function $F$ [3.19]. In addition this weighting will equalise the eigenvalues of the correlation matrix each direction so each coefficient error term will converge uniformly. Incorporating time dependency into (3.2.92) and using an instantaneous estimate for $\nabla F$ as similarly done for the Pseudo Linear Regression LMS algorithm in (3.2.83) gives,

$$\boldsymbol{\theta}_{n+1} = \boldsymbol{\theta}_n + \mu\widehat{\mathbf{R}}^{-1}_{\boldsymbol{\varphi}_o\boldsymbol{\varphi}_o}(n)\boldsymbol{\varphi}_o(n)e(n), \tag{3.2.93}$$

where $\widehat{\mathbf{R}}^{-1}_{\boldsymbol{\varphi}_o\boldsymbol{\varphi}_o}(n)$ is an estimate of the inverse of the correlation matrix $\mathbf{R}_{\boldsymbol{\varphi}_o\boldsymbol{\varphi}_o}$. Equation (3.2.93) is named the Pseudo Linear Regression LMS Newton (LMSN) adaptive IIR algorithm. Like the Simplified Gradient LMS Newton algorithm an update constant $\mu$ has been introduced to allow a greater degree of control of the algorithm since a noisy instantaneous gradient estimate is used.

Using similar assumptions to that of the Simplified Gradient LMS Newton algorithm bounds on the stepsize can be derived for convergence in the mean of the Pseudo Linear Regression LMS Newton algorithm of (3.2.93). Convergence in the mean about a local minimum point on the cost function $F$ will occur provided,

$$0 < \mu < 2, \tag{3.2.94}$$

and the echo path to be modelled in general, satisfies the SPR condition of (3.2.87). Like the Pseudo Linear Regression LMS algorithm the upper bounds of (3.2.94) may be too large and in practice the stepsize $\mu$ may have to be much less than for convergence. We shall see in Chapter 5 the stable range for stepsize $\mu$ for Acoustic Echo Cancellation on a mobile handset.

As for the Simplified Gradient LMS Newton algorithm the weighting by $\hat{\mathbf{R}}^{-1}_{\varphi_o\varphi_o}(n)$ will ideally make the Pseudo Linear Regression LMS Newton independent of the eigenvalue spread of the covariance matrix $\hat{\mathbf{R}}_{\varphi_o\varphi_o}(n)$. Using the matrix inversion lemma the inverse covariance estimate $\hat{\mathbf{R}}^{-1}_{\varphi_o\varphi_o}(n)$ may be computed as follows,

$$\hat{\mathbf{R}}^{-1}_{\varphi_o\varphi_o}(n)=\frac{1}{\lambda}\left(\hat{\mathbf{R}}^{-1}_{\varphi_o\varphi_o}(n-1)-\frac{\hat{\mathbf{R}}^{-1}_{\varphi_o\varphi_o}(n-1)\varphi_o(n)\varphi_o{}^T(n)\hat{\mathbf{R}}^{-1}_{\varphi_o\varphi_o}(n-1)}{\frac{\lambda}{\alpha}+\varphi_o{}^T(n)\hat{\mathbf{R}}^{-1}_{\varphi_o\varphi_o}(n-1)\varphi_o(n)}\right), \tag{3.2.95}$$

where $\lambda$ is termed the forgetting factor which weights the most recent output errors. This is useful to exclude old data that is less appropriate in non-stationary environments. $\alpha$ is a convergence factor.

Like the Simplified Gradient LMS Newton algorithm the choice of fixed stepsize $\mu$ in (3.2.93) can be difficult for non-stationary environments and signals. Instead a variable convergence factor $\mu(n)$ is chosen as follows to minimise a posteriori error,

$$\mu(n)=\frac{1}{\varphi_o{}^T(n)\hat{\mathbf{R}}^{-1}_{\varphi_o\varphi_o}(n)\varphi_o(n)}, \tag{3.2.96}$$

Introducing (3.2.96) into (3.2.93) we get ,

$$\boldsymbol{\theta}_{n+1}=\boldsymbol{\theta}_n+\mu\frac{\hat{\mathbf{R}}^{-1}_{\varphi_o\varphi_o}(n)\varphi_o(n)e(n)}{\varphi_o{}^T(n)\hat{\mathbf{R}}^{-1}_{\varphi_o\varphi_o}(n)\varphi_o(n)}, \tag{3.2.97}$$

Equation (3.2.83) is termed the Pseudo Linear Regression Normalised LMS Newton adaptive IIR algorithm, and incorporates an additional reduction factor $\mu$ , like the Simplified Gradient NLMS Newton algorithm, to control convergence speed at the expense of steady state error.

### 3.2.8. The Simplified Hyperstable Adaptive Recursive (SHARF) LMS Output Error Algorithm

In order overcome the convergence problem associated with the SPR conditions of (3.2.85) and (3.2.87) the output error can be filtered by a moving average filter $\mathbf{C}(q^{-1})$ giving the filter update,

$$\boldsymbol{\theta}_{n+1}=\boldsymbol{\theta}_n+\mu e_o(n)\left[1+\mathbf{C}(q^{-1})\right]\varphi_o(n), \tag{3.2.98}$$

Equation (3.2.98) is known as the Filtered Error Pseudo Linear Regression algorithm or more commonly as the SHARF (Simplified Hyperstable Adaptive Recursive Filtering) algorithm [3.12],[3.13],[3.23]. The coefficients $\mathbf{C}(q^{-1})$ are normally fixed throughout adaptation of the filter. The convergence limits of the Pseudo Linear Regression LMS algorithm in (3.2.86) also apply to the SHARF

algorithm of (3.2.98). The structure of the SHARF algorithm is illustrated in Figure 3.8. In Figure 3.8 $\mathbf{C}(q^{-1})$ is defined as a length N+1 MA filter with element one equal to unity ( $c_0 = 1$ ).

The SHARF algorithm by filtering the output error signal essentially expands the SPR region within the unit circle of the z domain to include more echo path coefficient values. However as the coefficients $\mathbf{C}(q^{-1})$ are fixed, like the Pseudo Linear Regression algorithm some knowledge of $1-\mathbf{A}_*(z^{-1})$ is required. As a rule a placement of a zero in the vicinity of each echo path model pole provides a reasonable set of coefficients for $\mathbf{C}(q^{-1})$ to ensure the following SPR (Strict Positive Real) condition is satisfied for the SHARF,

$$\mathrm{Re}\left[\frac{1+\mathbf{C}(z^{-1})}{1-\mathbf{A}_*(z^{-1})}\right]-\gamma > 0 \ , |z|=1, \tag{3.2.99}$$

where $\gamma$ is a scalar constant equal to 1/2 [3.12], [3.23].

We shall see later in Chapter 5 from the SPR (Strict Positive Real) nature of the measured acoustic echo paths for a mobile handset, how the SHARF $\mathbf{C}(q^{-1})$ coefficients are selected.

### 3.2.9. SHARF Normalised LMS Output Error adaptive IIR algorithm

In the same way the Pseudo Linear Regression algorithm is normalised to cope with the variation in input signal powers, the same normalisation can be used on the SHARF LMS algorithm of (3.2.98) giving,

$$\boldsymbol{\theta}_{n+1} = \boldsymbol{\theta}_n + \frac{\mu}{\delta + \boldsymbol{\varphi}_o^T(n)\boldsymbol{\varphi}_o(n)} e_o(n)\left[1+\mathbf{C}(q^{-1})\right]\boldsymbol{\varphi}_o(n), \tag{3.2.100}$$

where $\delta$ is a small positive constant to prevent division by zero when information vector power is zero. Equation (3.2.100) is termed SHARF Normalised LMS (NLMS) adaptive IIR algorithm.

From (3.2.88) it can be seen that the stepsize $\mu$ is normalised by the $l_2$ norm of the information vector $\boldsymbol{\varphi}_o(n)$. Despite becoming invariant to input signal power variations the same dependency on the eigenvalue spread of the correlation matrix $\mathbf{R}_{\varphi_o\varphi_o}$ will still exist as for the both the SHARF and Pseudo Linear Regression LMS algorithms.

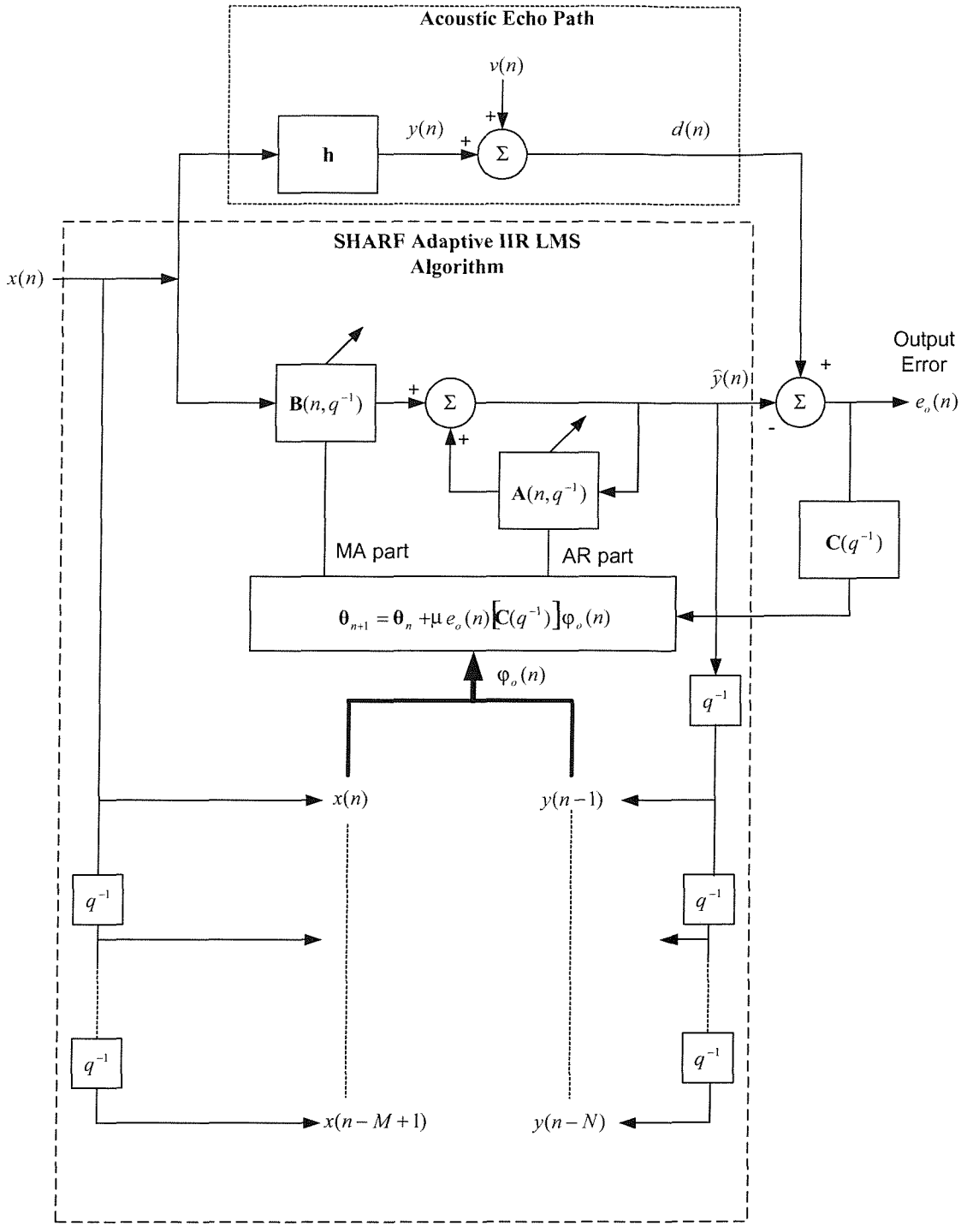


$$C(q^{-1}) = c_0 + c_1 q^{-1} + c_2 q^{-2} + \ldots\ldots + c_N q^{-(N)}, c_o = 1$$

**Figure 3.8 : The SHARF Adaptive IIR LMS algorithm structure**

### 3.2.9.1. The SHARF LMS Newton Output Error adaptive IIR algorithm

Mathematically the iterative solution to the recursive normal equations of (3.2.21) using Newton's Method is given by [3.12],

$$\boldsymbol{\theta}_{n+1} = \boldsymbol{\theta}_n - \mathbf{H}^{-1}(\boldsymbol{\theta}_n)\nabla F_n, \tag{3.2.101}$$

where $\mathbf{H}(\boldsymbol{\theta}_n)$ is the Hessian matrix of the mean squared error cost function $F$ of (3.2.11) and is $\mathbf{H}^{-1}(\boldsymbol{\theta}_n)$ its inverse. Using Feintuch's simplifications of (3.2.78) the Hessian matrix for the SHARf algorithm can be computed as follows,

$$\mathbf{H}^{-1}(\boldsymbol{\theta}_n) = \frac{\partial^2 F}{\partial \boldsymbol{\theta}_n \partial \boldsymbol{\theta}_n} = \frac{\partial}{\partial \boldsymbol{\theta}_n}\left[-2\mathbf{r}_{d\boldsymbol{\varphi}_o} + 2\mathbf{R}_{\boldsymbol{\varphi}_o\boldsymbol{\varphi}_o}\boldsymbol{\theta}\right], \tag{3.2.102}$$

giving

$$\mathbf{H}(\boldsymbol{\theta}_n) = 2\mathbf{R}_{\boldsymbol{\varphi}_o\boldsymbol{\varphi}_o}, \tag{3.2.103}$$

Substituting (3.2.103) into (3.2.101) we get an equation for the solution to the recursive normal equations using Newton's method as ,

$$\boldsymbol{\theta}_{n+1} = \boldsymbol{\theta}_n - \frac{1}{2}\mathbf{R}^{-1}_{\boldsymbol{\varphi}_o\boldsymbol{\varphi}_o}\nabla F_n. \tag{3.2.104}$$

Incorporating time dependency into (3.2.104) and using an instantaneous estimate for $\nabla F$ gives,

$$\boldsymbol{\theta}_{n+1} = \boldsymbol{\theta}_n + \mu\hat{\mathbf{R}}^{-1}_{\boldsymbol{\varphi}_o\boldsymbol{\varphi}_o}(n)e_o(n)\left[1 + \mathbf{C}(q^{-1})\right]\boldsymbol{\varphi}_o(n), \tag{3.2.105}$$

where $\hat{\mathbf{R}}^{-1}_{\boldsymbol{\varphi}_o\boldsymbol{\varphi}_o}(n)$ is an estimate of the inverse of the correlation matrix $\mathbf{R}_{\boldsymbol{\varphi}_o\boldsymbol{\varphi}_o}$. Equation (3.2.105) shall be termed the SHARF LMS Newton adaptive IIR algorithm. The coefficients $\mathbf{C}(q^{-1})$ like the SHARF LMS algorithm of (3.2.98) are normally fixed throughout adaptation of the filter. The convergence limits of (3.2.94) and SPR condition of (3.2.99) also apply to the SHARF LMS Newton algorithm. Like the PLR LMS Newton algorithm, the choice of fixed stepsize $\mu$ in (3.2.105) can be difficult for non-stationary environments and signals. Instead a variable convergence factor $\mu(n)$ as can be chosen to minimise a posteriori error giving,

$$\boldsymbol{\theta}_{n+1} = \boldsymbol{\theta}_n + \mu\frac{\hat{\mathbf{R}}^{-1}_{\boldsymbol{\varphi}_o\boldsymbol{\varphi}_o}(n)\boldsymbol{\varphi}_o(n)\left[1 + \mathbf{C}(q^{-1})\right]e_o(n)}{\boldsymbol{\varphi}_o{}^T(n)\hat{\mathbf{R}}^{-1}_{\boldsymbol{\varphi}_o\boldsymbol{\varphi}_o}(n)\boldsymbol{\varphi}_o(n)}, \tag{3.2.106}$$

Equation (3.2.106) is termed the SHARF Normalised LMS Newton algorithm, and incorporates an additional reduction factor, $\mu$ , like the PLR Normalised LMS Newton algorithm to control convergence speed at the expense of steady state error.

## 3.3. Equation Error Adaptive IIR Filtering

This section describes the most common adaptive IIR filtering algorithms based on the equation error formulation [3.4][3.12].

### 3.3.1. The Optimal Equation Error IIR Filter

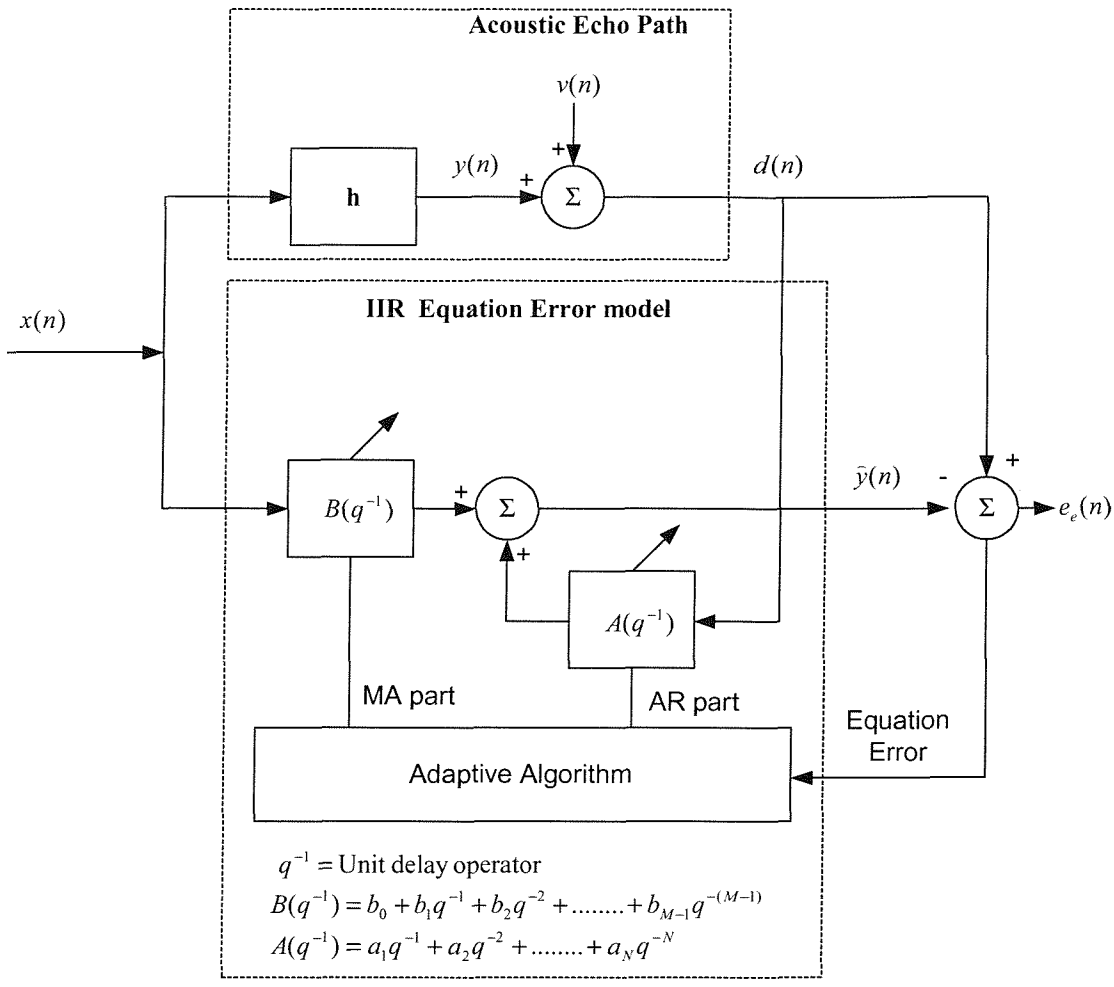


**Figure 3.9 : System Identification of echo path using an equation error adaptive IIR filter**

The same echo path model described by equation (3.1.1) and (3.1.2) is used for the unknown echo path to be modelled. Like the output error IIR filter to cancel the echo signal $d(n)$, a replica of the echo path output $y(n)$, denoted $\hat{y}(n)$, must be created by the IIR equation error filter which models the echo path transfer function and subtracted from $d(n)$. For a fixed time invariant equation error IIR filter model of order (M, N), the output $\hat{y}(n)$ becomes,

$$\hat{y}(n) = \mathbf{B}(q^{-1})x(n) + \mathbf{A}(q^{-1})d(n) = \sum_{i=0}^{M-1} b_i x(n-i) + \sum_{j=1}^{N} a_j d(n-j), \tag{3.3.1}$$

Re-writing (3.3.1) in more compact notation using vector notation we get,

$$\hat{y}(n) = \boldsymbol{\theta}^T \boldsymbol{\varphi}_e, \tag{3.3.2}$$

where $\boldsymbol{\theta}$ is the (M+N) x 1 coefficient vector as defined in (3.2.3) and $\boldsymbol{\varphi}_o$ is a (M+N) x 1 information regression vector defined as:

$$\boldsymbol{\varphi}_e = [x(n),...,x(n-M+1),d(n-1),...,d(n-N)]^T = [\mathbf{x}(n)^T, \mathbf{d}(n-1)^T]^T, \quad (3.3.3)$$

where $\mathbf{x}(n)$ is a Mx1 vector of echo path input samples defined in (3.2.5) and $\mathbf{d}(n-1)$ is a Nx1 vector echo path output samples defined as:

$$\mathbf{d}(n-1) = [d(n-1),.....,d(n-N)]^T, \quad (3.3.4)$$

From equation (3.3.2) we can see the filter output is a linear function of the coefficients $\boldsymbol{\theta}$ as it depends on signals $x(n)$ and $d(n)$ only, which do not depend on previous coefficient values. Equation (3.3.2) is often termed a linear regression [3.12]. Consider the equation error signal $e_e(n)$,

$$e_e(n) = d(n) - \hat{y}(n) = d(n) - \boldsymbol{\theta}^T \boldsymbol{\varphi}_e = d(n) - \sum_{j=1}^{N} a_j d(n-j) - \sum_{i=0}^{M-1} b_i x(n-i), \quad (3.3.5)$$

Re-writing (3.3.5) we get [3.12],

$$e_e(n) = [1 - \mathbf{A}(q^{-1})]d(n) - \mathbf{B}(q^{-1})x(n). \quad (3.3.6)$$

From (3.3.6) we can see the reason for terming the IIR model of (3.3.2) an equation error IIR filter model, as the error signal, $e_e(n)$, is generated by subtracting two difference equations: $[1 - \mathbf{A}(q^{-1})]d(n)$ and $\mathbf{B}(q^{-1})x(n)$. Since the coefficients $a_j$ of the equation error model are adjusted in response to delayed samples of the desired response $d(n)$, which does not depend on the filter output $\hat{y}(n)$, the error signal of (3.3.6) is a linear function of the filter coefficients $b_i$ and $a_j$. In the case of no output noise $v(n)$ we get an true IIR filter structure, otherwise the equation error IIR adaptive filter can be interpreted as two FIR filters $\mathbf{B}(q^{-1})$ and $\mathbf{A}(q^{-1})$. As long as FIR filter $\mathbf{A}(q^{-1})$ remains minimum phase the filter output of (3.3.2) will remain stable [3.13]. Comparing equation (3.3.6) to (3.2.7) we can define a relationship between the equation error and output error as [3.12],[3.26],

$$e_e(n) = [1 - \mathbf{A}(q^{-1})]e_o(n). \quad (3.3.7)$$

For a minimum equation error signal the fixed equation error IIR filter coefficients must be chosen to minimise some cost function. Like we have already seen for the optimal FIR and output error IIR filter models the cost function normally used in system identification theory is the minimisation of the mean square error. Consider now the design of an equation error IIR filter model of order (M,N) to minimise the mean square equation error. The cost function $F$ to be minimised is denoted as,

$$F = E[e_e^2(n)]. \quad (3.3.8)$$

Rewriting (3.3.8) using (3.3.6) and (3.3.2) we get an equation for the cost function $F$ in terms of the filter coefficient vector $\boldsymbol{\theta}$, which is termed the Mean Square Equation Error (MSEE) surface, as follows [3.4],[3.13],[3.26],

$$F = E[e_e^{\,2}(n)] = E\left[\left(d(n) - \boldsymbol{\theta}^T \boldsymbol{\varphi}_e\right)^2\right]. \tag{3.3.9}$$

Re-writing (3.3.10) we get,

$$F = E[d^2(n)] - 2\boldsymbol{\theta}^T \mathbf{r}_{d\varphi} + \boldsymbol{\theta}^T \mathbf{R}_{\varphi_e\varphi_e} \boldsymbol{\theta}. \tag{3.3.10}$$

Where $\mathbf{R}_{\varphi_e\varphi_e}$ is a (M+N) x (M+N) covariance matrix defined as [21]:

$$\mathbf{R}_{\varphi_e\varphi_e} = E[\boldsymbol{\varphi}_e \boldsymbol{\varphi}_e^{\,T}] = \begin{bmatrix} \mathbf{R}_{xx} & \mathbf{R}_{xd} \\ \mathbf{R}_{xd}^T & \mathbf{R}_{dd} \end{bmatrix}. \tag{3.3.11}$$

And $\mathbf{r}_{d\varphi}$ is a cross correlation vector defined as:

$$\mathbf{r}_{d\varphi} = E[d(n)\boldsymbol{\varphi}_e(n)], \tag{3.3.12}$$

with:

$$\mathbf{R}_{xd} = \text{M x N cross correlation matrix } E[\mathbf{x}(n)\mathbf{d}^T(n)], \tag{3.3.13}$$

$$\mathbf{R}_{dd} = \text{N x N autocorrelation matrix } E[\mathbf{d}(n)\mathbf{d}^T(n)], \tag{3.3.14}$$

From (3.3.10) we can clearly see that the Mean Square Equation Error (MSEE) surface for the equation error IIR filter model, like the FIR filter model, is a quadratic function of the filter coefficients $b_i$ and. As a result a single global minimum will exist in $F$ with respect to $\boldsymbol{\theta}$, with no local minima. The same techniques used for the selection of optimal coefficients for the FIR filter model described earlier applies here. To minimise this cost function $F$ of (3.3.8) with respect to the filter coefficient vector $\boldsymbol{\theta}$, differentiate F in (3.3.9) with respect to $\boldsymbol{\theta}$ and equate to zero. This yields,

$$\frac{\partial F}{\partial \boldsymbol{\theta}} = -\mathbf{r}_{d\varphi_e} + \mathbf{R}_{\varphi_e\varphi_e}\boldsymbol{\theta} = \mathbf{0}, \tag{3.3.15}$$

giving,

$$\mathbf{R}_{\varphi_e\varphi_e}\boldsymbol{\theta} = \mathbf{r}_{d\varphi_e}. \tag{3.3.16}$$

Equation (3.3.16) represents the equation error recursive form of the normal equations of (3.1.15). Like the FIR model equation (3.3.16) requires the orthogonality of the input regression vector and the equation error signal. Using (3.3.2), (3.3.8) and (3.3.15) this gives,

$$\frac{\partial F}{\partial \boldsymbol{\theta}} = \frac{\partial E[e_e^2(n)]}{\partial \boldsymbol{\theta}} = -2E[e_e(n)\frac{\partial e_e(n)}{\partial \boldsymbol{\theta}}] = -2E[e_e(n)\boldsymbol{\varphi}_e]. \tag{3.3.17}$$

The optimal least squares filter coefficients selected to minimise the mean square equation error (MSEE) are found by solving (3.3.16) for $\boldsymbol{\theta}$ as follows,

$$\boldsymbol{\theta}_{opt} = \mathbf{R}_{\varphi_e\varphi_e}^{\,-1}\mathbf{r}_{d\varphi_e}. \tag{3.3.18}$$

Equation (3.3.18) is the solution to the problem of designing a linear time invariant equation error IIR model to minimise the mean square equation error (MSEE) for wide sense stationary input signals.

From equation (3.3.18) we can see the selection of equation error IIR model coefficients $\boldsymbol{\theta}_{opt}$ to minimise the mean square estimation error (MSE) involves a direct matrix inversion.

### 3.3.2. Bias in the Equation Error Adaptive IIR Formulation

Despite the advantages of the quadratic Equation Error cost function in (3.3.10), the equation error formulation of an IIR filter model suffers from a bias problem. Re-writing (3.3.9) using (3.3.6) and Parseval's theorem to be in the same form as the output error IIR filter model in (3.2.24), we get [3.13],

$$F = \frac{1}{2\pi}\int_{-2\pi}^{2\pi} S_{xx}(e^{j\omega})\left|[1-A(e^{j\omega})][H(e^{j\omega})-B(e^{j\omega})]\right|^2 d\omega + \frac{1}{2\pi}\int_{-2\pi}^{2\pi} S_{vv}(e^{j\omega})\left|1-A(e^{j\omega})\right|^2 d\omega \qquad (3.3.19)$$

Comparing the equation error cost function to minimised in (3.3.19) to the output error cost function of (3.2.24) we can see unlike the output error model the minimisation of (3.3.19) due to the second term on the RHS of (3.3.19) will give a bias in the estimated pole vector. To see the effects of this bias more clearly from the optimal solution consider the sufficient order system identification case where the output $y(n)$ for an unknown IIR system of order (M,N) is to be modelled by an equation error IIR model of order (M,N) as shown in Figure 3.10 below.

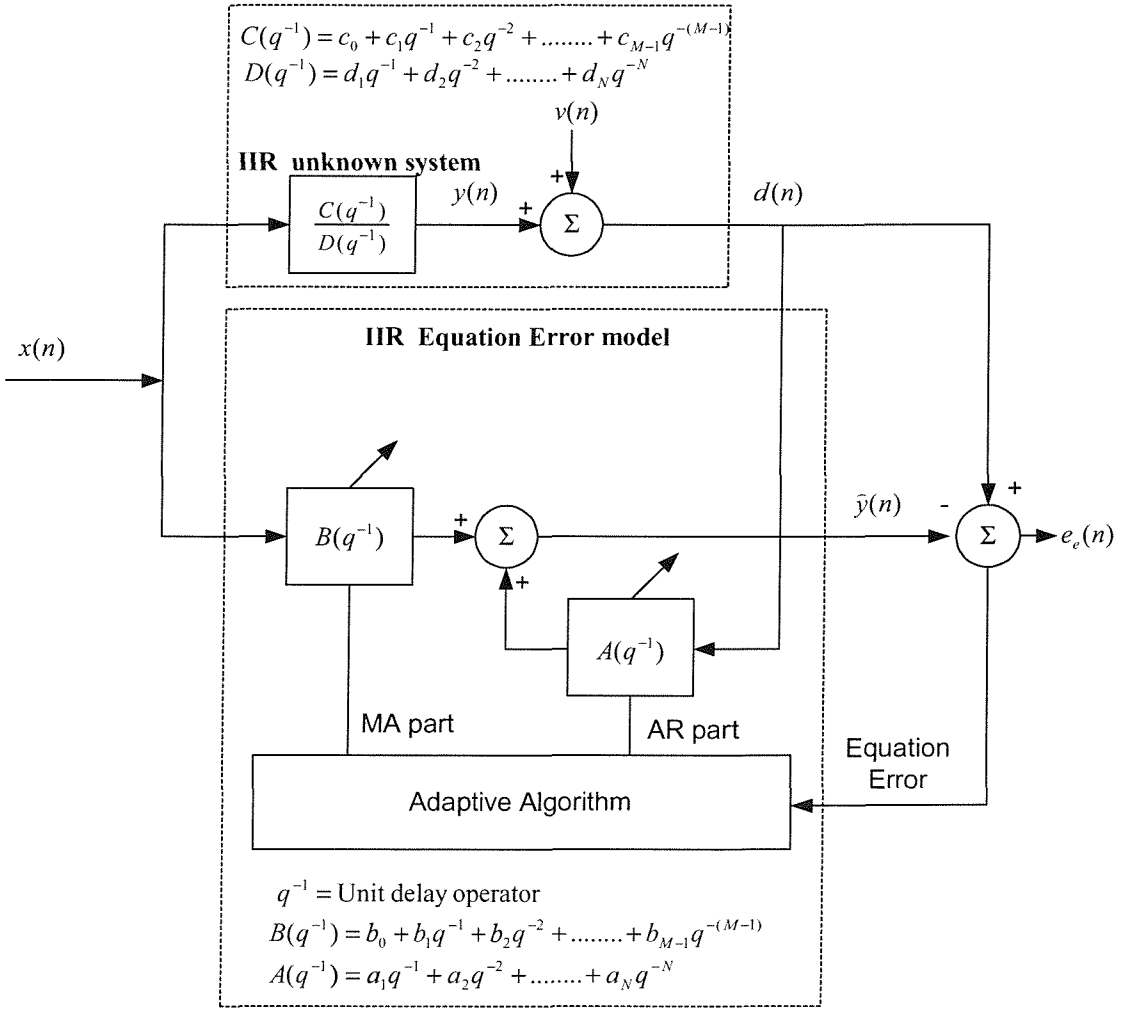


**Figure 3.10 : System Identification of IIR system using an equation error adaptive IIR filter**

The output of system $d(n)$ input to the equation error model is corrupted by a disturbance signal $v(n)$ that is independent of the input signal $x(n)$ giving,

$$d(n) = y(n) + v(n), \tag{3.3.20}$$

where $y(n)$ is the true system output to be modelled by the equation error IIR filter model. Rewriting the cost function of (3.3.10) using (3.3.20) to show more clearly the effects of the noise bias we get [3.26],[3.27],

$$F = E[y^2(n)] - 2\boldsymbol{\theta}^T\left[\begin{bmatrix}\mathbf{0}\\ \mathbf{r}_{vv}\end{bmatrix} - \mathbf{r}_{y\varphi_*}\right] + \boldsymbol{\theta}^T\left[\mathbf{R}_{\varphi_*\varphi_*} + E\begin{bmatrix}\mathbf{0} & \mathbf{0}\\ \mathbf{0} & \mathbf{R}_{vv}\end{bmatrix}\right]\boldsymbol{\theta} + E[v^2(n)], \tag{3.3.21}$$

where $\mathbf{v}(n)$ is a Nx1 vector of noise samples defined as:

$$\mathbf{v}(n) = [v(n-1),.....,v(n-N)]^T, \tag{3.3.22}$$

and $\varphi_*$ is the information vector of the IIR system to be modelled defined as:

$$\varphi_* = [x(n),...,x(n-M+1), y(n-1),..., y(n-N)]^T, \tag{3.3.23}$$

with:

$$\mathbf{r}_{vv} = \text{N x N cross correlation vector } E[v(n)\mathbf{v}(n)], \tag{3.3.24}$$

$$\mathbf{R}_{vv} = \text{N x N autocorrelation matrix } E[\mathbf{v}(n)\mathbf{v}^T(n)], \tag{3.3.25}$$

Comparing (3.3.21) with (3.3.10) and (3.3.11), we see that the disturbance signal $v(n)$ introduces additional bias to the cross correlation vector $\mathbf{r}_{d\varphi}$ and matrix $\mathbf{R}_{dd}$. This is a consequence of using the desired signal $d(n)$ in the feedback path of the equation error filter model which my corrupted by additive noise. To see the effects of this bias in the equation error cost function consider firstly the case where there is no disturbance noise at the output of the echo path to be identified. In this case $d(n) = y(n)$ and the cost function of (3.3.21) becomes,

$$F = E[y^2(n)] - 2\boldsymbol{\theta}^T\mathbf{r}_{y\varphi_*} + \boldsymbol{\theta}^T\mathbf{R}_{\varphi_*\varphi_*}\boldsymbol{\theta}. \tag{3.3.26}$$

For the noiseless case the optimum filter coefficients, $\boldsymbol{\theta}_{opt}$, may then be found by differentiating (3.3.26) with respect to $\boldsymbol{\theta}$ and equating to zero, which gives,

$$\boldsymbol{\theta}_{opt} = \mathbf{R}_{\varphi_*\varphi_*}^{-1}\mathbf{r}_{y\varphi_*}. \tag{3.3.27}$$

Considering now the case where the disturbance term $v(n)$ is not zero, the optimum solution $\boldsymbol{\theta}_{opt}$ found by differentiating (3.3.21)with respect to $\boldsymbol{\theta}$ and setting the result to zero giving,

$$\boldsymbol{\theta}_{opt} = \left[\mathbf{R}_{\varphi_*\varphi_*} + \begin{bmatrix}\mathbf{0} & \mathbf{0}\\ \mathbf{0} & \mathbf{R}_{vv}\end{bmatrix}\right]^{-1}\left[\mathbf{r}_{y\varphi_*} - \begin{bmatrix}\mathbf{0}\\ \mathbf{r}_{vv}\end{bmatrix}\right]. \tag{3.3.28}$$

Comparing (3.3.27) and (3.3.28) we can see that the optimum Wiener solution in the presence of a disturbance signal $v(n)$ at the output of the echo path, would attempt to select the $a_j$ coefficients in $\boldsymbol{\theta}_{opt}$ to both minimise the noise variance of $v(n)$ and to identify the poles of the echo path. This results in a bias in feedback coefficients $a_j$ of the optimum coefficient vector solution $\boldsymbol{\theta}_{opt}$. For a special case where the noise process $v(n)$ is white, with variance $\sigma_v^2$, we get [3.26],

$$\boldsymbol{\theta}_{opt} = \left[\mathbf{R}_{\varphi_*\varphi_*} + \begin{bmatrix} \mathbf{0} & \mathbf{0} \\ \mathbf{0} & \sigma_v^2\mathbf{I} \end{bmatrix}\right]^{-1} \left[\mathbf{r}_{y\varphi_*}\right]. \tag{3.3.29}$$

From (3.3.29) it can be seen that when $v(n)$ is white, a constant offset term is produced for the each AR coefficient, allowing any bias to be more simply compensated for. However as $v(n)$ in general is coloured a constant offset term will not be present since $\mathbf{R}_{vv}$ will no longer be identity in form. The disturbance noise signal $v(n)$ may be more widely interpreted to include, not only any disturbances picked up on the handset microphone at the output of the echo path, but also undermodelling noise. This undermodelling would be caused by the equation error IIR model order being lower than the order of the echo path to be modelled [3.29].

Like the optimal FIR solution of (3.1.18) a direct solution of the optimal equation error solution in equation (3.3.18) is impractical due to the difficulty and high computational complexity involved in constructing and inverting the auto covariance matrix $\mathbf{R}_{\varphi_e\varphi_e}$. A more practical solution is the development of iterative solutions to the normal equations of (3.3.16), which will continuously track changes in the optimal solution of (3.3.18) as each new data samples becomes available.

### 3.3.3. The Equation Error LMS (EELMS) adaptive algorithm

As was similarly done for the FIR LMS algorithm earlier in the chapter the steepest descent update for the iterative solution to the recursive normal equations of (3.3.16) is given by,

$$\boldsymbol{\theta}_{n+1} = \boldsymbol{\theta}_n - \frac{\mu}{2}\nabla F_n, \tag{3.3.30}$$

where $\mu$ is a step size parameter to control the size of change in $\theta_{n+1}$ from $\theta_n$. The gradient of the mean square equation error surface $\nabla F_n$ using (3.3.16) and (3.3.17) can be written as,

$$\nabla F_n = -2E\left[e_e(n)\varphi_e(n)\right], \tag{3.3.31}$$

giving the iteration,

$$\boldsymbol{\theta}_{n+1} = \boldsymbol{\theta}_n + \mu E\left[e_e(n)\varphi_e(n)\right]. \tag{3.3.32}$$

Since $E\left[e_e(n)\varphi_e(n)\right]$ is generally unknown an estimate can be used. In line with the FIR LMS philosophy used earlier in the chapter the gradient $\nabla F_n$ is replaced by an instantaneous estimate,

$$\nabla \hat{F}_n = \frac{\partial e_e^2(n)}{\partial \boldsymbol{\theta}_n}, \tag{3.3.33}$$

where,

$$\frac{\partial e_e^2(n)}{\partial \boldsymbol{\theta}_n} = -2\varphi_e(n)e_e(n), \tag{3.3.34}$$

giving the coefficient update,

$$\boldsymbol{\theta}_{n+1} = \boldsymbol{\theta}_n + \mu\varphi_e(n)e_e(n), \tag{3.3.35}$$

Equation (3.3.35) is known as the Equation Error LMS (EELMS) adaptive IIR algorithm[3.4],[3.13],[3.26]. The weight vector $\boldsymbol{\theta}_n$ is altered only by a small amount $\mu$ in order to ensure that the new weight vector is influenced by all previous error values and not just $e_e(n)$. This ensures the weight vector will converge to the optimal weight vector solution without excessive random wandering. The structure of the Equation Error Adaptive IIR algorithm is shown in Figure 3.11.

Consider the convergence of the EELMS algorithm in the mean. As done for the FIR LMS algorithm if we define a coefficient error vector $\boldsymbol{\varepsilon}_n$ which represents the difference between each element of the filter coefficient vector $\boldsymbol{\theta}_n$ and the optimal solution $\boldsymbol{\theta}_{opt}$ of (3.3.16) we get [3.26],

$$\boldsymbol{\varepsilon}_{n+1} = \left(\mathbf{I} - \mu\mathbf{R}_{\varphi_e\varphi_e}\right)\boldsymbol{\varepsilon}_n, \tag{3.3.36}$$

Consequently each coefficient error term j of $\boldsymbol{\varepsilon}_n$ will decay to zero provided that,

$$\left|(1-\mu\lambda_j)\right| < 1, \tag{3.3.37}$$

where $\lambda_j$ is the $j^{\text{th}}$ eigenvalue of covariance matrix $\mathbf{R}_{\varphi_e\varphi_e}$. From (3.3.37) the Equation Error LMS algorithm will converge in the mean provided that input is persistently exciting and the eigenvalues of covariance matrix $\mathbf{R}_{\varphi_e\varphi_e}$ have a magnitude less than unity. For a positive definite matrix $\mathbf{R}_{\varphi_e\varphi_e}$ the Equation Error LMS algorithm will converge in the mean provided that,

$$0 < \mu < \frac{2}{\lambda_{\max}}, \tag{3.3.38}$$

where $\lambda_{\max}$ is the maximum eigenvalue of covariance matrix $\mathbf{R}_{\varphi_e\varphi_e}$. For a positive semidefinite matrix $\mathbf{R}_{\varphi_e\varphi_e}$ that has Toeplitz form, the trace of the covariance matrix $\mathbf{R}_{\varphi_e\varphi_e}$ can be used for the upper bound of (3.3.38) in a similar fashion to what was done for the FIR algorithm. Due to the Teoplitz form of $\mathbf{R}_{\varphi_e\varphi_e}$ the upper bound of (3.3.38) can be reduced further to,

$$0 < \mu < \frac{2}{\left\|\varphi_e(n)\right\|_2}, \tag{3.3.39}$$

where $\left\|\varphi_e(n)\right\|_2$ is the $l_2$ norm of information vector $\varphi_e(n)$ which can be written as,

$$\left\|\varphi_e(n)\right\|_2 = \sum_{i=0}^{M-1} x^2(n-i) + \sum_{j=1}^{N} d^2(n-j), \tag{3.3.40}$$

From (3.3.37) we can see the convergence in the mean for each coefficient error term for the Equation Error LMS algorithm will be dependent on the eigenvalue spread of the covariance matrix $\mathbf{R}_{\varphi_e\varphi_e}$. The eigenvalue spread was defined earlier in (3.1.47).

Equation (3.3.35) is specified in a group adaption form where the same stepsize $\mu$ is used to control the adaption of all coefficients in the IIR filter coefficient vector $\boldsymbol{\theta}_n$. We shall see later in the Chapter 5 that homogenous adaption forms will be used due to echo path attenuation [3.16]. A homogenous adaption form uses separate stepsize factors, $\mu_b$ and $\mu_a$, to control adaption of the MA and AR parts of the coefficient vector.

### 3.3.4. Normalised LMS Equation Error adaptive IIR algorithms

In the same way the output error LMS algorithms will vary with the power of the information regression vector $\boldsymbol{\varphi}_o(n)$ or $\boldsymbol{\varphi}_f(n)$, the Equation Error adaptive IIR LMS algorithm will vary with the power of the information regression vector $\boldsymbol{\varphi}_e(n)$. This presents a problem for choosing a fixed step size $\mu$ for the Equation Error LMS algorithm. By incorporating normalisation into the filter update, proportional to the power of the information vector $\boldsymbol{\varphi}_e(n)$, the filter update can be made independent of input and output signal powers [3.30][3.31]. For the Equation Error LMS algorithm, normalisation by the $l_2$ norm of information vector $\boldsymbol{\varphi}_e(n)$ gives the filter update,

$$\boldsymbol{\theta}_{n+1} = \boldsymbol{\theta}_n + \frac{\mu}{\delta + \boldsymbol{\varphi}_e^T(n)\boldsymbol{\varphi}_e(n)} e_e(n)\boldsymbol{\varphi}_e(n), \tag{3.3.41}$$

where $\delta$ is a small positive constant to prevent division by zero when information vector power is zero. Equation (3.3.41) is called the Equation Error Normalised LMS (NLMS) algorithm. Like the other NLMS algorithms seen so far, the Equation Error NLMS algorithm will still suffer from the same dependency on the eigenvalue spread of the correlation matrix, $\mathbf{R}_{\varphi_e\varphi_e}$. Equation (3.3.41) is in group adaption form.

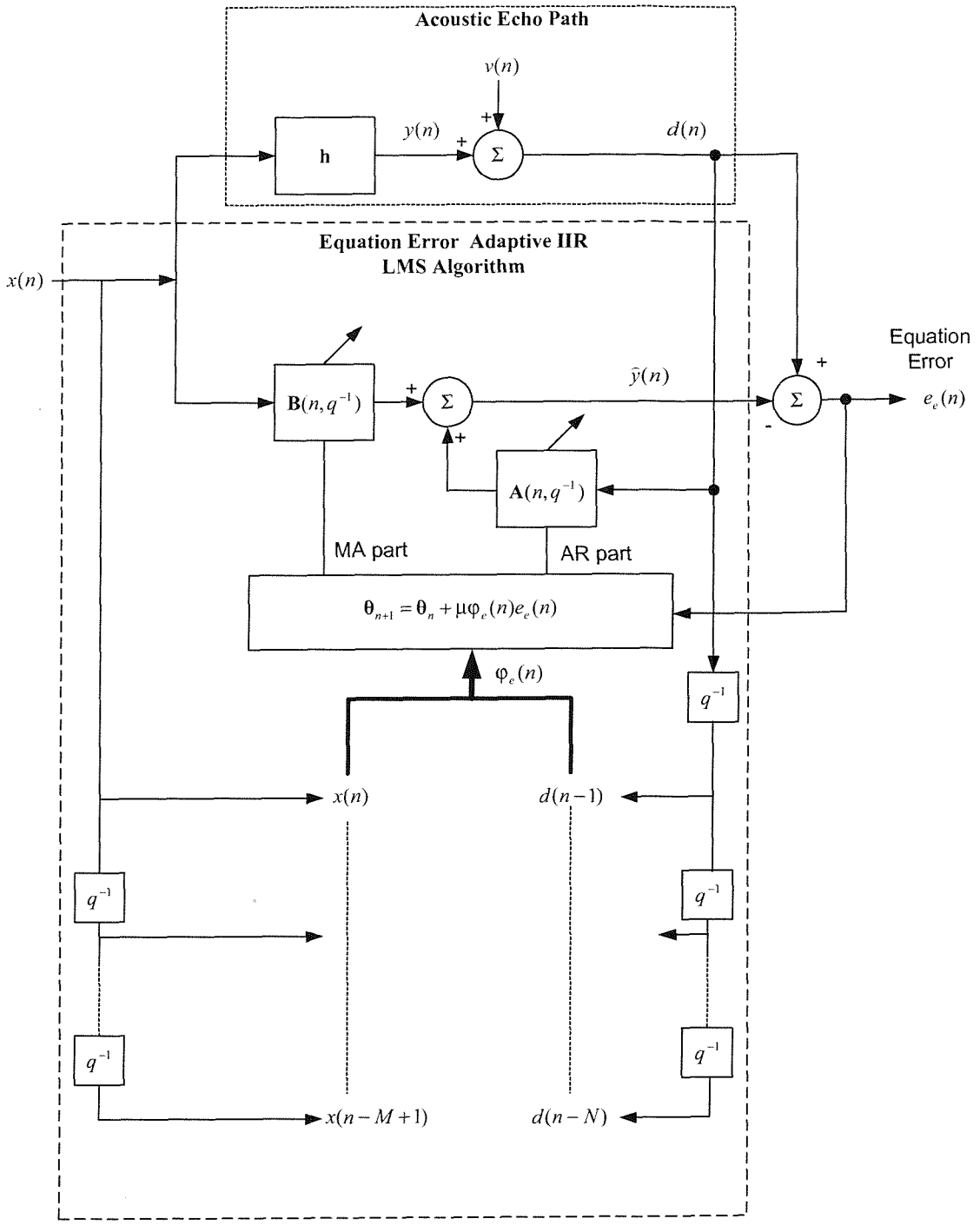


**Figure 3.11 : The structure of the Equation Error LMS adaptive IIR algorithm.**

### 3.3.5. Newton's method and the Equation Error LMS Newton adaptive IIR algorithm

Using the iterative solution to the recursive normal equations of (3.3.16) using Newton's Method gives,

$$\boldsymbol{\theta}_{n+1} = \boldsymbol{\theta}_n - \mu \mathbf{H}^{-1}(\boldsymbol{\theta}_n)\nabla F_n, \tag{3.3.42}$$

where $\mathbf{H}(\boldsymbol{\theta}_n)$ is the Hessian matrix of the mean squared error cost function $F$ of (3.3.10), and $\mathbf{H}^{-1}(\boldsymbol{\theta}_n)$ is its inverse. As we have discussed already the Hessain matrix defined in (3.1.55) is the second derivative of the cost function with respect to the filter coefficients. Using (3.3.10) the Hessain matrix for the equation error formulation can be computed as follows,

$$\mathbf{H}(\boldsymbol{\theta}_n) = \frac{\partial^2 F}{\partial \boldsymbol{\theta}_n \partial \boldsymbol{\theta}_n} = \frac{\partial}{\partial \boldsymbol{\theta}_n} 2E[-r_{y\varphi_e} + \mathbf{R}_{\varphi_e\varphi_e}\boldsymbol{\theta}], \tag{3.3.43}$$

giving,

$$\mathbf{H}(\boldsymbol{\theta}_n) = 2\mathbf{R}_{\varphi_e\varphi_e}, \tag{3.3.44}$$

Substituting (3.3.44) into (3.3.42) we get an equation for the solution to the normal equations using Newton's method as folows,

$$\boldsymbol{\theta}_{n+1} = \boldsymbol{\theta}_n - \mathbf{R}^{-1}_{\varphi_e\varphi_e}\nabla F_n, \tag{3.3.45}$$

Comparing (3.3.45) to (3.3.25) we can see that Newton's method can be expected to converge quicker due to the weighting by $\mathbf{R}^{-1}_{\varphi_e\varphi_e}$ which essentially modifies the search direction to point to a minimum (local or global) point on the cost function $F$. Like the other LMS Newton algorithms discussed so far this weighting will equalise the eigenvalues of the correlation matrix each direction so each coefficient error term will converge uniformly. Incorporating time dependency into (3.3.45) and using an instantaneous estimate for $\nabla F$ as in the Equation Error LMS philosophy of (3.2.28) gives,

$$\boldsymbol{\theta}_{n+1} = \boldsymbol{\theta}_n + \mu \widehat{\mathbf{R}}^{-1}_{\varphi_e\varphi_e}(n)\varphi_e(n)e_e(n), \tag{3.3.46}$$

Equation (3.3.46) is termed the Equation Error LMS Newton adaptive IIR algorithm. Like the FIR LMS Newton algorithm of (3.1.58) an update constant $\mu$ has been introduced to allow a greater degree of control of the algorithm since a noisy instantaneous gradient estimate is used. Convergence in the mean about a local minimum point on the cost function $F$ will occur provided,

$$|1-\mu| < 1, \tag{3.3.47}$$

or,

$$0 < \mu < 2, \tag{3.3.48}$$

Like the Simplified Gradient LMS Newton algorithm in practice the stepsize $\mu$ may have to be much lower than the upper bound of (3.3.48) for convergence. From (3.3.46) we can see the weighting by $\mathbf{R}^{-1}_{\varphi_e\varphi_e}(n)$ essentially will ideally make the Equation Error LMS Newton algorithm independent of the

eigenvalue spread of the covariance matrix $\mathbf{R}^{-1}_{\varphi_e\varphi_e}(n)$. This is a major advantage of the Equation Error LMS Newton algorithm over Equation Error LMS and NLMS algorithms because of the dependence of convergence speed on the eigenvalue spread of the covariance matrix $\mathbf{R}^{-1}_{\varphi_e\varphi_e}(n)$. Since the stepsize $\mu$ has to be sufficiently small for stability, a potentially slow convergence speed may result for coloured signals where the eigenvalue spread is greater than unity. However due to the requirement of the computation of an estimate of the inverse covariance matrix $\mathbf{R}^{-1}_{\varphi_e\varphi_e}(n)$ every iteration n, the Equation Error LMS Newton algorithm has a far higher computational requirement. To reduce complexity of the inverse covariance matrix calculation the same techniques employed for the FIR LMS Newton algorithm can be used. Using the matrix inversion lemma the inverse covariance estimate $\mathbf{R}^{-1}_{\varphi_e\varphi_e}(n)$ may be computed as follows [3.19],

$$\hat{\mathbf{R}}^{-1}_{\varphi_e\varphi_e}(n)=\frac{1}{\gamma}\left(\hat{\mathbf{R}}^{-1}_{\varphi_e\varphi_e}(n-1)-\frac{\hat{\mathbf{R}}^{-1}_{\varphi_e\varphi_e}(n-1)\varphi_e(n)\varphi_e{}^T(n)\hat{\mathbf{R}}^{-1}_{\varphi_e\varphi_e}(n-1)}{\frac{\gamma}{\alpha}+\varphi_e{}^T(n)\hat{\mathbf{R}}^{-1}_{\varphi_e\varphi_e}(n-1)\varphi_e(n)}\right), \tag{3.3.49}$$

where $\gamma=1-\alpha$ is termed the forgetting factor which weights the most recent output errors. This is useful to exclude old data that is less appropriate in non-stationary environments. $\alpha$ is a convergence factor.

Like the other LMS Newton algorithms discussed so far the choice of fixed stepsize $\mu$ in (3.3.46) can be difficult for non-stationary environments and signals. Instead a variable convergence factor $\mu(n)$ can be chosen to minimise a posteriori error as follows,

$$\mu(n)=\frac{1}{\varphi_e{}^T(n)\hat{\mathbf{R}}^{-1}_{\varphi_e\varphi_e}(n)\varphi_e(n)}, \tag{3.3.50}$$

Introducing (3.3.50) into (3.3.46) we get,

$$\theta_{n+1}=\theta_n+\mu\frac{\hat{\mathbf{R}}^{-1}_{\varphi_e\varphi_e}(n)\varphi_e(n)e_e(n)}{\varphi_e{}^T(n)\hat{\mathbf{R}}^{-1}_{\varphi_e\varphi_e}(n)\varphi_e(n)}, \tag{3.3.51}$$

Equation (3.3.51) is termed the Equation Error Normalised LMS Newton algorithm and incorporates an additional reduction factor, $\mu$, like the other Normalised LMS Newton algorithms discussed so far, to control convergence speed at the expense of steady state error.

### 3.3.6. Bias Removal in the Equation Error LMS algorithm and the Bias Remedy Equation Error LMS adaptive algorithm

The Equation Error LMS algorithm of (3.3.35) will still suffer the same bias in the AR coefficients once converged as illustrated in equation (3.3.29). This bias in the Equation Error LMS solution once converged is due to the fact the information vector $\varphi_e(n)$ in (3.3.3) includes not only the echo path output information $y(n)$, but also contributions disturbance signal $v(n)$ as follows,

$$\boldsymbol{\varphi}_e(n) = \boldsymbol{\varphi}_*(n) + \begin{bmatrix} \mathbf{v}(n) \\ \mathbf{0} \end{bmatrix}, \tag{3.3.52}$$

where $v(n)$ and $\boldsymbol{\varphi}_*(n)$ are defined in (3.3.22) and (3.3.23) respectively.

This additive disturbance signal $v(n)$ is however normally not directly available to allow a simple subtraction from the information vector to order to eliminate the bias. An alternative solution developed in [3.26],[3.28] is to use the output error signal $e_o(n)$, since this signal is a good estimate for the perturbation noise once the adaptive algorithm converges. Using this technique the adjusted information vector $\boldsymbol{\varphi}_{br}(n)$ can be expressed as,

$$\boldsymbol{\varphi}_{br}(n) = \boldsymbol{\varphi}_e(n) - \tau \mathbf{e}_o(n-1), \tag{3.3.53}$$

where $\mathbf{e}_o(n-1)$ is a N+M x1 vector defined as:

$$\mathbf{e}_o(n-1) = [0,.....0, e_o(n-1),...., e_o(n-N)]^T, \tag{3.3.54}$$

and the remedy parameter $\tau$ ($0 \le \tau \le 1$) is a parameter used to control the amount of bias that is eliminated from the information vector $\boldsymbol{\varphi}_e(n)$. Using this adjusted information vector in (3.3.53) gives the coefficient update,

$$\boldsymbol{\theta}_{n+1} = \boldsymbol{\theta}_n + \mu \boldsymbol{\varphi}_{br}(n) e_e(n), \tag{3.3.55}$$

Equation (3.3.55) is known as the Bias Remedy Equation Error LMS algorithm [3.4],[3.26],[3.28]. In comparison to the Equation Eroor LMS update of equation (3.3.35) the only additional complexity is the remedy parameter $\tau$, and an FIR filter who's zeros are the same as the poles of the IIR model to generate the equation error signal $e_e(n)$ from the output error signal $e_o(n)$. The structure of the Bias Remedy Equation Error LMS Adaptive IIR algorithm is shown in Figure 3.12.

In terms of the stability of the Bias Remedy Equation Error LMS algorithm of (3.3.59) the smaller $\tau$ is the closer the Bias Remedy Equation Error LMS algorithm is to the Equation Error LMS algorithm of (3.3.32) since from (3.3.53) $\boldsymbol{\varphi}_{br}(n)$ will be similar to $\boldsymbol{\varphi}_e(n)$. As a result for a smaller $\tau$ a larger the bias will exist in the AR coefficients when echo path output noise is present. However with a smaller $\tau$ the more stable the Bias Remedy Equation Error LMS algorithm becomes [3.4],[3.26],[3.28].
For the BR EELMS algorithm to be globally stable $\tau$ must satisfy [3.26],[3.28],

$$0 \le \tau \le \min\left[ k \frac{\|\boldsymbol{\varphi}_e(n)\|_2}{\|\mathbf{e}_o(n)\|_2}, 1 \right], \tag{3.3.56}$$

where $k$ is a non-zero scalar constant which must be determined practically, and $\mu$ must satisfy,

$$0 < \mu < \min\left( \frac{2}{\mathbf{R}_{\varphi_{br}\varphi_{br}}}, \sigma \right), \tag{3.3.57}$$

where $\lambda_{max}$ is the largest eigenvalue of covariance matrix $\mathbf{R}_{\varphi_{br}\varphi_{br}}$, and $\sigma$ is a sufficiently small positive real constant [3.26],[3.28]. The covariance matrix $\mathbf{R}_{\varphi_{br}\varphi_{br}}$ is defined as,

$$\mathbf{R}_{\varphi_{br}\varphi_{br}} = E[\varphi_{br}(n)\varphi_{br}{}^{T}(n)], \tag{3.3.58}$$

For a positive definite matrix $\mathbf{R}_{\varphi_{br}\varphi_{br}}$, which is Toeplitz in form, the upper bound of equation (3.3.61) becomes,

$$0 < \mu < \min\left(\frac{2}{\|\varphi_{br}(n)\|_2}, \sigma\right), \tag{3.3.59}$$

where $\|\varphi_{br}(n)\|_2$ is the $l_2$ norm of adjusted information vector $\varphi_{br}(n)$. In practice some experimentation is needed to define the constant $\sigma$ in the upper limit of (3.3.59) for convergence, as $\mu$ may have to be much lower than $\frac{2}{\|\varphi_{br}(n)\|_2}$ to remain stable.

Like the Equation Error LMS algorithm of (3.3.35) the Bias Remedy Equation Error LMS algorithm of (3.3.55) is specified in a group adaption form. We will see in Chapter 5 that like all LMS based adaptive IIR algorithms presented so far, a homogenous adaption forms may be required to echo path attenuation.

### 3.3.7. The Normalised LMS Bias Remedy Equation Error adaptive IIR algorithm

In the same way the Equation Error adaptive IIR LMS algorithm will vary with the power of the information regression vector $\varphi_e(n)$ the Bias Remedy Equation Error adaptive IIR LMS algorithm will vary with the power of information vector $\varphi_{br}(n)$. This presents a problem for choosing a fixed step size $\mu$ for the Bias Remedy Equation Error LMS algorithm. By incorporating normalisation into the filter update [3.30], proportional to the power of the information vector $\varphi_{br}(n)$, the filter update can be made independent this power variation. For the Bias Remedy Equation Error LMS algorithm, normalisation by the $l_2$ norm of information vector $\varphi_{br}(n)$ gives the filter update,

$$\boldsymbol{\theta}_{n+1} = \boldsymbol{\theta}_n + \frac{\mu}{\delta + \varphi_{br}^{T}(n)\varphi_{br}(n)} e_e(n)\varphi_{br}(n), \tag{3.3.60}$$

where $\delta$ is a small positive constant to prevent division by zero when information vector power is zero. Equation (3.3.60) is called the Normalised LMS (NLMS) Bias Remedy Equation Error algorithm. Like the other NLMS algorithms seen so far, the Bias Remedy Equation Error NLMS algorithm will still suffer from the same dependency on the eigenvalue spread of the correlation matrix, $\mathbf{R}_{\phi_{br}\phi_{br}}$.

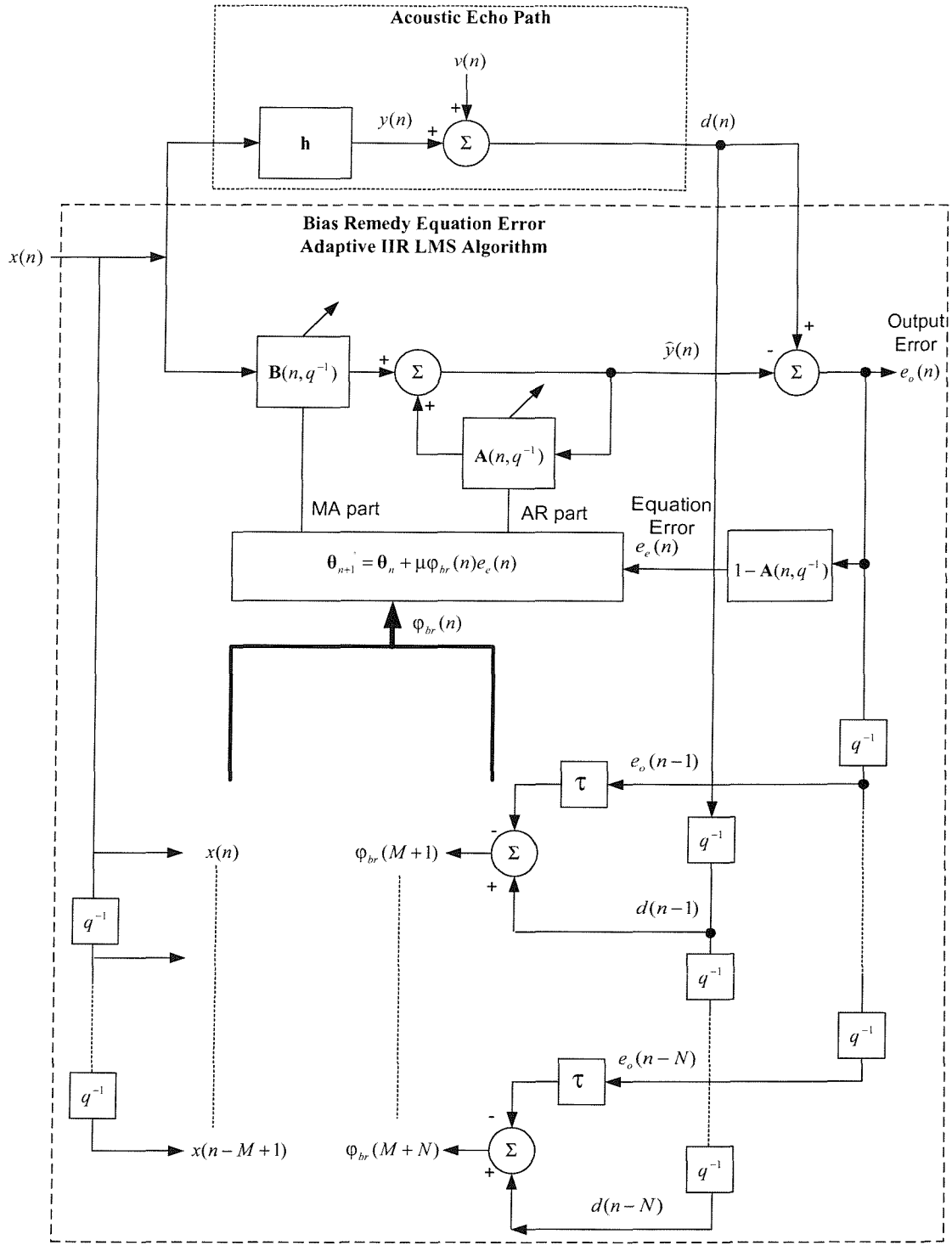


**Figure 3.12 : The structure of the Bias Remedy Equation Error LMS adaptive IIR algorithm.**

### 3.3.8. The Newton's method and Bias Remedy Equation Error LMS Newton adaptive IIR algorithm

Using the iterative solution to the recursive normal equations of (3.3.16) using Newton's Method gives,

$$\boldsymbol{\theta}_{n+1} = \boldsymbol{\theta}_n - \mu \mathbf{H}^{-1}(\boldsymbol{\theta}_n)\nabla F_n, \tag{3.3.61}$$

where $\mathbf{H}(\boldsymbol{\theta}_n)$ is the Hessian matrix of the mean squared error cost function $F$ of (3.3.10), and $\mathbf{H}^{-1}(\boldsymbol{\theta}_n)$ is its inverse. As we have discussed already the Hessain matrix defined in (3.1.55) is the second derivative of the cost function with respect to the filter coefficients. Using (3.3.10) and the modified information vector $\boldsymbol{\varphi}_{br}(n)$ the Hessain matrix for the bias remedy equation error formulation can be computed as follows,

$$\mathbf{H}^{-1}(\boldsymbol{\theta}_n) = \frac{\partial^2 F}{\partial \boldsymbol{\theta}_n \partial \boldsymbol{\theta}_n} = \frac{\partial}{\partial \boldsymbol{\theta}_n}\left[-2\mathbf{r}_{d\boldsymbol{\varphi}_{br}} + 2\mathbf{R}_{\boldsymbol{\varphi}_{br}\boldsymbol{\varphi}_{br}}\boldsymbol{\theta}\right], \tag{3.3.62}$$

giving,

$$\mathbf{H}(\boldsymbol{\theta}_n) = 2\mathbf{R}_{\boldsymbol{\varphi}_{br}\boldsymbol{\varphi}_{br}}, \tag{3.3.63}$$

Substituting (3.3.44) into (3.3.42) we get an equation for the solution to the normal equations using Newton's method as folows,

$$\boldsymbol{\theta}_{n+1} = \boldsymbol{\theta}_n - \mathbf{R}^{-1}_{\boldsymbol{\varphi}_{br}\boldsymbol{\varphi}_{br}}\nabla F_n, \tag{3.3.64}$$

Comparing (3.3.45) to (3.3.25) we can see that Newton's method can be expected to converge quicker due to the weighting by $\mathbf{R}^{-1}{}_{\boldsymbol{\varphi}_{br}\boldsymbol{\varphi}_{br}}$ which essentially modifies the search direction to point to a minimum (local or global) point on the cost function $F$. Like the other LMS Newton algorithms discussed so far this weighting will equalise the eigenvalues of the correlation matrix each direction so each coefficient error term will converge uniformly. Incorporating time dependency into (3.3.64) and using an instantaneous estimate for $\nabla F$ as in the Equation Error LMS philosophy of (3.2.28) gives,

$$\boldsymbol{\theta}_{n+1} = \boldsymbol{\theta}_n + \mu \hat{\mathbf{R}}^{-1}_{\boldsymbol{\varphi}_{br}\boldsymbol{\varphi}_{br}}(n)\boldsymbol{\varphi}_{br}(n)e_e(n), \tag{3.3.65}$$

Equation (3.3.65) is termed the Bias Remedy Equation Error LMS Newton adaptive IIR algorithm. Like the FIR LMS Newton algorithm of (3.1.58) an update constant $\mu$ has been introduced to allow a greater degree of control of the algorithm since a noisy instantaneous gradient estimate is used. Convergence in the mean about a local minimum point on the cost function $F$ will occur provided,

$$|1-\mu| < 1, \tag{3.3.66}$$

or,

$$0 < \mu < 2, \tag{3.3.67}$$

Like the Equation Error LMS Newton algorithm in practice the stepsize $\mu$ may have to be much lower than the upper bound of (3.3.67) for convergence. From (3.3.65) we can see the weighting by

$\mathbf{R}^{-1}_{\varphi_{br}\varphi_{br}}(n)$ essentially will ideally make the Bias Remedy Equation Error LMS Newton algorithm independent of the eigenvalue spread of the covariance matrix $\mathbf{R}_{\varphi_{br}\varphi_{br}}$. This is a major advantage of the Equation Error LMS Newton algorithm over Equation Error LMS and NLMS algorithms because of the dependence of convergence speed on the eigenvalue spread of the covariance matrix $\mathbf{R}_{\varphi_{br}\varphi_{br}}$. Since the stepsize $\mu$ has to be sufficiently small for stability, a potentially slow convergence speed may result for coloured signals where the eigenvalue spread is greater than unity. However due to the requirement of the computation of an estimate of the inverse covariance matrix $\mathbf{R}^{-1}_{\varphi_e\varphi_e}(n)$ every iteration n, the Equation Error LMS Newton algorithm has a far higher computational requirement. To reduce complexity of the inverse covariance matrix calculation the same techniques employed for the FIR LMS Newton algorithm can be used. Using the matrix inversion lemma the inverse covariance estimate $\mathbf{R}^{-1}_{\varphi_{br}\varphi_{br}}(n)$ may be computed as follows [3.19],

$$\mathbf{R}^{-1}_{\varphi_{br}\varphi_{br}}(n)=\frac{1}{\gamma}\left(\mathbf{R}^{-1}_{\varphi_{br}\varphi_{br}}(n-1)-\frac{\mathbf{R}^{-1}_{\varphi_{br}\varphi_{br}}(n-1)\varphi_{br}(n)\varphi_{br}{}^{T}(n)\mathbf{R}^{-1}_{\varphi_{br}\varphi_{br}}(n-1)}{\frac{\gamma}{\alpha}+\varphi_{br}{}^{T}(n)\mathbf{R}^{-1}_{\varphi_{br}\varphi_{br}}(n-1)\varphi_{br}(n)}\right), \tag{3.3.68}$$

where $\gamma=1-\alpha$ is termed the forgetting factor which weights the most recent output errors. This is useful to exclude old data that is less appropriate in non-stationary environments. $\alpha$ is a convergence factor.

Like the other LMS Newton algorithms discussed so far the choice of fixed stepsize $\mu$ in (3.3.65) can be difficult for non-stationary environments and signals. Instead a variable convergence factor $\mu(n)$ can be chosen to minimise a posteriori error as follows,

$$\mu(n)=\frac{1}{\varphi_{br}{}^{T}(n)\hat{\mathbf{R}}^{-1}_{\varphi_{br}\varphi_{br}}(n)\varphi_{br}(n)}, \tag{3.3.69}$$

Introducing (3.3.69) into (3.3.65)we get,

$$\theta_{n+1}=\theta_n+\mu\frac{\hat{\mathbf{R}}^{-1}_{\varphi_{br}\varphi_{br}}(n)\varphi_{br}(n)e_e(n)}{\varphi_{br}{}^{T}(n)\hat{\mathbf{R}}^{-1}_{\varphi_{br}\varphi_{br}}(n)\varphi_{br}(n)}, \tag{3.3.70}$$

Equation (3.3.70) is termed the Bias Remedy Equation Error Normalised LMS Newton algorithm and incorporates an additional reduction factor, $\mu$, like the other Normalised LMS Newton algorithms discussed so far, to control convergence speed at the expense of steady state error.

### 3.3.9. Bias Removal Using the Steiglitz McBride Equation Error Method

The Steiglitz McBride method of system identification essentially overcomes the bias problem of the standard Equation Error model of Figure 3.9 by pre-filtering the input signals by the poles of the adaptive model. As we shall see this essentially distorts the Equation Error surface in (3.3.19) to be minimised, to appear more like the Output Error cost function of (3.3.24), while still remaining a linear function of the adaptive filter coefficients. Consider the pre-filtered input signals [3.12], [3.19],

$$x_f(n) = \frac{x(n)}{1 - \mathbf{A}(q^{-1}, k)}, \tag{3.3.71}$$

and,

$$d_f(n) = \frac{d(n)}{1 - \mathbf{A}(q^{-1}, k)}, \tag{3.3.72}$$

where k is an iteration index, and $\mathbf{A}(q^{-1}, k)$ are poles of the adaptive model for iteration k. Using the relationship of (3.3.7) we can formulate a filtered equation error signal as follows,

$$e_{fe}(n) = \frac{e_e(n)}{\left[1 - \mathbf{A}(q^{-1}, k)\right]} = \frac{\left[1 - \mathbf{A}(q^{-1}, n)\right] e_o(n)}{\left[1 - \mathbf{A}(q^{-1}, k)\right]}, \tag{3.3.73}$$

Rewriting this gives,

$$e_{fe}(n) = \frac{\left[1 - \mathbf{A}(q^{-1}, n)\right]}{\left[1 - \mathbf{A}(q^{-1}, k)\right]} d(n) - \frac{\mathbf{B}(q^{-1}, n) x(n)}{\left[1 - \mathbf{A}(q^{-1}, k)\right]}, \tag{3.3.74}$$

By running a series of iterations k on time series data $x(n)$ and $d(n)$, where each iteration the pre-filters $\mathbf{A}(q^{-1}, k)$ are fixed during adaption of the filters coefficients, it is clear from (3.3.73) that $e_{fe}(n)$ is a filtered equation error, such that $F = E[e_{fe}^2(n)]$ would be a quadratic with respect to the filter coefficients. Thus the Steiglitz McBride method consists of a series of quadratic optimisation problems at each iteration k [3.12]. From (3.3.74) if the pre-filters $\mathbf{A}(q^{-1}, k)$ were time varying such that $k = n - 1$ then $e_{fe}(n)$ becomes similar in form to an Output Error signal $e_o(n)$ of (3.2.7).

Consider the modified equation error model output as a result of the pre-filtering processes of (3.3.71) and (3.3.72),

$$\hat{y}(n) = \boldsymbol{\theta}^T \boldsymbol{\varphi}_{fe}, \tag{3.3.75}$$

where $\boldsymbol{\theta}$ is as defined in (3.2.3) and $\boldsymbol{\varphi}_{fe}$ is the (M+N) x 1 filtered information vector defined as:

$$\boldsymbol{\varphi}_{fe} = [x_f(n), \ldots, x_f(n - M + 1), d_f(n - 1), \ldots, d_f(n - N)]^T = [\mathbf{x}_f(n)^T, \mathbf{d}_f(n - 1)^T]^T, \tag{3.3.76}$$

and where $\mathbf{x}_f(n)$ and $\mathbf{d}_f(n - 1)$ are a Nx1 vectors defined as:

$$\mathbf{x}_f(n - 1) = [x_f(n - 1), \ldots\ldots, x_f(n - M + 1)]^T, \tag{3.3.77}$$

$$\mathbf{d}_f(n - 1) = [d_f(n - 1), \ldots\ldots, d_f(n - N)]^T, \tag{3.3.78}$$

The error signal for the Steiglitz M$^c$Bride scheme then becomes,

$$e_{fe}(n) = d_f(n) - \boldsymbol{\theta}^T \boldsymbol{\varphi}_{fe}, \tag{3.3.79}$$

Comparing this error signal to the standard equation error signal of (3.3.6) we get the relationship [32],

$$e_{fe}(n) = \frac{e_e(n)}{\left[1 - \mathbf{A}(q^{-1}, n - 1)\right]}, \tag{3.3.80}$$

The cost function $F$ for the Steiglitz McBride Equation Error model to be minimised is defined as,

$$F = E[e_{fe}^2(n)] = E[(d_f(n) - \boldsymbol{\theta}^T \boldsymbol{\varphi}_{fe})^2], \tag{3.3.81}$$

Rewriting (3.3.38) this gives,

$$F = E[d_f^2(n)] - 2\boldsymbol{\theta}^T \mathbf{r}_{d_f\varphi_f} + \boldsymbol{\theta}^T \mathbf{R}_{\varphi_{fe}\varphi_{fe}} \boldsymbol{\theta}, \tag{3.3.82}$$

where $\mathbf{R}_{\varphi_{fe}\varphi_{fe}}$ is a (M+N) x (M+N) covariance matrix defined as [41]:

$$\mathbf{R}_{\varphi_{fe}\varphi_{fe}} = E[\boldsymbol{\varphi}_{fe}\boldsymbol{\varphi}_{fe}^T] = \begin{bmatrix} \mathbf{R}_{x_f x_f} & \mathbf{R}_{x_f d_f} \\ \mathbf{R}_{x_f d_f}^T & \mathbf{R}_{d_f d_f} \end{bmatrix}, \tag{3.3.83}$$

where $\mathbf{r}_{d_f\varphi_f}$ is a cross correlation vector defined as:

$$\mathbf{r}_{d_f\varphi_f} = E[d_f(n)\boldsymbol{\varphi}_{fe}(n)], \tag{3.3.84}$$

with:

$$\mathbf{R}_{x_f d_f} = \text{M x N cross correlation matrix } E[\mathbf{x}_f(n)\mathbf{d}_f^T(n)], \tag{3.3.85}$$

$$\mathbf{R}_{d_f d_f} = \text{N x N autocorrelation matrix } E[\mathbf{d}_f(n)\mathbf{d}_f^T(n)]. \tag{3.3.86}$$

Since at each iteration k the Steiglitz McBride model is inherently an equation error model and the cost function of (3.3.44) is linear with respect to the filter coefficients of the adaptive model. The same methods used for the equation error model to derive an optimum set of filter coefficients to minimise (3.3.39) can hence be used.

To minimise this cost function $F$ of (3.3.81) with respect to the filter coefficient vector $\boldsymbol{\theta}$, differentiate F in (3.3.82) with respect to $\boldsymbol{\theta}$ and equate to zero. This yields,

$$\frac{\partial F}{\partial \boldsymbol{\theta}} = -\mathbf{r}_{d_f\varphi_{fe}} + \mathbf{R}_{\varphi_{fe}\varphi_{fe}}\boldsymbol{\theta} = \mathbf{0}, \tag{3.3.87}$$

giving,

$$\mathbf{R}_{\varphi_{fe}\varphi_{fe}}\boldsymbol{\theta} = \mathbf{r}_{d_f\varphi_{fe}}, \tag{3.3.88}$$

Equation (3.3.46) represents the recursive form of the normal equations of (3.1.16) for the pre-filtered equation error filter model. Like the FIR model equation (3.3.16) requires the orthogonality of the input regression vector and the equation error signal of (3.3.36). Using (3.3.36) and (3.3.38) this gives,

$$\frac{\partial F}{\partial \boldsymbol{\theta}} = \frac{\partial E[e_{fe}^2(n)]}{\partial \boldsymbol{\theta}} = -2E[e_{fe}(n)\frac{\partial e_{fe}(n)}{\partial \boldsymbol{\theta}}] = -2E[e_{fe}(n)\boldsymbol{\varphi}_{fe}(n)], \tag{3.3.89}$$

The optimal least squares filter coefficients selected to minimise the cost function $F$ of (3.3.81) are found by solving (3.3.46) for $\boldsymbol{\theta}$ as follows,

$$\boldsymbol{\theta}_{opt} = \mathbf{R}_{\varphi_{fe}\varphi_{fe}}^{-1}\mathbf{r}_{d_f\varphi_{fe}}. \tag{3.3.90}$$

From equation (3.3.90) we can see the selection of equation error IIR model coefficients $\boldsymbol{\theta}_{opt}$ to minimise the the cost function $F$ of (3.3.81) involves a direct matrix inversion.

### 3.3.10. The method of Steepest Descent and the Steiglitz M$^c$Bride Equation Error LMS adaptive IIR algorithm

The development of the adaptive form of the Steiglitz M$^c$Bride method requires some simplifications must be made to the pre-filters $\mathbf{A}(q^{-1},k)$ [3.13],[3.27]. Instead of a sequence of

quadratic optimisation problems with stationary pre-filters $\mathbf{A}(q^{-1},k)$ for each iteration, time varying pre-filters $\mathbf{A}(q^{-1},n-1)$ are used on the input signals giving [3.13],[3.27],

$$x_f(n)=\frac{x(n)}{1-\mathbf{A}(q^{-1},n-1)}=x(n)-\sum_{j=1}^{N}a_j(n)x_f(n-j), \tag{3.3.91}$$

$$d_f(n)=\frac{d(n)}{1-\mathbf{A}(q^{-1},n-1)}=d(n)-\sum_{j=1}^{N}a_j(n)d_f(n-j), \tag{3.3.92}$$

From (3.3.91) and (3.3.92) it can be seen at time index $n$ the input signals $x(n)$ and $d(n)$ are pre-filtered by the poles of the adaptive model at previous time index $n-1$. The resulting error signal then becomes [3.13],

$$e_{fe}(n)=d_f(n)-\hat{y}(n)=\frac{e_e(n)}{\left[1-\mathbf{A}(q^{-1},n-1)\right]}=\frac{\left[1-\mathbf{A}(q^{-1},n)\right]e_o(n)}{\left[1-\mathbf{A}(q^{-1},n-1)\right]}, \tag{3.3.93}$$

From (3.3.93) it can be seen that the filtered error signal $e_{fe}(n)$ to be minimised is similar in form to an instantaneous output error signal. However for a "suffiently small" stepsize $\mu$, the filter coefficients vary "sufficiently slowly" such that prefilters $\mathbf{A}(q^{-1},n-1)$ are close to those preoduced by a stationary pre-filter at each step of adaption $n$ [3.13]. Thus $x_f(n)$ and $d_f(n)$ can be assumed to be independent of the filter coeffients $\boldsymbol{\theta}_n$ at each iteration n, such that minimisation of $F=E[e_{fe}^2(n)]$ will be a quadratic optimisation problem [3.13],[3.27].

Let us now continue with development of steepest descent adaptive LMS form of the Steiglitz M$^c$Bride equation error method. For this adaptive method our objective is to choose the filter coefficients $\boldsymbol{\theta}_n$ at each iteration n, to minimise the mean squared error cost function cost function of (3.3.81) [3.32], [3.33],

$$F=E[e_{fe}^2(n)]. \tag{3.3.94}$$

Using the steepest descent iterative method to provide an iterative solution to the recursive normal equations of (3.3.88) we get the update,

$$\boldsymbol{\theta}_{n+1}=\boldsymbol{\theta}_n-\frac{\mu}{2}\nabla F_n. \tag{3.3.95}$$

where $\mu$ is a step size parameter to control the size of change in $\theta_{n+1}$ from $\theta_n$. The gradient of the mean square equation error surface $\nabla F_n$ using (3.3.88) and (3.3.89) can be written as,

$$\nabla F_n=-2E\left[e_{fe}(n)\varphi_{fe}(n)\right], \tag{3.3.96}$$

giving the iteration,

$$\boldsymbol{\theta}_{n+1}=\boldsymbol{\theta}_n+\mu E\left[e_e(n)\varphi_e(n)\right]. \tag{3.3.97}$$

Since $E\left[e_{fe}(n)\varphi_{fe}(n)\right]$ is generally unknown an estimate can be used. In line with the FIR LMS philosophy used earlier in the chapter the gradient $\nabla F_n$ is replaced by an instantaneous estimate,

$$\nabla \hat{F}_n = \frac{\partial e_{fe}^2(n)}{\partial \boldsymbol{\theta}_n}, \tag{3.3.98}$$

where,

$$\frac{\partial e_{fe}^2(n)}{\partial \boldsymbol{\theta}_n} = -2\varphi_{fe}(n)e_{fe}(n), \tag{3.3.99}$$

giving the coefficient update,

$$\boldsymbol{\theta}_{n+1} = \boldsymbol{\theta}_n + \mu\varphi_{fe}(n)e_{fe}(n), \tag{3.3.100}$$

Equation (3.3.100) is known as the Steiglitz McBride Equation Error LMS adaptive IIR algorithm [3.13],[3.27],[3.32],[3.33]. The structure of the Steiglitz McBride Equation Error Adaptive IIR algorithm is shown in Figure 3.13.

Consider the convergence of the Steiglitz McBride Equation Error LMS algorithm in the mean for a "sufficiently small" step size and for a sufficient order model [3.13]. As done for the FIR LMS algorithm if we define a coefficient error vector $\boldsymbol{\varepsilon}_n$ which represents the difference between each element of the filter coefficient vector $\boldsymbol{\theta}_n$ and the optimal solution $\boldsymbol{\theta}_{opt}$ of (3.3.89) we get,

$$\boldsymbol{\varepsilon}_{n+1} = \left(\mathbf{I} - \mu\mathbf{R}_{\varphi_f\varphi_f}\right)\boldsymbol{\varepsilon}_n, \tag{3.3.101}$$

Consequently each coefficient error term j of $\boldsymbol{\varepsilon}_n$ will decay to zero provided that,

$$\left|(1-\mu\lambda_j)\right| < 1, \tag{3.3.102}$$

where $\lambda_{\max}$ is the maximum eigenvalue of covariance matrix $\mathbf{R}_{\varphi_{fe}\varphi_{fe}}$. For a positive semidefinite matrix $\mathbf{R}_{\varphi_{fe}\varphi_{fe}}$ that has Toeplitz form, the trace of the covariance matrix $\mathbf{R}_{\varphi_{fe}\varphi_{fe}}$ can be used for the upper bound of (3.3.102) in a similar fashion to what was done for the FIR algorithm. Due to the Teoplitz form of $\mathbf{R}_{\varphi_{fe}\varphi_{fe}}$ the upper bound of (3.3.102) can be reduced further to,

$$0 < \mu < \frac{2}{\left\|\varphi_{fe}(n)\right\|_2}, \tag{3.3.103}$$

where $\left\|\varphi_{fe}(n)\right\|_2$ is the $l_2$ norm of information vector $\varphi_e(n)$ which can be written as,

$$\left\|\varphi_e(n)\right\|_2 = \sum_{i=0}^{M-1} x_f^2(n-i) + \sum_{j=1}^{N} d_f^2(n-j), \tag{3.3.104}$$

From (3.3.102) we can see the convergence in the mean for each coefficient error term for the Equation Error LMS algorithm will be dependent on the eigenvalue spread of the covariance matrix $\mathbf{R}_{\varphi_{fe}\varphi_{fe}}$. The eigenvalue spread was defined earlier in (3.1.47).

Equation (3.3.100) is specified in a group adaption form where the same stepsize $\mu$ is used to control the adaption of all coefficients in the IIR filter coefficient vector $\boldsymbol{\theta}_n$. We shall see later in the Chapter 5 that homogenous adaption forms will be used due to echo path attenuation [3.16]. A homogenous adaption form uses separate stepsize factors, $\mu_b$ and $\mu_a$, to control adaption of the MA and AR parts of the coefficient vector.

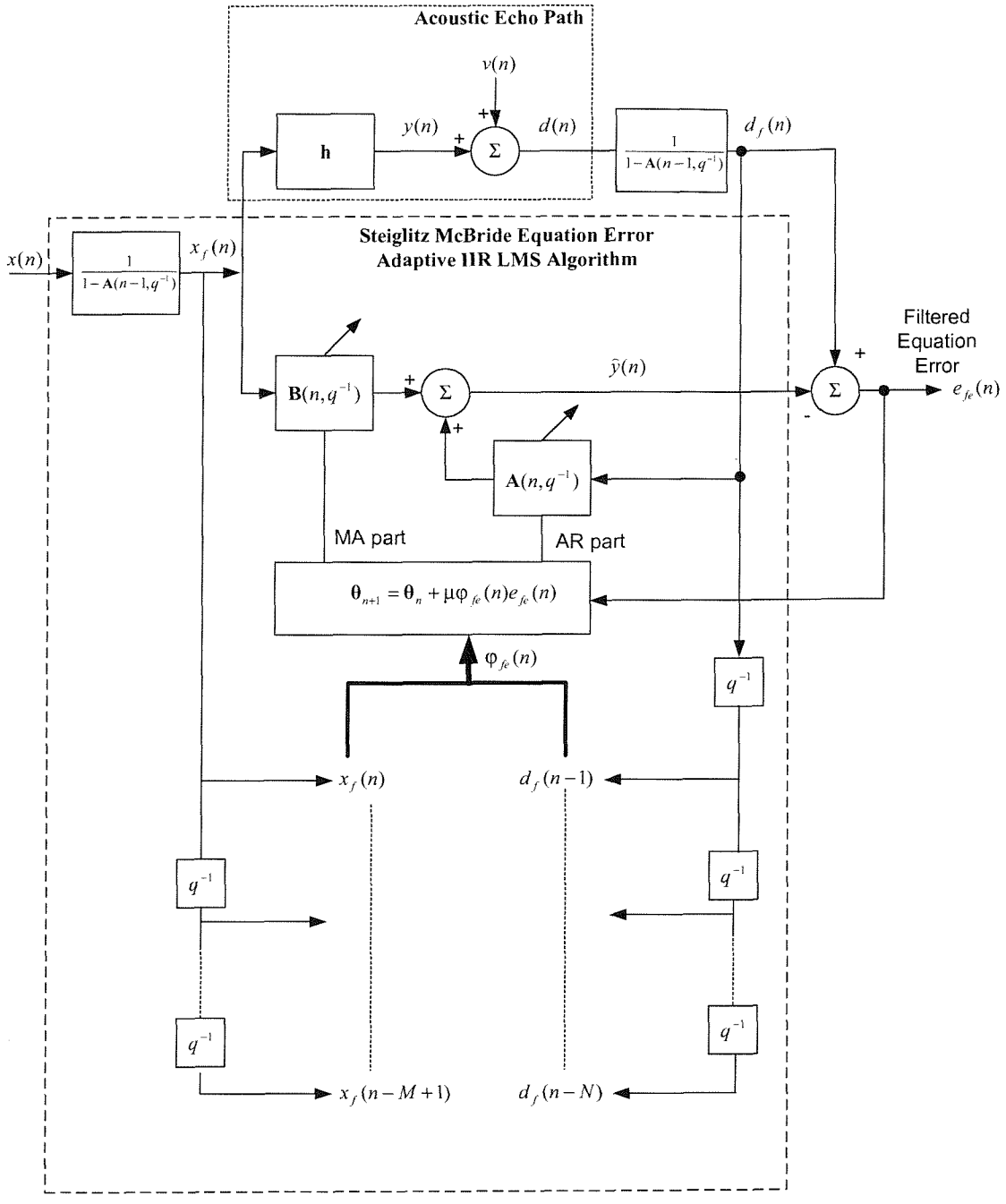


**Figure 3.13 : The structure of the Steiglitz McBride Equation Error LMS adaptive IIR algorithm.**

### 3.3.11. Normalised LMS Steiglitz McBride Equation Error adaptive IIR algorithm

In the same way the Equation Error LMS algorithm will vary with the power of the information regression vector $\boldsymbol{\varphi}_e(n)$, the adaptive IIR Steiglitz McBride Equation Error LMS algorithm will vary with the power of the information regression vector $\boldsymbol{\varphi}_{fe}(n)$. This presents a problem for choosing a fixed step size $\mu$ for the adaptive IIR Steiglitz McBride Equation Error LMS algorithm. By incorporating normalisation into the filter update, proportional to the power of the information vector $\boldsymbol{\varphi}_{fe}(n)$, the Steiglitz McBride Equation Error LMS filter update can be made independent of input and output signal powers [3.17],[3.30]. For the Steiglitz McBride Equation Error LMS algorithm normalisation by the $l_2$ norm of the filtered information vector $\boldsymbol{\varphi}_o(n)$ gives the filter update,

$$\boldsymbol{\theta}_{n+1} = \boldsymbol{\theta}_n + \frac{\mu}{\delta + \boldsymbol{\varphi}_{fe}^T(n)\boldsymbol{\varphi}_{fe}(n)} e_{fe}(n)\boldsymbol{\varphi}_{fe}(n), \tag{3.3.105}$$

Equation (3.3.105) is called the Steiglitz McBride Equation Error Normalised LMS adaptive IIR algorithm. Like the other NLMS algorithms seen so far, the Steiglitz McBride Equation Error NLMS algorithm will still suffer from the same dependency on the eigenvalue spread of the correlation matrix, $\mathbf{R}_{\varphi_{fe}\varphi_{fe}}$.

### 3.3.12. Newton's method and the Steiglitz M$^c$Bride Equation Error LMS Newton adaptive IIR algorithm

Using the iterative solution to the recursive normal equations of (3.3.88) using Newton's Method gives,

$$\boldsymbol{\theta}_{n+1} = \boldsymbol{\theta}_n - \mu \mathbf{H}^{-1}(\boldsymbol{\theta}_n)\nabla F_n, \tag{3.3.106}$$

where $\mathbf{H}(\boldsymbol{\theta}_n)$ is the Hessian matrix of the mean squared error cost function $F$ of (3.3.82), and $\mathbf{H}^{-1}(\boldsymbol{\theta}_n)$ is its inverse. As we have discussed already the Hessain matrix defined in (3.1.55) is the second derivative of the cost function with respect to the filter coefficients. Using (3.3.82) the Hessain matrix for the Steiglitz McBride equation error formulation can be computed as follows,

$$\mathbf{H}(\boldsymbol{\theta}_n) = \frac{\partial^2 F}{\partial \boldsymbol{\theta}_n \partial \boldsymbol{\theta}_n} = \frac{\partial}{\partial \boldsymbol{\theta}_n} 2E[-r_{y\varphi_{fe}} + \mathbf{R}_{\varphi_{fe}\varphi_{fe}}\boldsymbol{\theta}], \tag{3.3.107}$$

giving,

$$\mathbf{H}(\boldsymbol{\theta}_n) = 2\mathbf{R}_{\varphi_e\varphi_e}, \tag{3.3.108}$$

Substituting (3.3.108) into (3.3.106) we get an equation for the solution to the normal equations of (3.3.88) using Newton's method as folows,

$$\boldsymbol{\theta}_{n+1} = \boldsymbol{\theta}_n - \mathbf{R}^{-1}_{\varphi_{fe}\varphi_{fe}} \nabla F_n, \tag{3.3.109}$$

Comparing (3.3.109) to (3.3.100) we can see that Newton's method can be expected to converge quicker due to the weighting by $\mathbf{R}^{-1}_{\varphi_{fe}\varphi_{fe}}$ which essentially modifies the search direction to point to a minimum (local or global) point on the cost function $F$. Like the other LMS Newton algorithms discussed so far this weighting will equalise the eigenvalues of the correlation matrix each direction so each coefficient error term will converge uniformly. Incorporating time dependency into (3.3.109) and using an instantaneous estimate for $\nabla F$ as in the Steiglitz McBride Equation Error LMS philosophy of (3.3.98) gives,

$$\boldsymbol{\theta}_{n+1} = \boldsymbol{\theta}_n + \mu \hat{\mathbf{R}}^{-1}_{\varphi_{fe}\varphi_{fe}}(n) \varphi_{fe}(n) e_{fe}(n), \tag{3.3.110}$$

Equation (3.3.110) is termed the Steiglitz McBride Equation Error LMS Newton adaptive IIR algorithm. Like the FIR LMS Newton algorithm of (3.1.58) an update constant $\mu$ has been introduced to allow a greater degree of control of the algorithm since a noisy instantaneous gradient estimate is used. Convergence in the mean about a local minimum point on the cost function $F$ will occur provided,

$$|1 - \mu| < 1, \tag{3.3.111}$$

or,

$$0 < \mu < 2, \tag{3.3.112}$$

Like the Equation Error LMS Newton algorithm, in practice the stepsize $\mu$ may have to be much lower than the upper bound of (3.3.112) for convergence. From (3.3.110) we can see the weighting by $\mathbf{R}^{-1}_{\varphi_{fe}\varphi_{fe}}(n)$ essentially will ideally make the Steiglitz McBride Equation Error LMS Newton algorithm independent of the eigenvalue spread of the covariance matrix $\mathbf{R}_{\varphi_{fe}\varphi_{fe}}$. This is a major advantage of the Steiglitz McBride Equation Error LMS Newton algorithm over Steiglitz McBride Equation Error LMS and NLMS algorithms because of the dependence of convergence speed on the eigenvalue spread of the covariance matrix $\mathbf{R}_{\varphi_{fe}\varphi_{fe}}$. Since the stepsize $\mu$ has to be sufficiently small for stability, a potentially slow convergence speed may result for coloured signals where the eigenvalue spread is greater than unity. However due to the requirement of the computation of an estimate of the inverse covariance matrix $\mathbf{R}^{-1}_{\varphi_{fe}\varphi_{fe}}(n)$ every iteration n, the Steiglitz McBride Equation Error LMS Newton algorithm has a far higher computational requirement. To reduce complexity of the inverse covariance matrix calculation the same techniques employed for the FIR LMS Newton algorithm can be used. Using the matrix inversion lemma the inverse covariance estimate $\mathbf{R}^{-1}_{\varphi_{fe}\varphi_{fe}}(n)$ may be computed as follows [3.19],

$$\hat{\mathbf{R}}^{-1}_{\varphi_{fe}\varphi_{fe}}(n) = \frac{1}{\gamma}\left( \hat{\mathbf{R}}^{-1}_{\varphi_{fe}\varphi_{fe}}(n-1) - \frac{\hat{\mathbf{R}}^{-1}_{\varphi_{fe}\varphi_{fe}}(n-1)\varphi_{fe}(n)\varphi_{fe}{}^{T}(n)\hat{\mathbf{R}}^{-1}_{\varphi_{fe}\varphi_{fe}}(n-1)}{\frac{\gamma}{\alpha} + \varphi_{fe}{}^{T}(n)\hat{\mathbf{R}}^{-1}_{\varphi_{fe}\varphi_{fe}}(n-1)\varphi_{fe}(n)} \right), \tag{3.3.113}$$

where $\gamma = 1 - \alpha$ is termed the forgetting factor which weights the most recent output errors. This is useful to exclude old data that is less appropriate in non-stationary environments. $\alpha$ is a convergence factor.

Like the other LMS Newton algorithms discussed so far the choice of fixed stepsize $\mu$ in (3.3.110) can be difficult for non-stationary environments and signals. Instead a variable convergence factor $\mu(n)$ can be chosen to minimise a posteriori error as follows,

$$\mu(n) = \frac{1}{\varphi_{fe}^{T}(n)\hat{\mathbf{R}}^{-1}_{\varphi_{fe}\varphi_{fe}}(n)\varphi_{fe}(n)}, \tag{3.3.114}$$

Introducing (3.3.114) into (3.3.110) we get,

$$\boldsymbol{\theta}_{n+1} = \boldsymbol{\theta}_{n} - \mu \frac{\hat{\mathbf{R}}^{-1}_{\varphi_{fe}\varphi_{fe}}(n)\varphi_{fe}(n)e_{fe}(n)}{\varphi_{fe}^{T}(n)\hat{\mathbf{R}}^{-1}_{\varphi_{fe}\varphi_{fe}}(n)\varphi_{fe}(n)}, \tag{3.3.115}$$

Equation (3.3.115) is termed the Steiglitz McBride Equation Error Normalised LMS Newton algorithm and incorporates an additional reduction factor, $\mu$, like the other Normalised LMS Newton algorithms discussed so far, to control convergence speed at the expense of steady state error.

## 3.4. Adaptive IIR Algorithm Summary

A complete summary of the IIR adaptive algorithms detailed in the thesis can be formulated from (4.4.1) as shown in the table below,

| Initialisation: $\boldsymbol{\theta}_n = \mathbf{0}, \varphi_s(n) = \mathbf{0}, \forall n < 0$ | | | |
|---|---|---|---|
| **Algorithm** | $\hat{y}(n)$ | $e_s(n)$ | $\varphi_s(n)$ |
| Simplified Gradient Output Error | $\boldsymbol{\theta}_n^T \varphi_o(n)$ | $e_o(n)$ | $\varphi_f(n)$ |
| Pseudo Linear Regression Output Error | $\boldsymbol{\theta}_n^T \varphi_o(n)$ | $e_o(n)$ | $\varphi_o(n)$ |
| SHARF Output Error | $\boldsymbol{\theta}_n^T \varphi_o(n)$ | $e_{fo}(n)$ | $\varphi_o(n)$ |
| Equation Error | $\boldsymbol{\theta}_n^T \varphi_e(n)$ | $e_e(n)$ | $\varphi_e(n)$ |
| Bias Remedy Equation Error | $\boldsymbol{\theta}_n^T \varphi_o(n)$ | $e_e(n)$ | $\varphi_{br}(n)$ |
| Steiglitz McBride Equation Error | $\boldsymbol{\theta}_n^T \varphi_{fe}(n)$ | $e_{fe}(n)$ | $\varphi_{fe}(n)$ |
| $e_s(n) = d(n) - \hat{y}(n)$ | | | |
| **Algorithm Adaption Method** | $\mathbf{H}_n$ | $\mu(n)$ | |
| LMS | $\mathbf{I}$ | $\mu$ | |
| NLMS | $\mathbf{I}$ | $\dfrac{\mu}{\varphi_s^T(n)\varphi_s(n)}$ | |
| LMS Newton | $\mathbf{R}_{\varphi_s\varphi_s}^{-1}(n)$ | $\mu$ | |
| NLMS Netwon | $\mathbf{R}_{\varphi_s\varphi_s}^{-1}(n)$ | $\dfrac{\mu}{\varphi_s^T(n)\mathbf{R}_{\varphi_s\varphi_s}^{-1}(n)\varphi_s(n)}$ | |
| $\boldsymbol{\theta}_{n+1} = \boldsymbol{\theta}_n + \mu(n)\mathbf{H}_n\varphi_s(n)e_s(n)$ | | | |

**Table 3-2 : IIR adaptive algorithm summary**

where $e_o(n)$ is the output error signal, $e_e(n)$ is the equation error signal, $\hat{y}(n)$ is the output of the adaptive filter model and $d(n)$ is the output of the echo path to be modelled.

# Chapter 4

## 4. Modelling the acoustic echo path of a mobile handset

### 4.1. Introduction

In chapter 2, acoustic echo path responses were presented for typical mobile handset designs. It was established that, for the handset designs tested that acoustic echo cancellation was required. It was also seen that the variation of echo path response during normal handset use can be very large and in some configurations tested a resonant handset response is measured.

In chapter 3 we have introduced the fundamentals of optimal filtering using FIR (Finite Impulse Response) and IIR (Infinite Impulse Response) filter models. A longstanding question of the acoustic echo cancellation field is whether the use of an IIR model gives any significant performance advantages over the much simpler and more widely used FIR model. Modelling results in the acoustic echo cancellation literature concerning the relative performance of FIR and IIR filter models have tended to be based on room acoustic echo path impulse responses [4.1],[4.2],[4.3]. As correctly pointed out in [4.1] these modelling results are specific only to these particular application areas, and general conclusions on the modelling of an acoustic echo path using an IIR model should be avoided. To the author's knowledge no previous publications have documented the modelling of an acoustic echo path of a mobile handset using FIR or IIR models. The main aim of this chapter is to determine whether an FIR or IIR filter model is more suitable for modelling the echo path response of a mobile handset based on the echo path responses recorded in chapter 2.

In chapter 2 a sampling frequency of 12.8kHz was used to see clearly the characteristics of the acoustic echo path response. The topic of narrowband and wideband codec ADC systems was discussed. The main aim of this chapter is towards narrowband codec systems, as found in current GSM handset designs and fixed line telephony. To model the total echo path response, the echo path as seen by an acoustic echo cancellation device within the handset DSP (not only the acoustic response) must be considered. Sections 4.2 and 4.3 of this chapter deal with the complete echo path to be modelled (including the effect of codec filters). The issue of the sample rate conversion to the codec sample rate is discussed. Converted Echo path response results and Terminal Coupling Loss levels are presented for the handset test configurations of chapter 2 at actual the codec sample rate, including the effects of codec filtering.

In Section 4.4 a procedure for comparing the relative performance of FIR and IIR filter models is established. In Sections 4.5 and 4.6 modelling results are then presented using the converted echo path responses of Section 4.3. These results show there is a clear benefit of using an IIR filter model for modelling the acoustic echo path of a mobile handset.

Finally in Section 4.7 the need for an adaptive IIR model is established. The achievable performance of adaptive IIR filters over adaptive FIR filters using the adaptive algorithm techniques of chapter 3 are presented in detail in chapter 5.

## 4.2. The actual echo path of a mobile handset

In chapter 2 we looked only at the acoustic echo path of a mobile handset and how this response changes with the handset orientation in normal use. Consider now the actual echo path of a mobile a handset which an echo canceller must model, including all filtering as shown in Figure 4.1.

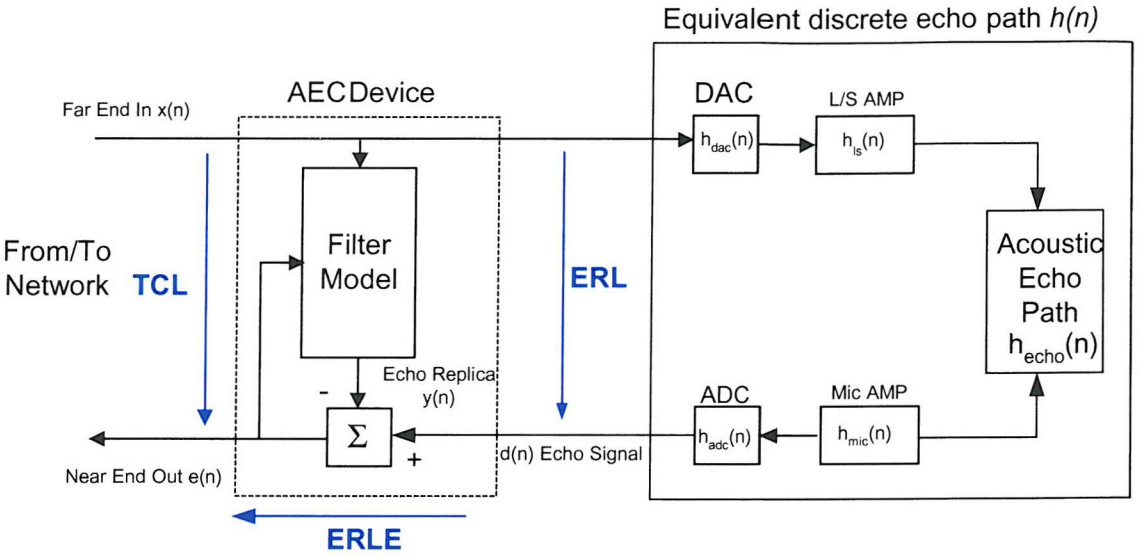


**Figure 4.1: The actual echo path response of a handset to be modelled**

As shown in Figure 4.1 above, the echo path response to be modelled by an echo canceller will contain filtering contributions from the ADC and DAC of the codec, and the handset loudspeaker and microphone amplifiers. The echo canceller would be implemented in digital form within the DSP of the handset, where the input and output samples $x(n)$, $d(n)$ and $e(n)$ would be at the sample rate of the handset codec device. For a narrowband codec this would be 8kHz. For a wideband codec this would be 16kHz. To relate a FIR or IIR discrete filter model to the filter model required by an echo canceller, the discrete echo path responses recorded in the chapter 2 at a sampling frequency of 12.8kHz must be converted. For a mobile handset with a narrowband codec the echo path response must be converted to 8kHz. To simulate a wideband codec system the actual echo path response sampled at 12.8kHz is used.

The equivalent discrete filter responses for the ADC and DAC of the handset codec device, $h_{adc}(n)$ and $h_{dac}(n)$, and loudspeaker and microphone amplifiers, $h_{ls}(n)$ and $h_{mic}(n)$, must also be included in the echo path response to be modelled by the echo canceller discrete filter model. The overall echo path to be modelled, $h(n)$, by the echo canceller can be written as follows,

$$h(n) = h_{echo}(n) * h_{dac}(n) * h_{adc}(n) * h_{mic}(n) * h_{ls}(n), \tag{4.1}$$

where $h_{echo}(n)$ is the equivalent discrete functions of the re-sampled acoustic echo path.

The contributions from the handset microphone and the microphone amplifier are already included in the acoustic echo path responses recorded in chapter 2. The converted echo path response, $h_{echo}(n)$, will as a result contain all $h_{mic}(n)$ contributions, and these terms in (4.1) can be neglected. As we shall see shortly it is difficult to measure separate responses for $h_{adc}(n)$ and $h_{dac}(n)$. A combined codec filter response $h_{codec}(n)$ can only be measured which will include all $h_{ls}(n), h_{adc}(n)$ and $h_{dac}(n)$ terms. The resulting echo path response $h(n)$ can be re-written as follows,

$$h(n) = h_{echo}(n) * h_{codec}(n), \tag{4.2}$$

The diagrams of Figure 4.1 may be re-dawn in Figure 4.2 to show the measurable echo path components to be modelled by the echo canceller.

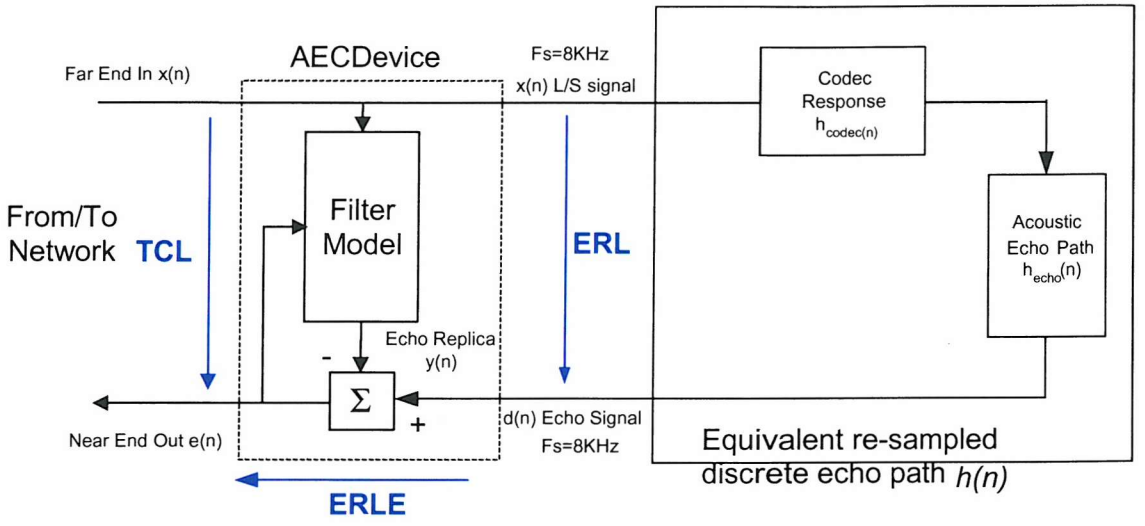


**Figure 4.2: Representation of the echo path to be modelled by an echo canceller containing measurable components $h_{echo}(n)$ and $h_{codec}(n)$.**

### 4.2.1. Measuring the filter response of conversion devices in a mobile handset

The transfer function estimation procedure of chapter 2 is used to measure the combined filter response of the conversion devices within the mobile handset as illustrated in Figure 4.3. A band-limited white noise input excitation signal is used. Both the original excitation sequence $x(n)$ and the output $d(n)$ of the echo path are recorded simultaneously. All data signals were recorded in an anechoic environment give a low ambient noise level for all experiments. The components $h_{fadc}(t)$ and $h_{aa}(t)$ represent the analogue responses of the ADC device, and anti-aliasing filters of [4.3]. The

components $h_{fdac}(t)$ and $h_{lsamp}(t)$ represent the analogue responses of the DAC device, and codec loudspeaker amplifier of [4.3].

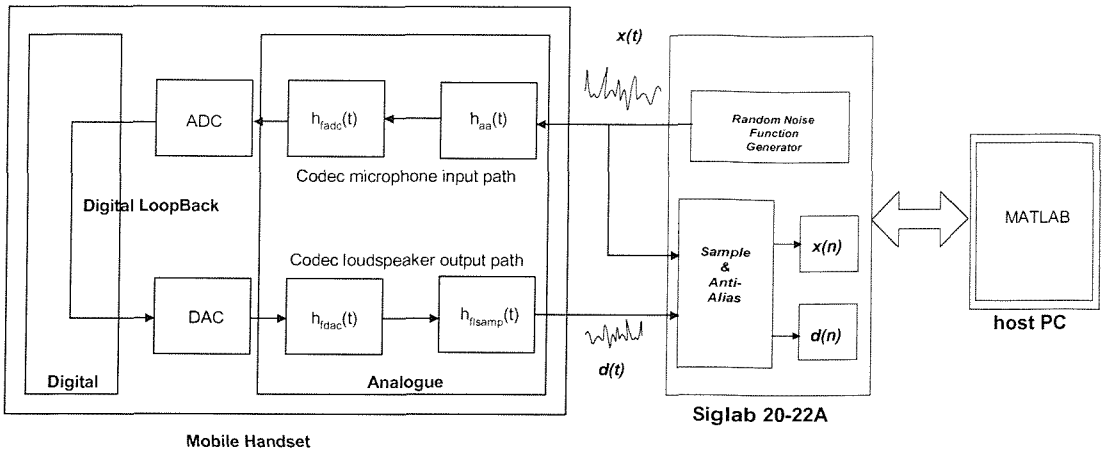


**Figure 4.3: Measurement set-up of handset codec filter responses**

In order to measure the codec filter response, the handset device is placed in a digital loop back mode. In this mode all data digitised by the handset ADC device is fed directly to the DAC filter path for reconstruction and output on the actual handset loudspeaker amplifier. Data record lengths of 320000 samples were recorded for both $x(n)$ and $d(n)$. A Hanning window size of 4096 was used allowing approximately 500 averages to be used in the computation of auto- and cross-spectrum estimates for $H_1(j\omega)$ and $\gamma^2_{xd}(\omega)$ to get accurate results. The codec filter magnitude, phase and impulse responses are shown in Figure 4.4. For a narrowband codec a sampling frequency of 12.8kHz is used. For a wideband codec a sampling frequency of 25.6kHz would be used. During the thesis only measurement results for a narrowband GSM codec were performed. These results are described next. The wideband codec response is not considered in the modelling experiments of this chapter. Only the original echo path signal response with bandwidth 0 to 6400Hz is used.

Figure 4.4 shows the measurement results for a narrowband GSM codec. The magnitude response has a distinct band pass response with sharp roll-off at the lower frequency of 240Hz and the higher frequency of 3600Hz. The stopband attenuation of the complete codec filter response is approximately 80dB. The passband gain is approximately 1dB. The complete echo path to be modelled, as shown in Figure 4.2, would result in all frequency information below 240Hz and above 3600Hz, effectively being eliminated, due to steep roll-off of the filter response and high stopband attenuation.

The impulse response of the codec filters as shown Figure 4.4(c) contains a delay period of approximately 0.6ms before any significant activity. This delay period can be attributed to the group delays of the filters in the codec ADC/DAC combined path. Following this delay period, a region of high activity is observed from 0.3ms to 4ms, which can be attributed mainly to the high frequency activity (upper cut off frequency) in the magnitude response. Impulse response activity after 4ms has a slowly decaying tail, which can mainly be attributed to the low frequency activity (lower cut off frequency) in the magnitude response. The complete echo path to be modelled, as shown in Figure 4.2, would hence contain

an additional delay period of approximately 0.6ms in additional to any delay in the acoustic echo path response.

From Figure 4.4(b) we can see the phase response of the codec filter is non-linear. The overall echo path phase response would as a result contain a non-linear phase response. This would also imply the impulse response would not be symmetrical.

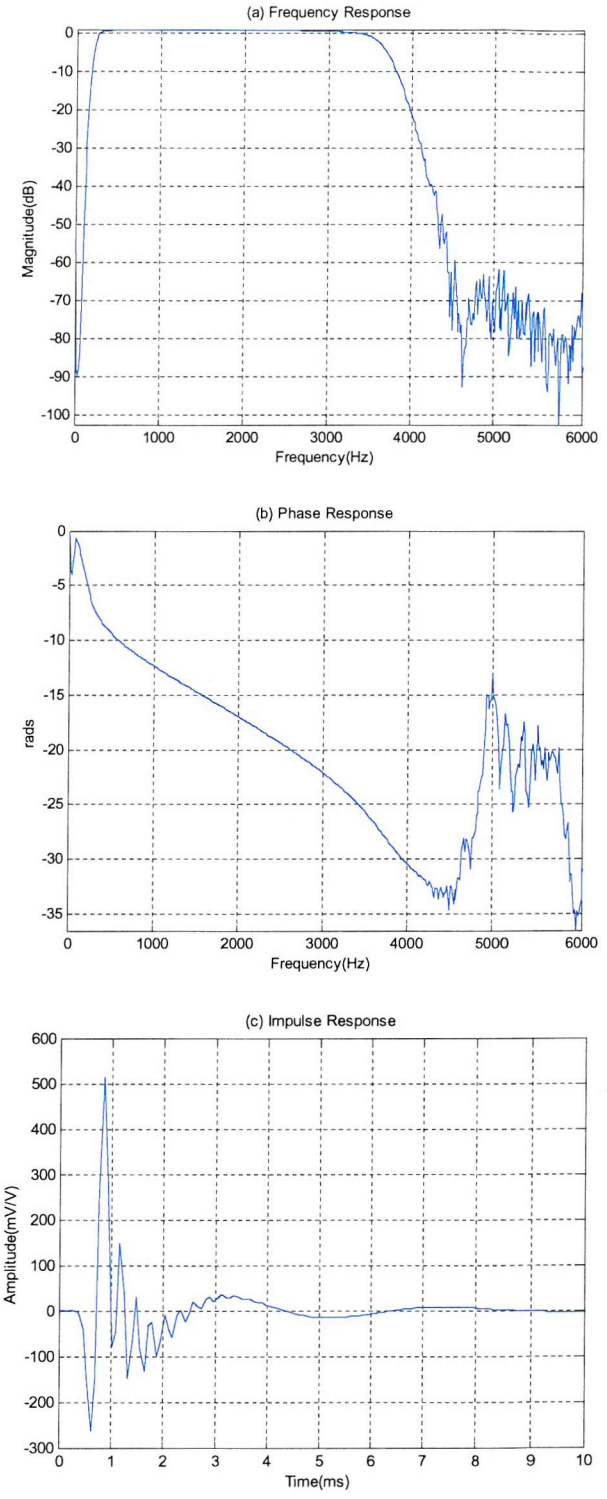


**Figure 4.4: The measured ADC/DAC combined codec filter response for a GSM narrowband codec.**

The filter frequency response is shown in (a). The phase response is shown in (b) and the impulse response is shown in (c).

## 4.3. The actual echo path response to be modelled

In order to create an overall echo path function for a narrowband codec sampled at 8kHz the conversion process of Figure 4.5 is used.

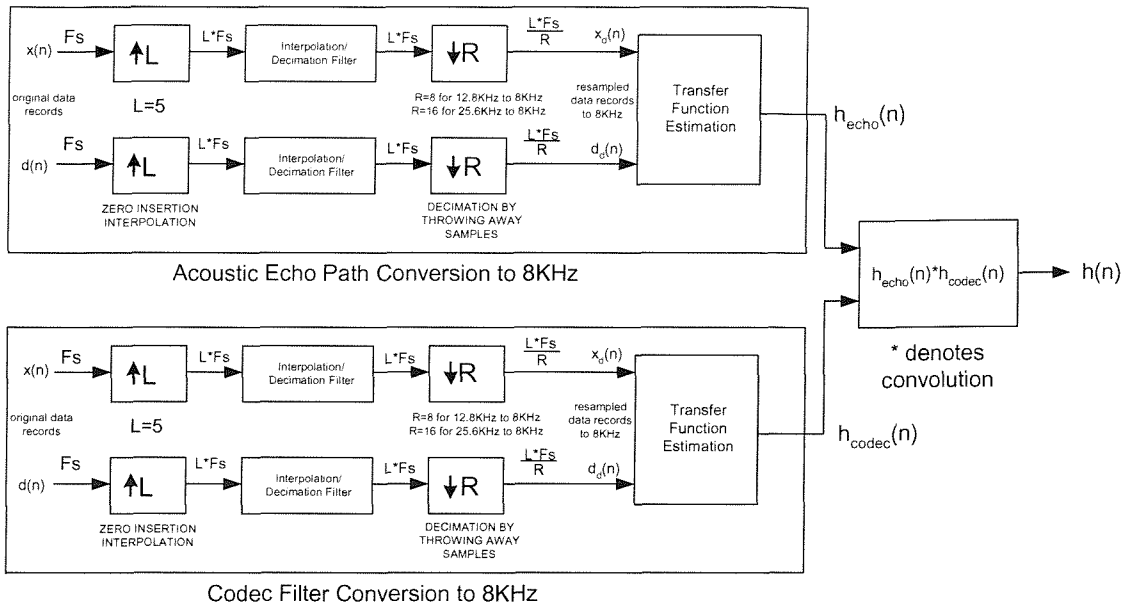


**Figure 4.5: Echo path conversion process**

As shown in Figure 4.5 above, both original input and output sequences *x(n)* and *d(n)* are re-sampled to 8Khz. The same transfer function estimation process in section 2.3 is then re-used to create an 8kHz sampled echo path transfer function. The re-sampled acoustic echo path function is then combined with the re-sampled codec filter response to create the overall 8kHz sampled echo path transfer function to be modelled by an echo canceller.

The interpolation/decimation filter design used is a linear phase FIR filter design, produced using the MATLAB fir1() design with a Kaiser window. The filter magnitude response of Fig 4.5(a) is unity across the terminal coupling loss measurement region of 300Hz to 3400Hz so as not to effect the echo loss of the converted echo path response. Re-sampling both input and output sequences to 8kHz before measuring the echo path transfer function will take into account all scaling involved in the interpolation and decimation processes. The MATLAB function resample() is used to perform the interpolation and decimation process.

For a wideband codec system the sampling rate is 16kHz, with an audio bandwidth 50-7000Hz. To investigate the effect of this higher audio bandwidth on FIR and IIR modelling performance, the actual 12.8kHz echo path responses of chapter 2 are used with no additional conversions or filtering.

## 4.4. Narrowband 8kHz Echo Path Results

All the echo path responses in chapter 2 are converted using the process described in the last section. The converted echo path responses are shown in Figure 4.6 to Figure 4.7. The Terminal Coupling Loss (TCL) and required Echo Return Loss Enhancement (ERLE) levels of these converted echo path responses are summarised in Table 4-1 below:-

| Handset Configuration | TCL(dB) | Effective Duration (ms) | ERLE (dB) |
|---|---|---|---|
| Artificial ear loudspeaker sealed test configuration of [1] | 46.13 | 9.62 | 0 |
| Face up configuration with no transducer seals | 32.84 | 4.63 | 13 |
| Face up configuration with adhesive tape loudspeaker seal | 41.86 | 7.88 | 4 |
| Face up configuration with adhesive tape microphone and loudspeaker seal | 39.43 | 8.88 | 6 |
| Face up configuration with adhesive tape microphone seal | 36.42 | 9.13 | 9 |
| Face down handset configuration | 29.91 | 10.25 | 16 |

**Table 4-1: Terminal Coupling Loss (TCL) levels and required Echo Return Loss Enhancement (ERLE) levels calculated for NEC G9 converted (8kHz narrowband) echo path responses.**

From Table 4-1 above we can see the terminal coupling loss and echo return loss enhancement levels calculated in chapter 2 remain largely unaffected when the complete echo path response is considered. This is not surprising since the codec response is flat in rolls off at frequencies less than 240Hz and greater than 3600Hz, outside the echo loss measurement bandwidth of 300Hz to 3400Hz .The requirement for additional ERLE in normal handset use as discussed in chapter 2 clearly still exits.

From these echo path results the same resonant behaviour still exists in these combined echo path responses in the range 240 to 3600Hz. All frequency information in the echo path responses presented in chapter 2 have been filtered out by the conversion process and the codec response above 3.6kHz and below 240Hz. Additionally the delay period before significant impulse response activity has now increased to 0.8ms due to additional delay in codec filter response. The overall effective duration of the impulse response to be modelled has also increased.

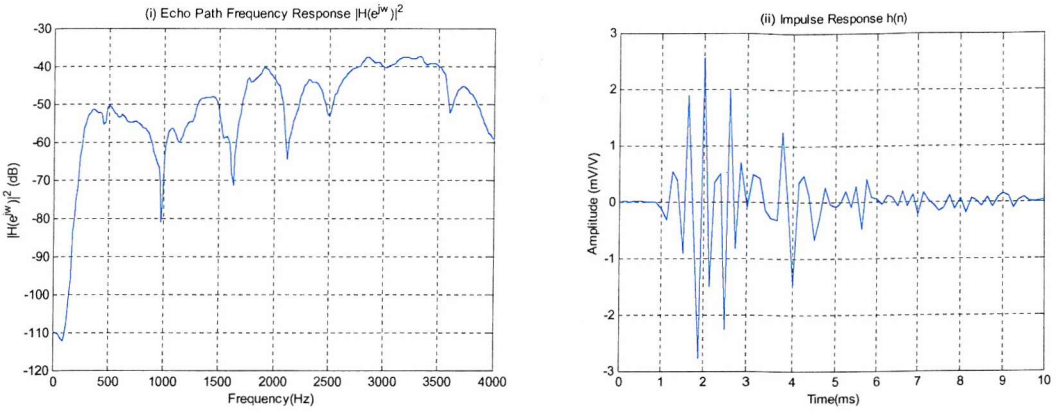


(a) Complete echo path response to be modelled for the artificial ear sealed handset configuration

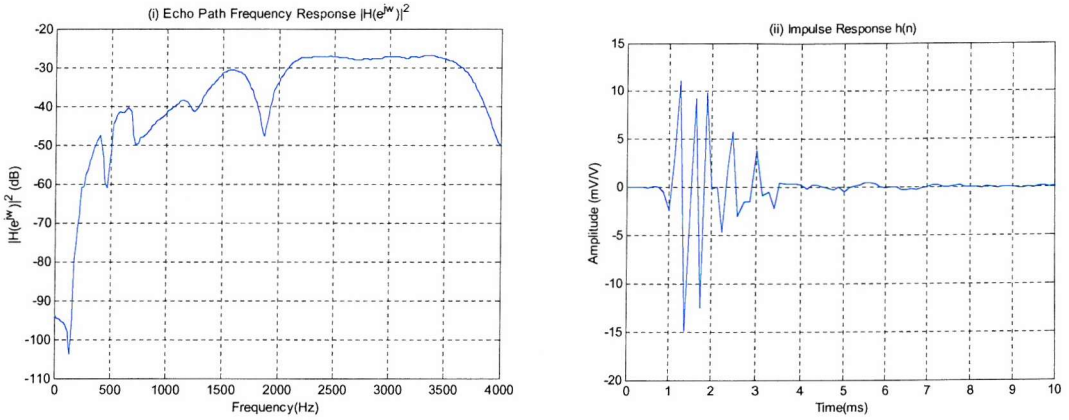


(b) Complete echo path response to be modelled for the face up no seals handset configuration

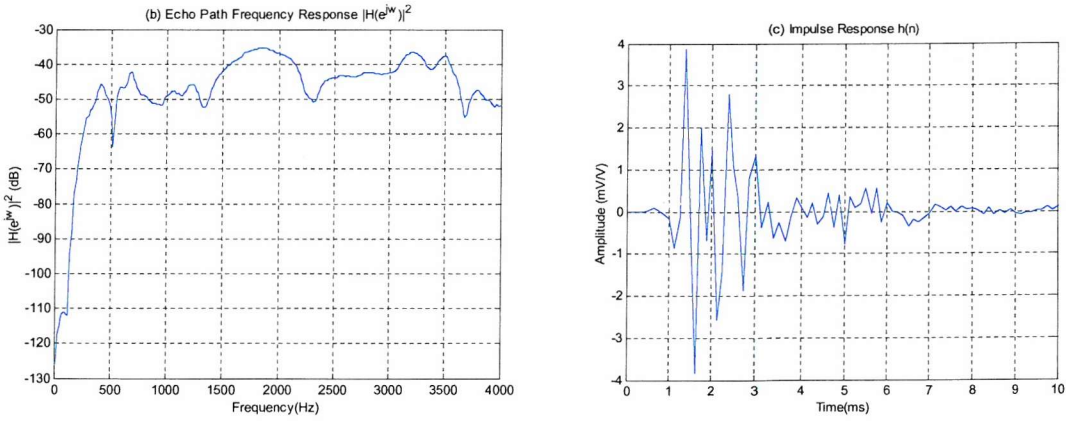


(c) Complete echo path response to be modelled for the loudspeaker tape adhesive sealed handset configuration

**Figure 4.6: The narrowband echo path responses for the artificial ear sealed, face up no seals and loudspeaker adhesive tape sealed handset configurations.**

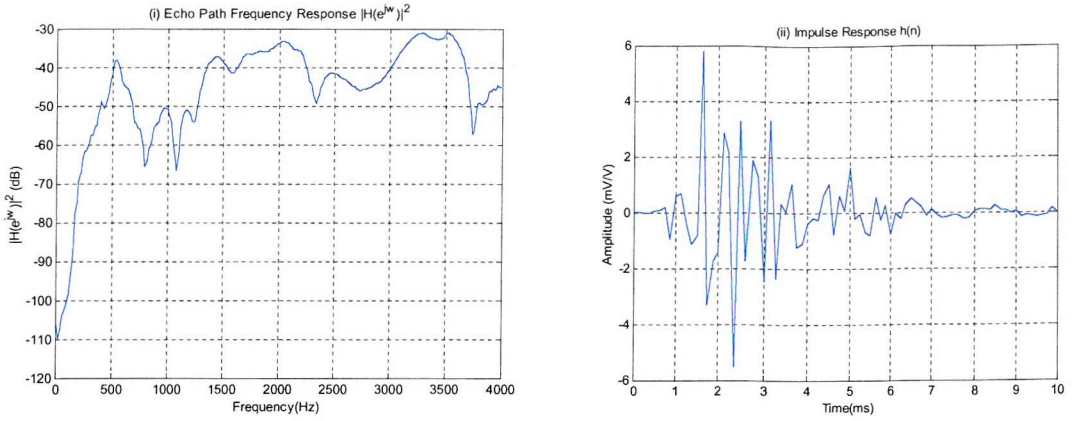


d) Complete echo path response to be modelled for the loudspeaker and microphone tape sealed handset configuration

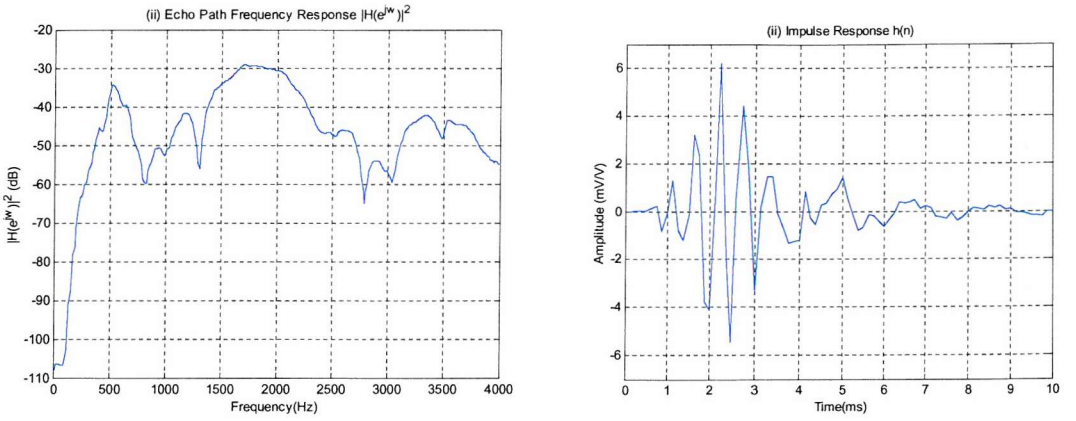


e) Complete echo path response to be modelled for the microphone tape sealed handset configuration

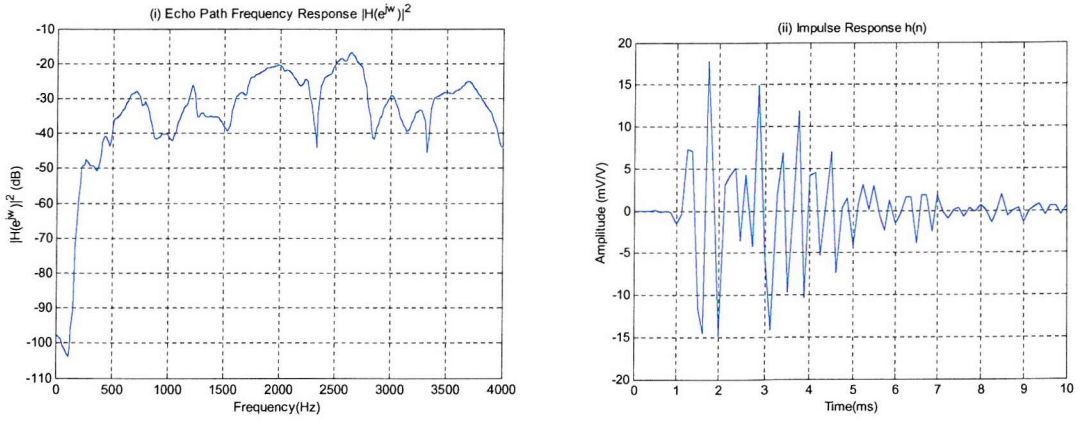


f) Complete echo path response to be modelled for the face down handset configuration

**Figure 4.7: The narrowband echo path responses for the artificial ear sealed, face up no seals and loudspeaker adhesive tape sealed handset configurations.**

## 4.5. Modelling the Acoustic Echo Path of a mobile handset using FIR and IIR filter models

In chapter 3 we have introduced the 3 main types of filter model used in most adaptive filtering applications - the FIR (Finite Impulse Response) filter model, the OE (Output Error) IIR (Infinite Impulse Response) filter model and the EE (Equation Error) IIR (Infinite Impulse Response) filter model. As a reminder of the general structure of these filter models Figure 4.8 shows each of these models connected in a system identification configuration.

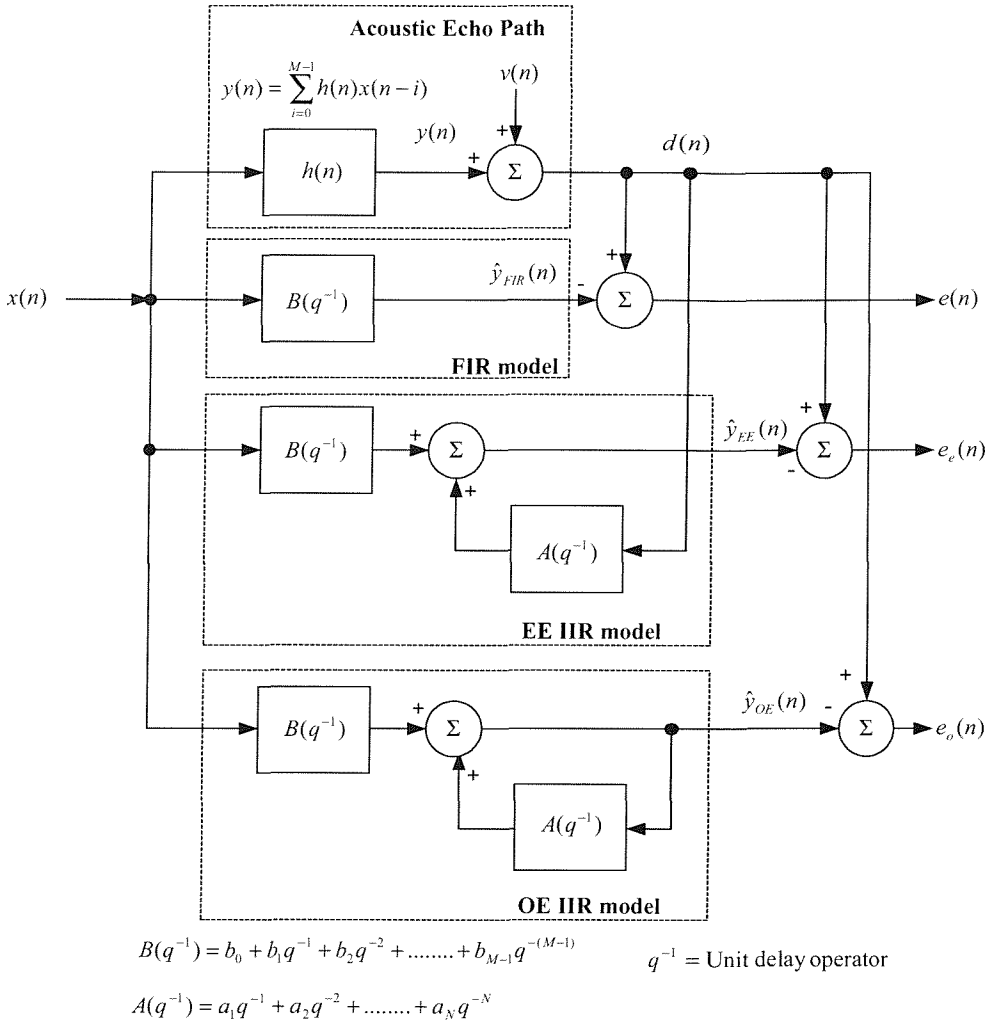


**Figure 4.8 : System Identification of echo path using FIR, OE IIR and EE IIR filter models**

In this section the aim is to assess the relative performance of FIR and IIR filter models for modelling the complete acoustic echo path responses of Section 4.3. In the next section we will review the criteria used to verify the performance of both types of model, and the parameter estimation methods used to select the optimum filter coefficients of each model. In Section 4.5 we will present the actual modelling results. Finally the issue of whether an adaptive model is needed will be addressed in Section 4.6.

### 4.5.1. Performance Comparison of FIR and IIR filter models

The primary measure of echo canceller performance is normally the level of ERLE (Echo Return Loss Enhancement) that is obtained while modelling an echo path in a system. The actual performance of each filter model will be established by using ERLE performance curves, where the ERLE level for both FIR and IIR models are plotted on the same axis against the number of coefficients used in both the models as illustrated in Figure 4.9.

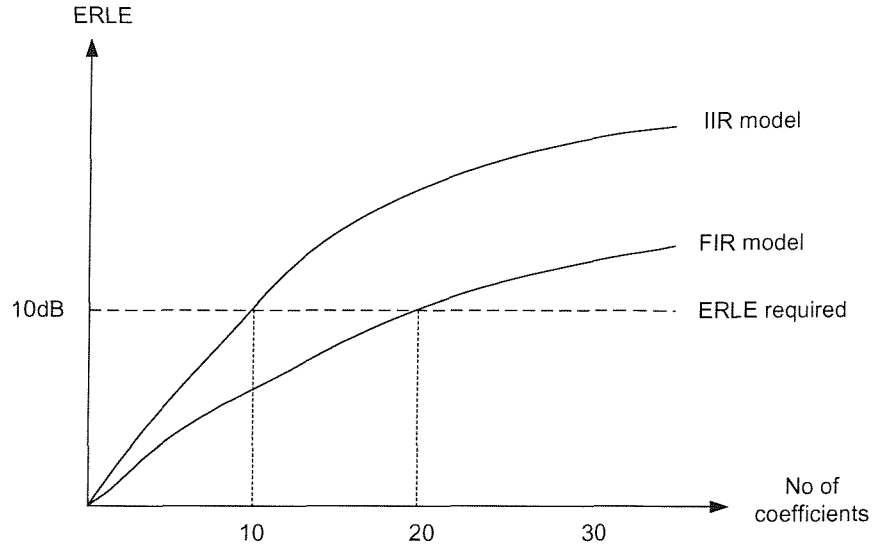


**Figure 4.9 : ERLE performance curve example**

When the required ERLE level is calculated for each handset acoustic echo path being modelled and superimposed on each curve as shown in Figure 4.9 the minimum filter orders for each model can be established to meet this required ERLE level. It is then straightforward to determine which model type is most suitable for this application, and the CRF (Coefficient Reduction Factor) possible by using this model type. It will be shown later in Section 4.5 that an IIR filter model is most suitable for acoustic echo cancellation on a mobile handset.

The system identification configuration of Figure 4.8 shall be used. The offline parameter estimation algorithms presented in Chapter 3 were used to calculate the filter model coefficients for each model order and each echo path to be modelled to maximise the ERLE (Echo Return Loss Enhancement or equivalently to minimising the mean squared error of each model type.

#### 4.5.1.1. FIR model offline parameter estimation

The optimal FIR least squares filter coefficients selected to minimise the mean square estimation error was established in (3.1.19) in Chapter 3 to be,

$$\mathbf{b}_{opt} = \mathbf{R}_{xx}^{-1}\mathbf{r}_{xd}, \tag{3.1.19}$$

Consider the definition of ERLE from (2.21), where ERLE is defined as,

$$ERLE_{dB} = 10.\log_{10}\left[\frac{E[d^2(n)]}{E[e^2(n)]}\right], \tag{2.21}$$

The mean square error (MSE) output is defined in (3.1.8) as,

$$MSE_{dB} = 10.\log_{10}\left[E[e^2(n)]\right], \tag{3.18}$$

From (3.18) and (2.21) we can see, for a stationary echo path system we have constant echo path output term $E[d^2(n)]$, that the ERLE is inversely proportional to the MSE. Minimising the MSE with respect to the model coefficients for the FIR model is equivalent to maximising the ERLE with respect to the filter model coefficients. The techniques used in Chapter 3 to minimise the MSE for an FIR filter model can be applied here directly.

From Equation (3.1.18) we can see the selection of FIR model coefficients $\mathbf{b}_{opt}$ of order M to minimise the mean square estimation error (MSE) involves a direct matrix inversion. However for the offline modelling results of this section, the computational burden of direct matrix inversion is satisfactory.

In this section of the report the FIR model coefficients of order M are found using a MATLAB implementation of equation (3.1.18). As the correlation matrix $\mathbf{R}_{xx}$ structure is of *Toeplitz* form computational simplifications can be used to compute its inverse. By computing the autocorrelation vector of the input signal over M lags using the MATLAB function xcorr(), the autocorrelation matrix $\mathbf{R}_{xx}$ can be easily constructed using the function teoplitz(). The matrix inverse may then be computed using Cholesky factorisation, implemented by the function chol(). The optimum filter coefficient vector may then be found using equation (3.1.18) in MATLAB.

#### 4.5.1.2. Output Error IIR model offline parameter estimation

The optimal Output Error IIR least squares filter coefficients are selected to minimise the mean square output estimation error (MSOE) create the recursive equations of (3.2.22) in Chapter 3,

$$\begin{aligned} E\left\{e_o(n)\left[x(n-i)+\sum_{m=1}^{N}a_m\frac{\partial\hat{y}(n-m)}{\partial b_i}\right]\right\}&=0 \quad ;0\le i\le M-1,\\ E\left\{e_o(n)\left[\hat{y}(n-j)+\sum_{m=1}^{N}a_m\frac{\partial\hat{y}(n-m)}{\partial a_j}\right]\right\}&=0 \quad ;1\le j\le N, \end{aligned} \tag{3.2.21}$$

From (3.2.22) we can see this equation is non-linear with respect to the filter coefficients $b_i$ and $a_j$. Local minima may exist, and hence it is difficult to solve directly as done n the FIR normal equations. Instead a recursive estimate is normally employed.

For the OE IIR offline modelling results the MATLAB system identification toolbox function ***oe()*** is used to compute optimum coefficients for the Output Error IIR model of order (M,N) , where M is the

number of feedforward coefficients and N is the number of feedback coefficients in the IIR model. This function uses the recursive prediction error method to minimise the MSOE [4.5].

Like the FIR filter model, minimising the MSOE with respect to the model coefficients is equivalent to maximising the ERLE for the Output Error IIR filter model with respect to the model coefficients.

#### 4.5.1.3. Equation Error IIR model offline parameter estimation

In chapter 3 we have seen in (3.3.28) and (3.2.29) that the standard Equation Error IIR model despite having a linear mean square equation error (MSEE) surface with respect to the model coefficients is subject to parameter bias in the $a_j$ coefficients when noise term $v(n)$ in Figure 4.8 is non-zero. This is also the case as discussed in chapter 3 for system identification when under modelling noise exists. To overcome this an extension to basic Equation Error model can be used based on the Steiglitz McBride system identification method. As we have shown in Chapter 3 Section 3.3.3 this gives a modified MSEE surface which is still linear with respect to the filter coefficients in the IIR model, allowing the similar techniques as the FIR model to be used.

Like the FIR filter model, minimising the MSEE with respect to the model coefficients is equivalent to maximising the ERLE for the Equation Error IIR filter model with respect to the model coefficients. Using the Steiglitz McBride scheme the IIR optimal least squares filter coefficients selected to minimise the mean square equation error (MSEE) with respect to the model coefficients is as follows,

$$\boldsymbol{\theta}_{opt} = \mathbf{R}_{\varphi_{fe}\varphi_{fe}}^{-1}\mathbf{r}_{d_f\varphi_{fe}}, \tag{3.3.88}$$

From equation (3.3.48) we can see the selection of equation error IIR model coefficients $\boldsymbol{\theta}_{opt}$ to minimise the mean square estimation equation error (MSEE) involves a direct matrix inversion. For the offline modelling results of this section, the computational burden of direct covariance matrix inversion is satisfactory.

For the EE IIR offline modelling results the signal processing toolbox function ***stmbc()*** is used to compute optimum coefficients for the Equation Error IIR model of order (M,N) , where M is the number of feedforward coefficients and N is the number of feedback coefficients in the IIR model. This function employs a MATLAB implementation of equation (3.3.48). Initial pole vector pre-filtering is done using a prony() initialisation. A direct inversion of pre-filtered covariance matrix is then used over a number of iterations to compute optimum coefficients for the Steiglitz McBride Equation Error IIR model of order (M,N).

#### 4.5.1.4. Model Order Distribution

Having established the process for selecting coefficients to maximise ERLE in each model it is necessary to establish what respective filter orders need to be used for each of these models. An IIR model of order (M,N) coefficients is equivalent to an FIR model of M+N coefficients as follows,

$$M_{FIR} = M_{IIR} + N_{IIR}, \tag{4.3}$$

For the modelling results presented in this Chapter the model coefficient range of 18,22,26 to 62 coefficients is used. For FIR filter models the total number of coefficients $M_{FIR}$ is simply equal to the total number of coefficients in each experiment, so $M_{FIR}$ varies from 18,22,26 to 62.

For IIR filter models different numbers of feedforward and feedback coefficients are used. The total model coefficient order ranges varies from 18 to 62 as with the FIR model. Different numbers of feedback coefficients $N_{IIR}$ are used of 7 to 27 coefficients are used. The feedforward coefficients $M_{IIR}$ in the IIR model are adjusted so (4.3) holds for each experiment. For the coefficient range of 18,22,26 to 62 coefficients a feedforward coefficient vector of $N_{IIR}$=7 coefficients, gives the IIR filter model orders (11,7), (15,7),(19,7) to (35,7).

#### 4.5.1.5. Coefficient Reduction Factor

A coefficient reduction factor can then be computed for both models, for the number of coefficients to meet the required ERLE level, defined as,

$$CRF = \frac{\text{Number of FIR coeffcients to meet ERLE}_{\text{req}}}{\text{Number of IIR coefficients to meet ERLE}_{\text{req}}}, \tag{4.4}$$

A simple inspection of both the ERLE curve and the CRF value indicates the most suitable filter model for modelling the echo path impulse response. The higher the CRF value, the lower the number of coefficients required in the IIR model to meet the ERLE requirements in comparison to the FIR model. A CRF greater than unity is needed to offset any increase in complexity or degradation in performance when using adaptive IIR models instead of adaptive FIR models for a particular application. From the simple example of Figure 4.9, for a required ERLE of 10dB, a CRF of 2 is calculated from (4.4). In this example the IIR model clearly is the most suitable filter model for modelling the echo path.

## 4.6. Narrowband 8kHz Echo Path Modelling Results

In this section FIR and IIR modelling results are presented for the narrowband echo path impulse responses of section 4.4. The modelling results showing the performance of FIR and IIR models (both Equation and Output Error) for each echo path response are shown in Figure 4.10 to Figure 4.15. These modelling results are summarised in Table 4-2 and Table 4-3.

| Echo Path Response | ERLE Required (dB) | Required Model Order | | | CRF |
|---|---|---|---|---|---|
| | | FIR | Equation Error | Output Error | |
| Artificial Ear Sealed response | 0 | - | - | - | - |
| Face Up No Seals response | 13 | 22 | (15,11) | (15,7) | 1 |
| Loudspeaker Adhesive Tape Sealed Response | 4 | 18 | (11,7) | (11,7) | 1 |
| Loudspeaker and Microphone Adhesive Tape Sealed Response | 6 | 22 | (15,7) | (11,11) | 1 |
| Microphone Adhesive Tape Sealed Response | 9 | 34 | (19,7) | (19,7) | 1.55 |
| Face Down response | 16 | 54 | (31,11) | (27,15) | 1.29 |

**Table 4-2: Required model orders for FIR and IIR filter models to meet the required ERLE of each echo path. The Coefficient Reduction (CRF) is calculated for each echo path**

From Table 4-2 it can be seen the face down echo path response represents the worst acoustic conditions in terms of the number of modelling coefficients required. A maximum model order of 42 coefficients is required for an IIR filter model to meet the required ERLE of each echo path. For an output error IIR filter model the model order required is (27,15) – 27 feedforward coefficients and 15 feedback coefficients. For an equation error IIR filter model the model order required is (31,11) – 31 feedforward coefficients and 11 feedback coefficients. For an FIR filter model 54 coefficients are required giving a Coefficient Reduction Factor of up to 1.29.

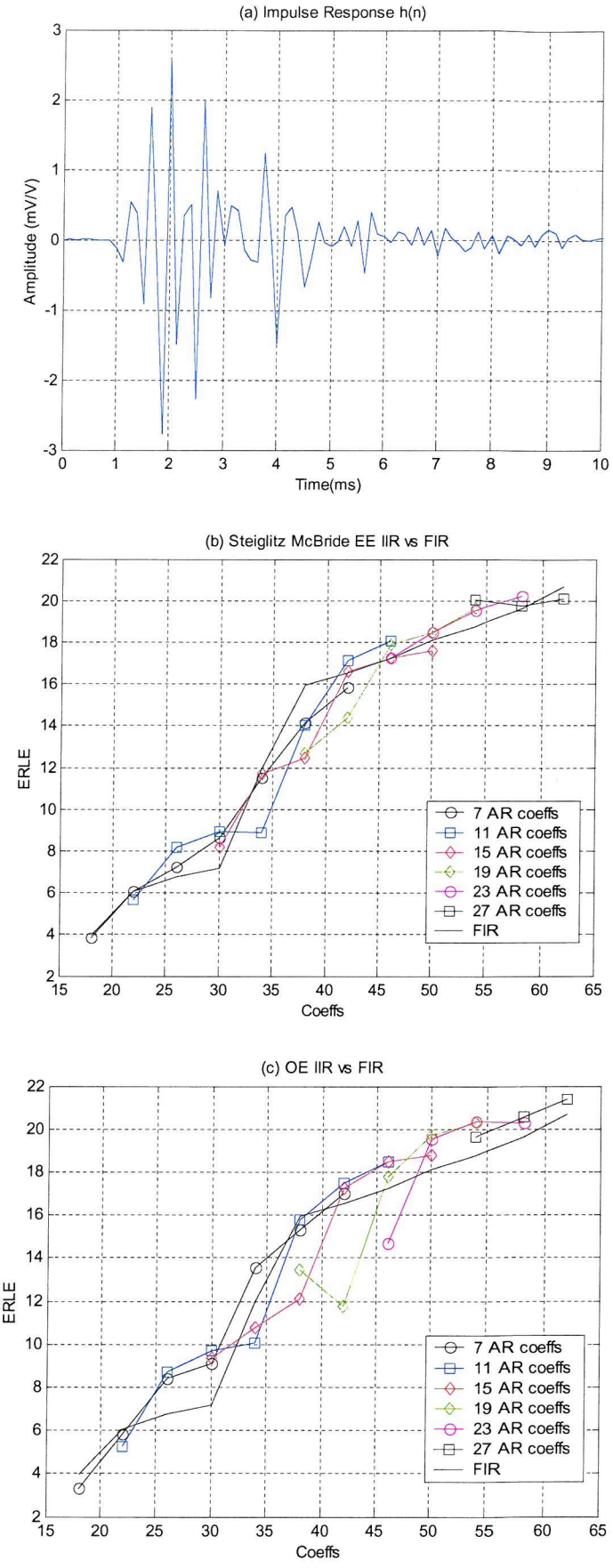


**Figure 4.10: Offline Modelling results for the narrowband artificial ear sealed echo path response**

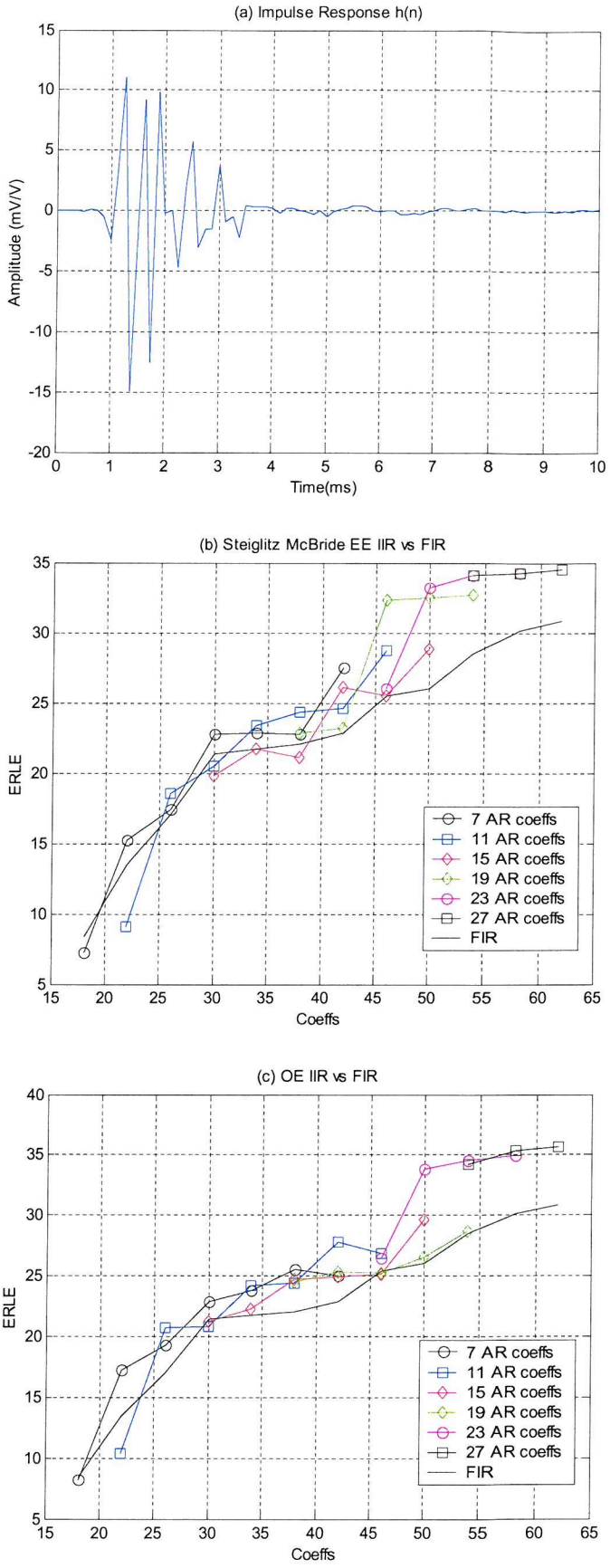


**Figure 4.11: Offline Modelling results for the narrowband artificial ear sealed echo path response**

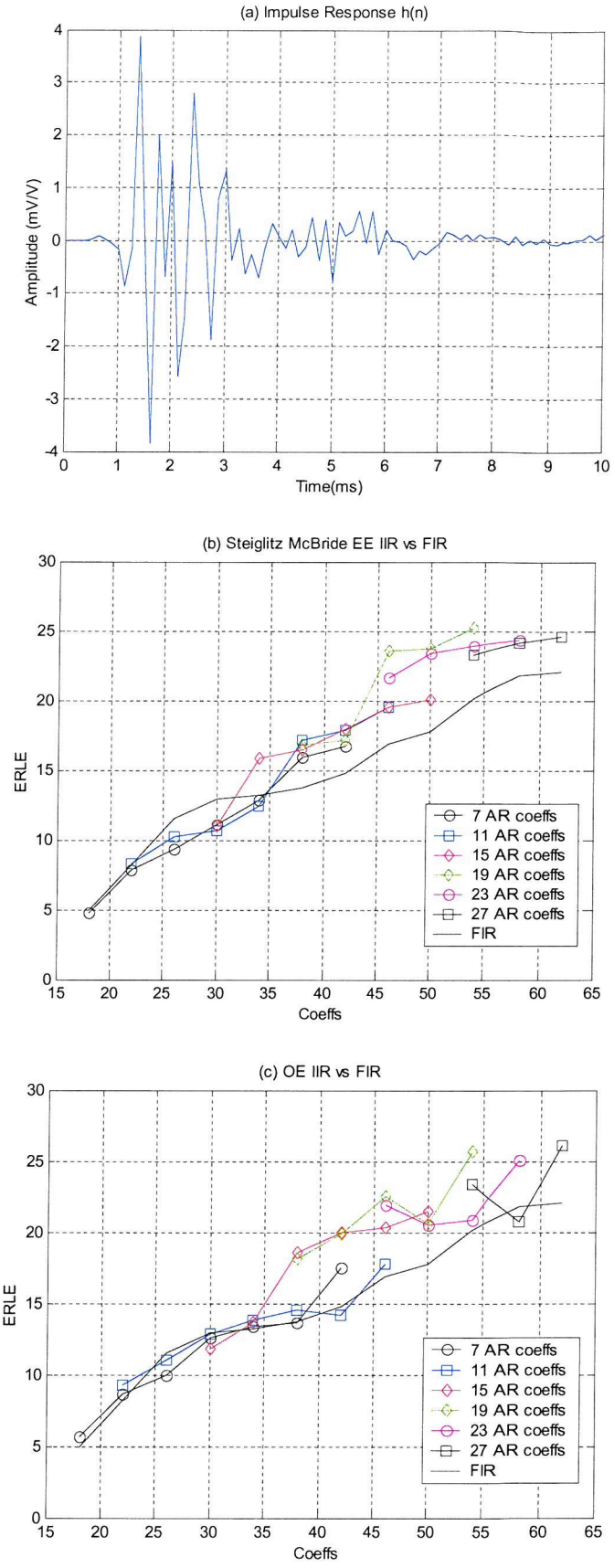


**Figure 4.12 : Offline Modelling results for the narrowband loudspeaker adhesive tape sealed echo path response**

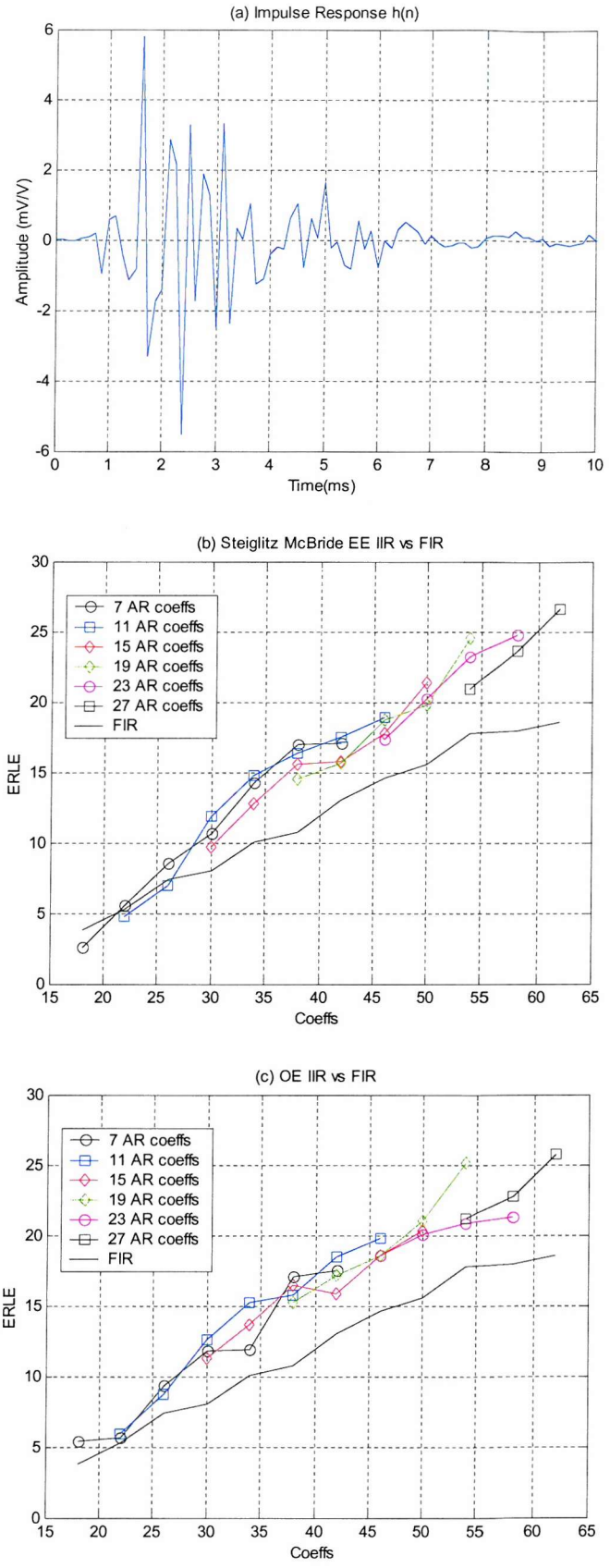


**Figure 4.13 : Offline Modelling results for the narrowband loudspeaker and microphone adhesive tape sealed echo path response**

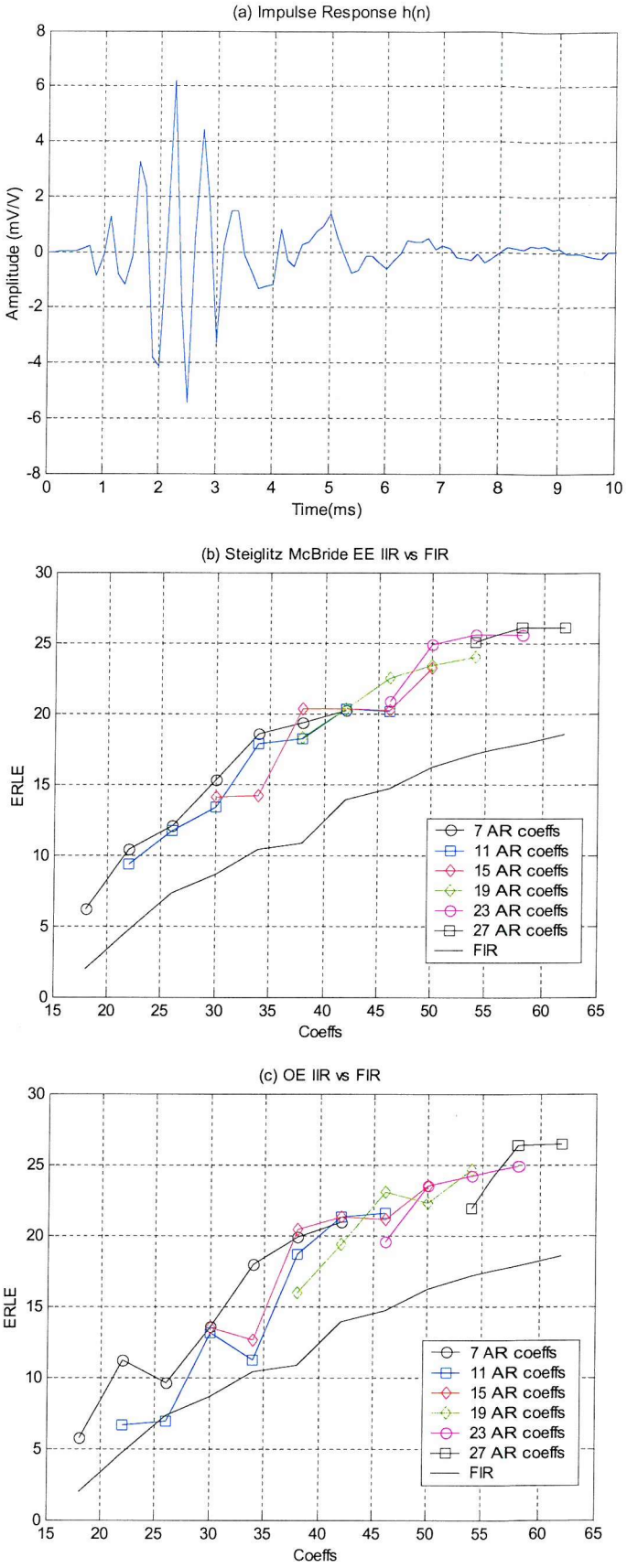


**Figure 4.14 : Offline Modelling results for the narrowband microphone adhesive tape sealed echo path response**

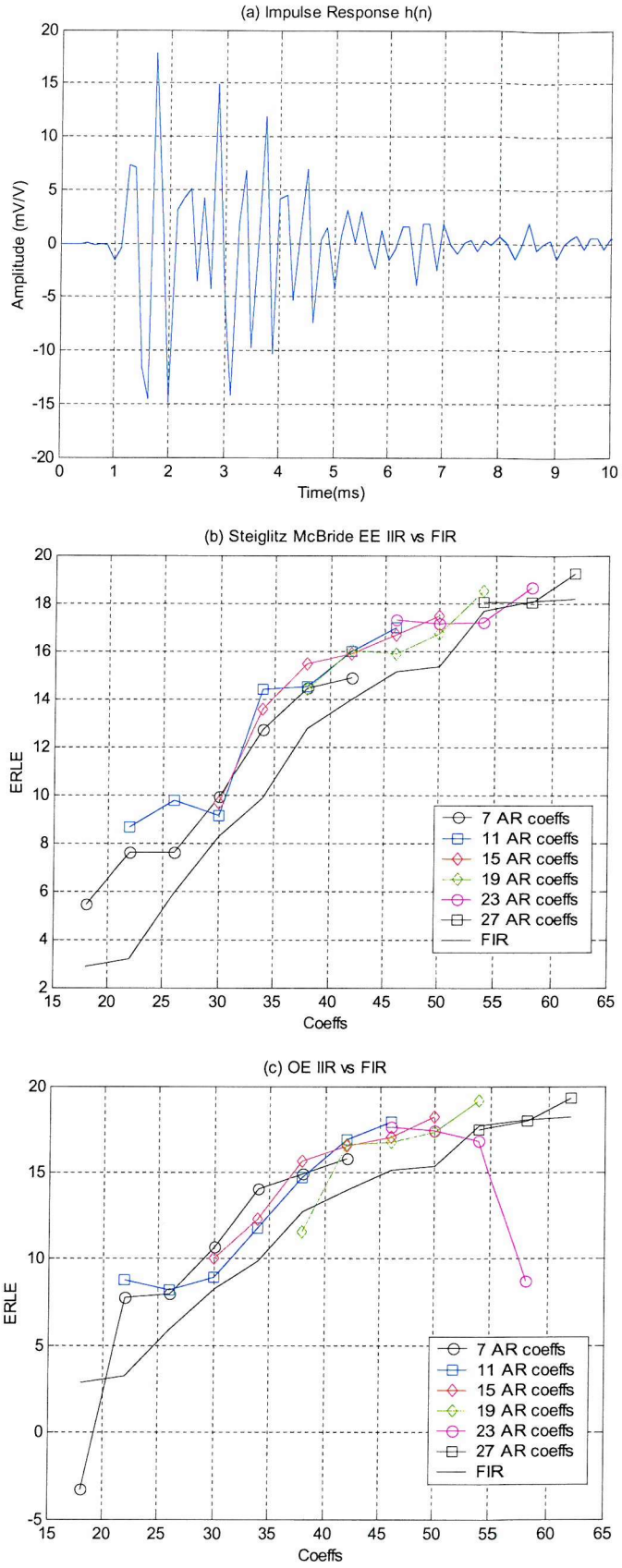


**Figure 4.15: Offline Modelling results for the narrowband face down tape sealed echo path response**

| Echo Path Response | ERLE gain over FIR model for total model order of 42 coefficients | |
|---|---|---|
| | Equation Error | Output Error |
| Artificial Ear Sealed response | 1.8 | 2 |
| Face Up No Seals response | 0.6 | 0.7 |
| Loudspeaker Adhesive Tape Sealed Response | 3.1 | 5.2 |
| Loudspeaker and Microphone Adhesive Tape Sealed Response | 4.5 | 2.8 |
| Microphone Adhesive Tape Sealed Response | 6.5 | 7.4 |
| Face Down response | 2 | 2.5 |

**Table 4-3: ERLE gain of IIR filter models over FIR filter models for a total model order of 42 coefficients.**

From Table 4-3 it can be seen for an output error IIR filter model of order (27,15) an ERLE gain of up to 7.4dB is possible over an FIR filter model with the same number of coefficients. For an equation error IIR filter model of order (31,11) an ERLE gain of up to 6.5dB is possible over an FIR filter model with the same number of coefficients.

It should also be noted at this point that incorporating a tap delay line in both the FIR and IIR models can be used to account for the small activity of 1ms (8 coefficients) in echo path responses presented in section 4.4. Incorporating this delay line makes no differences to the relative ERLE performance of both FIR and IIR models, and will only serve to shift the ERLE curves to the left (by approximately 8 coefficients on the x-axis). This will be considered at a later stage in the thesis when complexity issues are discussed.

In summary it can be concluded that from the offline modelling results presented there is a clear benefit in using an IIR filter over an FIR filter to model the narrowband acoustic echo path of a mobile handset. Fewer filter coefficients are required (CRF upto 1.29) and a gain in ERLE performance can be obtained (upto 7.4dB).

## 4.7. Wideband Echo Path Modelling Results

In this section FIR and IIR modelling results are presented for the wideband echo path impulse responses of chapter 2. The modelling results showing the performance of FIR and IIR models (both Equation and Output Error) for each echo path response are shown in Figure 4.16 to Figure 4.21.

Using the knowledge that the face down echo path response represents the worst acoustic conditions in terms of the number of modelling coefficients required. The number of model coefficients needed to obtain the required ERLE of this echo path response will determine the required model order for this application. A maximum model order of 50 coefficients is required for an IIR filter model to meet the required ERLE of each echo path. For an output error IIR filter model the model order required is (31,19) – 31 feedforward coefficients and 19 feedback coefficients. For an equation error IIR filter model the model order required is (27,23) – 27 feedforward coefficients and 13 feedback coefficients. For an FIR filter model 74 coefficients are required giving a Coefficient Reduction Factor of up to 1.48.

From Table 4-3 it can be seen for an output error IIR filter model of order (31,19) an ERLE gain of up to 9.4dB is possible over an FIR filter model with the same number of coefficients. For an equation error IIR filter model of order (27,23) an ERLE gain of up to 9.1dB is possible over an FIR filter model with the same number of coefficients.

| **Echo Path Response** | **ERLE gain over FIR model for total model order of 50 coefficients** | |
|---|---|---|
| | Equation Error | Output Error |
| Artificial Ear Sealed response | 1.6 | 2.1 |
| Face Up No Seals response | 7.1 | 4.7 |
| Loudspeaker Adhesive Tape Sealed Response | 4.9 | 2.8 |
| Loudspeaker and Microphone Adhesive Tape Sealed Response | 6.1 | 6.5 |
| Microphone Adhesive Tape Sealed Response | 9.4 | 9.1 |
| Face Down response | 4 | 4 |

**Table 4-4: ERLE gain of IIR filter models over FIR filter models for a total model order of 42 coefficients.**

In summary it can be concluded that from the offline modelling results presented there is a clear benefit in using an IIR filter over an FIR filter to model the narrowband acoustic echo path of a mobile handset. Fewer filter coefficients are required (CRF upto 1.48) and a gain in ERLE performance can be obtained (upto 9.4dB).

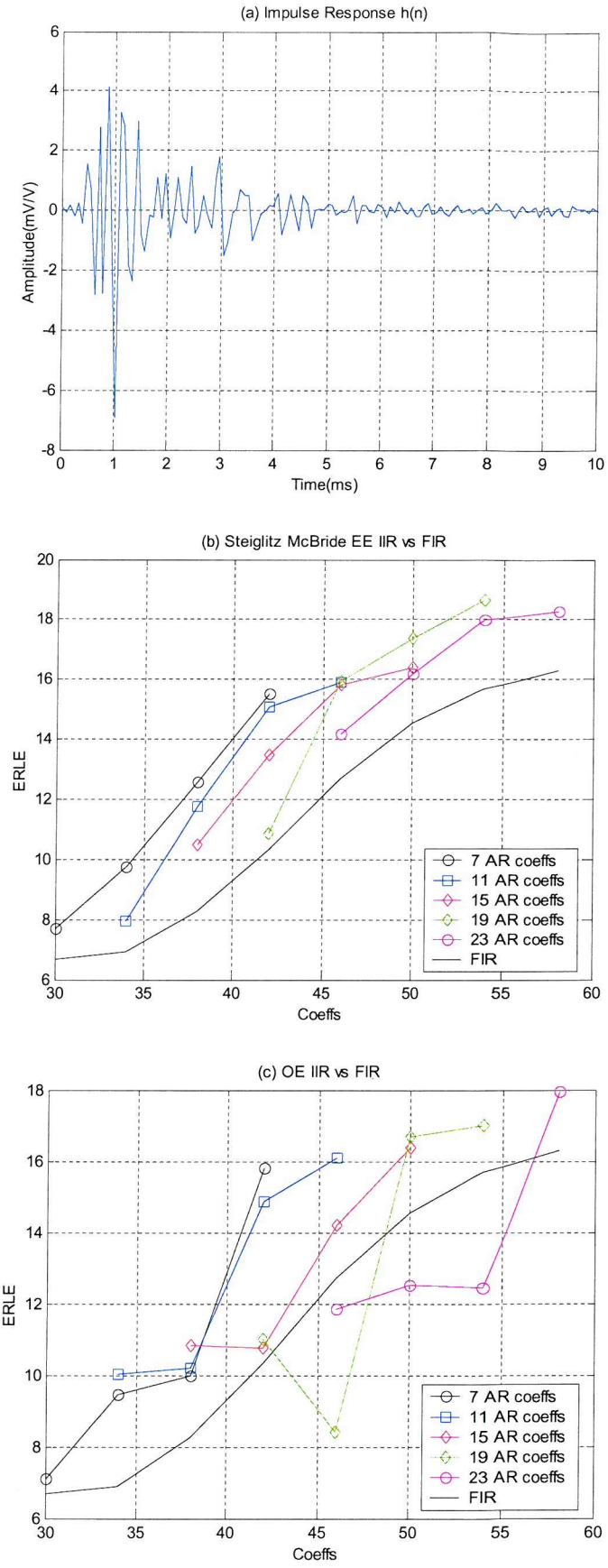


**Figure 4.16: Offline Modelling results for the wideband artificial ear sealed echo path response**

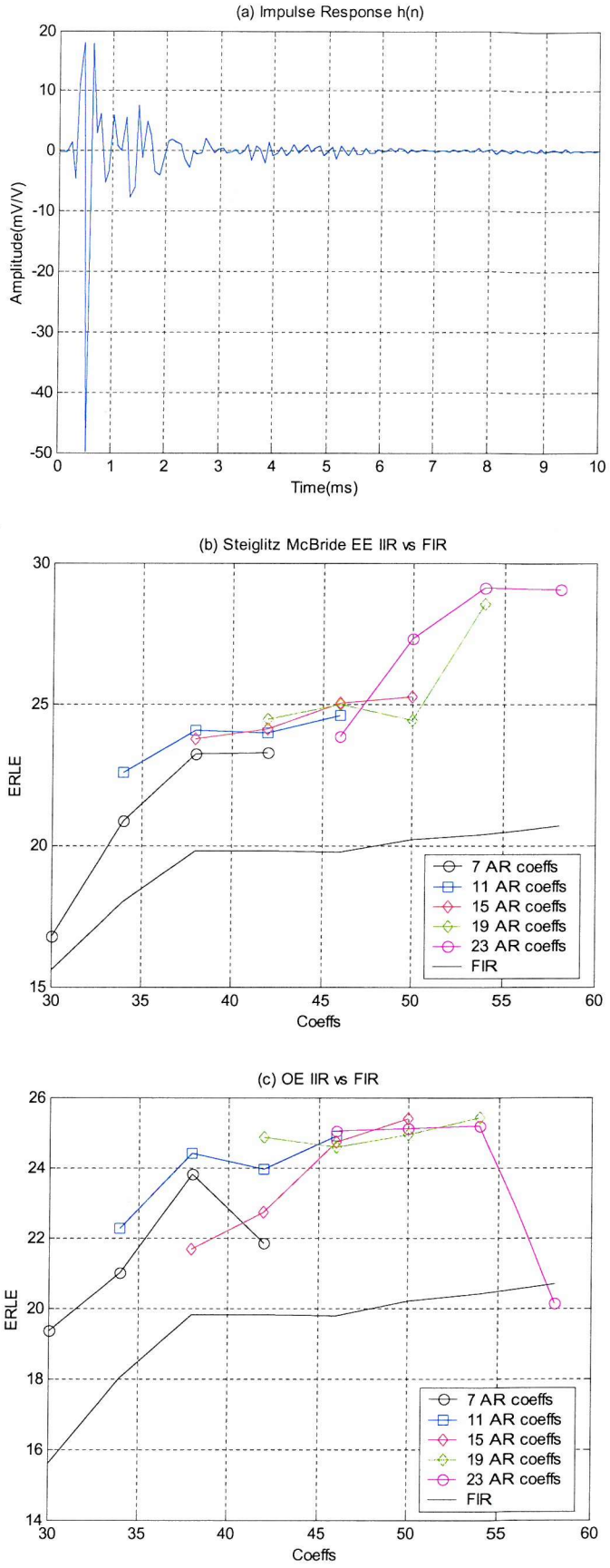


**Figure 4.17: Offline Modelling results for the wideband face up no seals echo path response**

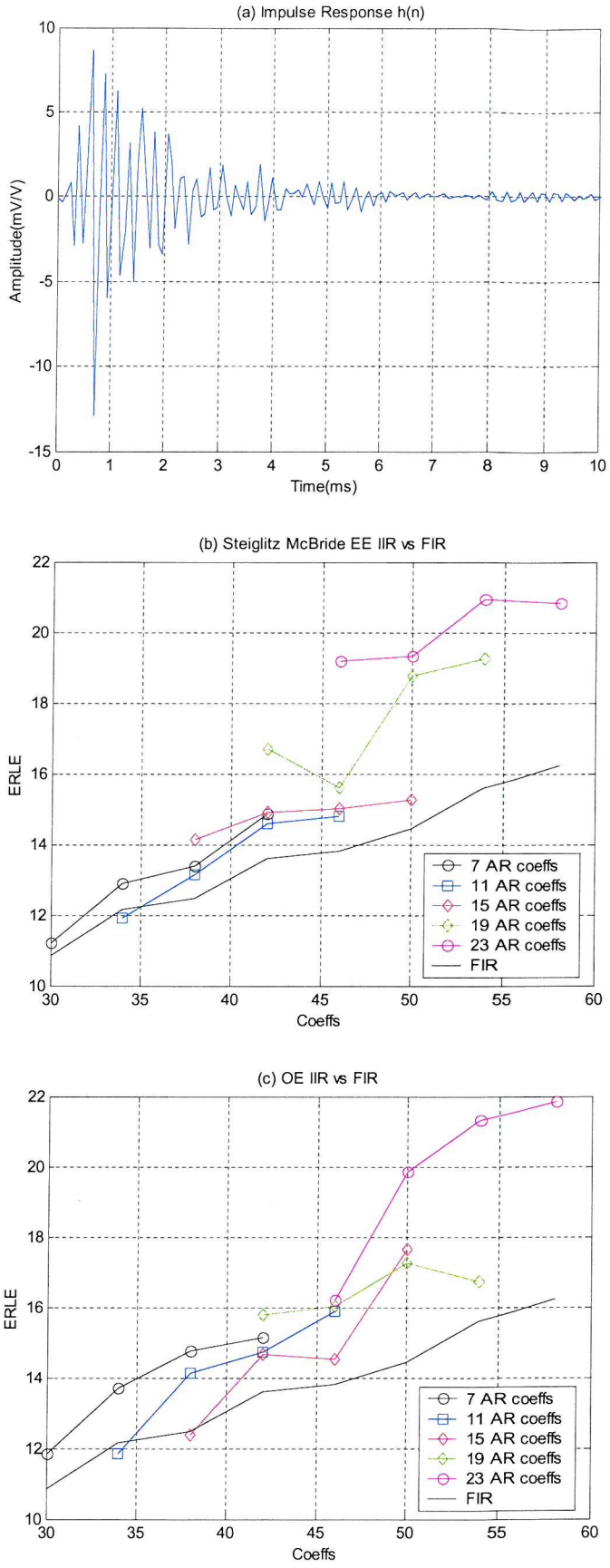


**Figure 4.18: Offline Modelling results for the wideband loudspeaker adhesive tape sealed echo path response**

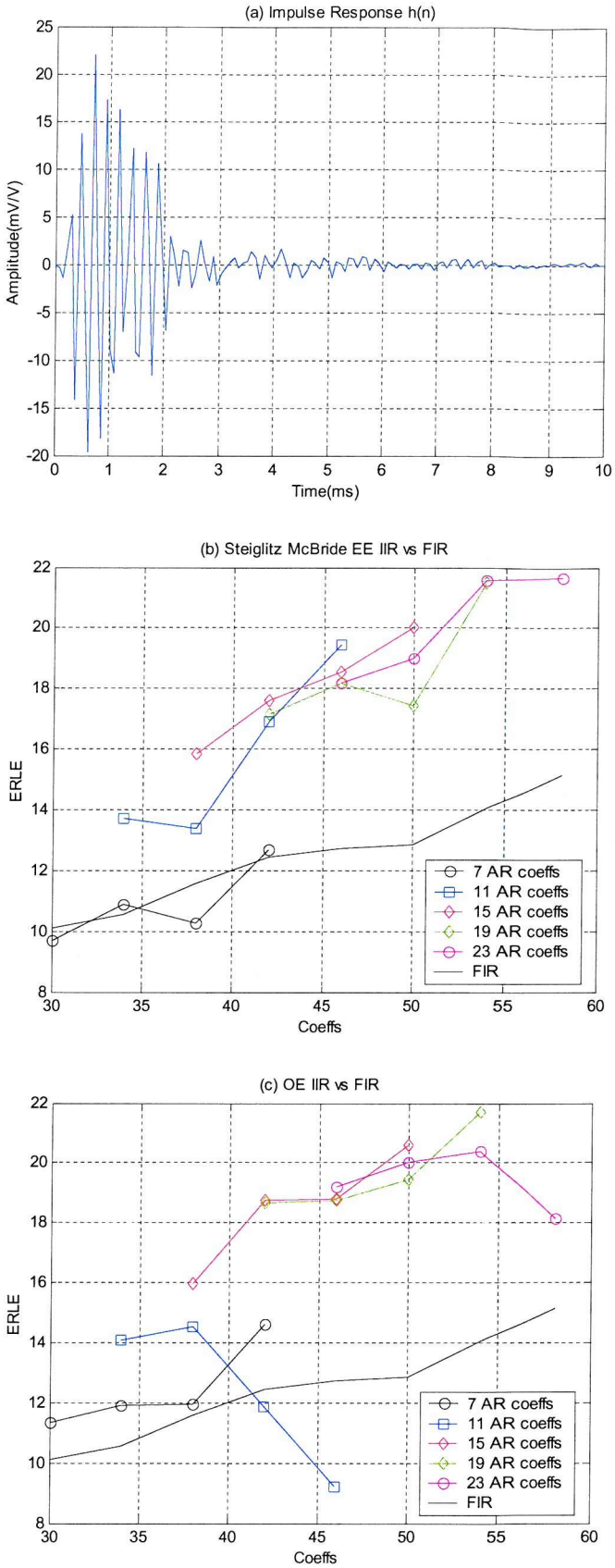


**Figure 4.19: Offline Modelling results for the wideband loudspeaker and microphone adhesive tape sealed echo path response**

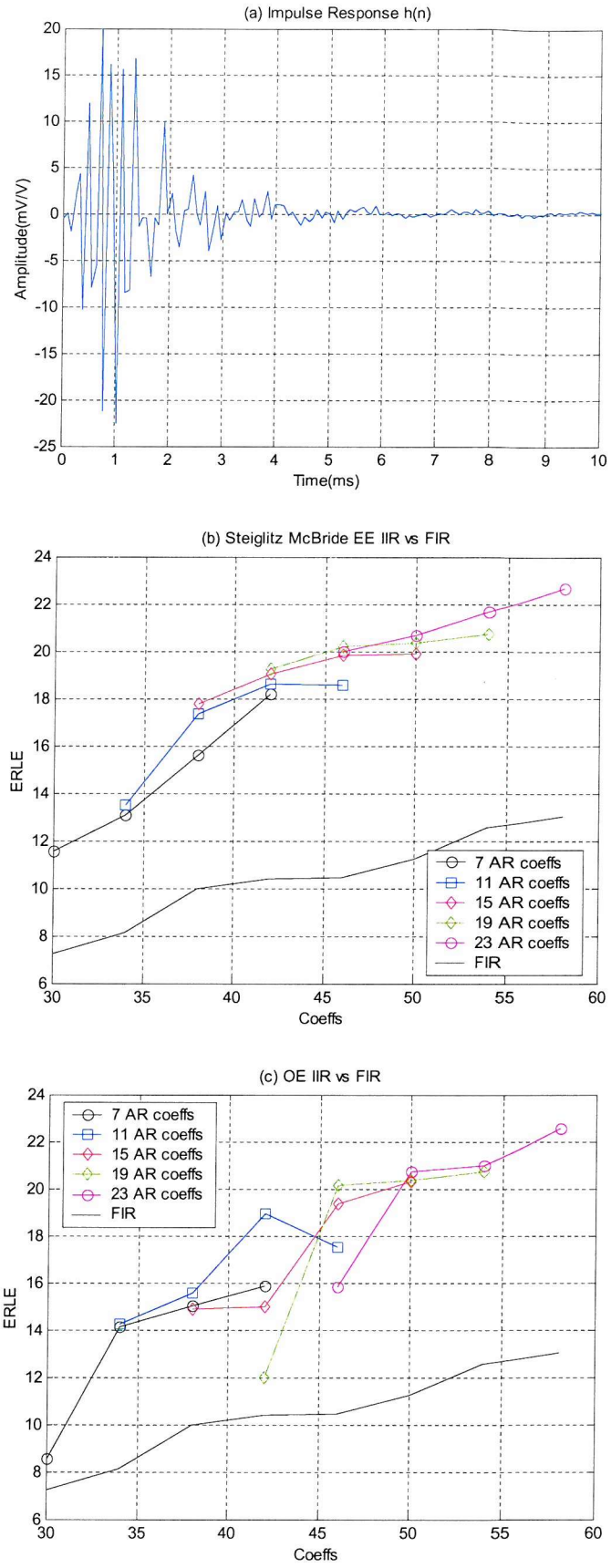


**Figure 4.20: Offline Modelling results for the wideband microphone adhesive tape sealed echo path response**

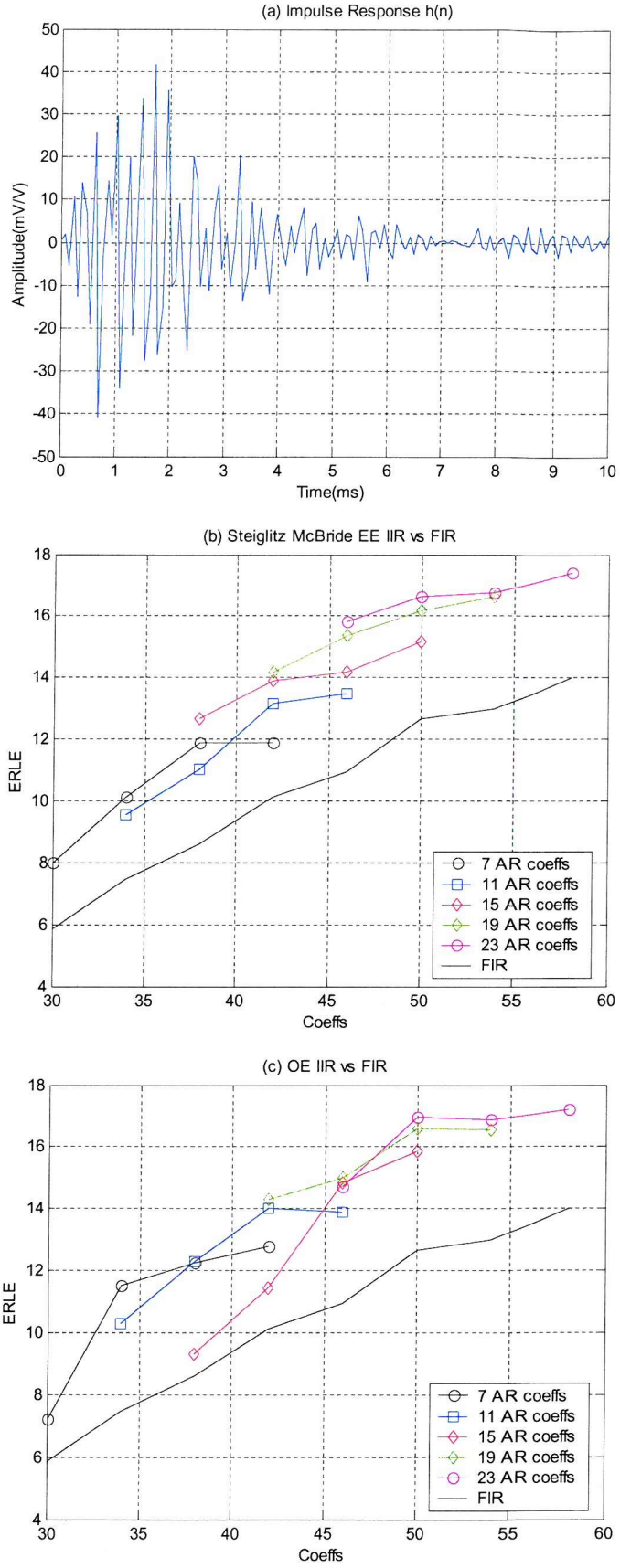


**Figure 4.21: Offline Modelling results for the wideband face down echo path response**

## 4.8. The need for an adaptive IIR filter model

An important point often neglected in most filter model analysis literature [4.2],[4.3] is whether the filter model type used is required to be adaptive. In chapter 2 we have seen how the echo path variation can be large depending on the handset configuration/orientation. We have seen in sections 4.6 and 4.7 how an IIR filter model is best suited to model the full range of echo path variation possible in normal handset use. What is not clear so far however is whether the IIR filter model is required to be adaptive to model the full echo path variation in normal use. If an adaptive IIR model is needed, do the feedforward and feedback sections of the IIR filter model are required to be adaptive?

To determine whether the IIR filter model for echo cancellation on a mobile handset is required to be adaptive an output error IIR filter model used of order (25,17). Only the variation in the narrowband echo path responses of section 4.5 are considered.

To determine whether an adaptive IIR model is needed, the feedforward and feedback coefficient vectors produced by this output error model when modelling the narrowband echo path models of section 4.4 are analysed. From the results presented is a strong indication a fixed IIR filter model will not be able to model the full echo path variation that may exist in normal handset use. The impact of using an IIR filter model a single set of feedforward and feedback coefficients is then investigated using an output error IIR filter model. It is clear from the modelling results presented that an adaptive IIR model is required.

To determine whether both feedforward and feedback section are required to be adaptive the impact on modelling performance of using only an adaptive feedforward section is investigated (fixed pole adaptive IIR filter). From the modelling results presented it is clear the adaptive IIR filter model must have adaptive feedforward and feedback sections when modelling the possible echo path variation in normal handset use.

### 4.8.1. The Coefficient vectors of an IIR model for narrowband echo path modelling

In previous sections we have seen modelling results for different echo path models sowing the benefit of IIR filer models for the handset echo cancellation application. What has not been established is how close the filter model coefficient values are for each of these echo path responses. That is, can an IIR model with fixed feedforward and feedback coefficient values be used to meet the ERLE requirement of each echo path?

Figure 4.22 shows the offline feedforward and feedback coefficient values calculated for an output error IIR filter model of order (27,15) for each narrowband echo path response. It can be seen clearly from this figure when modelling the possible variation of the echo path response of a mobile handset, a significant variation in the feedforward and feedback coefficient values can occur in the IIR filter model. This is a strong indication that an IIR filter model with fixed feedforward and feedback coefficients is unsuitable. An IIR filter model with adaptive coefficient values is required for this application.

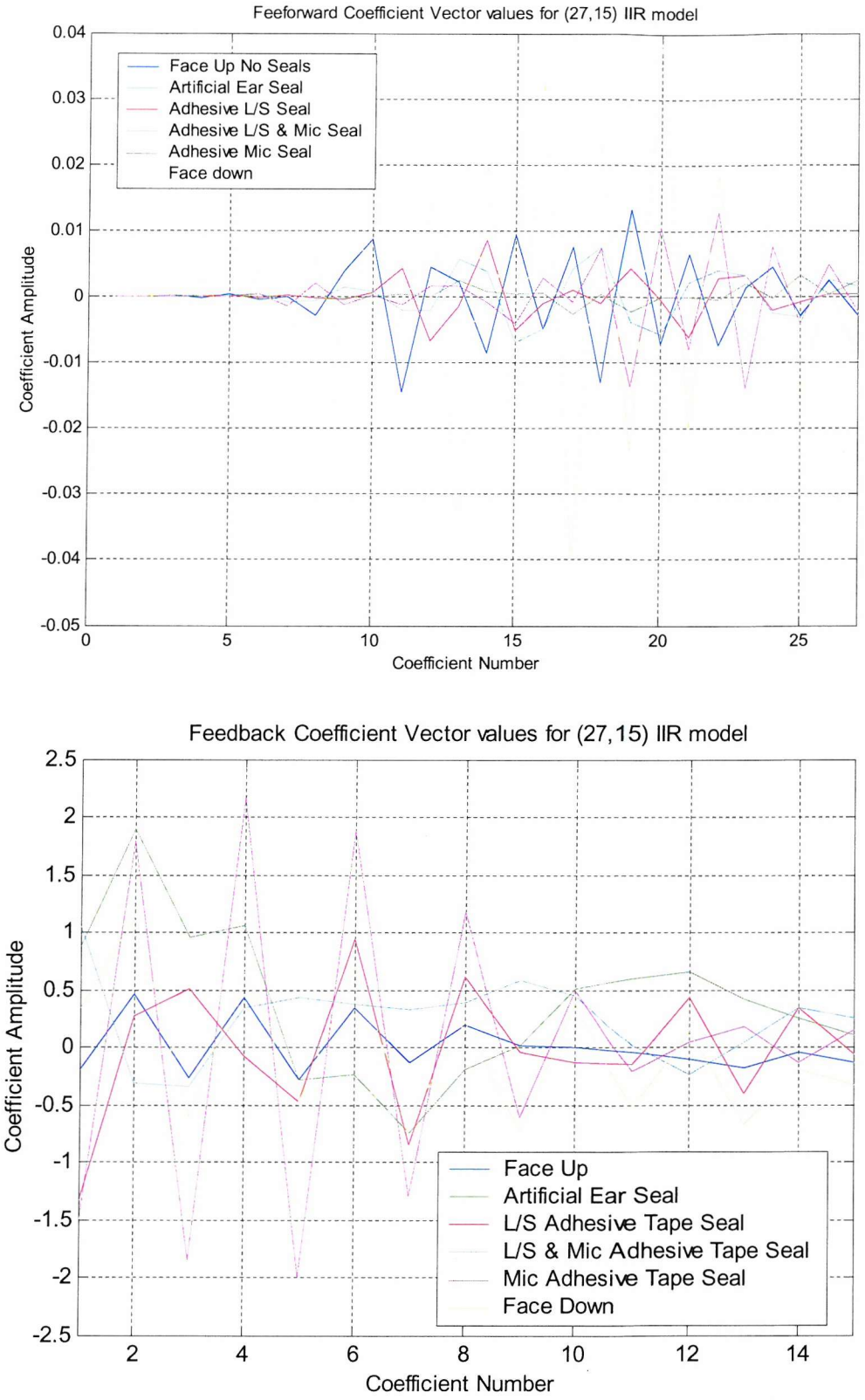


**Figure 4.22: Feedforward and Feedback Coefficient values for Output Error (27,15) IIR model**

### 4.8.2. ERLE possible using an IIR filter model with fixed feedforward and feedback coefficients

Table 4-5 shows the impact of using fixed feedforward and feedback coefficients used to model the variation in the narrowband echo path response. An IIR model of order (27,15) is used. The fixed IIR model coefficient used are the final calculated coefficient values resulting from the output error offline modelling results for each echo path in section 4.6

| Echo Path Modelled | ERLE Required | ERLE achievable in (27,15) fixed IIR model | | | | | |
|---|---|---|---|---|---|---|---|
| | | Face Up IIR model | Artificial Ear IIR model | L/S Tape Seal IIR model | L/S & Mic Tape Seal IIR model | Mic Tape Seal IIR model | Face Down IIR model |
| Face Up No Seals | 13 | 25.1 | -0.2 | -1 | -0.4 | -2.7 | -4.6 |
| Artificial Ear Seal | - | -13.6 | 16 | -5.7 | -6.7 | -9.4 | -16.3 |
| Loudspeaker Adhesive Tape Seal | 4 | -10.4 | -1.8 | 20 | -6.4 | -8.2 | -11.8 |
| Loudspeaker and Microphone Adhesive Tape Seal | 6 | -7.5 | -0.5 | -4.1 | 18.1 | -2.2 | -10.6 |
| Microphone Adhesive Tape Seal | 9 | -6.5 | 0.1 | -2.6 | 1.1 | 21.1 | -6.6 |
| Face Down | 16 | -1.9 | -0.25 | 0.3 | -0.7 | -0.1 | 16.6 |

**Table 4-5 : ERLE achievable using a fixed IIR model for each echo path for NEC G9 handset**

From Table 4-5 the IIR model coefficients calculated for each echo path response modelled are used to model the echo path variations of all other echo paths. It is clear from the poor ERLE levels of Table 4-5 that a single fixed IIR filter model cannot be used to model all possible echo path variations in normal handset use. An adaptive IIR filter model is required.

### 4.8.3. ERLE possible using an IIR filter model with fixed feedback coefficients

In the last section it was established that an adaptive IIR model is required to model the handset variation in normal handset use. However it is not clear whether the IIR model has to be fully adaptive, that is, do both the feedforward and feedback coefficients need to be adapted to satisfy the required ERLE of each echo path modelled.

Figure 4.23 shows the structure of a fixed feedback section adaptive IIR model. This is also referred to as a fixed pole adaptive IIR model [4.6][4.7]. Table 4-6 shows the ERLE modelling performance using the structure of Figure 4.23 in order to determine whether both feedforward and feedback coefficients need to be adaptive to model the possible echo path variation in normal handset use. An IIR model order of (27,15) is used. The fixed pole/coefficient vectors used are the final calculated coefficients resulting from the output error offline modelling results for each echo path in section 4.6. Only the narrowband echo path variations in normal handset use are modelled.

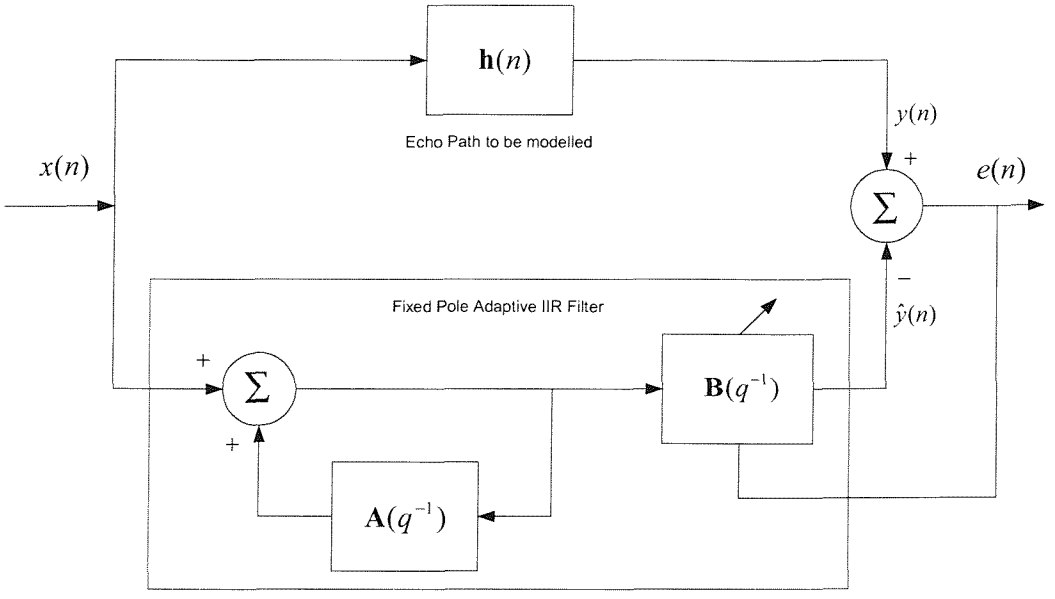


**Figure 4.23: Fixed Pole Adaptive IIR filter model**

From Table 4-6 it is clear that an adaptive IIR model with fixed feedback coefficients cannot sufficiently model the possible echo path variation in normal handset use. An adaptive IIR filter model is required with adaptive feedforward and feedback coefficients.

## 4.9. Summary

In this chapter converted echo path responses were presented showing the variation in the complete echo path response to be modelled by an echo canceller in normal handset use. Using these echo path responses modelling results were presented showing the benefits of using an IIR filter model over the more traditional FIR filter model for acoustic echo cancellation on a mobile handset.

| Echo Path Modelled | ERLE Required | ERLE achievable in (27,15) fixed pole Adaptive IIR model | | | | | |
|---|---|---|---|---|---|---|---|
| | | Face Up IIR model | Artificial Ear IIR model | L/S Tape Seal IIR model | L/S & Mic Tape Seal IIR model | Mic Tape Seal IIR model | Face Down IIR model |
| Face Up No Seals | 13 | 25.1 | -16.3 | 13.9 | 11.7 | 16.2 | 11.7 |
| Artificial Ear Seal | - | -11 | 16 | 5.6 | 5.6 | 6.8 | 6.3 |
| Loudspeaker Tape Seal | 4 | 11 | 4 | 20 | 8.5 | 12.4 | 8.7 |
| Loudspeaker and Microphone Tape Seal | 6 | -4.8 | 6.5 | 7.7 | 18.1 | 12.3 | 6.7 |
| Microphone Tape Seal | 9 | 7.9 | 6.7 | 8.4 | 5.4 | 21.1 | 5.2 |
| Face Down | 16 | 6.2 | -16.8 | 3.9 | 5.7 | 4.3 | 16.6 |

**Table 4-6 : ERLE achievable using a fixed pole IIR model for each echo path for NEC G9 handset**

During the thesis the main objective was the narrowband echo path response with a bandwidth of 300 to 3400Hz, as found in most GSM handsets today. Modelling results presented in this chapter show that a Coefficient Reduction Factor of up to 1.29 is possible using an IIR filter to model the variation possible in the narrowband echo path response of a mobile handset in normal use. An Output Error IIR model of (27,15) was identified to achieve this Coefficient Reduction Factor. For this model order an ERLE gain of up to 7.4dB is possible over an FIR filter model with the same total number of coefficients. An Equation Error IIR model of (31,11) was also identified to achieve this Coefficient Reduction Factor. For this model order an ERLE gain of up to 6.5dB is possible over an FIR filter model with the same total number of coefficients.

At the time of writing this thesis, due to new audio and video applications, wideband speech codecs have been developed with an audio bandwidth of 50-7000Hz. Modelling results are presented showing that with an IIR filter model a Coefficient Reduction Factor of up to 1.48 can be obtained with an ERLE gain of up to 9.4dB over an FIR filter model with the same total number of coefficients. These results show for future mobile handsets with wideband codecs, an IIR filter model is more suited to handset acoustic echo cancellation than a more traditional FIR filter model.

In the final part of this chapter modelling results are presented to show that an adaptive IIR model must be used to model the possible variation in the handset echo path response in normal handset use. Having established in this chapter that an IIR model is more suited to model the echo path response of a mobile handset, and that the IIR model needs to be adaptive, the next chapter looks at the modelling performance of adaptive IIR algorithms over adaptive FIR algorithms.

# Chapter 5

## 5. System Identification of the Acoustic Echo Path of a Mobile Handset using Adaptive IIR Filtering

### 5.1. Introduction

In chapter 4 complete acoustic echo path responses were presented which represent the full range of echo path variation likely in normal handset use. Modelling results were presented for narrowband and wideband echo path models using non-adaptive FIR and IIR filter models over a range of model orders. The coefficient values for each model were computed offline. A clear benefit in modelling performance was observed by using an IIR filter model to model the echo path of a mobile handset.

The main goal of this chapter is to assess whether adaptive IIR filters models have benefits in modelling performance over adaptive FIR filters when modelling the narrowband acoustic echo path of a mobile handset. In order to achieve this chapter 5 is split into 2 main parts.

The first part is section 5.2. Section 5.2 is a direct extension of chapter 4, where adaptive FIR and IIR filter models are now used to model the narrowband echo path of a mobile handset in normal use. No echo path output noise is used. Using the adaptive algorithms presented in chapter 3, the steady state modelling performance of adaptive FIR and IIR algorithms is established using stationary input signals. It is clear from the results presented that adaptive IIR algorithms do offer benefits in modelling performance over adaptive FIR algorithms, and that the gains in performance reported in chapter 4 are still valid for adaptive IIR filter models. It is also clear that LMS Newton based adaptive IIR filters are required to model the handset echo path effectively.

The second part is section 5.3. Since in the handset echo cancellation application environment noise will also be present on the handset microphone in addition to acoustic echo, it is important to also assess the steady state modelling performance of adaptive algorithms in the presence of echo path output noise. Section 5.3 repeats all the modelling experiments of Section 5.2 for the LMS Newton based adaptive algorithms presented in chapter 3 over a range of Echo to Noise Ratios (ENR). From the results presented it is clear an Output Error adaptive IIR filtering algorithm is required for this application. The low ENR levels possible in the handset acoustic echo path application make Equation Error adaptive IIR algorithms unsuitable for this application. In particular only the Simplified Gradient LMS Newton based algorithms of chapter 3 can maintain the gains in performance reported in chapter 4 when modelling the acoustic echo path of a mobile handset in the presence of output noise. The Simplified Gradient LMS Newton based algorithms of chapter 3 will be used for further algorithm development in later chapters.

## 5.2. System Identification of the Echo Path Response of a Mobile Handset in the Absence of Output Noise

### 5.2.1. Assessment Criteria

In order to determine the modelling performance benefits of adaptive IIR algorithms over their FIR counterparts when modelling the acoustic echo path of a mobile handset, it is first of necessary to establish what criteria will be used to compare the modelling performance of both types of adaptive algorithms.

In Chapter 3 the misadjustment of an adaptive FIR algorithm was introduced. In a stationary context, this Misadjustment level can be related to accuracy of convergence to the optimal solution in the steady state [5.1]. The misadjustment of an adaptive filter can be defined as [5.1],

$$\mathcal{M} = \frac{F_{ex\infty}}{F_{\min}} = \frac{E[\left(e(n) - e_{opt}(n)\right)^2]}{E[e_{opt}^2(n)]}, \tag{5.1}$$

which is the ratio of excess steady state mean square error $F_{ex\infty}$ of the adaptive model, to the minimum mean square error $F_{\min}$. For adaptive FIR algorithms $F_{\min}$ is the minimum mean square error as a result of the optimal solution of (3.1.19). At first thought the misadjustment would seem a good method for assessing tracking performance for an adaptive IIR algorithm, since the smaller $\mathcal{M}$ is the more accurate the adaptive filtering solution is for the echo path being modelled. The main problem of using the misadjustment for adaptive IIR algorithms arises in the calculation of the minimum mean square error ($F_{\min}$) for an Output Error adaptive IIR algorithm, as we have already seen in Chapter 3. The other problem is that the misadjustment measure alone contains no information about the convergence of the adaptive algorithm, only the steady state accuracy after convergence.

As an alternative to misadjustment, a measure more suited for adaptive IIR algorithms is the ensemble averaged ERLE level. This measure also serves as a more direct way of comparing the steady state modelling capabilities of adaptive algorithms to the offline results of Chapter 4. For convenience the ERLE is firstly redefined as follows,

$$ERLE_{dB} = 10\log_{10}\left[\frac{E[d^2(n)]}{E[e^2(n)]}\right] = 10\log_{10}\left[\frac{\sum_{n=0}^{M-1} d^2(n)}{\sum_{n=0}^{M-1} e^2(n)}\right], \tag{5.2}$$

From (5.2) we can see the ERLE is defined as the ratio of echo path output power $E[d^2(n)]$ to the modelling error signal power $E[e^2(n)]$ in decibels, calculated as a time average, where M represents the length of recorded sequences $d(n)$ and $e(n)$. The ensemble averaged ERLE level is then defined as follows,

$$ERLE_{en}(m) = 10\log_{10}\left[\frac{1}{P}\sum_{p=1}^{P}\left(\frac{\sum_{j=0}^{L-1} d_p^2(mL+j)}{\sum_{j=0}^{L-1} e_p^2(mL+j)}\right)\right], \tag{5.3}$$

where $P$ is the number of repeated trials for each modelling experiment required for ensemble average estimate $ERLE_{en}(m)$. Each $ERLE_{en}(m)$ is calculated in 32ms frames (L=256 @ 8kHz) from sequences $d_p(n)$ and $e_p(n)$ in each trial $p = 1 \cdots P$. The steady state ensemble averaged ERLE value is finally defined as

$$ERLEss_{dB} = 10\log_{10}\left[\frac{1}{K}\sum_{k=N-K}^{N-1} 10^{\left\{\frac{ERLE_{en}(k)}{10}\right\}}\right]. \tag{5.4}$$

From (5.4), due to practicalities of simulation time, the steady state ERLE value, the $ERLEss_{dB}$ level is calculated from the last K=288ms of the ensemble averaged ERLE level, $ERLE_{en}(n)$. For slower converging algorithms or inappropriate choice of parameters, this will result in a final state, but not steady state ERLE level, during the allowed 10s adaption period.

In assessing the steady state modelling performance it is important to calculate the final converged steady state ERLE level for comparison with the reported levels in Chapter 4. However for the acoustic echo cancellation application the time taken to reach this steady state level, and the required ERLE level of each echo path modelled is also important. As a result, two additional measures of convergence speed are used. The first is measure of the time taken for the adaptive model to reach the required ERLE level for the echo path being modelled. This measure is termed $TIC_{req}$ and is defined as,

$$TIC_{req} = m * 32ms \text{ for } ERLE_{en}(m) = ERLE_{req}. \tag{5.5}$$

where $ERLE_{req}$ is the required ERLE level of the echo path response being modelled . The second convergence speed measure is the time taken for the adaptive model to reach its steady state ERLE level for the echo path being modelled. This measure is termed $TIC_{ss}$ and is defined as,

$$TIC_{ss} = m * 32ms \text{ for } ERLE_{en}(m) = ERLEss_{dB}. \tag{5.6}$$

where $ERLEss_{dB}$ is the steady state ERLE level for the adaptive algorithm for the echo path response being modelled.

### 5.2.2. Adaptive Algorithms used for Modelling Experiments

A large number of possible adaptive IIR algorithms were presented in Chapter 3. To simplify the presentation of results and to reduce the number of experiments required in this section it is desirable to choose only a subset of the algorithms of Chapter 3 to answer the two main points of this section. The first point is what the most suitable model order is for Equation Error and Output Error adaptive IIR

algorithms, and what Coefficient Reduction Factor is possible? The second point is of the possible LMS and LMS Newton based adaptive IIR algorithm forms presented in Chapter 3, which are most suitable in terms of steady state ensemble averaged ERLE level and convergence time when modelling the acoustic echo path of a mobile handset.

In this section only four of the adaptive algorithms of Chapter 3 are used to establish the steady state modelling properties of adaptive IIR algorithms over adaptive FIR algorithms for the handset acoustic echo cancellation application in the absence of output noise. For stationary input signals and a suitable choice of stepsize, similar performance is obtained for LMS and Normalised LMS algorithms, and LMS Newton and Normalised LMS Newton algorithms, so only Normalised LMS and LMS Newton forms are simulated.

To assess modelling capabilities of Output Error adaptive IIR LMS based algorithms, the Normalised LMS Simplified Gradient algorithm is used. To assess modelling capabilities of Output Error Adaptive IIR LMS Newton based algorithms, the LMS Newton Simplified Gradient algorithm is used.

To assess modelling capabilities of Equation Error adaptive IIR LMS based algorithms, the Normalised LMS Equation Error algorithm is used. To assess modelling capabilities of Equation Error Adaptive IIR LMS Newton based algorithms, the LMS Newton Equation Error algorithm is used.

### 5.2.3. System Identification Experiment Configuration

In order to answer the question of what input signals will be used, and what echo path responses will be modelled, the system identification configuration used in each modelling experiment will now be discussed.

Figure 5.1 shows the system identification configuration used to perform the required modelling experiments of this section [5.1]. It can be seen no echo path output noise is present, and the echo paths to be modelled are fixed for the duration of each system identification experiment. To begin with only the face up no seals echo path response of Chapter 4 is used to determine the effect of algorithm parameters on modelling performance. Once the most suitable parameters have been chosen for each adaptive algorithm modelling results for all the echo path responses of Chapter 4 will be presented.

From Figure 5.1 each modelling experiment consists of a single adaptive algorithm operating on echo path input signal $x(n)$ and output signal data $d(n)$ from a single echo path response $\mathbf{h}$. The echo path response $\mathbf{h}$ is defined as a vector of L echo path response samples given by,

$$\mathbf{h} = [h(0), h(1), ...., h(L-1)]^T, \tag{5.7}$$

For each system identification experiment an input signal of duration 10s and sample rate 8 kHz (N=80000 samples) is used. A band-limited pink noise signal input $x(n)$ as used in Chapter 4 to represent the long-term average spectrum characteristics of a speech signal is re-used in this Chapter to allow the convergence behaviour of adaptive algorithms to be investigated. Note for a FIR adaptive filter $\mathbf{A}(n, q^{-1}) = \mathbf{0}$.

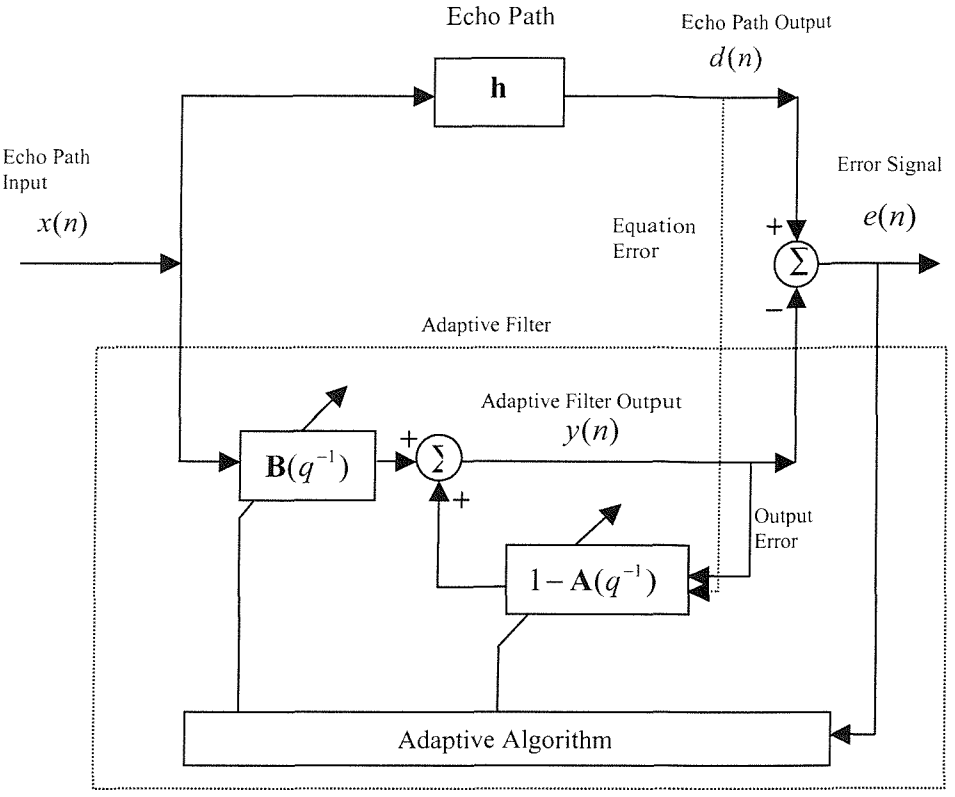


**Figure 5.1 : System Identification Configuration**

A model order range of 30 to 58 coefficients is simulated for each adaptive algorithm and echo path to be modelled, with different feedforward to feedback coefficient ratios. The echo path responses presented in Chapter 4 are used here to represent the variation in handset response to be modelled by an echo canceller in normal use. Each modelling experiment is repeated $P$=20 times, where different random noise seeds are used for the band-limited pink noise signal input $x(n)$ in each repeated trial, in order to compute ensemble average estimate $ERLE_{en}(n)$. Once the ensemble averaged level $ERLE_{en}(n)$ is computed the steady state ERLE value, $ERLEss_{dB}$, and convergence times $TIC_{ss}$ and $TIC_{req}$ are recorded. Once $ERLEss_{dB}$ is computed for each echo path to be modelled over a range of model orders for each adaptive algorithm a Coefficient Reduction Factor as defined in Chapter 4 can be computed to see whether the performance benefits presented in Chapter 4 are still valid.

The adaptive algorithm parameters chosen for each modelling experiment are selected as a trade off between steady state ensemble averaged ERLE level, and convergence time. The effect of adaptive algorithm parameters on $ERLEss_{dB}$ and convergence time is discussed in the following sections.

### 5.2.4. The effect of NLMS Adaptive Algorithm design parameters on Steady State modelling performance

To establish the effect of NLMS algorithm parameters on steady state modelling performance the FIR NLMS algorithm, the Simplified Gradient Output Error NLMS adaptive IIR algorithm, and the Equation Error NLMS adaptive IIR algorithms will be used. Consider the original forms of these algorithms as follows,

$$\mathbf{b}_{n+1} = \mathbf{b}_n + \frac{\mu}{\delta + \mathbf{x}^T(n)\mathbf{x}(n)}\mathbf{x}(n)e(n), \tag{3.1.51}$$

$$\boldsymbol{\theta}_{n+1} = \boldsymbol{\theta}_n + \frac{\mu}{\delta + \boldsymbol{\varphi}_f^T(n)\boldsymbol{\varphi}_f(n)}e_o(n)\boldsymbol{\varphi}_f(n), \tag{3.2.66}$$

$$\boldsymbol{\theta}_{n+1} = \boldsymbol{\theta}_n + \frac{\mu}{\delta + \boldsymbol{\varphi}_e^T(n)\boldsymbol{\varphi}_e(n)}e_e(n)\boldsymbol{\varphi}_e(n), \tag{3.3.41}$$

From the discussion on FIR adaptive algorithms presented in Chapter 3 it was seen that algorithm stability and Misadjustment for NLMS algorithms depends on the filter order, input signal characteristics and the stepsize $\mu$. From (5.1) and (5.2) it can be seen that the Misadjustment is approximately inversely proportional to the ERLE level. In order see the effect of NLMS adaptive algorithm parameters on the modelling performance, the relationships between convergence time, steady state $ERLEss_{dB}$ level, stepsize $\mu$, filter order, and the input signal characteristics need to be investigated for both adaptive FIR and adaptive IIR algorithms. To explore the relationship between model order, stepsize, convergence time and $ERLEss_{dB}$ three different model orders are used. A lowest model order range for all modelling experiments of 30 coefficients is used, in addition to a middle range model order of 42 coefficients, and a maximum model order of 58 coefficients.

#### 5.2.4.1. The FIR NLMS adaptive algorithm

Figure 5.2 to Figure 5.5 shows the $ERLEss_{dB}$ and convergence times achievable for these model orders for a FIR NLMS algorithm for both a white noise and band limited pink noise signal input. This is the outcome of modelling the face up handset echo path response with no transducer seals of Chapter 4.

The achievable $ERLEss_{dB}$ vs. stepsize $\mu$ has a well-defined behaviour for the FIR NLMS algorithm. By looking at the resulting convergence times in Figure 5.4 and Figure 5.5 it can be seen at low stepsize values below $10^{-4}$ for white noise input, and $10^{-3}$ for a band-limited pink noise input the convergence of the FIR NLMS algorithm is much slower. This will result in a roll-off of $ERLEss_{dB}$ achievable within the 10s adaption period used. The achievable $ERLEss_{dB}$ level levels off

between stepsize levels of $10^{-4}$ and $10^{-3}$ to for white noise input, and $10^{-3}$ and $10^{-2}$ for band-limited pink noise input. Above these ranges the $ERLEss_{dB}$ level rolls off due to the dependency of the Misadjustment of (3.1.47) for the FIR NLMS on the stepsize value $\mu$ as discussed in Chapter 3. Beyond stepsize levels of approximately 0.025, instability rapidly occurs. The $ERLEss_{dB}$ level for white noise input is clearly higher than that obtained when bandlimited pink noise input is used. At the lowest model order a larger stepsize can be tolerated, due to the dependency of the stability limit of (3.1.45) on the model order of the filter.

From Figure 5.4 and Figure 5.5 it can be seen that slower algorithm convergence occurs with bandlimited pink noise signals for the same input signal powers and stepsize value. This is expected, as discussed in Chapter 3, due to the of the FIR NLMS algorithm on the eigenvalue spread of the covariance matrix $\mathbf{R}_{xx} = E[\mathbf{x}^T(n)\mathbf{x}(n)]$. Convergence times only become similar at higher stepsize values before instability occurs where the Misadjustment becomes larger. Also for lower filter orders convergence to the steady state can be seen to occur quicker. This is due to the fact the eigenvalue spread of $\mathbf{R}_{xx}$ is a monotonically non-decreasing function of the filter length M for a coloured input signal $x(n)$, for smaller orders the eigenvalue spread may be less [5.2].

### 5.2.4.2. Homogenous Adaption Coefficients for adaptive IIR NLMS algorithms

Before looking at these relationships of the stepsize parameter $\mu$ for the Simplified Gradient NLMS and Equation Error NLMS adaptive IIR algorithms, consider the performance of these algorithms using a single stepsize $\mu$ to control the adaption of both feedforward and feedback coefficients. This is termed Group Adaption [5.3]. The ensemble averaged ERLE curves of Figure 5.6 show the relative performance of these algorithms with respect to an adaptive FIR algorithm for a bandlimited noise input signal. A stepsize $\mu$ =0.005 is used for all algorithms. This is the outcome of modelling the face up handset echo path response with no transducer seals of Chapter 4.

From Figure 5.6 it can seen that both adaptive IIR NLMS algorithms of order (27,15) have similar ensemble averaged steady state ERLE level performance to that of an adaptive FIR algorithm of 27 coefficients. This can be explained by considering the effect of the attenuation of the echo path being modelled. In Chapter 3 the equation error information vector $\varphi_e(n)$ was introduced as

$$\varphi_e(n) = [x(n),...,x(n-M+1),d(n-1),...,d(n-N)]^T, \tag{5.8}$$

From Figure 5.1 and (5.8) we can see that the information vector $\varphi_e(n)$ contains both echo path input and output signal terms. As the echo path attenuation loss of a typical mobile handset in normal use can vary between -30dB and -46dB, the echo loss of $\mathbf{h}$ will result in the echo path output signal $d(n)$ being much lower in level than the echo path input signal $x(n)$. The normalisation of both feedforward

and feedback coefficients by the term $\varphi_e^T(n)\varphi_e(n)$ occurs in (3.3.41). If we write the inner product $\varphi_e^T(n)\varphi_e(n)$ in full we get the following

$$\varphi_e^T(n)\varphi_e(n) = \sum_{i=0}^{M-1} x^2(n-i) + \sum_{j=1}^{N} d^2(n-j), \tag{5.9}$$

Since $\sum_{i=0}^{M-1} x^2(n-i) >> \sum_{j=1}^{N} d^2(n-j)$, due to the attenuation of the echo path being modelled, the normalisation of $\mu$ by $\delta + \varphi_e^T(n)\varphi_e(n)$ in (3.3.41) will lead to an inappropriately small step size value selected for the update of feedback coefficients in $\boldsymbol{\theta}_n$. This in turn will lead to virtually no AR coefficient adaption in (3.3.41), resulting in the ERLE performance of the Equation Error NLMS algorithm of order (M,N) being similar to that of an FIR NLMS algorithm of M coefficients. A similar problem also occurs with the Simplified Gradient NLMS algorithm of (3.2.66).

In order to overcome this problem it is necessary to separate the step size normalisation process for both feedforward and feedback coefficients within the vector $\boldsymbol{\theta}_n$, so as to account for the gain difference between $x(n)$ and $d(n)$ or $x_f(n)$ and $y_f(n)$. This is termed Homogenous Adaption [5.3]. The Equation Error NLMS algorithm of (3.3.41) and the Simplified Gradient Output Error NLMS algorithm of (3.2.66) can be re-written in the Homogenous Adaption forms below,

$$\mathbf{b}_{n+1} = \mathbf{b}_n + \frac{\mu_b}{\delta + \mathbf{x}_f^T(n)\mathbf{x}_f(n)} e_o(n)\mathbf{x}_f(n), \tag{3.2.66a}$$

$$\mathbf{a}_{n+1} = \mathbf{a}_n + \frac{\mu_a}{\delta + \mathbf{y}_f^T(n)\mathbf{y}_f(n)} e_o(n)\mathbf{y}_f(n), \tag{3.2.66b}$$

and

$$\mathbf{b}_{n+1} = \mathbf{b}_n + \frac{\boldsymbol{\mu}_{IIR}}{\delta + \mathbf{x}^T(n)\mathbf{x}\ (n)} e_e(n)\mathbf{x}(n), \tag{3.3.41a}$$

$$\mathbf{a}_{n+1} = \mathbf{a}_n + \frac{\mu_a}{\delta + \mathbf{d}^T(n)\mathbf{d}\ (n)} e_e(n)\mathbf{d}(n), \tag{3.3.41b}$$

where $\mathbf{x}(n)$, $\mathbf{d}(n)$, $\mathbf{x}_f(n)$ and $\mathbf{y}_f(n)$ are defined in Chapter 3. The improved performance of these Homogenous Adaption forms is shown in Figure 5.7.

The Homogenous Adaption Normalised LMS forms in (3.2.66) and (3.3.41) will be used all modelling experiments presented in this chapter. For simplicity the stepsizes $\mu_b = \mu_a$ are used in all modelling experiments.

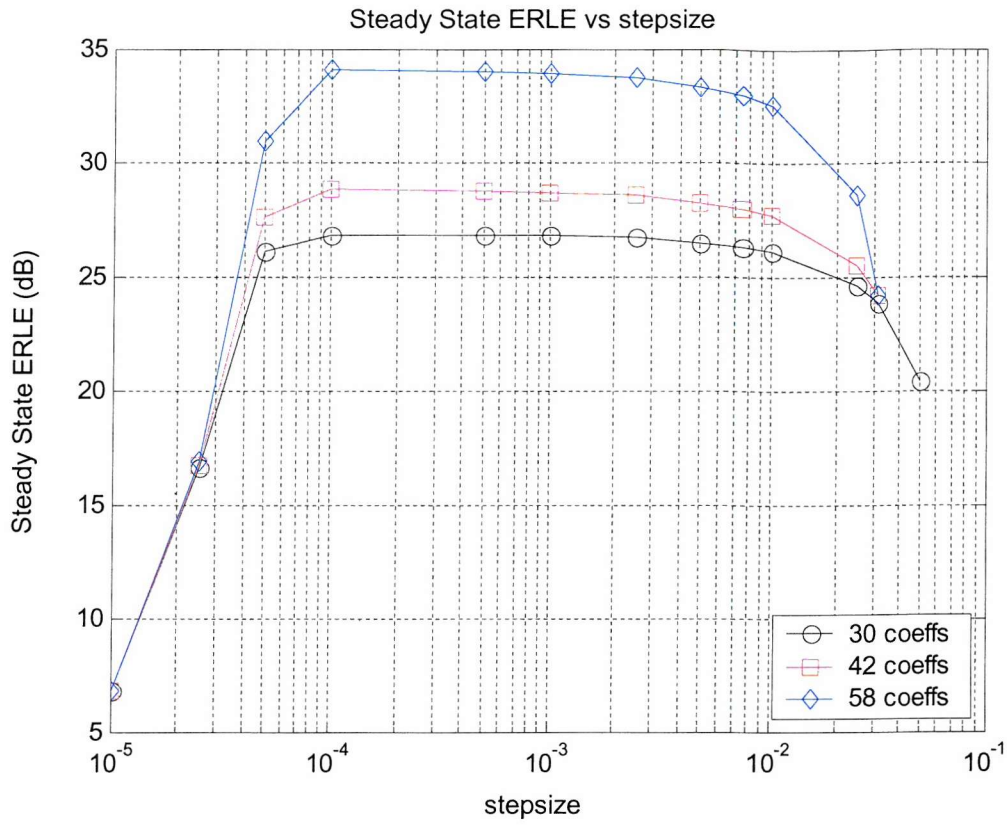


**Figure 5.2 : Steady State ERLE for the FIR NLMS vs. stepsize, for different filter orders, for white noise input**

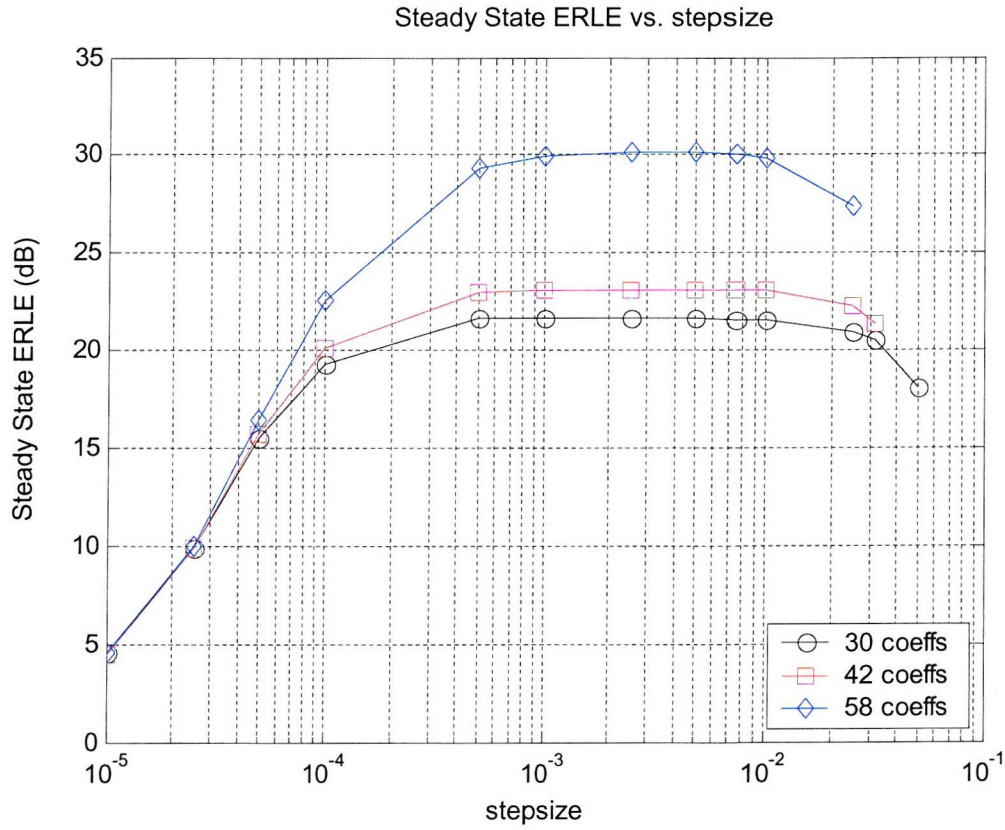


**Figure 5.3 : Steady State ERLE for the FIR NLMS vs. stepsize, for different filter orders, for band limited pink noise input**

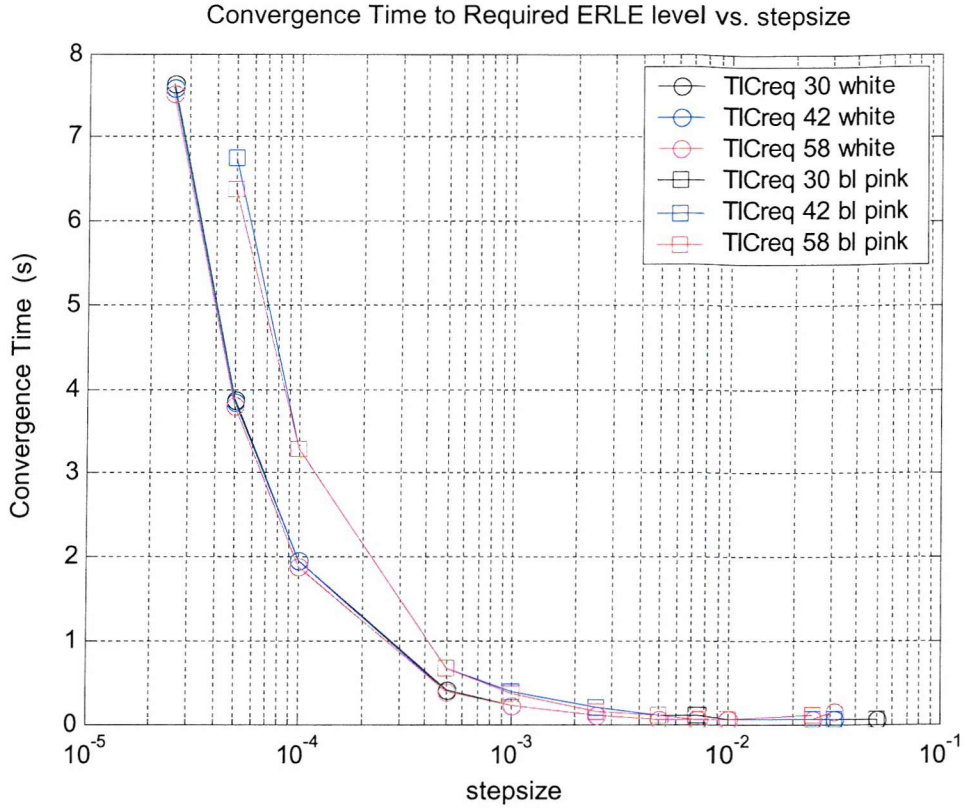


**Figure 5.4 : Convergence time to required ERLE for FIR NLMS vs. stepsize, for different filter orders**

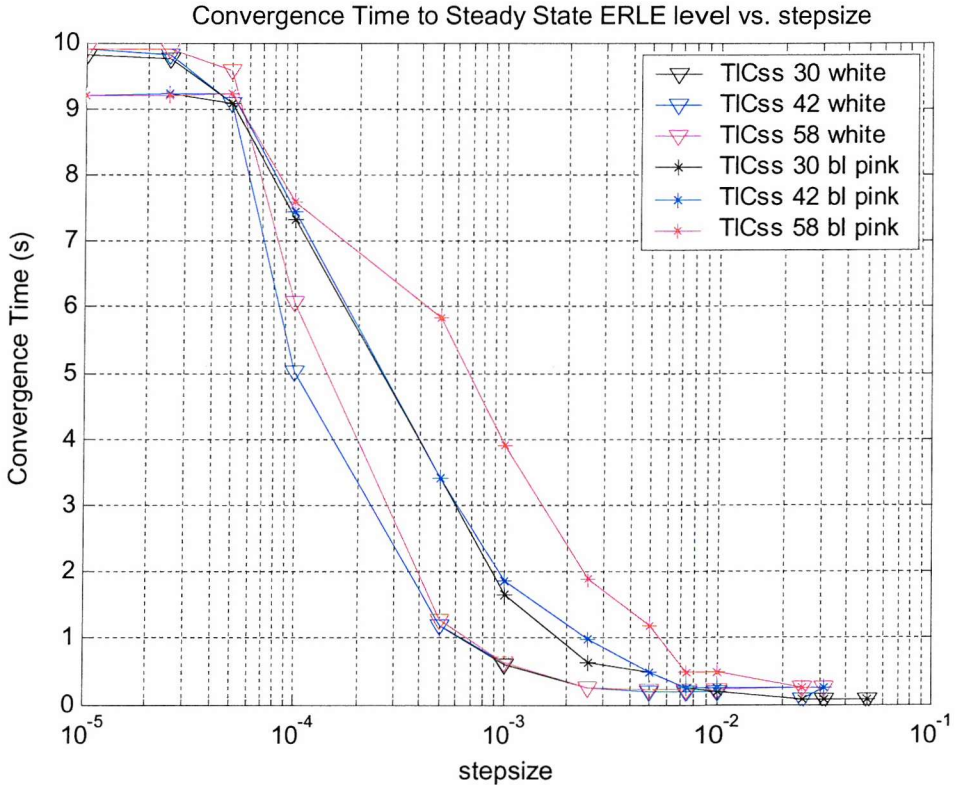


**Figure 5.5 : Convergence time to Steady State ERLE level for FIR NLMS vs. stepsize, for different filter orders**

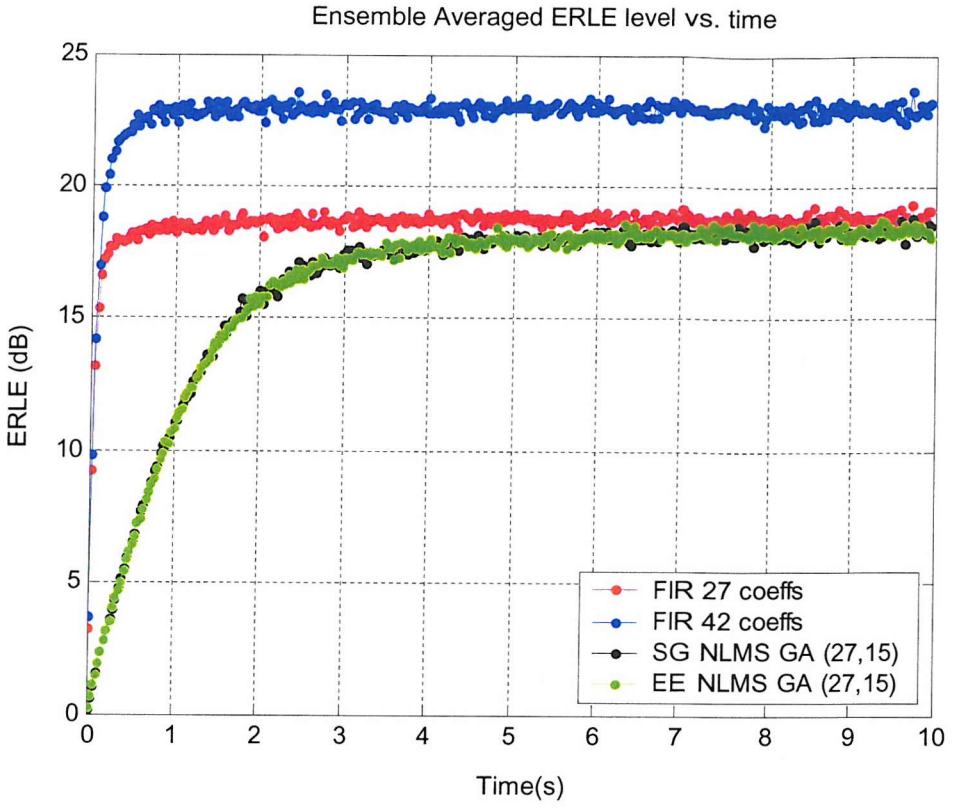


**Figure 5.6 : Adaptive IIR NLMS adaption using single stepsize for feedback and feedforward coefficients**

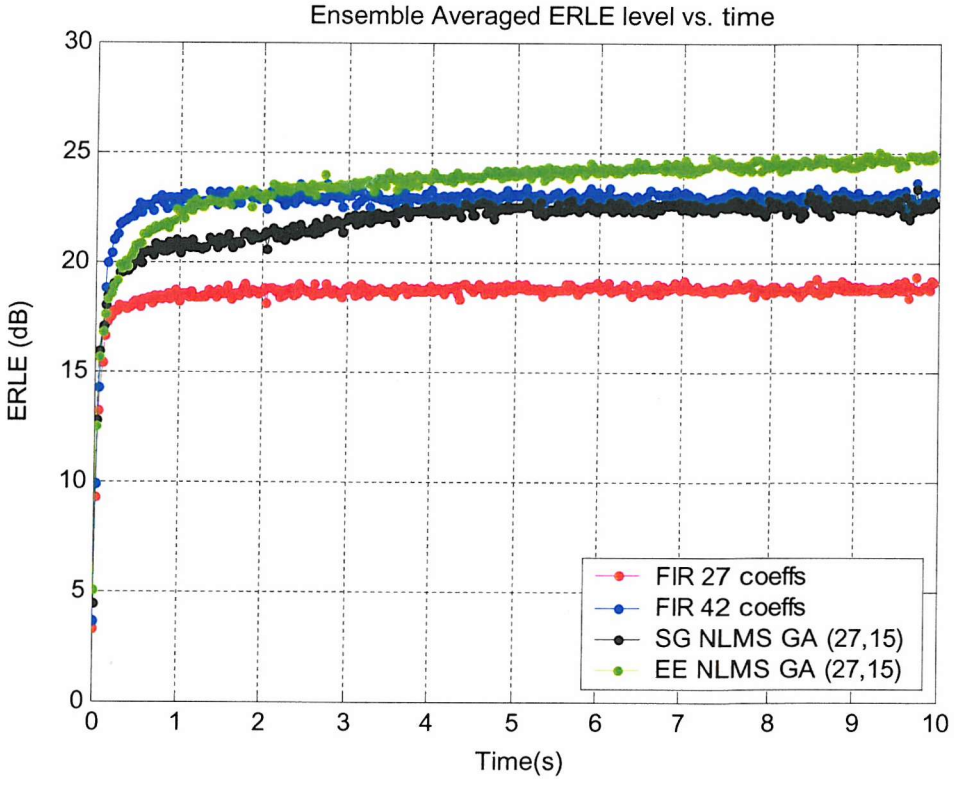


**Figure 5.7 : Adaptive IIR NLMS adaption using separate stepsizes for feedback and feedforward coefficients**

### 5.2.4.3. The Equation Error NLMS adaptive IIR algorithm

Figure 5.8 to Figure 5.11 shows the $ERLEss_{dB}$ and convergence times achievable for these model orders for the Equation Error Adaptive IIR NLMS algorithm for both a white noise and band limited pink noise signal input. This is the outcome of modelling the face up handset echo path response with no transducer seals of Chapter 4.

From Figure 5.8 and Figure 5.9 the achievable $ERLEss_{dB}$ level levels off between a narrow range of stepsizes, between values of 0.00075 and 0.0025 for a white noise input, and $10^{-2}$ and 0.0025 for a band-limited pink noise input. Above these ranges the $ERLEss_{dB}$ level rolls off due to the dependency of the Misadjustment of the Equation Error NLMS algorithm on the stepsize value $\mu$. Below a stepsize of $10^{-4}$ there is a noticeably sharper roll-off for the white noise case. For the pink noise case there is a more gradual roll-off in the achievable $ERLEss_{dB}$ level below $10^{-2}$.

From Figure 5.10 the Equation Error NLMS algorithm exhibits a similar relationship with stepsize and convergence time $TIC_{req}$, as we have already seen for the FIR NLMS algorithm. Slower convergence occurs below stepsize level of $10^{-3}$ for a bandlimited pink noise signal input, for the echo path being modelled. Above stepsize levels of $10^{-3}$ the $TIC_{req}$ values are similar for both white and bandlimited pink noise signals for this echo path being modelled. The $TIC_{ss}$ behaviour of the Equation Error NLMS algorithm in Figure 5.10 and Figure 5.11 with the stepsize value is however different to that of the FIR NLMS seen earlier, and does not follow the same form as the $TIC_{req}$ curve.

To explain the different behaviour the Equation Error NLMS algorithm with the respect to the stepsize value in terms of the $TIC_{ss}$ and $ERLEss_{dB}$ levels, consider the form of covariance matrix $\mathbf{R}_{\varphi_e\varphi_e}$ which applies to the Equation Error NLMS algorithm of (3.3.41) as follows,

$$\mathbf{R}_{\varphi_e\varphi_e} = E\left[\boldsymbol{\varphi}_e(n)\boldsymbol{\varphi}_e^T(n)\right] = \begin{bmatrix} \mathbf{R}_{xx} & \mathbf{R}_{xd} \\ \mathbf{R}_{xd}^T & \mathbf{R}_{dd} \end{bmatrix}, \tag{5.10}$$

where $\mathbf{R}_{xx}$, $\mathbf{R}_{xd}$ and $\mathbf{R}_{dd}$ are defined as,

$$\mathbf{R}_{xx} = E\left[\mathbf{x}(n)\mathbf{x}^T(n)\right], \tag{5.11}$$

$$\mathbf{R}_{xd} = E\left[\mathbf{x}(n)\mathbf{d}^T(n)\right], \tag{5.12}$$

$$\mathbf{R}_{dd} = E\left[\mathbf{d}(n)\mathbf{d}^T(n)\right], \tag{5.13}$$

and $\mathbf{x}(n)$ and $\mathbf{d}(n)$ are as defined in Chapter 3. Consider firstly a white noise signal $x(n)$. The $\mathbf{R}_{xx}$ component in $\mathbf{R}_{\varphi_e\varphi_e}$ is dependent only on the white noise signal input $x(n)$ and hence will be almost an identify matrix in form. However the $\mathbf{R}_{dd}$ of $\mathbf{R}_{\varphi_e\varphi_e}$ will contain significant off diagonal components, primarily due to the colouration of the echo path output signal $d(n)$ by the echo path $\mathbf{h}$

being modelled. The components of $\mathbf{R}_{dd}$ will also be much lower than the $\mathbf{R}_{xx}$ component due to the echo path loss of $\mathbf{h}$. The cross correlation matrix term $\mathbf{R}_{xd}$ in $\mathbf{R}_{\varphi_e\varphi_e}$ is negligible in practice for this system identification experiment compared to $\mathbf{R}_{xx}$ or $\mathbf{R}_{dd}$ and may effectively be treated as a null matrix. The resulting $\mathbf{R}_{\varphi_e\varphi_e}$ for a white noise input can then be written as,

$$\mathbf{R}_{\varphi_e\varphi_e} = \begin{bmatrix} \sigma_x^2\mathbf{I} & \mathbf{0} \\ \mathbf{0}^T & \mathbf{R}_{dd} \end{bmatrix}, \tag{5.14}$$

where $\mathbf{0}$ is a N x M matrix of zeros and $\sigma_x^2$ is the variance of white noise input $x(n)$. Equation (5.14) effectively means that the eigenvalue spread of $\mathbf{R}_{\varphi_e\varphi_e}$ is dependent mainly on $\mathbf{R}_{dd}$. The mean coefficient error terms of the feedforward coefficients of the Equation Error NLMS algorithm will decay at a similar rate, whereas the mean coefficient error terms of the feedback coefficients will converge at different rates even for a white noise signal input $x(n)$.

Equation (5.14) is the main contributory factor to the convergence behaviour of the Equation Error NLMS adaptive IIR algorithm of order (M,N) with the stepsize value $\mu$. From (5.14) for Equation Error adaptive IIR algorithms the upper stability limit will be dependant on both filter model order, input signal type and the echo path being modelled. At lower stepsizes below $10^{-4}$ will result in mainly only the feedforward coefficients of the Equation Error NLMS converging, resulting in the sharp roll-off in both the $ERLEss_{dB}$ levels and $TIC_{req}$ values achievable with stepsize in Figure 5.8 and Figure 5.10. As mainly only feedforward coefficients of the Equation Error NLMS algorithm adapt, similar $ERLEss_{dB}$ behaviour to that of an FIR NLMS of M coefficients will occur at these lower stepsize values. As a result $ERLEss_{dB}$ levels for both (35,23) and (31,11) orders at these lower stepsize values are similar. At larger stepsizes above $10^{-4}$ the feedback coefficients of the Equation Error NLMS will begin to converge resulting in the gradual increase of $ERLEss_{dB}$ level achievable with these large stepsizes. The $ERLEss_{dB}$ levels for both (35,23) and (31,11) orders begin to show a difference. For the lower model order (23,7) in Figure 5.8 the $ERLEss_{dB}$ curve with respect to stepsize shows a more peaked response in comparison to the other model orders used. With fewer feedback coefficients the eigenvalue spread $\mathbf{R}_{dd}$ can be assumed to be smaller resulting in increased convergence with stepsize levels exceeding $10^{-4}$.

The general ERLE convergence profile behaviour for the Equation Error NLMS algorithm with stepsize value, and the $TIC_{ss}$ value behaviour with stepsize can be explained using Figure 5.13 for an order of (23,7). One may initially expect a similar relationship of $TIC_{ss}$ with stepsize for an Equation Error algorithm, as obtained for a FIR NLMS algorithm in Figure 5.5 for a white noise input. However from Figure 5.13 we can see the ERLE convergence profile behaviour of both adaptive FIR and Equation Error NLMS algorithms are different. For the Equation Error NLMS algorithm a rapid initial convergence period is obtained due to convergence of the feedforward coefficients similar to an FIR NLMS algorithm, followed by a slower convergence period dominated by convergence of any feedback coefficient error

terms. This is the reason an increase in $TIC_{ss}$ values exists for stepsizes above 0.0005, as the steady state level is not effectively reached within the 10s adaption period since not all feedback coefficients will converge within the 10s adaption period due to the eigenvalue spread of $\mathbf{R}_{dd}$. For a FIR NLMS algorithm the steady state ERLE level would be reached after the initial convergence period.

Consider next the behaviour for a band limited pink noise input $x(n)$. The resulting $\mathbf{R}_{\varphi_e\varphi_e}$ can now be written as,

$$\mathbf{R}_{\varphi_e\varphi_e} = \begin{bmatrix} \mathbf{R}_{xx} & \mathbf{0} \\ \mathbf{0}^T & \mathbf{R}_{dd} \end{bmatrix}, \tag{5.15}$$

where both $\mathbf{R}_{xx}$ and $\mathbf{R}_{dd}$ have now off diagonal components due to the a band limited pink noise input $x(n)$. The resulting eigenvalue spread of $\mathbf{R}_{\varphi_e\varphi_e}$ is now a combination of the spreads of $\mathbf{R}_{xx}$ and $\mathbf{R}_{dd}$. Both the mean feedforward and feedback coefficient error terms will decay at different rates due to the eigenvalue spreads of $\mathbf{R}_{xx}$ and $\mathbf{R}_{dd}$. Like the white noise case the eigenvalue spread of $\mathbf{R}_{dd}$ is likely to be larger than that of $\mathbf{R}_{xx}$ due to the additional colouration of input signal $x(n)$ by echo path vector $\mathbf{h}$.

For the bandlimited pink noise case the colouration of $\mathbf{R}_{xx}$ causes a more gradual roll off in the achievable $ERLEss_{dB}$ levels below a stepsize of $10^{-2}$. The ERLE convergence behaviour of the Equation Error NLMS algorithm with the stepsize value is similar to that already discussed for the white noise case, except that now $ERLEss_{dB}$ and convergence are much lower within the 10s adaption period as shown in Figure 5.14. Like the FIR NLMS for the bandlimited pink noise signal, due to the larger eigenvalue spread of both $\mathbf{R}_{xx}$ and $\mathbf{R}_{dd}$ some feedforward and feedback coefficient error terms will not decay sufficiently within the 10s adaption period, resulting in a lower achievable $ERLEss_{dB}$ level compared to the white noise case. We shall see later how the Equation Error LMS Newton algorithm can result in much improved modelling performance for coloured input signals where the eigenvalue spread of $\mathbf{R}_{\varphi_e\varphi_e}$ will be larger.

It is expected in general all other Equation Error NLMS based algorithms presented in Chapter 3 will exhibit similar behaviour in terms of steady state modelling performance and convergence with regards to the stepsize value $\mu$, as discussed here for the Equation Error NLMS algorithm. A stepsize of $\mu$ =0.00075 is chosen for the Equation Error NLMS algorithm for satisfactory steady state modelling performance for all echo paths to be modelled. Using different feedforward and feedback coefficients has negligible impact on modelling performance.

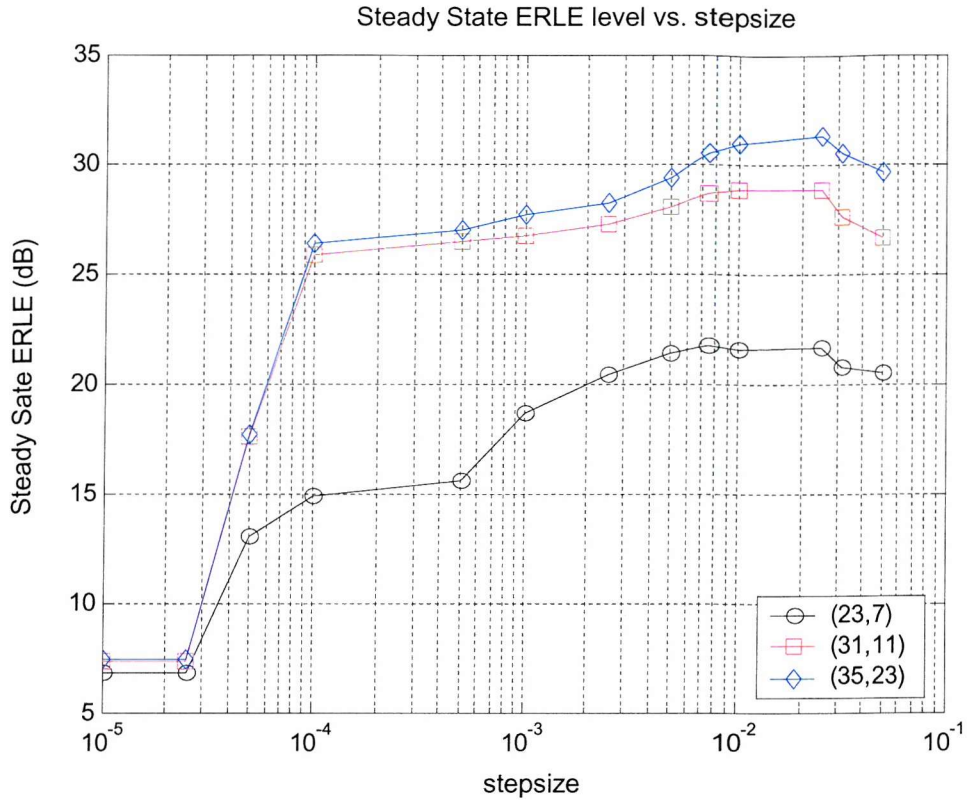


**Figure 5.8 : Steady State ERLE level for Equation Error NLMS vs. stepsize, for different filter orders, for white noise input**

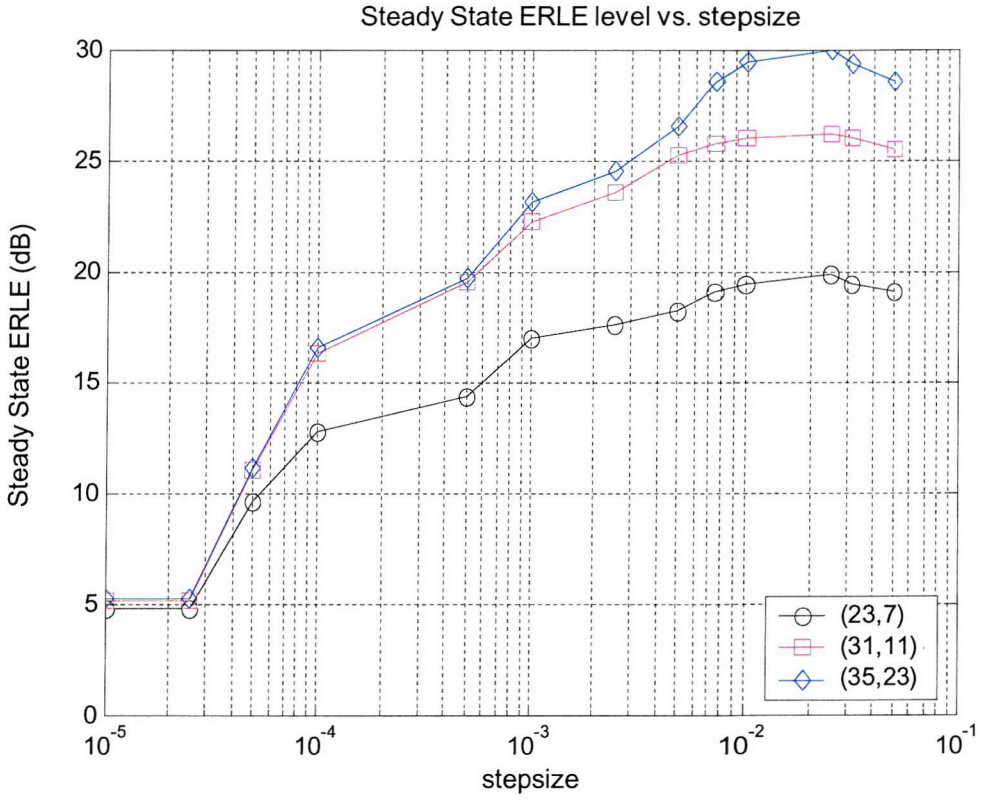


**Figure 5.9 : Steady State ERLE level for Equation Error NLMS vs. stepsize, for different filter orders, for bandlimited pink noise input**

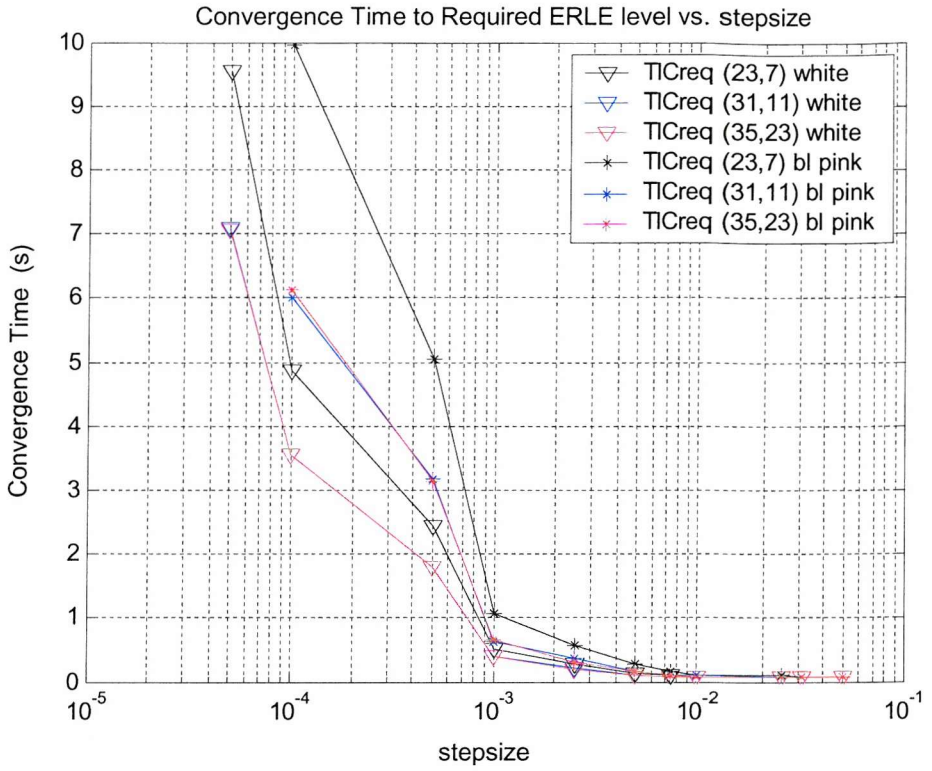


**Figure 5.10 : Convergence time to required ERLE level for Equation Error NLMS vs. stepsize, for different filter orders**

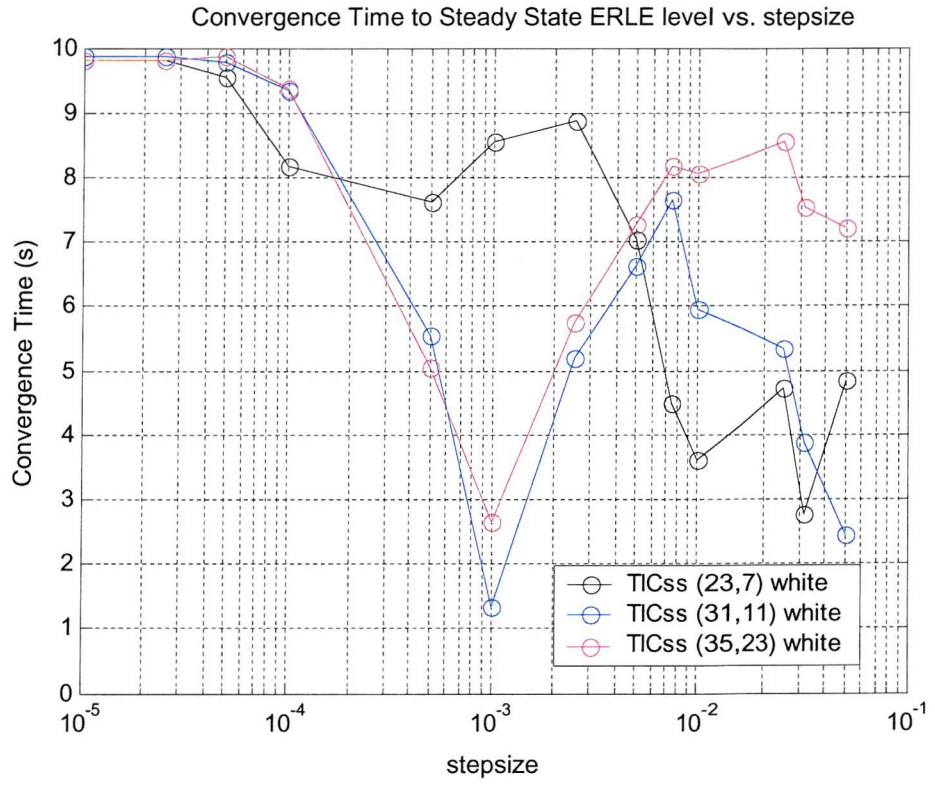


**Figure 5.11 : Convergence time to Steady State ERLE level for Equation Error NLMS vs. stepsize, for different filter orders for white noise input**

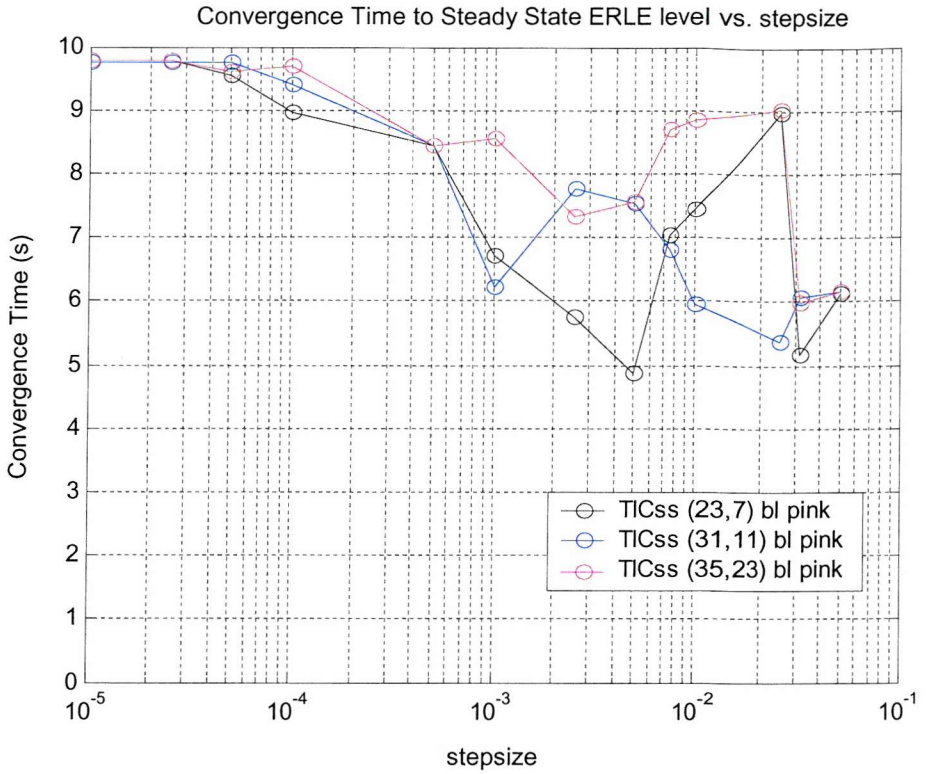


**Figure 5.12 : Convergence time to the Steady State ERLE level for Equation Error NLMS vs. stepsize, for different filter orders for bandlimited pink noise input**

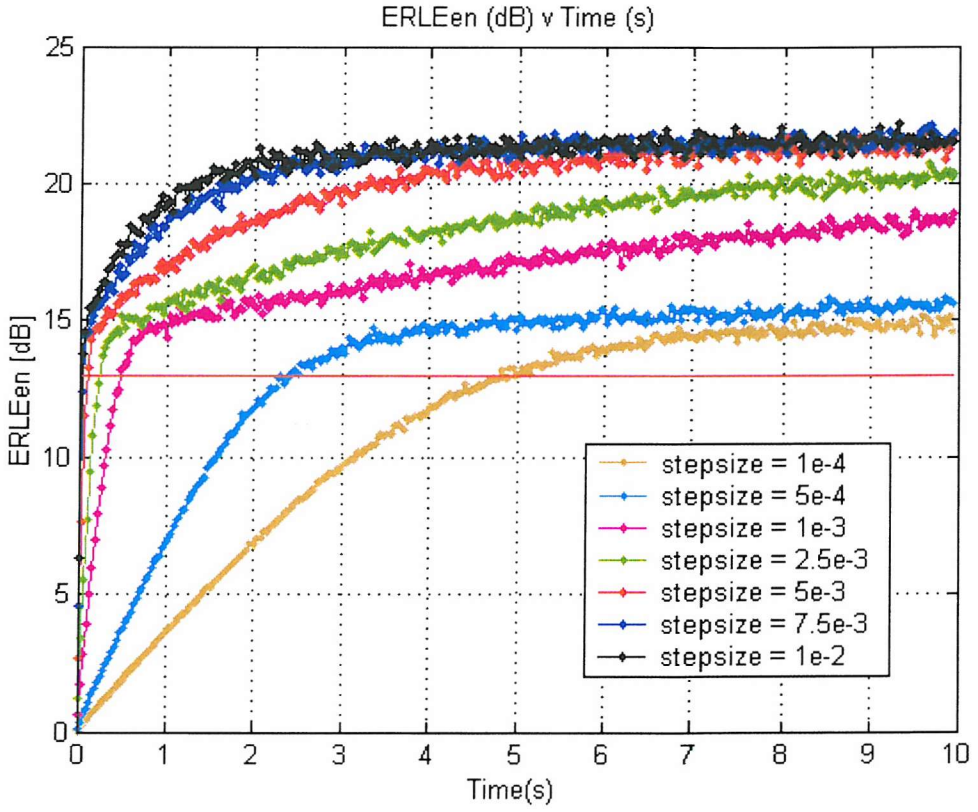


**Figure 5.13 : EE NLMS ensemble averaged ERLE level vs. time, for (23,7) order for white noise input, for different stepsizes**

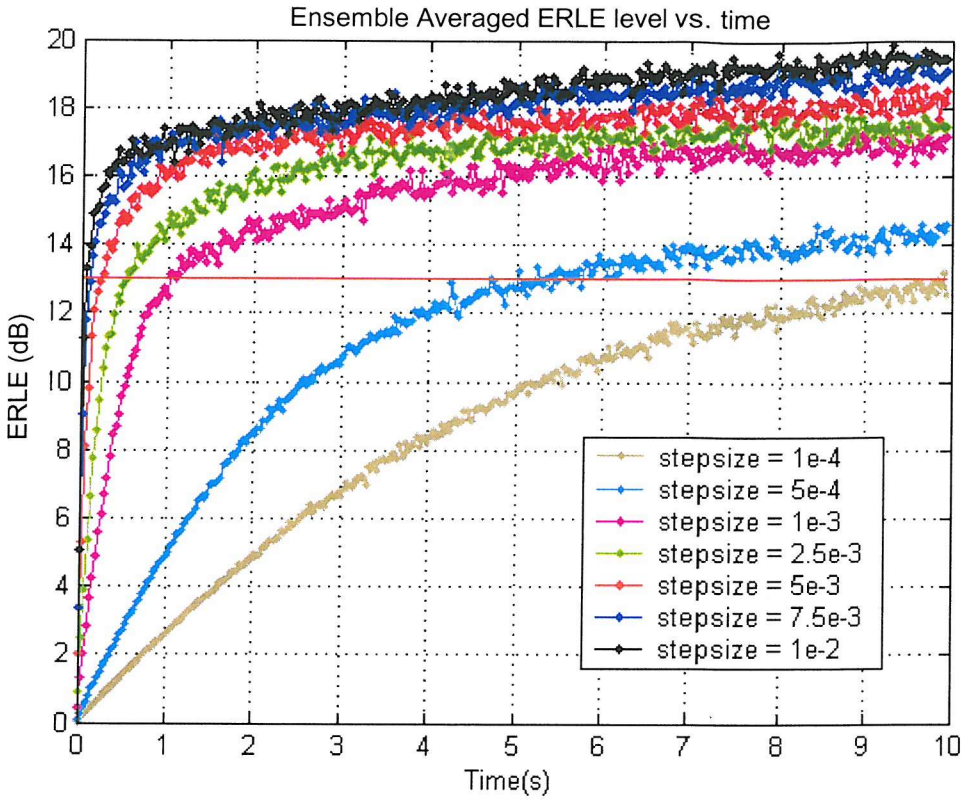


**Figure 5.14 : EE NLMS ensemble averaged ERLE vs. time, for (23,7) order for bandlimited pink noise input, for different stepsizes**

### 5.2.4.4. The Simplified Gradient NLMS Output Error Adaptive IIR Algorithm

Consider now the performance of the Simplified Gradient NLMS Output Error adaptive IIR algorithm of (3.2.66). Figure 5.15 to Figure 5.19 shows the $ERLEss_{dB}$ and convergence times achievable for these model orders for the Simplified Gradient Adaptive IIR NLMS algorithm for both a white noise and band limited pink noise signal input. This is the outcome of modelling the face up handset echo path response with no transducer seals of Chapter 4.

From Figure 5.15 and Figure 5.16 the achievable $ERLEss_{dB}$ level levels are similar in form to those of the FIR NLMS algorithm. Consider the white noise case of Figure 5.15 , below a stepsize of $10^{-4}$ and above a stepsize of $10^{-2}$ the $ERLEss_{dB}$ level rolls off. The roll off above $10^{-2}$ is due to the dependency of the misadjustment of the Simplified Gradient NLMS algorithm on the stepsize value $\mu$ , and above a stepsize of 0.05 instability occurs.

In Figure 5.19 the Simplified Gradient NLMS algorithm exhibits a similar relationship for the convergence time $TIC_{req}$ with stepsize, as we have already seen for the FIR NLMS algorithm. Slower convergence occurs below stepsize level of $10^{-3}$ for a bandlimited pink noise signal input for the echo path

being modelled. Above stepsize levels of $10^{-3}$ the $TIC_{req}$ values are similar for both white and bandlimited pink noise signals for this echo path being modelled.

To explain the different behaviour the Simplified Gradient NLMS algorithm with the respect to the stepsize value in terms of the $TIC_{ss}$ and $ERLEss_{dB}$ levels, consider the form of covariance matrix $\mathbf{R}_{\varphi_f\varphi_f}$ which applies to the Simplified Gradient NLMS algorithm of (3.2.66) as follows

$$\mathbf{R}_{\varphi_{of}\varphi_{of}} = E\left[\boldsymbol{\varphi}_f(n)\boldsymbol{\varphi}_f^T(n)\right] = \begin{bmatrix} \mathbf{R}_{\mathbf{x}_f\mathbf{x}_f} & \mathbf{R}_{\mathbf{x}_f\mathbf{y}_f} \\ \mathbf{R}_{\mathbf{x}_f\mathbf{y}_f}^T & \mathbf{R}_{\mathbf{y}_f\mathbf{y}_f} \end{bmatrix}, \tag{5.16}$$

where $\mathbf{R}_{\mathbf{x}_f\mathbf{x}_f}$, $\mathbf{R}_{\mathbf{x}_f\mathbf{y}_f}$ and $\mathbf{R}_{\mathbf{y}_f\mathbf{y}_f}$ are defined as,

$$\mathbf{R}_{\mathbf{x}_f\mathbf{x}_f} = E\left[\mathbf{x}_f(n)\mathbf{x}_f^T(n)\right], \tag{5.17}$$

$$\mathbf{R}_{\mathbf{x}_f\mathbf{y}_f} = E\left[\mathbf{x}_f(n)\mathbf{y}_f^T(n)\right], \tag{5.18}$$

$$\mathbf{R}_{\mathbf{y}_f\mathbf{y}_f} = E\left[\mathbf{y}_f(n)\mathbf{y}_f^T(n)\right], \tag{5.19}$$

and $\mathbf{x}_f(n)$ and $\mathbf{y}_f(n)$ are as defined in Chapter 3 in (3.2.46) and (3.2.47). The input signal, $x(n)$, and output of the adaptive model, $y(n)$, for the Simplified Gradient NLMS algorithm are filtered by the feedback coefficients of the adaptive filter, which is time varying in nature.

If we simplistically neglect the long term cross components $\mathbf{R}_{\mathbf{x}_f\mathbf{y}_f}$ in $\mathbf{R}_{\varphi_f\varphi_f}$ to make the eigenvalue spread of $\mathbf{R}_{\varphi_f\varphi_f}$ simply dependent on $\mathbf{R}_{\mathbf{x}_f\mathbf{x}_f}$ and $\mathbf{R}_{\mathbf{y}_f\mathbf{y}_f}$ we get,

$$\mathbf{R}_{\varphi_f\varphi_f} = \begin{bmatrix} \mathbf{R}_{\mathbf{x}_f\mathbf{x}_f} & \mathbf{0} \\ \mathbf{0}^T & \mathbf{R}_{y_fy_f} \end{bmatrix}, \tag{5.20}$$

Consider firstly a white noise signal $x(n)$. In the longer term as the adaptive algorithm converges $\mathbf{R}_{\mathbf{x}_f\mathbf{x}_f}$ will be coloured, due to filtering with the feedback coefficients of the adaptive filter, even for a white noise input signal. The adaptive filter output signal $y(n)$ will be coloured by the filtering of input signal $x(n)$ by the feedforward and feedback coefficients of the adaptive filter. The filtered signal $y_f(n)$ from which $\mathbf{R}_{\mathbf{y}_f\mathbf{y}_f}$ is formed will hence be strongly coloured as the algorithm converges, resulting in $\mathbf{R}_{\mathbf{y}_f\mathbf{y}_f}$ being strongly coloured. The resulting eigenvalue spread of $\mathbf{R}_{\varphi_f\varphi_f}$ depend on both $\mathbf{R}_{\mathbf{x}_f\mathbf{x}_f}$ and $\mathbf{R}_{\mathbf{y}_f\mathbf{y}_f}$, but is expected to be dominated by the larger spread of $\mathbf{R}_{\mathbf{y}_f\mathbf{y}_f}$ (neglecting the influence of $\mathbf{R}_{\mathbf{x}_f\mathbf{y}_f}$ terms)

Equation (5.16) is the main contributory factor to the convergence behaviour of the Simplified Gradient NLMS adaptive IIR algorithm of order (M,N) with the stepsize value $\mu$. From the simplification of (5.16) in (5.20) for Output Error adaptive IIR algorithms the upper stability limit will be dependant on the filter model order, input signal type and the echo path being modelled (since this will

influence the colouration of $y(n)$). Like the Equation Error NLMS algorithm, lower stepsizes below $10^{-4}$ will result in mainly only the feedforward coefficients converging. At these lower stepsizes due to small adaption in the feedback coefficients even for a white noise input signal, the input signal $x(n)$ will not be strongly coloured by the feedback coefficients of the adaptive model resulting in a $\mathbf{R}_{\mathbf{x}_f\mathbf{x}_f}$ component being strongly identity like in form. Due to converging feedforward coefficients the component $\mathbf{R}_{\mathbf{y}_f\mathbf{y}_f}$ will still be coloured in form. The mean feedforward coefficient error terms will hence decay at similar rates, whereas the mean feedback coefficient error terms will decay at different rates.

The resulting achievable $ERLEss_{dB}$ below stepsize levels of $10^{-4}$ for the Simplified Gradient NLMS of order (M,N) will hence be similar to an FIR NLMS of M coefficients. At larger stepsizes above $10^{-4}$ the feedback coefficients of the Simplified Gradient NLMS algorithm will begin to converge resulting in the gradual increase of $ERLEss_{dB}$ level achievable. For the lower model order (23,7) in Figure 5.15 the $ERLEss_{dB}$ curve with respect to stepsize shows a more peaked response in comparison to the other model orders used. With fewer feedback coefficients the eigenvalue spread of $\mathbf{R}_{\mathbf{y}_f\mathbf{y}_f}$ will be less, resulting in increased convergence with stepsize levels exceeding $10^{-4}$.

The general ERLE convergence profile behaviour for the Simplified Gradient NLMS algorithm with stepsize value, and the $TIC_{ss}$ value behaviour with stepsize can be explained using Figure 5.20 for an order of (23,7). A similar relationship of $TIC_{ss}$ with stepsize exists as for the Equation Error NLMS algorithm. The ERLE convergence profiles of the FIR NLMS algorithm and the Simplified Gradient NLMS algorithm are different. Like the Equation Error NLMS algorithm the Simplified Gradient NLMS algorithm profile contains a rapid initial convergence period, to convergence of the feedforward coefficients similar to an FIR NLMS algorithm, followed by a slower convergence period dominated by convergence of any feedback coefficient error terms. This is the reason an increase in $TIC_{ss}$ values exists for stepsizes above $10^{-3}$, as the steady state level is not effectively reached within the 10s adaption period. For a FIR NLMS algorithm the steady state ERLE level would be reached after the initial convergence period. Even at the largest stepsizes prior to instability the steady state level is clearly not still reached within the 10s adaption period due mainly to the eigenvalue spread of both $\mathbf{R}_{\mathbf{x}_f\mathbf{x}_f}$ and $\mathbf{R}_{\mathbf{y}_f\mathbf{y}_f}$. We shall see later how the Simplified Gradient LMS Newton algorithm can be used to improve the modelling performance of the Simplified Gradient algorithm, due to the resulting eigenvalue spread of $\mathbf{R}_{\boldsymbol{\varphi}_f\boldsymbol{\varphi}_f}$ even for a white noise input signal.

For a band limited pink noise signal $x(n)$, a larger eigenvalue spread will result in $\mathbf{R}_{\mathbf{x}_f\mathbf{x}_f}$ and $\mathbf{R}_{\mathbf{y}_f\mathbf{y}_f}$. This creates slowly converging feedback filter coefficients and lower achievable $ERLEss_{dB}$ within the 10s adaption period as shown in Figure 5.16. The mean feedforward and feedback coefficient error terms will now both decay at different rates due to the larger eigenvalue spread of both

$\mathbf{R}_{\mathbf{x}_f\mathbf{x}_f}$ and $\mathbf{R}_{\mathbf{y}_f\mathbf{y}_f}$. These in turn lead to slower convergence performance with stepsize as seen for the white noise input case as shown in Figure 5.17 and Figure 5.19. The lower $ERLEss_{dB}$ levels achievable is a result of coefficient error terms not decaying sufficiently within the 10s adaption period due to the eigenvalue spread of $\mathbf{R}_{\varphi_f\varphi_f}$. We shall see later how the Simplified Gradient LMS Newton algorithm can result in much improved modelling performance over the Simplified Gradient NLMS algorithm for coloured input signals where the eigenvalue spread of $\mathbf{R}_{\varphi_f\varphi_f}$ will be larger.

A stepsize of $\mu$ =0.00075 is chosen for the Simplified Gradient NLMS algorithm for satisfactory steady state modelling performance for all echo paths to be modelled. Using different feedforward and feedback coefficients has negligible impact on modelling performance.

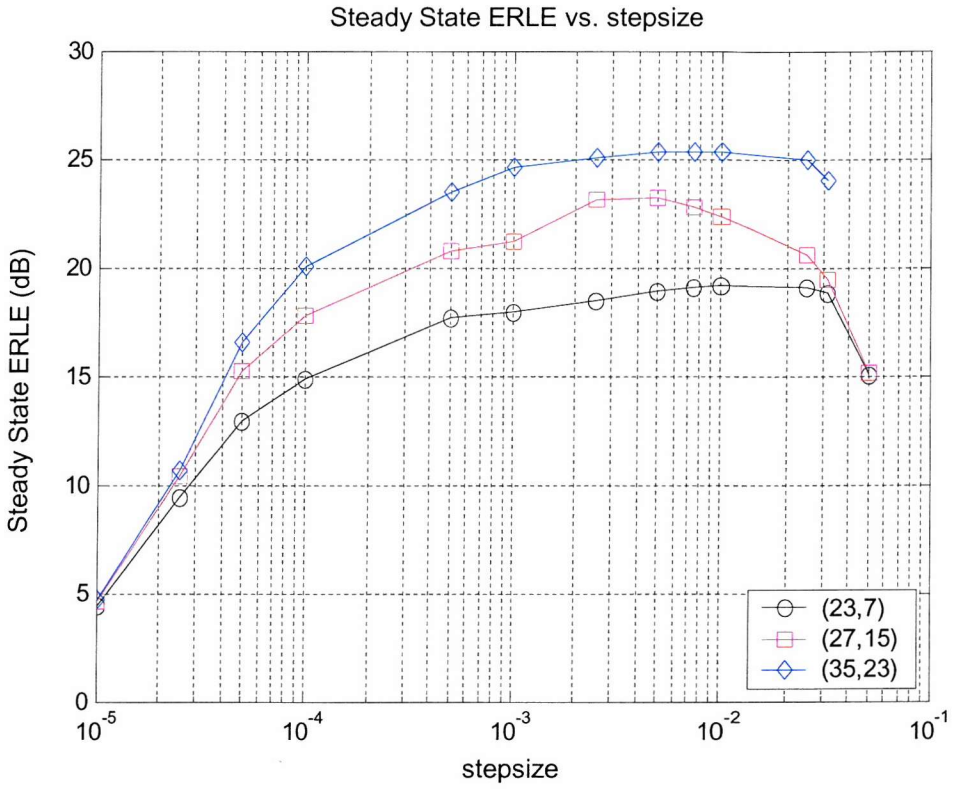


**Figure 5.15 : Steady State ERLE level for Simplified Gradient NLMS vs. stepsize, for different filter orders, for white noise input**

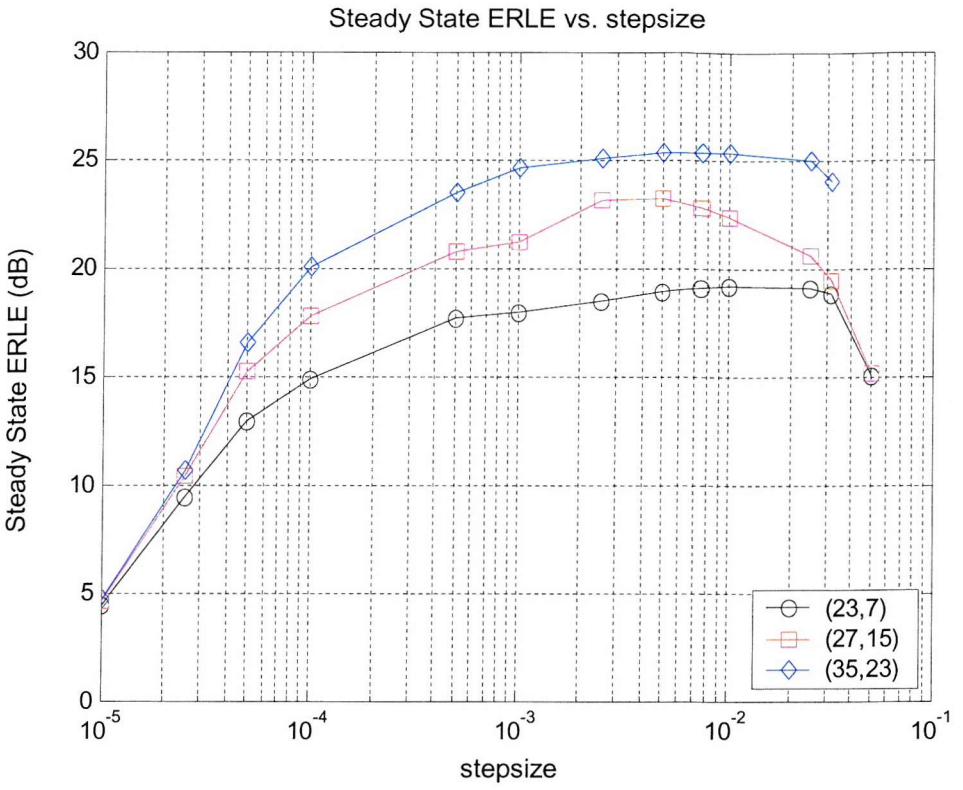


**Figure 5.16 : Steady State ERLE level for Simplified Gradient NLMS vs. stepsize, for different filter orders, for bandlimited pink noise input**

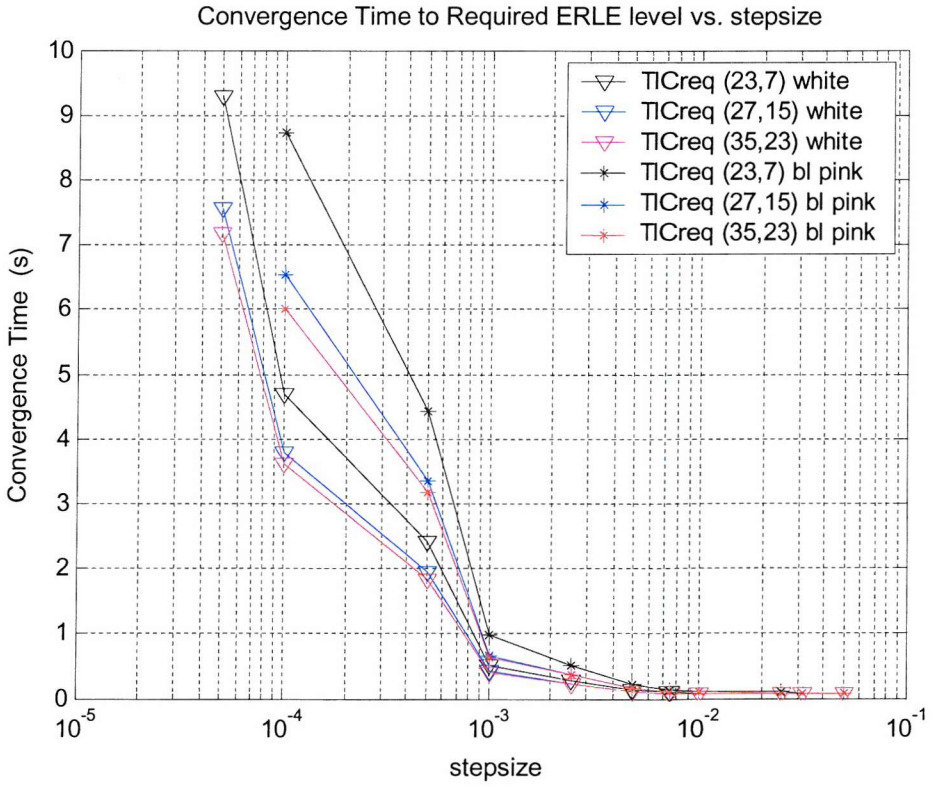


**Figure 5.17 : Convergence time to the required ERLE level for Simplified Gradient NLMS vs. stepsize, for different filter orders**

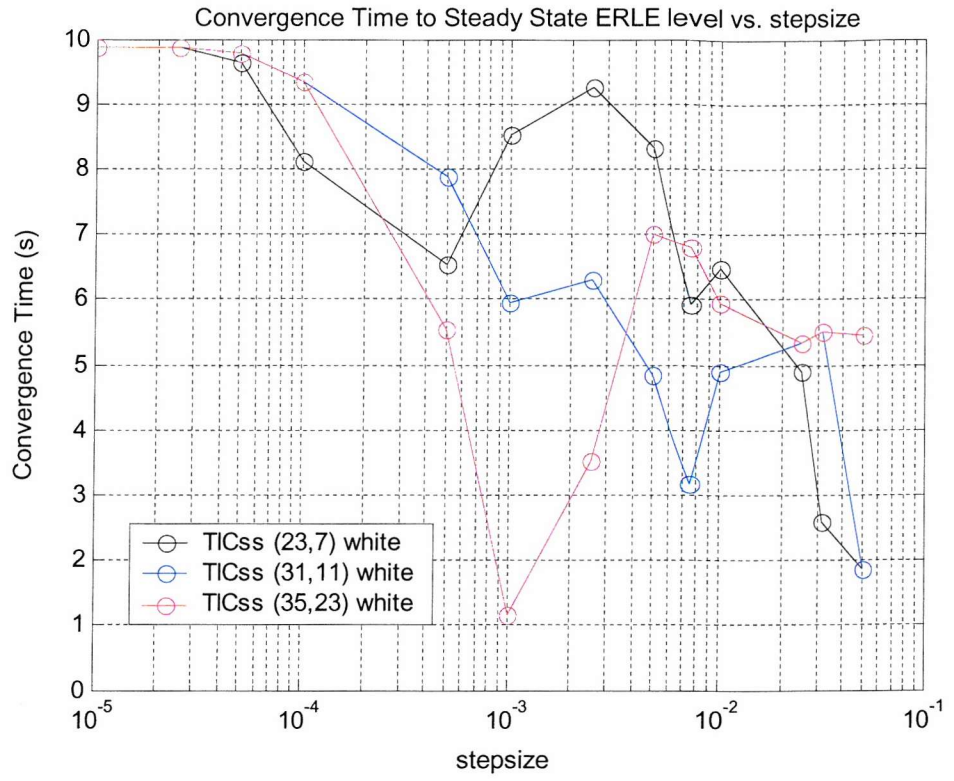


**Figure 5.18 : Convergence time to the Steady State ERLE level for Simplified Gradient NLMS vs. stepsize, for different filter orders for white noise**

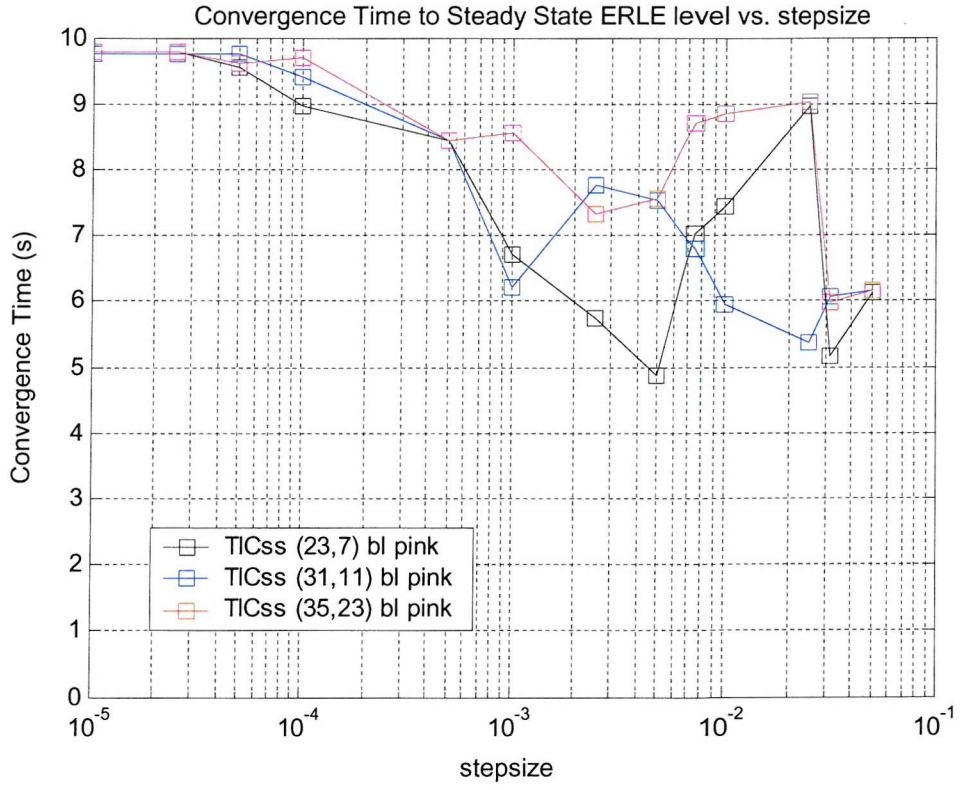


**Figure 5.19 : Convergence time to the Steady State ERLE level for Simplified Gradient NLMS vs. stepsize, for different filter orders for band limited pink noise**

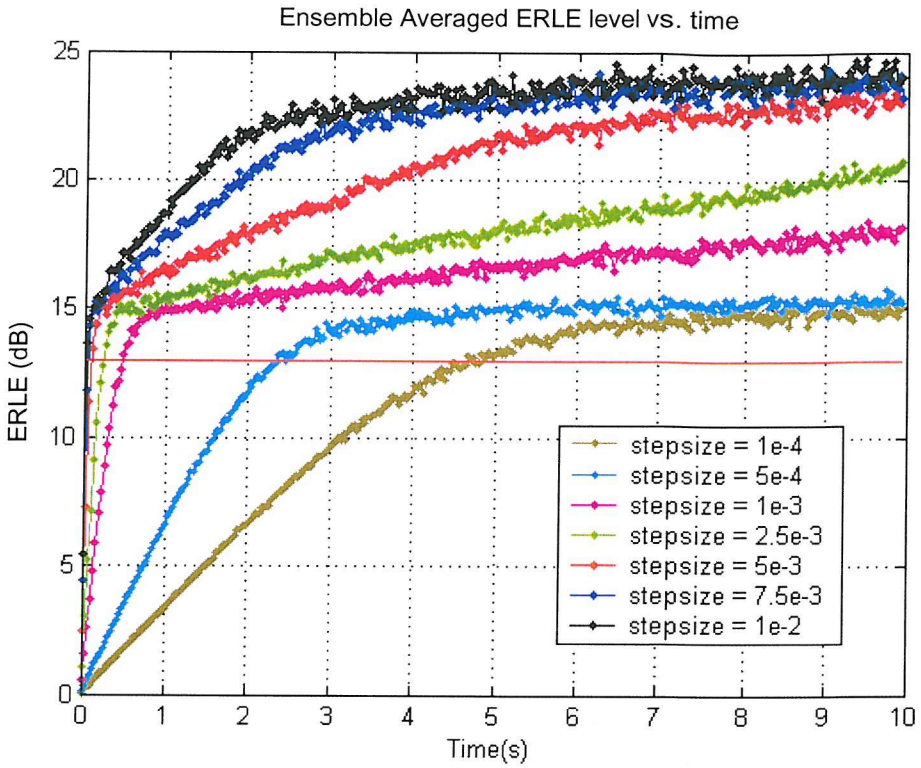


**Figure 5.20 : Ensemble averaged ERLE for Simplified Gradient NLMS vs. time for different stepsizes for white noise with filter order (23,7)**

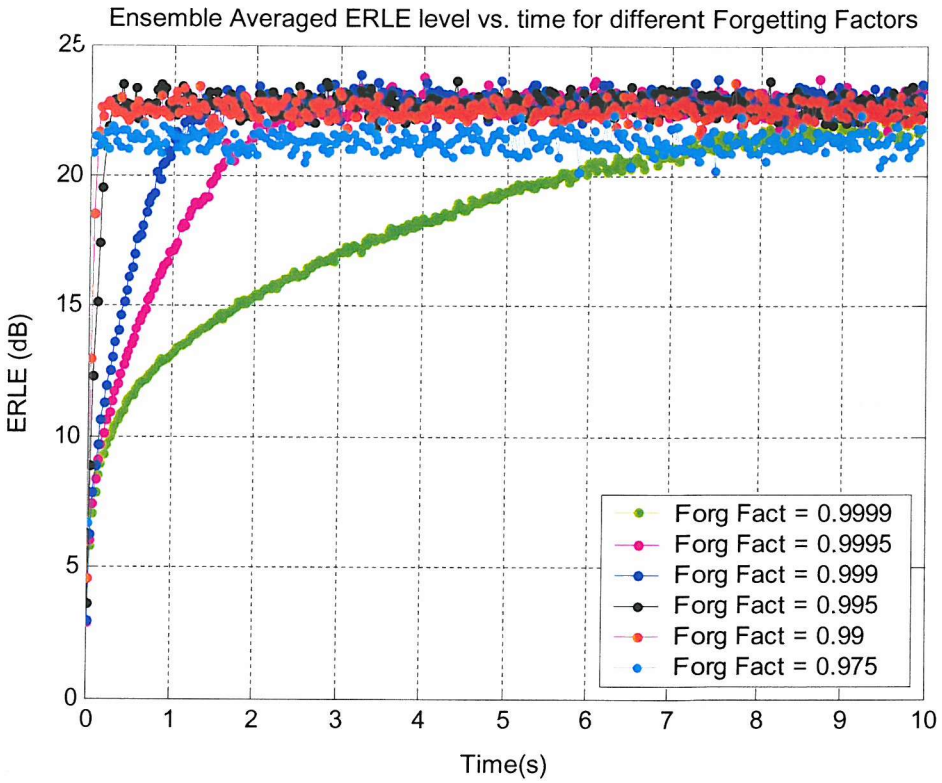


**Figure 5.21 : FIR LMS Newton ERLE performance with different forgetting factors $\lambda$**

### 5.2.5. The effect of LMS Newton adaptive algorithm design parameters on steady state modelling performance

To establish the effect of LMS Newton algorithm parameters on steady state modelling performance the FIR LMS Newton algorithm, the Simplified Gradient Output Error LMS Newton adaptive IIR algorithm, and the Equation Error LMS Newton adaptive IIR algorithms will be used. Consider the original forms of these algorithms as follows,

$$\mathbf{b}_{n+1} = \mathbf{b}_n + \mu\hat{\mathbf{R}}_{xx}^{-1}(n)\mathbf{x}(n)e(n), \tag{3.1.58}$$

$$\boldsymbol{\theta}_{n+1} = \boldsymbol{\theta}_n + \mu\hat{\mathbf{R}}_{\varphi_f\varphi_f}^{-1}(n)\boldsymbol{\varphi}_f(n)e(n) \tag{3.2.71}$$

$$\boldsymbol{\theta}_{n+1} = \boldsymbol{\theta}_n + \mu\hat{\mathbf{R}}_{\varphi_e\varphi_e}^{-1}(n)\boldsymbol{\varphi}_e(n)e_e(n), \tag{3.3.46}$$

From the above algorithms, like the NLMS algorithms, the stepsize parameter $\mu$ is one of the most important parameters of LMS Newton based algorithms. However there are also additional important algorithm parameters for LMS Newton based algorithms used in the computation of the inverse covariance matrix estimates $\hat{\mathbf{R}}_{xx}^{-1}(n)$, $\hat{\mathbf{R}}_{\varphi_f\varphi_f}^{-1}(n)$, and $\hat{\mathbf{R}}_{\varphi_e\varphi_e}^{-1}(n)$. As discussed in Chapter 3 estimates of the covariance matrices may be computed as follows [5.1],[5.2],[5.4]-[5.6].

$$\hat{\mathbf{R}}_{xx}(n) = \lambda\hat{\mathbf{R}}_{xx}(n-1) + \alpha\mathbf{x}(n)\mathbf{x}^T(n), \tag{5.21}$$

$$\hat{\mathbf{R}}_{\varphi_f\varphi_f}(n) = \lambda\hat{\mathbf{R}}_{\varphi_f\varphi_f}(n-1) + \alpha\boldsymbol{\varphi}_f(n)\boldsymbol{\varphi}_f{}^T(n), \tag{5.22}$$

$$\hat{\mathbf{R}}_{\varphi_e\varphi_e}(n) = \lambda\hat{\mathbf{R}}_{\varphi_e\varphi_e}(n-1) + \alpha\boldsymbol{\varphi}_e(n)\boldsymbol{\varphi}_e{}^T(n), \tag{5.23}$$

where $\lambda$ is a forgetting factor to weight previous estimates depending on the stationarity of input data, and $\alpha$ is a convergence factor . Normally $\lambda = 1-\alpha$ so the covariance matrix estimates of (5.21), (5.22) and (5.23) are an exponentially weighted average of the outer product $\mathbf{x}(n)\mathbf{x}^T(n)$, $\boldsymbol{\varphi}_f(n)\boldsymbol{\varphi}_f{}^T(n)$ and $\boldsymbol{\varphi}_e(n)\boldsymbol{\varphi}_e{}^T(n)$. However the general forms of (5.21), (5.22) and (5.23) allow the convergence factor $\alpha$ to be altered independently of the forgetting factor $\lambda$ to slow the update rate of these covariance matrix estimates in the presence of any disturbances[5.6]. Using the matrix inversion lemma on (5.21), (5.22) and (5.23) the following covariance matrix estimates $\hat{\mathbf{R}}_{xx}^{-1}(n)$, $\hat{\mathbf{R}}_{\varphi_f\varphi_f}^{-1}(n)$, and $\hat{\mathbf{R}}_{\varphi_e\varphi_e}^{-1}(n)$ are formed,

$$\hat{\mathbf{R}}_{xx}^{-1}(n) = \frac{1}{\lambda}\left(\hat{\mathbf{R}}_{xx}^{-1}(n-1) - \frac{\hat{\mathbf{R}}_{xx}^{-1}(n-1)\mathbf{x}(n)\mathbf{x}^T(n)\hat{\mathbf{R}}_{xx}^{-1}(n-1)}{\frac{\lambda}{\alpha} + \mathbf{x}^T(n)\hat{\mathbf{R}}_{xx}^{-1}(n-1)\mathbf{x}(n)}\right), \tag{5.24}$$

$$\hat{\mathbf{R}}_{\varphi_f\varphi_f}^{-1}(n) = \frac{1}{\lambda}\left(\hat{\mathbf{R}}_{\varphi_f\varphi_f}^{-1}(n-1) - \frac{\hat{\mathbf{R}}_{\varphi_f\varphi_f}^{-1}(n-1)\boldsymbol{\varphi}_f(n)\boldsymbol{\varphi}_f{}^T(n)\hat{\mathbf{R}}_{\varphi_f\varphi_f}^{-1}(n-1)}{\frac{\lambda}{\alpha} + \boldsymbol{\varphi}_f{}^T(n)\hat{\mathbf{R}}_{\varphi_f\varphi_f}^{-1}(n-1)\boldsymbol{\varphi}_f(n)}\right), \tag{5.25}$$

$$\hat{\mathbf{R}}^{-1}_{\varphi_e\varphi_e}(n)=\frac{1}{\lambda}\left(\hat{\mathbf{R}}^{-1}_{\varphi_e\varphi_e}(n-1)-\frac{\hat{\mathbf{R}}^{-1}_{\varphi_e\varphi_e}(n-1)\varphi_e(n)\varphi_e{}^T(n)\hat{\mathbf{R}}^{-1}_{\varphi_e\varphi_e}(n-1)}{\frac{\lambda}{\alpha}+\varphi_e{}^T(n)\hat{\mathbf{R}}^{-1}_{\varphi_e\varphi_e}(n-1)\varphi_e(n)}\right), \tag{5.26}$$

where the following initialisations are used,

$$\hat{\mathbf{R}}^{-1}_{xx}(0)=\hat{\mathbf{R}}^{-1}_{\varphi_f\varphi_f}(0)=\hat{\mathbf{R}}^{-1}_{\varphi_e\varphi_e}(0)=\delta\mathbf{I}, \tag{5.27}$$

and $\delta$ is a large scalar constant >>1.

From equations (5.21) to (5.27), in addition to the stepsize parameter $\mu$, the parameters $\lambda$, $\alpha$, and $\delta$ are also important in determining the convergence and steady state $ERLEss_{dB}$ level performance behaviour of the LMS Newton algorithms of (3.1.58), (3.2.71) and (3.3.46). In order to see the effects of LMS Newton algorithm parameters on the steady state modelling performance of adaptive FIR and IIR algorithms, the relationships between filter order, convergence time, steady state $ERLEss_{dB}$ level, stepsize $\mu$, covariance matrix estimation parameters $\lambda$, $\alpha$, and $\delta$, and input signal characteristics need to be investigated

To explore these relationships with filter order three different model orders are used again. A lowest model order range for all modelling experiments of 30 coefficients is used, in addition to a middle range model order of 42 coefficients, and a maximum model order of 58 coefficients.

#### 5.2.5.1. FIR LMS Newton Adaptive Algorithm

The effect of the forgetting factor $\lambda$ on the convergence and steady state $ERLEss_{dB}$ level achievable by the FIR LMS Newton algorithm is firstly established. Figure 5.21 shows the ensemble averaged ERLE level results achieved for a model order of 42 coefficients for modelling experiments with different forgetting factors for the face up no seals handset echo path response of Chapter 4. The same stepsize $\mu$, convergence factor $\alpha$ and initialisation factor $\delta$ are used for all these experiments. A stationary band limited pink noise signal $x(n)$ is used. From the results presented it can be clearly seen fro stationary signals the higher the forgetting factor $\lambda$ results in much slower convergence to both the required ERLE level ($TIC_{req}$) and the steady state ERLE level ($TIC_{ss}$) for the FIR LMS Newton algorithm. A larger forgetting factor gives more weight to previous estimates $\mathbf{R}_{xx}(n-1)$, and thus slower convergence for the inverse covariance matrix estimate $\hat{\mathbf{R}}^{-1}_{xx}(n)$ due to the larger weighting by $1/\lambda$. Only at the high factors of $\lambda$ =0.9999 and above does the steady state $ERLEss_{dB}$ level become affected during the 10s adaption period. At low forgetting factors $\lambda$ below 0.99 the steady state $ERLEss_{dB}$ level achievable becomes lower, and below $\lambda$ =0.975 instability occurs. The same trends in modelling performance with the forgetting factor $\lambda$ can be observed for different model orders and other stationary input signal types for the FIR LMS Newton algorithm.

A value of $\lambda$ =0.999 can be selected for the FIR LMS Newton algorithm from the assessment of ERLE performance with the forgetting factor $\lambda$ with other stationary signal input types, model orders and echo paths modelled.

Consider now the effect of the initialisation factor $\delta$ on the convergence and steady state $ERLEss_{dB}$ level achievable by the FIR LMS Newton algorithm. The same stepsize $\mu$, convergence factor $\alpha$ and two different forgetting factors $\lambda$ =0.999 and $\lambda$ =0.9999 are used for all these experiments. A stationary band limited pink noise signal $x(n)$ is used. From the results presented it can be clearly seen for stationary signals the higher the initialisation factor $\delta$ results in much slower convergence to both the required ERLE level ($TIC_{req}$) and the steady state ERLE level ($TIC_{ss}$) for the FIR LMS Newton algorithm. This is because the inverse covariance matrix estimate $\widehat{\mathbf{R}}_{xx}^{-1}(n)$ will take longer to converge from its initial state for lower initialisation factors. The impact of the initialisation factor $\delta$ is also more pronounced for higher forgetting factors. It can be seen from Figure 5.22 for lower forgetting factors (below $\lambda$ =0.99975) the initialisation factor will only effect the convergence times $TIC_{req}$ and $TIC_{ss}$ and not the achievable steady state $ERLEss_{dB}$ level within the 10s adaption period. The same trends in modelling performance with the initialisation factor $\delta$ can be observed for different model orders and other stationary input signal types for the FIR LMS Newton algorithm. A choice of approximately $\delta \leq 100/\sigma_x^2$ is recommended for stationary signals, where $\sigma_x^2$ is the input signal variance. A value around $\delta$ =100 can be selected for the FIR LMS Newton algorithm from the assessment of ERLE performance with the initialisation factor $\delta$ with other stationary signal input types of similar input power, model orders and echo paths modelled.

The effect of the convergence factor $\alpha$ on the convergence and steady state $ERLEss_{dB}$ level achievable by the FIR LMS Newton algorithm is shown in Figure 5.23. Figure 5.23 shows the ensemble averaged ERLE level results achieved for a model order of 42 coefficients for modelling experiments with different forgetting factors for the face up no seals handset echo path response of Chapter 4. The same stepsize $\mu$, initialisation factor $\delta$ and two different forgetting factors $\lambda$ =0.999 and $\lambda$ =0.9999 are used for all these experiments. A stationary band limited pink noise signal $x(n)$ is used. From the results presented it can be clearly seen for stationary signals the higher the convergence factor $\alpha$ results in much slower convergence to both the required ERLE level ($TIC_{req}$) and the steady state ERLE level ($TIC_{ss}$) for the FIR LMS Newton algorithm. The impact of the convergence factor can be clearly seen to be much more pronounced in Figure 5.23 for larger forgetting factors ($\lambda$ =0.9999 and above), and effects both the convergence times $TIC_{req}$ and $TIC_{ss}$, and the steady state $ERLEss_{dB}$ level. Where a larger forgetting factor is needed in an application the convergence factor $\alpha$ can be reduced to improve the convergence performance of the FIR LMS Newton algorithm. Like wise where required a larger convergence factor $\alpha$ is used the convergence of the FIR LMS Newton can effectively be slowed down or halted. At lower

forgetting factors (below $\lambda$=0.99975) the convergence factor $\alpha$ effects only convergence performance ($TTC_{req}$ and $TIC_{ss}$) and not the achievable steady state $ERLEss_{dB}$ level. The same trends in modelling performance with the convergence factor $\alpha$ can be observed for different model orders and other stationary input signal types for the FIR LMS Newton algorithm. A value between $\alpha$=0.001 and $\alpha$=0.005 can be selected for the FIR LMS Newton algorithm from the assessment of ERLE performance with the initialisation factor $\alpha$ with other stationary signal input types, model orders and echo paths modelled.

Now the impact of inverse covariance matrix parameters, $\lambda, \alpha$ and $\delta$ on the steady state modelling performance of the FIR LMS Newton algorithm has been analysed and a suitable range for these parameters has been established, consider the effect of the stepsize value $\mu$ on the convergence and steady state $ERLEss_{dB}$ level achievable by the FIR LMS Newton algorithm. Figure 5.24 to Figure 5.27 show the impact on steady state modelling performance and convergence of the FIR LMS Newton algorithm for different stepsize levels for both a white noise and bandlimited pink noise signal input.

From Figure 5.24 and Figure 5.25 for stepsize levels in the range 0.0005 to $10^{-2}$ the maximum $ERLEss_{dB}$ is achievable within the 10s adaption period for the FIR LMS Newton algorithm. Comparing to Figure 5.2 and Figure 5.3 for the FIR NLMS algorithm, it is clear that for a suitably chosen stepsize level the FIR Normalised LMS and LMS Newton algorithms have the same Misadjustment and achieve the same $ERLEss_{dB}$ level within the 10s adaption period [5.2]. Unlike the FIR NLMS algorithm in Figure 5.4 and Figure 5.5, it can be seen in Figure 5.26 and Figure 5.27 that LMS Newton based adaption overcomes the larger eigenvalue spread associated with a band limited pink noise signal input. The convergence rate behaviour to both the required and steady state ERLE levels are very similar for both a white noise input and a bandlimited pink noise signal input with stepsize. This is due to the component $\mathbf{R}_{xx}^{-1}(n)$ in the LMS Newton algorithm update of (3.1.51) which will essentially equalise the eigenvalues of the correlation matrix of the input signal in each direction.

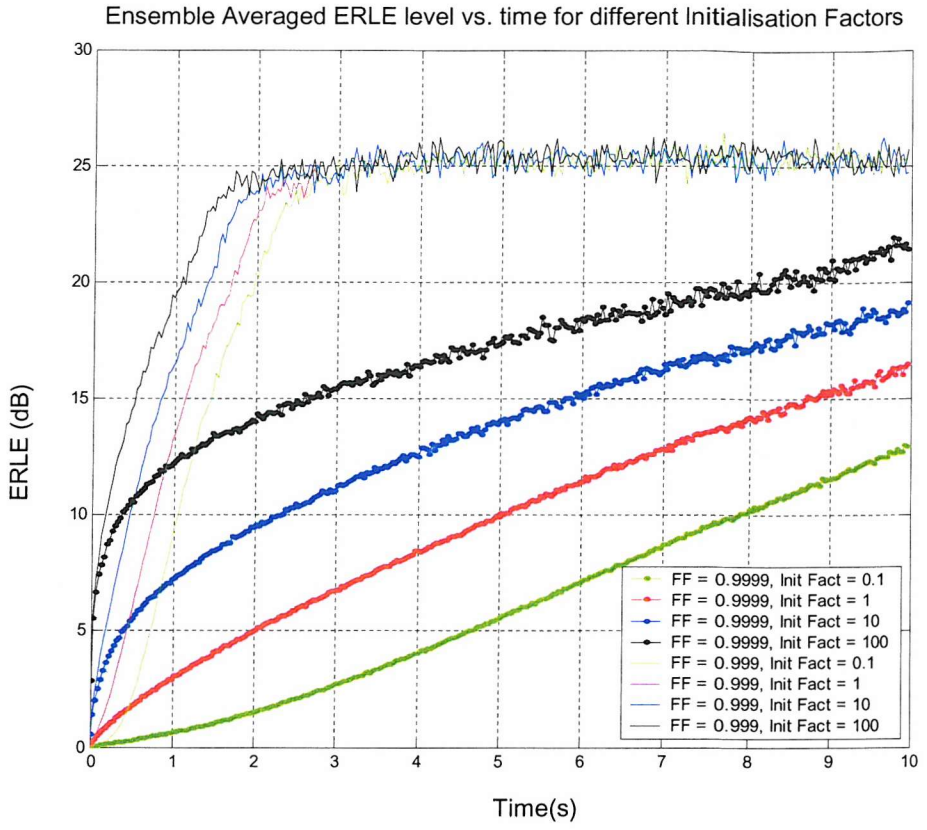


**Figure 5.22 : FIR LMS Newton ERLE performance with different Initialisation Factors $\delta$**

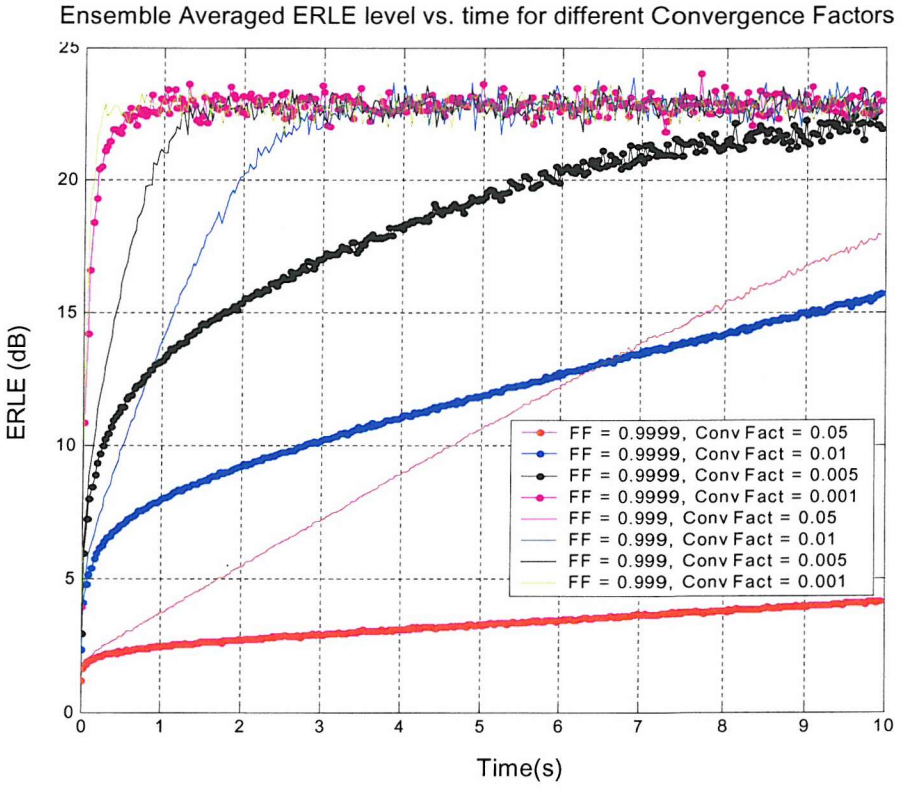


**Figure 5.23 : FIR LMS Newton ERLE performance with different Convergence Factors $\alpha$**

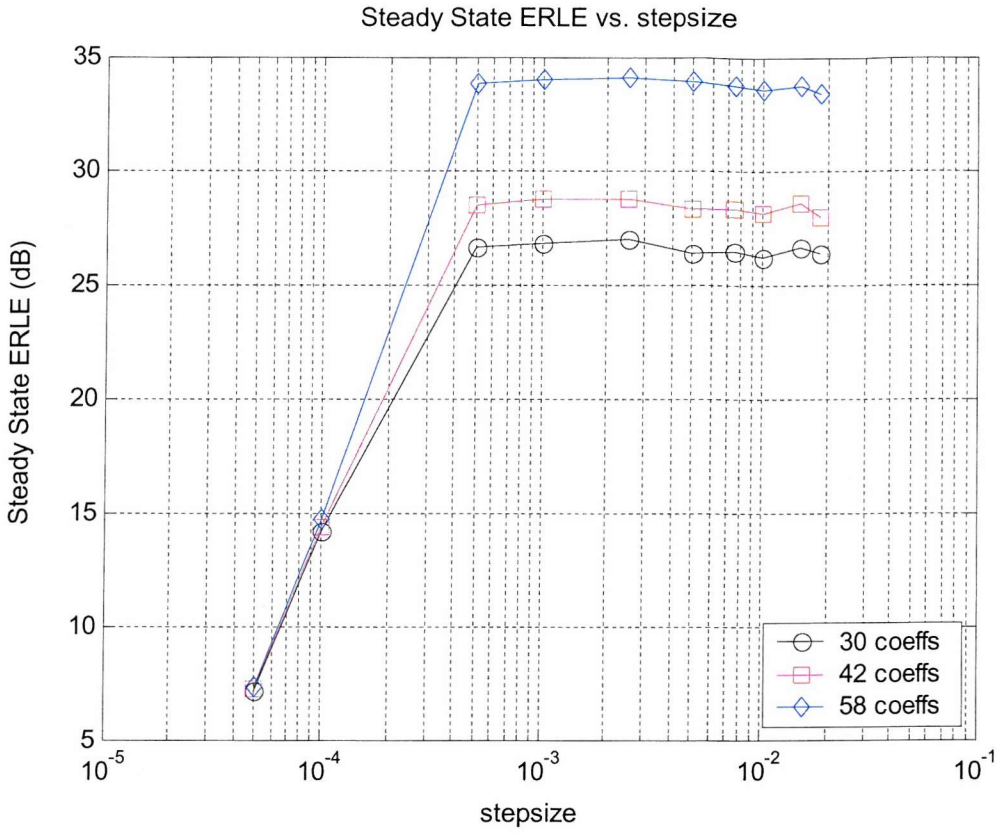


**Figure 5.24 : Steady State ERLE level for FIR LMS Newton vs. stepsize, for different filter orders, for white noise input**

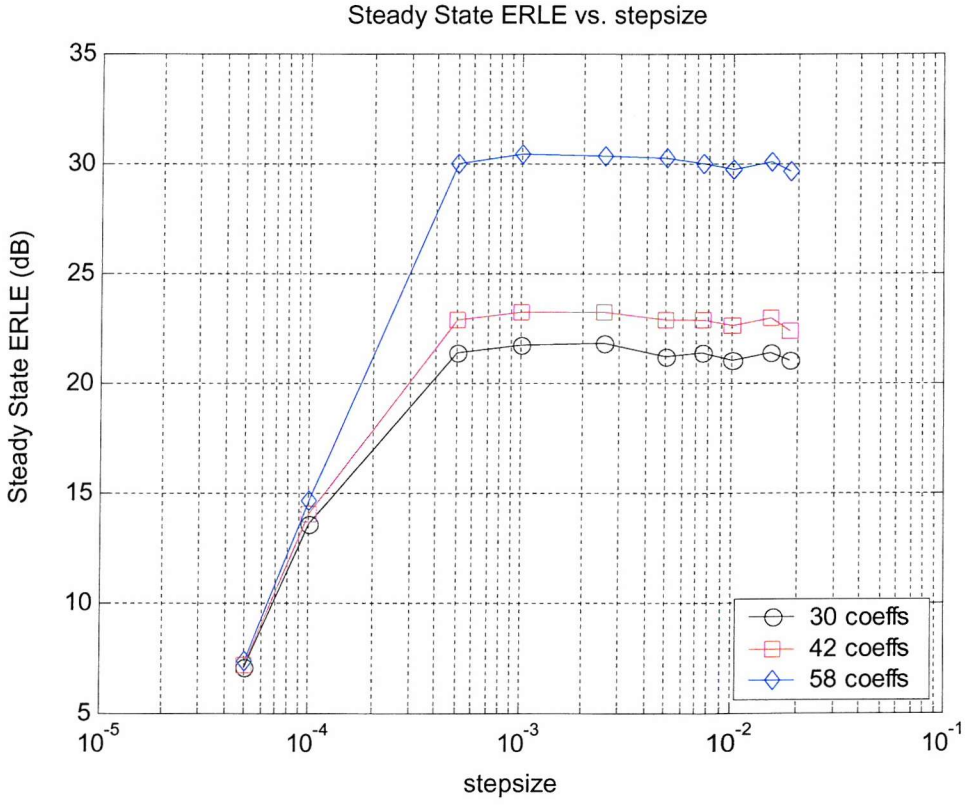


**Figure 5.25 : Steady State ERLE level for FIR LMS Newton vs. stepsize, for different filter orders, for band limited pink noise input**

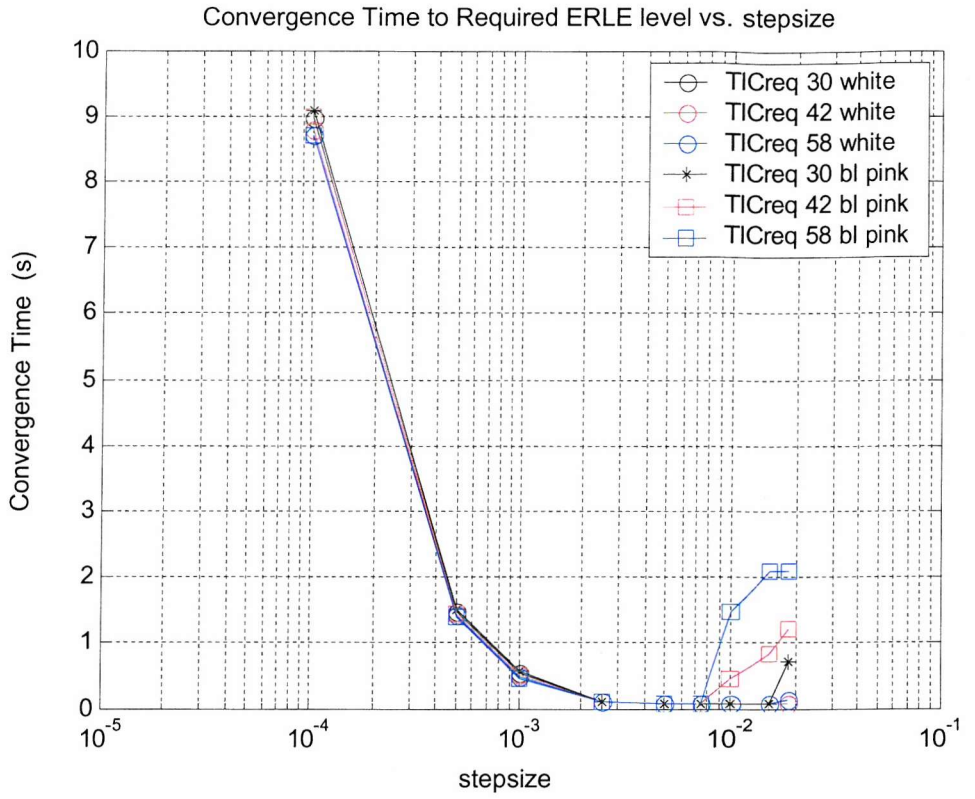


**Figure 5.26 : Convergence time to required ERLE level for FIR LMS Newton vs. stepsize, for different filter orders**

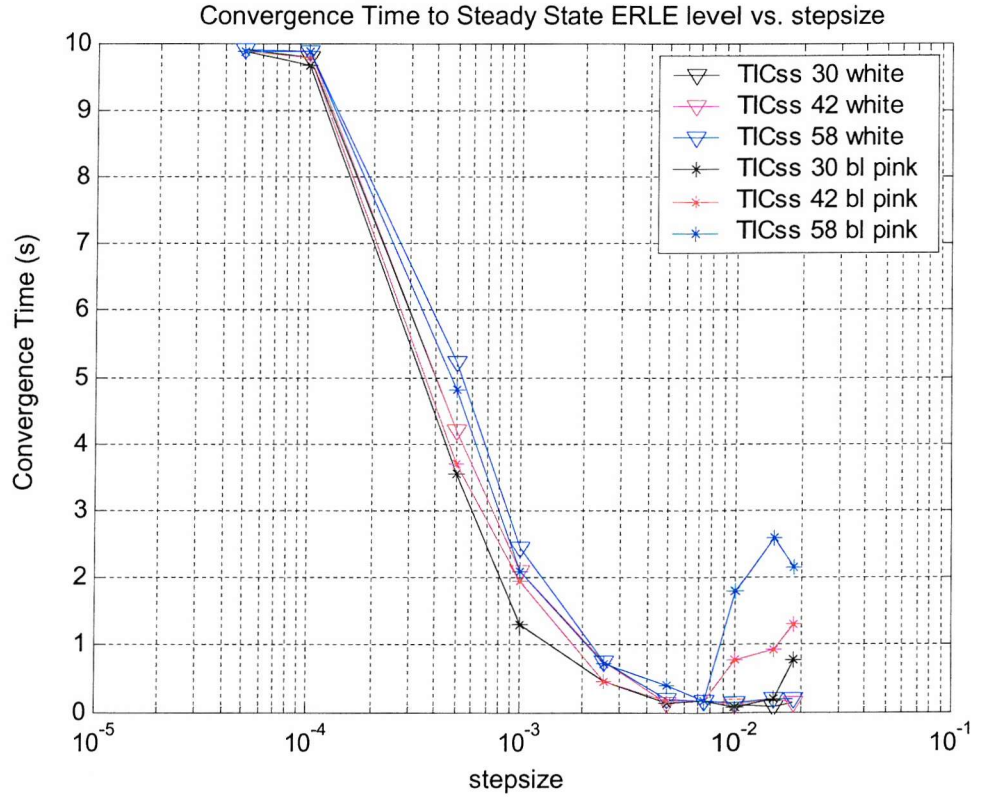


**Figure 5.27 : Convergence time to the Steady State ERLE level for FIR LMS Newton vs. stepsize, for different filter orders**

### 5.2.5.2. The Equation Error LMS Newton Adaptive IIR Algorithm

Consider now the effect of the forgetting factor $\lambda$ on the convergence and steady state $ERLEss_{dB}$ level achievable by the Equation Error LMS Newton algorithm. Figure 5.21 shows the ensemble averaged ERLE level results achieved for a model order of (31,11) for modelling experiments with different forgetting factors for the face up handset echo path response of Chapter 4. The same stepsize $\mu$, convergence factor $\alpha$ and initialisation factor $\delta$ are used for all these experiments. A stationary band limited pink noise signal $x(n)$ is used. From the results presented in Fig Figure 5.28 it can be clearly seen similar modelling performance is obtained as for the FIR LMS Newton algorithm discussed earlier with respect to the forgetting factor $\lambda$. Much slower convergence can be observed with higher forgetting factors $\lambda$ to both the required ERLE level ($TIC_{req}$) and the steady state ERLE level ($TIC_{ss}$). A larger forgetting factor gives more weight to previous estimates $\hat{\mathbf{R}}_{\varphi_e\varphi_e}(n-1)$, and thus slower convergence for the inverse covariance matrix estimate $\hat{\mathbf{R}}^{-1}_{\varphi_e\varphi_e}(n)$ due to the larger weighting by $1/\lambda$. At $\lambda$=0.9999 and above the steady state $ERLEss_{dB}$ level become affected during the 10s adaption period. At low forgetting factors $\lambda$ below 0.99 the steady state $ERLEss_{dB}$ level achievable becomes lower, and below $\lambda$=0.975 instability occurs.

A value of $\lambda$=0.999 can be selected for the Equation Error LMS Newton algorithm from the assessment of ERLE performance with the forgetting factor $\lambda$ with other stationary signal input types, model orders and echo paths modelled.

Consider now the effect of the initialisation factor $\delta$ on the convergence and steady state $ERLEss_{dB}$ level achievable by the Equation Error LMS Newton algorithm. Figure 5.29 shows the ensemble averaged ERLE level results achieved for a model order of (31,11) for modelling experiments with different forgetting factors for the face up no seals handset echo path response of Chapter 4. The same stepsize $\mu$, convergence factor $\alpha$ and two different forgetting factors $\lambda$=0.999 and $\lambda$=0.9999 are used for all these experiments. A stationary band limited pink noise signal $x(n)$ is again used. From the results presented it can be seen that the higher the initialisation factor $\delta$ results in much slower convergence for the Equation Error LMS Newton algorithm. This due to the fact the inverse covariance matrix estimate $\hat{\mathbf{R}}^{-1}_{\varphi_e\varphi_e}(n)$ will take longer to converge from its initial state for lower initialisation factors. A choice of approximately $\delta \leq 100/\sigma_x^2$ is recommended for stationary signals, where $\sigma_x^2$ is the input signal variance. Like the FIR LMS Newton algorithm a value around $\delta$ =100 can be selected for the Equation Error LMS Newton algorithm from the assessment of ERLE performance with the initialisation factor $\delta$ with other stationary signal input types of similar input power, model orders and echo paths modelled.

Consider lastly the effect of the convergence factor $\alpha$ on the convergence and steady state $ERLEss_{dB}$ level achievable by the Equation Error LMS Newton algorithm is shown in Figure 5.30. Figure 5.30 shows the ensemble averaged ERLE level results achieved for a model order of (31,11) for modelling experiments with different forgetting factors for the face up no seals handset echo path response of Chapter 4. The same stepsize $\mu$, initialisation factor $\delta$ and two different forgetting factors $\lambda$=0.999 and $\lambda$=0.9999 are used for all these experiments. A stationary band limited pink noise signal $x(n)$ is again used. The convergence to both the required ERLE level ($TIC_{req}$) and the steady state ERLE level ($TIC_{ss}$) is impacted by the value of $\alpha$, the higher the convergence factor $\alpha$ the slower convergence is to both the required ERLE level ($TIC_{req}$) and the steady state ERLE level ($TIC_{ss}$) for the Equation Error LMS Newton algorithm. A value between $\alpha$ =0.001 and $\alpha$ =0.005 can be selected for the Equation Error LMS Newton algorithm from the assessment of ERLE performance with the convergence factor $\alpha$ for different stationary signal input types, model orders and echo paths modelled.

Now the impact of inverse covariance matrix parameters, $\lambda$, $\alpha$ and $\delta$ on the steady state modelling performance of the Equation LMS Newton algorithm has been analysed and a suitable range for these parameters has been established, consider the effect of the stepsize value $\mu$ on the convergence and steady state $ERLEss_{dB}$ level achievable by the Equation Error LMS Newton algorithm. Figure 5.24 to Figure 5.27 show the impact on steady state modelling performance and convergence of the FIR LMS Newton algorithm for different stepsize levels for both a white noise and bandlimited pink noise signal input.

From Figure 5.31 and Figure 5.32 for stepsize levels in the range 0.00075 to $10^{-2}$ the maximum $ERLEss_{dB}$ is achievable within the 10s adaption period for the Equation Error LMS Newton algorithm. Comparing to Figure 5.8 and Figure 5.9 for the Equation Error NLMS algorithm, it is clear that for the 10s adaption period higher $ERLEss_{dB}$ is achievable using the Equation Error LMS Newton based adaption, particularly at higher model orders. From Figure 5.33 and Figure 5.34, unlike the Equation Error NLMS algorithm, the convergence rate behaviour to both the required and steady state ERLE levels are very similar for both a white noise input and a bandlimited pink noise signal input with stepsize for all model orders. Improved convergence to the steady state ERLE level is clearly obtained by using the Equation Error LMS Newton algorithm. This is due to the component $\hat{\mathbf{R}}^{-1}_{\varphi_e\varphi_e}(n)$ in the LMS Newton algorithm update of (3.3.46) which will essentially equalise the eigenvalues of the correlation matrix $\hat{\mathbf{R}}_{\varphi_e\varphi_e}(n)$ in each direction, improving the decay rate of any coefficient error modes.

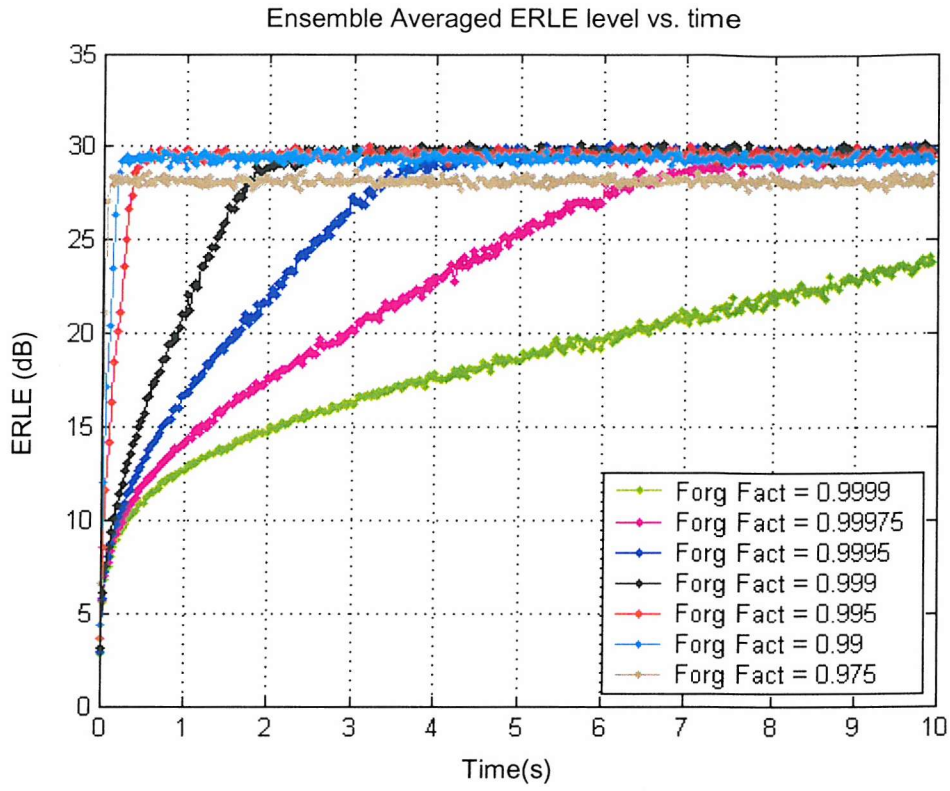


**Figure 5.28 : Equation Error LMS Newton ERLE performance with different forgetting factors $\lambda$**

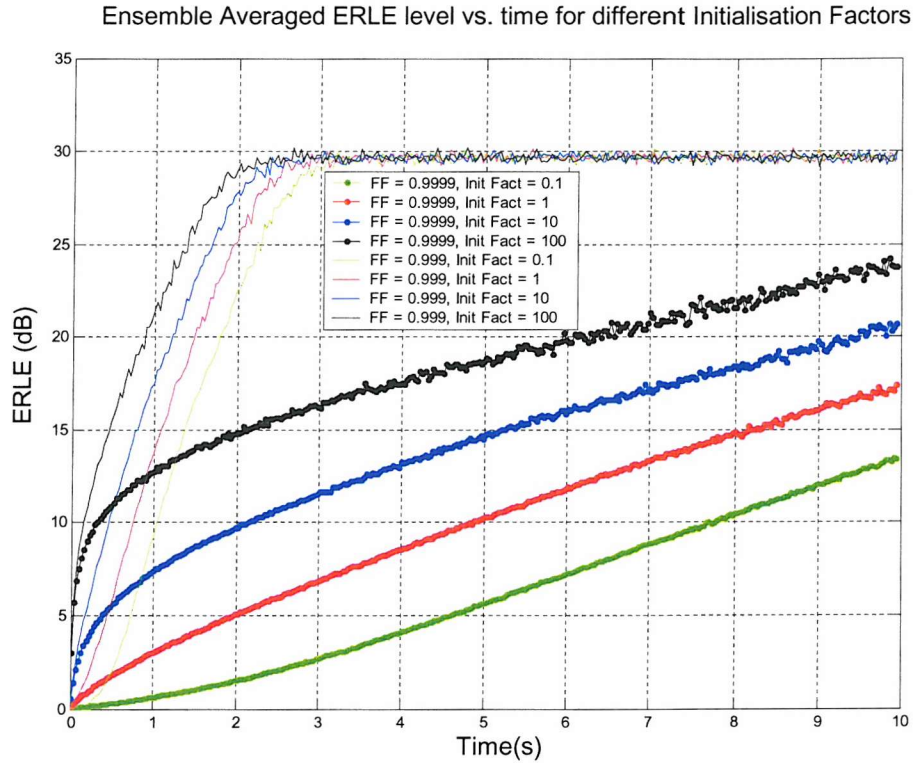


**Figure 5.29 : Equation Error LMS Newton ERLE performance with the initialisation factor $\delta$**

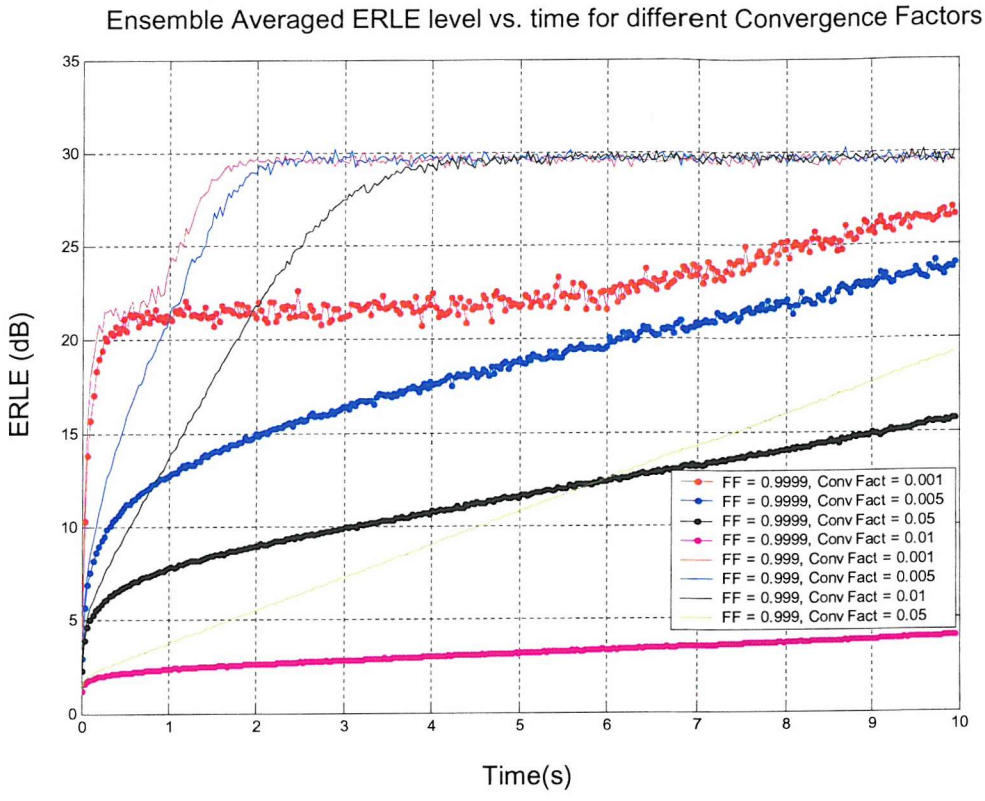


**Figure 5.30 : Equation Error LMS Newton ERLE performance with the convergence factor $\alpha$**

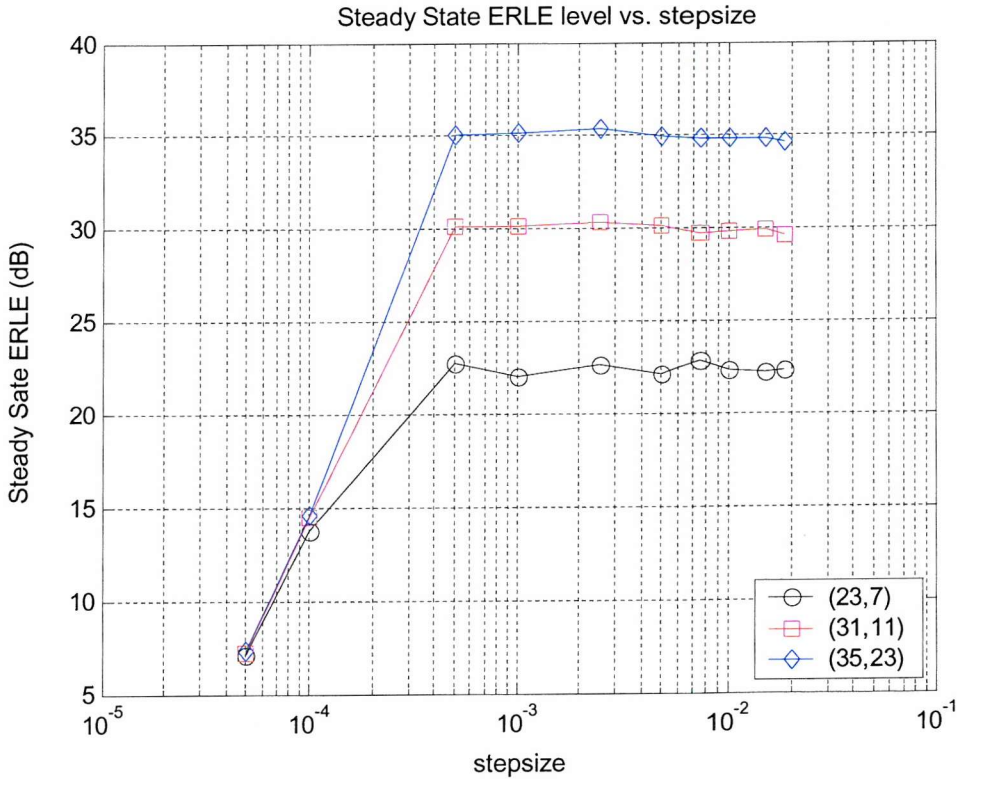


**Figure 5.31 : Steady State ERLE level for Equation Error LMS Newton vs. stepsize, for different filter orders, for white noise input**

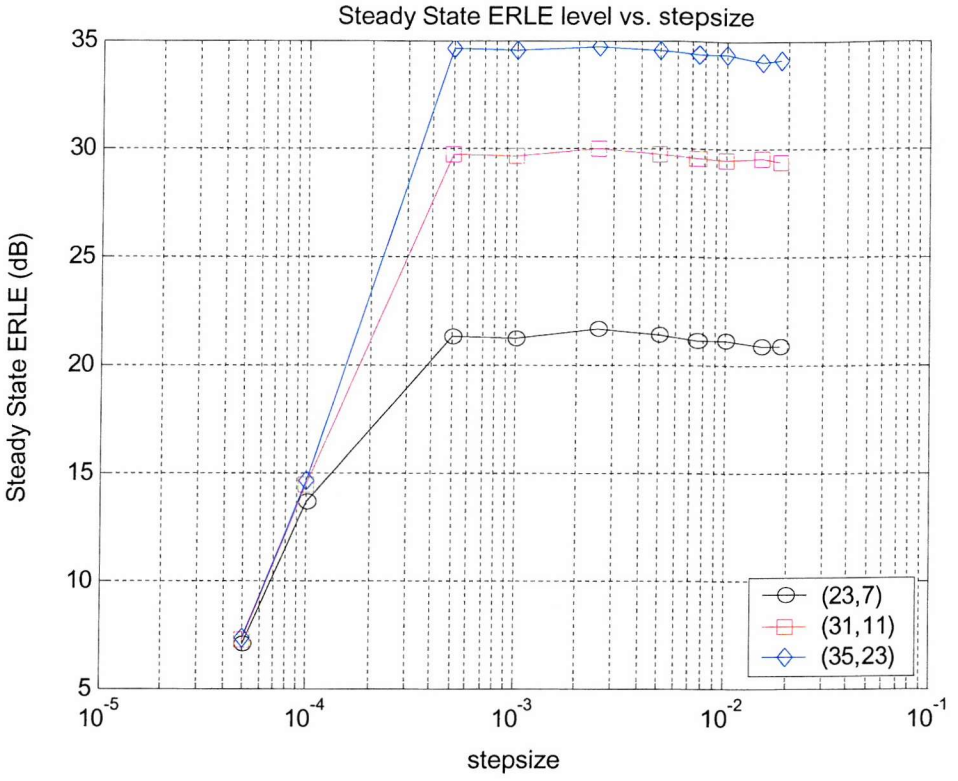


**Figure 5.32 : Steady State ERLE level for Equation Error LMS Newton vs. stepsize, for different filter orders, for band limited pink noise input**

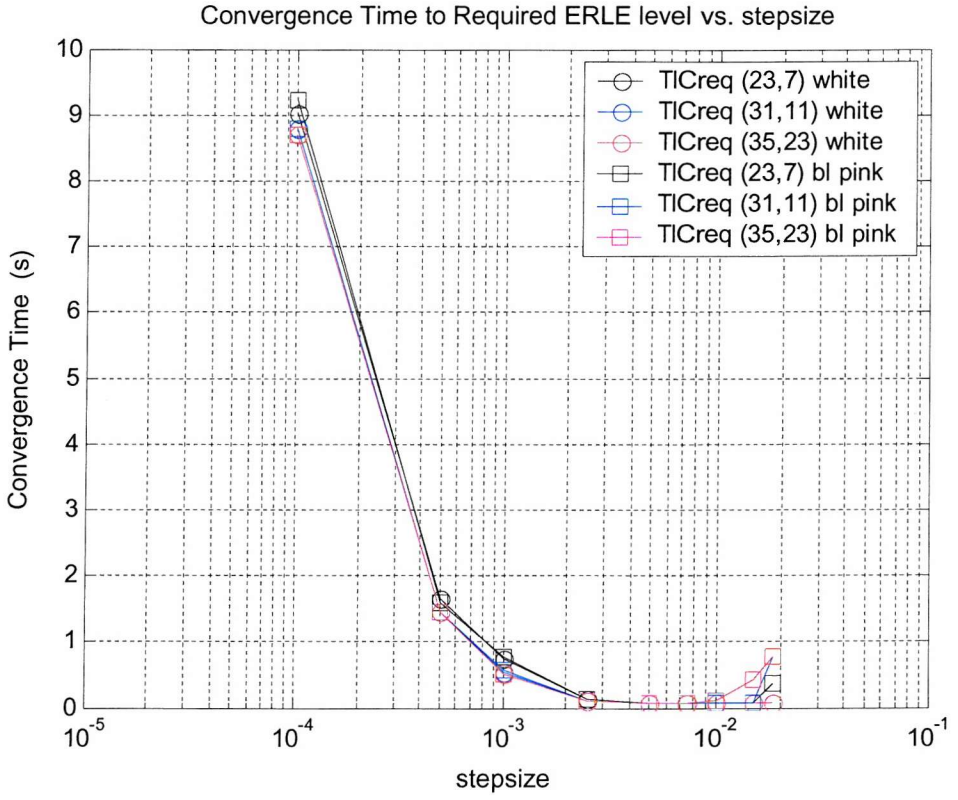


**Figure 5.33 : Convergence time to the required ERLE level for Equation Error LMS Newton vs. stepsize, for different filter orders**

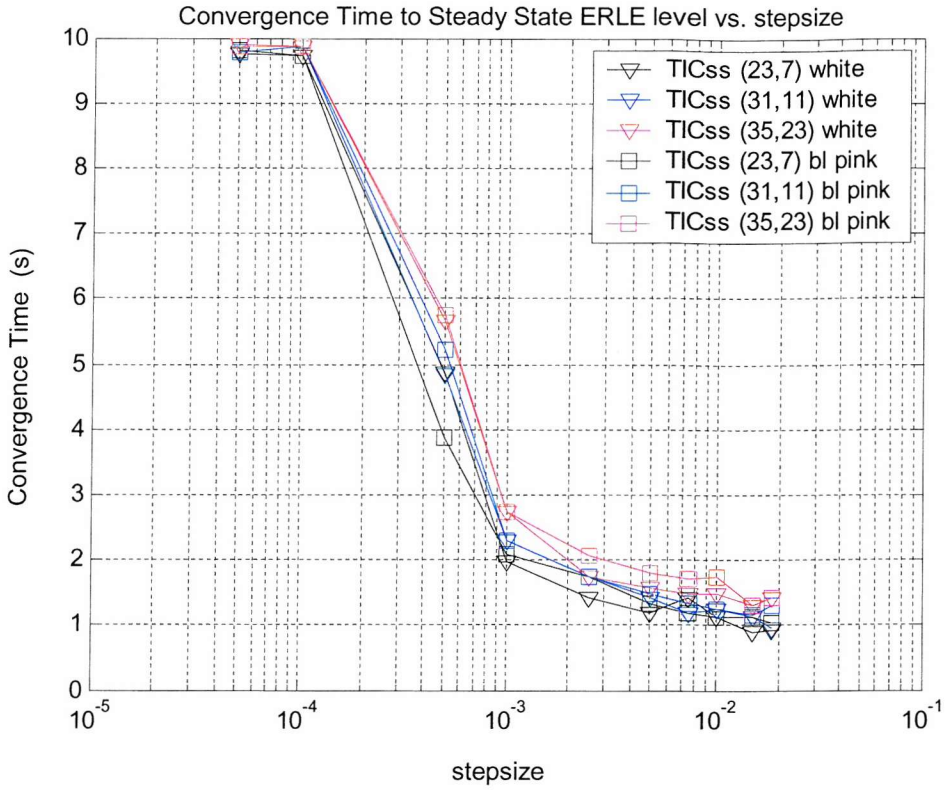


**Figure 5.34 : Convergence time to the Steady State ERLE level for Equation Error LMS Newton vs. stepsize, for different filter orders**

### 5.2.5.3. The Simplified Gradient LMS Newton Adaptive IIR Algorithm

Consider now the effect of the forgetting factor $\lambda$ on the convergence and steady state $ERLEss_{dB}$ level achievable by the Simplified Gradient LMS Newton algorithm. Figure 5.35 shows the ensemble averaged ERLE level results achieved for a model order of (27,15) for modelling experiments with different forgetting factors for the face up no seals handset echo path response of Chapter 4. The same stepsize $\mu$, convergence factor $\alpha$ and initialisation factor $\delta$ are used for all these experiments. A stationary band limited pink noise signal $x(n)$ is used. From the results presented in Figure 5.35 it can be clearly seen similar modelling performance is obtained as for the other LMS Newton algorithms discussed earlier with respect to the forgetting factor $\lambda$. Much slower convergence can be observed with higher forgetting factors $\lambda$ to both the required ERLE level ($TIC_{req}$) and the steady state ERLE level ($TIC_{ss}$) A larger forgetting factor gives more weight to previous estimates $\hat{\mathbf{R}}_{\varphi_f\varphi_f}(n-1)$, and thus slower convergence for the inverse covariance matrix estimate $\hat{\mathbf{R}}^{-1}_{\varphi_f\varphi_f}(n)$ due to the larger weighting by $1/\lambda$. At above $\lambda$ =0.99975 the steady state $ERLEss_{dB}$ levels become affected during the 10s adaption period. At

low forgetting factors $\lambda$ below 0.9975 the steady state $ERLEss_{dB}$ level achievable becomes lower, and below $\lambda$ =0.995 instability occurs.

A value of $\lambda$ =0.999 can be selected for the Simplified Gradient LMS Newton algorithm from the assessment of ERLE performance with the forgetting factor $\lambda$ with other stationary signal input types, model orders and echo paths modelled.

Consider now the effect of the initialisation factor $\delta$ on the convergence and steady state $ERLEss_{dB}$ level achievable by the Simplified Gradient LMS Newton algorithm. Figure 5.36 shows the ensemble averaged ERLE level results achieved for a model order of (27,15) for modelling experiments with different forgetting factors for the face up no seals handset echo path response of Chapter 4. The same stepsize $\mu$ , convergence factor $\alpha$ and two different forgetting factors $\lambda$ =0.999 and $\lambda$ =0.9999 are used for all these experiments. A stationary band limited pink noise signal $x(n)$ is again used. From the results presented it can be seen that the higher the initialisation factor $\delta$ results in much slower convergence for the Equation Error LMS Newton algorithm. This due to the fact the inverse covariance matrix estimate $\hat{\mathbf{R}}^{-1}_{\varphi_f\varphi_f}(n)$ will take longer to converge from its initial state for lower initialisation factors. A choice of approximately $\delta \leq 100/\sigma_x^2$ is recommended for stationary signals, where $\sigma_x^2$ is the input signal variance. Like other LMS Newton algorithms discussed a value around $\delta$ =100 can be selected for the Simplified Gradient LMS Newton algorithm from the assessment of ERLE performance with the initialisation factor $\delta$ with other stationary signal input types of similar input power, model orders and echo paths modelled.

Consider lastly the effect of the convergence factor $\alpha$ on the convergence and steady state $ERLEss_{dB}$ level achievable by the Equation Error LMS Newton algorithm is shown in Figure 5.37. Figure 5.37 shows the ensemble averaged ERLE level results achieved for a model order of (27,15) for modelling experiments with different forgetting factors for the face up no seals handset echo path response of Chapter 4. The same stepsize $\mu$ , initialisation factor $\delta$ and two different forgetting factors $\lambda$ =0.999 and $\lambda$ =0.9999 are used for all these experiments. A stationary band limited pink noise signal $x(n)$ is again used. The convergence to both the required ERLE level ($TIC_{req}$) and the steady state ERLE level ($TIC_{ss}$) is impacted by the value of $\alpha$ , the higher the convergence factor $\alpha$ the slower convergence is to both the required ERLE level ($TIC_{req}$) and the steady state ERLE level ($TIC_{ss}$) for the Equation Error LMS Newton algorithm. Like the other LMS Newton based algorithms discussed a value between $\alpha$ =0.001 and $\alpha$ =0.005 can be selected for the Simplified Gradient LMS Newton algorithm from the assessment of ERLE performance with the convergence factor $\alpha$ for different stationary signal input types, model orders and echo paths modelled.

Now the impact of inverse covariance matrix parameters, $\lambda$ ,$\alpha$ and $\delta$ on the steady state modelling performance of the Simplified Gradient LMS Newton algorithm has been analysed and a suitable range for these parameters has been established, consider the effect of the stepsize value $\mu$ on the

convergence and steady state $ERLEss_{dB}$ level achievable by the Equation Error LMS Newton algorithm. Figure 5.38 to Figure 5.41 show the impact on steady state modelling performance and convergence of the Simplified Gradient LMS Newton algorithm for different stepsize levels for both a white noise and bandlimited pink noise signal input.

From Figure 5.38 and Figure 5.39 for stepsize levels in the range $10^{-3}$ to 0.0075 the maximum $ERLEss_{dB}$ is achievable within the 10s adaption period for the Simplified Gradient LMS Newton algorithm. Comparing to Figure 5.15 and Figure 5.16 for the Simplified Gradient NLMS algorithm, it is clear that for the 10s adaption period higher $ERLEss_{dB}$ is achievable using the Simplified Gradient LMS Newton based adaption. From Figure 5.40, unlike the Simplified gradient NLMS algorithm, the convergence rate behaviour to both the required and steady state ERLE levels are very similar for both a white noise input and a bandlimited pink noise signal input with stepsize for all model orders. From Figure 5.41 the same general trend on decreasing convergence rate to the steady state ERLE level is observable for all model orders and both input signal types. These different convergence time values are due to the component $\hat{\mathbf{R}}^{-1}_{\varphi_f\varphi_f}(n)$ in the LMS Newton algorithm update of (3.2.71) which will essentially equalise the eigenvalues of the correlation matrix $\hat{\mathbf{R}}_{\varphi_f\varphi_f}(n)$ in each direction, improving the decay rate of any coefficient error modes.

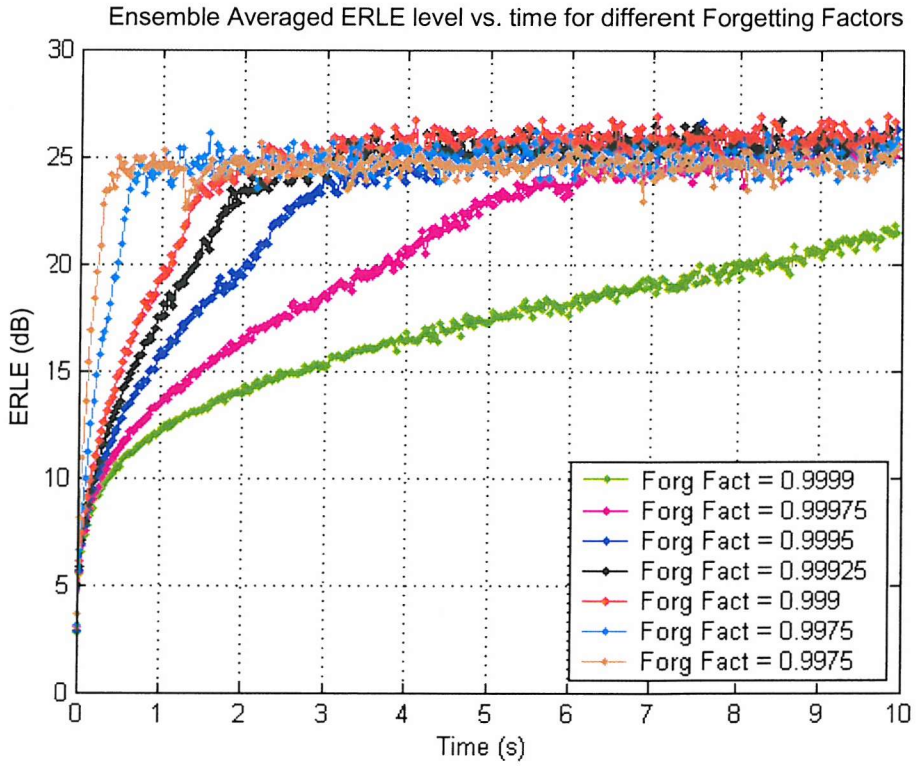


**Figure 5.35: Simplified Gradient LMS Newton ERLE performance vs. forgetting factors $\lambda$**

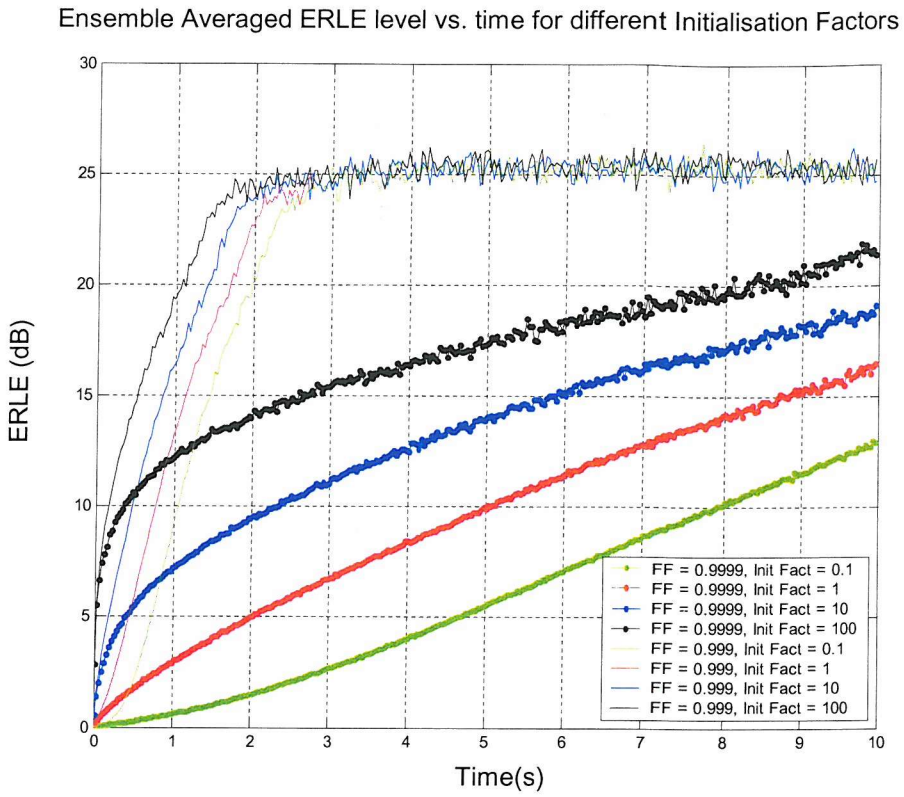


**Figure 5.36: Simplified Gradient LMS Newton ERLE performance vs. initialisation factor $\delta$**

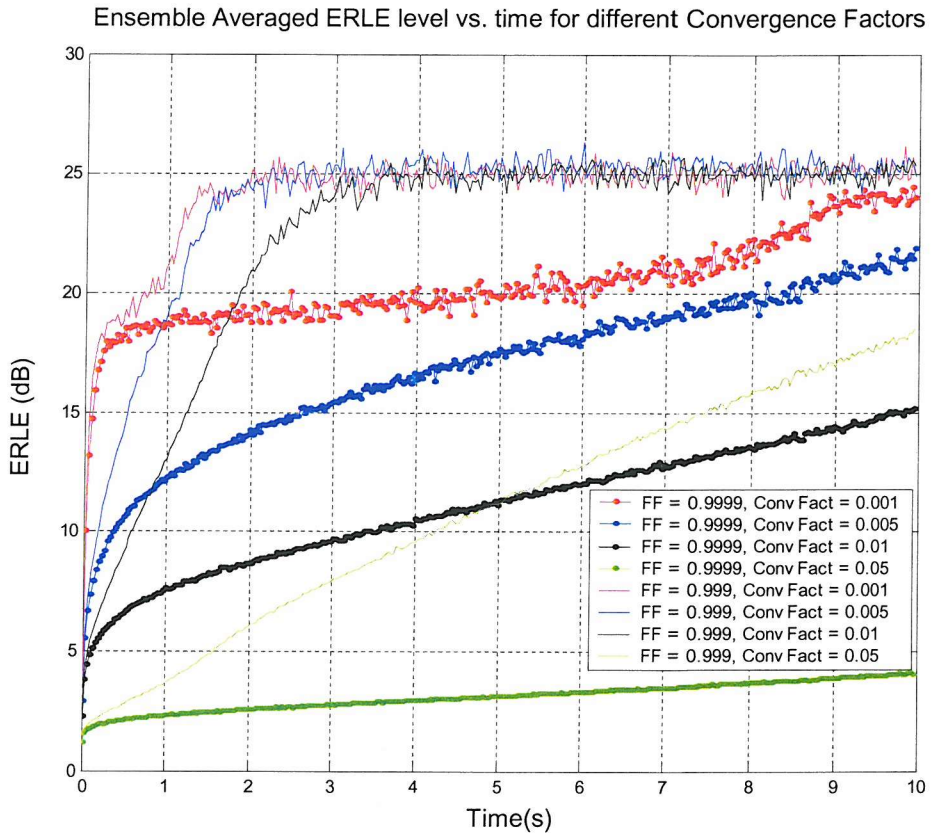


**Figure 5.37 : Simplified Gradient LMS Newton ERLE performance vs. convergence factors $\alpha$**

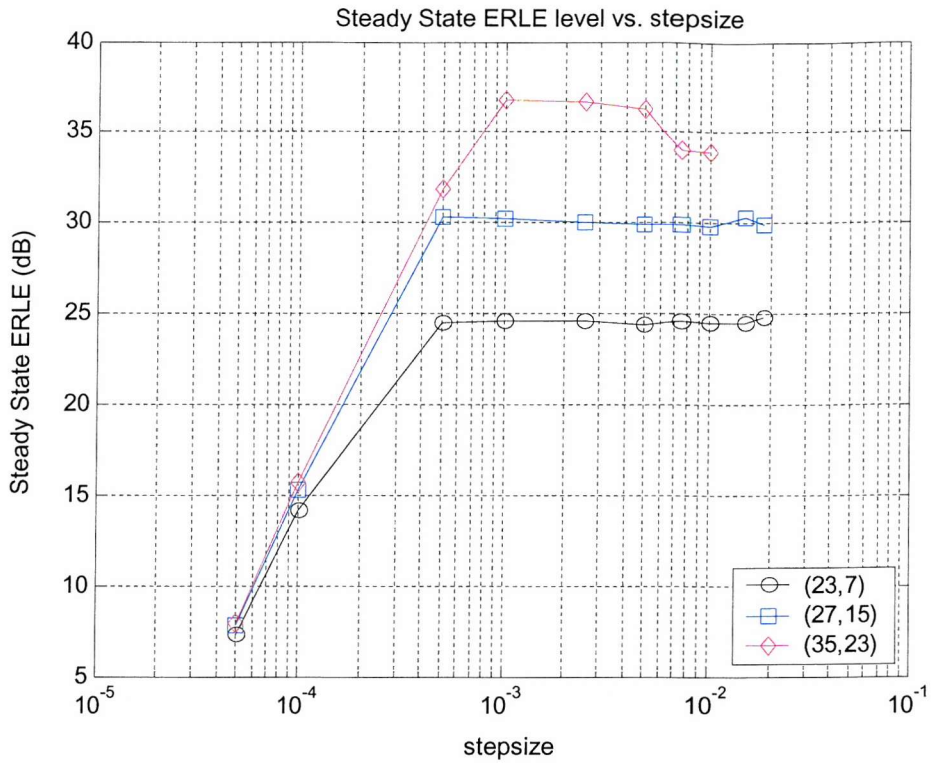


**Figure 5.38 : Steady State ERLE level for Simplified Gradient LMS Newton vs. stepsize, for different filter orders, for white noise input**

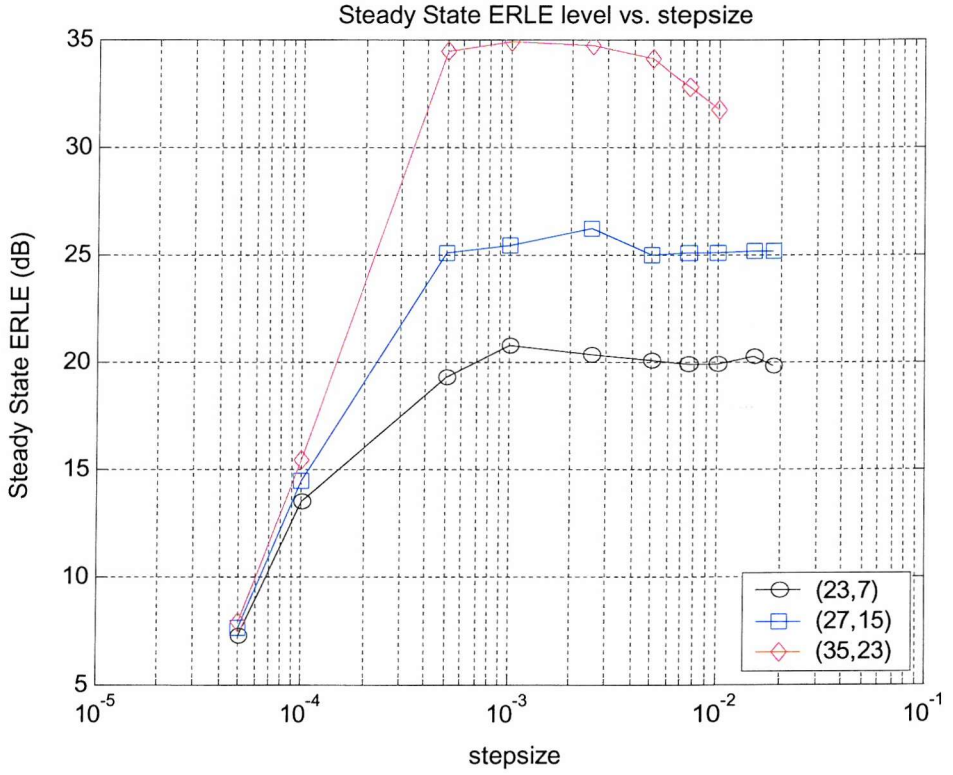


**Figure 5.39 : Steady State ERLE level for Simplified Gradient LMS Newton vs. stepsize, for different filter orders, for band limited pink noise input**

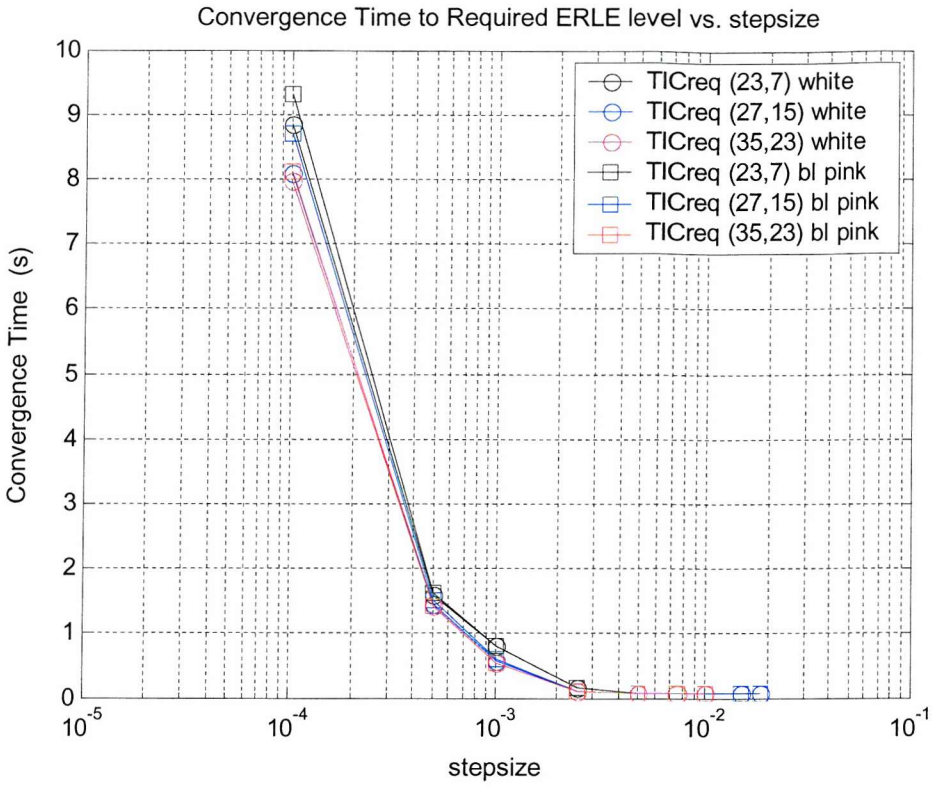


**Figure 5.40 : Convergence time to the required ERLE level for Simplified Gradient LMS Newton vs. stepsize, for different filter orders**

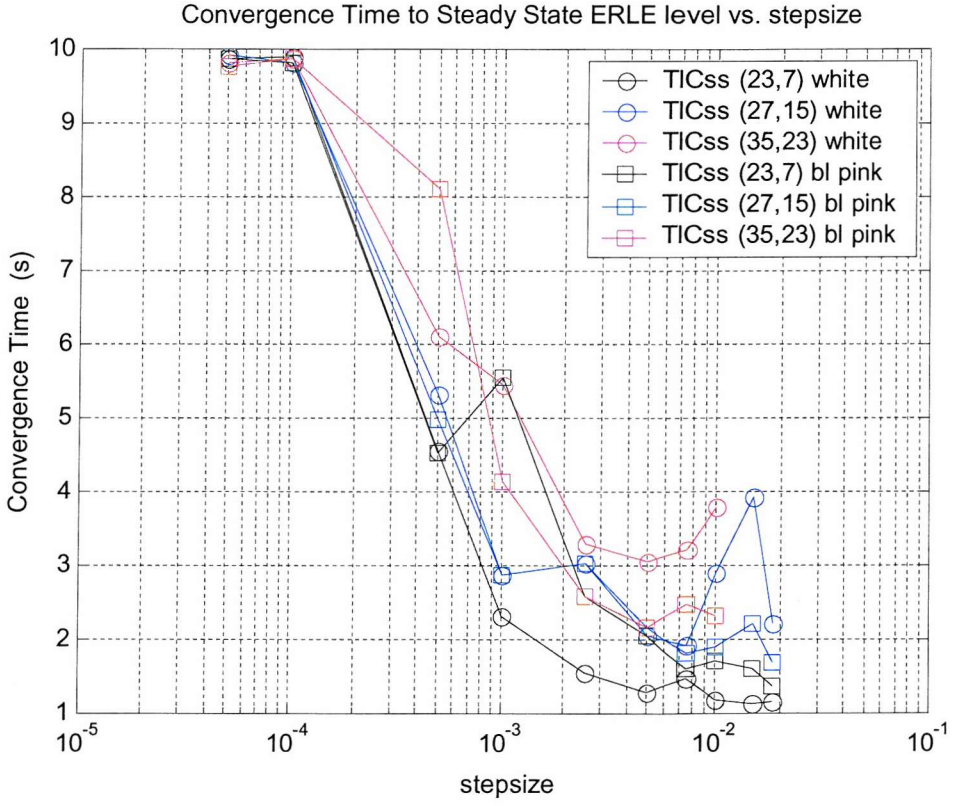


**Figure 5.41 : Convergence time to the Steady State ERLE level for Simplified Gradient LMS Newton vs. stepsize, for different filter orders**

### 5.2.6. Steady State Modelling results of Adaptive FIR and Equation Error Adaptive IIR algorithms

Having established the choice of algorithm design parameters on the modelling performance of both adaptive FIR and Equation Error adaptive algorithms used in this Chapter, modelling results for all the echo paths of Chapter 4 over a range of model orders can be presented. A single set of algorithm parameters are used for all experiments, using the recommendations discussed earlier.

The steady state ensemble averaged modelling results are shown in Figure 5.42 to Figure 5.53 for a range of different model orders for each echo path of Chapter 4. For Equation Error adaptive IIR algorithms different distributions of feedforward and feedback coefficients are used. The number of feedback coefficients used is fixed at 7,11,15,19 and 23 in these modelling experiments, where the number of feedforward coefficients is adjusted to keep the same total number of filter coefficients the same for both FIR and IIR adaptive algorithms. The total number of coefficients used is varied between 30 and 58 coefficients. To improve clarity on these figures only the most important points (up to a maximum of 4 points) are plotted at each different (M,N) model distribution for Equation Error adaptive IIR algorithms. Results for both Normalised LMS and LMS Newton adaptive FIR and IIR algorithms are presented using the same axis for easy comparison.

From the results presented in Figure 5.42 to Figure 5.53 it is clear the face down echo path configuration determines the minimum order for both adaptive FIR and Equation Error adaptive IIR algorithms needed to meet the required ERLE of each handset (shown as a horizontal red line in Figure 5.42 to Figure 5.53). A minimum model order of 42 coefficients, with 31 feedforward and 11 feedback coefficients, (31,11), is required by both the Equation Error Normalised LMS adaptive IIR algorithm and the Equation Error LMS Newton adaptive IIR algorithm. For the adaptive FIR algorithms a minimum order of 54 coefficients is required. A maximum Coefficient Reduction Factor (CRF) of up to 1.29 is possible with Equation Error adaptive IIR algorithms. At the model order of (31,11) the ensemble averaged ERLE levels and convergence times are summarised in Table 5-1 below.

| Echo Path | FIR LMSN | | | Equation Error NLMS | | | Equation Error LMSN | | |
|---|---|---|---|---|---|---|---|---|---|
| | $TIC_{re}$ (ms) | $TIC_{ss}$ (ms) | $ERLE_{ss}$ (dB) | $TIC_{re}$ (ms) | $TIC_{ss}$ (ms) | $ERLE_{ss}$ (dB) | $TIC_{re}$ (ms) | $TIC_{ss}$ (ms) | $ERLE_{ss}$ (dB) |
| Face Up No Seals | 96 | 608 | 23.1 | 64 | 5376 | 26.2 | 96 | 1824 | 29.6 |
| Artificial Ear Seal | 32 | 384 | 16.2 | 32 | 8032 | 13.4 | 32 | 1824 | 15 |
| Loudspeaker Seal | 32 | 832 | 15.4 | 32 | 7136 | 16.1 | 32 | 1686 | 17.5 |
| Loudspeaker and Microphone Seal | 64 | 160 | 13.9 | 64 | 5440 | 19.8 | 256 | 1824 | 21.3 |
| Microphone Seal | 64 | 160 | 12.6 | 64 | 1984 | 15.9 | 64 | 1440 | 16.7 |
| Face Down | - | 256 | 13.6 | 3424 | 3424 | 16 | 1120 | 1376 | 16.9 |

**Table 5-1 : Summary of steady state ERLE and convergence results of FIR and Equation Error Algorithms for model order (31,11), total order 42 coefficients.**

From the ERLE levels presented in Table 5-2 it is clear both Equation Error Normalised LMS and LMS Newton algorithms cannot exceed the modelling performance of an equivalent FIR adaptive algorithm for all echo paths. However an ERLE gain of up to 5.7dB for the Equation Error Normalised LMS algorithms over an equivalent FIR adaptive algorithm is still possible. For Equation Error LMS Newton algorithms an ERLE gain of up to 7.2 dB is possible.

From Table 5-2 it can be seen that the convergence times to the required ERLE of each echo path ($TIC_{req}$) for all adaptive algorithms is similar. For the convergence times to the steady state ensemble averaged ERLE level($TIC_{ss}$) it is clear to see that the convergence of both Normalised LMS and LMS Newton Equation Error adaptive IIR algorithms is longer than that of an equivalent adaptive FIR algorithm. For Equation Error NLMS algorithms much slower convergence occurs to the steady state ensemble averaged ERLE than Equation Error LMS Newton based algorithms due to the dependency on the eigenvalue spread of $\mathbf{R}_{\varphi_e\varphi_e}$, which has off-diagonal components even for a white noise input signal due to the colouration of the echo path output signal. As a result the eigenvalue spread of $\mathbf{R}_{\varphi_e\varphi_e}$ depends on the echo path to be modelled, the slowest convergence occurring for the artificial ear sealed handset configuration. Faster convergence of Equation Error LMS Newton based algorithms for a bandlimited pink noise input also results in an improvement of the achievable steady state ensemble averaged ERLE level of up to 3.2dB during the 10s adaption period.

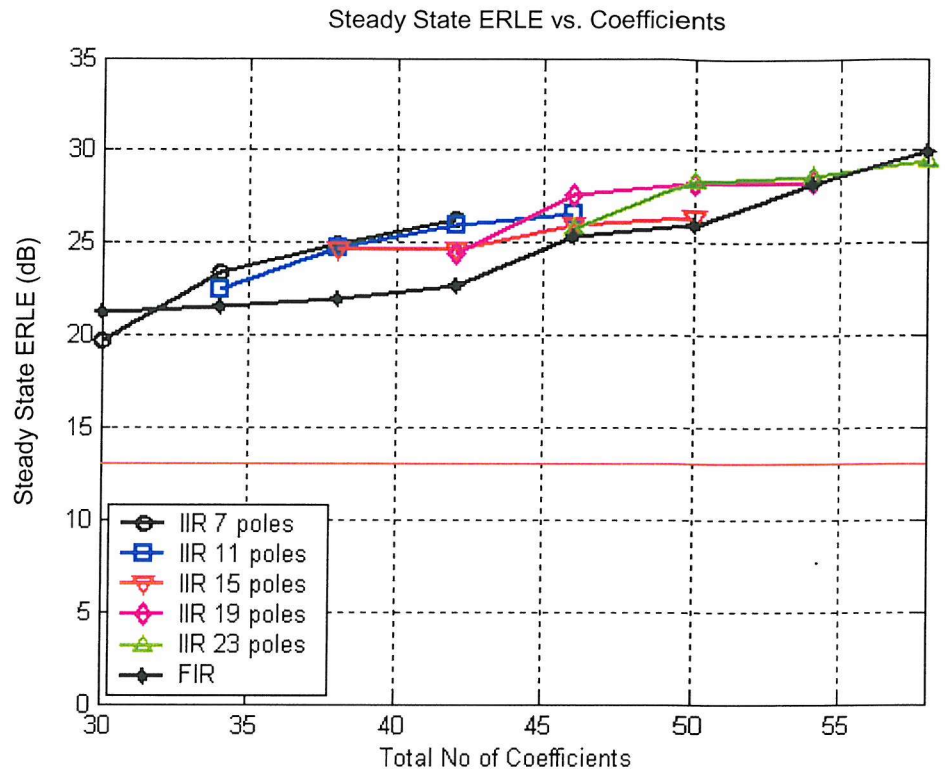


**Figure 5.42 : FIR vs. Equation Error Normalised LMS modelling results for the face up handset configuration with no transducer seals**

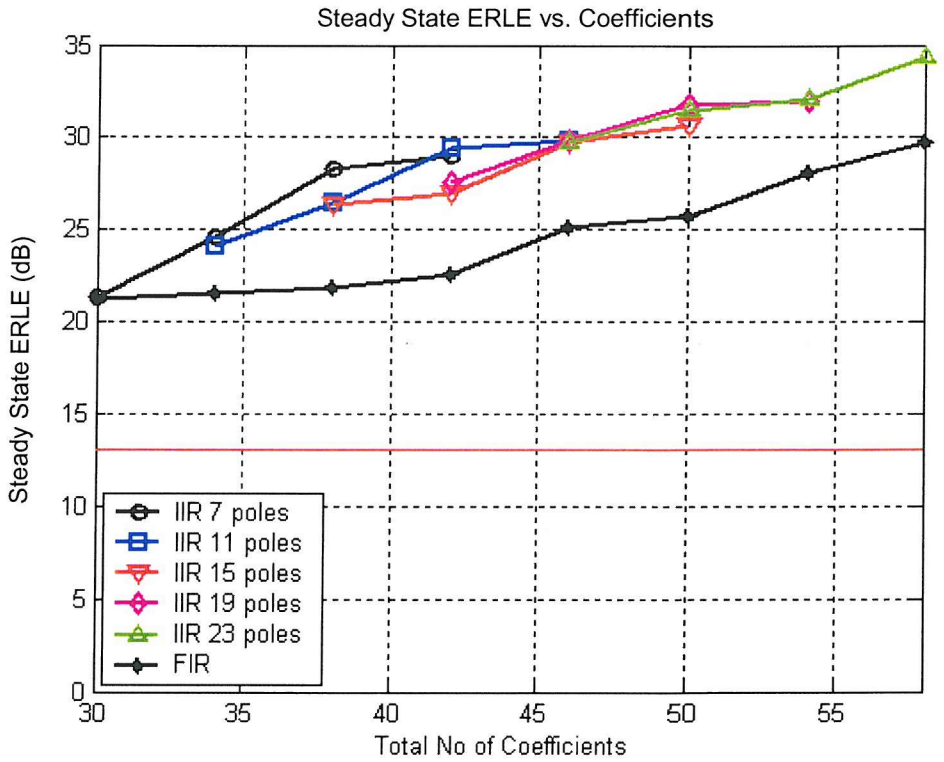


**Figure 5.43 : FIR vs. Equation Error LMS Newton modelling results for the face up handset configuration with no transducer seals**

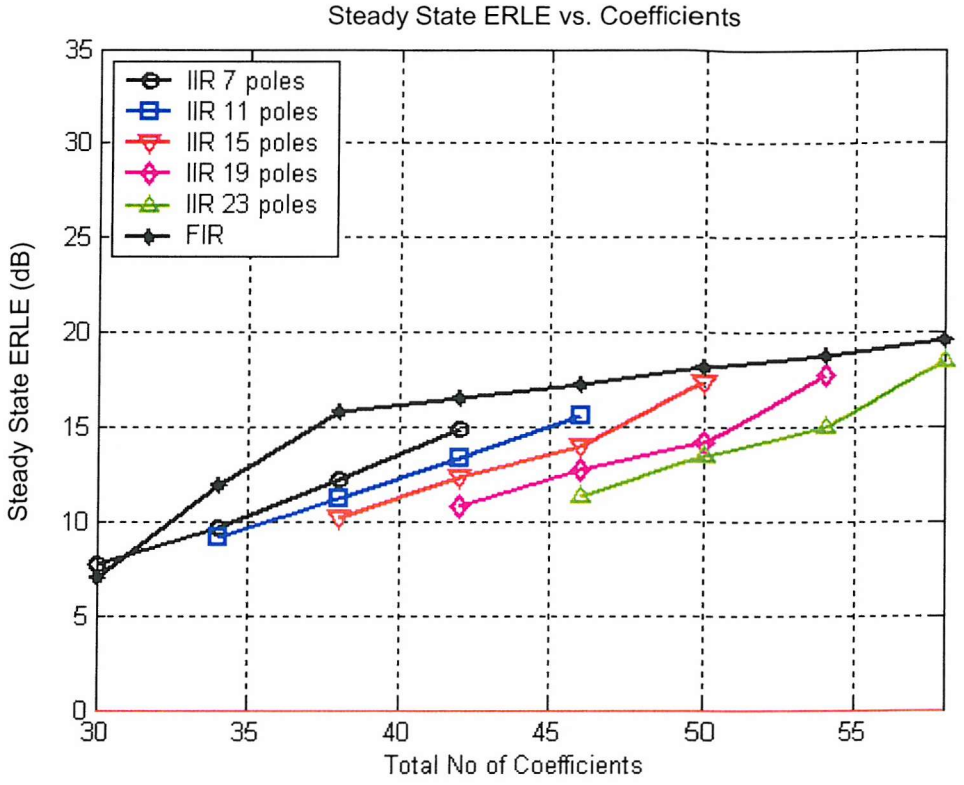


**Figure 5.44 : FIR vs. Equation Error Normalised LMS modelling results for the artificial ear sealed handset configuration**

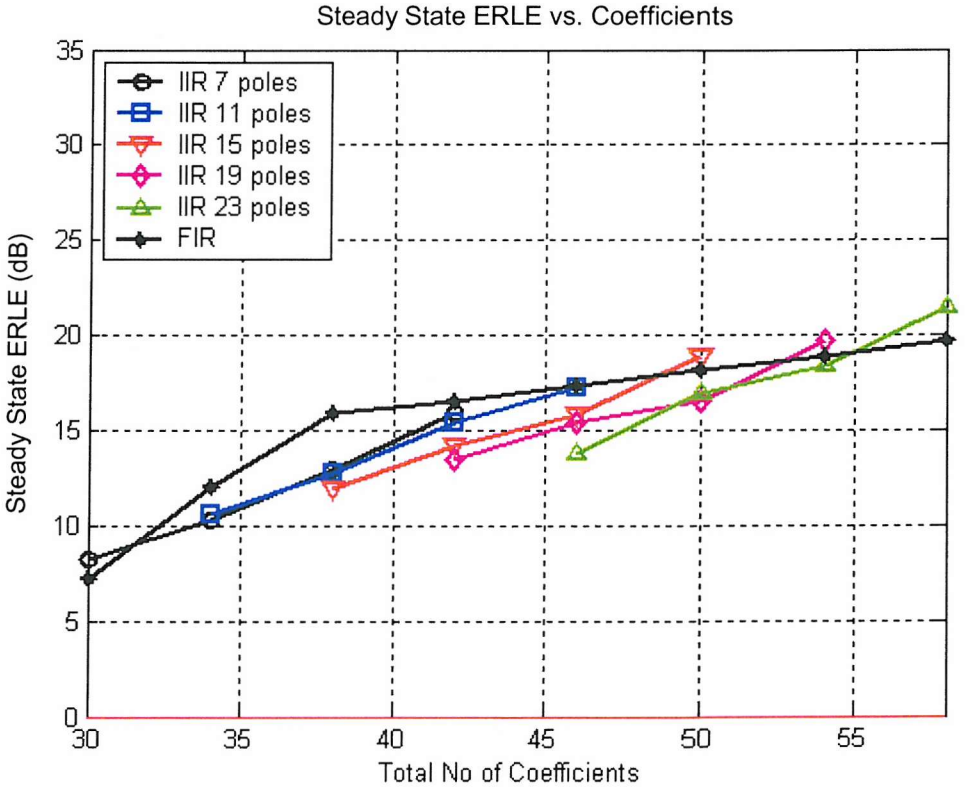


**Figure 5.45 : FIR vs. Equation Error LMS Newton modelling results for the artificial ear sealed handset configuration**

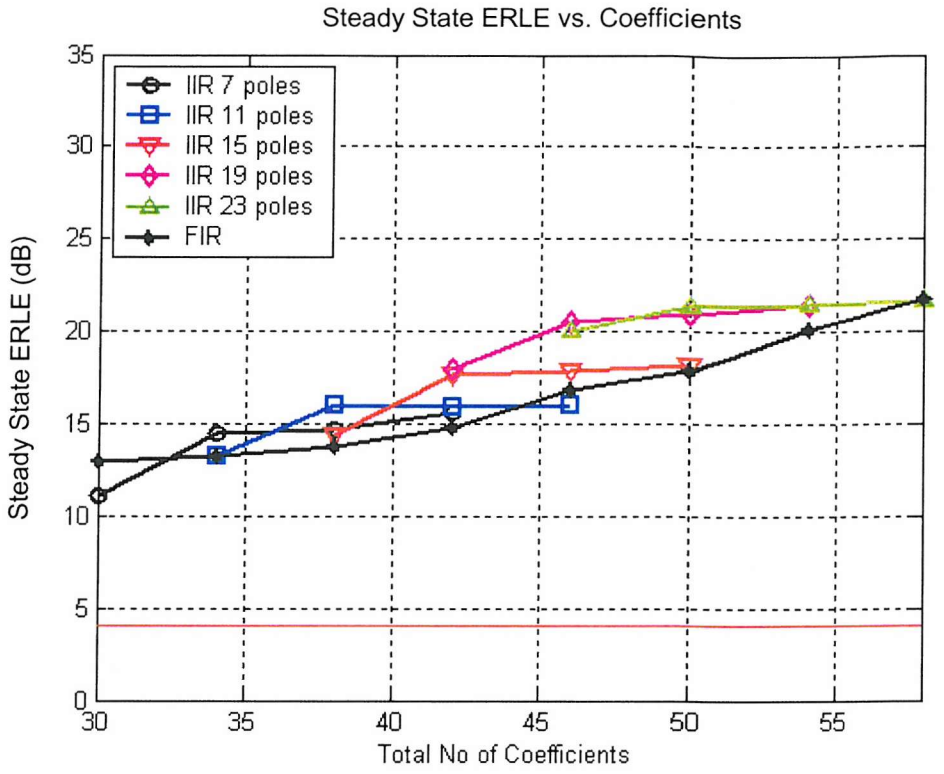


**Figure 5.46 : FIR vs. Equation Error Normalised LMS modelling results for the loudspeaker adhesive tape sealed handset configuration**

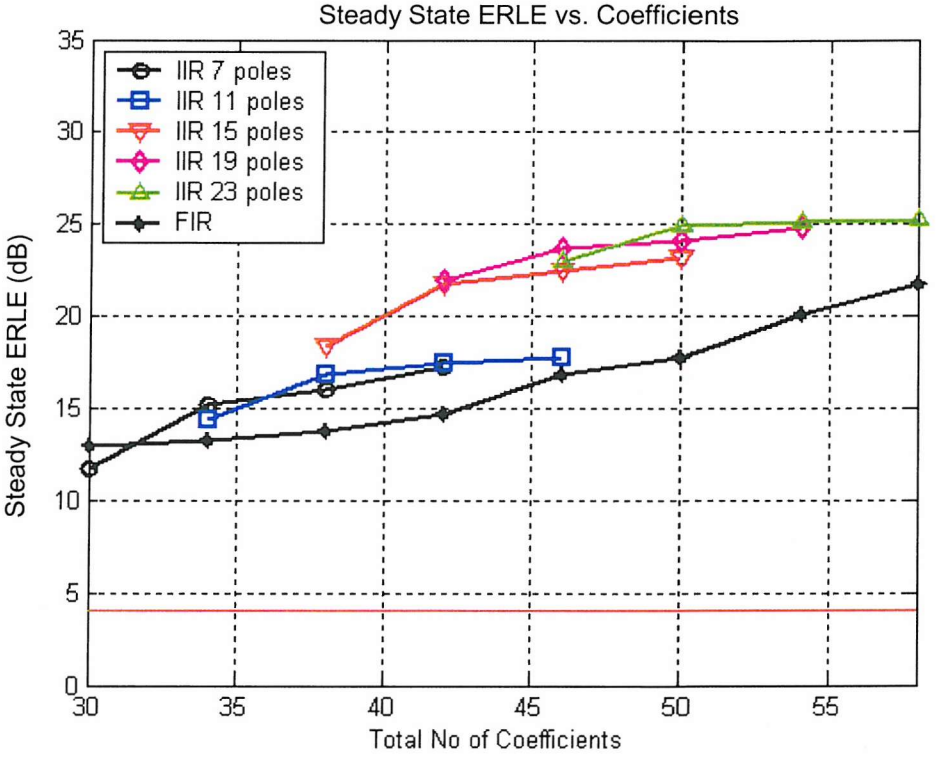


**Figure 5.47 : FIR vs. Equation Error LMS Newton modelling results for the loudspeaker adhesive tape sealed handset configuration**

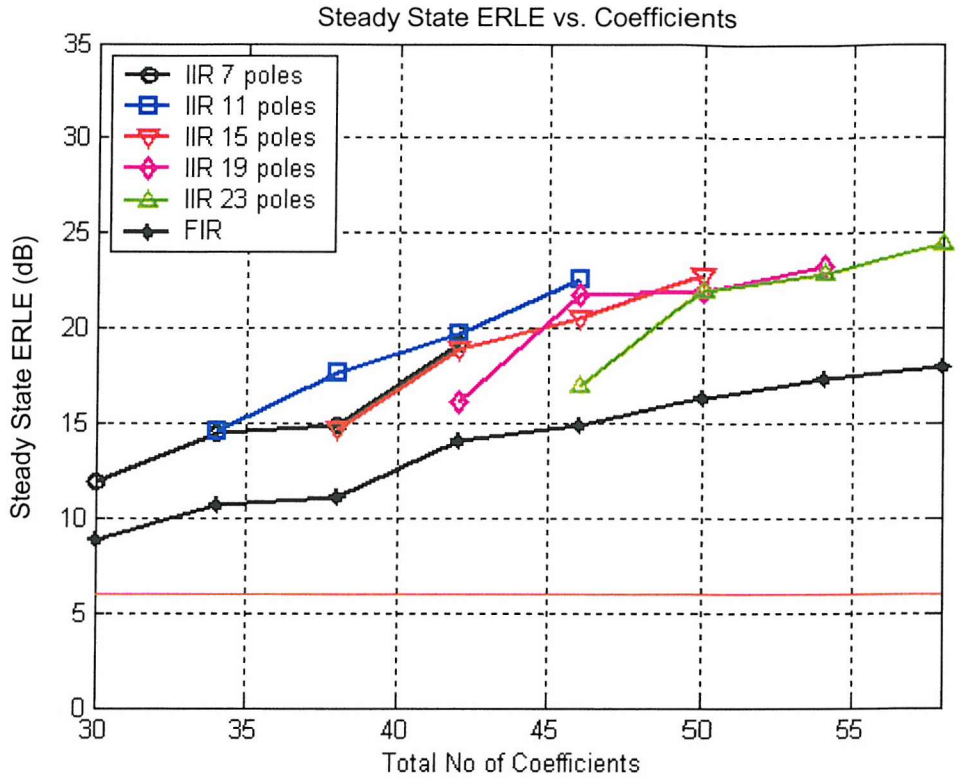


**Figure 5.48 : FIR vs. Equation Error Normalised LMS modelling results for the loudspeaker and microphone adhesive tape sealed handset configuration.**

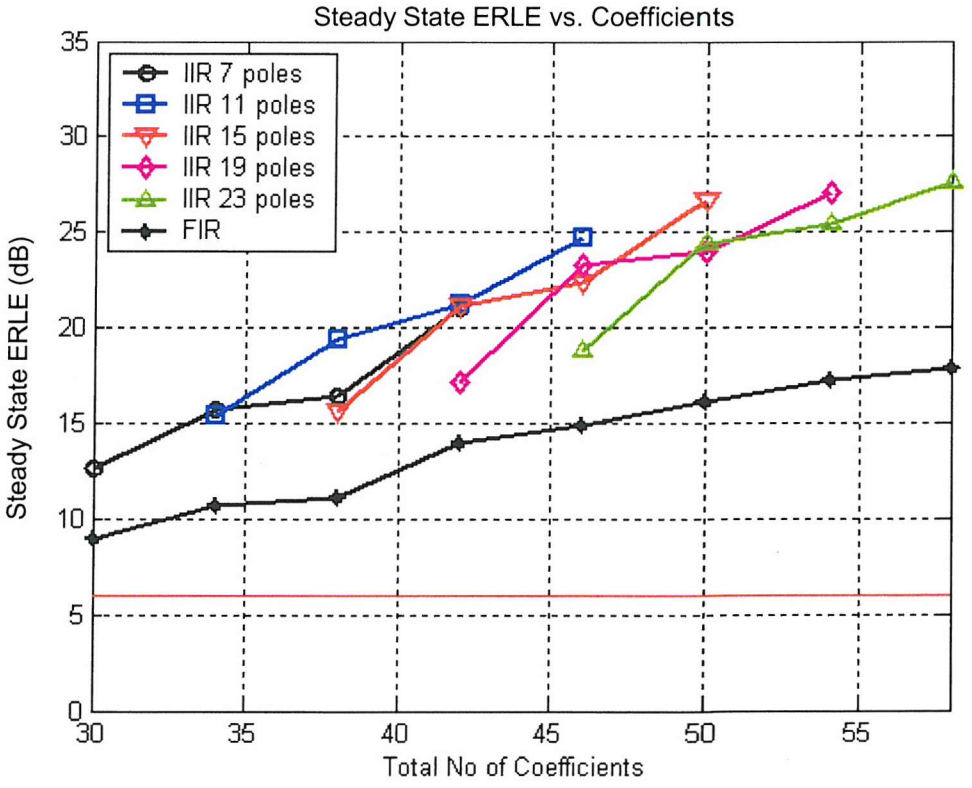


**Figure 5.49 : FIR vs. Equation Error LMS Newton modelling results for the loudspeaker and microphone adhesive tape sealed handset configuration.**

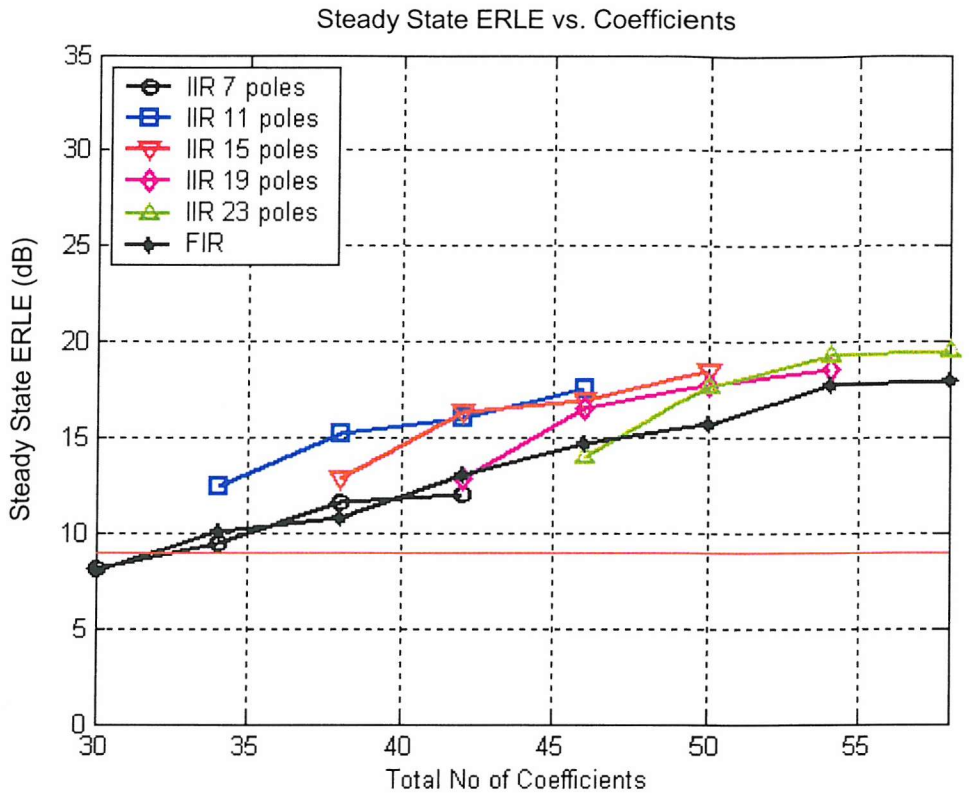


**Figure 5.50 : FIR vs. Equation Error Normalised LMS modelling results for the microphone adhesive tape sealed handset configuration.**

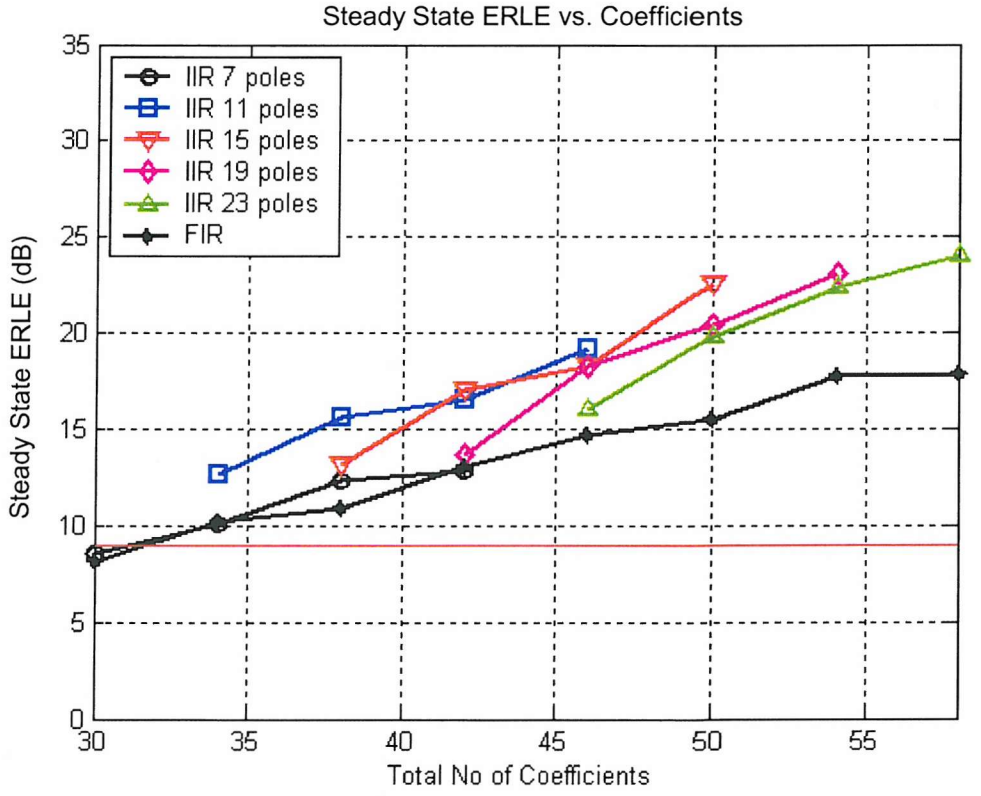


**Figure 5.51: FIR vs. Equation Error LMS Newton modelling results for the microphone adhesive tape sealed handset configuration.**

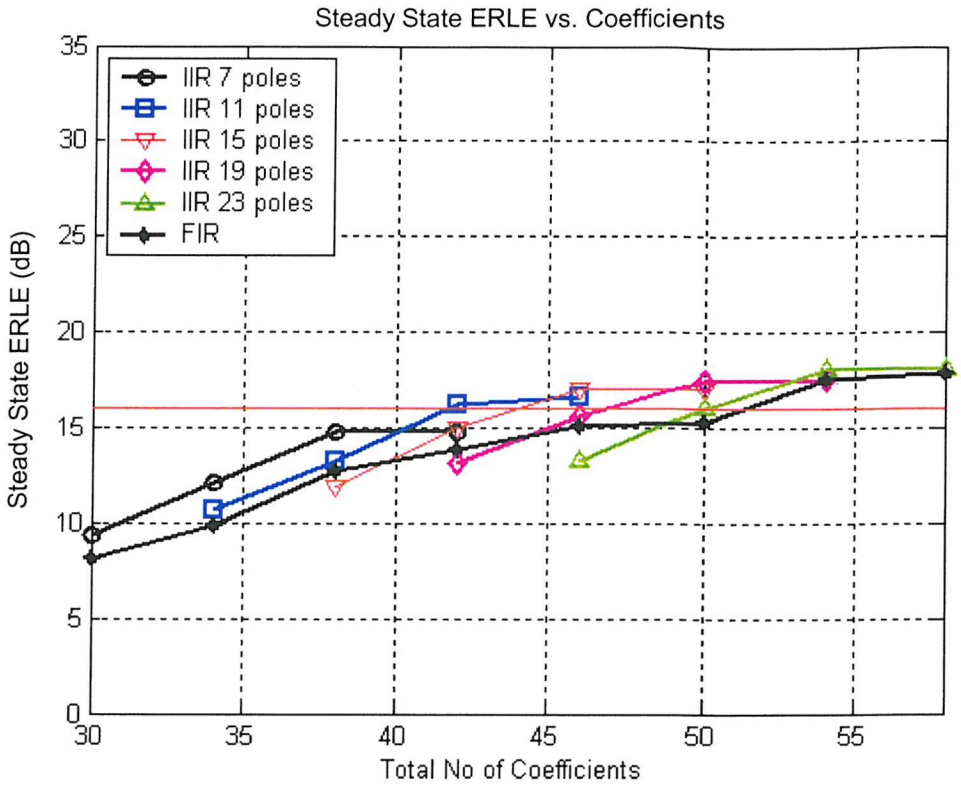


**Figure 5.52 : FIR vs. Equation Error Normalised LMS modelling results for the face down handset configuration**

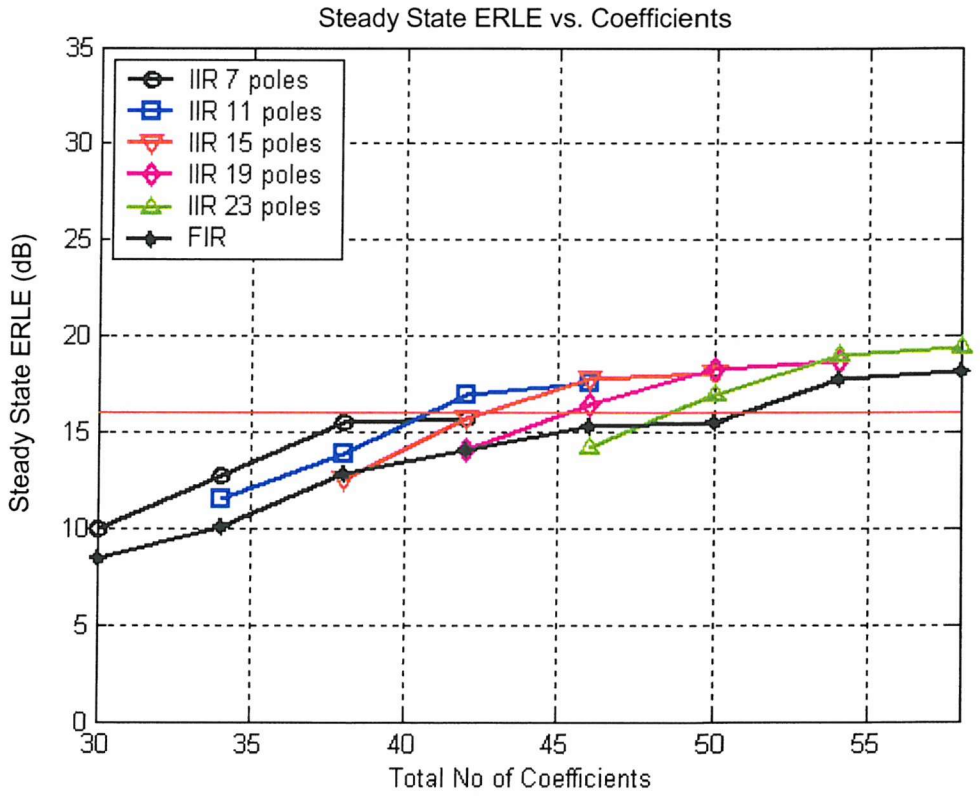


**Figure 5.53 : FIR vs. Equation Error LMS Newton modelling results for the face down handset configuration**

### 5.2.7. Steady State Modelling results of Adaptive FIR and Output Error Adaptive IIR algorithms

Earlier in Chapter the choice of algorithm design parameters on the modelling performance of Output Error adaptive algorithms was discussed using the Simplified Gradient algorithm. A single set of algorithm parameters is used for all experiments presented in this section.

The steady state ensemble averaged modelling results are shown in Figure 5.54 to Figure 5.65 for a range of different model orders for each echo path of Chapter 4. For Output Error adaptive IIR algorithms different distributions of feedforward and feedback coefficients are used. The number of feedback coefficients used is fixed at 7,11,15,19 and 23 in these modelling experiments, where the number of feedforward coefficients is adjusted to keep the same total number of filter coefficients the same for both FIR and IIR adaptive algorithms. The total number of coefficients used is varied between 30 and 58 coefficients, where again only the most important points (up to a maximum of 4 points) are plotted at each different (M,N) model distribution. Results for both Normalised LMS and LMS Newton adaptive FIR and IIR algorithms are presented using the same axis scaling for easy comparison.

From the results presented in Figure 5.54 to Figure 5.65 it is clear the face down echo path configuration determines the minimum order for both adaptive FIR and Simplified Gradient adaptive IIR algorithms needed to meet the required ERLE of each handset. A minimum model order of 42 coefficients, with 27 feedforward and 15 feedback coefficients, (27,15), is required by the Simplified Gradient Output Error LMS Newton adaptive IIR algorithm. For the Simplified Gradient Output Error NLMS adaptive IIR algorithm a minimum order of 54 coefficients is required, with 39 feedforward and 15 feedback coefficients, (39,15). The ERLE levels and convergence times are summarised in Table 5-2 below for a total model order of 42 coefficients.

| Echo Path | FIR LMSN | | | Simplified Gradient NLMS | | | Simplified Gradient LMSN | | |
|---|---|---|---|---|---|---|---|---|---|
| | $TIC_{rt}$ (ms) | $TIC_{ss}$ (ms) | $ERLE_{ss}$ (dB) | $TIC_{rt}$ (ms) | $TIC_{ss}$ (ms) | $ERLE_{ss}$ (dB) | $TIC_{rt}$ (ms) | $TIC_{ss}$ (ms) | $ERLE_{ss}$ (dB) |
| Face Up No Seals | 96 | 608 | 23.1 | 96 | 4416 | 23 | 96 | 3232 | 26.2 |
| Artificial Ear Seal | 32 | 384 | 16.2 | 32 | 2624 | 9.8 | 32 | 3008 | 17 |
| Loudspeaker Seal | 0 | 832 | 15.4 | 0 | 3680 | 14.2 | 0 | 1856 | 19.4 |
| Loudspeaker and Microphone Seal | 64 | 160 | 13.9 | 128 | 8128 | 16.7 | 576 | 2016 | 20.9 |
| Microphone Seal | 64 | 160 | 12.6 | 64 | 3200 | 14.6 | 64 | 1504 | 17.5 |
| Face Down | - | 256 | 13.6 | - | 2272 | 13.3 | 1344 | 2112 | 16.5 |

**Table 5-2 : Summary of steady state ERLE and convergence results of FIR and Simplified Gradient Output Error Algorithms for model order (27,15), total order 42 coefficients.**

From the ERLE levels presented in Table 5-2 using the Simplified Gradient adaptive IIR algorithm a maximum Coefficient Reduction Factor (CRF) of up to 1.29 is possible with Output Error LMS Newton based adaptive IIR algorithms. A Coefficient Reduction Factor (CRF) of unity is only possible for Output Error Normalised LMS adaptive IIR algorithms. However an ERLE gain of up to 2.8dB for the Output Error Normalised LMS algorithms over an equivalent FIR adaptive algorithm is still possible. For Output Error LMS Newton algorithms an ERLE gain of up to 7 dB is possible over an equivalent FIR adaptive algorithm.

From Table 5-2 it can be seen that the convergence times to the required ERLE of each echo path ($TTC_{req}$) for all adaptive algorithms again similar. For the convergence times to the steady state ensemble averaged ERLE level($TIC_{ss}$) it is clear to see that the convergence of both Normalised LMS and LMS Newton Output Error adaptive IIR algorithms is longer than that of an equivalent adaptive FIR algorithm. For Output Error NLMS algorithms much slower convergence occurs to the steady state ensemble averaged ERLE than Output Error LMS Newton based algorithms due to the dependency on the eigenvalue spread of $\mathbf{R}_{\varphi_f\varphi_f}$, limiting the achievable steady state ERLE during the 10s adaption period. Faster convergence of Output Error LMS Newton based algorithms for a bandlimited pink noise input results in an improvement of the achievable steady state ensemble averaged ERLE level of up to 7.2dB over Output Error NLMS algorithms.

### 5.2.8. Summary of Section 5.2 modelling results

From the modelling results presented in Section 5.2 it is clear that the steady state ERLE gains and Coefficient Reduction Factor possible presented in Chapter 4 for offline (non-adaptive) IIR models are also achievable with adaptive IIR algorithms. These results are for no echo path output noise.

Due to much slower convergence performance it was concluded that Equation Error NLMS are unsuitable for modelling the echo path of a mobile handset for the handset acoustic echo cancellation application. Only Equation Error LMS Newton based algorithms are suitable for handset acoustic echo cancellation application. It was found that a model order of (31,11) is needed for an Equation Error LMS Newton algorithm to meet the required ERLE of each echo path. With this model order an ERLE gain of up to 7.2 dB is possible over an equivalent FIR adaptive algorithm, with a CRF of up to 1.29 achievable. For Output Error NLMS algorithms it was found that in due to the dependency of convergence on the eigenvalue spread of $\mathbf{R}_{\varphi_f\varphi_f}$ the achievable steady state ERLE during the 10s adaption period with model order is unsatisfactory. Only LMS Newton based Output Error adaptive IIR algorithms are suitable for this application area. It was found that a model order of (27,15) is needed for an Output Error LMS Newton algorithm to meet the required ERLE of each echo path. With this model order an ERLE gain of up to 7 dB is possible over an equivalent FIR adaptive algorithm, with a CRF of up to 1.29 achievable.

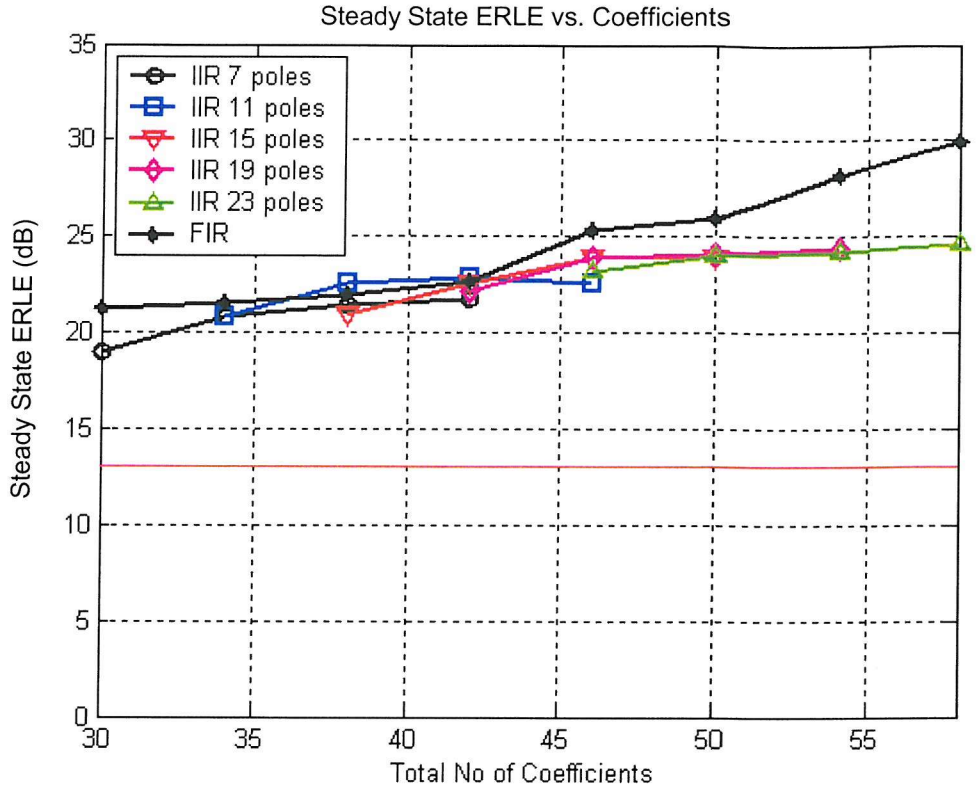


**Figure 5.54 : FIR vs. Output Error Normalised LMS Modelling results for the face up handset configuration with no transducer seals**

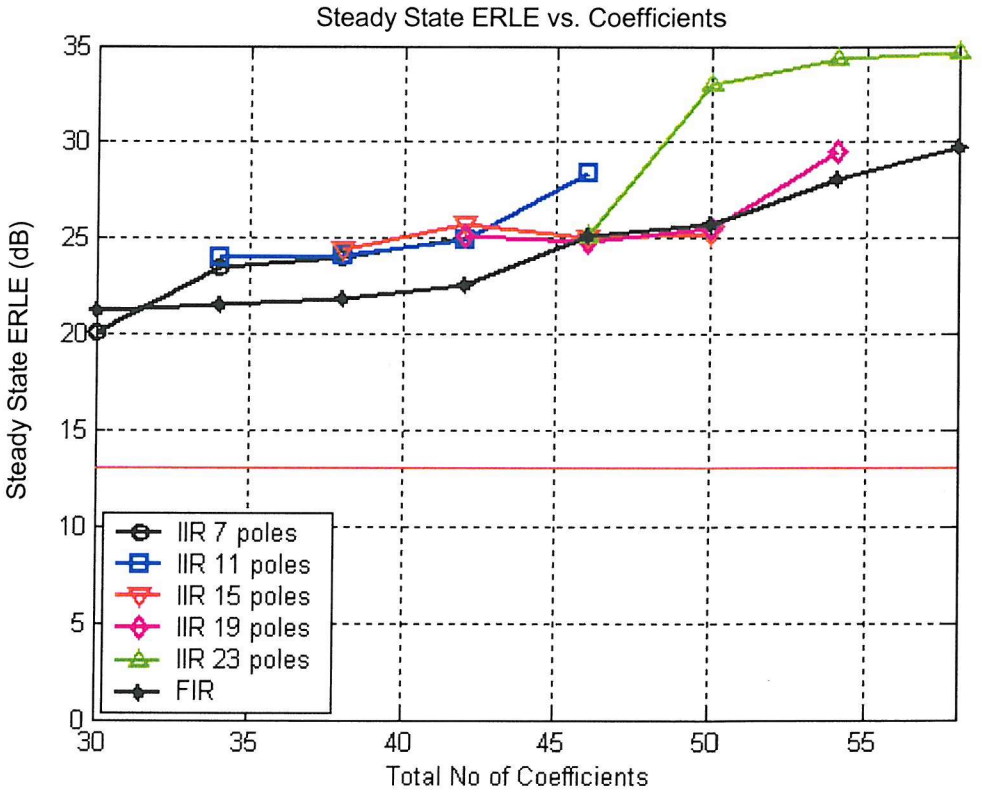


**Figure 5.55 : FIR vs. Output Error LMS Newton Modelling results for the face up handset configuration with no transducer seals**

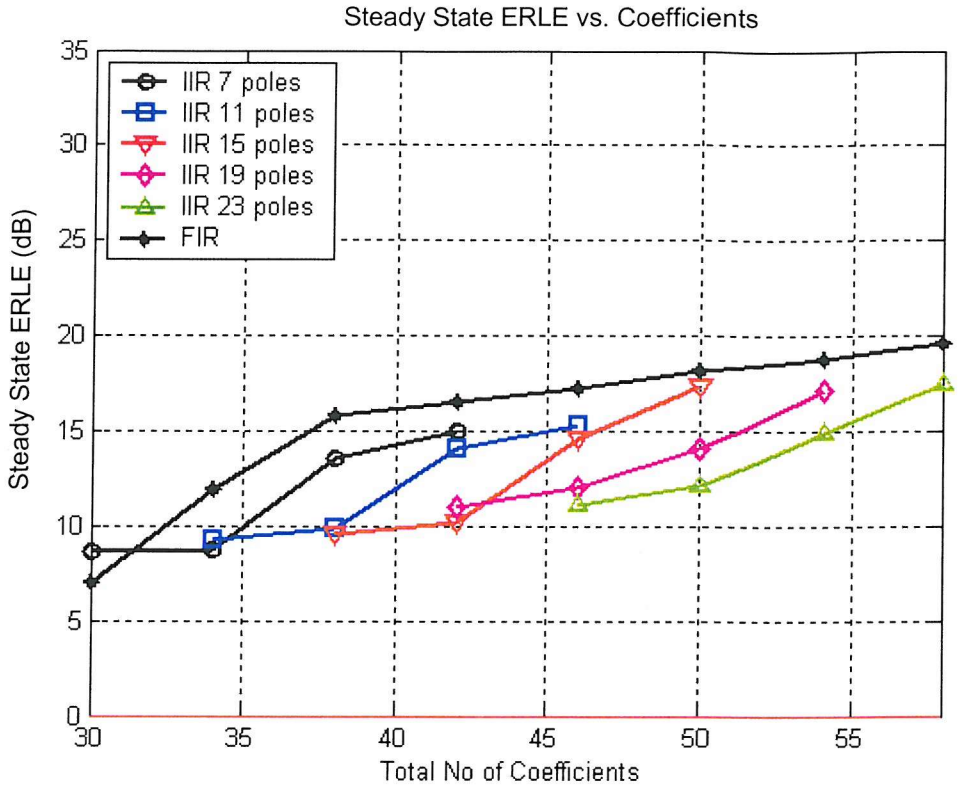


**Figure 5.56 : FIR vs. Output Error Normalised LMS Modelling results for the artificial ear sealed handset configuration**

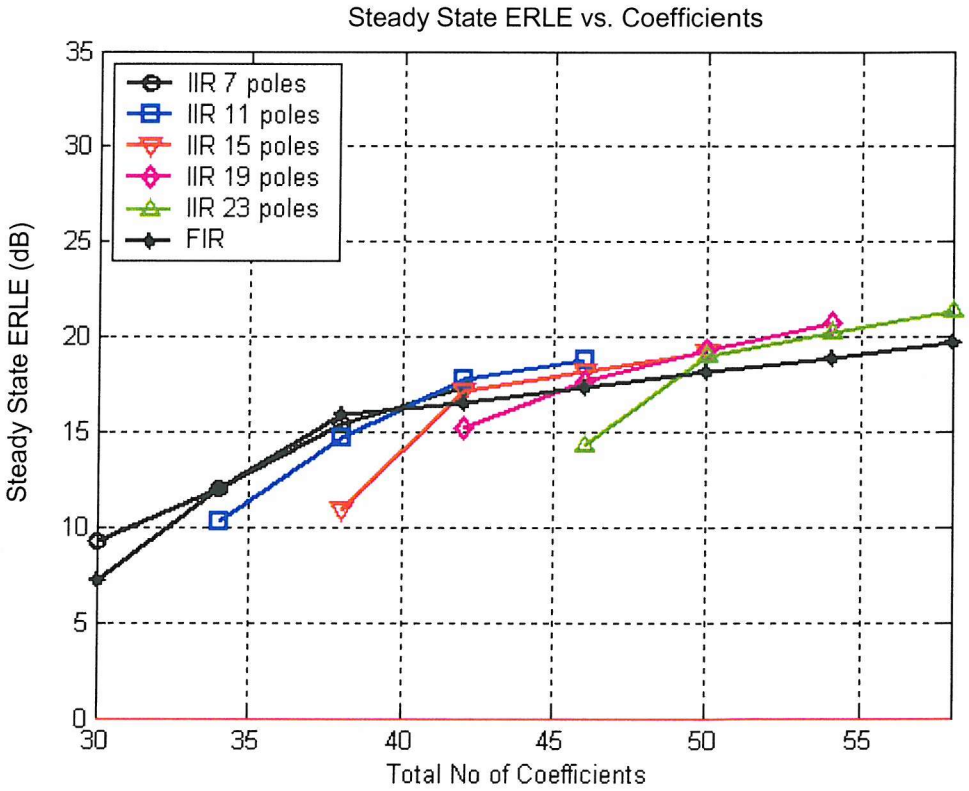


**Figure 5.57 : FIR vs. Output Error LMS Newton Modelling results for the artificial ear sealed handset configuration**

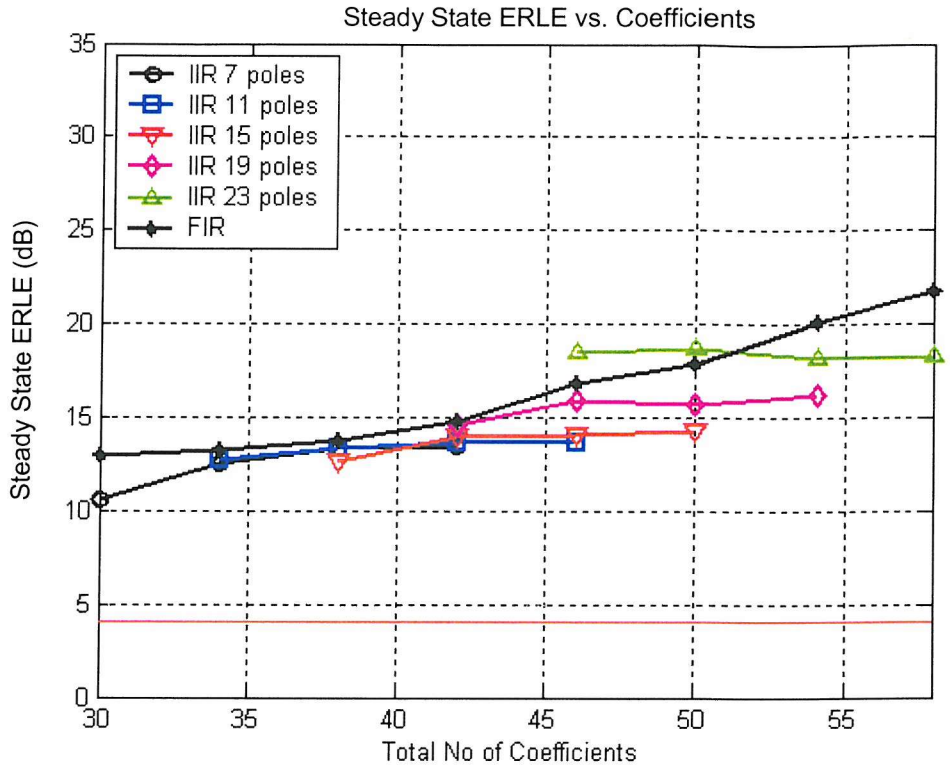


**Figure 5.58 : FIR vs. Output Error Normalised LMS Modelling results for the loudspeaker adhesive tape sealed handset configuration**

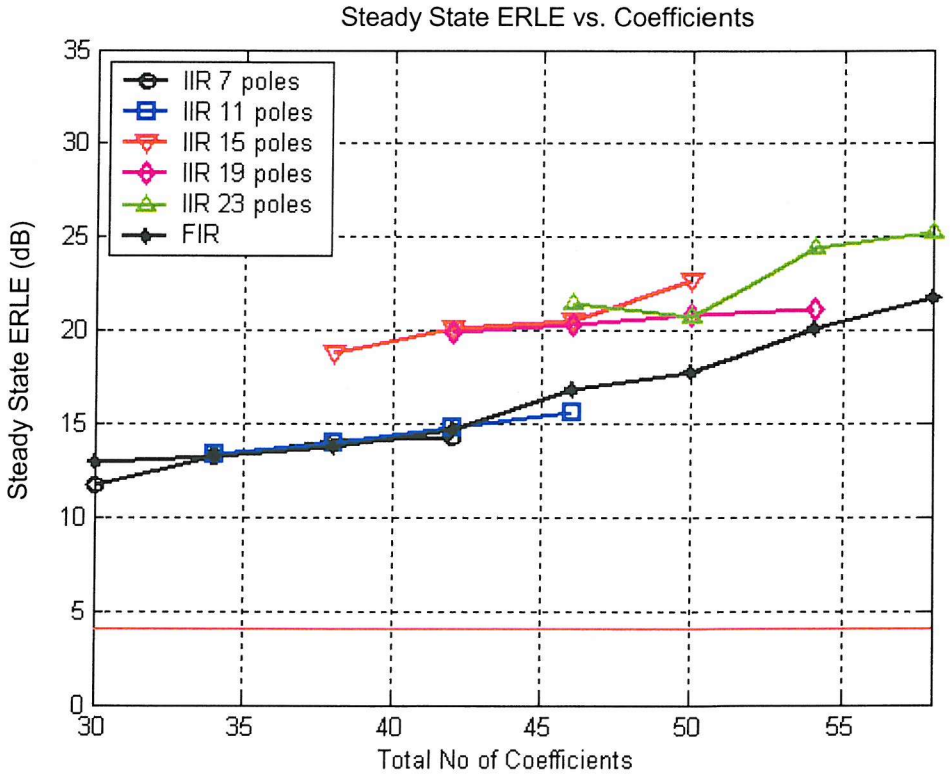


**Figure 5.59 : FIR vs. Output Error LMS Newton Modelling results for the loudspeaker adhesive tape sealed handset configuration**

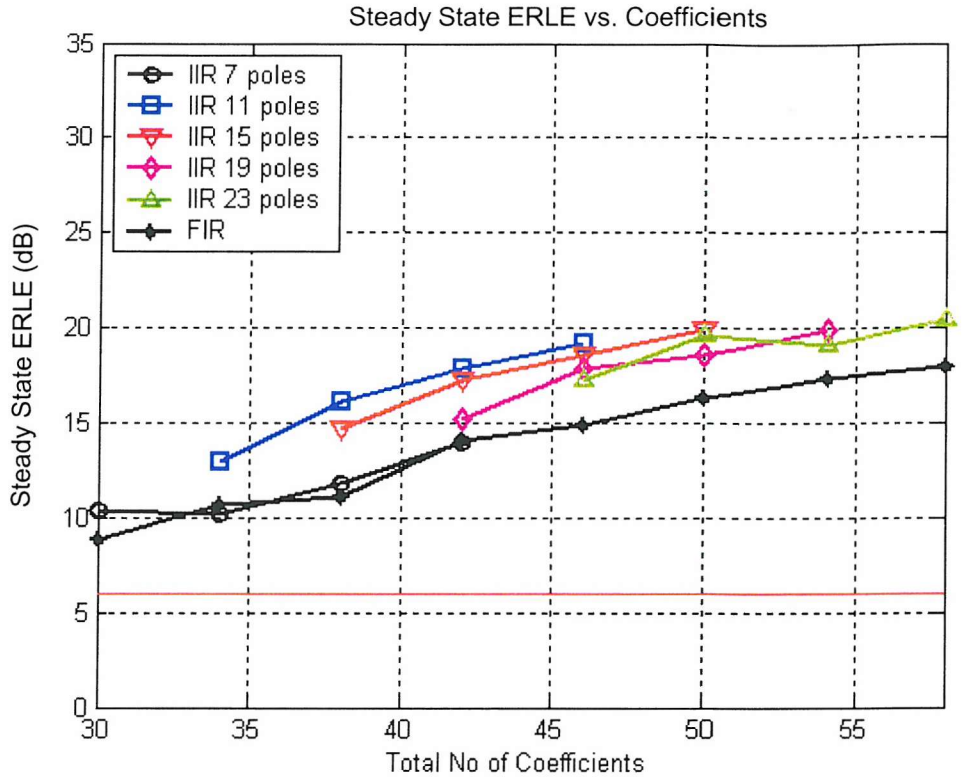


**Figure 5.60 : FIR vs. Output Error Normalised LMS Modelling results for the loudspeaker and microphone adhesive tape sealed handset configuration.**

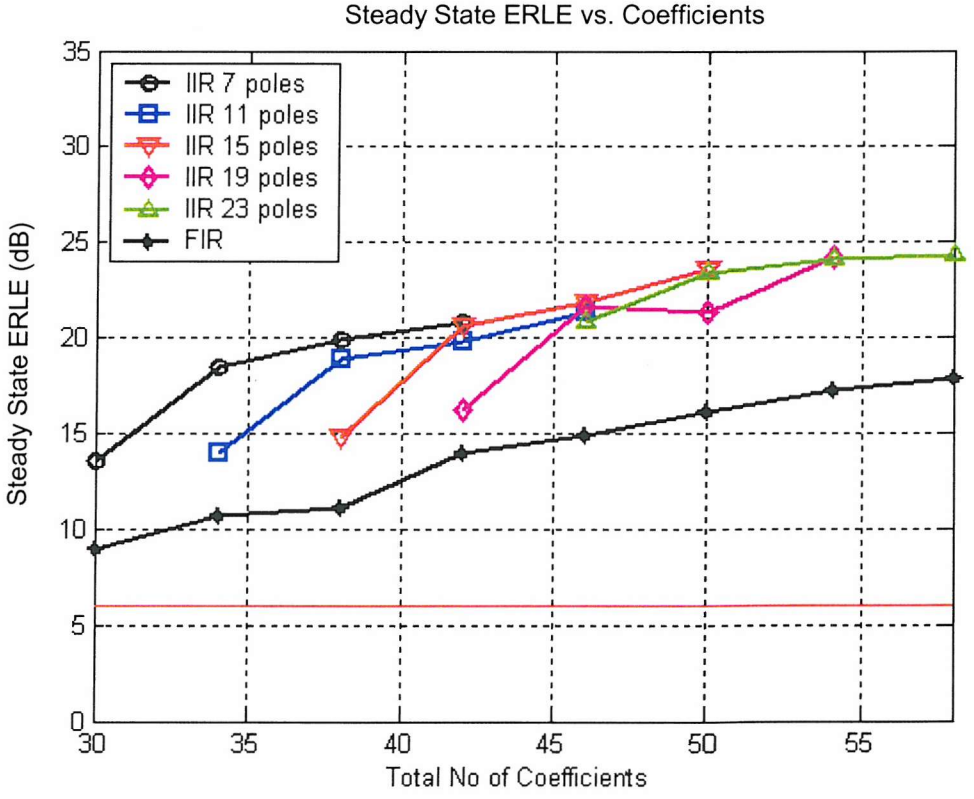


**Figure 5.61 : FIR vs. Output Error LMS Newton Modelling results for the loudspeaker and microphone adhesive tape sealed handset configuration.**

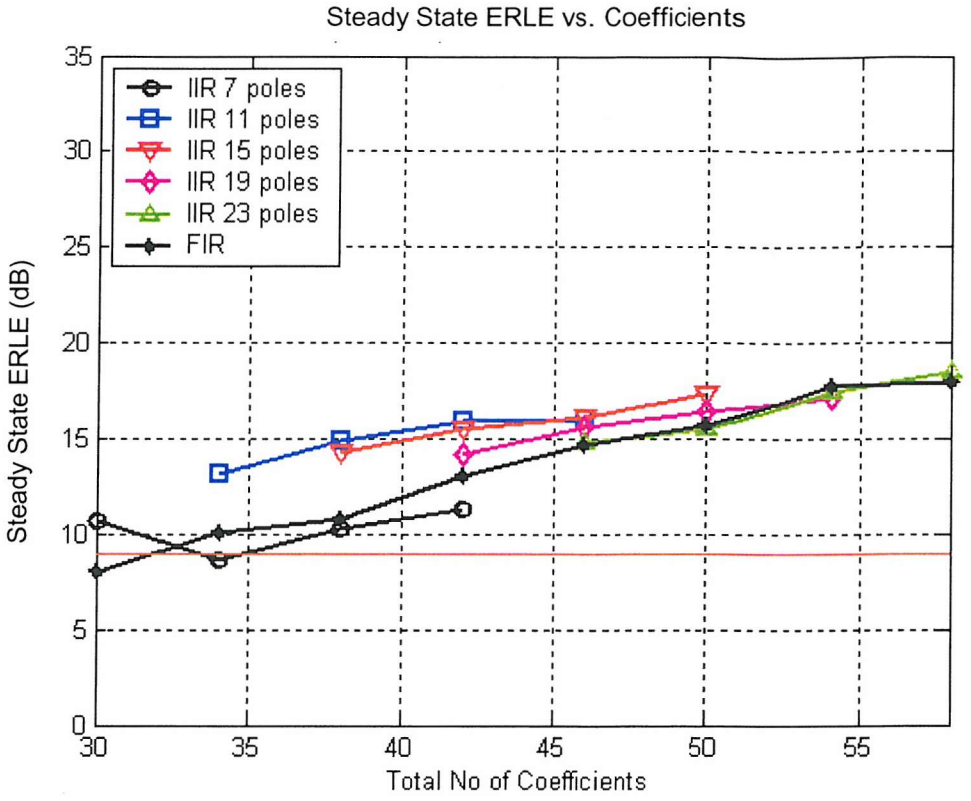


**Figure 5.62 : FIR vs. Output Error Normalised LMS Modelling results for the microphone adhesive tape sealed handset configuration.**

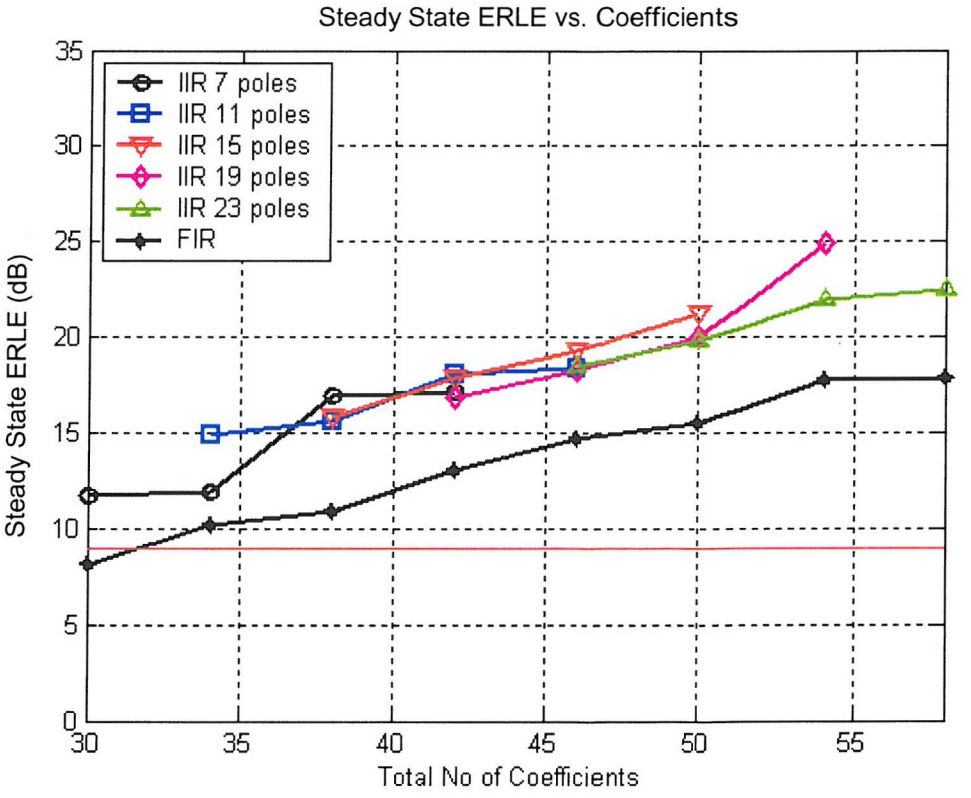


**Figure 5.63: FIR vs. Output Error LMS Newton Modelling results for the microphone adhesive tape sealed handset configuration.**

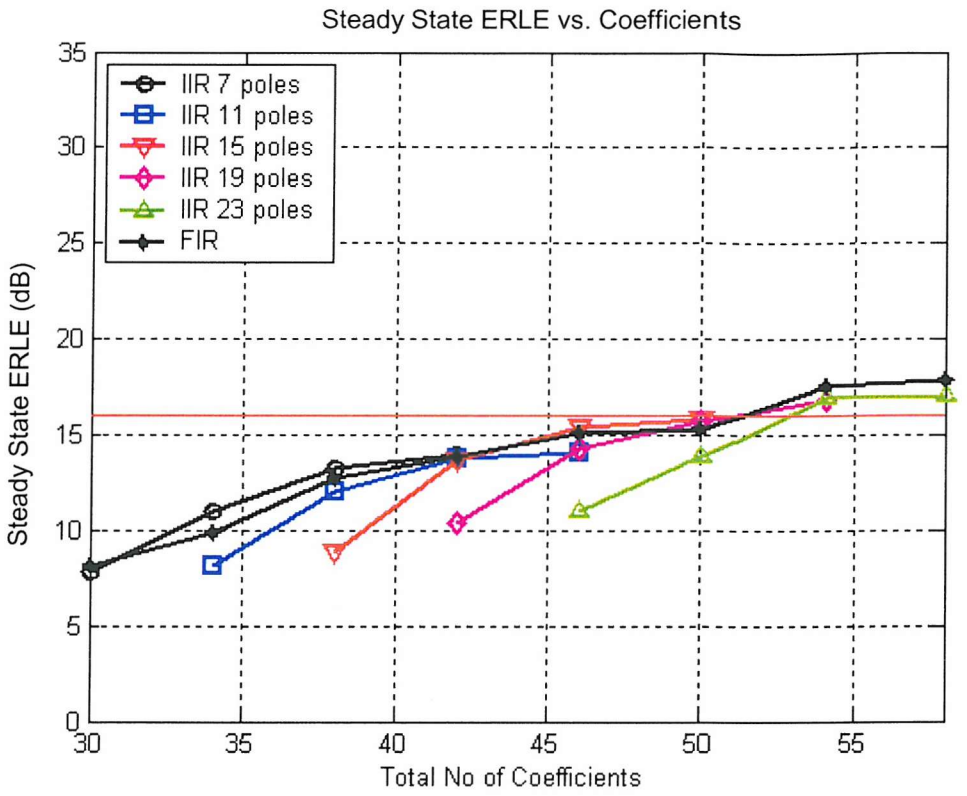


**Figure 5.64 : FIR vs. Output Error Normalised LMS Modelling results for the face down handset configuration**

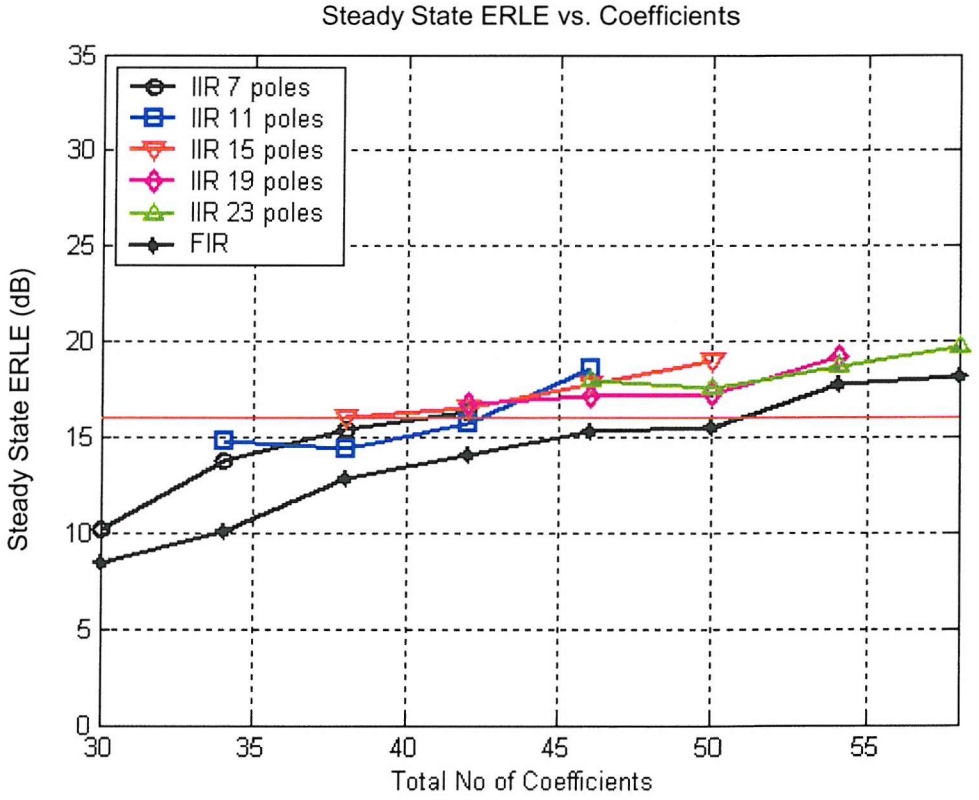


**Figure 5.65 : FIR vs. Output Error LMS Newton Modelling results for the face down handset configuration**

## 5.3. System Identification of the Echo Path Response of a Mobile Handset in the Presence of Echo Path Output Noise

In section 5.2 of this chapter it was shown that only a subset of all the adaptive IIR algorithms of chapter 3 were suitable for modelling the echo path of a mobile handset. These conclusions were based on steady state modelling performance and the achievable Coefficient Reduction Factor of a subset of adaptive algorithms. No echo path output noise was present.

In the application of adaptive IIR filtering algorithms to acoustic echo cancellation on a mobile handset, an echo path disturbance noise source will almost always exist. This noise source is due to pressure fluctuations from the operating environment being picked up on the handset microphone. In order to establish whether the gains in modelling performance presented in section 5.2 can be obtained in noisy environments more modelling experiments are needed with echo path output noise present.

This section of the chapter establishes the modelling performance of the subset of LMS Newton adaptive IIR algorithms in the presence of echo path output noise in order both establish these gains in modelling performance are still possible, and to make a selection of the most suitable adaptive IIR filtering algorithms for acoustic echo cancellation on a mobile handset.

### 5.3.1. Adaptive Algorithms used for Modelling Experiments in presence of output noise

In section 5.2 it was established that LMS Newton based adaptive IIR algorithms are required for modelling the acoustic echo path of a mobile handset. In this section only the LMS Newton based adaptive algorithms of Chapter 3 are used to establish the modelling performance of adaptive algorithms in the presence of output noise. For stationary input signals and a suitable choice of stepsize, similar performance is obtained for LMS Newton and Normalised LMS Newton algorithms, so only LMS Newton forms are simulated.

To assess modelling capabilities of Output Error LMS Newton based algorithms in the presence of echo path output noise, the Simplified Gradient, Pseudo Linear Regression and SHARF LMS Newton adaptive IIR algorithms are used. To assess modelling capabilities of Equation Error LMS Newton based algorithms in the presence of echo path output noise, the Equation Error, Steiglitz McBride and Bias Remedy Equation Error LMS Newton adaptive IIR algorithms are used.

### 5.3.2. System Identification Experiment Configuration and Assessment Criteria

A standard system identification configuration is used as illustrated in Figure 5.66 to perform the required system identification experiments of this section in the presence of each path output noise. It can be seen an additive echo path output noise signal $v(n)$ is present throughout each system identification experiment. The echo path response $\mathbf{h}$ is as defined in (5.7). The echo paths to be modelled are fixed for the duration of each system identification experiment. The same format as used in section 5.2 is repeated for this section. To start with only the face up no seals echo path response will be used to determine the

effect of LMS Newton algorithm parameters on modelling performance when echo path output noise is present. Once the most suitable parameters have been chosen for each adaptive algorithm, modelling results for all the echo path responses of chapter 4 will be presented.

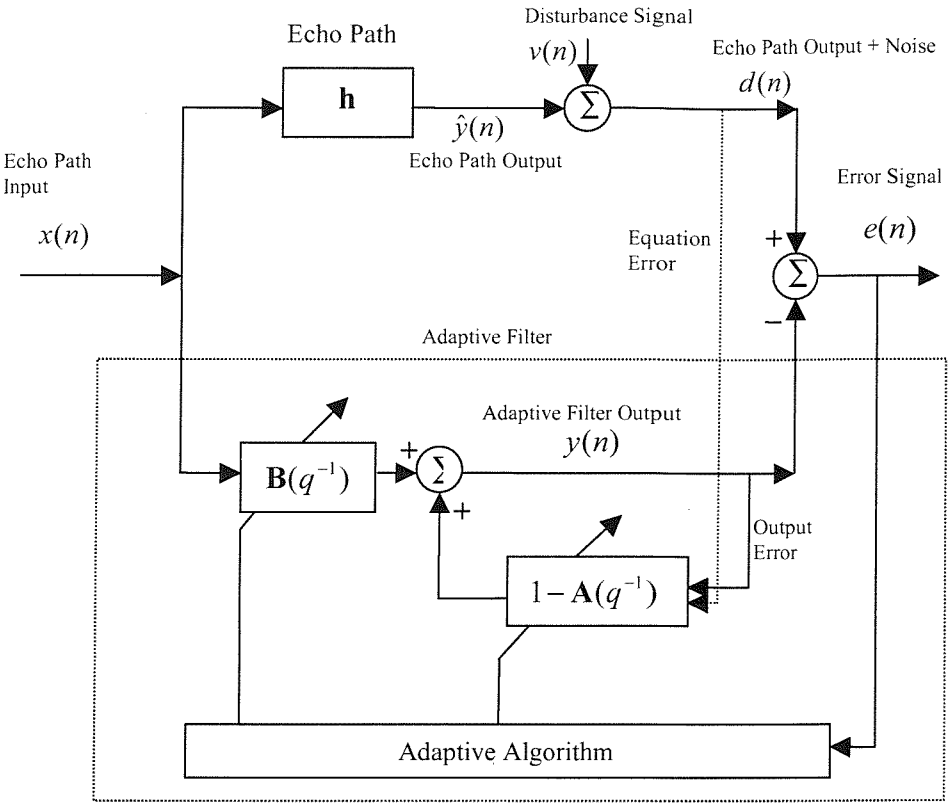


**Figure 5.66 : System Identification Configuration for echo path output noise**

A system identification experiment is defined as an adaptive algorithm of fixed order operating on input signal $x(n)$ and noisy echo path output $d(n)$ .For each system identification experiment an input signal of duration 10s and sample rate 8 kHz (N=80000 samples) is used. A band-limited pink noise signal input $x(n)$ is employed here.

To investigate the steady state modelling performance of each adaptive algorithm in the presence of echo path output noise two different noise signals are used for signal $v(n)$ . Due to codec ADC filtering of the noise source recorded on the handset microphone the spectrum of the additive noise source will be strongly band limited in form. Both band limited white noise signal and band limited pink noise signal $v(n)$ are used, uncorrelated with signal input $x(n)$ , to allow the performance of adaptive algorithms to be tested in the presence of echo path output noise.

For each experiment the fixed model orders detailed in the last section will be used – (27,15) for the Output Error LMS Newton algorithms and (31,11) for the Equation Error LMS Newton algorithms. The noise signal $v(n)$ will be scaled in each experiment to give a certain Echo to Noise Ratio (ENR) levels. The Echo to Noise Ratio is defined as follows,

$$ENR_{dB} = 10\log_{10}\left[\frac{E[\hat{y}^2(n)]}{E[v^2(n)]}\right] = 10\log_{10}\left[\frac{\sum_{n=0}^{M-1}\hat{y}^2(n)}{\sum_{n=0}^{M-1}v^2(n)}\right], \quad (5.28)$$

From (5.28) we can see the ENR is defined as the ratio of echo path output power in the absence of noise, $E[\hat{y}^2(n)]$, to the echo path output disturbance noise power, $E[v^2(n)]$, in decibels, calculated as a time average. M represents the length of recorded sequences $\hat{y}(n)$ and $v(n)$. The ENR level for each experiment is held constant over the simulation duration. For quiet indoor environments the ENR level is typically around 5 to 10dB. For noisy indoor environments and outdoor environments the ENR level will be less than 5dB. In this Chapter an ENR range of 0dB to 20dB is used for each echo path modelled is simulated.

In terms of assessment criteria used to establish steady state modelling performance in the presence of echo path output noise, the same measures used in last section are employed – the steady state ERLE value, $ERLEss_{dB}$, and convergence times $TIC_{ss}$ and $TIC_{req}$ defined in (5.4) to (5.6). The only difference is that in the presence of echo path output noise a slight modification to the ERLE level calculated is recorded. The Echo Return Loss Enhancement must be established from the true echo path output $\hat{y}(n)$ and not the total output including the disturbance signal $d(n)$ as in the previous Section of the Chapter. The ERLE recorded in this section is defined as follows.

$$ERLE_{dB}(m) = 10\log_{10}\left[\frac{\sum_{n=0}^{N-1}\hat{y}^2(m-n)}{\sum_{n=0}^{N-1}e^2(m-n)}\right], \quad (5.29)$$

where N is the sample duration corresponding to 32ms window duration at a 8kHz sample rate (256 samples). The index m denotes 32ms time sample instants in the recorded sequences $\hat{y}(n)$ and $e(n)$. The ensemble averaged ERLE level, the steady state ensemble averaged ERLE value, $ERLEss_{dB}$, and convergence times $TIC_{ss}$ and $TIC_{req}$ defined in (5.3) to (5.6) are calculated from the ERLE definition of (5.29) in each modelling experiment.

Each modelling experiment is repeated $P$=20 times, where different random noise seeds are used for the band-limited pink noise signal input $x(n)$ and noise signal $v(n)$ in each repeated trial, in order to compute ensemble average estimate $ERLE_{en}(n)$. Once the ensemble averaged level $ERLE_{en}(n)$ is computed the steady state ERLE value, $ERLEss_{dB}$, and convergence times $TIC_{ss}$ and $TIC_{req}$ are recorded. Once $ERLEss_{dB}$ is computed for each echo path to be modelled over a range of Echo to Noise Ratios for each adaptive algorithm of fixed order. A minimum Coefficient Reduction Factor as defined in Chapter 4 can be computed to see whether the performance benefits presented in Chapter 4 are still valid in the presence of echo path output noise.

### 5.3.3. The effect of Echo Path output noise on the choice of LMS Newton adaptive algorithm design parameters

In section 5.2 of this chapter the convergence and steady state $ERLEss_{dB}$ level performance behaviour of only the LMS Newton algorithms of (3.1.58), (3.2.71) and (3.3.46) was discussed with respect to adaptive algorithm parameters $\mu$, $\lambda$, $\alpha$, and $\delta$. These observations were for the case where no echo path output noise is present.

In this section of the Chapter we wish to establish convergence and steady state $ERLEss_{dB}$ level performance behaviour for all LMS Newton algorithms presented in Chapter 3 with respect to main adaptive algorithm parameters, in the presence of echo path output noise. The lowest considered ENR level of 0dB will be used. This ensures the most suitable set of adaptive algorithm parameters are used for the modelling results of section 5.3. A bandlimited pink noise source will be used be used for both input signal $x(n)$ and disturbance signal $v(n)$. A single filter model order of 42 coefficients (identified as the most suitable order in Section 5.2) will be used for all algorithms.

#### 5.3.3.1. The FIR LMS Newton adaptive FIR algorithm

Consider firstly the choice of design parameters for the FIR LMS Newton algorithm when echo path noise is present. As the input signal characteristics have not changed, the parameter value recommended for $\delta$ in Section 5.2, which determines the initial covariance matrix estimate $\delta\mathbf{I}$ will remain unchanged. This is the case for all algorithms. For the FIR LMS Newton algorithm the stepsize $\mu = 0.0025$ recommended in Section 5.2 will be adopted, only the values of forgetting factor $\lambda$ and convergence factor $\alpha$ will be changed to give robust performance at low ENR levels.

Consider now the effect of the forgetting factor $\lambda$ on the convergence and steady state $ERLEss_{dB}$ level achievable by the FIR LMS Newton in the presence of echo path output noise, for a convergence factor of $\alpha = 0.0075$. Figure 5.67 shows the ensemble averaged ERLE level results achieved for a model order of 42 coefficients for modelling experiments with different forgetting factors for the face up no seals handset echo path response of Chapter 4. As in the no noise case of Figure 5.21 the same general trends in performance occur with the forgetting factor $\lambda$ where higher values slow convergence and improve the steady state $ERLEss_{dB}$ level, and lower values improve convergence and lower the steady state $ERLEss_{dB}$ level. However when echo path noise is present at such low levels a minimum forgetting factor value of $\lambda$ =0.999 is needed for stability. It can also be observed that for higher forgetting factor values at low ENR levels, the convergence rate is improved over the no noise case. The improvement in achievable steady state $ERLEss_{dB}$ level over that achieved with lower forgetting factors at low ENR levels is more pronounced than in the no noise case, due to less filter weight perturbation as they converge with higher forgetting factors at low ENR levels. In comparison to the no noise case of Figure 5.21 only a small degradation in achievable steady state $ERLEss_{dB}$ level results for

lower ENR levels, when noise source $v(n)$ is present. A value of $\lambda$ =0.9995 is recommended for stability and performance over a range of different ENR levels and echo paths.

Consider next the effect of the convergence factor $\alpha$ on the convergence and steady state $ERLEss_{dB}$ level achievable by the FIR LMS Newton in the presence of echo path output noise, for a fixed stepsize of $\mu = 0.0025$ and forgetting factor $\lambda = 0.9995$. Figure 5.68 shows the ensemble averaged ERLE level results achieved for a model order of 42 coefficients for modelling experiments with different convergence factors for the face up no seals handset echo path response of Chapter 4. As in the no noise case of Figure 5.23 the same performance trends occur with the value of $\alpha$. However at larger values of $\alpha$ the slower convergence results in less filter weight perturbation at lower ENR levels and as a result the achievable steady state $ERLEss_{dB}$ level increases for values up to $\alpha$ =0.025. A value of $\alpha$ =0.01 is recommended for stability and performance over a range of different ENR levels and echo paths.

#### 5.3.3.2. The Simplified Gradient LMS Newton adaptive IIR algorithm

Like the FIR LMS Newton algorithm a fixed stepsize value will be used. However due to stability problems below an ENR level of 10dB, a lower fixed stepsize value of $\mu = 0.00125$ from the recommended value chosen in Section 5.2 will be used. Only the values of forgetting factor $\lambda$ and convergence factor $\alpha$ will be investigated for robust operation at low ENR levels.

Figure 5.69 shows the ensemble averaged ERLE level results achieved for a model order of 42 coefficients (27,15) for modelling experiments with different forgetting factors, for the face up no seals handset echo path response of Chapter 4. As in the no noise case of Figure 5.35 the same general trends in performance occur with the forgetting factor $\lambda$. However when echo path noise is present at such low levels as in Figure 5.69, a very narrow range of forgetting factors exists for algorithm stability and performance. A value of $\lambda$ =0.9998 is recommended for stability and performance over a range of different ENR levels and echo paths.

Figure 5.68 shows the ensemble averaged ERLE level results achieved for a model order of 42 coefficients for modelling experiments with different convergence factors for the face up no seals handset echo path response of Chapter 4. As in the no noise case of Figure 5.37 the same performance trends occur with the value of $\alpha$. A value of $\alpha$ =0.0075 is recommended for stability and performance over a range of different ENR levels and echo paths. Below this value at low ENR levels of 0 or below algorithm instability will occur. As we shall see in later Chapters, the convergence factor $\alpha$ can be varied depending on the ENR level to maintain fast convergence and robust operation in noisy environments.

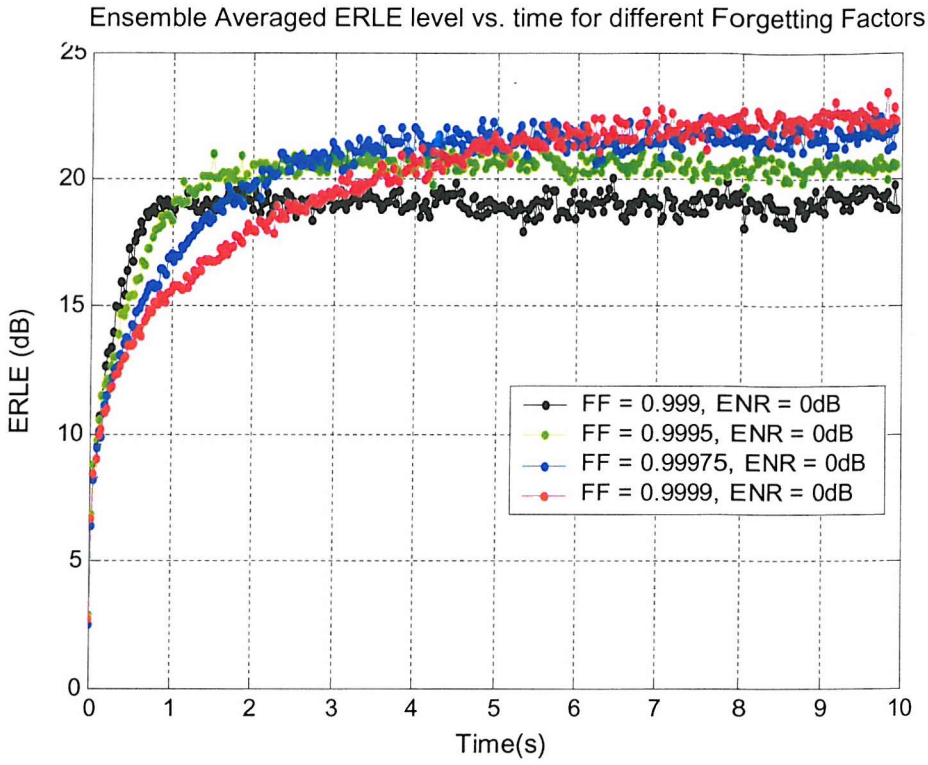


**Figure 5.67 : FIR LMS Newton ERLE performance with different forgetting factors $\lambda$ for ENR level of 0dB**

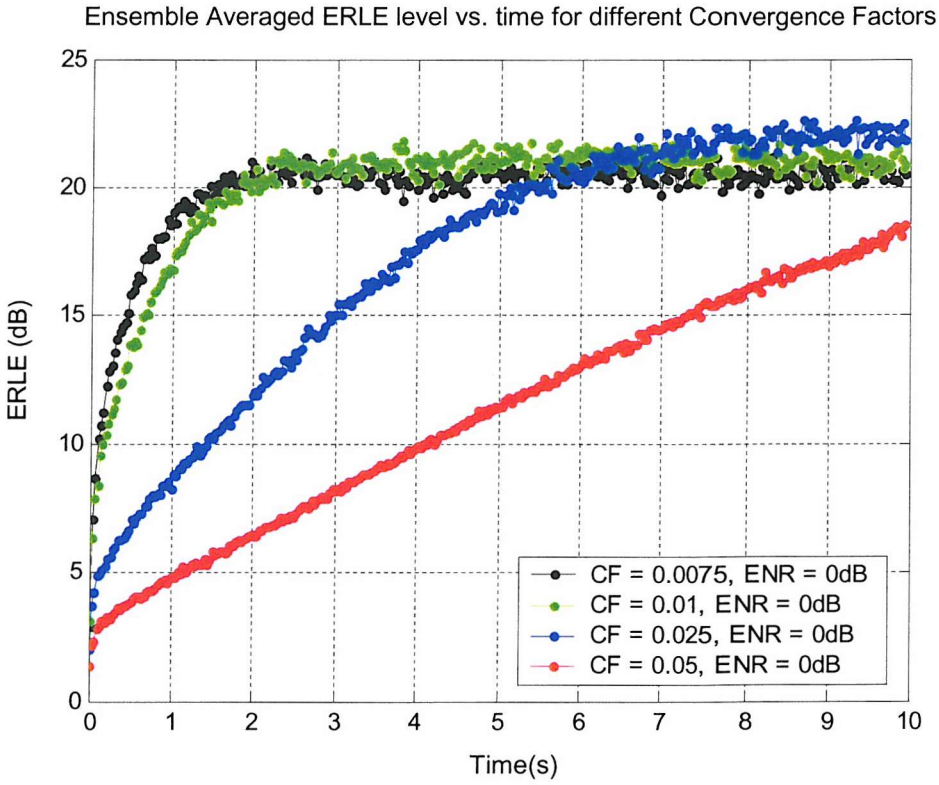


**Figure 5.68 : FIR LMS Newton ERLE performance with different convergence factors $\alpha$ for ENR level of 0dB**

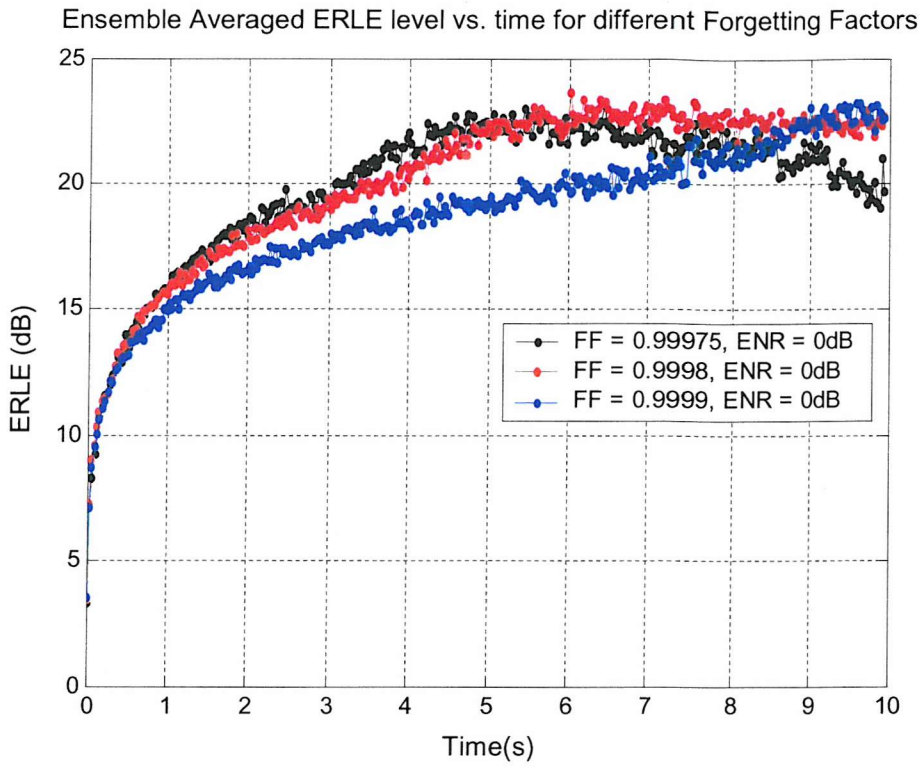


**Figure 5.69 : Simplified Gradient LMS Newton ERLE performance with different forgetting factors $\lambda$ for ENR level of 0dB ($\alpha$ =0.0075)**

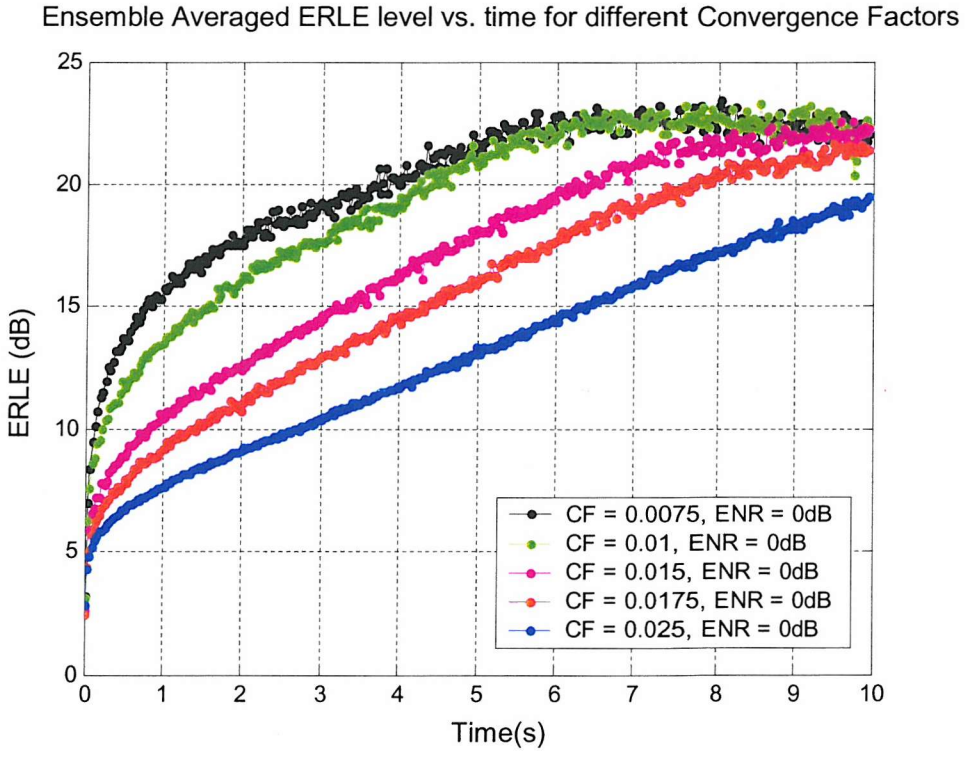


**Figure 5.70 : Simplified Gradient LMS Newton ERLE performance with different convergence factors $\alpha$ for ENR level of 0dB ($\lambda$ =0.9998)**

### 5.3.3.3. The Pseudo Linear Regression LMS Newton adaptive IIR algorithm

From the results presented in Section 5.2 we have seen in a general sense how the performance of adaptive IIR output error LMS Newton algorithms vary with algorithm parameters $\mu$, $\lambda$, $\alpha$, and $\delta$, for no echo path output noise. Now we will see how these parameters specifically affect the Pseudo Linear Regression LMS Newton algorithm when echo path output noise is present.

The Pseudo Linear Regression LMS Newton algorithm is re-written for convenience below,

$$\boldsymbol{\theta}_{n+1} = \boldsymbol{\theta}_n + \mu \hat{\mathbf{R}}^{-1}_{\varphi_o\varphi_o}(n)\varphi_o(n)e_o(n), \tag{3.2.92}$$

where

$$\hat{\mathbf{R}}^{-1}_{\varphi_o\varphi_o}(n) = \frac{1}{\lambda}\left(\hat{\mathbf{R}}^{-1}_{\varphi_o\varphi_o}(n-1) - \frac{\hat{\mathbf{R}}^{-1}_{\varphi_o\varphi_o}(n-1)\varphi_o(n)\varphi_o{}^T(n)\hat{\mathbf{R}}^{-1}_{\varphi_o\varphi_o}(n-1)}{\frac{\lambda}{\alpha} + \varphi_o{}^T(n)\hat{\mathbf{R}}^{-1}_{\varphi_o\varphi_o}(n-1)\varphi_o(n)}\right), \tag{3.2.93}$$

and the following initialisations is used,

$$\hat{\mathbf{R}}^{-1}_{\varphi_o\varphi_o}(0) = \delta\mathbf{I}, \tag{5.30}$$

In Chapter 3 the term Strict Positive Real (SPR) was introduced for the Pseudo Linear Regression algorithm as,

$$\mathrm{Re}\left[\frac{1}{1-\mathbf{A}_*(z^{-1})}\right] > 0 \ , |z| = 1, \tag{3.2.84}$$

where Re(u) denotes the real part of u and $1-\mathbf{A}_*(z^{-1})$ denotes the poles of the system to be modelled. It was discussed how that this condition should in general be satisfied to ensure convergence. In some cases however, despite violation of (3.2.84) the algorithm will still converge if it has sufficient degrees of freedom to approximate the echo path being modelled. Figure 5.71 shows the SPR condition for the echo paths of Chapter 4 (which approximates the handset variation in normal handset use). The poles $A_*(q^{-1})$ here, are the poles estimated for each echo path using the Simplified Gradient LMS Newton with no echo path output noise and a model order of (27,15). From Figure 5.71 it can be seen that there is a 'mild' violation of the SPR condition of most of the echo path responses to be modelled. As we shall see shortly for all of these echo paths when modelling results for the Pseudo Linear Regression LMS Newton algorithm are discussed, that convergence and stability for a suitable choice of algorithm parameters is obtained despite the violation of (3.2.84). The condition of (3.2.84) is clearly overly restrictive for this application, and can be termed as 'sufficient' but 'not necessary' for algorithm convergence. It is assumed the model order of (27,15) seems to give this algorithm sufficient degrees of freedom to model the echo path response of a mobile handset to achieve convergence.

As an example of the convergence performance of this algorithm Figure 5.72 shows the ensemble averaged ERLE level results achieved for a model order of 42 coefficients (27,15) when modelling the face up no seals handset echo path response of Chapter 4. Different forgetting factors $\lambda$ are used. As expected the same general trends in performance occur with the forgetting factor $\lambda$ as did for the FIR

LMS Newton and Simplified Gradient LMS Newton algorithms. Unlike the Simplified Gradient LMS Newton algorithm the Pseudo Linear Regression LMS Newton algorithm does not have such a restrictive range with respect to the forgetting factor $\lambda$ in order to achieve stability at lower ENR levels.

A value of $\lambda$ =0.9995 is recommended for stability and performance over a range of different ENR levels and echo paths. A fixed value of stepsize is employed based on recommendations from Section 5.2. A value $\mu = 0.00125$ is recommended for robust operation at low ENR levels for all echo paths.

From Figure 5.73 it can be seen that the same general trends also exist for the convergence factor $\alpha$ for the Pseudo Linear Regression LMS Newton algorithms, as did for both the FIR LMS Newton and Simplified Gradient LMS Newton algorithms. A value of $\alpha$ =0.005 is recommended for stability and performance over a range of different ENR levels and echo paths.

#### 5.3.3.4. The SHARF LMS Newton adaptive IIR algorithm

As discussed in Chapter 3 an additional fixed FIR error filter $\mathbf{C}(q^{-1})$ can be used in the Pseudo Linear Regression algorithm structure, giving the filter update,

$$\boldsymbol{\theta}_{n+1} = \boldsymbol{\theta}_n + \mu \hat{\mathbf{R}}^{-1}_{\varphi_o\varphi_o}(n) e_o(n)\left[1 + \mathbf{C}(q^{-1})\right]\varphi_o(n), \tag{3.2.104}$$

Equations (3.2.93) and (5.30) of Pseudo Linear Regression LMS Newton algorithm also apply to the SHARF LMS Newton algorithm. The coefficients $\mathbf{C}(q^{-1})$ are normally fixed throughout adaptation of the filter and are chosen to meet the following SPR condition,

$$\mathrm{Re}\left[\frac{1+\mathbf{C}(z^{-1})}{1-\mathbf{A}_*(z^{-1})}\right] > 0 \ , |z| = 1, \tag{3.2.98}$$

By using this fixed filter $\mathbf{C}(q^{-1})$ the SPR region within the unit circle of the z domain is expanded to include more echo path coefficient values, thus allowing the SPR condition of (3.2.98) to be satisfied even for those echo paths whose poles $A_*(q^{-1})$ fail to satisfy the SPR condition of (3.2.84).

Since the Pseudo Linear Regression LMS Newton algorithm converges satisfactorily for all echo paths of Chapter 4 to be modelled despite the violation of most echo paths of the SPR condition of (3.2.84) it can be concluded that this additional fixed filter is not actually required for stability and convergence reasons for this application. Additionally the problem of choosing a fixed filter $\mathbf{C}(q^{-1})$ when the echo path response is unknown, and can change during a call due to handset movements is both difficult and impractical. To investigate whether the application of SHARF algorithm with this fixed filter $\mathbf{C}(q^{-1})$ may hold any performance or convergence benefits over the standard Pseudo Linear Regression LMS Newton Figure 5.74shows ensemble averaged ERLE level results achieved for a model order of 42 coefficients (27,15) when modelling the face up no seals handset echo path response of Chapter 4. Different forgetting factors $\lambda$ are used and an ENR level of 0dB is present. The coefficients $\mathbf{C}(q^{-1})$ are chosen to place a zero in the vicinity of each pole $\widetilde{A}_*(q^{-1})$, where $\widetilde{A}_*(q^{-1})$ are the estimated poles for the face up no seals echo path modelled using the Pseudo Linear Regression LMS Newton algorithm with an order of (27,15) with no echo path noise present.

In comparison to the results of the Pseudo Linear Regression LMS Newton in Figure 5.72 it can be clearly seen there are no performance or convergence benefits using the SHARF LMS Newton algorithm structure. This is also the case for other echo paths modelled over a range of ENR levels. The SHARF algorithm will not be considered further in this thesis for the handset echo cancellation application.

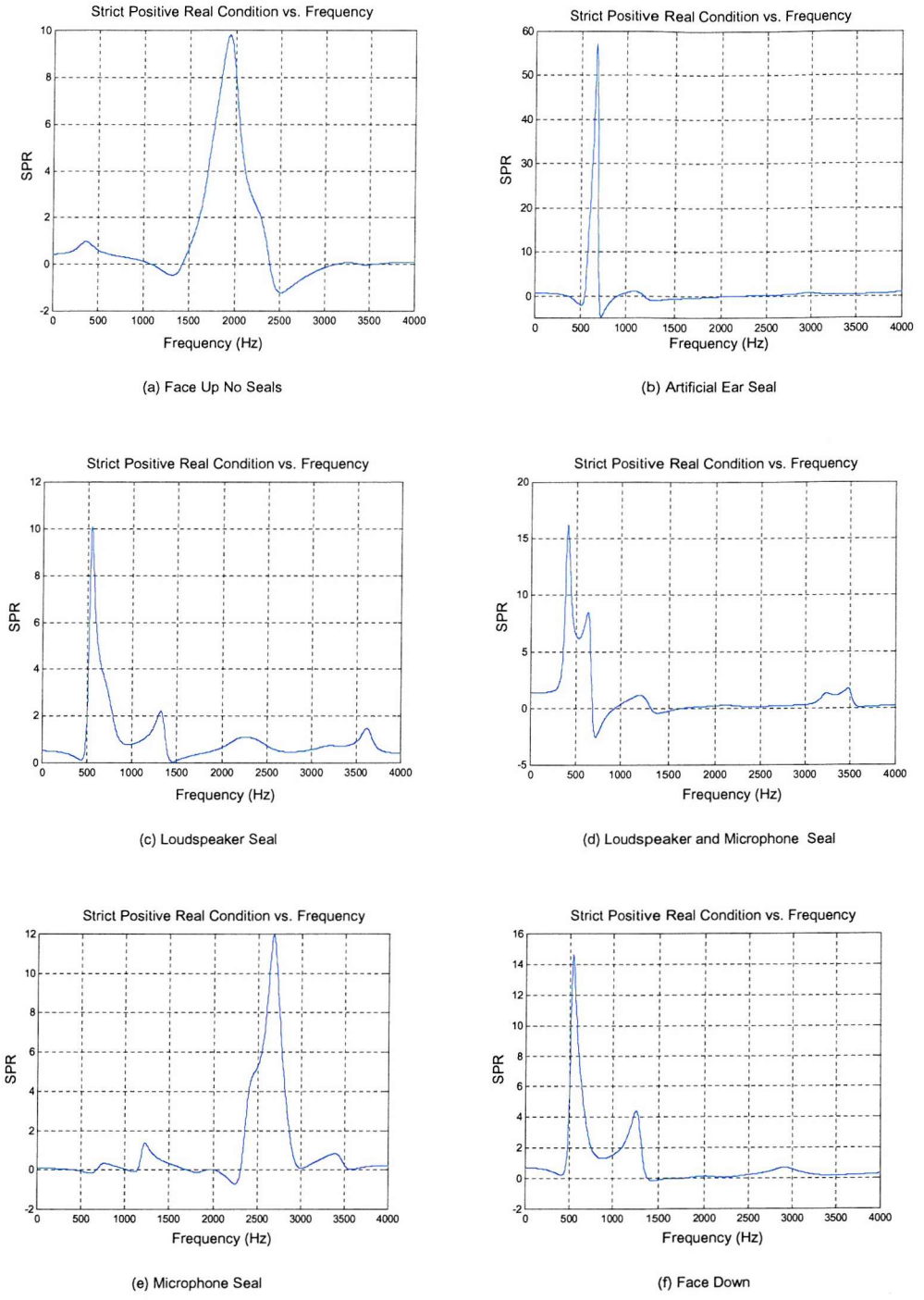


**Figure 5.71 : SPR condition of the poles of each handset echo path**

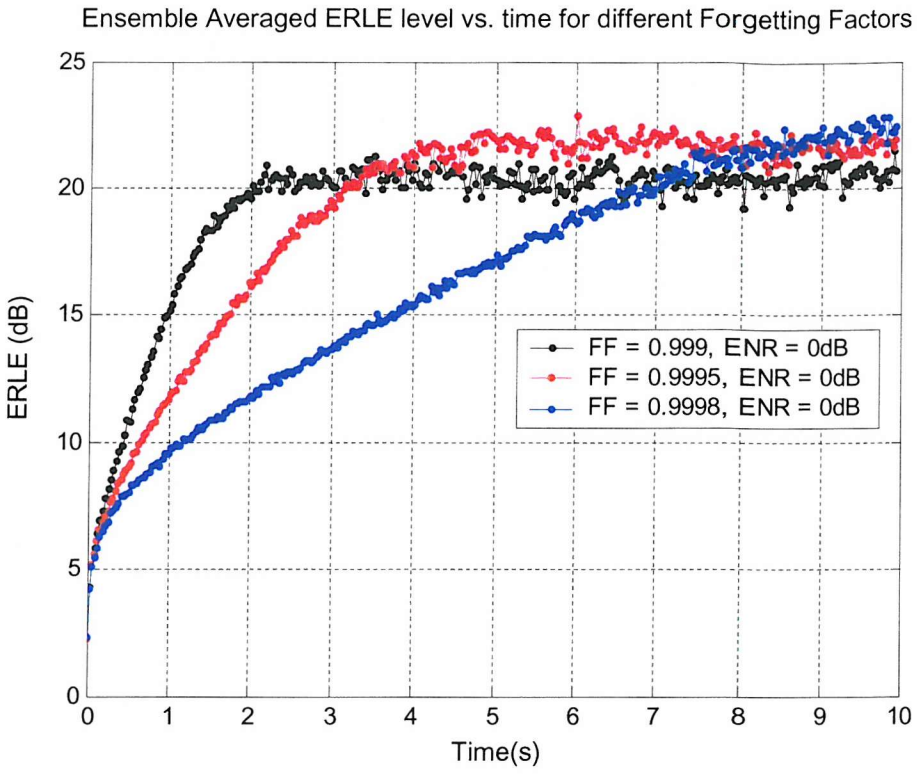


**Figure 5.72 : Pseudo Linear Regression LMS Newton ERLE performance with different forgetting factors $\lambda$ for ENR level of 0dB ($\alpha$ =0.0075).**

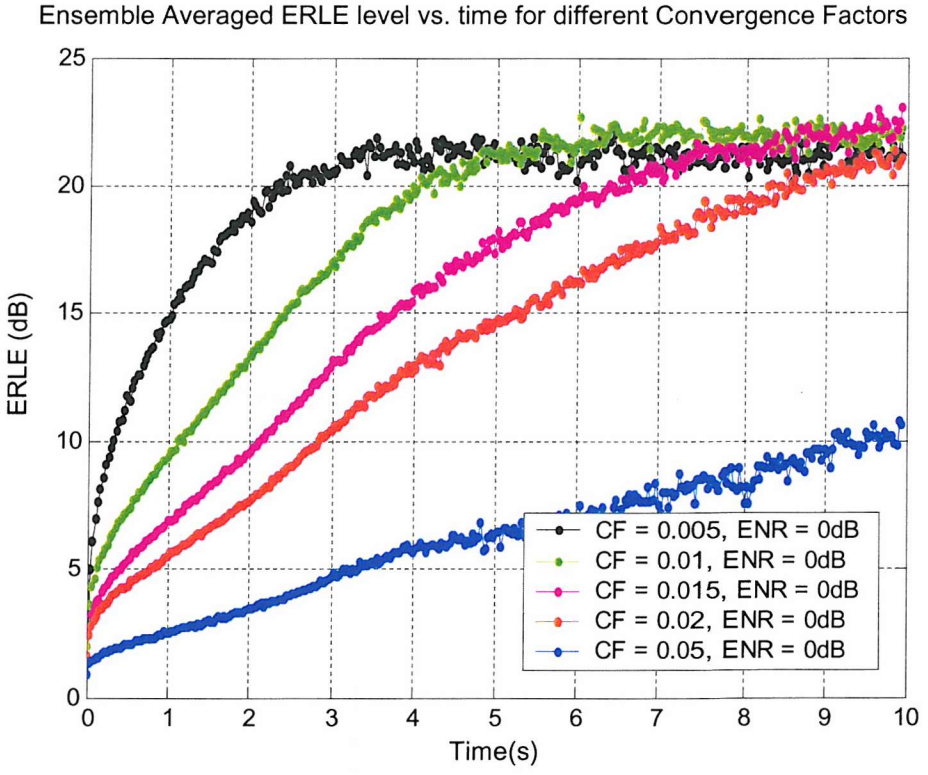


**Figure 5.73 : Pseudo Linear Regression LMS Newton ERLE performance with different convergence factors $\alpha$ for ENR level of 0dB ($\lambda$ =0.9995).**

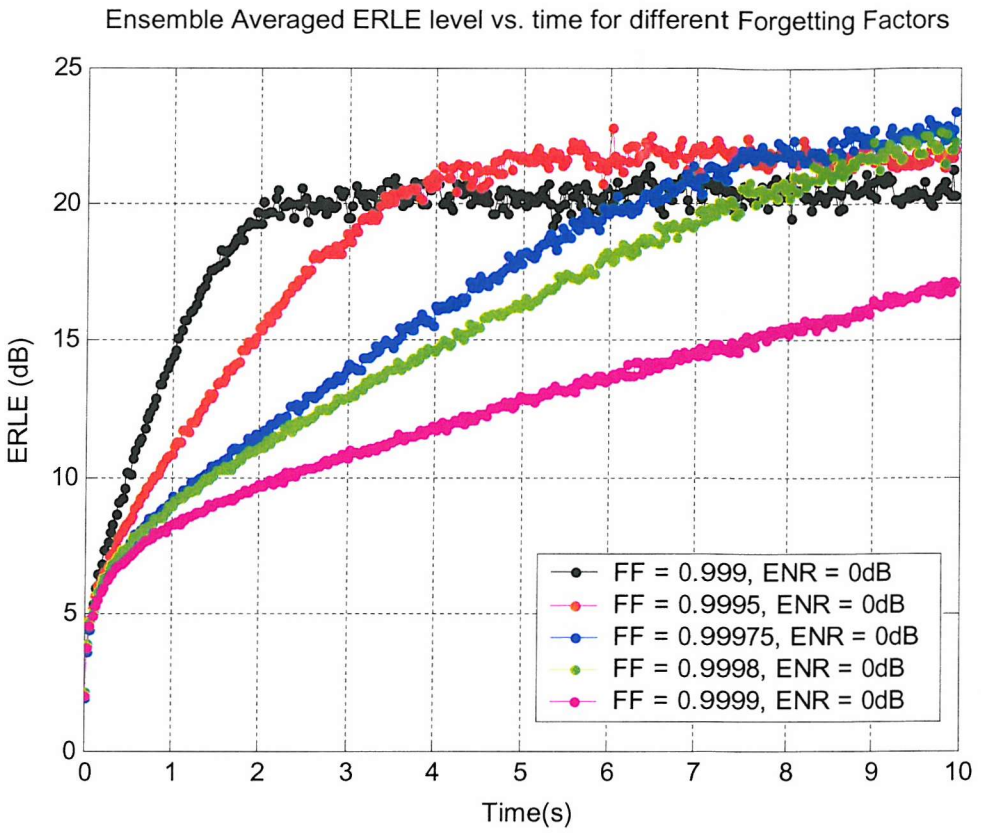


**Figure 5.74 : SHARF LMS Newton ERLE performance with different forgetting factors $\lambda$ for ENR level of 0dB ($\alpha$ =0.0075).**

#### 5.3.3.5. The Equation Error LMS Newton adaptive IIR algorithm

Consider next the choice of design parameters for the Equation Error LMS Newton adaptive IIR algorithm when echo path noise is present. For the Equation Error LMS Newton algorithm the stepsize $\mu = 0.0025$ recommended in Section 5.2 will be adopted, only the values of forgetting factor $\lambda$ and convergence factor $\alpha$ will be changed to give robust performance at low ENR levels.

Consider the effect of the forgetting factor $\lambda$ on the convergence and steady state $ERLEss_{dB}$ level achievable by the Equation LMS Newton algorithm. Figure 5.75 shows the ensemble averaged ERLE level results achieved for a model order of 42 coefficients (31,11) when modelling the face up no seals handset echo path response of Chapter 4. Different forgetting factors are used with a fixed convergence factor of $\alpha = 0.0075$. It is clear to see the bias effect at lower ENR levels from Figure 5.75 . As the feedforward coefficients begin to converge the ensemble averaged ERLE level increases. However once the feedback coefficients begin to adapt the bias caused by the high disturbance noise signal levels in the estimation of the optimum feedback coefficients causes the ensemble averaged ERLE level to significantly reduce. As a result from these initial results is not difficult to determine that the Equation LMS Newton algorithm is unsuitable for the handset echo cancellation application due to the low ENR levels possible. The Equation Error LMS Newton algorithm will still be considered in further

modelling experiments to serve a reference to compare other bias removal Equation Error methods against.

For the Equation LMS Newton algorithm despite the bias problem the same general trends still exits with respect to the forgetting factor $\lambda$ and convergence factor $\alpha$ as with the other LMS Newton algorithms considered so far. A forgetting factor of $\lambda$ =0.9995 and convergence factor $\alpha$ =0.0075 are recommended for the Equation LMS Newton algorithm for robust performance in the presence of echo path noise, and to obtain optimal performance at higher ENR levels where the bias effect will be less. Where the Equation LMS Newton algorithm is used in environments where the ENR level can occasionally be low, the values of $\lambda$ and $\alpha$ should be increased to slow adaption and reduce bias during low ENR periods.

#### 5.3.3.6. The Steiglitz McBride Equation Error LMS Newton adaptive IIR algorithm

The results presented in Section 5.2 demonstrated how the performance of adaptive IIR equation error LMS Newton algorithms vary with algorithm parameters $\mu$ , $\lambda$ , $\alpha$ , and $\delta$ , for no echo path output noise. In this section we will see how these parameters specifically affect the Steiglitz McBride LMS Newton algorithm when echo path output noise is present.

The Steiglitz McBride LMS Newton algorithm is re-written for convenience below,

$$\boldsymbol{\theta}_{n+1} = \boldsymbol{\theta}_n - \alpha \hat{\mathbf{R}}^{-1}_{\varphi_{fe}\varphi_{fe}}(n)\varphi_{fe}(n)e_{fe}(n) \tag{3.3.94}$$

where,

$$\hat{\mathbf{R}}^{-1}_{\varphi_{fe}\varphi_{fe}}(n) = \frac{1}{\gamma}\left(\hat{\mathbf{R}}^{-1}_{\varphi_{fe}\varphi_{fe}}(n-1) - \frac{\hat{\mathbf{R}}^{-1}_{\varphi_{fe}\varphi_{fe}}(n-1)\varphi_{fe}(n)\varphi_{fe}{}^{T}(n)\hat{\mathbf{R}}^{-1}_{\varphi_{fe}\varphi_{fe}}(n-1)}{\frac{\gamma}{\alpha} + \varphi_{fe}{}^{T}(n)\hat{\mathbf{R}}^{-1}_{\varphi_{fe}\varphi_{fe}}(n-1)\varphi_{fe}(n)}\right) \tag{3.3.96}$$

and the following initialisations is used,

$$\hat{\mathbf{R}}^{-1}_{\varphi_{fe}\varphi_{fe}}(n) = \delta\mathbf{I}\,, \tag{5.31}$$

For the Steiglitz McBride LMS Newton algorithm a fixed stepsize $\mu = 0.00125$ is used and only the values of forgetting factor $\lambda$ and convergence factor $\alpha$ will be investigated for robust operation at low ENR levels.

Figure 5.77 shows the ensemble averaged ERLE level results achieved for a model order of 42 coefficients (31,11) for modelling experiments with different forgetting factors, for the face up no seals handset echo path response of Chapter 4. The Equation Error LMS Newton algorithm is also drawn on the same axes to show the bias remedy capabilities of the Steiglitz McBride LMS Newton over the standard equation error approach.

Despite removing much of the bias due to the equation error formulation the Steiglitz McBride method does produce a slower convergence rate as a higher forgetting factor of $\lambda$ =0.9998 is needed for

robust convergence at low ENR levels for all echo paths. Below a forgetting factor of $\lambda$ =0.9996 instability occurs at low ENR levels. Like other algorithms presented so far with a higher forgetting factor algorithm convergence time to the steady state ensemble averaged ERLE level increases.

Figure 5.78 shows the effect on ensemble averaged ERLE level for different values of convergence factor $\alpha$ . The same trends of increasing algorithm convergence time to the steady state ensemble averaged ERLE level can be observed for higher values of $\alpha$ . Below $\alpha$ =0.0075 instability occurs. A value of $\alpha$ =0.0075 is recommended for stability and performance over a range of different ENR levels and echo paths.

### 5.3.3.7. The Bias Remedy Equation Error LMS Newton adaptive IIR algorithm

Consider now the choice of design parameters for the Bias Remedy Equation Error LMS Newton adaptive IIR algorithm when echo path noise is present. The Bias Remedy Equation Error LMS Newton algorithm is re-written for convenience below,

$$\boldsymbol{\theta}_{n+1} = \boldsymbol{\theta}_n + \mu \hat{\mathbf{R}}^{-1}_{\varphi_{br}\varphi_{br}}(n)\varphi_{br}(n)e_e(n), \tag{3.3.65}$$

where

$$\hat{\mathbf{R}}^{-1}_{\varphi_{br}\varphi_{br}}(n) = \frac{1}{\gamma}\left( \hat{\mathbf{R}}^{-1}_{\varphi_{br}\varphi_{br}}(n-1) - \frac{\hat{\mathbf{R}}^{-1}_{\varphi_{br}\varphi_{br}}(n-1)\varphi_{br}(n)\varphi_{br}{}^{T}(n)\hat{\mathbf{R}}^{-1}_{\varphi_{br}\varphi_{br}}(n-1)}{\frac{\gamma}{\alpha} + \varphi_{br}{}^{T}(n)\hat{\mathbf{R}}^{-1}_{\varphi_{br}\varphi_{br}}(n-1)\varphi_{br}(n)} \right), \tag{3.3.68}$$

and the following initialisations is used,

$$\hat{\mathbf{R}}^{-1}_{\varphi_{br}\varphi_{br}}(n-1) = \delta \mathbf{I}, \tag{5.32}$$

From (3.3.94) and (3.3.96) the same algorithm design parameters $\mu$ , $\lambda$ , $\alpha$ , and $\delta$ as for the Steiglitz McBride LMS Newton algorithm exist for this algorithm also. However an additional parameter $k$ is also used in the Bias Remedy Equation Error LMS Newton in order to alter level of bias in information vector $\varphi_{br}(n)$ in (3.3.53) and (3.3.56). For the Bias Remedy Equation Error LMS Newton algorithm a fixed stepsize $\mu = 0.00125$ is used and only the values of forgetting factor $\lambda$ , convergence factor $\alpha$ and bias constant $k$ will be investigated for robust operation at low ENR levels.

Figure 5.79 shows the ensemble averaged ERLE level results achieved for a model order of 42 coefficients (31,11) for modelling experiments with different forgetting factors, for the face up no seals handset echo path response of Chapter 4. Two different bias constants are shown also. From Figure 5.79 it can be seen that a bias constant of $k$ =0 gives the same performance as the standard Equation Error LMS Newton algorithm. A value of $k$ =0.5 gives the best trade off between algorithm stability across all echo paths and the level of bias reduction.

From Figure 5.79 it can be seen that as for other algorithms discussed so far increasing the forgetting factor increases the convergence time. Below a forgetting factor of $\lambda$ =0.9996 instability occurs at low ENR levels. A value of $\lambda$ =0.9996 is recommended.

The same trends of increasing algorithm convergence time to the steady state ensemble averaged ERLE level exist as in all other algorithms discussed so far. A value of $\alpha$ =0.0075 is recommended for stability and performance over a range of different ENR levels and echo paths.

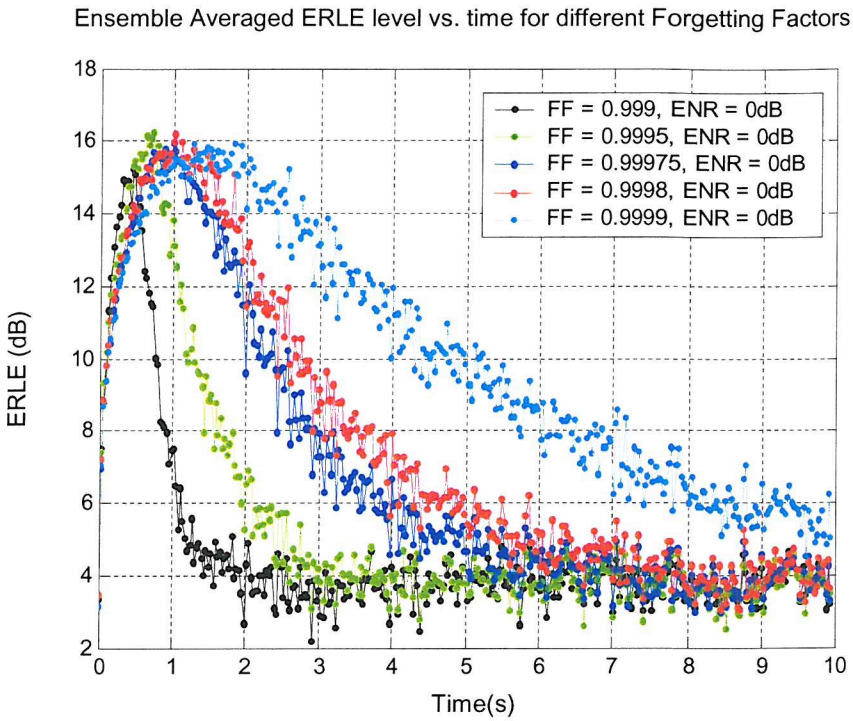


**Figure 5.75 : Equation Error LMS Newton ERLE performance with different forgetting factors $\lambda$ for ENR level of 0dB ($\alpha$ =0.0075).**

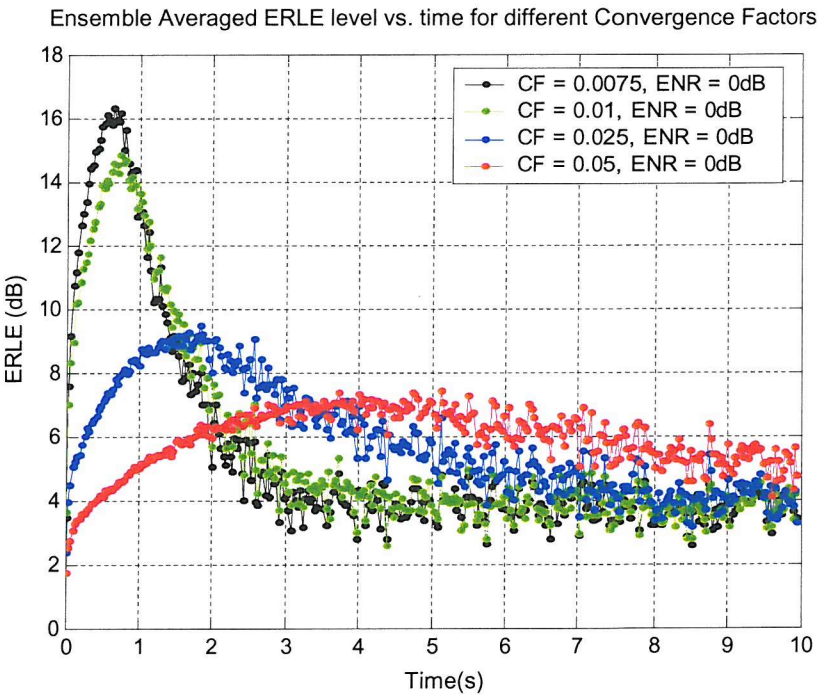


**Figure 5.76 : Equation Error LMS Newton ERLE performance with different convergence factors $\alpha$ for ENR level of 0dB ($\lambda$ =0.9995)**

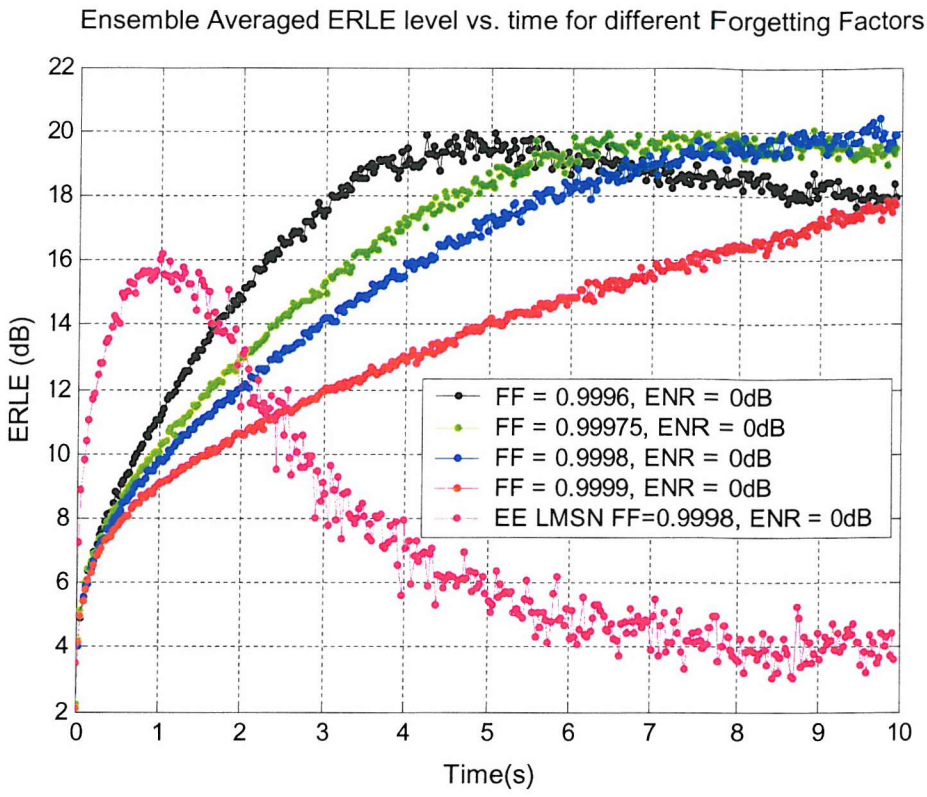


**Figure 5.77 : Steiglitz McBride Equation Error LMS Newton ERLE performance with different forgetting factors $\lambda$ for ENR level of 0dB ($\alpha$ =0.0075).**

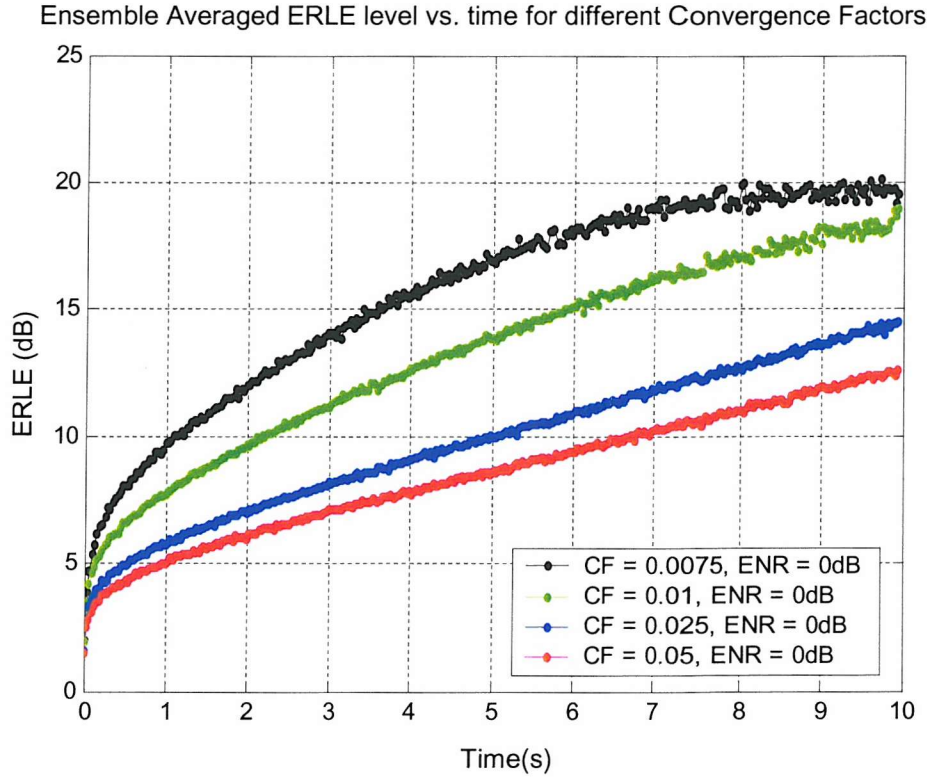


**Figure 5.78 : Steiglitz McBride Equation Error LMS Newton ERLE performance with different convergence factors $\alpha$ for ENR level of 0dB ($\lambda$ =0.9998)**

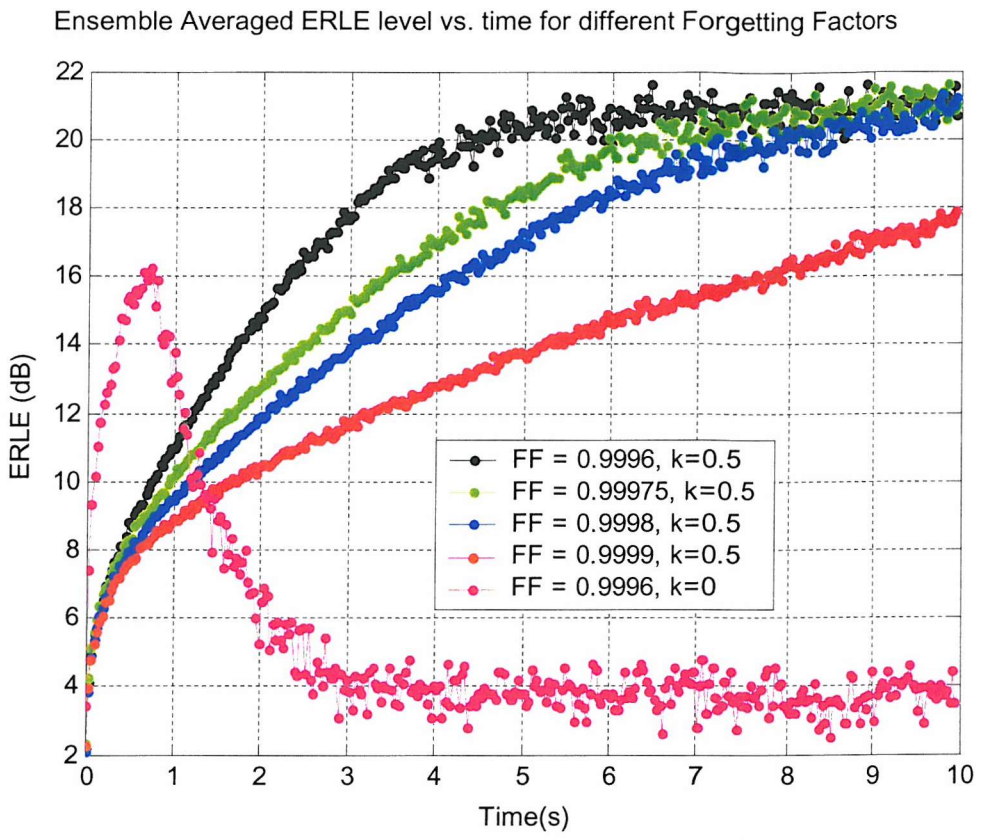


**Figure 5.79 : Bias Remedy Equation Error LMS Newton ERLE performance with different forgetting factors $\lambda$ for ENR level of 0dB ($\alpha$ =0.0075).**

### 5.3.4. LMS Newton Modelling Results in the Presence of Echo Path Output Noise

The adaptive algorithm parameters chosen for each modelling experiment is a single set of parameters, selected as a trade off between steady state ensemble averaged ERLE level and convergence time, using the recommendations discussed in the last section.

The steady state ensemble averaged modelling results are shown in Figure 5.80 to Figure 5.85 for a range of ENR levels for each narrowband echo path of chapter 4. A filter model order of 42 coefficients is used for all LMS Newton algorithms. The main results in Table 5-3 are summarised in below for an ENR level of 3dB.

| Echo Path | Adaptive Algorithms | | | | | |
|---|---|---|---|---|---|---|
| | FIR LMS Newton | Simplified Gradient LMS Newton | Pseudo Linear Regression LMS Newton | Equation Error LMS Newton | Bias Remedy Equation Error LMS Newton | Steiglitz McBride LMS Newton |
| Face Up No Seals | 21.5 | 23.3 | 22.5 | 6.8 | 22.8 | 20.2 |
| Artificial Ear Seal | 15.5 | 14.9 | 12 | 5.7 | 10.8 | 11.4 |
| Loudspeaker Seal | 14.8 | 19 | 16.9 | 6.2 | 12.9 | 13 |
| Loudspeaker and Microphone Seal | 13.4 | 20.1 | 17.1 | 5.8 | 18.3 | 14 |
| Microphone Seal | 12.8 | 17.6 | 16 | 5.9 | 14.4 | 12.2 |
| Face Down | 14 | 16.2 | 13.9 | 5 | 14.8 | 12.8 |

**Table 5-3 : Summary of steady state ERLE results for LMS Newton adaptive algorithms for a total order of 42 coefficients. The ENR level is 3dB**

From the results presented in Table 5-3 it is clear that the Simplified Gradient LMS Newton algorithm is the only algorithm capable of meeting the required ERLE level for each echo path down to an ENR level of 3dB. An ERLE gain of up to 6.7dB is achievable over an equivalent FIR algorithm even at ENR levels as low as 3dB. Similar ERLE gains as those presented in chapter 4 (for offline IIR models in the absence of echo path output noise) are clearly achievable using output error adaptive IIR algorithms in the presence of echo path output noise. Only the Simplified Gradient LMS Newton based algorithms will be considered in future chapters.

From Figure 5.80 to Figure 5.85 the bias effect of the Equation Error LMS Newton algorithm is clear. Only at ENR levels above 25dB(not shown) is the Equation Error LMS Newton algorithm capable of meeting the required ERLE of each echo path response. Despite both the Bias Remedy Equation Error LMS Newton algorithm and the Steiglitz McBride LMS Newton algorithm overcoming this bias, their performance does not match that of the output error Simplified Gradient LMS Newton algorithm.

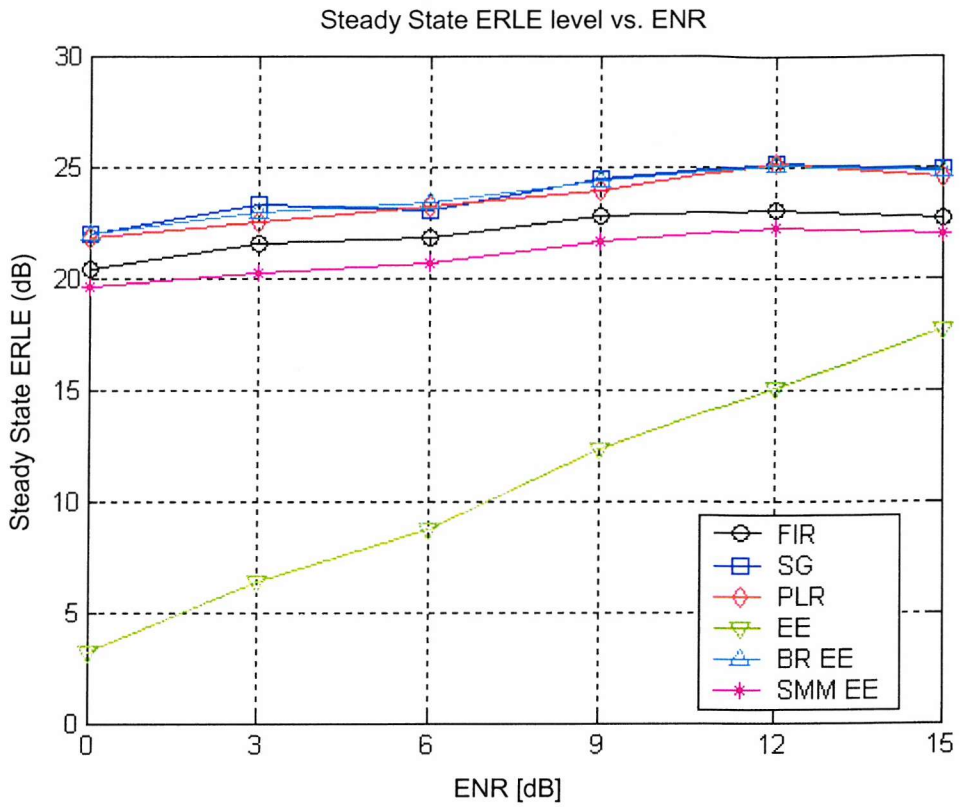


**Figure 5.80 : LMS Newton modelling results for the Face Up No Seals Echo Path Response.**

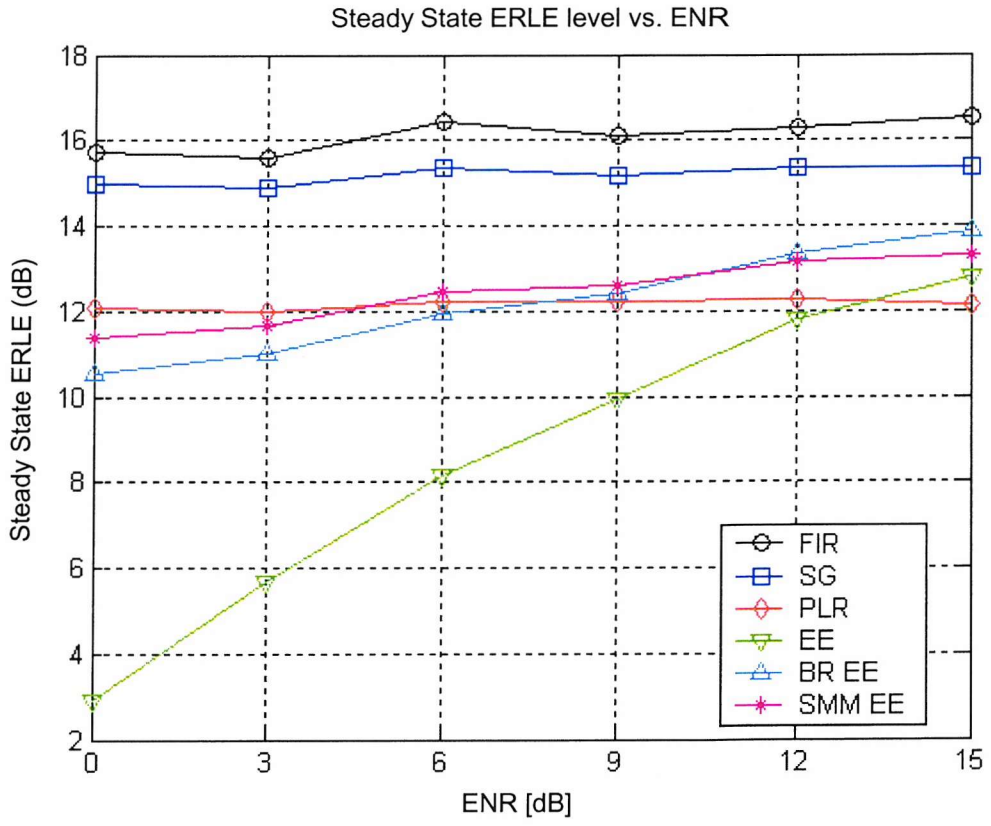


**Figure 5.81 : LMS Newton modelling results for the Artificial Ear Sealed Echo Path Response**

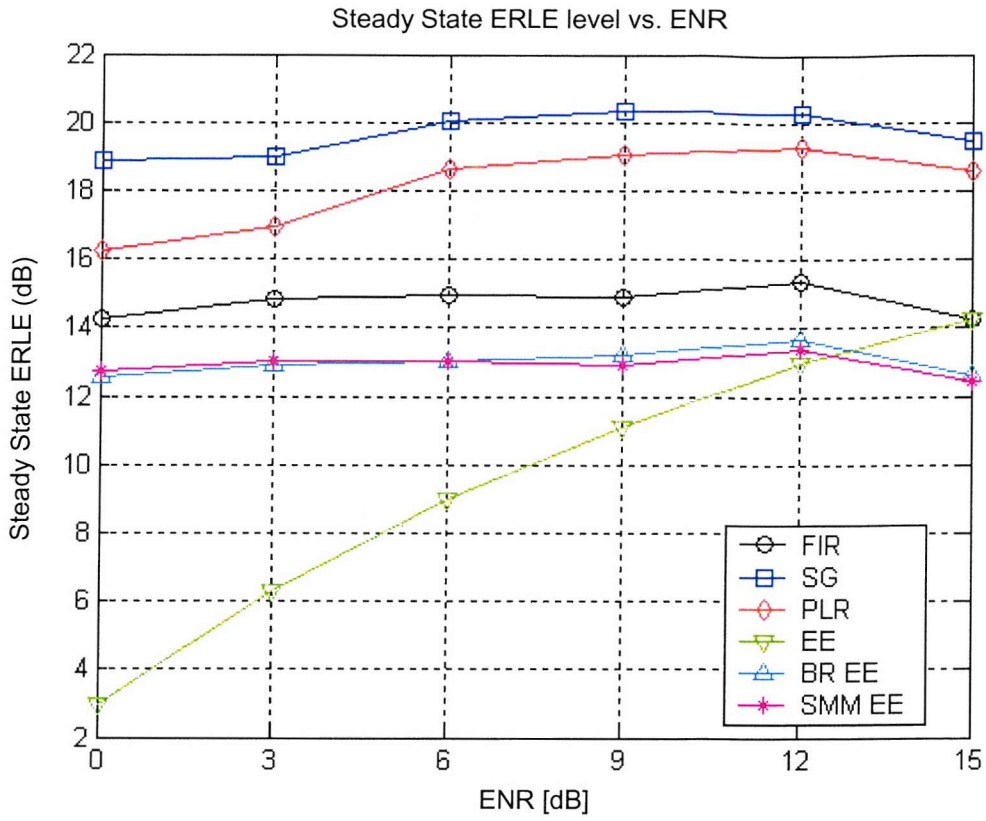


**Figure 5.82 : LMS Newton modelling results for the Loudspeaker Adhesive Tape Sealed Echo Path Response.**

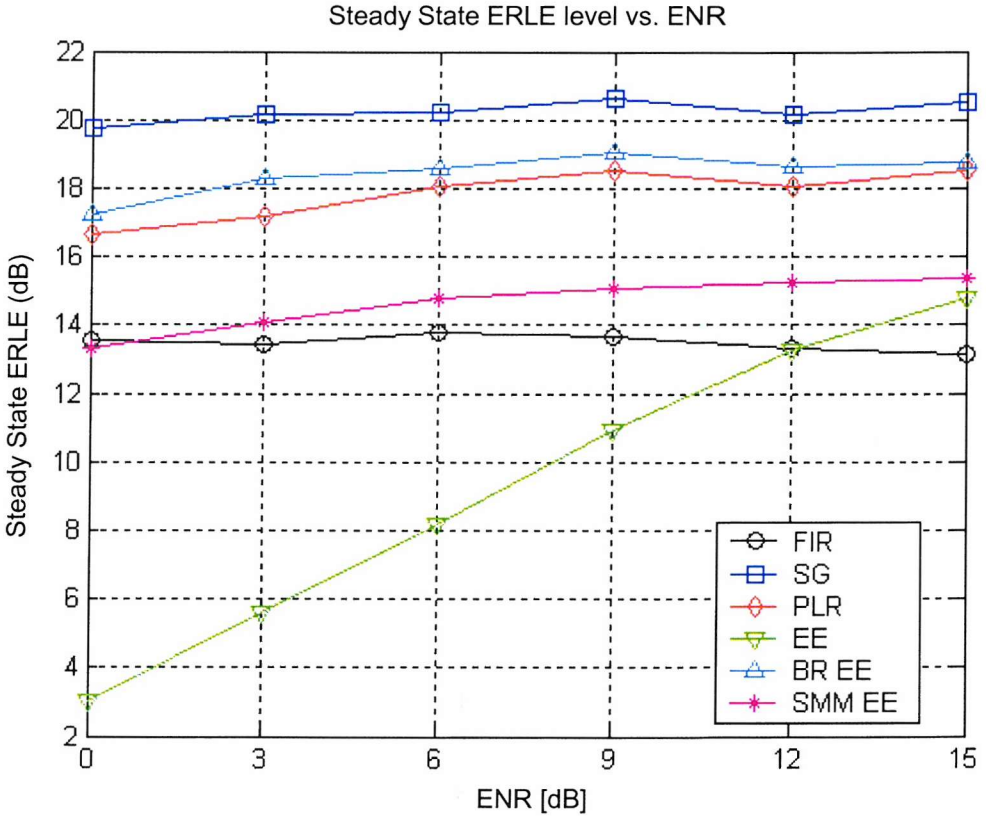


**Figure 5.83 : LMS Newton modelling results for the Loudspeaker and Microphone Adhesive Tape Sealed Echo Path Response.**

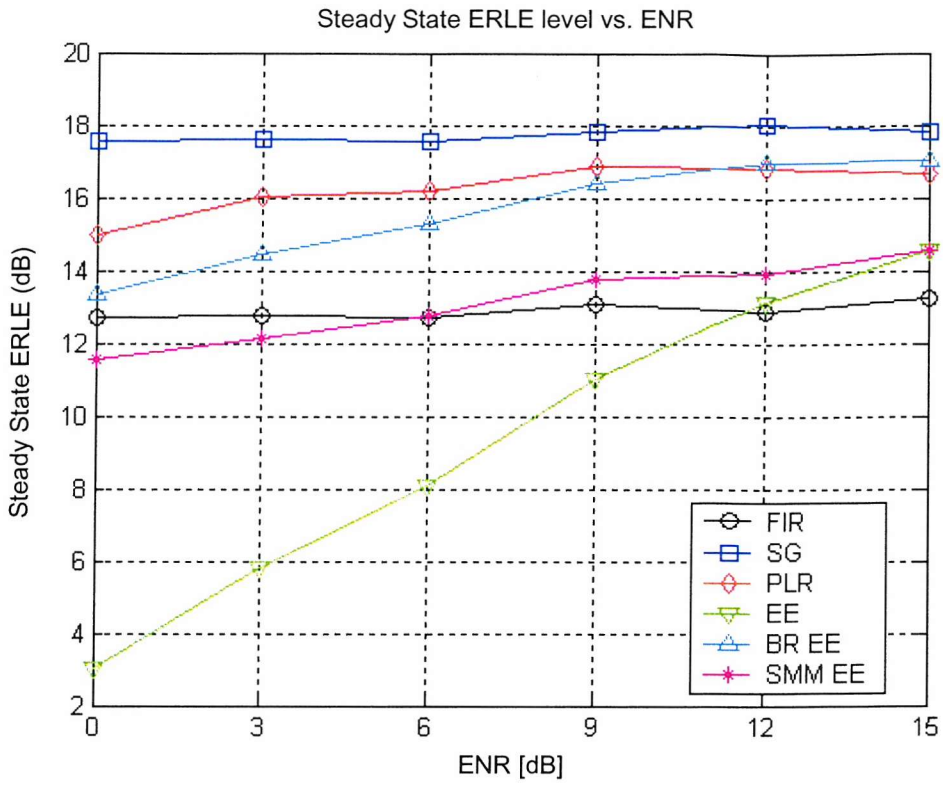


**Figure 5.84 : LMS Newton modelling results for the Microphone Adhesive Tape Sealed Echo Path Response.**

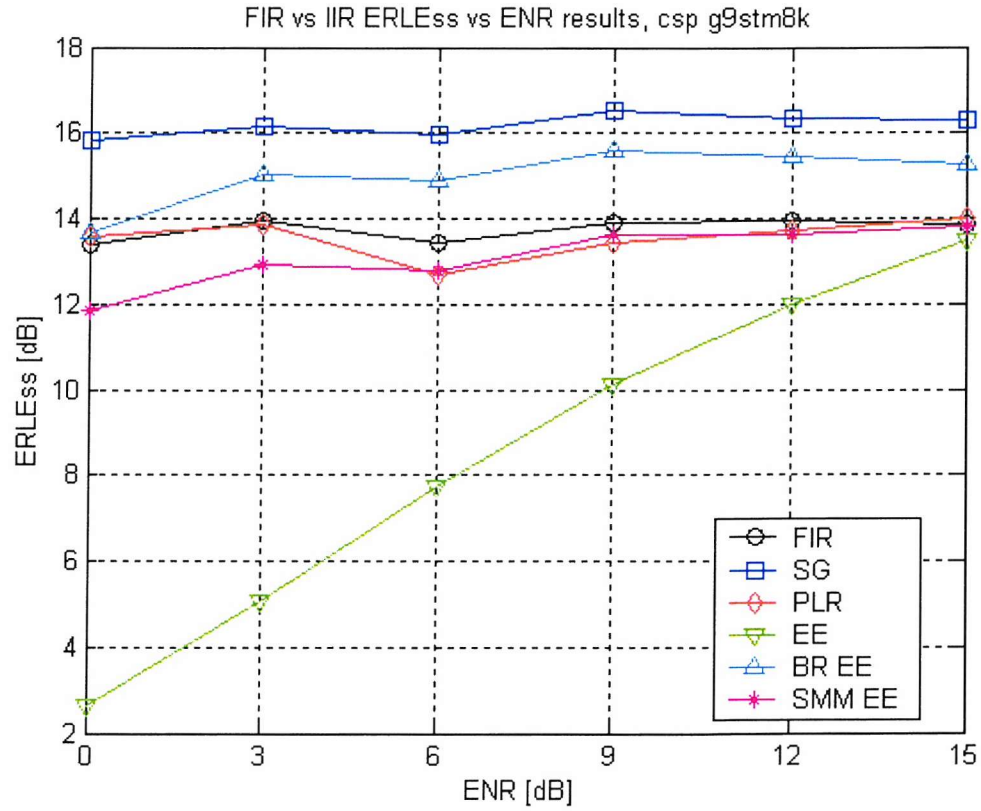


**Figure 5.85 : LMS Newton modelling results for the Face Down Echo Path Response.**

### 5.3.5. Summary of Chapter

The main goal of this chapter was to assess whether adaptive IIR filters have any benefits in terms of modelling performance over more traditional FIR adaptive models when modelling the narrowband echo path responses of chapter 4. A secondary aim of this chapter is to discuss the advantages and disadvantages of the adaptive algorithms presented in chapter 3, when modelling the echo path of a mobile handset is also addressed, and their performance with respect to algorithm design parameters.

The main goal of this chapter was undertaken in two stages. The first stage was section 5.2, which was a direct extension of chapter 4 with adaptive FIR and IIR modelling experiments. No echo path output noise is present in these modelling experiments. As part of this section adaptive IIR algorithm performance with respect to algorithm design parameters is also analysed. From the modelling results presented in section 5.2 it is clear that the steady state ERLE gains and Coefficient Reduction Factor possible presented in chapter 4 for offline (non-adaptive) IIR models are also achievable with adaptive IIR LMS Newton based algorithms. Even for a white noise signal input the eigenvalue spread is too large to enable adaptive IIR LMS and Normalised LMS algorithm forms to converge.

In section 5.3 it was found that a model order of (31,11) is needed for an equation error LMS Newton algorithm to meet the required ERLE of each echo path. With this model order an ERLE gain of up to 7.2 dB is possible over an equivalent FIR adaptive algorithm, with a CRF of up to 1.29 achievable. For an output error LMS Newton algorithm it was found that a model order of (27,15) is needed to meet the required ERLE of each echo path. With this model order an ERLE gain of up to 7 dB is possible over an equivalent FIR adaptive algorithm, with a CRF of up to 1.29 achievable

The second stage was section 5.3. The main aim of this section is to assess the steady state modelling performance of adaptive FIR and IIR algorithms in the presence of echo path output noise. The modelling results of section 5.2 are repeated using different LMS Newton adaptive algorithms at specific model orders in the presence of echo path output noise. The modelling performance over a range of different ENR levels is presented. Due to the low ENR levels possible in the handset echo cancellation application it was found that only output error LMS Newton adaptive IIR algorithms are suitable. For the Simplified Gradient output error LMS Newton algorithm of order (27,15) it was found an ERLE gain of up to 6.7dB is achievable over an equivalent FIR algorithm even at ENR levels as low as 3dB.

For acoustic echo cancellation on a mobile handset the Simplified Gradient output error LMS Newton algorithms of chapter 3 will be used in the next chapter to assess the tracking performance of adaptive IIR algorithms for input and echo path time variations at different input SNR and output ENR levels.

# 6. Tracking Time Variations using Adaptive IIR Filtering Algorithms

## 6.1. Introduction

In the thesis so far only the steady state or asymptotic modelling performance of the adaptive algorithms has been discussed. In chapter 3 the most commonly used adaptive IIR algorithms were presented. In chapter 5 it was found that only Simplified Gradient Output Error LMS and NLMS Newton algorithms from the many algorithms considered were suitable for modelling the echo path of a mobile handset in line with the main aim of this thesis. However during handset acoustic echo cancellation time variations will exist in both the echo path to be modelled, and the input signals to the echo canceller.

The main aim of this chapter is to discuss the effects of time variations algorithms in both the handset echo path response and the input signals used, on the modelling performance of adaptive IIR algorithms, since convergence (as studied in chapter 5) does not guarantee tracking [6.2]. This chapter is split into two main parts. Section 6.2 continues from the modelling work presented in chapter 5. Results are presented showing the capability of adaptive IIR algorithms to track time variations in the handset echo path response in normal use. Linear gain variations are simulated in section 6.2.2. In section 6.2.3 step variation from one echo path response to another are simulated.

Section 6.3 assesses the capability of adaptive IIR algorithms to provide sufficient ERLE performance for speech signal inputs. The influence of input noise (noisy speech) on adaptive IIR algorithm performance over a range of SNR levels is also established. The effects of output noise on the estimated filter coefficients during silent periods of speech are also discussed. A new adaptive IIR algorithm, the Correlation Simplified Gradient NLMS Newton algorithm is presented to provide robust modelling performance at low ENR conditions satisfying the main aim of this thesis.

## 6.2. System Identification of a Time Varying Echo Path Response

As already presented in chapter 2 the acoustic echo path response of a mobile handset will vary dependent on the handset orientation. In normal use during a call it is vital the adaptive filtering algorithm of the echo canceller within the mobile handset can track these echo path changes in order maintain the required levels of ERLE during a call. To the author's knowledge no literature has been presented to date on the ability of adaptive IIR algorithms for tracking the acoustic echo path of a mobile handset. The purpose of this section is to analyse the performance of adaptive IIR algorithms for tracking the time varying acoustic echo path of a mobile handset.

Using the modelling results of chapter 5 two adaptive algorithms - the Simplified LMS and NLMS Newton algorithms - will be used to assess the tracking ability of adaptive IIR algorithms. The choice of algorithm parameters influencing tracking performance will be discussed. The FIR LMS Newton

algorithm will also be used to allow a performance comparison to be made between the tracking performance of adaptive FIR and IIR algorithms to be made for a time varying echo path.

During the thesis only echo path measurements were made in fixed handset orientations, and no measurements were made recording time variations in the handset response due to changing handset positions. As a result echo path time variations must be simulated in this chapter. Two different time variations are simulated to assess tracking ability – persistent linear time variations in the acoustic echo path response and non-linear transitional time variations in the acoustic echo path response. Results and conclusions on echo path tracking performance are presented.

### 6.2.1. Criteria for Assessing Tracking Performance

Different criteria for tracking assessment of adaptive FIR algorithms have been proposed in [6.1]-[6.3]. In chapter 3 the Misadjustment of an adaptive FIR algorithm was introduced. In a stationary context this Misadjustment level can be related to accuracy of convergence to the optimal solution in the steady state [6.1],[6.2]. At first thought the Misadjustment would seem a good method for assessing tracking performance for an adaptive IIR algorithm. However as we have already seen in chapter 5 due to the difficulty in the calculation of the optimal steady state solution for an output error formulation, the Misadjustment is deemed unsuitable. It previously demonstrated in chapter 5 the ERLE definition is closely related to the Misadjustment level, and is of far more importance in the selection of adaptive algorithms for the acoustic echo cancellation application. The criteria for tracking assessment used in this chapter shall be the ensemble averaged ERLE level as follows,

$$ERLE_{en}(m) = 10\log_{10}\left[\frac{1}{P}\sum_{p=1}^{P}\left(\frac{\sum_{j=0}^{L-1} d_p^2(mL-j)}{\sum_{j=0}^{L-1} e_p^2(mL-j)}\right)\right], \tag{6.1}$$

where $P$ is the number of repeated trials for each modelling experiment required for ensemble average estimate $ERLE_{en}(m)$. As in Chapter 5 each ensemble averaged estimate, $ERLE_{en}(m)$, is computed in m=32ms frames (L=256 @ 8kHz) across the recorded sequences $d_p(n)$ and $e_p(n)$ for each trial $p = 1 \cdots P$. In analogy with the Mean Square Deviation level of [6.1] the ERLE definition of (6.1) may be decomposed into two terms as follows,

$$ERLE_{en}(n) = ERLE_{ss}(n) - ERLE_{lag}(n), \tag{6.2}$$

where $ERLE_{ss}(n)$ is the asymptotic ERLE level reached during a normal convergence period as presented in chapter5, and may be termed the estimation ERLE level and is always present. The term $ERLE_{lag}(n)$ is the reduction in ERLE level due to adaptive filter coefficient vector lag resulting from a time varying echo path. The tracking results presented in the following section will contain ensemble averaged ERLE curves and tabulated asymptotic and lag ERLE levels from which tracking performance comparisons and selection of parameters involving adaptive IIR algorithms can be made.

### 6.2.2. Tracking Linear Time Variations in the Acoustic Echo Path response

In a call where the handset position does not remain fixed, time variations echo path response will exist. In addition to handset movement, the handset volume control (which is after the echo canceller input and part of the echo path to be modelled) can introduce linear gain changes in the handset echo path response. This section of the chapter is used to assess tracking performance for slow time variations in the echo path response as illustrated in Figure 6.1.

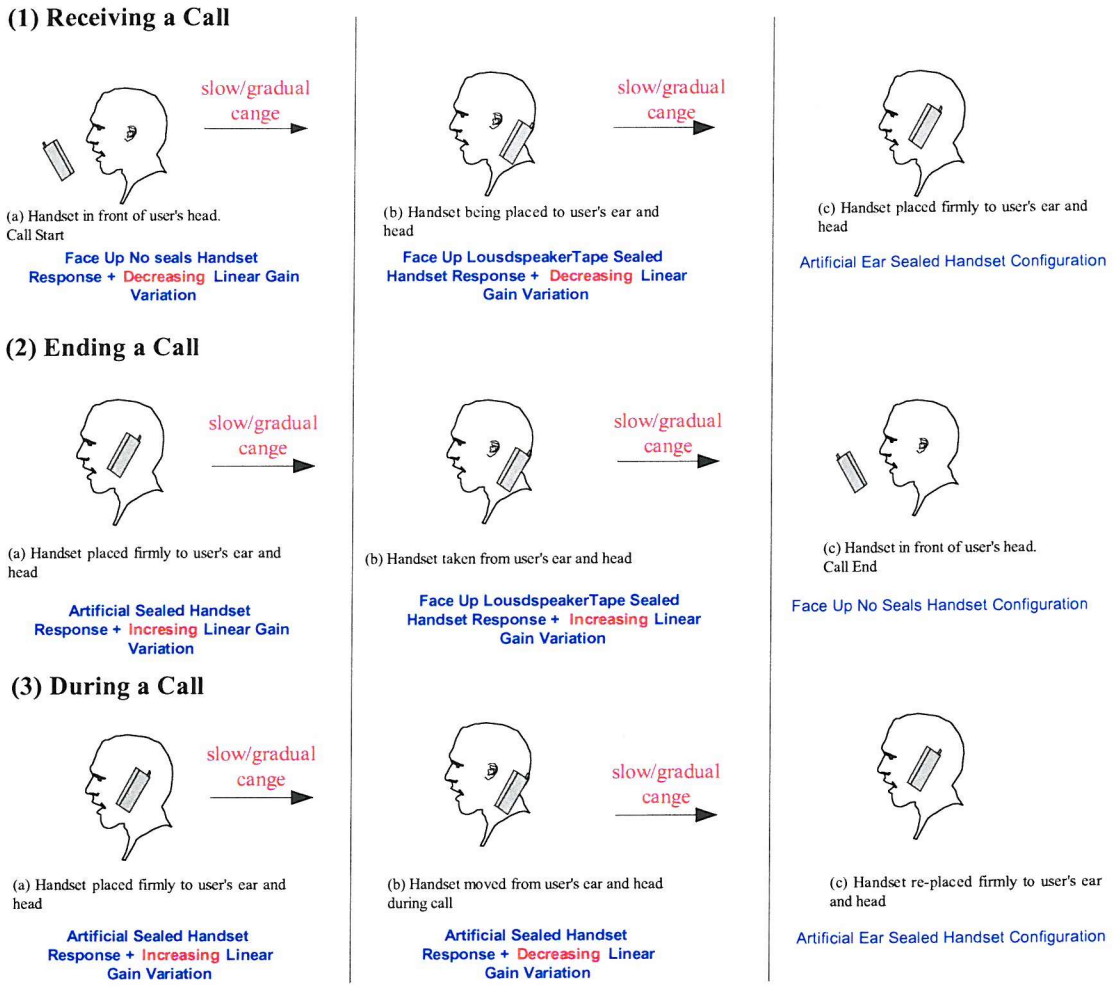


**Figure 6.1 : Echo path sequences during normal call**

From Figure 6.1 it is clear that both increasing and decreasing variations in the echo path response to be modelled can occur.

### 6.2.2.1. Experimental Design

In chapter2 it was established that the acoustic echo path response of a mobile handset was linear in nature, but the echo path response varies dependent on the handset orientation. Only the acoustic echo path responses of different fixed handset positions were measured. In a call where the handset position does not remain fixed a time varying acoustic echo path response results. A reasonable approximation to simulate this time variation is to use linear echo path gain changes at the output of the echo path responses measured during chapter 2. By varying the rate of these linear gain changes tracking performance behaviour for slow and fast echo path variations can be assessed.

The system identification configuration illustrated in Figure 6.2 is used to perform the system identification experiments with a time varying echo path response. From Figure 6.2 a variable gain block is added to the output of the echo path $\mathbf{h}$ being modelled, which contains the input $g(n)$ to control the gain of the block with respect to time. From Figure 6.2 it can be seen the gain profile of input $g(n)$ provides duration T1 to allow the adaptive algorithm to initially converge to its steady state level $ERLE_{ss}(n)$, or to settle to its steady state ERLE level after any output gain changes. Duration T2 is used to linearly ramp up or down the gain at the output of $\mathbf{h}$ between gains G1 to G2 to allow the component $ERLE_{lag}(n)$ to be calculated.

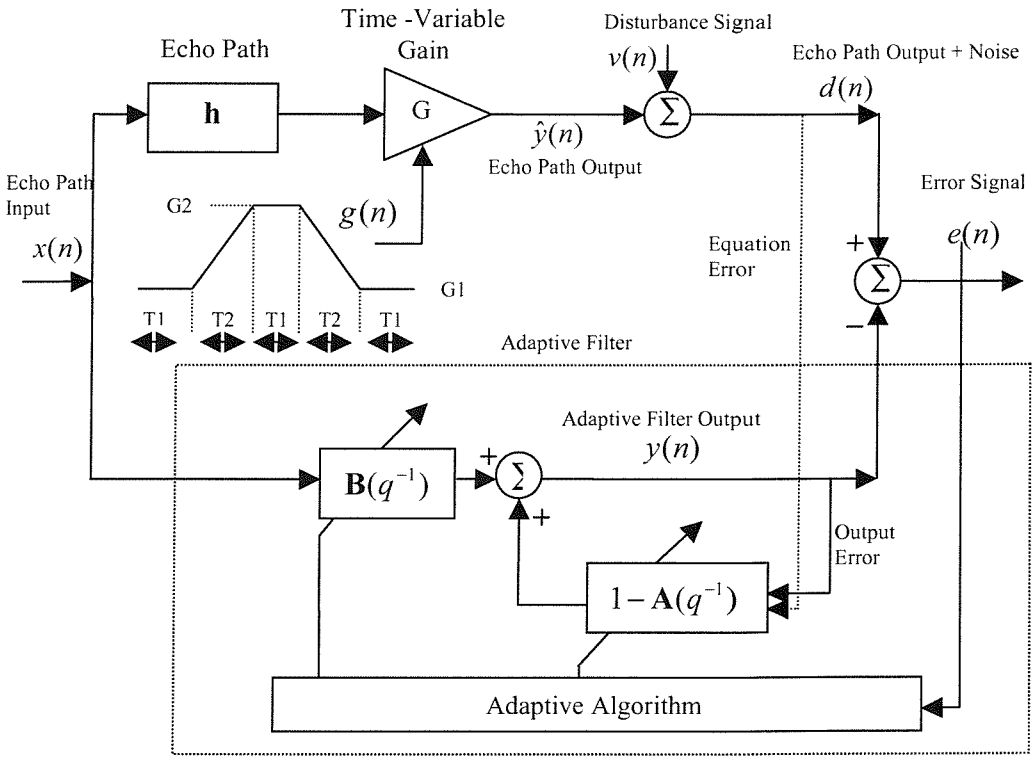


**Figure 6.2 : System identification experiment configuration for linear echo path time variations.**

The values of T1, T2, G1 and G2 can be altered to simulate fast and slow linear echo path variations. For the tests in this section G1 is unity and T1 is 10secs as in chapter 5 modelling results. Duration T2 is 5 seconds and gain level G2 is chosen depending on $\mathbf{h}$ to represent the minimum and maximum gain changes likely in normal handset use.

Stationary input signals are used to allow the effects of time variation in the echo path response on the tracking performance of adaptive algorithms to be analysed in isolation. Later in this Chapter the effects of time varying signals on algorithm performance is considered. A band-limited pink noise signal is used for both input signal $x(n)$ and disturbance signal $v(n)$. The additive noise signal $v(n)$ is scaled o allow algorithm echo path tracking performance to be assessed over a range of Echo to Noise Ratio (ENR) levels. Both $x(n)$ and $v(n)$ are uncorrelated. The choice of adaptive filtering parameters is discussed in the next section.

#### 6.2.2.2. The effect of adaptive filter design parameters on the tracking performance of adaptive IIR algorithms

The Simplified Gradient LMS and NLMS Newton algorithms are summarised in Table 6-1. From Table 6-1 both adaptive IIR algorithms have the following design parameters - $\mu$, $\lambda$, $\alpha$ and $\delta$. In the modelling experiments of chapter 5 these parameters were chosen for maximum steady state ERLE level $ERLE_{ss}(n)$ and minimum convergence time across all echo paths $\mathbf{h}$ modelled. No consideration was given to tracking time variation at that stage and the effect of these parameters on the levels of $ERLE_{lag}(n)$ when the echo path being modelled exhibits time variations. Tracking and convergence to the steady state ERLE level are two different entities [6.2].

The variable $\delta$ is used for the initialisation of autocorrelation estimate $\mathbf{R}^{-1}(0)$ in Table 6-1 for both algorithms to a multiple of the identity matrix [6.5]. The choice of $\delta$ is straightforward - a smaller value leads to slower convergence and vice versa. The choice of $\delta$ depends mostly on the input signal statistics [6.5]. For stationary signals the optimised setting as used in chapter 5 is employed and no variation of $\delta$ is considered. Additionally the choice of stepsize $\mu$ in both algorithms is also straightforward and the parameter selected for optimising ERLE convergence and $ERLE_{ss}(n)$ levels of Chapter 5 is re-used in these experiments. Only the effect of parameters $\lambda$ and $\alpha$ on algorithm tracking performance is considered.

For both the LMS Newton and NLMS Newton algorithms of Table 6-1 the choice of the forgetting factor $\lambda$ is the most crucial and influences the stability, convergence and tracking performance of the algorithm. The smaller the value of $\lambda$, the faster the convergence and the better the tracking performance will be [6.4],[6.5]. However the lower the value of $\lambda$ the more unstable both algorithm becomes. The influence of different forgetting factors $\lambda$ on tracking linear time variations in the echo

path response is illustrated in Figure 6.3 for stationary inputs and the artificial ear sealed echo path response for an ENR level of 20dB.

| | |
|---|---|
| Initialisation: $\hat{\mathbf{R}}^{-1}_{\varphi_f\varphi_f}(0)=\delta\mathbf{I}, \boldsymbol{\theta}_n=\mathbf{0}, \forall n<0$ | |
| $\varphi(n)=[x(n),...,x(n-M+1),y(n-1),...y(n-N)]^T$ | |
| $\hat{y}(n)=\boldsymbol{\theta}_n^T\varphi(n)$<br>$e_s(n)=d(n)-\hat{y}(n)$ | |
| $x_f(n)=x(n)+\sum_{j=1}^{N}\boldsymbol{\theta}_n(M+j)x_f(n-j)$<br>$y_f(n)=y(n-1)+\sum_{j=1}^{N}\boldsymbol{\theta}_n(M+j)y_f(n-j)$<br>$\varphi_f(n)=[x_f(n),...,x_f(n-M+1),y_f(n-1),...y_f(n-N)]^T$ | |
| **LMS Newton** | $\mu(n)=\mu$ |
| **NLMS Newton** | $\mu(n)=\dfrac{\mu}{\varphi_f^T(n)\mathbf{R}^{-1}_{\varphi_f\varphi_f}(n-1)\varphi_f(n)}$ |
| $\boldsymbol{\theta}_n=\boldsymbol{\theta}_{n-1}+\mu(n)\mathbf{R}^{-1}_{\varphi_f\varphi_f}(n-1)\varphi_f(n)e(n)$ | |
| $\hat{\mathbf{R}}^{-1}_{\varphi_f\varphi_f}(n)=\dfrac{1}{\lambda}\left(\hat{\mathbf{R}}^{-1}_{\varphi_f\varphi_f}(n-1)-\dfrac{\hat{\mathbf{R}}^{-1}_{\varphi_f\varphi_f}(n-1)\varphi_f(n)\varphi_f{}^T(n)\hat{\mathbf{R}}^{-1}_{\varphi_f\varphi_f}(n-1)}{\frac{\lambda}{\alpha}+\varphi_f{}^T(n)\hat{\mathbf{R}}^{-1}_{\varphi_f\varphi_f}(n-1)\varphi_f(n)}\right)$ | |

**Table 6-1: Simplified Gradient LMS Newton and NLMS Newton Adaptive IIR Algorithms**

From Figure 6.3 the gain profile used to create linear time variations at the echo path output is displayed. A normal convergence period (T1) occurs at times 0 to 10s, 15 to 25s and 30 to 40s during which the adaptive algorithm will settle to its asymptotic ERLE level, and during which no time variation exists. At times 10 to 15s and 25 to 30s (T2) the linear echo path gain increments are applied to the output of the echo path response. During times 10 to 15s the echo path gain is increased from G1 to G2, and during times 25 to 30s the echo path gain is reduced from G2 back down to G1. Here G1 and G2 are chosen to give a gain difference of 9dB in the power of the modelled echo path as illustrated in Figure 6.3. Most tracking experiments in the literature often consider only the first part of the gain profile when the echo path gain is increased [6.4],[6.5]. However in the handset acoustic echo cancellation area, echo path time variations could occur due to the placement and removal of a handset to the user's head, thus resulting in both decreasing and increasing echo path loss respectively. Also the handset volume control can also create increasing and decreasing gain changes in the echo path response. It is thus important to look at the tracking response of adaptive algorithms to both linear increasing and decreasing gain steps at the echo path output.

From Figure 6.3 it can be observed that a lower $\lambda$ increases convergence speed to the asymptotic ERLE level during a normal convergence periods (T1), and results in a lower $ERLE_{lag}$ level during non-stationary periods (T2) when linear echo path time variations are applied.

At this point it is worth noting the profile of ERLE levels during non-stationary periods (T2) when linear time variations are applied. From Figure 6.3 it can be seen that for positive linear gain increments, the delay in adaptive filter response to this time variations results in a drop in ERLE level, which remains around this level until the adaptive filter begins to track these time variations. The delay or lag in tracking response is proportional to the length of the adaptive filter [6.2],[6.3],[6.4]. For a larger number of coefficients the $ERLE_{lag}$ level is more pronounced [6.3]. For the IIR filter order size (27,15), consisting of 27 feedforward and 15 feedback coefficients the delay in adaptive filter response is small enabling linear echo path time variations to be quickly tacked during the non-stationary period and results in convergence towards the asymptotic ERLE level during this period. For the application of longer adaptive FIR filter to give similar asymptotic ERLE level performance, as discussed in chapter 5, would result in a longer lag delay and inferior tracking performance. This maximum drop in ERLE level during the non-stationary periods (T2) is termed the $ERLE_{lag}$ level. The value of this $ERLE_{lag}$ level depends on the echo path gain rate change and the adaptive filter parameters used.

For the periods when decreasing echo path gain increments are applied (T2) the ERLE tracking profiles are very different to those when positive gain increments were applied. The most notable difference is the larger maximum $ERLE_{lag}$ level. The second different is that this maximum level occurs at the end and not the start of the decreasing gain period from 25 to 30s. Convergence towards the asymptotic ERLE level only occurs at the end of the non-stationary period, and not during this period, as we have seen already during the positive gain increment period. This is due to the fact during the positive gain increment period the adaptive filter output power level rises towards the desired response level that is increasing, resulting in a positive ERLE level. When decreasing gain increments are applied the opposite happens. Extensive simulations have shown that to guarantee stability of adaptive IIR algorithms during handset echo path tracking experiments with linear time variations it is the deceasing gain increment period from 25 to 30s that is the most crucial. This is most likely the case for other adaptive algorithms that employ some form of normalisation in the filter coefficient update, when decreasing echo signal levels are produced. In the case of the Simplified Gradient LMS Newton algorithm this normalisation is the estimate of the inverse of the covariance matrix. For the adaptive IIR NLMS Newton algorithm this is both the stepsize normalisation and the estimate of the inverse of the covariance matrix.

Consider the effect of forgetting factor $\lambda$ on tracking performance of Simplified Gradient LMS Newton based algorithms. From Figure 6.3 a larger $\lambda$ can result in a much larger $ERLE_{lag}$ level, particularly during time period 25 to 30s when decreasing linear gain variations are applied. A value of $\lambda$ larger between $1-\frac{1}{50*(M+N)}$ and $1-\frac{1}{100*(M+N)}$ is required for stationary inputs for stability and reasonable tracking performance for the Simplified Gradient LMS Newton algorithm, where M is the number of feedforward coefficients and N is the number of feedback coefficients. For the

Simplified Gradient NLMS Newton algorithm a value of $\lambda$ between $1-\frac{1}{25*(M+N)}$ and $1-\frac{1}{100*(M+N)}$ is required. We shall see in later sections considerations for the choice of $\lambda$ with respect to non-stationary input signals.

Consider now the effect of variable $\alpha$ on tracking performance. The variable $\alpha$ is a convergence control parameter in both algorithms. The influence of convergence parameter $\alpha$ on tracking linear time variations in the echo path response is illustrated in Figure 6.4 for stationary inputs and the artificial ear sealed echo path response for an ENR level of 20dB. The tracking performance of the Simplified Gradient LMS Newton algorithm is shown in Figure 6.4. Like the forgetting factor $\lambda$ the smaller the value of$\alpha$ , the faster the convergence and the better the tracking performance. The values of $\alpha$ displayed in Figure 6.4 has a small effect on convergence and asymptotic ERLE performance during normal periods (T1), has a large effect on tracking performance during non-stationary periods (T2) when linear echo path time variations are present. A value for convergence parameter $\alpha$ between $\mu$ and $2\mu$ is recommended for reasonable tracking performance and algorithm stability.

For the Simplified Gradient NLMS Newton algorithm in Figure 6.4 the tracking performance behaves differently with respect to parameter $\alpha$ due to the effective normalisation of the stepsize $\mu$ in Table 6-1. A larger value, closer to unity, is most suitable to increase the convergence time to the asymptotic ERLE level during the initial convergence period. During non-stationary periods (T1) the influence of $\alpha$ on tracking performance is small.

From numerous simulations at different ENR levels for all echo paths of chapter 4 the following design parameters are chosen for both algorithms, as a trade off between convergence speed and ERLE performance during both normal convergence periods (T1) and non-stationary periods (T2).

| **Parameters** | **Simplified Gradient LMS Newton** | **Simplified Gradient NLMS Newton** |
|---|---|---|
| Stepsize $\mu$ | 0.005 | 0.0125 |
| Forgetting Factor $\lambda$ | 0.9995 | 0.999 |
| Convergence parameter $\alpha$ | 0.0075 | 1 |
| Initialisation Parameter $\delta$ | 100 | 100 |

**Table 6-2 : Adaptive IIR algorithm design parameters for echo path tracking tests**

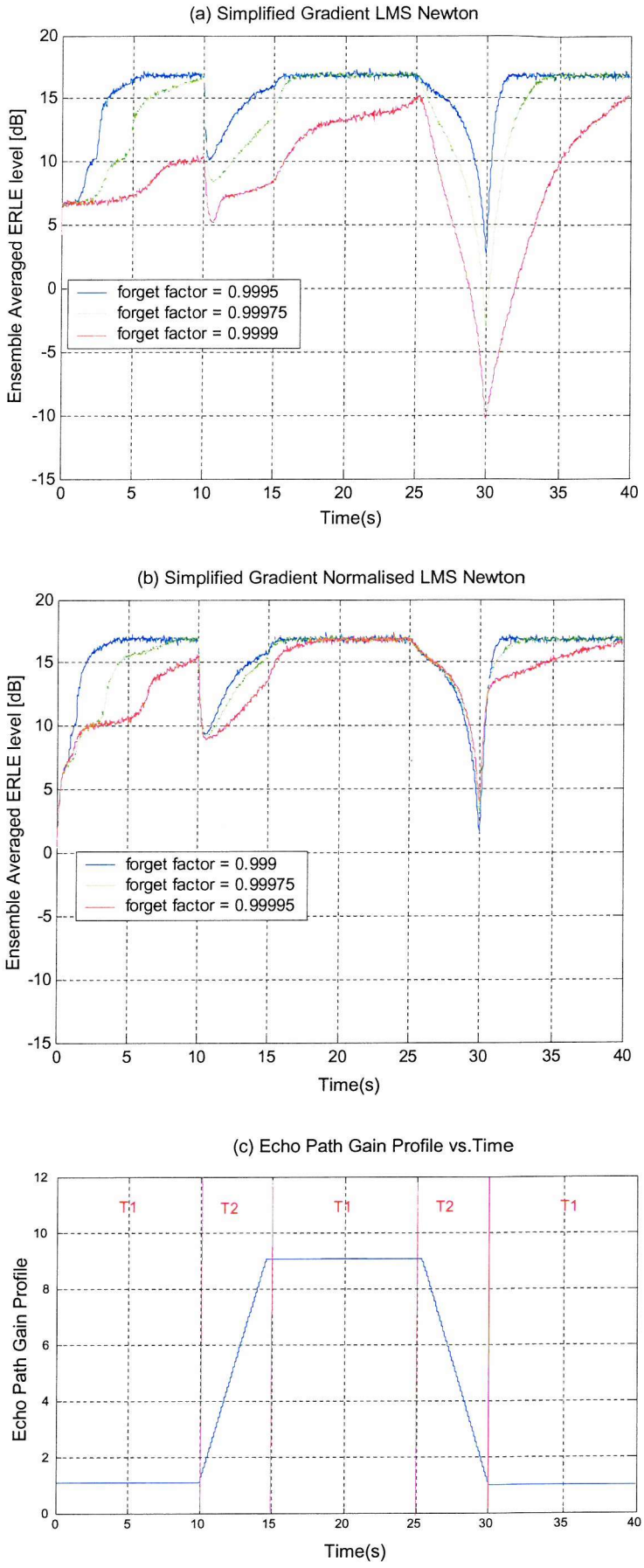


**Figure 6.3: Tracking performance for different forgetting factors $\lambda$**

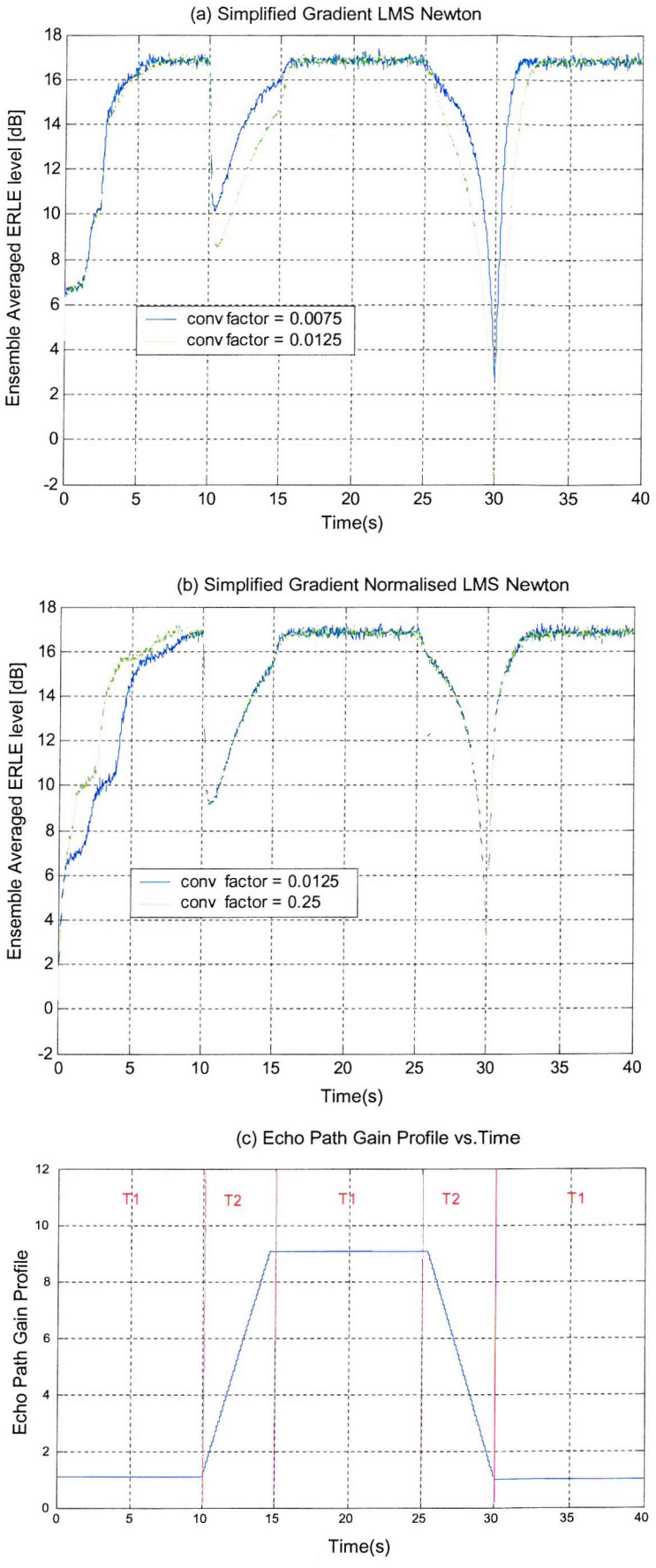


**Figure 6.4 : Tracking performance for different convergence factors $\alpha$**

#### 6.2.2.3. Tracking Performance Results

In this section the comparative tracking performance of adaptive FIR and IIR algorithms for non-linear echo path time variations is established. As in the last section the Simplified Gradient LMS Newton and NLMS Newton algorithms of Table 6-1 are used to establish adaptive IIR algorithm performance. The FIR LMS Newton is used to establish adaptive FIR algorithm performance during these tests. For the tracking experiments of this section the following echo paths are used,

1) The artificial ear sealed handset echo path response,
2) The loudspeaker adhesive tape sealed handset echo path response
3) The face up handset response with no transducer seals.

From Figure 6.1 it can be seen that by applying linear gain variations at the output of these three echo paths the gradual change in the handset echo path response during normal use can be simulated. From Figure 6.1 it can be clearly seen that both increasing and decreasing gain changes are needed to simulate echo path behaviour in normal handset use. The gain changes used in this section are representative of the maximum increasing or decrease in gain envisaged for that echo path response in normal handset use as illustrated in Figure 6.1. For example, the artificial ear sealed response will have a linear output gain profile which will increase the terminal coupling loss from the 46dB level calculated in chapter 2, to match the terminal coupling loss levels of both the face up no seals handset response and the adhesive tape sealed response. To establish the ability of both adaptive FIR and IIR algorithms to track linear time variations in the presence of microphone disturbance noise, an additive band limited noise signal is used to create different ENR levels. The ENR levels of 5 and 10dB are used to show how tracking performance varies with low and medium noise environments.

Consider firstly the tracking results for the artificial ear sealed handset echo path response. The gain profile as used in Figure 6.3 is re-used here to give an echo path loss gain-time variation of around 9dB possible over 5 seconds (~1.8dB/second). The tracking performance of both adaptive FIR and IIR algorithms are shown in Figure 6.5. The results are summarised in Table 6-3. It can be seen that both Simplified Gradient LMS Newton based algorithms have similar tracking performance to an equivalent adaptive FIR algorithm, albeit slightly inferior during the first period up to 10s. The $ERLE_{lag}$ levels are similar for all algorithms. The asymptotic ERLE levels for both adaptive IIR algorithms are slightly larger than the adaptive FIR LMS Newton algorithm. It is also worth mentioning that the Simplified Gradient IIR LMS Newton algorithm shows faster tracking performance over the Simplified Gradient IIR NLMS Newton algorithm during the periods when linear gain increments at the echo path output exist, but inferior convergence in the first convergence period up to 10s.

The effect of output noise component $v(n)$ at the echo path output has negligible effect on tracking performance of all algorithms at ENR levels of 5 and 10dB. Only the asymptotic ERLE level is reduced as a result of this additive component. This remains the case for all echo path responses tested so from this point forward only results for an ENR of 10dB are presented to simplify presentation of results in the remainder of this section.

| Algorithm | Asymptotic ERLE(dB) | | Lag ERLE (dB) | | | |
|---|---|---|---|---|---|---|
| | | | Positive Gain Inc | | Negative Gain Inc | |
| | ENR 10dB | ENR 5dB | ENR 10dB | ENR 5dB | ENR 10dB | ENR 5dB |
| FIR LMS Newton | 16.3 | 16 | 10.2 | 10.2 | 2.6 | 2.6 |
| Simplified Gradient LMS Newton | 16.7 | 16.3 | 9.8 | 9.8 | 1.9 | 1.9 |
| Simplified Gradient NLMS Newton | 16.7 | 16.3 | 9.5 | 9.5 | 1.7 | 1.7 |

**Table 6-3 : Summary of ERLE results for artificial ear sealed echo path tracking experiments**

Consider next the tracking results for the loudspeaker adhesive tape sealed handset echo path response. The tracking performance of both adaptive FIR and IIR algorithms are shown in Figure 6.6. These results are summarised in Table 6-4. It can be clearly seen that both Simplified Gradient LMS Newton based algorithms have superior asymptotic ERLE levels to the adaptive FIR LMS Newton algorithm during non-time varying/non-stationary periods. The $ERLE_{lag}$ level for all algorithms is similar.

Finally consider the face up no seals handset echo path response. The tracking performance of both adaptive FIR and IIR algorithms are shown in Figure 6.6. The results are summarised in Table 6-5.
Both Simplified Gradient LMS Newton based algorithms have superior asymptotic ERLE levels to the adaptive FIR LMS Newton algorithm during non-time varying/non-stationary periods. The $ERLE_{lag}$ levels and tracking performance of both adaptive IIR algorithms differ largely for this experiment. The Simplified Gradient NLMS Newton algorithm has clearly superior tracking performance, whereas the Simplified Gradient LMS Newton algorithm has superior asymptotic ERLE level. The tracking performance different between adaptive IIR algorithms is most noticeable when decreasing gain increments are applied. Again the Simplified Gradient NLMS Newton algorithm achieves the best performance overall.

Using the adaptive FIR LMS Newton and Simplified Gradient Simplified Gradient LMS and NLMS Newton algorithms the tracking performance of adaptive IIR and FIR algorithms has been compared for linear echo path time variations. From the results presented it has been show that for linear time variations in the handset echo path response the tracking performance of both adaptive FIR and output error LMS Newton based algorithms is similar, but depends largely on the echo path response being modelled.

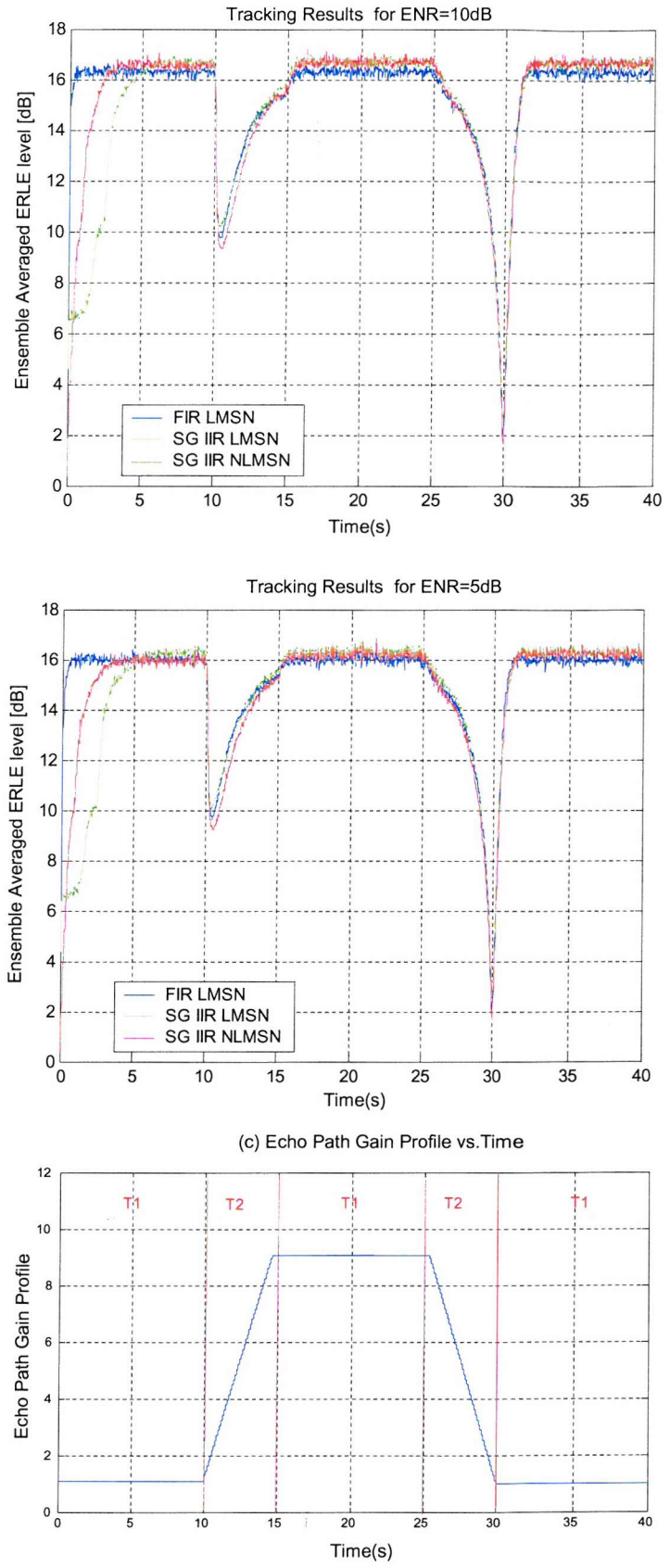


**Figure 6.5 : Tracking performance for artificial ear sealed handset echo response**

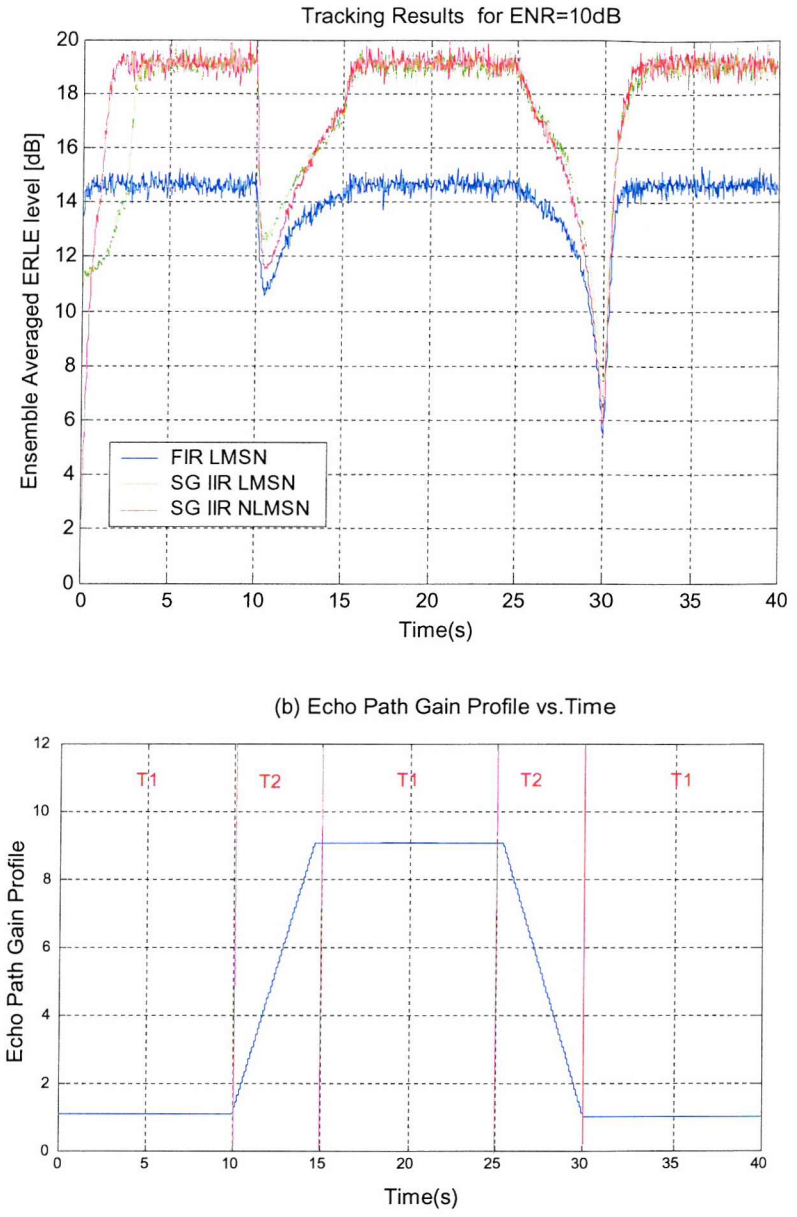


**Figure 6.6 : Tracking performance for loudspeaker adhesive tape sealed handset echo response**

| Algorithm | Asymptotic ERLE(dB) | Lag ERLE (dB) | |
|---|---|---|---|
| | | Positive Gain Inc | Negative Gain Inc |
| FIR LMS Newton | 14.6 | 10.7 | 5.5 |
| Simplified Gradient LMS Newton | 19.2 | 12.7 | 6.7 |
| Simplified Gradient NLMS Newton | 19.2 | 11.6 | 5.8 |

**Table 6-4 : Summary of ERLE results for loudspeaker adhesive tape sealed echo path tracking experiments**

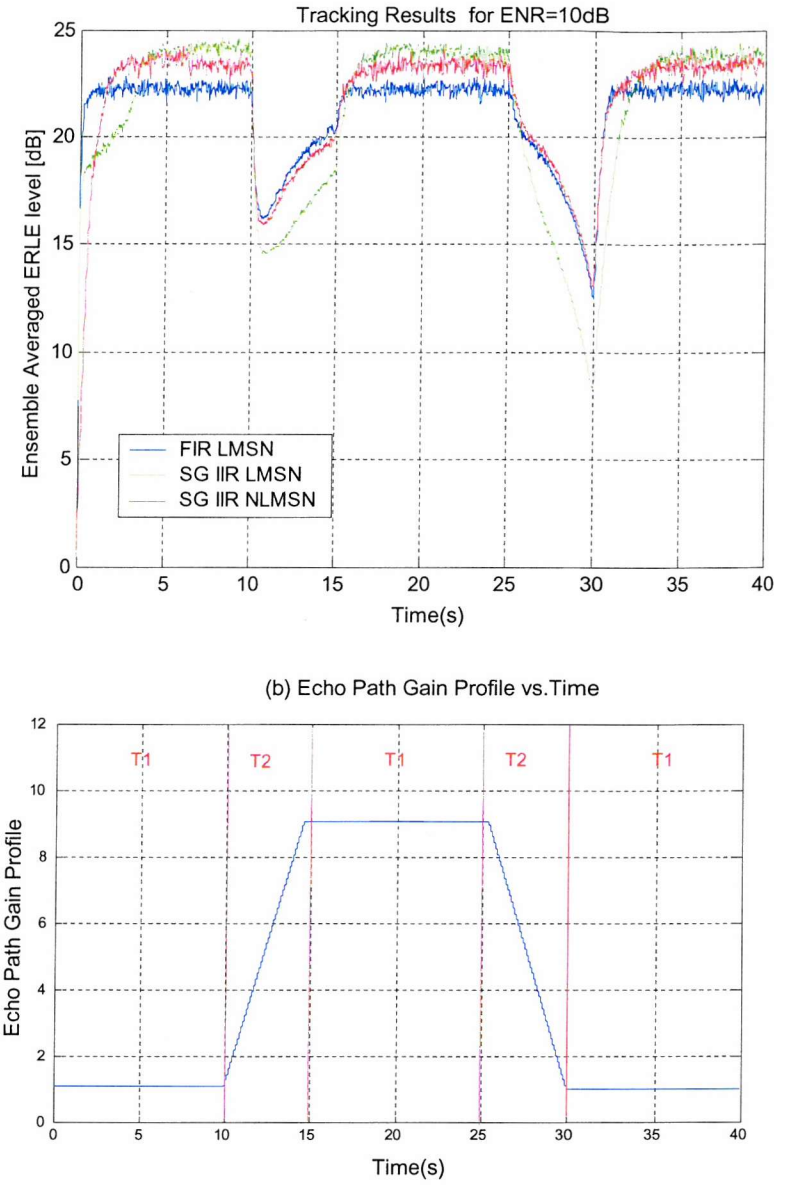


**Figure 6.7 : Tracking performance of adaptive FIR and IIR algorithms.**

| Algorithm | Asymptotic ERLE(dB) | Max Lag ERLE (dB) | |
|---|---|---|---|
| | | Positive Gain Inc | Negative Gain Inc |
| FIR LMS Newton | 22.25 | 16.3 | 12.7 |
| Simplified Gradient LMS Newton | 24.2 | 14.7 | 13 |
| Simplified Gradient NLMS Newton | 23.5 | 16 | 8.3 |

**Table 6-5 : Summary of ERLE results for face up no seals echo path tracking experiments**

### 6.2.3. Tracking Non-linear Transitional Time Variations in the Acoustic Echo Path response

#### 6.2.3.1. Experiment Design

The system identification configuration illustrated in Figure 6.8 below is used to perform the system identification experiments with a time varying echo path response.

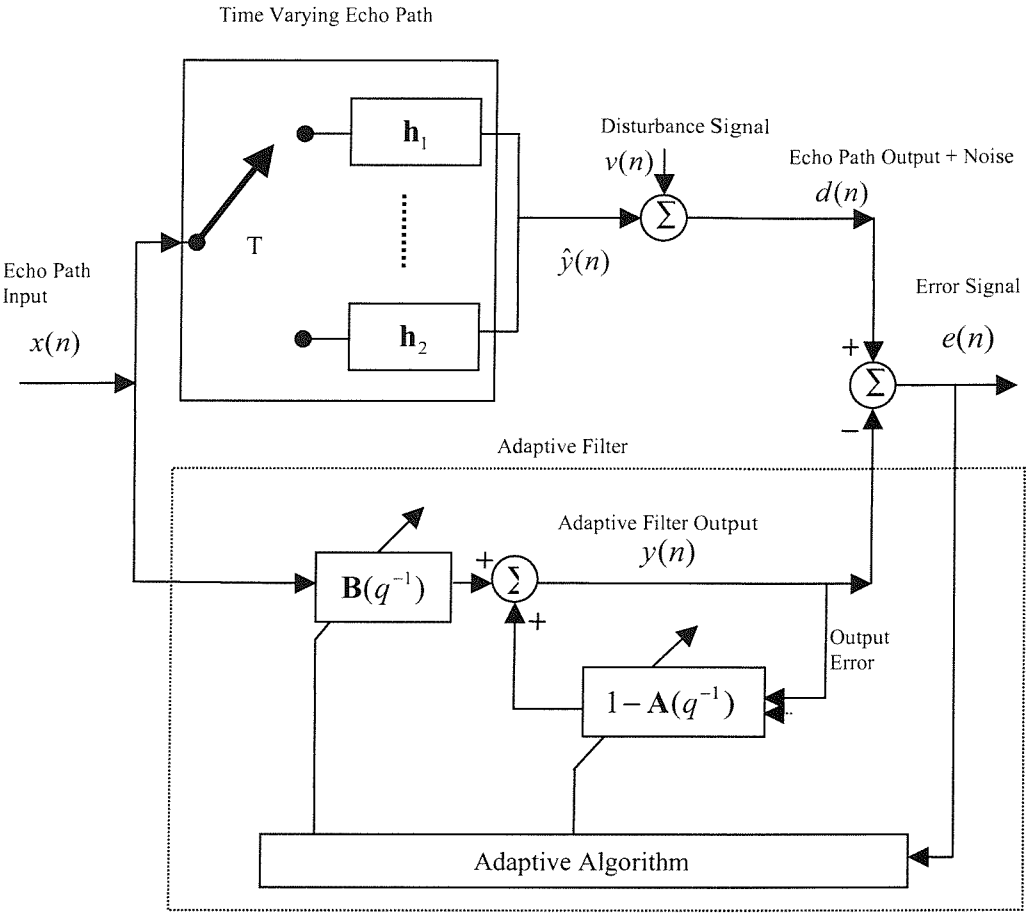


**Figure 6.8 : System identification experiment configuration for non-linear echo path time variations.**

From Figure 6.8 we can see that time variation is incorporated into the modelling experiments of this section by using a time switch, where every T seconds a different echo path response may be switched to contribute the echo output $y(n)$. The rate of change of echo path change is made equal to 10s to allow convergence behaviour of adaptive algorithms to be analysed. The echo path responses $\mathbf{h}_1$ and $\mathbf{h}_2$ are vectors of echo path response samples as defined in (5.1), and could be any of the 6 measured echo path responses of Chapter 4. As we shall discuss shortly, the echo response vectors $\mathbf{h}_1$ and $\mathbf{h}_2$ are arranged to simulate the most likely ***sequence*** of fast or extreme echo path changes during normal handset use.

Stationary input signals are again used to allow the effects of time variations in the echo path response to be analysed. As in the previous section of tracking experiments a band-limited pink noise signal is used for both input signal $x(n)$ and disturbance signal with both $x(n)$ and $v(n)$ being uncorrelated. Again the signal $v(n)$ is scaled to allow the tracking performance to be assessed in the presence of different echo path output noise levels.

In the last section the effect of design parameters on the tracking performance of the adaptive IIR Simplified Gradient LMS and NLMS Newton algorithms were discussed. The same tracking performance variations that existed for linear echo path time variations with respect to the forgetting factor $\lambda$ and convergence factor $\alpha$ also exist for non-linear echo path time variations simulated in this section. The design parameters of Table 6-2 are re-used in this section.

#### 6.2.3.2. Tracking Results

In this section the comparative tracking performance of adaptive FIR and IIR algorithms for non-linear/step echo path time variations is established. As in the previous section the Simplified Gradient LMS Newton and NLMS Newton algorithms of Table 6-1 are used to establish adaptive IIR algorithm performance. The FIR LMS Newton is used to establish adaptive FIR algorithm performance during these tests.

In section 6.2.2 it was illustrated how linear echo path time variations can simulate the most likely sequence of gradual echo path variations during a normal call using 3 handset orientations. In this section step transitions in time are used rather than linear gain increments over a period of time, to simulate the most likely sequence of fast or extreme echo path variations that may occur during a call. To accomplish this, the following echo paths are used as illustrated in,

1. The artificial ear sealed handset echo path response
2. The loudspeaker adhesive tape sealed handset echo path response
3. The face up handset response with no transducer seals.
4. The face down handset response.

From Figure 6.9 it can be seen how the above 4 handset orientations can approximate the most likely ***sequence*** of fast or extreme echo path variations during a normal call.

Consider firstly the tracking results for the artificial ear sealed to loudspeaker tape sealed echo path response transitions as shown in Figure 6.10. From Figure 6.10 what is immediately clear is that when transitional echo path variations occur in normal use the ERLE profile produced will appear like two(or more) normal convergence periods. On the step transition, the ERLE level falls to zero or less (if echo path $\mathbf{h}_1$ has lower echo loss than $\mathbf{h}_2$ ). The tracking performance reduces to the algorithm stability on the step boundary and the time taken to subsequently converge to the new echo path response from the previously converged condition. The $ERLE_{lag}$ levels for this section are not used since the time variation

is instant. Only asymptotic ERLE levels and convergence times are important for very fast or transitional type echo path non-stationary periods in normal handset use.

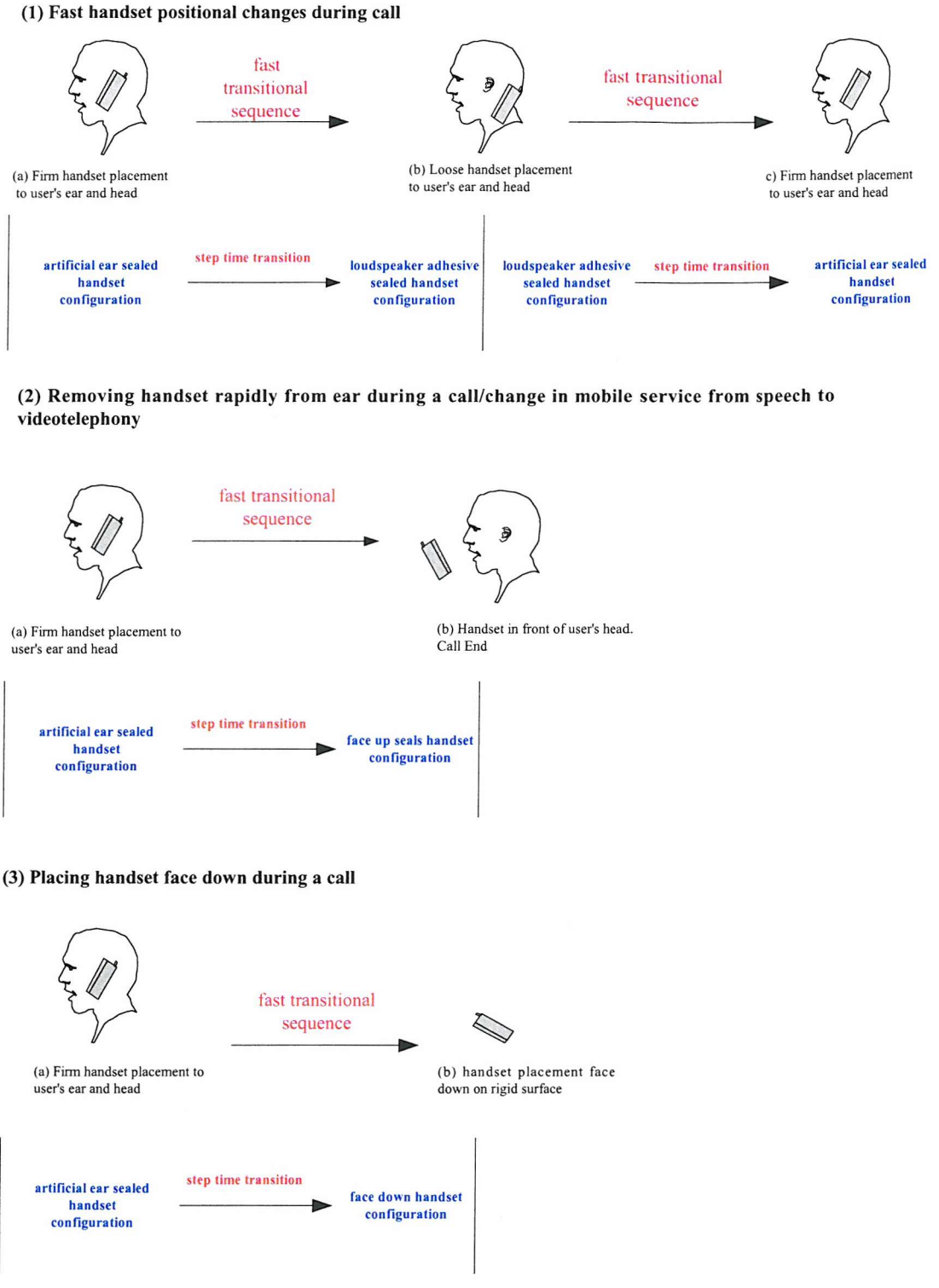


**Figure 6.9 : Echo path fast transitional sequences during normal call**

From Figure 6.10 as expected (from the results in Chapter 5), the FIR LMSN algorithm has the fastest convergence to the asymptotic ERLE level. However for the artificial ear sealed to loudspeaker tape sealed echo path response transition experiment the convergence time to the required ERLE of each

echo path is similar for the adaptive FIR and IIR LMS Newton based algorithms tested. It is clear both Simplified Gradient LMS Newton algorithms have superior asymptotic ERLE level performance for this experiment. What is also clear is that like section 6.2.2 the effect of output noise component $v(n)$ at the echo path output has negligible effect on tracking performance of all algorithms at ENR levels of 5 and 10dB. Only the asymptotic ERLE level is reduced as a result of this additive component. Only results for an ENR of 10dB are presented to simplify presentation of results in the remainder of this section. As we have seen so far in the thesis for all experiments convergence time to the asymptotic ERLE level for adaptive IIR algorithms is slower than equivalent adaptive FIR algorithms. Overall the Simplified Gradient NLMS Newton algorithm has the fastest convergence of both the adaptive IIR algorithms tested.

Consider next the tracking results for the loudspeaker tape to artificial ear sealed echo path response transitions, and the artificial ear sealed to face up no seals echo path response transitions of Figure 6.11 and Figure 6.12. From both these figures it is clear that again the Simplified Gradient LMS Newton base algorithms have superior asymptotic ERLE level performance over and equivalent adaptive FIR algorithm and similar convergence times to the required ERLE level of each echo path. Again the convergence time to the asymptotic ERLE level is fastest for the adaptive LMS Newton algorithm and overall the Simplified Gradient NLMS Newton algorithm has the fastest convergence of both the adaptive IIR algorithms tested. It is worth noting that for all algorithms in Figure 6.11 as the step transition occurs between echo path response such that $\mathbf{h}_1$ has lower echo loss than $\mathbf{h}_2$ then briefly after the step transition the ERLE level is negative until the adaptive algorithm begins to track and model the new echo path response switched in.

Finally consider the tracking results for the artificial ear sealed to face down echo path response transitions of Figure 6.13. The face down echo path response as discussed in previous Chapters represents the worst-case acoustic conditions, and is also the most problematic response to model for both adaptive FIR and IIR algorithms. From Figure 6.13 a fast transition to this echo path is the worst case possible transitional sequence likely to occur in normal handset use (and the maximum instantaneous shift in echo loss level most likely). The convergence time to the asymptotic ERLE level is fastest for the adaptive LMS Newton algorithm, and overall the Simplified Gradient NLMS Newton algorithm has the fastest convergence of both the adaptive IIR algorithms tested. It is clear only the Simplified Gradient LMS Newton based algorithms have sufficient asymptotic ERLE levels to meet the required ERLE levels for the face down echo path (as we have seen already in chapter 5).

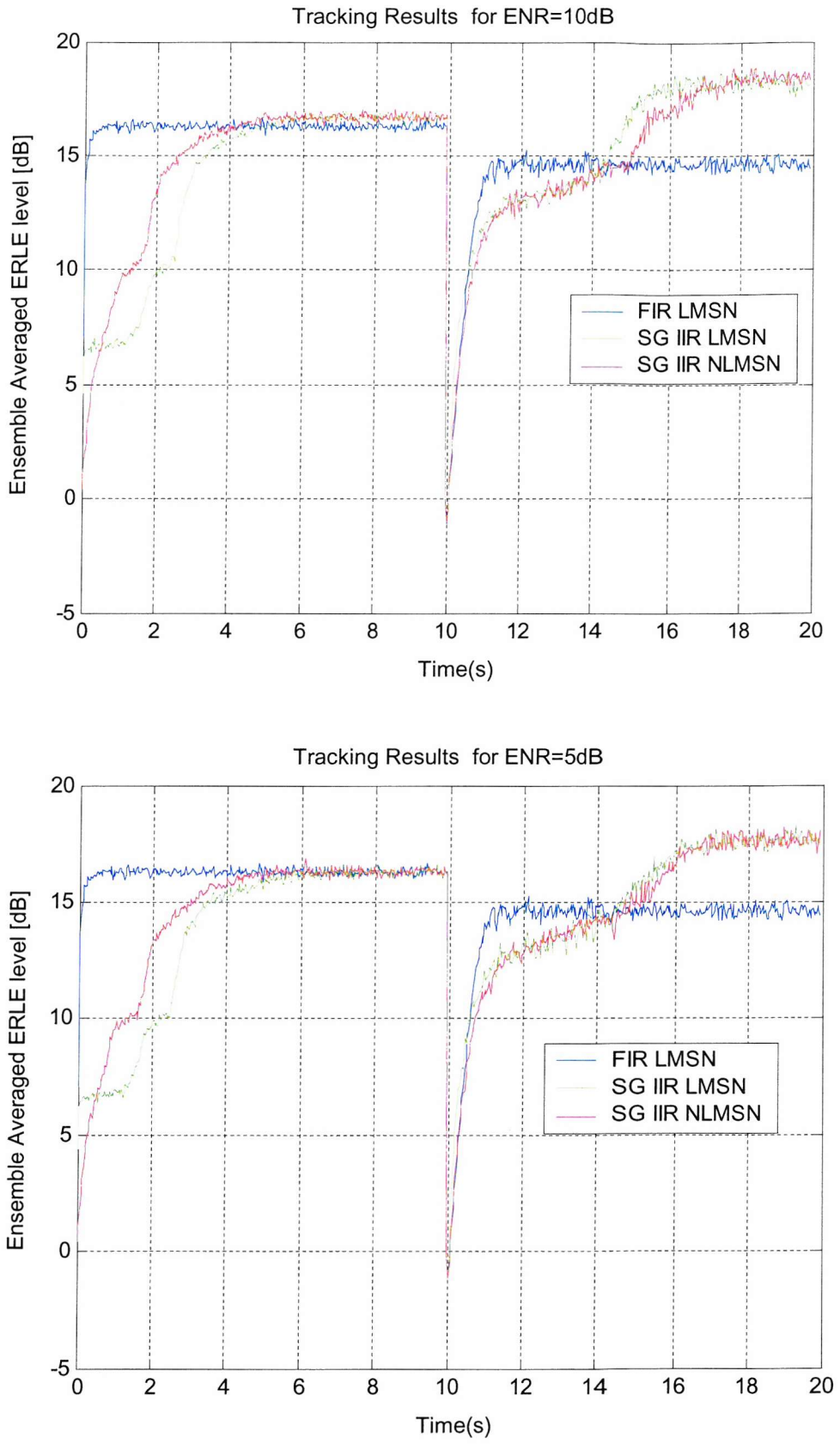


**Figure 6.10 : Tracking performance for the artificial ear sealed response to the loudspeaker adhesive tape sealed response transitions.**

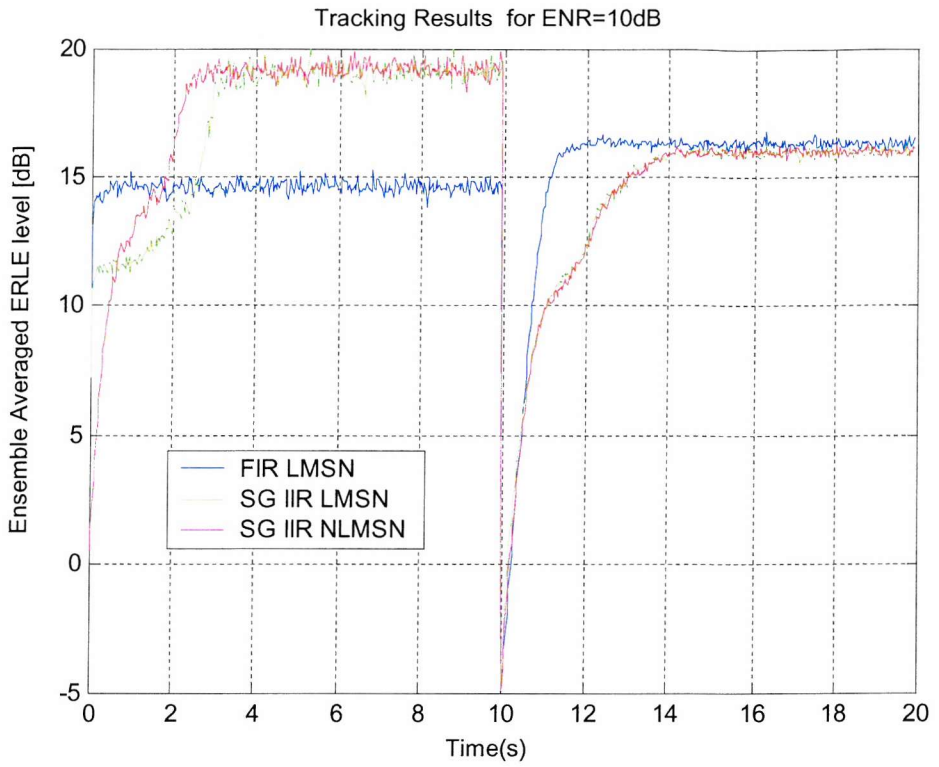


**Figure 6.11: Tracking performance for the loudspeaker adhesive tape sealed response to the artificial ear sealed response to the transitions**

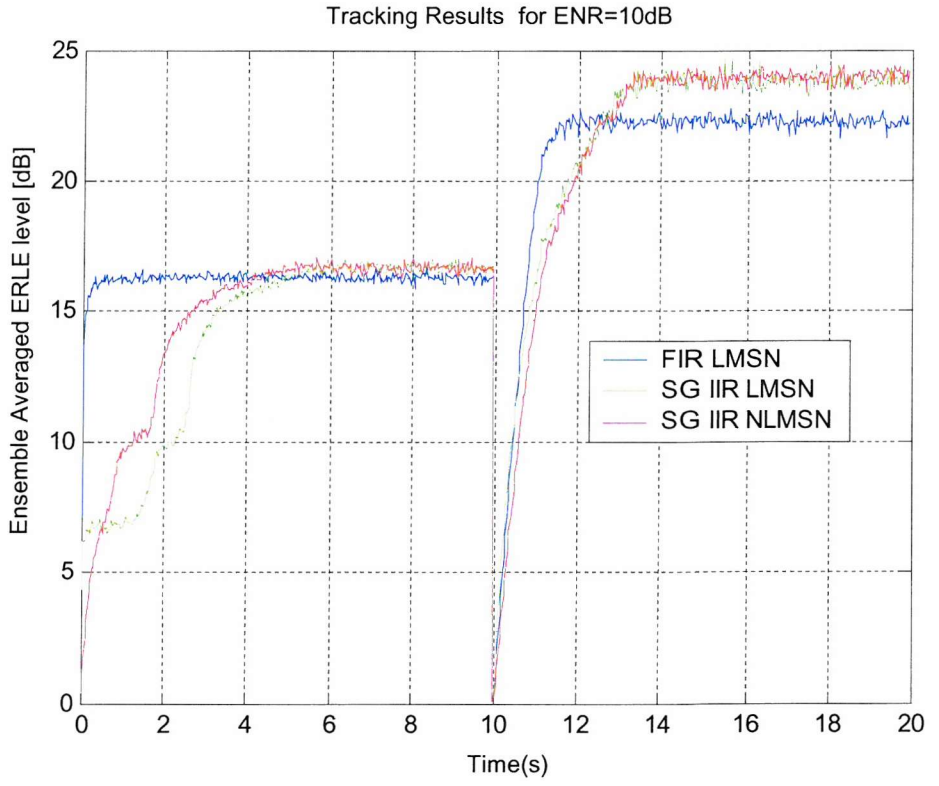


**Figure 6.12: Tracking performance for the artificial ear sealed response to the face up no seals response transitions.**

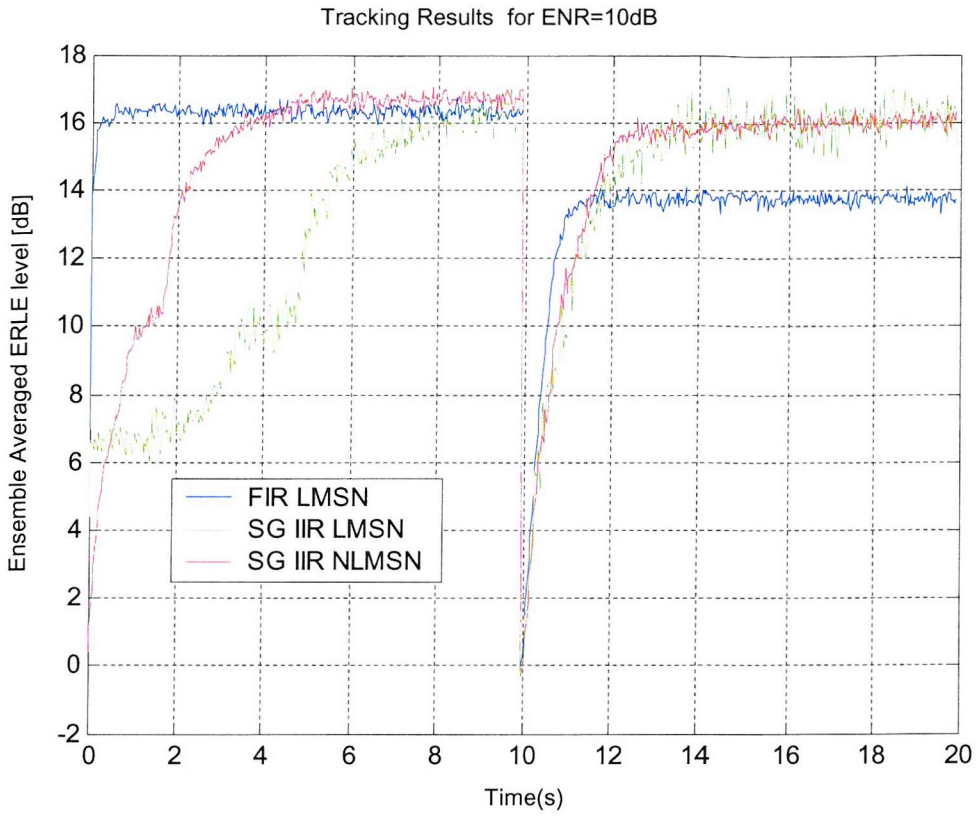


**Figure 6.13 : Tracking performance for the artificial ear sealed response to the face down response transitions.**

### 6.2.3.3. Summary of Tracking Results

The tracking performance for adaptive FIR and output error IIR LMS Newton algorithms has been analysed for both linear time variations and step variations in the echo path response to be modelled in the handset echo cancellation application. The effects of echo path output noise on tracking performance have also been examined.

For linear time variations the tracking performance during transitional periods when the time variations are applied depends on the echo path being modelled. Overall the Simplified Gradient NLMS Newton algorithm has superior tracking performance over the un-normalised version of the algorithm. The tracking performance of this algorithm is similar to the FIR LMS Newton algorithm.

From the results of the step variation experiments the adaptive FIR LMS Newton has faster convergence to its steady state ERLE level after each echo path transition. Whereas the adaptive IIR LMS Newton algorithms normally have higher steady state ERLE level once they have reach their steady state levels. Echo path output noise has negligible impact on tracking step variations of all algorithms. To meet the required ERLE of each echo path after the step transitions for a model order of 42 coefficients requires an adaptive IIR algorithm to be used.

## 6.3. System Identification of an Echo Path response with Time Varying Input Signals

In previous sections of this Chapter we have looked at tracking time variations in the echo path response to be modelled. In the handset acoustic echo cancellation application in addition to a time varying echo path, the input signals most commonplace are speech signals, which are also time varying or non-stationary in nature. In this section of the Chapter the modelling performance of adaptive IIR algorithms with input speech signals over a range of input SNR and output ENR levels is established. The results presented show that the performance benefits we have seen in previous Chapters for stationary input signals are still valid for speech signal inputs.

### 6.3.1. Experimental Configuration and ERLE measures for time varying speech signals

The system identification configuration of Figure 6.14 below is used.

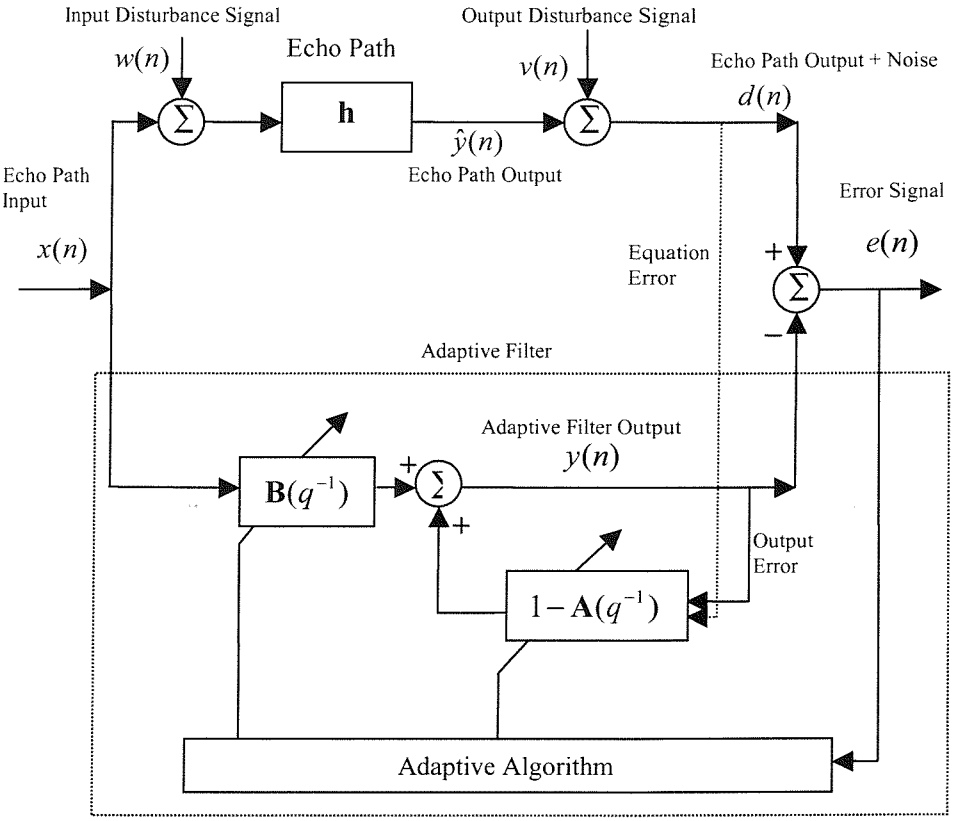


**Figure 6.14 : System Identification configuration for speech input signals**

The input signal $x(n)$ consists of both a male and female speech recordings up to approximately 40 seconds in duration. These recordings are in English and contain approximately 35 utterances that are a

mixture of natural conversational speech and energetic speech utterances. Different pause durations are present between utterances in part of these recordings as we shall see later, to allow the robustness of adaptive algorithms to be tested during silent speech periods when input and output noise sources $w(n)$ and $v(n)$ are present. As in previous sections of this chapter a band-limited pink noise signal is used for additive output noise signal $v(n)$ to represent the typical coloured spectrum of a noisy environment. Similarly for the additive input noise source $w(n)$ a band-limited pink noise signal is also used. Both $w(n)$ and $v(n)$ are uncorrelated. The power of output noise signal $v(n)$ is scaled to allow adaptive algorithm performance to be assessed over a range of output Echo to Noise Ratio (ENR) levels. The power of input noise signal $w(n)$ is scaled to allow adaptive algorithm performance to be assessed over a range of input Signal to Noise Ratio (ENR) levels.

Before discussing these modelling results it is first necessary to construct some definitions of ERLE performance for speech signals. So far the input signal $x(n)$ has been stationary, where the input power level is relatively constant over time, allowing the definitions of (5.3) and (6.1) to be used to measure ERLE performance after an initial convergence period. With speech input signals, although the input signal is relatively stationary over the 32ms frame calculation used in (6.1), the ERLE measure of (6.1) will fluctuate considerably over time due to the power fluctuations of input signal $x(n)$. This makes performance comparisons between different adaptive algorithms difficult using (6.1) alone. In addition to (6.1) some statistical measures of ERLE performance are needed to summarise the ERLE variation over the input test sequences to make algorithm comparison easier. The following parameters in Table 6-6 will be used [6.6].

| Measure | Definition |
|---|---|
| $ERLE_{en}$ | Ensemble averaged ERLE level as measured in (6.1) in dB. Calculated in 32ms frames |
| $ERLE_{mean}$ | Average value of $ERLE_{en}$ in dB over entire input signal duration |
| $ERLE_{std}$ | Standard deviation of $ERLE_{en}$ in dB about $ERLE_{mean}$ |
| $ERLE_{\max}$ | Maximum value of $ERLE_{en}$ in dB obtained across entire input signal duration |
| $TIC_{mean}$ | The time in ms for $ERLE_{en}$ to attain $ERLE_{mean}$ |
| $TIC_{req}$ | The time in ms for $ERLE_{en}$ to attain the required ERLE for echo path modelled. |

**Table 6-6 : Evaluation Criteria for input speech signals**

### 6.3.2. Modelling results

In this section the comparative performance of adaptive FIR and IIR algorithms for speech input signals are discussed. As in the previous sections the Simplified Gradient LMS Newton and NLMS Newton algorithms of Table 6-1 are used to establish adaptive IIR algorithm performance. The FIR LMS Newton is used to establish adaptive FIR algorithm performance.

This section will consist of three main parts. Firstly the ERLE performance in idealistic input SNR and output ENR conditions will be established for both adaptive FIR and adaptive IIR algorithms. Next the ERLE performance of adaptive IIR algorithms for different input SNR levels (noisy speech) is discussed. Finally the ERLE performance at different output ENR levels is presented.

#### 6.3.2.1. Modelling results for high input SNR and output ENR conditions

Consider firstly the ERLE performance at an input SNR and output ENR level of 40dB. These conditions are representative of the echo loss test conditions of [6.1]. Only the single talk case is considered where there is no microphone speech signal present only low-level background noise. In the actual echo loss test of [6.1] a 20 s male artificial voice recording is used as an input signal. The first 10s is used to allow any echo cancellation devices to converge then during the second 10s the terminal coupling loss is evaluated as discussed in Chapter 2. This test is repeated for a female artificial voice recording and the terminal coupling loss re-calculated. The overall terminal coupling loss value for the handset is the average of the terminal coupling levels obtained from the male and female speech experiments. In this section the ERLE performance of adaptive IIR algorithms for the anechoic handset echo path responses of Chapter 4 will be established in a similar way to the echo loss tests of [6.1]. A 20 second actual male speech recording for input signal is firstly used and the ERLE evaluation parameters of Table 6.4 calculated. A 20 second actual female speech recording for input signal is then used and the ERLE evaluation parameters of Table 6.4 re-calculated. The overall ERLE performance of an adaptive algorithm is simply the average of the results from these two experiments.

Consider firstly the modelling performance of adaptive FIR and IIR algorithms for the face up no seals handset configuration as shown in Figure 6.15. A summary of the ERLE performance is given in Table 6-7. It is clear even from Figure 6.15 the Simplified Gradient NLMS Newton algorithm has superior ERLE performance for this echo path response. From Figure 6.15 it can be seen without the additional ERLE parameter summary in Table 6-7 it is difficult to compare the relative performance of adaptive IIR and FIR algorithms, particularly between FIR LMS Newton and Simplified Gradient LMS Newton algorithms. From the summary in Table 6-7 it can be seen that for input speech signals the Simplified Gradient NLMS Newton adaptive IIR algorithm can achieve approximately 4dB more $ERLE_{mean}$ performance and less ERLE variation about this mean level, over an equivalent adaptive FIR algorithm. The convergence time to the required ERLE level of this echo path, $TIC_{req}$, is also smaller.

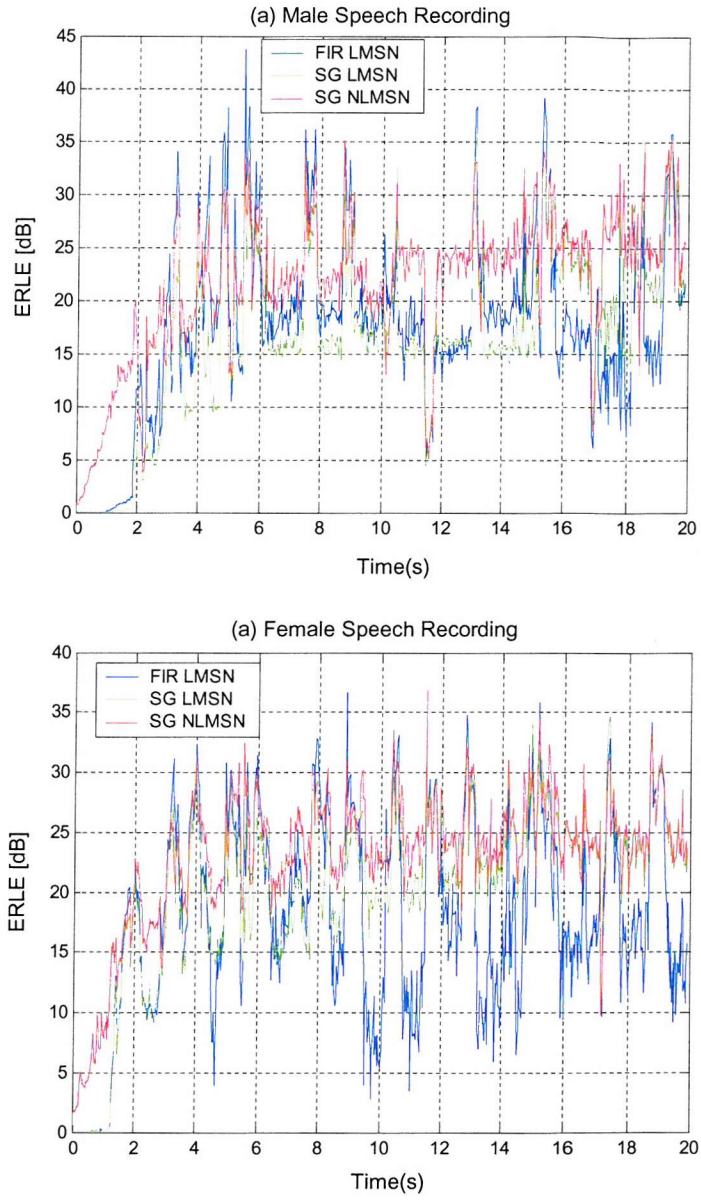


**Figure 6.15 : Modelling performance of adaptive FIR and IIR algorithms for the face up no seals handset configuration.**

This ERLE performance superiority of the Simplified Gradient NLMS Newton algorithm over the other LMS Newton based algorithms tested also occurs for most of the remainder of the echo path responses modelled as summarised in Table 6-8 to Table 6-12.

| Algorithm | $ERLE_{mean}$ | $ERLE_{\max}$ | $ERLE_{std}$ | $TIC_{mean}$ | $TIC_{req}$ |
|---|---|---|---|---|---|
| FIR LMS Newton | 18.16dB | 34.16dB | 8.37dB | 1.9ms | 1.79ms |
| IIR LMS Newton | 18.22dB | 35.03dB | 7.7dB | 2.99ms | 2.72ms |
| IIR NLMS Newton | 22.04dB | 35.88dB | 6.1dB | 2.61ms | 1.3ms |

**Table 6-7 : Summary of ERLE results for the face up no seals echo path experiments**

| Algorithm | $ERLE_{mean}$ | $ERLE_{\max}$ | $ERLE_{std}$ | $TIC_{mean}$ | $TIC_{req}$ |
|---|---|---|---|---|---|
| FIR LMS Newton | 11.63dB | 26.53dB | 5.75dB | 1.3ms | 1.76ms |
| IIR LMS Newton | 10.92dB | 24.94dB | 5.25dB | 2.83ms | 4.26ms |
| IIR NLMS Newton | 15.07dB | 26.48dB | 4.4dB | 1.68ms | 2.67ms |

**Table 6-8 : Summary of ERLE results for the face down echo path experiments**

| Algorithm | $ERLE_{mean}$ | $ERLE_{\max}$ | $ERLE_{std}$ | $TIC_{mean}$ | $TIC_{req}$ |
|---|---|---|---|---|---|
| FIR LMS Newton | 11.96dB | 33.18dB | 7.53dB | 1.73ms | 1.68ms |
| IIR LMS Newton | 11.65dB | 31.13dB | 6.56dB | 2.67ms | 1.71ms |
| IIR NLMS Newton | 16.2dB | 33.82dB | 5.51dB | 2.56ms | 0.244ms |

**Table 6-9 : Summary of ERLE results for the loudspeaker tape sealed echo path experiments**

| Algorithm | $ERLE_{mean}$ | $ERLE_{\max}$ | $ERLE_{std}$ | $TIC_{mean}$ | $TIC_{req}$ |
|---|---|---|---|---|---|
| FIR LMS Newton | 10.11dB | 28.22dB | 6.82dB | 1.7ms | 1.68ms |
| IIR LMS Newton | 10.84dB | 26.51dB | 5.81dB | 2.7ms | 1.74ms |
| IIR NLMS Newton | 14.89dB | 26.98dB | 9.75dB | 1.7ms | 0.53ms |

**Table 6-10 : Summary of ERLE results for the loudspeaker and microphone tape sealed echo path experiments**

| Algorithm | $ERLE_{mean}$ | $ERLE_{\max}$ | $ERLE_{std}$ | $TIC_{mean}$ | $TIC_{req}$ |
|---|---|---|---|---|---|
| FIR LMS Newton | 11.27dB | 22.75dB | 4.98dB | 1.73ms | 0ms |
| IIR LMS Newton | 5.15dB | 18.22dB | 4.21dB | 1.82ms | 0ms |
| IIR NLMS Newton | 10.33dB | 20.68dB | 4.32dB | 3.77ms | 0ms |

**Table 6-11 : Summary of ERLE results for the artificial ear sealed echo path experiments**

| Algorithm | $ERLE_{mean}$ | $ERLE_{\max}$ | $ERLE_{std}$ | $TIC_{mean}$ | $TIC_{req}$ |
|---|---|---|---|---|---|
| FIR LMS Newton | 11dB | 32.19dB | 7.32dB | 1.7ms | 1.71ms |
| IIR LMS Newton | 11.56dB | 30.05dB | 7.15dB | 1.79ms | 1.78ms |
| IIR NLMS Newton | 16.52dB | 32.36dB | 5.97dB | 1.3ms | 0.88ms |

**Table 6-12 : Summary of ERLE results for the microphone tape sealed echo path experiments**

From these tables a $ERLE_{mean}$ performance improvement of up to approximately 5.5dB over the FIR LMS Newton algorithm and 5dB over the Simplified Gradient LMS Newton algorithm is achieved. This higher $ERLE_{mean}$, lower can be attributed to the stepsize normalisation in the NLMS Newton algorithm update in Table 6-1 [6.7]. Unlike the NLMS Newton algorithm normalised stepsize which will

adapt with time depending on the short term energy variations of the input speech signal, LMS Newton based algorithms have a fixed convergence factor resulting poorer convergence and higher sensitivity to short term input signal variations.

In conclusion from the results presented the most appropriate adaptive IIR algorithm has been shown to be the Simplified Gradient NLMS Newton algorithm for the handset acoustic echo cancellation application. The Simplified Gradient LMS Newton algorithm will be considered no further in this thesis. The adaptive FIR NLMS Newton algorithm will be used from this point forward in order to compare performance to an equivalent adaptive FIR algorithm in line with the main aims of this thesis.

#### 6.3.2.2. The effect of input SNR on modelling performance

In the handset echo cancellation application we have already identified that speech signals are most likely to be input to the Acoustic Echo Canceller. However as shown in Figure 6.16, depending on the local environment of the other handset in the call the input speech signal may be degraded with some form of disturbance noise. For example the other caller may be using a hands free unit in a car where the environment noise level $w(n)$ would be high in comparison to the microphone signal $x(n)$. This input disturbance signal $w(n)$ results in a Signal to Noise Ratio (SNR) at the input of the echo canceller.

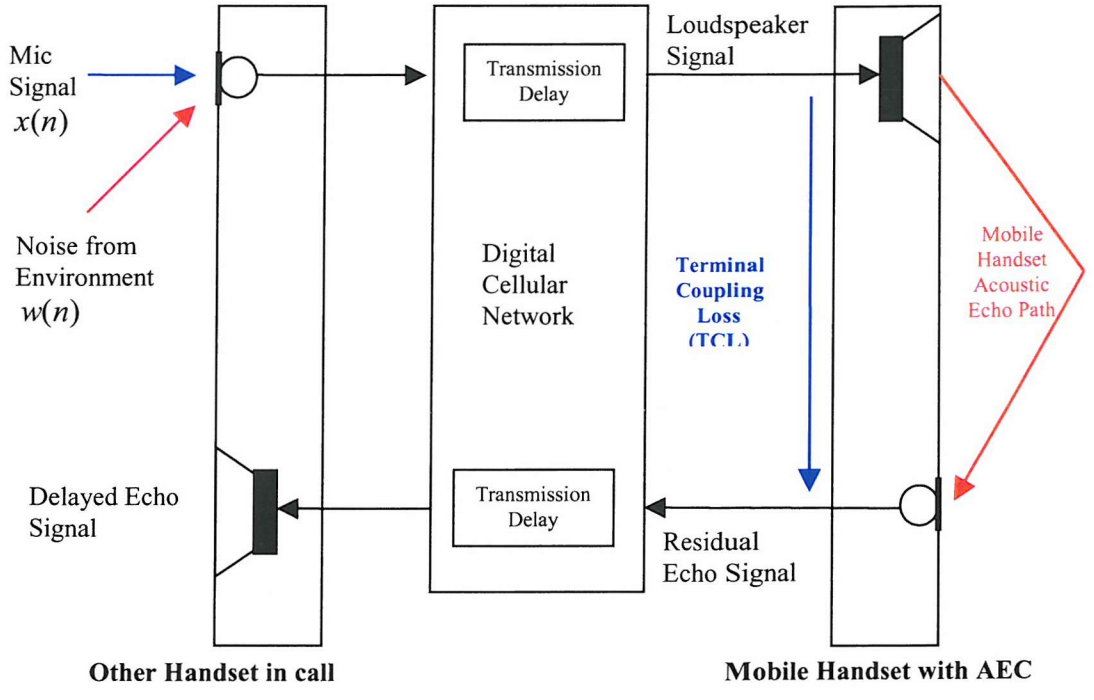


**Figure 6.16 : Noisy Loudspeaker Signal input to handset with Acoustic Echo Canceller**

The Signal to Noise Ratio (SNR) is defined as follows,

$$SNR_{dB} = 10\log_{10}\left[\frac{E[x^2(n)]}{E[w^2(n)]}\right] = 10\log_{10}\left[\frac{\sum_{n=0}^{M-1} x^2(n)}{\sum_{n=0}^{M-1} w^2(n)}\right], \quad (6.3)$$

From (6.3) we can see the SNR is defined as the ratio of echo path output power in the absence of noise $E[x^2(n)]$, to the echo path output disturbance noise power $E[w^2(n)]$ in decibels, calculated as a time average, where M represents the length of sequences $x(n)$ and $w(n)$. Both $x(n)$ and $w(n)$ are uncorrelated. The power of input noise signal $w(n)$ is scaled to allow adaptive algorithm performance to be assessed over a range of input Signal to Noise Ratio (SNR) levels from 0 to 40dB. A typical level of SNR for input speech signals is between 10 and 20dB. The SNR level for each experiment is held constant over the simulation duration. As already discussed the input noise disturbance used is band limited pink noise to approximate the spectral characteristics of typical environment noise.

The results for different input SNR levels is shown in Figure 6.17 for the face up artificial ear sealed handset configuration using the Simplified Gradient NLMS Newton adaptive IIR algorithm. A summary of these results for different input SNR levels is shown in Table 6-13.

From Figure 6.17(a) to Figure 6.17 (c) it can be clearly seen at lower input SNR levels the power variation of the echo signal to be cancelled (and the input to the adaptive filter) is less, as these input signals now become more noise like in nature. As a result of this improved ERLE performance is obtained as seen in Figure 6.17 at lower input SNR levels. From Table 6-13 the main improvements are slightly higher $ERLE_{mean}$ level performance and less ERLE variation. These results for the artificial ear sealed echo path response are also valid for all other echo path responses of chapter 4.

In conclusion from the results presented it can be seen that the Simplified Gradient NLMS Newton adaptive IIR algorithm gives robust ERLE performance for low input SNR conditions.

| **SNR** | $ERLE_{mean}$ | $ERLE_{\max}$ | $ERLE_{std}$ | $TIC_{mean}$ | $TIC_{req}$ |
|---|---|---|---|---|---|
| 40dB | 11.23dB | 22.84dB | 4.89dB | 7.3ms | 0ms |
| 20dB | 11.64dB | 22.91dB | 4.65dB | 7.74ms | 0ms |
| 0dB | 12.33dB | 21.11dB | 4.22dB | 7.74ms | 0ms |

**Table 6-13 : Summary of ERLE results for the artificial ear sealed handset configuration for different input SNR levels using the Simplified Gradient NLMS Newton adaptive IIR algorithm**

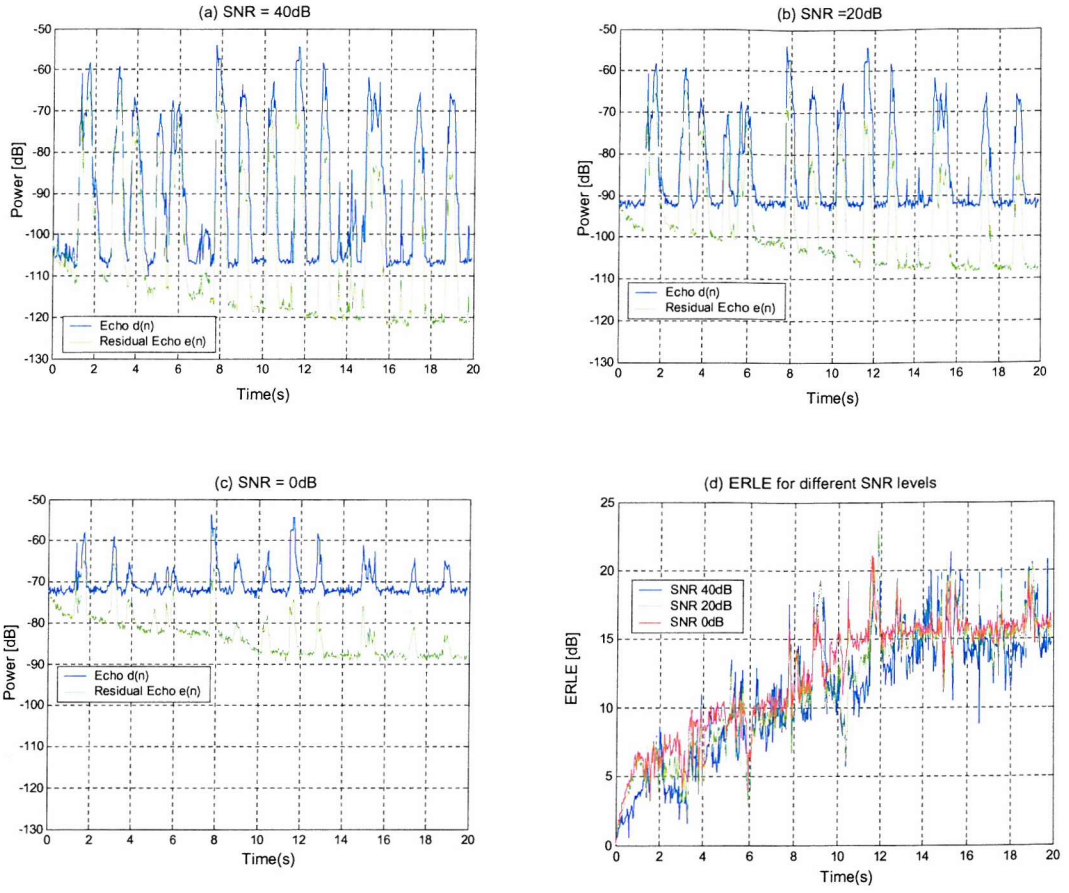


**Figure 6.17 : Modelling performance for the artificial ear sealed handset configuration for different input SNR levels using the Simplified Gradient NLMS Newton adaptive IIR algorithm**

(a) to (c) show the echo and residual echo signals at an input SNR of 40, 20 and 0dB. The Ensemble averaged ERLE curves for different input SNR levels is shown in (d). The simplified Gradient NLMS Newton algorithm is used for all curves in this figure.

### 6.3.2.3. The effect of output ENR on modelling performance

So far only modelling performance for speech signals at a high output Echo to Noise Ratio (ENR) has been considered. In the real handset echo cancellation however, the input speech signal $x(n)$ will contain silent periods of low energy during normal conversational speech. It is during these silent periods the effects of a microphone noise source will be most severe and may cause the adaptive algorithm coefficients to move away from their previously converged values [6.4]. An adaptive algorithm for this application must provide robust modelling performance for input speech signals at ENR levels as low as 5dB as we have discussed already in Chapter 5.

Consider the speech segment whose average power in 32ms frames is shown in Figure 6.18. From Figure 6.18 it can be seen there exists a significant silent period between two groups of speech utterances around 5s and, about a 1s silent period between each individual speech utterance. The input SNR used is 15dB. The modelling performance using the Simplified Gradient NLMS Newton algorithm for the face up

no seals handset configuration echo path response is shown in Figure 6.18 for different ENR levels. The ERLE modelling results are summarised in Table 6-14.

From Figure 6.18 it can be clearly seen that during the large silent period (between 7 to 12s) the ERLE level drops significantly, particularly at lower ENR levels. At the lowest ENR level of 10dB displayed the ERLE performance drops significantly even between each individual speech utterance, as the adaptive algorithm filter coefficients move away from their previously converged values during active speech periods. At ENR levels below 10dB stability is a problem for the Simplified Gradient NLMS Newton algorithm. The same modelling performance arises when modelling the other echo path responses of Chapter 4.

The reason for this stability problem and poor performance at low ENR levels becomes clear from Figure 6.19. In Figure 6.19 the speech utterance is displayed together with the time varying stepsize $\mu(n) = \dfrac{\mu}{\varphi_f^T(n)\mathbf{R}^{-1}_{\varphi_f\varphi_f}(n-1)\varphi_f(n)}$. The stepsize normalisation factor $\varphi_f^T(n)\mathbf{R}^{-1}_{\varphi_f\varphi_f}(n-1)\varphi_f(n)$ is proportional to the input signal power. During the silent speech periods the factor $\varphi_f^T(n)\mathbf{R}^{-1}_{\varphi_f\varphi_f}(n-1)\varphi_f(n)$ is small resulting in a large stepsize, and during active speech periods this factor is larger resulting in a smaller stepsize. However during these silent speech periods the microphone disturbance noise has the greatest effect, and a large stepsize causes the poor ERLE performance, as the filter coefficients will move away quickly from their previously converged values during the active speech period. At low ENR levels below 10dB this large stepsize results in stability problems for the Simplified Gradient NLMS Newton algorithm.

In conclusion for lower noise environments where the ENR level remains above 15dB the Simplified Gradient NLMS Newton algorithm provides good ERLE performance. However as this cannot be guaranteed in practical handset use the Simplified Gradient NLMS Newton algorithm must be modified for robust operation at lower ENR levels. The next section introduces a modified form of the Simplified Gradient NLMS Newton algorithm.

| **ENR** | $ERLE_{mean}$ | $ERLE_{\max}$ | $ERLE_{std}$ | $TIC_{mean}$ | $TIC_{req}$ |
|---|---|---|---|---|---|
| 20dB | 22.45dB | 36.24dB | 5.56dB | 2.02ms | 1.06ms |
| 15dB | 20.39dB | 34.38dB | 5.5dB | 1.89ms | 1.09ms |
| 10dB | 17.15dB | 32.1dB | 6dB | 1.63ms | 1.12ms |

**Table 6-14 : Summary of ERLE results for the face up no seals handset configuration for different output ENR levels using the Simplified Gradient NLMS Newton adaptive IIR algorithm**

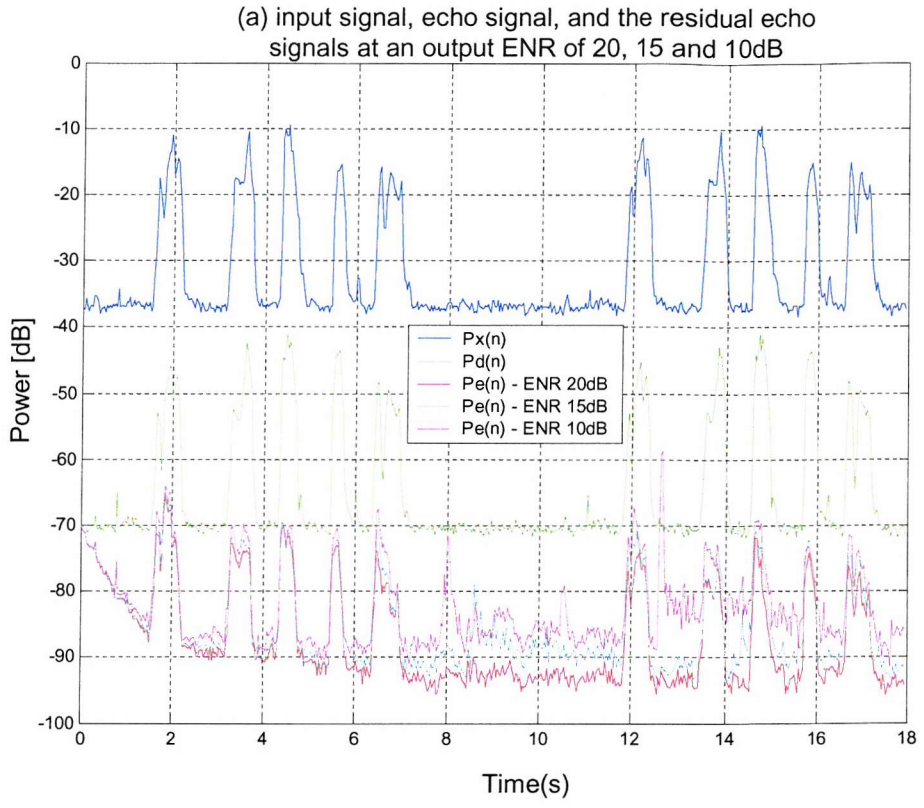


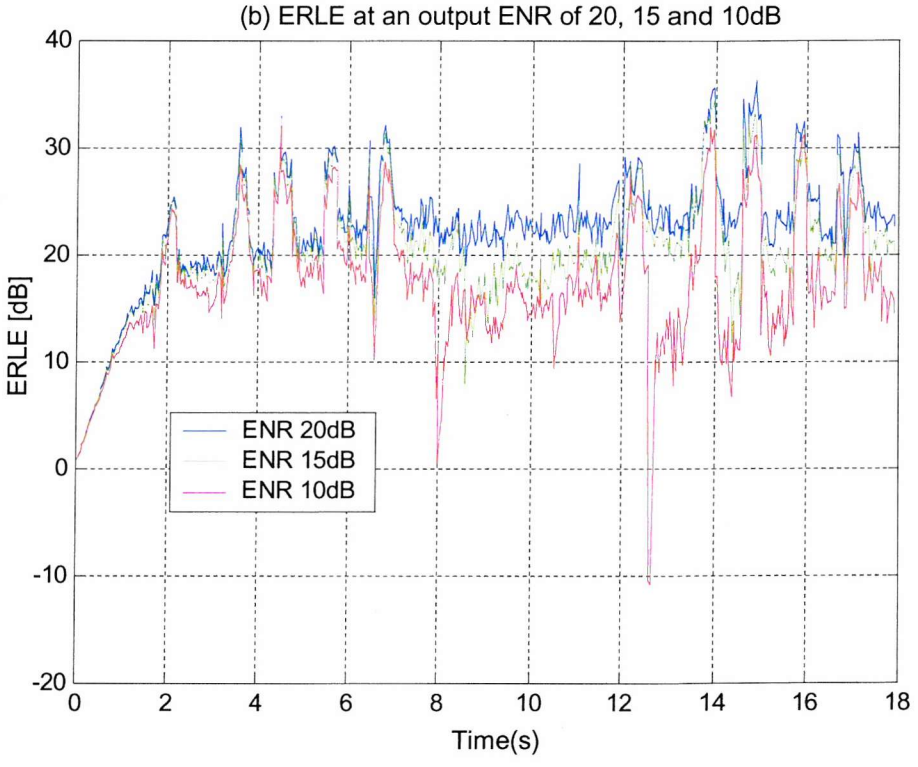


**Figure 6.18 : Modelling performance for the face up no seals handset configuration for different output ENR levels using the Simplified Gradient NLMS Newton adaptive IIR algorithm.**

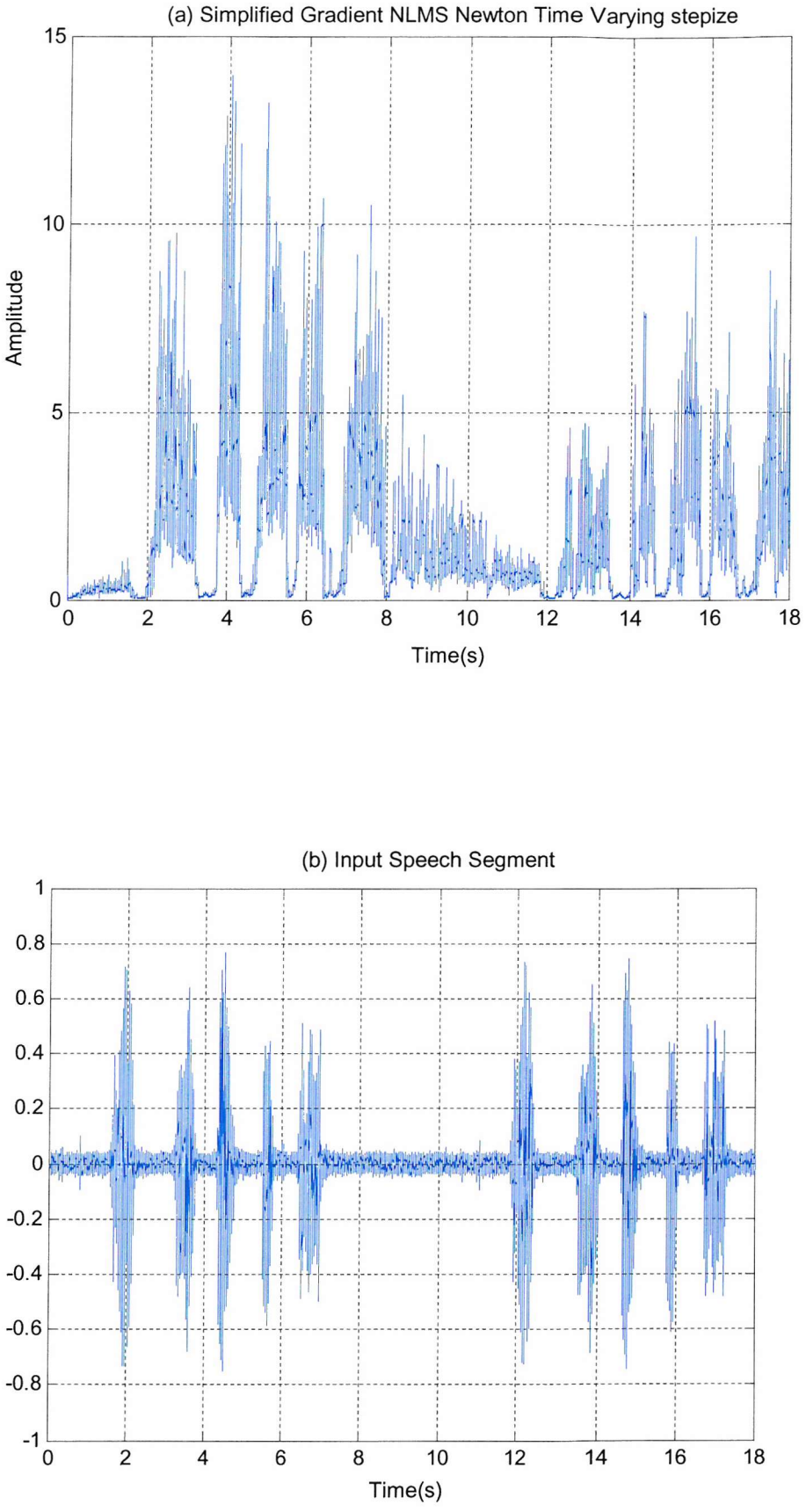


**Figure 6.19 : Example of time varying stepsize for an input speech signal.**

## 6.4. A modified Simplified Gradient Adaptive IIR NLMS Newton algorithm for Robust Acoustic Echo Cancellation on a mobile handset

It is clear from the previous section that the adaption rate of the Simplified Gradient NLMS Newton algorithm must be modified to slow the update rate when the algorithm has sufficiently converged to the echo path response being modelled, or when the input activity is low in order to make the algorithm robust in low ENR environments.

One method of achieving these aims is to use a method similar to that proposed in [6.8]and [6.9]. Let us first quickly recap how the Simplified Gradient NLMS algorithm was arrived at. In Chapter 3 the solution for an output error filter model to the recursive normal equations of (3.2.70) using Newton's Method was presented, as follows,

$$\boldsymbol{\theta}_{n+1} = \boldsymbol{\theta}_n - \mathbf{R}^{-1}_{\varphi_f \varphi_f} \nabla F_n, \tag{6.4}$$

where $\nabla F_n$ is the resulting gradient of the cost function $F$ (mean square output error) with respect to the coefficients $b_i$ and $a_j$ at time index n. The gradient of the mean square output error surface $\nabla F_n$ from (4.2.56) can be written as,

$$\nabla F_n = -2E[e_o(n)\nabla\hat{y}(n)], \tag{6.5}$$

Using the slowly varying filter coefficients assumption we get,

$$\nabla F_n = -2E[e_o(n)\phi_f(n)], \tag{6.6}$$

For the Simplified Gradient NLMS Newton algorithm an instantaneous estimate of $\nabla F_n$ is used giving,

$$\nabla F_n = -2e_o(n)\phi_f(n), \tag{6.7}$$

Incorporating time dependency into the coefficient update of (3.2.70), and using (6.7) in conjunction with stepsize parameter $\mu$ for greater update control, and incorporating the normalisation of (3.2.75) to deal with non-stationary signals we arrive at the Simplified Gradient NLMS Newton algorithm of Table 6-1.

Consider now the gradient of the mean square output error surface $\nabla F_n$ from (6.6). From (6.6) we can see that $\nabla F_n$ is simply the cross correlation of the filtered information vector $\phi_f(n)$ with the output error $e_o(n)$. By incorporating a more accurate estimate of this cross correlation into the Simplified Gradient NLMS Newton update of (3.2.76) it becomes apparent that we can slow the update rate when the algorithm has sufficiently converged to the echo path response being modelled, or when the input activity is low in order to make the algorithm robust in lower ENR environments for independent microphone disturbance signals. For non-stationary input signals such as speech this also solves the problem of high adaption gain during silent periods of speech at lower ENR levels..

Consider now how a correlation factor estimate proportional to $\rho = E[e_o(n)\phi_f(n)]$ can be incorporated into the Simplified Gradient NLMS Newton algorithm of Table 6-1 to provide robust

adaption at low ENR levels. One of the simplest estimates of $\rho = E[e_o(n)\phi_f(n)]$ is to use the following recursive estimate,

$$\hat{\rho}(n) = (1-\lambda_c)\hat{\rho}(n-1) + \lambda_c \bar{\phi}_f(n) e_o(n), \tag{6.8}$$

where $\bar{\phi}_f(n)$ is defined as,

$$\bar{\phi}_f(n) = \frac{1}{M+N} \sum_{i=1}^{M+N} \phi_{f,i}(n), \tag{6.9}$$

and $\bar{\phi}_{f,i}(n)$ is the i$^{th}$ element of filtered information vector $\phi_f(n)$ and $\lambda_c$ is a smoothing parameter to deal with the non-stationarities of the adaption process. Now to slow the adaption rate of the Simplified Gradient NLMS Newton algorithm a modification is made to both the convergence of the inverse covariance matrix estimate, and the stepsize. Consider the estimate of covariance matrix estimate $\hat{\mathbf{R}}_{\varphi_f\varphi_f}(n)$ every update period as follows [6.10],

$$\hat{\mathbf{R}}_{\varphi_f\varphi_f}(n) = (1-\lambda)\hat{\mathbf{R}}_{\varphi_f\varphi_f}(n-1) - \alpha\phi_f(n)\phi_f{}^T(n), \tag{6.10}$$

where $\lambda$ is the forgetting factor and $\alpha$ is a convergence parameter as discussed earlier in the Chapter. Using a modified update to slow the rate of adaption once the algorithm has converged we get

$$\hat{\mathbf{R}}_{\varphi_f\varphi_f}(n) = (1-\lambda)\hat{\mathbf{R}}_{\varphi_f\varphi_f}(n-1) - g(n)\phi_f(n)\phi_f{}^T(n), \tag{6.11}$$

where $g(n)$ is defined as,

$$g(n) = \alpha\left|\hat{\rho}(n)\right|, \tag{6.12}$$

The inverse covariance matrix estimate using the Matrix Inversion Lemma becomes,

$$\hat{\mathbf{R}}^{-1}_{\varphi_f\varphi_f}(n) = \frac{1}{\lambda}\left(\hat{\mathbf{R}}^{-1}_{\varphi_f\varphi_f}(n-1) - \frac{\hat{\mathbf{R}}^{-1}_{\varphi_f\varphi_f}(n-1)\varphi_f(n)\varphi_f{}^T(n)\hat{\mathbf{R}}^{-1}_{\varphi_f\varphi_f}(n-1)}{\frac{\lambda}{g(n)} + \varphi_f{}^T(n)\hat{\mathbf{R}}^{-1}_{\varphi_f\varphi_f}(n-1)\varphi_f(n)}\right), \tag{6.13}$$

Consider now the time-varying stepsize estimate $\mu(n)$ from Table 6-1,

$$\mu(n) = \frac{\mu}{\varphi_f^T(n)\mathbf{R}^{-1}_{\varphi_f\varphi_f}(n-1)\varphi_f(n)}, \tag{6.14}$$

In addition to slowing the covariance matrix update, the stepsize must also be altered to stop the variation of filter coefficients once the algorithm has converged or during silent periods in the input speech signal. The stepsize $\mu(n)$ is modified as follows,

$$\mu(n) = \frac{\mu}{\lambda/g(n) + \varphi_f^T(n)\mathbf{R}^{-1}_{\varphi_f\varphi_f}(n-1)\varphi_f(n)}. \tag{6.15}$$

The stepsize of (6.13) now becomes more like an RLS type update [6.8]. From (6.11) to (6.15) as the adaptive algorithm converges to the echo path modelled $g(n)$ tends towards zero. This slows the rate at which the covariance matrix and its inverse is updated and also reduces the effective stepsize $\mu(n)$. This effectively slows the response of the adaptive algorithm to any independent microphone disturbances.

Equations (6.11) to (6.13) constitute a modified Simplified Gradient NLMS Newton algorithm for robust acoustic echo cancellation on a mobile handset. From this point forward this shall be referred to as the Correlation Simplified Gradient NLMS Newton algorithm. The full Correlation Simplified Gradient NLMS Newton algorithm process is shown in Table 6-15.

| | |
|---|---|
| Initialisation: $\hat{\mathbf{R}}^{-1}_{\varphi_f\varphi_f}(0)=\delta\mathbf{I}, \boldsymbol{\theta}_n=\mathbf{0}, \hat{p}(0)=0, \forall n<0$ | |
| $\varphi(n)=[x(n),...,x(n-M+1),y(n-1),...y(n-N)]^T$ | |
| $\hat{y}(n)=\boldsymbol{\theta}_n^T\varphi(n)$<br>$e_s(n)=d(n)-\hat{y}(n)$ | |
| $x_f(n)=x(n)+\sum_{j=1}^{N}\boldsymbol{\theta}_n(M+j)x_f(n-j)$<br>$y_f(n)=y(n-1)+\sum_{j=1}^{N}\boldsymbol{\theta}_n(M+j)y_f(n-j)$<br>$\varphi_f(n)=[x_f(n),...,x_f(n-M+1),y_f(n-1),...y_f(n-N)]^T$ | |
| **Correlation Estimate** | $\bar{\phi}_f(n)=\frac{1}{M+N}\sum_{i=1}^{M+N}\phi_{f,i}(n)$<br>$\hat{\rho}(n)=(1-\lambda_c)\hat{\rho}(n-1)+\lambda_c\bar{\phi}_f(n)e_o(n)$<br>$g(n)=\alpha\lvert\hat{\rho}(n)\rvert$ |
| **Stepsize** | $\mu(n)=\frac{\mu}{\lambda/g(n)+\varphi_f^T(n)\mathbf{R}^{-1}_{\varphi_f\varphi_f}(n-1)\varphi_f(n)}$ |
| $\boldsymbol{\theta}_n=\boldsymbol{\theta}_{n-1}+\mu(n)\mathbf{R}^{-1}_{\varphi_f\varphi_f}(n-1)\varphi_f(n)e(n)$ | |
| $\hat{\mathbf{R}}^{-1}_{\varphi_f\varphi_f}(n)=\frac{1}{\lambda}\left(\hat{\mathbf{R}}^{-1}_{\varphi_f\varphi_f}(n-1)-\frac{\hat{\mathbf{R}}^{-1}_{\varphi_f\varphi_f}(n-1)\varphi_f(n)\varphi_f{}^T(n)\hat{\mathbf{R}}^{-1}_{\varphi_f\varphi_f}(n-1)}{\frac{\lambda}{g(n)}+\varphi_f{}^T(n)\hat{\mathbf{R}}^{-1}_{\varphi_f\varphi_f}(n-1)\varphi_f(n)}\right)$ | |

**Table 6-15 : Correlation Simplified Gradient NLMS Newton Adaptive IIR Algorithm**

The robust nature of the Correlation Simplified Gradient NLMS Newton algorithm is illustrated in Figure 6.20 for the face up no seals handset configuration at different low ENR levels using the same input speech signal as was used in Figure 6.19. From Figure 6.20 it can be clearly seen unlike the original Simplified Gradient NLMS Newton algorithm of Figure 6.2 as we have seen earlier, little ERLE variation occurs during the during the large silent period (between 7 to 12s) even at very low ENR levels. This is because during the silent speech periods of speech, both the covariance matrix update is slowed and the stepsize reduced, putting the adaptive filter into an effective sleep state. This produces little or no filter coefficient variation even at low ENR levels maintaining ERLE levels.

In line with the main aims of the thesis Figure 6.20 to Figure 6.20 shows the tabulated ERLE level results comparing the ERLE performance of the new the Correlation Simplified Gradient NLMS Newton algorithm presented in this section and the standard FIR NLMS Newton algorithm for different ENR levels. For these tabulated results both a male and female speech recording is used of up to approximately 40 seconds in duration. These recordings are in English and contain approximately 35 utterances, which are a mixture of natural conversational speech, and energetic speech utterances. Different pause durations are present between utterances in part of these recordings. An ENR level 0dB is used to demonstrate robust AEC operation. Due to the small acoustic echo signal coupled into the handset microphone in relation to the background noise level of a typical operating environment an ENR level of 0dB or lower is quite likely.

From the results presented it is clear the Correlation Simplified Gradient NLMS Newton algorithm performs significantly better than a standard FIR NLMS Newton algorithm with the same number of coefficients, satisfying the main aim of the thesis.

## 6.5. Summary of Chapter

The main aim of this chapter was to study the effects of time variations algorithms in both the handset echo path response and the input signal to the adaptive filter on the modelling performance of adaptive IIR algorithms.

In section 6.2 results were presented on the tracking performance of equivalent adaptive FIR and IIR algorithms for a time varying echo path response. Both linear and non-linear time variations were considered. From the results presented it is clear that output error adaptive IIR algorithms can satisfactorily track time variations in the echo path response during normal handset use, even in the presence of echo path output noise. The tracking performance with respect to an equivalent FIR adaptive algorithm for NLMS Newton based adaptive IIR algorithms is similar.

In section 6.3 results were presented on the modelling performance of equivalent adaptive FIR and IIR algorithms for speech input signals. Both male and female speech recordings have been used over a range of input SNR and output ENR levels. From the results presented it is clear adaptive IIR algorithms can have superior modelling performance over adaptive FIR algorithms for the mobile handset acoustic echo cancellation application. A new algorithm, the Correlation Simplified Gradient NLMS Newton adaptive IIR algorithm is presented for robust acoustic echo cancellation on a mobile handset where ENR levels can typically be less than or equal to 0dB in practice.

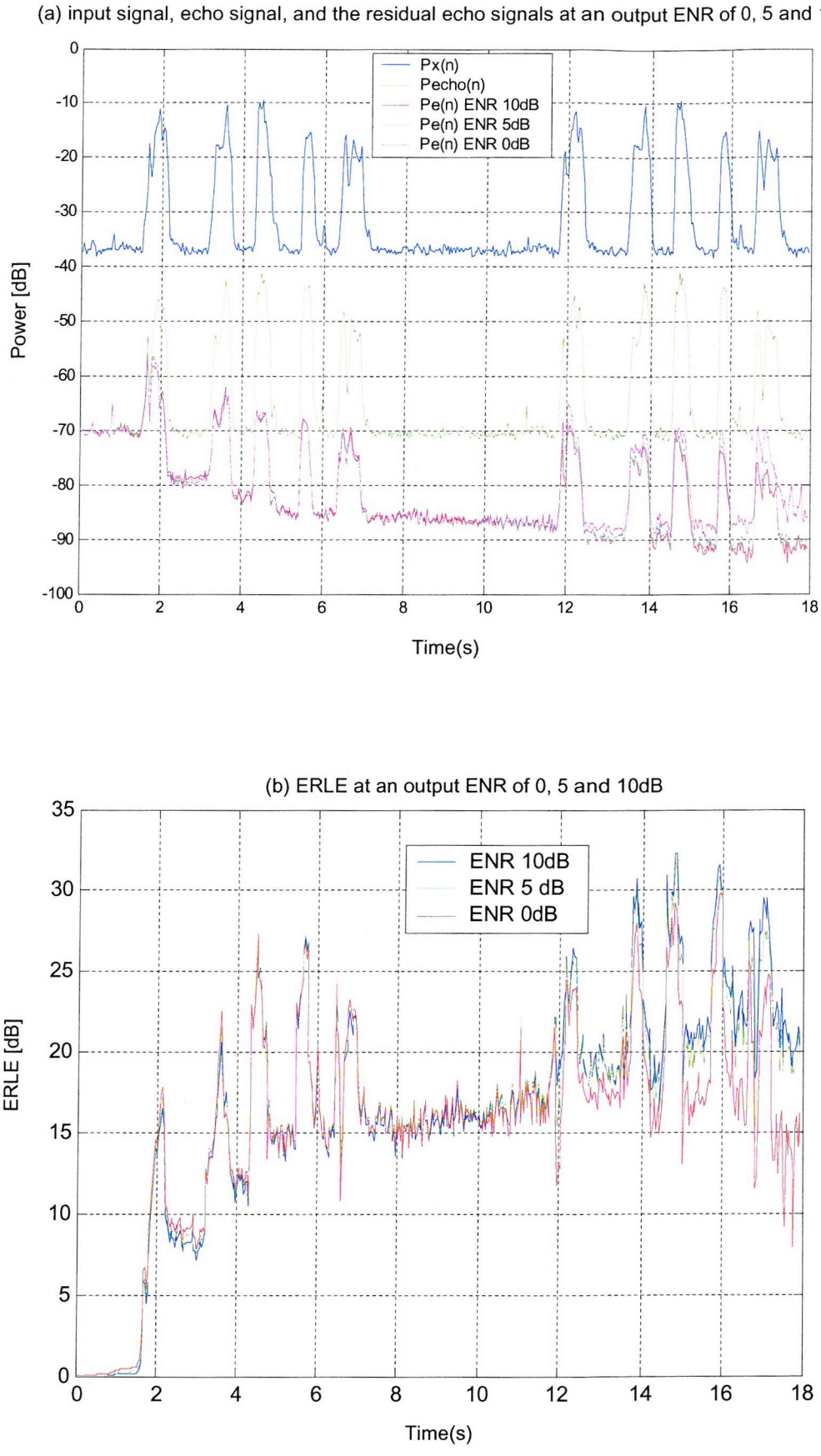


**Figure 6.20 : Robust handset acoustic echo cancellation using the Correlation Simplified Gradient NLMS Newton adaptive IIR algorithm.**

| Algorithm | $ERLE_{mean}$ | $ERLE_{\max}$ | $ERLE_{std}$ | $TIC_{mean}$ | $TIC_{req}$ |
|---|---|---|---|---|---|
| FIR NLMS Newton | 11.93dB | 25.17dB | 4.21dB | 1.76ms | 1.76ms |
| Correlation SG NLMS Newton | 15.4dB | 30.78dB | 5.64dB | 3.81ms | 3.23ms |

**Table 6-16 : Summary of ERLE results for the face up echo path response.**

| Algorithm | $ERLE_{mean}$ | $ERLE_{\max}$ | $ERLE_{std}$ | $TIC_{mean}$ | $TIC_{req}$ |
|---|---|---|---|---|---|
| FIR NLMS Newton | 9.06dB | 26.48dB | 5.143dB | 1.248ms | 1.248ms |
| Correlation SG NLMS Newton | 11.6dB | 30.29dB | 5.09dB | 1.6ms | 1.664ms |

**Table 6-17 : Summary of ERLE results for the loudspeaker sealed echo path experiments.**

| Algorithm | $ERLE_{mean}$ | $ERLE_{\max}$ | $ERLE_{std}$ | $TIC_{mean}$ | $TIC_{req}$ |
|---|---|---|---|---|---|
| FIR NLMS Newton | 8.34dB | 26.53dB | 5.32dB | 1.248ms | 1.248ms |
| Correlation SG NLMS Newton | 11.35dB | 29.36dB | 5.57dB | 1.632ms | 1.376ms |

**Table 6-18 : Summary of ERLE results for the microphone sealed echo path experiments.**

| Algorithm | $ERLE_{mean}$ | $ERLE_{\max}$ | $ERLE_{std}$ | $TIC_{mean}$ | $TIC_{req}$ |
|---|---|---|---|---|---|
| FIR NLMS Newton | 8.85dB | 23.54dB | 4.41dB | 1.248ms | 1.312ms |
| Correlation SG NLMS Newton | 10.54dB | 25.4dB | 4.91dB | 1.376ms | 3.776ms |

**Table 6-19 : Summary of ERLE results for the face down echo path experiments.**

# Chapter 7

## 7. Summary and Conclusions

The aim of the research documented in this thesis was to develop adaptive IIR filtering techniques suitable for acoustic echo cancellation on a mobile handset, and investigate their benefits in terms of complexity and performance over more traditional adaptive FIR filtering techniques.

The motivation behind this research is explained in chapter 1. In order to prevent disruption to speech communication, most telecommunication systems, such as GSM, impose restrictions on the maximum level of acoustic echo allowable on a handset. At the time of writing this thesis trends in mobile handset over the last five years have been to have increasingly smaller handset designs, with flip phone type designs becoming increasingly more popular. The need for acoustic echo control of some kind on a mobile handset has thus become more widespread, as the level of acoustic coupling between a handset loudspeaker and microphone will have increased significantly on newer handset designs over the last few years. Due to large amount of handset model variants produced by each manufacturer, and the concept removable front casings, the most favoured method of acoustic echo control is in the form of acoustic echo cancellation within the handset electronics. From the handset echo path measurements and modelling results reported in this thesis, the purpose of researching the benefits of Adaptive IIR filtering techniques for acoustic echo cancellation on a mobile handset is clear.

### 7.1. The Acoustic Echo Path of a Mobile Handset

The nature of the acoustic echo path has been discussed in chapter 2. Although the GSM handset design tested at the earlier stages of this thesis has larger dimensions than current GSM handset designs available today, it is still expected that the same general behaviour in the echo path response will exist for modern handset designs constructed in a similar way. Indeed the measured Terminal Coupling Loss levels of modern designs may require higher levels of Echo Return Loss Enhancement than those reported in this thesis, as the relative distance between handset loudspeaker and microphone will be less, resulting in a much smaller Terminal Coupling Loss. The conclusions drawn from the handset design tested are however still valid for cordless handset designs of similar construction found today in the home and office, as these cordless handsets have similar dimensions to the GSM mobile handset design tested during this thesis.

The handset orientations used in chapter 2 are fixed orientations that are measured in an anechoic environment. The responses measured from these orientations represent the likely variation of the acoustic echo path response of a mobile handset in normal handset use. It is clear from the results presented that the single artificial ear sealed handset test condition, used in GSM standards to measure the Terminal Coupling Loss of a mobile handset in normal use, does not reflect the actual variation of Terminal Coupling Loss in a mobile handset possible in normal use. When compared to actual echo path responses recorded in reverberant environments these fixed handset orientations can be seen to provide a more

robust method of ensuring the Terminal Coupling Loss of a mobile handset remains below the required level in normal use.

The handset responses recorded in chapter 2 show that the main source of echo reflections due to the environment occurs after 10ms, corresponding to reflections from surfaces 3-4m away. As these reflections occur after the main anechoic region of the response and are significantly lower in level, the acoustic echo canceller within the mobile handset electronics can ignore these echo reflections. Reflections due to the user's head and body are likely to occur within a 1m range and within the anechoic region of the echo path response up to 7ms. From an observation of the measured echo path responses, it is concluded that the reflections due to the user's head and body can be concluded are negligible and can be ignored.

From the most likely echo path sources identified in chapter 2, only the internal and external echo path components have influence on the overall acoustic echo path response. If no loudspeaker or microphone seal or obstruction exists, or the effect of these is small on a mobile handset during normal use, the external echo path will dominate the overall acoustic echo path response. The resulting Terminal Coupling Loss may be as low as 33dB with an effective duration of up to 4ms. If a loudspeaker seal or obstruction exists and the seal is very good, such as with the firm placement to a user's ear and head in normal use, the internal echo path will dominate the overall acoustic echo path response. The resulting Terminal Coupling Loss may be as high as 46dB with an effective duration of up to 4ms. For a poorer loudspeaker seal the resulting Terminal Coupling Loss may be as low as 42dB. If a microphone seal or obstruction exists the internal echo path will dominate the overall acoustic echo path response. The resulting Terminal Coupling Loss may be as low as 37dB with an effective duration of up to 7ms. The echo path response is clearly resonant in nature. When placed face down on a rigid surface the worst case acoustic condition is produced where the echo path response is clearly resonant in nature with an effective duration of up to 10ms and a Terminal Coupling Loss as low as 29dB.

## 7.2. Can IIR Filter Models Offer Better Modelling Capabilities than FIR Filter Models?

The echo path responses reported in chapter 2 did not include the effects of the handset codec filtering and the actual audio sample rate used in the mobile handset. To determine whether IIR filter models have better modelling capabilities than FIR filter models in normal handset use these effects must be included in the echo path responses to be modelled. In chapter 4 the measurements of the fixed handset orientations of chapter2, used to represent the possible handset response variation in normal use are converted to represent the handset variation modelled by an acoustic echo canceller within the handset electronics. Since the Terminal Coupling Loss level being calculated in the range 300 to 3400 Hz, within the passband of the codec filters, the Terminal Coupling Loss levels of the modified echo path responses are relatively unchanged. Information in the echo path measurements reported in chapter 2 above 3600Hz will be eliminated in these modified responses, due to heavy attenuation by the codec filter response. Additionally a larger delay period and longer decaying tail will exist in the modified echo path responses to be modelled.

Using a system identification configuration various offline FIR filter models are investigated, using the optimal Wiener solution, an Output Error filter model using a recursive prediction error adaptive model, and an Equation Error IIR Filter model using an offline Steiglitz McBride method. These are used to determine the modelling capabilities of FIR and IIR filters, for modelling the variation in handset response in normal use. By calculating the ERLE level for each filter model, over a range of different filter model coefficients for each echo path response, a Coefficient Reduction Factor can be calculated which allows the benefits in terms of ERLE performance and complexity of each model to be directly compared. From the modelling results presented and the required ERLE levels needed for each echo path it is clear that the face down echo path response is the worst-case echo path response to be modelled.

For the Equation Error offline IIR filter model a coefficient reduction factor of up to 1.13 can be obtained. A model order of at least 46 coefficients is required for the Equation Error IIR Filter model with 11 AR coefficients, (35,11). For this model order an ERLE gain of up to 6dB is possible for the Equation Error IIR filter model over an FIR filter model. For the Output Error offline IIR filter model a coefficient reduction factor of up to 1.29 can be obtained with at least 42 coefficients with 15 AR coefficients, (27,15). For this model order an ERLE gain of up 7dB is possible for the Output Error IIR filter model over an FIR filter model. The larger model order required for the Equation Error model is attributed to bias in the form of under modelling noise. It is clear from the ERLE gains calculated and the Coefficient Reduction Factors greater than unity that IIR Filter models have benefits in terms of performance and complexity over more traditional FIR filter models.

## 7.3. Is an Adaptive IIR Model Needed?

The offline modelling results of chapter 4 show the clear benefits of using an IIR filter model. From these modelling results the Z domain representation of a (27,15) output error IIR filter model for some of the echo path modelled are analysed. Despite these echo path responses modelled having the same fixed codec filter contributions to its frequency and impulse response, it is clear from the pole and zero positions of the (27,15) IIR models can be significantly different. This indicates that to model the handset echo path response in normal use with an IIR filter model, both feedforward and feedback sections must be adapted in the IIR filter model.

To show the impacts on modelling performance of using the same feedforward and feedback section or only just the same feedback section, the offline IIR models are re-computed for each echo path response to be modelled. Poor ERLE performance was obtained using the same the same feedforward and feedback section or only the same feedback section for each IIR model. This clearly shows that these cannot be used in the IIR filter model within the echo canceller to model the variation of the handset response in normal use. The IIR filter model within the echo canceller must be adaptive.

## 7.4. Can Adaptive IIR Filters offer better modelling capabilities than Adaptive FIR Filters?

In order to determine the modelling performance benefits of adaptive IIR algorithms over their FIR counterparts when modelling the acoustic echo path of a mobile handset a number of questions must be addressed. Firstly, what criteria will be used for comparing the steady state modelling performance of both adaptive FIR and IIR algorithms? Secondly, what adaptive algorithms will be used to assess modelling performance of adaptive FIR and IIR algorithms? Thirdly, for the adaptive algorithms chosen what parameters values were chosen and how do these parameters impact modelling performance? Next, is whether only the steady state performance is to be modelled for comparison purposes? Lastly, what input signals will be used, what echo path responses will be modelled, and will modelling performance in the presence of echo path output noise be considered?

As part of chapter 5 the results of many system identification experiments are presented in order to assess the modelling performance of adaptive IIR filters. In order to establish whether the same performance benefits are obtained as for the offline IIR filter models of chapter 4, only the steady state modelling performance will be considered. Additionally, no echo path output noise is present. As the steady state modelling performance is to be established the input signal used for each experiment is stationary. A long experiment run of 80000 samples or 10 seconds is used for each experiment to allow sufficient convergence time for each algorithm to reach its steady state solution for this application.

In comparing algorithm performance two factors are important. The criteria selected must first of all allow a direct comparison with the offline modelling results of chapter 4 to be made. Secondly the criteria selected must represent not only the steady state converged solution of each adaptive algorithm in a consistent way but must represent the time taken to converge to this solution, and the effects of adaptive algorithm parameters. In chapter 5 the ensemble averaged steady state ERLE level is used as a method of comparing the steady state modelling performance of adaptive FIR and IIR algorithms in this thesis. In addition the convergence time to both the steady state solution and the required ERLE level of acoustic each path modelled is reported.

In chapter 5 the Normalised LMS and LMS Newton forms of all adaptive algorithms presented in chapter 3 are used to both address whether adaptive IIR algorithms have any benefits over adaptive FIR algorithms for this application. However in order to reduce the number of experiments needed, initially the required model order for Output Error and Equation Error adaptive IIR algorithms is determined using only the Equation Error NLMS and LMS Newton algorithms, and the Simplified Gradient NLMS and LMS Newton Output Error adaptive IIR algorithms. The effect of algorithm design parameters for these NLMS and LMS Newton adaptive IIR algorithms on the convergence rate and the steady state ensemble averaged ERLE levels are also established in chapter 5. The initial modelling results reported in chapter 5, over a range of model orders, show that for Output Error adaptive IIR algorithms a model order of (27,15) is the most suitable. A gain in the steady state ensemble averaged ERLE level of 6.6dB over a FIR adaptive algorithm is possible, with a coefficient reduction factor of up to 1.29 achievable. The convergence rate to the required ERLE level for each echo path is similar to adaptive FIR algorithms, but

generally slower convergence is achieved to steady state ERLE level for Output Error adaptive IIR algorithms. In order to achieve these gains with adaptive IIR Output Error algorithms it is necessary to use LMS Newton based algorithms. Since the mean feedforward and feedback coefficient error terms will decay at different rates due to eigenvalue spread of $\mathbf{R}_{\phi_f\phi_f}$ a slow convergence rate exists, particularly for the feedback coefficients in the NLMS based algorithms. This is not the case for LMS Newton algorithms where the term $\mathbf{R}^{-1}_{\phi_f\phi_f}$ equalises the rate of decay of each coefficient error term, resulting is faster convergence and higher steady state ERLE level within the 10s experiment duration.

For the Equation Error adaptive IIR algorithms a model order of (31,11) is the most suitable. A gain in the steady state ensemble averaged ERLE level of 7.2dB over a FIR adaptive algorithm is possible, with a coefficient reduction factor of up to 1.29 again achievable. Although Equation Error NLMS algorithms may achieve a sufficient gain in the steady sate ensemble averaged ERLE level in comparison to an equivalent FIR adaptive algorithm for some echo paths modelled, this does not occur for all echo paths. Additionally the convergence time to the required ERLE level and steady state ERLE level is too slow in comparison to an adaptive FIR algorithm. This is due to the eigenvalue spread of $\mathbf{R}_{\phi_e\phi_e}$ that causes the mean feedforward and feedback coefficient error terms to decay at different rates, resulting in slow convergence. A LMS Newton based Equation Error adaptive IIR algorithm overcomes this slow convergence rate due to the term $\mathbf{R}^{-1}_{\phi_e\phi_e}$, achieving higher steady state ensemble averaged ERLE levels. In conclusion from these initial results presented in chapter 5, adaptive IIR algorithms offer clear benefits in modelling performance over adaptive FIR algorithms. The benefits reported in chapter 4 of IIR filter models over FIR filter models are still valid for adaptive filters, provided LMS Newton based algorithms are employed.

For the handset acoustic echo cancellation environment, noise will be present on the handset microphone in addition to acoustic echo. To fully answer the question of "Can Adaptive IIR Filters offer better modelling capabilities than Adaptive FIR Filters?" the steady state modelling performance of adaptive IIR algorithms in the presence of echo path output noise is also established in chapter 5. Since the steady state modelling performance is to be measured, only stationary input signals are used with no time variation in the response to be modelled. A band-limited pink noise source is re-used as the adaptive filter input. Both band-limited white and pink noise echo path output noise sources, uncorrelated with the adaptive filter input source, are used. Only the LMS Newton based adaptive algorithms of chapter 3 are used, with a total model order of 42 coefficients - (27,15) for the output error algorithms, (31,11) for the equation error algorithms. The same assessment criterions used in modelling experiments earlier in chapter 5 are used again.

Using the Simplified Gradient LMS Newton Output Error adaptive IIR algorithm and the Equation Error LMS Newton adaptive IIR algorithm the effect of echo output path noise level on the steady state modelling performance and choice of algorithm design parameters is analysed. For the Simplified Gradient LMS Newton algorithm it is clear that a much lower stepsize is required to maintain stability and reasonable steady state ERLE level performance at lower ENR levels. This is also the case for the Equation Error LMS Newton algorithm, but it is clear that a significantly lower steady state ERLE level is

produced, compared with that measured earlier in the chapter with no echo path output noise due to bias introduced into the estimation of the feedback coefficients. At the lowest levels of Echo to Noise Ratio, the performance of a (31,11) Equation Error LMS Newton algorithm is similar to the performance of a 31-coefficient FIR LMSN algorithm. The algorithm design parameters for all other LMS Newton adaptive algorithms are then chosen in a similar fashion.

In order to maintain the required ERLE for each echo path when modelling the acoustic echo path of a mobile handset in the presence of echo path output noise, it is clear from the modelling results reported in chapter 5 that an Output Error adaptive IIR algorithm is required. Despite the improved performance of the Steiglitz McBride LMS Newton and Bias Remedy LMS Newton adaptive IIR algorithms over the Equation Error LMS Newton algorithm, at the lower ENR levels bias is still significant, particularly for a coloured echo path output noise source. Of the adaptive IIR algorithms considered, only the Simplified Gradient LMS Newton Output Error algorithm can achieve the required ERLE for each echo path down to ENR levels of 5dB, while maintaining an ERLE gain of up to 5.9dB.

In conclusion it can be said that Output Error LMS Newton based adaptive IIR filtering algorithms do offer benefits in terms of modelling performance over an equivalent adaptive FIR algorithm even in the presence of echo path output noise.

## 7.5. Acoustic Echo Cancellation using Adaptive IIR Filters

In the mobile handset acoustic echo cancellation application a number of real world factors need to be considered when using an adaptive IIR algorithm. The first factor is that in real handset use, the handset position will change and will not remain in a fixed position. Also the volume control on the handset normally controls the gain of the handset loudspeaker after the acoustic echo canceller in the handset electronics, and so forms part of the echo path system to be modelled. As a results gain changes in the echo path response can occur during a call if the volume control is adjusted. The resulting echo path to be modelled will contain time variations during a call that must be tracked by the adaptive IIR algorithm in the acoustic echo canceller

The second real world factor is the nature of actual input signals encountered in the acoustic echo cancellation application. For this application speech signals will form the input signal to the echo canceller, which are non-stationary in nature. An adaptive IIR algorithm for use in the handset acoustic echo cancellation application must give sufficient performance for speech signal inputs.

The third factor is the impact of the environment on performance. If the user of a handset receives a call from a person who is in a noisy environment the input speech signal to the echo canceller will be contaminated with noise. Additionally when the user is in a noisy environment during silent speech periods the Echo to Noise Ratio will be much lower than that during active speech periods. An adaptive IIR algorithm for use in the handset acoustic echo cancellation application must have robust performance with low input SNR and low output ENR when speech signals are used.

Chapter 6 of this thesis follows on from the modelling experiments reported in chapter 5. The capability of adaptive IIR algorithms for tracking time variations in the echo path response to be modelled is established in comparison to an equivalent adaptive FIR algorithm. Many possible adaptive IIR

algorithms exist for use in this application. Using the results of chapter 5, only the Simplified Gradient Output Error adaptive IIR algorithms have been shown to be suitable for modelling the acoustic echo path of a mobile handset from all the algorithms presented in chapter 3. These algorithms will be used to establish the tracking performance of adaptive IIR filters.

Two different types of time variations in the handset echo path response to be modelled by an echo canceller are simulated in chapter 6 to establish tracking performance of adaptive IIR algorithms. Linear gain time variations in each echo path response modelled simulate both slow variations in the handset response, and gain increments due to changing volume control during a call. Non-linear (or step) variations in each echo path response modelled simulate rapid changes in the handset echo path response to be modelled during a call. The effects of both these linear and non-linear time variations in the echo path response are simulated in chapter 6 using different system identification experiments with stationary input signals. The effects of algorithm design parameters on tracking performance are firstly assessed, since those parameters chosen for optimal steady state performance will differ from those selected for fast echo path tracking performance. Tracking results presented in chapter 6 clearly show that Output error adaptive IIR algorithms can exhibit similar tracking performance to adaptive FIR algorithms.

Using slightly modified ERLE definitions to account for the non-stationary nature of speech signals the performance of adaptive FIR and Output Error IIR algorithms is investigated in chapter 6 of the thesis. From the results reported, it is clear that Normalised LMS Newton based adaption in the Simplified Gradient Output Error adaptive IIR algorithm gives superior ERLE performance due to the time varying normalisation factor in the filter update equation, which can take into account the shorter term energy fluctuation in the input speech signal which does not occur with the fixed convergence factor of LMS Newton based algorithms. An improved convergence rate and a gain in the mean ERLE performance of up to 5dB is achieved over a FIR LMS Newton algorithm and up to 5.5dB over a Simplified Gradient LMS Newton Output Error adaptive IIR algorithm, is achieved using the Simplified Gradient Normalised LMS Newton Output Error adaptive IIR algorithm.

The effect on adaptive IIR performance for different input SNR and output ENR levels with speech signal inputs are established in chapter 6 of this thesis. Using input speech signals contaminated with band limited pink noise the performance at low input SNR levels of adaptive IIR algorithms is established. With increasing levels of noise at lower SNR levels, the input signal becomes more noise like or stationary in nature, resulting in improved convergence rate and less variation in the ERLE level. Using speech signals with an input SNR of 15dB (typical for a lower noise office type environment) the ERLE performance of adaptive IIR algorithms is investigated in chapter 6, using the Simplified Gradient Normalised LMS Newton Output Error adaptive IIR algorithm. At low ENR levels during silent periods of speech large deviations in the ERLE level can occur, resulting in poor ERLE performance and instability for ENR levels below 10dB. This behaviour is due to the time varying convergence factor of the Normalised LMS Newton filter update which during silent speech periods gives a large stepsize, resulting in the filter coefficients moving from their previously converged values in active speech periods causing instability in some cases. To overcome this problem a modification to the Simplified Gradient Normalised LMS Newton Output Error adaptive IIR algorithm is presented to slow filter adaption during silent speech

periods. The Correlation Simplified Gradient Normalised LMS Newton adaptive IIR algorithm is presented in chapter 6 for robust Acoustic Echo Cancellation on a mobile handset.

## 7.6. Future Work and Research Directions

The performance benefits of Output Error adaptive IIR filtering algorithms for acoustic echo cancellation on a mobile handset have been successfully demonstrated in this thesis. With some further development an adaptive IIR algorithm could be successfully implemented within a handset DSP and tested in the field.

The echo path measurements used to establish the performance benefits of adaptive IIR algorithms have been largely based on measurements carried out on a particular type of handset construction. In today's market, flip-phone type designs are becoming increasingly popular due to their small and compact size. An interesting area of future work would be to investigate the acoustic echo path response of these flip-phone handsets. The construction of these handsets is different to the construction of the handset used for echo path measurements in this thesis. For flip-phones the handset loudspeaker and microphone are normally in two separate sections separated by some sort of hinging mechanism. It would be interesting to establish the benefits of adaptive IIR filtering for handsets of this type of construction, as well as more modern and smaller handsets of the same construction type as reported in this thesis, as this would indicate the widespread use of adaptive IIR filters for this application is beneficial.

During this thesis it was not possible to study complexity issues of adaptive IIR filtering. Due to the speech frame structure arrive in blocks every 20ms it is possible that block adaptive IIR filtering schemes would be very suitable for this application. Transform Domain adaptive IIR filtering techniques such as Frequency Domain adaptive IIR filtering, based on an output error criterion, could lead to additional savings in complexity and improved convergence.

Genetic algorithms have been successfully applied to the area of output error adaptive IIR filtering in recent years. An interesting area of future research would be to study the performance and complexity of different genetic adaptive IIR algorithm solutions for this application area, with the hope of enhanced modelling and tracking performance over more conventional Output Error adaptive IIR filtering schemes reported in this thesis.

# 8. Glossary

## 8.1. Abbreviations

| | |
|---|---|
| ADC | Analogue to Digital Converter |
| AEC | Acoustic Echo Cancellation |
| CRF | Coefficient Reduction Factor |
| DAC | Digital to Analogue Converter |
| DECT | Digital European Cordless Telephone |
| DSP | Digital Signal Processor |
| EE | Equation Error |
| ERLE | Echo Return Loss Enhancement |
| ENR | Echo to Noise Ratio |
| FIR | Finite Impulse Response |
| FFT | Fast Frequency Transform |
| GSM | Gobal System for Mobile commmunications |
| IFFT | Inverse Fast Frequency Transform |
| IIR | Infinite impulse Response |
| ISDN | Integrated Services Development Network |
| LCD | Liquid Crystal Display |
| LMS | Least Mean Squares |
| LMSN | LMS Newton |
| MSE | Mean Square Error |
| MSEE | Mean Square Equation Error |
| MSOE | Mean Square Output Error |
| NLMS | Normalised LMS |
| NLMSN | Normalised LMS Newton |
| OE | Output Error |
| PDA | Personal Digital Assistant |
| PSTN | Public Switched Telephone Network |
| PLR | Pseudo Linear Regression |
| RLS | Recursive Least Squares |

| | |
|---|---|
| SG | Simplified Gradient |
| SHARF | Simplified Hyperstable Adaptive Recursive Filter |
| SPR | Strict Positive Real |
| SNR | Signal to Noise Ratio |
| TCL | Terminal Coupling Loss |

## 8.2. Symbols

| | |
|---|---|
| $ERLE_{en}$ | Ensemble averged ERLE level. Calculated in 32ms frames |
| $ERLEss_{dB}$ | Steady state ensmeble averaged ERLE level |
| $ERLE_{mean}$ | Average value of $ERLE_{en}$ in dB over entire input signal duration |
| $ERLE_{std}$ | Standard deviation of $ERLE_{en}$ in dB about $ERLE_{mean}$ |
| $ERLE_{\max}$ | Maximum value of $ERLE_{en}$ in dB over entire input signal duration |
| $TIC_{req}$ | Convergence time to the required ERLE level |
| $TIC_{ss}$ | Convergence time to the steady state ERLE level |
| $t_{eff}$ | Effective echo path impulse response duration |
| $n$ | Discrete time index |
| $x(n)$ | Adaptive filter input signal |
| $d(n)$ | Adaptive filter desired signal input |
| $y(n)$ | Echo path output signal |
| $v(n)$ | Echo path output disturbance signal |
| $S_{xx}(\omega)$ | Auto power spectrum of the input excitation signal $x(n)$ |
| $S_{xy}(\omega)$ | Complex cross-power spectrum between echo path input $x(n)$ and output $y(n)$ |
| $H(e^{j\omega})$ | Complex frequency response |
| $h(n)$ | Echo path impulse response |
| $\gamma^2{}_{xd}(\omega)$ | Coherence function |
| $r_{xx}(k)$ | auto-correlation of echo path input $x(n)$ at lag k |
| $r_{xy}(k)$ | cross-correlation between echo path input $x(n)$ and output $y(n)$ at lag k |
| $\hat{y}(n)$ | Echo path replica at output of adaptive filter model |
| $e(n)$ | Estimation error signal |
| $\mathbf{h}$ | vector of L echo path impulse response samples |

| | |
|---|---|
| $M$ | Feedforward coefficient order |
| $N$ | Feedback coefficient order |
| $\mathbf{b}$ | FIR filter model coefficient vector |
| $F$ | Mean square error cost function |
| $\mathbf{R}_{xx}$ | M x M autocorrelation matrix of the input signal $x(n)$ |
| $\mathbf{r}_{dx}$ | M x 1 cross correlation vector between input signal $x(n)$ and output of the echo path $d(n)$ |
| $\mathbf{b}_{opt}$ | Optimum weight vector solution to the normal equations |
| $\mathbf{x}(n)$ | FIR adaptive filter information vector of M past input samples |
| $\mu$ | Stepsize parameter in adaptive algorithms |
| $\mathbf{p}_n$ | Vector which controls the search direction on the mean squared error surface of steepest descent algorithm |
| $F_{\min}$ | Minimum solution to cost function $F$ |
| $\nabla F_n$ | Gradient of the mean squared error cost function $F$ |
| $\mathbf{I}$ | Identity matrix |
| $\lambda_{\max}$ | Maximum eigenvalue of correlation matrix $\mathbf{R}$ |
| $\lambda_{\min}$ | Minimum eigenvalue of correlation matrix $\mathbf{R}$ |
| $\tilde{\boldsymbol{\varepsilon}}_n$ | Expectation of the error in the adaptive filter coefficient vector estimate at time index n and the optimal solution |
| $\boldsymbol{\varepsilon}_n$ | rotated error vector |
| $\mathbf{Q}$ | Matrix whose columns are the eigenvectors of correlation matrix $\mathbf{R}$ |
| $\boldsymbol{\Lambda}$ | Diagonal matrix whose elements consist of the eigenvalues of correlation matrix $\mathbf{R}$ |
| $tr[\mathbf{R}]$ | Trace of correlation matrix $\mathbf{R}$ |
| $\chi(\mathbf{R})$ | Eigenvalue spread of correlation matrix $\mathbf{R}$ |
| $\mathcal{M}$ | Misdajustment |
| $\boldsymbol{\varphi}_o$ | Output error IIR filter information vector |
| $\hat{\mathbf{y}}(n-1)$ | Vector of N past output samples of adaptive filter model |
| $\boldsymbol{\theta}$ | IIR filter coefficient vector of M feedforward and N feedback coefficients |
| $e_o(n)$ | Output error signal |
| $q^{-1}$ | Unit delay operator |
| $\mathbf{B}(q^{-1})$ | Feedforward coefficient vector |
| $\mathbf{A}(q^{-1})$ | Feedback coefficient vector |
| $\mathbf{R}_{\boldsymbol{\varphi}_o\boldsymbol{\varphi}_o}$ | (M+N) x (M+N) autocorrelation matrix of the information vector $\boldsymbol{\varphi}_o$ |

| | |
|---|---|
| $\mathbf{r}_{y\varphi_o}$ | (M+N) x 1 cross correlation vector between the output of IIR filter signal $y(n)$ and the information vector $\boldsymbol{\varphi}_o$ |
| $\mathbf{R}_{x\hat{y}}$ | M x N cross correlation matrix between input vector $\mathbf{x}(n)$ and IIR filter output vector $\hat{\mathbf{y}}(n-1)$ |
| $\mathbf{R}_{\hat{y}\hat{y}}$ | N x N cross correlation matrix of IIR filter output vector $\hat{\mathbf{y}}(n-1)$ |
| $b_i$ | Feedforward coefficient i |
| $a_j$ | Feedback coefficient j |
| $\boldsymbol{\varphi}_{FG}(n)$ | Full gradient output error AR filtered information vector |
| $\mathbf{x}_f(n)$ | Vector of M past AR filtered input samples |
| $\hat{\mathbf{y}}_f(n)$ | Vector of N past AR filtered IIR filter output samples |
| $\varphi_f(n)$ | Simplified gradient output error AR filtered information vector |
| $\boldsymbol{\theta}_*$ | IIR filter coefficient vector at minimum point on mean square error surface |
| $\mathbf{R}_{\varphi_f\varphi_f}$ | (M+N) x (M+N) autocorrelation matrix of the information vector $\varphi_f(n)$ |
| $\mathbf{R}_{x_f x_f}(n)$ | M x M auto correlation matrix of filtered IIR filter output vector $\mathbf{x}_f(n)$ |
| $\mathbf{R}_{x_f\hat{y}_f}$ | M x N auto correlation matrix between the filtered input vector $\mathbf{x}_f(n)$ and filtered IIR filter output vector $\hat{\mathbf{y}}_f(n)$ |
| $\mathbf{R}_{\hat{y}_f\hat{y}_f}$ | N x N auto correlation matrix of filtered IIR filter output vector $\hat{\mathbf{y}}_f(n)$ |
| $\mathbf{R}^{-1}_{\varphi_f\varphi_f}$ | Inverse of correlation matrix $\mathbf{R}_{\varphi_f\varphi_f}$ |
| $\mathbf{H}(\boldsymbol{\theta}_n)$ | Hessian matrix for filter coefficients $\boldsymbol{\theta}$ |
| $\mathbf{H}^{-1}(\boldsymbol{\theta}_n)$ | Inverse of Hessian matrix |
| $\hat{\mathbf{R}}^{-1}_{\varphi_f\varphi_f}$ | Estimate of the inverse of correlation matrix $\mathbf{R}_{\varphi_f\varphi_f}$ using matrix inversion lemma |
| $\rho$ | Stepsize control factor for use in Normalised LMS Newton algorithms |
| $\alpha$ | Convergence factor |
| $\mathbf{R}_{\varphi_o\varphi_o}$ | (M+N) x (M+N) autocorrelation matrix of the information vector $\varphi_o(n)$ |
| $\mathbf{R}^{-1}_{\varphi_o\varphi_o}$ | Inverse of correlation matrix $\mathbf{R}_{\varphi_o\varphi_o}$ |
| $\hat{\mathbf{R}}^{-1}_{\varphi_o\varphi_o}$ | Estimate of the inverse of correlation matrix $\mathbf{R}_{\varphi_o\varphi_o}$ using matrix inversion lemma |
| $\mathbf{C}(q^{-1})$ | Error filter coefficient vector |
| $\mathbf{d}(n-1)$ | Vector of N past desired signal samples |
| $e_e(n)$ | Equation error signal |
| $\boldsymbol{\varphi}_e(n)$ | Equation error IIR filter information vector |

| | |
|---|---|
| $\mathbf{R}_{\varphi_e\varphi_e}$ | (M+N) x (M+N) autocorrelation matrix of the information vector $\boldsymbol{\varphi}_e(n)$ |
| $\mathbf{r}_{d\varphi}$ | (M+N) x 1 cross correlation vector between the desired signal $d(n)$ and the information vector $\boldsymbol{\varphi}_e(n)$ |
| $\mathbf{R}_{xd}$ | M x N cross correlation matrix between the input vector $\mathbf{x}(n)$ and desired signal vector $\mathbf{d}(n-1)$ |
| $\mathbf{R}_{dd}$ | M x M auto correlation matrix of desired signal vector $\mathbf{d}(n-1)$ |
| $\mathbf{v}(n)$ | Vector of N past echo path output disturbance signal samples |
| $\mathbf{r}_{vv}$ | (N) x 1 cross correlation vector between the noise signal $v(n)$ and the noise vector $\mathbf{v}(n)$ |
| $\mathbf{R}_{vv}$ | N x N auto correlation matrix of noise signal vector $\mathbf{v}(n)$ |
| $\mathbf{R}^{-1}_{\varphi_e\varphi_e}$ | Inverse of correlation matrix $\mathbf{R}_{\varphi_e\varphi_e}$ |
| $\hat{\mathbf{R}}^{-1}_{\varphi_e\varphi_e}$ | Estimate of the inverse of correlation matrix $\mathbf{R}_{\varphi_e\varphi_e}$ using matrix inversion lemma |
| $\boldsymbol{\varphi}_{br}(n)$ | Bias remedied equation error IIR filter information vector |
| $\tau$ | Bias remedy parameter |
| $\mathbf{R}_{\varphi_{br}\varphi_{br}}$ | (M+N) x (M+N) autocorrelation matrix of the information vector $\boldsymbol{\varphi}_{br}(n)$ |
| $\mathbf{R}^{-1}{}_{\varphi_{br}\varphi_{br}}$ | Inverse of correlation matrix $\mathbf{R}_{\varphi_{br}\varphi_{br}}$ |
| $\hat{\mathbf{R}}^{-1}{}_{\varphi_{br}\varphi_{br}}$ | Estimate of the inverse of correlation matrix $\mathbf{R}^{-1}{}_{\varphi_{br}\varphi_{br}}$ using matrix inversion lemma |
| $e_{fe}(n)$ | Filtered equation error signal |
| $d_f(n)$ | Filtered desired response signal |
| $\mathbf{d}_f(n-1)$ | Vector of N past AR filtered desired signal samples |
| $\boldsymbol{\varphi}_{fe}(n)$ | Filtered equation error IIR filter information vector |
| $\mathbf{R}_{\varphi_{fe}\varphi_{fe}}$ | (M+N) x (M+N) autocorrelation matrix of the information vector $\boldsymbol{\varphi}_{fe}(n)$ |
| $\mathbf{R}_{x_f d_f}$ | M x N cross correlation matrix between the filtered input vector $\mathbf{x}_f(n)$ and filtered desired signal vector $\mathbf{d}_f(n-1)$ |
| $\mathbf{R}_{d_f d_f}$ | M x M auto correlation matrix of desired signal vector $\mathbf{d}(n-1)$ |
| $\mathbf{R}^{-1}_{\varphi_{fe}\varphi_{fe}}$ | Inverse of correlation matrix $\mathbf{R}_{\varphi_{fe}\varphi_{fe}}$ |
| $\hat{\mathbf{R}}^{-1}_{\varphi_{fe}\varphi_{fe}}$ | Estimate of the inverse of correlation matrix $\mathbf{R}_{\varphi_{fe}\varphi_{fe}}$ using matrix inversion lemma |

# 9. References


[1.1] G.W.K.Gritton and D.W.Lin, "Echo Cancellation Algorithms", IEEE ASSP Mag, April 1984, p31-38

[1.1] M.M.Sondhi and D.A. ,Berkley , " Silencing Echoes on the Telephone Network", Proc IEEE, Vol68, No8, August 1980, p948-963

[1.2] D.G. Messerschmitt, "Echo Cancellation in Speech and Data Transmission", IEEE Journal on Selected Areas in Comm, SAC-2, p283-297, 1984

[1.3] M.M.Sondhi, "An Adaptive Echo Canceller", Bell Sys Tech Journal, p497-511, 1967.

[1.4] "Acoustic Echo Controllers", ITU G.167 , March 1993

[1.5] S.H.Jensen, "Acoustic Echo Canceller for Hands-free Mobile Radiotelephony", Signal Processing VI: Theories and Applications, p1629-1632, 1992.

[1.6] A. Zitzerwitz, " Considerations on Acoustic Echo Cancelling based on Realtime Experiments", Signal Processing V: Theories and Applications, p1987-1990, 1986

[1.7] J.W.Emling and D.Mitchell, " The Effects of Time and Delay on Telephone Conversations", Bell Sys Tech Journal, 1963, p2869-2891.

[1.8] R.G. Gould and G.K.Helder, " Transmission Delay and Echo Suppression", IEEE Spectrum April 1970, p47-54.

[1.9] "Speech Teleservices: 30.6. Telephone Acoustic Coupling Loss", Digital Cellular Telecommunications System (Phase2): Mobile Station Conformance Specification; Part 1, GSM 11.10-1, version 4.21.0, p1154-1156, March 1998.

[1.10] "Terminal Acoustic Characteristics for Telephony: Requirements", 3GPP TS 26.131,v3.3, Sept 2001.

[1.11] P.A. Nelson and S.J. Elliott, " Active Control of Sound", Academic Press 1992.

[1.12] E.Hansler, "From Algorithms to Systems – It's a Rocky Road", International Workshop on Acoustic Echo and Noise Control, Sept 1997

[1.13] S.Gudvangen, S.J.Flockton, "Modelling of Acoustic Transfer Functions for echo cancellers", IEE Proc Vis Signal Image Process, Vol 142, No 1, Feb 1995

[2.1] "Speech Teleservices: 30.6. Telephone Acoustic Coupling Loss", Digital Cellular Telecommunications System (Phase2): Mobile Station Conformance Specification; Part 1, GSM 11.10-1, version 4.21.0, p1154-1156, March 1998.

[2.2] "Terminal Acoustic Characteristics for Telephony: Requirements", 3GPP TS 26.131,v3.3, Sept 2001.

[2.3] J.P Costa, et al, " Non-linear mechanical echo cancellation in a GSM terminal".

[2.4] J.Borwick, "Loudspeaker and Headphone Handbook", Focal Press, 1994.

[2.5] P.A. Nelson and S.J. Elliott, " Active Control of Sound", Academic Press 1992.

[2.6] D.E.Newland, " An Introduction to Random Vibrations, Spectral and Wavelet Analysis", Longman Scientific and Technical, 1993.

[2.7] P. D. Welch, "The use of the Fast Fourier Transform for the Estimation of Power Spectra: A Method Based on Time Averaging Over Short, Modified Periodograms", IEEE Trans. Audio Electroacoust. Vol. AU-15, p70-73, June 1967.

[2.8] Siglab Application Note 7.1, "Real-Time Processing Within Matlab", p1-12, Jan 1996

[2.9] Siglab Application Note 5.1, "Estimating Transfer Functions with Siglab", p1-20, Nov 1996
[2.10] MATLAB Signal Processing Toolbox User's Guide.
[2.11] "Terminal Coupling Loss Algorithm", CCITT G.122, March 1993.
[2.12] "Adaptive Multi-Rate Wideband codec", ITU Recommendation G.722.2

[3.1] P.A. Nelson and S.J. Elliott, " Active Control of Sound", Academic Press 1992.
[3.2] P.M.Clarkson, " Optimal and Adaptive Signal Processing", CRC Press, 1993.
[3.3] S.Gudvangen and P.Flockton, "Modelling of acoustic transfer functions for echo cancellers", IEEE Proc Vis Image Sig Proc, Vol 142, No 1, Feb 1995, p47-51.
[3.4] P.S.R Diniz and S.Netto, "Adaptive IIR Filtering Algorithms for System Identification: A General Framework", IEEE Trans Education, Vol 35, No 1, Feb 1995.
[3.5] B.Widrow & S.Stearns, "Adaptive Signal Processing", Prentice Hall, 1985.
[3.6] G.W. Gritton and D.W.Lin, "Echo Cancellation Algorithms", IEEE ASSP Mag, Vol 1, No 2, April 1984, p30-38.
[3.7] M.M.Sondhi, "An Adaptive Echo Canceller", Bell Sys Tech Journal, Vol 46, March 1967, p497-511.
[3.8] J.Lim and A.Oppenheim, "Advanced Topics in Signal Processing", Prentice Hall, 1987.
[3.9] P.S.R.Diniz, M.L.R.Campos, "Analysis of LMS Newton Adaptive Filtering Algorithms with variable convergence factor", IEEE Trans Sig Proc, Vol43, No3, p617-627, March 1995
[3.10] M.L.R.Campos, "A new Quasi-Newton Adaptive Filtering Algorithm", IEEE Trans Ccts and Sys II,, Vol44, No11, Nov 1997
[3.11] Simon Haykin, "Adaptive Filter Theory", Prentice Hall, 1996
[3.12] J.Shynk, "Adaptive IIR Filtering", IEEE ASSP Mag, April 1989
[3.13] P.A.Regalia, " Adaptive IIR Filtering in Signal Processing and Control", Marcel Dekker, 1995
[3.14] M.H.Hayes, "Statistical Digital Signal Processing and Modelling", John Wiley and Sons, 1996
[3.15] S.White, " An Adaptive Recursive Digital Filter".
[3.16] W.Mikhael, F.H.Wu, L.G.Kazovsky, "Adaptive Filters with Individual Adaption of Parameters", IEEE Trans Ccts & Sys, vol CAS-33, No 7, July 1986, p677-685.
[3.17] H.Fan, "An Investigation of an Adaptive IIR Echo Canceller: Advantages and Problems", IEEE Trans ASSP, vol 36, No 12, Dec 1998.
[3.18] S.Gee, M Rupp, " A comparison of Adaptive IIR Echo Canceller Hybrids", IEEE Conf 1991, p1541-1544.
[3.19] R.A.Soni, W.Jenkins, "A rapidly converging adaptive IIR filter", IEEE Conf 1996, p236-239.
[3.20] P.L. Feintuch, "An Adaptive Recursive LMS Filter", Proc IEE Nov 1976, p1622-1624.
[3.21] C.R.Johnson Jr, "Comments and Additions to An Adaptive Recursive LMS Filter", IEEE Electronic Letters, Sept 1997, p1399-1401.
[3.22] P.L. Feintuch,"Reply to Comments and Additions to An Adaptive Recursive LMS Filter", IEEE Electronic Letters, Sept 1977, p1401-1402.
[3.23] C.R.Johnson Jr, M.G.Larrimore, "SHARF: An algorithm for adapting IIR digital filters", IEEE Trans ASSP, vol 28, No 4, p428-440, Aug 1980.
[3.24] C.R.Johnson Jr, "Adaptive IIR Filtering: Current Results and Open Issues", IEEE Trans IT, vol 30, No 2, p237-249, March 1984.
[3.25] M.Rupp and A.Sayed, "On the stability and convergence of Feintuch's Algorithm for Adaptive IIR Filtering", IEEE Conf 1995, p1388-1390

[3.26] J.N.Lin, R.Unbehauen, " Bias Remedy Least Mean Square Equation Error Algorithm for IIR Parameter Recursive Eatimation", IEEE Trans Sig Proc, vol 40, No 1, Jan 1992, p62-69.

[3.27] H.Fan, W.Jenkins, " A new Adaptive IIR Filter", IEEE Trans Ccts & Sys, Vol 33, No 10, Oct 1986.

[3.28] J.N.Lin, R.Unbehauen, "A modification of the Bias Remedy LMSEE Algorithm for System Identication and adaptive filtering", IEEE Conf 1990, p3150-3153.

[3.29] S.Gudvangen, S.J Flockton, " Modelling of acoustic transter functions for echo cancellers", IEE Proc Vis Image Sig Proc, vol 142, No 1, Feb 1995, p47-51.

[3.30] M.Rupp, "A comparison of Adaptive IIR Echo Canceller Hybrids", IEEE Conf 1991.

[3.31] M.Rupp, "Adaptive IIR Echo Cancellers for Hybrids using the Motorolla 56001", Signal Proc V, p1487-1490.

[3.32] J.E. Cousseau, P. S. R. Diniz, " A consistent Steiglitz McBride Algorithm", IEEE conf 1993

[3.33] J.E. Cousseau, P. S. R. Diniz, " New adaptive IIR Filtering Algorithms Based on the Steiglitz-McBride Methos", IEEE Trans Signal Proc, Vol 45, No 5, May 1997.

[4.1] A P. Liavias, P. A. Regalia, "Acoustic Echo Cancellation: Do IIR Models Offer Better Modelling Capabilities than their FIR counterparts?", IEEE Transactions on Signal Processing, Vol. 46, No 9 , p2499-2504, Sept 1998

[4.2] S. Gudvangen, S.J. Flockton, "Modelling of acoustic transfer functions for echo cancellers"
IEE Proc Vis Image Signal Processing, Vol. 142, No 1, p47-51, Feb 1995.

[4.3] S. Gudvangen, S.J. Flockton, "Comparison of Pole-Zero and All Zero Modelling of Acoustic Transfer function", IEE Electronic Letters, Vol. 28, No 21, p1976-1978, Oct 92.

[4.4] "Lucent CSP1089 GSM Signal Processor for Cellular Handset and Modem Applications v1.0", May 1997, Lucent Technologies.

[4.5] MATLAB System Identification Toolbox User's Guide.

[4.6] Händel, P., and A. Nehorai (1994). Tracking Analysis of an Adaptive Notch Filter with Constrained Poles and Zeros. *IEEE Trans. Signal Processing*, vol.42, 2, pp.281-291.

[4.7] G.A. Williamson and S. Zimmermann, "Globally convergent adaptive IIR filters based on fixed pole locations," IEEE Trans. on Signal Processing, vol. 44, no. 6, pp. 1418-1427, June 1996.

[5.1] Simon Haykin , "Adaptive Filter Theory", Prentice Hall, 1996

[5.2] P.M.Clarkson, "Optimal and Adaptive Signal Processing", CRC Press, 1993.

[5.3] Wafsy B. Michael et al, "Adaptive Filters with Individual Adaption of Parameters", IEEE Trans Circuits and Systems, Vol 33, No 7, July 1996, p677-685

[5.4] J.S. Lim, A.V. Oppenhien, " Advance Topics in Signal Processing", Prentice Hall, 1988

[5.5] W.K. Jenkins, R.A. Soni, " Rapidly Converging Adaptive IIR Algorithms", IEEE Proc 1996.

[5.6] T.J. Shan, T. Kailath, "Adaptive Algorithms with an Automatic Gain Control Feature", IEEE Transactions Circuits and Systems, Vol 35, No 1, Jan 1988.

[5.7] C.Breining, E.Hansler, et al, "Acoustic Echo Control: An Application of Very-High -Order Adaptive Filters", IEEE Signal Proc Mag, July 1999.

[5.8] Sergio L. Netto, Paulo S.R.Diniz, "Adaptive IIR filtering Algorithms for System Identification: A General Framework", IEEE Trans Education, Vol 38, No 1, Feb 1995, p54-66

[5.9] Monson H.Hayes, "Statistical Digital Signal Processing and Modelling",

[5.10] P.L Feintuch, " An Adaptive Recursive LMS Filter", Proceedings IEEE, Nov 1976, p1622-1624

[6.1] Simon Haykin , "Adaptive Filter Theory", Prentice Hall, 1996

[6.2] O.Macchi , "A general methodology for comparison of adaptive filtering algorithms in a non-stationary context", Signal Processing V: Theories and Applications, p189-192, 1990.

[6.3] A.Gilliore. T.Petillion, "A comparison of NLMS and Fast RLS algorithms for identification of time-varying systems with noisy outputs", Signal Processing V: Theories and Applications, p417-420, 1990.

[6.4] T.Petillion , A Gilliore, "The Fast Newton Transversal Filter : An efficient scheme for Acoustic Echo Cancellation in Mobile Radio", IEEE Trans Sig Proc, Vol 42, No 3, March 1994.

[6.5] E.Hansler et al, "Acoustic Echo Control: An application of Very High Order Adaptive Filters", IEEE Signal Proc Mag, p42-52, July 1999

[6.6] P.Naylor, J.Boudy, Y.Grenier, "Enhancement of hands-free telecommunications", Ann Telecommun, Vol 49, No7-8, 1994

[6.7] Marcello de Campos, " A new Quasi-Newton Adaptive Filtering Algorithm", IEEE Trans Ccts and Sys - II, Vol 44, No 11, Nov 1997, p 924-934

[6.8] T.Shan and T.Kailath ,"Adaptive Algorithms with an Automatic Gain Control Feature", IEEE Trans Ccts and Sys, Vol 35, No 1, Jan 1998

[6.9] T.Shan and T.Kailath ,"Adaptive Algorithms with an Automatic Gain Control", Conf on Ccts Sys and Computers, p509-513, Nov 1985.

[6.10] Paulo S.R.Diniz, "Analysis of LMS Newton Adaptive Filtering algorithms with variable convergence factor", IEEE Trans on Signal Proc, Vol 43, No 3, March 1995